THIRD WINDOW SYNDROME

EDITED BY: P. Ashley Wackym, Carey David Balaban, Tetsuo Ikezono and Yuri Agrawal

PUBLISHED IN: Frontiers in Neurology

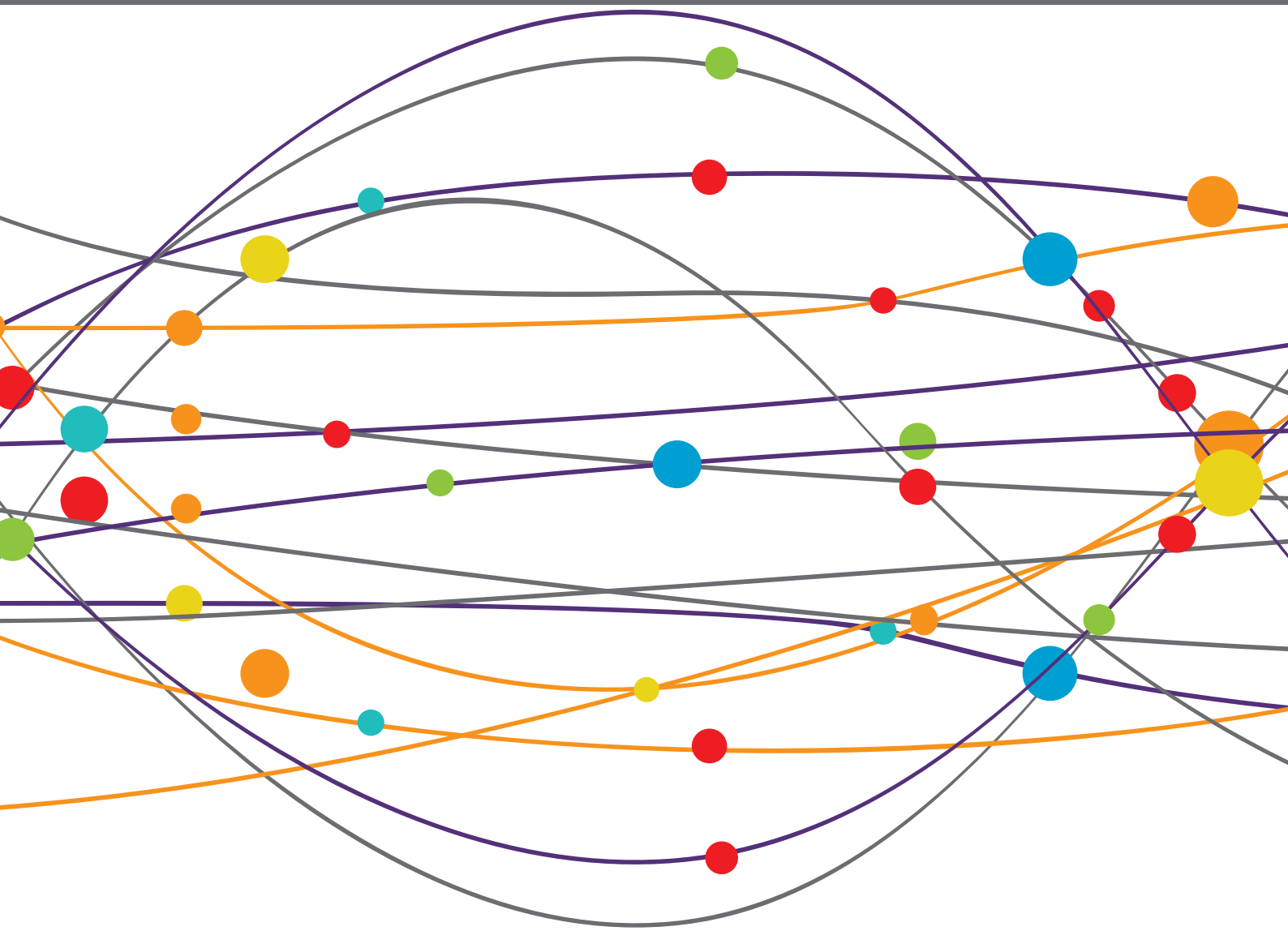

frontiers Research Topics

ISSN 1664-8714
ISBN 978-2-88971-190-1
DOI 10.3389/978-2-88971-190-1

About Frontiers

Frontiers is more than just an open-access publisher of scholarly articles: it is a pioneering approach to the world of academia, radically improving the way scholarly research is managed. The grand vision of Frontiers is a world where all people have an equal opportunity to seek, share and generate knowledge. Frontiers provides immediate and permanent online open access to all its publications, but this alone is not enough to realize our grand goals.

Frontiers Journal Series

The Frontiers Journal Series is a multi-tier and interdisciplinary set of open-access, online journals, promising a paradigm shift from the current review, selection and dissemination processes in academic publishing. All Frontiers journals are driven by researchers for researchers; therefore, they constitute a service to the scholarly community. At the same time, the Frontiers Journal Series operates on a revolutionary invention, the tiered publishing system, initially addressing specific communities of scholars, and gradually climbing up to broader public understanding, thus serving the interests of the lay society, too.

Dedication to Quality

Each Frontiers article is a landmark of the highest quality, thanks to genuinely collaborative interactions between authors and review editors, who include some of the world's best academicians. Research must be certified by peers before entering a stream of knowledge that may eventually reach the public - and shape society; therefore, Frontiers only applies the most rigorous and unbiased reviews.
Frontiers revolutionizes research publishing by freely delivering the most outstanding research, evaluated with no bias from both the academic and social point of view. By applying the most advanced information technologies, Frontiers is catapulting scholarly publishing into a new generation.

What are Frontiers Research Topics?

Frontiers Research Topics are very popular trademarks of the Frontiers Journals Series: they are collections of at least ten articles, all centered on a particular subject. With their unique mix of varied contributions from Original Research to Review Articles, Frontiers Research Topics unify the most influential researchers, the latest key findings and historical advances in a hot research area! Find out more on how to host your own Frontiers Research Topic or contribute to one as an author by contacting the Frontiers Editorial Office: frontiersin.org/about/contact

THIRD WINDOW SYNDROME

Topic Editors:
P. Ashley Wackym, Rutgers Robert Wood Johnson Medical School, NJ, United States
Carey David Balaban, University of Pittsburgh, PA, United States
Tetsuo Ikezono, Saitama Medical University, Japan
Yuri Agrawal, Johns Hopkins University, MD, United States

Citation: Wackym, P. A., Balaban, C. D., Ikezono, T., Agrawal, Y., eds. (2021). Third Window Syndrome. Lausanne: Frontiers Media SA.
doi: 10.3389/978-2-88971-190-1

Table of Contents

05 ***Editorial: Third Window Syndrome***
P. Ashley Wackym, Yuri Agrawal, Tetsuo Ikezono and Carey D. Balaban

11 ***Third Window Syndrome: Surgical Management of Cochlea-Facial Nerve Dehiscence***
P. Ashley Wackym, Carey D. Balaban, Pengfei Zhang, David A. Siker and Jasdeep S. Hundal

35 ***Ambient Pressure Tympanometry Wave Patterns in Patients With Superior Semicircular Canal Dehiscence***
Anthony Thai, Zahra N. Sayyid, Davood K. Hosseini, Austin Swanson, Yifei Ma, Ksenia A. Aaron and Yona Vaisbuch

43 ***Psychometric Tests and Spatial Navigation: Data From the Baltimore Longitudinal Study of Aging***
Eric X. Wei, Eric R. Anson, Susan M. Resnick and Yuri Agrawal

52 ***Vestibular Evoked Myogenic Potential (VEMP) Testing for Diagnosis of Superior Semicircular Canal Dehiscence***
Kimberley S. Noij and Steven D. Rauch

60 ***Changes in Vestibulo-Ocular Reflex Gain After Surgical Plugging of Superior Semicircular Canal Dehiscence***
Sang-Yeon Lee, Yun Jung Bae, Minju Kim, Jae-Jin Song, Byung Yoon Choi and Ja-Won Koo

71 ***Membranous or Hypermobile Stapes Footplate: A New Anatomic Site Resulting in Third Window Syndrome***
Arun K. Gadre, Ingrid R. Edwards, Vicky M. Baker and Casey R. Roof

83 ***Biomechanics of Third Window Syndrome***
Marta M. Iversen and Richard D. Rabbitt

94 ***Ocular Vestibular-Evoked Myogenic Potential Amplitudes Elicited at 4 kHz Optimize Detection of Superior Semicircular Canal Dehiscence***
Emma D. Tran, Austin Swanson, Jeffrey D. Sharon, Yona Vaisbuch, Nikolas H. Blevins, Matthew B. Fitzgerald and Kristen K. Steenerson

105 ***Investigation of Mechanisms in Bone Conduction Hyperacusis With Third Window Pathologies Based on Model Predictions***
Stefan Stenfelt

120 ***Perilymphatic Fistula: A Review of Classification, Etiology, Diagnosis, and Treatment***
Brooke Sarna, Mehdi Abouzari, Catherine Merna, Shahrnaz Jamshidi, Tina Saber and Hamid R. Djalilian

131 ***Audiovestibular Quantification in Rare Third Window Disorders in Children***
Soumit Dasgupta, Sudhira Ratnayake, Rosa Crunkhorn, Javed Iqbal, Laura Strachan and Shivaram Avula

146 ***Impact of Superior Canal Dehiscence Syndrome on Health Utility Values: A Prospective Case-Control Study***
Ibrahim Ocak, Vedat Topsakal, Paul Van de Heyning, Gilles Van Haesendonck, Cathérine Jorissen, Raymond van de Berg, Olivier M. Vanderveken and Vincent Van Rompaey

154 ***Cervical and Ocular Vestibular-Evoked Myogenic Potentials in Patients With Intracochlear Schwannomas***
Laura Fröhlich, Ian S. Curthoys, Sabrina Kösling, Dominik Obrist, Torsten Rahne and Stefan K. Plontke

164 ***Bone-Conducted oVEMP Latency Delays Assist in the Differential Diagnosis of Large Air-Conducted oVEMP Amplitudes***
Rachael L. Taylor, John S. Magnussen, Belinda Kwok, Allison S. Young, Berina Ihtijarevic, Emma C. Argaet, Nicole Reid, Cheryl Rivas, Jacob M. Pogson, Sally M. Rosengren, G. Michael Halmagyi and Miriam S. Welgampola

175 ***Congenital Membranous Stapes Footplate Producing Episodic Pressure-Induced Perilymphatic Fistula Symptoms***
Han Matsuda, Yasuhiko Tanzawa, Tatsuro Sekine, Tomohiro Matsumura, Shiho Saito, Susumu Shindo, Shin-ichi Usami, Yasuhiro Kase, Akinori Itoh and Tetsuo Ikezono

180 ***A Simple Specific Functional Test for SCD: VEMPs to High Frequency (4,000Hz) Stimuli—Their Origin and Explanation***
Ian S. Curthoys and Leonardo Manzari

184 ***Case Report: Local Anesthesia Round Window Plugging and Simultaneous Vibrant Soundbridge Implant for Superior Semicircular Canal Dehiscence***
Giulia Mignacco, Lorenzo Salerni, Ilaria Bindi, Giovanni Monciatti, Alfonso Cerase and Marco Mandalà

190 ***Detection of Wandering Behaviors Using a Body-Worn Inertial Sensor in Patients With Cognitive Impairment: A Feasibility Study***
Rebecca J. Kamil, Dara Bakar, Matthew Ehrenburg, Eric X. Wei, Alexandra Pletnikova, Grace Xiao, Esther S. Oh, Martina Mancini and Yuri Agrawal

196 ***Case Report: Could Hennebert's Sign Be Evoked Despite Global Vestibular Impairment on Video Head Impulse Test? Considerations Upon Pathomechanisms Underlying Pressure-Induced Nystagmus due to Labyrinthine Fistula***
Andrea Castellucci, Cecilia Botti, Margherita Bettini, Ignacio Javier Fernandez, Pasquale Malara, Salvatore Martellucci, Francesco Maria Crocetta, Martina Fornaciari, Francesca Lusetti, Luigi Renna, Giovanni Bianchin, Enrico Armato and Angelo Ghidini

207 ***Current Trends, Controversies, and Future Directions in the Evaluation and Management of Superior Canal Dehiscence Syndrome***
Kristine Elisabeth Eberhard, Divya A. Chari, Hideko Heidi Nakajima, Mads Klokker, Per Cayé-Thomasen and Daniel J. Lee

frontiers in Neurology

EDITORIAL
published: 18 June 2021
doi: 10.3389/fneur.2021.704095

Editorial: Third Window Syndrome

P. Ashley Wackym[1]*, *Yuri Agrawal*[2], *Tetsuo Ikezono*[3] and *Carey D. Balaban*[4]

[1] Department of Otolaryngology-Head and Neck Surgery, Rutgers Robert Wood Johnson Medical School, New Brunswick, NJ, United States, [2] Department of Otolaryngology-Head and Neck Surgery, Johns Hopkins University, Baltimore, MD, United States, [3] Department of Otorhinolaryngology, Graduate School of Medicine, Saitama Medical University, Saitama, Japan, [4] Departments of Otolaryngology, Neurobiology, Communication Science & Disorders, Bioengineering and Mechanical Engineering and Materials Science, University of Pittsburgh, Pittsburgh, PA, United States

Keywords: cognitive dysfunction, dizziness, perilymph fistula, sound-induced dizziness, superior semicircular canal dehiscence, third window syndrome, vestibular migraine

Editorial on the Research Topic

Third Window Syndrome

In this Research Topic, Third Window Syndrome, we brought together recent discoveries of the mechanisms of the associated spectrum of symptoms, dysfunction, novel diagnostic tools and interventions to identify and resolve Third Window Syndrome.

Nearly a century ago, Tullio described the physiologic outcomes of creating a third mobile window in the semicircular canals of pigeons. Since that time, many locations of third mobile windows have been described; however, the sound-induced dizziness and/or nystagmus has been memorialized by the eponym "Tullio phenomenon." Clinically, the most thoroughly characterized third mobile window is superior semicircular canal dehiscence. In 1998, Minor et al. first reported the diagnosis of CT positive superior semicircular canal dehiscence (SSCD) (1). Minor later reported a conductive hearing loss, which was recognized as a pseudoconductive hearing loss (bone-conduction hyperacusis), as well as a reduced cervical vestibular myogenic potential (cVEMP) threshold in patients with superior semicircular canal dehiscence. While superior semicircular canal dehiscence is well-recognized; it has been reported the existence of a CT negative third window syndrome with the same clinical phenotype of superior semicircular canal dehiscence exists. It has been reported that CT negative third window syndrome is associated with a pseudoconductive hearing loss and an abnormally reduced cVEMP threshold, among other objective findings typically found in superior semicircular canal dehiscence patients. The more general term of Third Window Syndrome has gained acceptance because the same spectrum of symptoms, signs on physical examination and audiological diagnostic findings are encountered with superior semicircular canal dehiscence, cochlea-facial nerve dehiscence, cochlea-internal carotid artery dehiscence, cochlea-internal auditory canal dehiscence, lateral semicircular canal-superior semicircular canal ampulla dehiscence, modiolus, "perilymph fistula," posterior semicircular canal dehiscence, posterior semicircular canal-jugular bulb dehiscence, superior semicircular canal dehiscence-subarcuate artery dehiscence, superior semicircular canal dehiscence-superior petrosal vein dehiscence, vestibule-middle ear dehiscence, lateral semicircular canal-facial nerve dehiscence, wide vestibular aqueduct in children, post-traumatic hypermobile stapes footplate and in patients with CT negative Third Window Syndrome. A common structural finding in all of these conditions is an otic capsule defect that creates a "third window."

Over the past 60 years, we have learned much regarding the clinical features, outcomes measured by validated survey instruments and neuropsychology testing as well as objective diagnostic studies in Third Window Syndrome. Beyond the hallmark symptoms of sound-induced otolithic

OPEN ACCESS

Edited and reviewed by:
Michael Strupp,
Ludwig Maximilian University of Munich, Germany

***Correspondence:**
P. Ashley Wackym
wackym@neurotology.org

Specialty section:
This article was submitted to Neuro-Otology, a section of the journal Frontiers in Neurology

Received: *01 May 2021*
Accepted: *07 May 2021*
Published: *18 June 2021*

Citation:
Wackym PA, Agrawal Y, Ikezono T and Balaban CD (2021) Editorial: Third Window Syndrome. Front. Neurol. 12:704095. doi: 10.3389/fneur.2021.704095

dysfunction (dizziness) and autophony, a wide range of other associated clinical manifestations have been reported, including: cognitive dysfunction, spatial disorientation, anxiety and migraine. The series of papers included in this Research Topic have provided important insights to both scientists and clinicians who deal with these fascinating areas of peripheral vestibular dysfunction and associated pathophysiology.

This Research Topic was truly global in effort and representation with four continents: Asia, Australia/Oceania, Europe, and North America. However, three were not represented: Africa, Antarctica, and South America. There were 15 countries represented: USA; Denmark; Israel; Korea; Germany; Australia; Switzerland; Belgium; Netherlands; Russia; Sweden; England/United Kingdom; New Zealand, Italy; and Japan. There were 118 authors.

In this summary, we highlight the 20 published studies included in this Research Topic and have organized these within the following categories: Diagnostic Studies and New Diagnostic Tools; Cognitive or Spatial Orientation; Health Utility Values; Biomechanics and Pathophysiology; Reviews; Sites of Dehiscence—Rare or Never Before Reported; and Surgical Advances.

DIAGNOSTIC STUDIES AND NEW DIAGNOSTIC TOOLS

Third Window Syndrome has been an important new clinical diagnosis, and worldwide thousands of patients have benefited from the discovery of this syndrome and the development of successful treatment. Additionally, Third Window Syndrome has also been a very useful pathologic phenomenon with which to better understand the physiology of the vestibular end-organs, and also develop and refine diagnostic tools that probe various elements of the vestibular system. In this Research Topic, several advances in our understanding of vestibular physiology and third window syndrome diagnosis have been reported. Many of these center around the vestibular-evoked myogenic potential (VEMP), which has found primary use in the detection of third mobile window physiology. An overall summary of the diagnostic value of VEMP in Third Window Syndrome has been provided by Noij and Rauch. In their comprehensive synthesis of the topic, the authors highlight that VEMP testing provides an efficient, accurate, and cost-effective screening and diagnostic tool for SSCD physiology, which can then be followed up by temporal bone CT. Noij and Rauch also discuss cutting edge enhancements of VEMP testing, including performing high frequency VEMP testing, which is further explored in detail by several other studies in this Research Topic.

Specifically, Tran et al. reported on the predictive value of using ocular VEMPs elicited at 4 kilohertz (kHz) in the diagnosis of SSCD. The conventional air-conducted sound stimulus for the VEMP test is a 500 Hz tone burst, given that this is thought to be within the physiologic frequency range of the otolith organs. However, the authors find a higher specificity for diagnosing SSCD with the higher frequency sound stimulus, possibly because the otoliths are less sensitive to sound at this higher frequency, and the low impedance system produced by a dehiscence results in the greatest difference in response compared to normal ears at the higher frequencies. Curthoys and Manzari also provide a report underscoring the diagnostic value of the higher frequency 4 kHz stimulus, and offer compelling data that superior canal afferents are activated in a dehiscent inner ear, which respond to 4 kHz stimulation and contribution to the enhancement of this higher frequency response. Curthoys and Manzari also note that performing a single-frequency VEMP has the benefit of reducing the sound exposure and time required for VEMP threshold testing, which requires presentation of multiple sound stimuli at different amplitudes to determine the threshold.

Another study that considers the role of VEMP in SSCD detection is the report from Taylor et al. which found that longer latencies in the bone-conducted ocular VEMP response provide additional diagnostic value in identifying SSCD. The authors provide the intriguing hypotheses that an additional inhibitory node in the stimulation of the inferior oblique muscle in the ocular VEMP response, or collision between ampullopetal and ampullofugal endolymph movement in the membranous canal may cause the delayed response. A final study that considered VEMP and Third Window Syndrome in this Research Topic is the report from Fröhlich et al.. The authors present intriguing data that patients with intracochlear schwannomas have evidence of VEMP abnormalities, including enhancement of VEMP responses. The authors provide the provocative hypothesis that the mass effect of the intracochlear schwannoma may affect inner ear fluid dynamics, and contribute to endolymphatic hydrops, which is some cases can parallel the physiology of Third Window Syndrome.

Additional studies in this Research Topic that have advanced new diagnostic tools include the study by Thai et al. which reported the use of ambient pressure tympanometry in patients with SSCD. Patients were observed to have rhythmic oscillations of their tympanic membranes, consistent with the dehiscence allowing transmission of vascular or cerebrospinal fluid pulsations through the membranous labyrinth, oval window, ossicular chain to the tympanic membrane. Two other studies provided insight into the frequency dynamics of the inner ear fluids. Lee et al. observed that following canal plugging, high frequency vestibular-ocular reflex responses in the plugged canal normalized over the long term, suggesting some preservation of high frequency responses despite resolution of symptoms and closure of the dehiscence. As a corollary, Castellucci et al. reported in a series of 3 patients with labyrinthine fistula that high-frequency responses were attenuated, although the patients still had evidence of canal function given a persistent Hennebert sign, possibly consistent with the preservation of low-frequency responses in a dehiscent state. This set of studies on new diagnostic tools provides evidence that Third Window Syndrome offers a window into the mechanisms of the inner ear!

COGNITIVE OR SPATIAL ORIENTATION

As has been noted previously, individuals with peripheral vestibular pathologies including semicircular canal dehiscence

have been shown to experience cognitive deficits that improve upon treatment of the vestibular pathology. As such, this Research Topic also explored the theme of cognitive sequelae associated with vestibular impairment. In one article by Wei et al. the link between two commonly-used cognitive outcome measures included in vestibular studies was investigated. Specifically, psychometric paper-and-pencil based cognitive tests and a dynamic test of spatial navigation—the Triangle Completion Task—were compared in ∼150 healthy older adults. The study reported that performance on the Triangle Completion Task was significantly associated with scores on tests of visuospatial ability, executive function, and motor processing speed, suggesting that spatial navigation ability taps into the cognitive skills of visuospatial processing, executive function, and motor processing speed. Interestingly, prior research has shown that vestibular function is also related to these cognitive outcome measures. Another study in this Research Topic by Kamil et al. further assessed a quantitative method to capture disoriented spatial navigation behavior—specifically wandering behavior—in a cohort of older adults with Alzheimer disease in whom wandering behaviors are common. Indeed, prior research has shown that patients with Alzheimer have an increased prevalence of vestibular impairment relative to cognitively-intact controls, and that vestibular impairment in turn is associated with spatial cognitive difficulties in Alzheimer patients. The Kamil et al. study established the feasibility of continuous accelerometric monitoring in Alzheimer patients, and provided preliminary data that characteristics of the turning behaviors in Alzheimer patients may identify individuals who wander. Taken together, this series of articles within this Research Topic provided further insight into relevant cognitive outcome measures that can be used in the study of patients with vestibular impairment.

HEALTH UTILITY VALUES

The most common third mobile window producing Third Window Syndrome is SSCD. Patients can experience disabling symptoms and may opt for surgical management. Limited data are available on the impact of SSCD on health-related quality of life (HRQoL) and disease-specific HRQoL more specifically. Ocak et al. performed a prospective analysis on generic HRQoL in SSCD patients compared to healthy age-matched controls. The study participants completed the Health Utility Index (HUI) Mark 2 (HUI2)/Mark 3 (HUI3) questionnaire. For the control group, age-matched participants without otovestibular pathology or other chronic pathology were recruited. The multi-attribute utility function (MAUF) score was calculated for the HUI2 and HUI3. Results of both groups were then compared using the Mann–Whitney *U*-test. For the SSCD case group, the median HUI2 MAUF score was 0.75 and median HUI3 MAUF score was 0.65. For the control group, the median scores were 0.88 and 0.86, respectively. There was a statistically significant difference for both HUI2 ($p = 0.024$) and HUI3 ($p = 0.011$) between the two groups. Not surprisingly, the SSCD patients had a worse generic HRQoL than age-matched healthy controls. Interestingly, one patient with unilateral SSCD had a negative HUI3 MAUF score (−0.07), indicating a health-state worse than death. Ocak et al. concluded that SSCD patients have significantly lower health utility values than an age-matched control group confirms the negative impact of SSCD on generic HRQoL using an instrument that is not designed to be disease-specific but to assess health state in general.

In a study of surgical outcomes in managing Third Window Syndrome caused by cochlea-facial dehiscence, Wackym et al. used the Dizziness Handicap Inventory (DHI) and also the Headache Impact Test (HIT-6) validated survey instruments to assess the changes in scores postoperatively compared to preoperatively for 8 patients who had round window reinforcement surgery for cochlea-facial nerve dehiscence causing third window syndrome and initially and at follow up for 8 patients who elected not to have surgery. The DHI is a 25-item self-assessment inventory designed to evaluate the self-perceived handicapping effects imposed by dizziness/vestibular dysfunction. The HIT-6 is a six-item self-assessment questionnaire used to measure the impact headaches have on a patient's ability to function on the job, at school, at home and in social situations. There was a highly significant improvement in DHI and HIT-6 at pre- vs. postoperative ($p < 0.0001$ and $p < 0.001$, respectively). These findings suggest that round reinforcement surgery for cochlea-facial nerve dehiscence reduces the handicap due to the secondary dizziness/vestibular dysfunction and impact of migraine headaches on their ability to function.

BIOMECHANICS AND PATHOPHYSIOLOGY

The current status of conceptual approaches to understanding the biomechanics and pathophysiology of Third Window Syndrome is reviewed and extended in the contributions by Iversen and Rabbitt and by Stenfelt. The former, very approachable review paper provides a comprehensive orientation to biomechanical issues in relation to auditory and vestibular findings. The audiometric results are discussed in the context of a simplified, lumped parameter model of the middle ear and inner ear that will serve well for didactic purposes. The separate sections on oculomotor findings, vestibular-evoked myogenic potentials, and electrocochleography also provide summaries of concepts and the current literature that orient the reader to the state-of-the-art.

The contribution by Stenfelt is an *in silico* study that adapts an earlier model to more deeply probe our formal understanding of basic principles underlying the relative contributions of bone conduction pathways [fluid inertia, middle ear inertial, compression, intracranial (CSF) pressure, and ear canal] to audition in the presence of third window syndromes. The findings predict that fluid inertial effects will have the greatest effect in a simulated semicircular canal dehiscence syndrome and that transmission via cerebrospinal fluid is unlikely to have a significant effect under the same conditions. Secondary predictions regarding the effects of vestibular aqueduct size, amenable to study.

REVIEWS

Over the past two decades, advances in diagnostic techniques have raised the awareness of SSCD and treatment approaches have been refined to improve patient outcomes. Eberhard et al. discuss contemporary and emerging diagnostic approaches for patients with Third Window Syndrome due to SSCD, focusing on four challenges: (1) the clinical testing algorithm for quantifying the effects of SSCD; (2) while high-resolution temporal bone CT remains the gold standard for detecting SSCD, a bony defect does not always result in signs and symptoms; (3) even when SSCD repair is indicated, there is a lack of consensus about nomenclature to describe the SSCD, ideal surgical approach, specific repair techniques, and type of materials used; and (4) there is no established algorithm in the evaluation of SSCD patients who fail primary repair and may be candidates for revision surgery. They concluded that comparative outcome studies are needed to assess challenging cases, such as patients with bilateral dehiscence, near dehiscence, revision cases, and concurrent SSCD and migraine disorder. It should be noted that many Third Window Syndrome sites of dehiscence, including SSCD, are associated with migraine headaches and the three variants of migraine (ocular migraine, vestibular migraine, and/or hemiplegic migraine) and are either comorbid, exacerbated by or caused by the otolithic asymmetry producing Third Window Syndrome.

An expanded discussion of Third Window Syndromes and how to distinguish them from PLF is found in the review by Sarna et al. Diagnosing PLFs has been a difficult task ever since their description over a century ago. The authors aimed at providing an update on the classification, diagnosis, and treatment of PLF. New diagnostic criteria are based on the inciting events and confirmation of a specific biomarker and leakage identification plus resolution symptoms after blood patch/surgical plugging. Presently, the novel biomarker cochlin-tomoprotein (CTP) is the best candidate for a specific biomarker, which has been approved by the Japan Ministry of Health, Labor, and Welfare (equivalent agency as the United States Food and Drug Administration [FDA] or the CE Mark for the European Union) for medical diagnosis. Advances in diagnostic criteria, high resolution imaging, and biomarker testing are paving the way for accurate preoperative diagnosis of Third Window Syndrome. The authors concluded that PLF is one of the few etiologies of dizziness, tinnitus, and hearing loss that can be treated surgically. They also emphasized that it is critical to remain vigilant and keep PLF in the differential diagnosis since prompt treatment has the potential to alleviate patients from debilitating vertigo and permanent hearing loss.

SITES OF DEHISCENCE—RARE OR NEVER BEFORE REPORTED

Dasgupta et al. completed a retrospective study of children (aged 5–17 years) diagnosed with rare third window disorders in a tertiary pediatric vestibular unit in the United Kingdom. They investigated the audiovestibular function in these children. The radiographic diagnosis was achieved by high resolution CT scan of the temporal bones. Of 920 children presenting for audiovestibular assessment over a 42 month period, rare third mobile windows were observed in 8 (<1%). These included posterior semicircular canal dehiscence (n = 3, 0.3%), posterior semicircular canal thinning (n = 2, 0.2%), X linked gusher (modiolus as the third mobile window) (n = 2, 0.2%), and a combination of dilated internal auditory meatus/irregular cochlear partition/deficient facial nerve canal (n = 1, 0.1%). The majority of these children (87.5%) demonstrated a mixed/conductive hearing loss with an air-bone gap in the presence of normal tympanometry (pseudoconductive hearing loss) in 100% of the children. Transient otoacoustic emissions were absent with a simultaneous cochlear pathology in 50% of the cohort. Features of disequilibrium were observed in 75% and about a third showed deranged vestibular function tests. Video head impulse test abnormalities were detected in 50% localizing to the side of the lesion. Cervical vestibular evoked myogenic potential test abnormalities were observed in all children in the cohort undergoing the test where low thresholds and high amplitudes classically found in third mobile window disorders localized to the side of the defects in 28.5%. In the series, 71.4% also demonstrated absent responses/amplitude asymmetry, some of which did not localize to the side of the third mobile window. Only two children presented with typical third window symptoms. This study suggests that pediatric third window disorders may not present with classical third mobile window features and are variable in their presentations and audiovestibular functions.

The prevalence and distribution of sites of dehiscence in 802 temporal bones of 401 patients with Third Window Syndrome was reported by Wackym et al. However, it should be emphasized that all of their patients had Third Window Syndrome symptoms, whereas the status of Third Window Syndrome symptoms was not reported for the subjects in other published prevalence studies. Wackym et al. identified 463 temporal bones [57.7% (463/802)] with a single site of dehiscence (SSCD, near-SSCD, CT negative Third Window Syndrome, CFD, cochlea-internal auditory canal, wide vestibular aqueduct, lateral semicircular canal, modiolus and posterior semicircular canal, SSCD and superior petrosal sinus, SSCD and subarcuate artery). If the CT negative Third Window Syndrome temporal bones were excluded, there was single site temporal bone dehiscence found in 366 [366/402 (91.0%)]. SSCD and near-SSCD were the most commonly observed site of dehiscence [59% (296/502)]. The second most commonly observed category of radiologic findings in the Third Window Syndrome cohort was CT negative Third Window Syndrome [19.3% (97/502)]. The third most commonly observed site of dehiscence was CFD [10.4% (52/502)]. Regarding multiple sites of dehiscence, there were 38 instances [38/405 (9.38%)] of two site dehiscence (SSCD and CFD, CFD and cochlea-internal auditory canal, CFD and wide vestibular aqueduct, SSCD and cochlea-internal auditory canal, SSCD and posterior semicircular canal-jugular bulb). The combination of SSCD and CFD accounted for 6% (30/502). There was one instance of three sites [3/405 (0.24%)] of dehiscence (SSCD and posterior semicircular canal and wide vestibular

aqueduct). The prevalence of multiple-site findings is important to consider when faced with recurrent or incompletely resolved Third Window Syndrome symptoms after plugging a SSCD. In light of their recent observations and the histologic, cadaveric and patient CT scan prevalence of CFD and concurrent SSCD and CFD, they concluded that careful assessment of the presence of CFD in patients with SSCD should be completed and factored into the surgical planning.

The pair of papers contributed by Gadre et al. and Matsuda et al. highlight that acquired or congenital defects in the stapes footplate can create Third Window Syndrome by creating a third mobile window. Gadre et al. reported an observational analytic case studies review of 28 patients (33 ears) managed over an 11-year interval. These patients suffered persistent dizziness following head trauma and demonstrated Tullio phenomena or Hennebert sign. All had neuroradiologists report normal otic capsules on high resolution temporal bone CT scans. However, when the gray-scale invert function was used to visualize the stapes footplate the absence of a normal footplate was evident, thus yielding the preoperative diagnosis. All cases had middle ear exploration to determine if perilymph leakage was present. Intraoperative Valsalva maneuvers were performed to visualize perilymph egress. They performed fat grafting of round and oval windows with none of the patients having deterioration of their hearing. Prior to surgery all patients reported dizziness in response to loud sounds and/or barometric pressure changes. Seven out of 33 ears had demonstrable perilymph leakage into the middle ear; the rest (26 ears) appeared to have membranous or hypermobile stapes footplates. Thirteen patients had a fistula sign positive bilaterally while 15 had unilateral pathology. Twenty-four of the 28 patients (85.7%) showed both subjective and objective improvement following surgery. They concluded that a membranous or hypermobile stapes footplate can occur following head trauma and can cause intractable dizziness typical of Third Window Syndrome.

The contribution by Matsuda et al. reported a patient with a congenital dehiscence of the right stapes footplate. This dehiscence caused long-standing episodic pressure-induced vertigo (Hennebert sign) with intervals of being asymptomatic and normal. At the time of presentation, her increased thoracic pressure changes induced the rupture of the membranous stapes footplate. She had experienced a sudden right-sided hearing loss and severe true rotational vertigo, immediately after nose-blowing. CT scan showed a vestibule pneumolabyrinth. Perilymphatic fistula (PLF) repair surgery was performed. During the operation, a bony defect of 0.5 mm at the center of the right stapes footplate, which was covered by a membranous tissue, and a tear was found in this anomalous membrane. A perilymph-specific protein CTP detection test was positive. The fistula in the footplate was sealed. Postoperatively, the vestibular symptoms resolved, and her hearing improved. A more detailed history revealed that, for 15 years, she experienced true rotational vertigo when she would blow her nose. After she stopped blowing her nose, she would again feel normal. They concluded that this case demonstrated that a congenital defect in the stapes footplate can result in a PLF by seemingly insignificant events such as nose-blowing. Appropriate recognition and treatment of PLF can improve a patient's condition and hence, the quality of life.

SURGICAL ADVANCES

Wackym et al. published a series of 16 patients with Third Window Syndrome due to cochlea-facial nerve dehiscence (CFD); 8 who had surgical management [round window reinforcement (RWR)] and 8 who did not. Pre- vs. postoperative Dizziness Handicap Inventory (DHI), Headache Impact Test (HIT-6), and audiometric data were compared statistically. The thresholds and amplitudes for cVEMP in symptomatic ears, ears with CFD and ears without CFD were compared statistically. All 8 in the surgical cohort had a history of trauma before the onset of their symptoms. The mean cVEMP threshold was 75 dB nHL (SD 3.8) for the operated ear and 85.7 dB (SD 10.6) for the unoperated ear. In contrast to superior semicircular canal dehiscence, where most ears have abnormal electrocochleography (ECoG) findings suggestive of endolymphatic hydrops, only 1 of 8 operated CFD ears (1 of 16 ears) had an abnormal ECoG study. The phenotype associated with CFD was typical of the spectrum of signs and symptoms seen in SSCD patients, including 5/16 (31%) who could hear their eyes move or blink and 13/16 (81%) with sound-induced dizziness. Other clinical findings often seen in SSCD were the presence of headache and migraine headaches 15/16 (94%), vestibular migraine with true rotational vertigo episodes 8/16 (50%) and ocular migraine 7/16 (44%); however, ocular migraines were infrequent as were vestibular migraine episodes. The one patient who did not have headaches or migraine headaches had vestibular migraine episodes intermittently. Overall there was a marked and clinically significant improvement in DHI, HIT-6, and Third Window Syndrome symptoms postoperatively for the CFD cohort who had RWR surgery. A statistically significant reduction in cVEMP thresholds was observed in patients with radiographic evidence of CFD. Surgical management with RWR in patients with CFD was associated with improved symptoms and outcomes measures. There was no statistically significant change of hearing in the patients with CFD who underwent RWR. It is emphasized that radiographic CFD is not in itself an indication for surgery and that the most important factor in decision-making should be in the context of clinical symptoms and other diagnostic findings. There are three important presenting symptoms and physical findings that are critical when identifying a Third Window Syndrome, including CFD: (1) sound-induced dizziness; (2) hearing internal sounds; and (3) hearing or feeling low frequency tuning forks in an involved ear when applied to a patient's knee or elbow. Another important observation in the study was that multiple sites of dehiscence in temporal bones with Third Window Syndrome occurs and this finding is important to consider when faced with recurrent or incompletely resolved Third Window Syndrome symptoms after plugging a SSCD.

Mignacco et al. reported a novel strategy in managing a patient with SSCD. While round window reinforcement has been used as a surgical alternative to plugging or resurfacing a SSCD, the

authors reported the outcomes of round window reinforcement surgery performed with the application of a Vibrant Soundbridge middle ear implant. The patient experienced recurrent sound-induced vertigo/dizziness, Tullio phenomenon, Hennebert sign, bone conduction hypersensitivity (pseudoconductive hearing loss), and bilateral moderate to severe mixed hearing loss. Cervical vestibular evoked myogenic potentials (cVEMP) and high-resolution CT confirmed bilateral superior semicircular canal dehiscence. The surgical procedure was performed in the right ear as it had worse vestibular and auditory symptoms, a poorer hearing threshold, more evident SSCD by CT and higher amplitude and lower threshold cVEMP findings. With local anesthesia and sedation, round window reinforcement surgery with perichondrium was performed with simultaneous positioning of a Vibrant Soundbridge on the round window niche. At the one and 3 months follow-up after surgery, Vibrant Soundbridge-aided hearing threshold in the right ear improved to mild, and loud sounds no longer elicited either dizziness in the patient.

CONCLUSIONS

In this Editorial, we highlight the 20 published studies included in this Research Topic and organized these in the following categories: Diagnostic Studies and New Diagnostic Tools; Cognitive or Spatial Orientation; Health Utility Values; Biomechanics and Pathophysiology; Reviews; Sites of Dehiscence—Rare or Never Before Reported; and Surgical Advances. The studies of new diagnostic tools provide evidence that Third Window Syndrome offers a window into the mechanisms of the inner ear. Fundamentally there are three important presenting symptoms and physical findings that are critical when identifying a Third Window Syndrome regardless of physical site of the dehiscence: (1) sound-induced dizziness; (2) hearing internal sounds; and (3) hearing or feeling low frequency tuning forks in an involved ear when applied to a patient's knee or elbow. The sound-induced auditory and vestibular activity is distinct from other balance disorders in the sense that the transient vestibular afferent activity is uncoupled from motion of the head or body in space (allocentric reference frame) or from motion of the environment around the head and body (egocentric reference frame). It will also be uncorrelated with contextual visual, somesthetic, and interoceptive sensory information and on-going (or planned) motor activity. Although the studies focused on cognitive and spatial orientation findings in TWS provided further insight into relevant cognitive outcome measures that can be used in the study of patients with vestibular impairments, neither their measures nor validated survey instruments for symptoms (e.g., DHI or HIT-6) are designed to consider the unique features of perceptual incongruities between Third Window Syndrome and other conditions While current tools may be useful for monitoring patient outcomes while managing patients with Third Window Syndrome, there is room for refinement. The biomechanics, pathophysiology and review studies provided useful conceptual and state-of-the-art frameworks to better understand peripheral bases for the signs and symptoms of common forms of Third Window Syndrome. These frameworks are essential for designing specific diagnostic tests and new, potentially therapeutic approaches. Finally, rare and newly identified sites creating a third mobile window were presented and surgical advances to manage various sites resulting in Third Window Syndrome were reported. Together, these 20 publications comprising this Research Topic present an overview of current knowledge and gaps to be filled in our understanding, diagnosis and management of patients with Third Window Syndrome.

AUTHOR CONTRIBUTIONS

PAW, YA, TI, and CDB contributed conception, design of the editorial, and wrote sections of the manuscript. PAW, YA, TI, and CDB wrote the first draft of the manuscript. All authors contributed to manuscript revision, then read and approved the submitted version.

REFERENCES

1. Minor LB, Solomon D, Zinreich JS, Zee DS. Sound- and/or pressure-induced vertigo due to bone dehiscence of the superior semicircular canal. *Arch Otolaryngol Head Neck Surg*. (2018) 124:249–258. Available online at: https://jamanetwork.com/journals/jamaotolaryngology/fullarticle/219008

Conflict of Interest: TI holds patents for the test to detect perilymph leakage using the novel biomarker cochlin-tomoprotein (CTP).

The remaining authors declare that the research was conducted in the absence of any commercial or financial relationships that could be construed as a potential conflict of interest.

frontiers in Neurology

ORIGINAL RESEARCH
published: 13 December 2019
doi: 10.3389/fneur.2019.01281

Third Window Syndrome: Surgical Management of Cochlea-Facial Nerve Dehiscence

P. Ashley Wackym[1†], Carey D. Balaban[2†], Pengfei Zhang[3], David A. Siker[4] and Jasdeep S. Hundal[5]*

[1] Department of Otolaryngology–Head and Neck Surgery, Rutgers Robert Wood Johnson Medical School, New Brunswick, NJ, United States, [2] Departments of Otolaryngology, Neurobiology, Communication Sciences & Disorders, and Bioengineering, University of Pittsburgh School of Medicine, Pittsburgh, PA, United States, [3] Department of Neurology, Rutgers Robert Wood Johnson Medical School, New Brunswick, NJ, United States, [4] Siker Medical Imaging and Intervention, Portland, OR, United States, [5] Department of Neurosurgery, Rutgers Robert Wood Johnson Medical School, New Brunswick, NJ, United States

Objective: This communication is the first assessment of outcomes after surgical repair of cochlea-facial nerve dehiscence (CFD) in a series of patients. Pre- and post-operative quantitative measurement of validated survey instruments, symptoms, diagnostic findings and anonymous video descriptions of symptoms in a cohort of 16 patients with CFD and third window syndrome (TWS) symptoms were systematically studied.

Study design: Observational analytic case-control study.

Setting: Quaternary referral center.

Patients: Group 1 had 8 patients (5 children and 3 adults) with CFD and TWS who underwent surgical management using a previously described round window reinforcement technique. Group 2 had 8 patients (2 children and 6 adults) with CFD who did not have surgical intervention.

Interventions: The Dizziness Handicap Inventory (DHI) and Headache Impact Test (HIT-6) were administered pre-operatively and post-operatively. In addition, diagnostic findings of comprehensive audiometry, cervical vestibular evoked myogenic potential (cVEMP) thresholds and electrocochleography (ECoG) were studied. Symptoms before and after surgical intervention were compared.

Main outcome measures: Pre- vs. post-operative DHI, HIT-6, and audiometric data were compared statistically. The thresholds and amplitudes for cVEMP in symptomatic ears, ears with cochlea-facial nerve dehiscence and ears without CFD were compared statistically.

Results: There was a highly significant improvement in DHI and HIT-6 at pre- vs. post-operative ($p < 0.0001$ and $p < 0.001$, respectively). The age range was 12.8–52.9 years at the time of surgery (mean = 24.7 years). There were 6 females and 2 males. All 8 had a history of trauma before the onset of their symptoms. The mean cVEMP threshold was 75 dB nHL (SD 3.8) for the operated ear and 85.7 dB (SD 10.6) for the unoperated ear. In contrast to superior semicircular canal dehiscence, where most ears have abnormal ECoG findings suggestive of endolymphatic hydrops, only 1 of 8 operated CFD ears (1 of 16 ears) had an abnormal ECoG study.

OPEN ACCESS

Edited by:
Vincent Van Rompaey, University of Antwerp, Belgium

Reviewed by:
Quinton Gopen, University of California, Los Angeles, United States
Elliott D. Kozin, Harvard Medical School, United States
Jae-Jin Song, Seoul National University Bundang Hospital, South Korea

****Correspondence:***
P. Ashley Wackym
wackym@neurotology.org

†These authors share first authorship

Specialty section:
This article was submitted to Neuro-Otology, a section of the journal Frontiers in Neurology

Received: *04 October 2019*
Accepted: *19 November 2019*
Published: *13 December 2019*

Citation:
Wackym PA, Balaban CD, Zhang P, Siker DA and Hundal JS (2019) Third Window Syndrome: Surgical Management of Cochlea-Facial Nerve Dehiscence. Front. Neurol. 10:1281. doi: 10.3389/fneur.2019.01281

Conclusions: Overall there was a marked improvement in DHI, HIT-6 and symptoms post-operatively. Statistically significant reduction in cVEMP thresholds was observed in patients with radiographic evidence of CFD. Surgical management with round window reinforcement in patients with CFD was associated with improved symptoms and outcomes measures.

Keywords: cochlea-facial nerve dehiscence, cognitive dysfunction, dizziness, perilymph fistula, spatial disorientation, superior semicircular canal dehiscence syndrome, traumatic brain injury, vestibular migraine

INTRODUCTION

Ninety years ago, Tullio described the physiologic outcomes of creating a third mobile window in the semicircular canals of pigeons (1). Since that time, many locations of third mobile windows have been described (2–43); however, the sound-induced dizziness and/or nystagmus has been memorialized by the eponym "Tullio phenomenon." Clinically, the most thoroughly characterized third mobile window is superior semicircular canal dehiscence (SSCD). In 1998, Minor and coworkers first reported the diagnosis of CT positive (CT+) SSCD (10). Minor later reported a conductive hearing loss, which was recognized as a pseudoconductive hearing loss (bone-conduction hyperacusis), as well as a reduced cervical vestibular myogenic potential (cVEMP) threshold in patients with SSCD to 81 ± 9 dB nHL (11). While SSCD is well-recognized; Wackym and colleagues reported the existence of a CT negative (CT–) third window syndrome (TWS) with the same clinical phenotype of SSCD that also exists (12–19). In three published series of such CT– TWS patients (no otic capsule dehiscence visible on imaging) all were treated with round window reinforcement (RWR) (12–14). In these publications, we reported that CT– TWS is associated with a pseudoconductive hearing loss and the abnormally reduced cVEMP threshold, among other objective findings typically found in SSCD patients (12–14). We have proposed the more general term of TWS or otic capsule dehiscence syndrome (OCDS) because the same spectrum of symptoms, signs on physical examination and audiological diagnostic findings are encountered with SSCD, cochlea-facial nerve dehiscence (CFD), cochlea-internal carotid artery dehiscence, cochlea-internal auditory canal dehiscence, lateral semicircular canal-superior semicircular canal ampulla dehiscence, modiolus, "perilymph fistula (PLF)," posterior semicircular canal dehiscence, posterior semicircular canal-jugular bulb dehiscence, SSCD-subarcuate artery dehiscence, SSCD-superior petrosal vein dehiscence, vestibule-middle ear dehiscence, lateral semicircular canal-facial nerve dehiscence, wide vestibular aqueduct in children, post-traumatic hypermobile stapes footplate, otosclerosis with internal auditory canal involvement and in patients with CT– TWS (2–43). A common structural finding in all of these conditions is an otic capsule defect that creates a "third window."

In 2014, Robert Jyung et al. were the first to identify CFD resulting in TWS; however, neither of their two patients were managed surgically (28). Interest in this clinical entity producing TWS has been mounting, as there have been three recent studies focused on the histologic, CT and cadaveric micro-CT prevalence of CFD (32, 44, 45). The relationship between CFD and facial nerve stimulation in cochlear implant recipients has also been described in a total of 5 patients (46, 47). In the series with 3 patients, no TWS symptoms were presented (46). In the other case report of the other 2 patients they reported that they had no balance problems or autophony; however, no cVEMP data or other TWS symptoms were presented (47). The present report represents the first description of clinical features and outcomes of CFD managed surgically with round window reinforcement (RWR). In addition to comparing the DHI and HIT-6 data, we compared the traditional metrics used in SSCD studies including audiometric data, resolution of symptoms as well as the cVEMP thresholds and amplitudes (8–14, 20, 21, 23, 27, 36, 37, 40, 41). However, because of the tissue placed in the middle ear during the RWR procedure interferes with air-conduction for the cVEMP studies, we did not routinely repeat these studies post-operatively.

MATERIALS AND METHODS

Subjects, Validated Survey Instruments and Surgical Intervention

High-Resolution Temporal Bone Computed Tomography (CT) Findings

The OsiriX MD (Pixmeo SARL, Bernex, Switzerland) database built by the neurotologist author (PAW) was used to identify cases of CFD among all of the high-resolution temporal bone CT scans performed in patients with TWS symptoms. Each CT was reviewed by the neurotologist author (PAW) and the neuroradiologist author (DAS) to determine the presence of a CFD and the other known sites of bony dehiscence cataloged in the Introduction; and also to ascertain cases of CT– TWS.

Subjects

The procedures followed were in accordance with the ethical standards of the responsible committee on human experimentation and with the Helsinki Declaration. The Rutgers Biomedical Health Sciences Institutional Review Board approved these observational analytic case-control studies (IRB Pro2019000726). The Institutional Review Board granted a consent waiver and also approved the use of age and gender as deidentified data. Inclusion criteria encompassed TWS patients

with an otic capsule bony dehiscence limited to CFD. Exclusion criteria included multiple sites of dehiscence, aural atresia, bilateral CFD with only one side operated, <6 months of post-operative follow up, those who did not complete their diagnostic testing and those involved in active litigation. After March 20, 2019, no data were collected from the clinical services provided.

Sixteen subjects with CFD were included in this study. There were two cohorts; Group 1 (CFD with RWR surgery) and Group 2 (CFD without RWR surgery) (**Tables 1**, **2**). The patient demographics and clinical features for each subject are summarized in **Tables 1**, **2**. The 16 patients were not identical in the reported TWS symptoms, but reflected the spectrum of symptoms seen in TWS (**Table 3**). The laterality of the TWS was determined by the ear that had sound-induced symptoms and heard internal sounds. To further confirm laterality, another useful technique was to ask patients (or parents) to use an ear plug in one ear while exposed to loud sounds or music and to alternate placement of the plug to determine which ear is responsible for sound-induced symptoms. Likewise, encouragement to use an earbud or headphone with sound delivered to individual ears often confirms the ear affected by a third mobile window. Low frequency sounds, particularly with prominent bass components, such as hip-hop music, were particularly useful in inducing symptoms. Clinically, pneumatic otoscopy while a patient wears Frenzel lenses (fistula test/Hennebert sign) was another useful intervention to confirm laterality.

For those with CFD who had RWR (Group 1), there were 5 children and 3 adults, and a F:M ratio of 6:2. There were 3 patients with a left CFD, 5 with a right CFD, 1 with an asymptomatic left near-CFD and in 1 subject, a left-sided CT– TWS was also present. The mean age at the time of RWR surgery was 24.3 years (range 12.8–52.9 years). The mean duration of follow-up after RWR surgery was 55 months (4 years and 5 months) with a range of 10–71 months.

For those with CFD and who did not have RWR (Group 2), there were 5 children and 3 adults, and a F:M ratio of 5:3. There were 3 bilateral CFD and 4 left CFD. The mean age at the time of initial presentation was 30.8 years (range 6.7–55.7 years).

Dizziness Handicap Inventory

As a routine part of their clinical care, all 16 subjects completed the DHI. The DHI is a 25-item self-assessment inventory designed to evaluate the self-perceived handicapping effects imposed by dizziness/vestibular dysfunction. There is a maximum score of 100 and a minimum score of 0. The higher the score, the greater the perceived handicap due to dizziness. For the subjects who underwent RWR, the DHI was also repeated 3–4 months after their final surgical procedure. For the subjects who did not elect surgical intervention, the DHI was performed at their initial evaluation and repeated at their routine follow-up appointment 3–6 months later. The DHI questionnaire responses were entered into each medical record by a nurse not involved with the clinical research and scored automatically via the electronic medical record DHI programming using the scoring system validated by Jacobson and Newman for this instrument ("Yes" = 4 points; "Sometimes" = 2 points; "No" = 0 points) (48). A score of 0–30 indicates mild impairment, a score of 31–60 indicates moderate impairment and a score of 61–100 indicates severe impairment (49). The pre- and post-treatment scores were then totaled, both for the combined total and for each domain score (physical, functional, emotional), difference scores were calculated, and all total scores were entered into an Excel database for analysis. All data were examined with standard descriptive statistics (mean, SD, range). When comparisons between the pre- and post-treatment scores were made in the RWR surgery group, as well as with the initial scores and follow-up scores in the no surgery group, the data were analyzed using repeated-measures analysis of variance and least significant differences tests for paired comparisons, establishing 0.05 as the criterion level of significance.

Statistical comparisons to answer the question, "do specific items change between the two DHI test applications in the CFD cohort who did not choose to have surgery group?," tested the hypothesis that there are significant differences in individual symptom report scores in that group in the early vs. later tests. This hypothesis was tested by paired t-tests (Bonferroni-corrected p-value for multiple tests, $p_{\text{corrected}} = 0.05/31$ tests) between the two test scores.

Statistical comparisons were made to determine if specific DHI scores by individual question changed between the pre- and post-treatment scores in the RWR surgery group. This hypothesis was tested by paired t-tests (Bonferroni-corrected p-value for multiple tests) between the two test scores.

Headache Impact Test

As a routine part of their clinical care, all 16 subjects completed the HIT-6. The HIT-6 is a six-item self-assessment questionnaire used to measure the impact headaches have on a patient's ability to function on the job, at school, at home and in social situations. For the subjects who underwent RWR, the DHI was also repeated 3–4 months after their final surgical procedure (**Tables 1**, **2**). For the subjects who did not elect surgical intervention, the HIT-6 was performed at their initial evaluation and repeated at their routine follow-up appointment 3–6 months later. The HIT-6 questionnaire responses were entered into each medical record by a nurse not involved with the clinical research and scored automatically via the electronic medical record HIT-6 programming using the scoring system validated for this instrument ("Never" = 6 points; "Rarely" = 9 points; "Sometimes" = 10 points; "Very often" = 11 points; "Always" = 13 points) (50, 51). The final HIT-6 score was obtained from simple summation of the six items and ranges between 36 and 78, with larger scores reflecting greater impact. Headache impact severity level was categorized using score ranges based on the HIT-6 interpretation guide (50, 51). The four headache impact severity categories are little or no impact [49 or less, (Class I)], some impact [50–55, (Class II)], substantial impact [56–59, (Class III)], and severe impact [60–78, (Class IV)]. The pre- and post-treatment scores were examined with standard descriptive statistics (mean, SD, range). When comparisons between the pre- and post-treatment scores were made, the data were analyzed using repeated-measures analysis of variance and least significant differences tests for paired comparisons, establishing 0.05 as the criterion level of significance. The classification of headache and migraine used in this study followed the International Headache

TABLE 1 | Patient third window syndrome symptoms, physical findings, and results of diagnostic studies in 16 patients with cochlea-facial nerve dehiscence.

Group 1: Cochlea-facial nerve dehiscence and third window syndrome patients who underwent round window reinforcement surgery

Patient (age at surgery)	Sex	Sound-induced	Hearing internal sounds	128 and 256 Hz tuning forks	Pseudoconductive hearing loss	Electrocochleography (SP/AP ratio)	cVEMP threshold (dB nHL)/amplitude (μV)	Surgery performed (length of follow-up)	High-resolution TB CT
1* (12.75)	M	Dizziness and nausea, increased headache	Heartbeat	Negative	None	L 0.36 R 0.32	L 75 dB/437 μV R 95 dB/458 μV	L RWR (52 months)	L CFD
2* (12.92)	M	Increased HA, dizziness, pain	Eyes moving and blinking (R > L)	Positive (back of head)	Left, Right (true conductive hearing loss)	L 0.43 (ELH) R 0.38	L 80 dB/77 μV R 95 dB/301 μV (with true conductive hearing loss)	L RWR R RWR (71 months)	L CT– TWS R CFD
3 (15.17)	F	Dizziness, headache	Eyes blinking, chewing, heel strike	Positive	Bilateral	L 0.38 R 0.46 (ELH)	L 80 dB/121 μV R 75 dB/148 μV	R RWR (10 months)	R CFD L near-CFD
4 (16.5)	F	Increased headache, no dizziness	Voice resonant (left)	Positive (back of head)	Left	L 0.33 R 0.34	L 75 dB/466 μV R 95 dB/358 μV	L RWR (49 months)	L CFD
5* (17.19)	F	Dizziness, migraine; severe sound sensitivity/pain	Eyes blinking, autophony	Positive	Bilateral	L 0.28 R 0.32	L 90 dB/415 μV R 70 dB/619 μV	R RWR (69 months)	R CFD
6* (19.0)	F	Dizziness, nausea, agitated, worsens postural dyscontrol	Voice resonant (L > R), eyes moving and blinking (R), heartbeat (R), chewing (R)	Positive	Bilateral	L 0.39 R 0.37	L 70 dB/194 μV R 70 dB/206 μV	R RWR (11 months)	R CFD
7* (51.42)	F	Dizziness, nausea, HA	Voice resonant, heartbeat	Positive	Left	L 0.36 R 0.35	L 75 dB/277 μV R 75 dB/296 μV	L RWR (12 months)	L CFD
8 (52.92)	F	Dizziness, nausea	Voice resonant	Negative	Bilateral	L 0.14 R 0.37	L 95 dB/3.3 μV R 80 dB/22 μV	R RWR (37 months)	R CFD

Group 2: Cochlea-facial nerve dehiscence and third window syndrome patients who did not undergo round window reinforcement surgery

Patient (age at presentation)	Sex	Sound-induced	Hearing internal sounds	128 and 256 Hz tuning forks	Pseudoconductive hearing loss	Electrocochleography (SP/AP ratio)	cVEMP threshold (dB nHL)/amplitude (μV)	Surgery performed	High-resolution TB CT
1 (6.65)	M	Dizziness; pain	Heel strike, face being touched	Positive	Left	L 0.36 R 0.17	L 70 dB/1,093 μV R 70 dB/531 μV	None	Bilateral CFD (R > L)
2 (7.58)	F	Dizziness; pain	Voice resonant	Positive	Left	L 0.26 R 0.30	L 70 dB/430 μV R 80 dB/387 μV	None	L CFD
3 (27.88)	F	Dizziness	Voice resonant	Positive	Left (small)	L 0.30 R 0.29	L 75 dB/180 μV R 80 dB/170 μV	None	L CFD
4 (28.71)	F	Dizziness, increased headache	No	Positive	Bilateral	L 0.39 R 0.23	L 70 dB/554 μV R 90 dB/539 μV	None	Bilateral CFD (L > R)
5 (30.27)	F	Dizziness, confusion, overwhelmed, headache	Eyes blinking, voice resonant, chewing, heartbeat	Positive	Bilateral	L 0.37 R 0.31	L 80 dB/134 μV R NR	None	Bilateral CFD
6 (34.61)	M	Head pain, bitter taste	No	Positive	Left	L 0.37 R 0.39	L 75 dB/400 μV R 80 dB/229 μV	None	L CFD or near-CFD
7 (54.71)	M	Agitated, sense of foreboding	Chewing	Positive	Bilateral	L 0.36 R 0.35	L 80 dB/100 μV R 80 dB/75 μV	None	L CFD
8 (55.67)	F	Dizziness	Chewing	Positive	Left	L NR R NR	L 85 dB/41 μV R 95 dB/20 μV	None	L CFD

**See video links in references (15–19) [Cohort 1: subject 1 (15), subject 2 (16), subject 5 (17), subject 6 (18), subject 7 (19)]; 128 and 256 Hz = ability to hear or feel the vibration of the tuning fork in the head when applied to knees and elbows; CFD, cochlea-facial nerve dehiscence; CT, computed tomography scan; CT–, CT negative (no dehiscence seen on CT); cVEMP, cervical vestibular evoked myogenic potential; dB nHL, decibel above normal adult hearing level; Dizziness, gravitational receptor asymmetry type of vertigo (e.g., as if on a boat, rocky, wavy, tilting, being pushed, pulled, flipped, or sense of floor falling out from under them); ELH, endolymphatic hydrops (abnormal summating potential/action potential [SP/AP] ratio >0.42 by electrocochleography); F, female; HA, headache; L, left; M, male; TB, temporal bone; R, right. The classification of headache and migraine used in this study followed the International Headache Society's International Classification of Headache Disorders, 3rd edition (ICHD3).*

TABLE 2 | Patient demographics, history, symptoms, and results of diagnostic studies in 16 patients with cochlea-facial nerve dehiscence.

Group 1: Cochlea-facial nerve dehiscence and third window syndrome patients who underwent round window reinforcement surgery

Patient (age at surgery)	Sex	Cognitive dysfunction	Spatial disorientation	Anxiety	Nausea	Migraine/ Migrainous Headache	Duration of medical migraine management before surgery	Pre-trauma migraine	Trauma	Surgery performed (length of follow-up)	High-resolution TB CT
1* (12.75)	M	Impaired attention and concentration; dysnomia, agrammatical speech and aprosdia; difficulty reading; Impaired memory	No	No	Yes	Daily migraine HA, infrequent ocular migraine	2.5 months	Rare migraine HA	Football concussion, TWS after vigorous nose blowing during acute sinusitis	L RWR (52 months)	L CFD
2* (12.92)	M	Impaired attention and concentration; difficulty reading; Impaired memory	Rare difficulty with judging distances and sense of detachment	No	No	24/7, light sensitivity	15 months	None	Snowboarding accident, LOC	L RWR R RWR (71 months)	L CT– TWS RCFD
3 (15.17)	F	Impaired attention and concentration; dysnomia, agrammatical speech and aprosdia; Impaired memory	No	No	No	3 days clusters of migraine HA, light sensitivity, occasional ocular migraine	27 months	Childhood migraine HA, infrequent	Mononucleosis/ pneumonia, severe coughing	R RWR (10 months)	R CFD Lnear-CFD
4 (16.5)	F	Impaired attention and concentration; dysnomia, agrammatical speech and aprosdia; difficulty in name finding; difficulty reading; Impaired memory	Mild difficulty judging distances, particularly in cars	No	Once	24/7, light sensitive, vestibular migraine with rotational vertigo, occasional ocular migraine	13 months	None	Concussion, basketball blow to head, sinus infection with vigorous nose blowing	L RWR (49 months)	L CFD
5* (17.19)	F	Impaired attention and concentration; dysnomia, agrammatical speech and aprosdia; slurred speech; difficulty in name finding; Impaired memory	Difficulty judging distances; sense of detachment	No	No	Constant headache and daily migraine HA	21 months		Concussions (3), onset of symptoms after severe vomiting during influenza infection	R RWR (69 months)	R CFD

(Continued)

TABLE 2 | Continued

Group 1: Cochlea-facial nerve dehiscence and third window syndrome patients who underwent round window reinforcement surgery

Patient (age at surgery)	Sex	Cognitive dysfunction	Spatial disorientation	Anxiety	Nausea	Migraine/ Migrainous Headache	Duration of medical migraine management before surgery	Pre-trauma migraine	Trauma	Surgery performed (length of follow-up)	High-resolution TB CT
6* (19.0)	F	Impaired attention and concentration; dysnomia, agrammatical speech and aprosdia; slurred speech; difficulty in name finding; Impaired memory (lost her photographic memory)	Difficulty judging distances; sense of detachment	Sense of impending doom	Yes (constant)	Frequent migraine HA, light sensitivity, ocular migraine (2), vestibular migraine with rotational vertigo	85 months	Migraine HA history began at age 11 years	Concussions (3)	R RWR (11 months)	R CFD
7* (51.42)	F	Impaired attention and concentration; dysnomia, agrammatical speech and aprosdia; slurred speech; difficulty in name finding; slurred speech; difficulty in name finding; Impaired memory	Difficulty in judging distances; sense of detachment; perception of walls breathing	Sense of impending doom	Yes	Daily migraine HA	22 months	None	MVA with airbag deployment	L RWR (12 months)	L CFD
8 (52.92)	F	Impaired attention and concentration; dysnomia, agrammatical speech and aprosdia; Impaired memory	Difficulty in judging distances; sense of detachment; occasional out of body experiences	No	Yes (extreme)	Chronic migraine HA, ocular migraine once monthly, infrequent vestibular migraine with rotational vertigo	16 months	Adult onset migraine HA clusters with menstrual cycle	MVA	R RWR (37 months)	R CFD

Group 2: Cochlea-facial nerve dehiscence and third window syndrome patients who did not undergo round window reinforcement surgery

Patient (age at presentation)	Sex	Cognitive dysfunction	Spatial disorientation	Anxiety	Nausea	Migraine/ Migrainous Headache	Duration of medical migraine management before surgery	Pre-trauma migraine	Trauma	Surgery performed	High-resolution TB CT
1 (6.65)	M	Unknown	Unknown	Unknown	Yes	Weekly migraine HA, intermittent vestibular migraine	NA	NA	None	None	Bilateral CFD (R > L)

(Continued)

TABLE 2 | Continued

Group 2: Cochlea-facial nerve dehiscence and third window syndrome patients who did not undergo round window reinforcement surgery

Patient (age at presentation)	Sex	Cognitive dysfunction	Spatial disorientation	Anxiety	Nausea	Migraine/ Migrainous Headache	Duration of medical migraine management before surgery	Pre-trauma migraine	Trauma	Surgery performed	High-resolution TB CT
2 (7.58)	F	Impaired attention and concentration; dysnomia, agrammatical speech and aprosdia; difficulty reading; Impaired memory	Difficulty judging distances	No	No	Weekly migraine HA, vestibular migraine with rotational vertigo 1 time per week	NA	NA	None	None	L CFD
3 (27.88)	F	Mild impaired attention, concentration and memory	No	No	Yes	Daily migraine HA, ocular migraines (2)	NA	Migraine HA 2 times per week, ocular migraine (1)	Taxi trunk lid "slammed" on head	None	L CFD
4 (28.71)	F	Impaired attention and concentration; dysnomia, agrammatical speech and aprosdia; difficulty reading; Impaired memory and forgetful	Difficulty in judging distances; sense of detachment; perception of walls and floor moving	No	Yes	Daily HA with severe migraine HA 2–3 times per week, occasional vestibular migraine with rotational vertigo	NA	None	MVA with mTBI	None	Bilateral CFD (L > R)
5 (30.27)	F	Impaired attention and concentration; dysnomia, agrammatical speech and aprosdia; occasional slurred speech; difficulty reading; Impaired memory	Difficulty in judging distances; sense of detachment; perception of walls moving	No	Yes	Migraine HA 2–3 times per week, occasional perimenstrual vestibular migraine with rotational vertigo, ocular migraine (1)	NA	Onset migraine HA age 5	None	None	Bilateral CFD
6 (34.61)	M	Impaired attention and concentration; dysnomia, agrammatical speech and aprosdia; occasional slurred speech; difficulty in name finding; Impaired memory	Perception of walls swaying; perceives room proportions distorted	No	Yes	Nearly constant migraine HA	NA	"Sinus headaches"	None; onset symptoms after 4 days of Adderall	None	L CFD or near-CFD
7 (54.71)	M	No	No	No	Yes	Vestibular migraine with rotational vertigo, no migraine HA	NA	NA	None	None	L CFD

(Continued)

TABLE 2 | Continued

Group 2: Cochlea-facial nerve dehiscence and third window syndrome patients who did not undergo round window reinforcement surgery										
Patient (age at presentation)	**Sex**	**Cognitive dysfunction**	**Spatial disorientation**	**Anxiety**	**Nausea**	**Migraine/ Migrainous Headache**	**Duration of medical migraine management before surgery**	**Pre-trauma migraine**	**Trauma**	**Surgery performed**	**High-resolution TB CT**
8 (55.67)	F	Impaired attention and concentration; dysnomia, agrammatical speech and aprosdia; occasional slurred speech; difficulty in name finding; Impaired memory	Difficulty in judging distances	No	Yes	Occasional migraine HA	NA	NA	None	None	L CFD

*See video links in references (15–19) [Cohort 1: subject 1 (15), subject 2 (16), subject 5 (17), subject 6 (18), subject 7 (19)]; 24/7 = migraine headache present constantly, 24 h per day and 7 days per week while awake; CFD, cochlea-facial nerve dehiscence; CT, computed tomography scan; CT–, CT negative (no dehiscence seen on CT); F, female; HA, headache; L, left; LOC, loss of consciousness; M, male; mTBI, mild traumatic brain injury; MVA, motor vehicle accident; TB, temporal bone; R, right. The classification of headache and migraine used in this study followed the International Headache Society's International Classification of Headache Disorders, 3rd edition (ICHD3).

Society's International Classification of Headache Disorders, 3rd edition (ICHD3) (52).

Statistical comparison to answer the question, "do specific items change between the two HIT-6 test applications in the CFD cohort who did not choose to have surgery group?" tested the hypothesis that there are significant differences in individual symptom report scores in that group in the early vs. later tests. This hypothesis was tested by paired *t*-tests (Bonferroni-corrected *p*-values for multiple tests) between the two test scores.

Statistical comparisons were made to determine if specific HIT-6 scores by individual question changed between the pre- and post-treatment scores in the RWR surgery group (Group 1) and between the initial evaluation and at their routine follow-up appointment 3–6 months later for Group 2 (the subjects who did not elect surgical intervention). This hypothesis was tested by paired *t*-tests (Bonferroni-corrected *p*-values for multiple tests) between the two test scores.

Round Window Reinforcement With the Perichondrial and Cartilage Graft Technique

For CFD patients who had RWR and the 1 patient with right-sided CT– TWS (Group 1, **Tables 1**, **2**), the perichondrial and cartilage graft technique described previously for RWR was ultimately performed in all 8 subjects (12–14). For details, see **Supplementary Material**.

Hearing and Balance Testing

Comprehensive Audiometric Testing

Pure-tone audiometry was performed over the frequency ranges of 250–8,000 Hz for air conduction and 250–3,000 Hz for bone conduction. Testing was performed in a sound-proof booth. Appropriate masking was used for bone conduction and, when needed, for air conduction. Tympanometry was also performed, and acoustic reflexes were tested for ipsilateral and contralateral presentation of tones. After noting the presence of a pseudoconductive hearing loss, a 4-frequency (500, 1,000, 2,000, and 4,000 Hz) air-bone gap was calculated before and after RWR and presented using the standardized format for reporting hearing outcome in clinical trials (53).

Tuning Fork Testing

As a screening tool for patients with TWS symptoms, low-frequency tuning forks were applied to the knees and elbows, and they were asked if they could hear or feel the vibration in their head; 128 and 256 Hz tuning forks were used (54). In addition, for most patients, they stood with feet together, and when possible with eyes closed, while a 256 Hz tuning fork was applied to the elbow on the side in which they most loudly heard or felt the vibration. This typically resulted in a sense of tilting and increased sway (18).

Cervical Vestibular Evoked Myogenic Potentials (cVEMP)

A commercial auditory evoked potential software system (ICS Chartr EP 200, Otometrics, Natus Medical Inc., Schaumburg, IL) was used for acoustic cVEMP testing. Sound stimuli were delivered monaurally via an intra-auricular transducer with

TABLE 3 | Spectrum of symptoms, signs or exacerbating factors seen in third window syndrome and diagnostic tools and metrics available to measure these clinically observed phenomenon.

Category	Symptom, sign, or exacerbating factors	Diagnostic tools and metrics
Sound-induced	Dizziness or otolithic dysfunction (see vestibular dysfunction below); nausea; cognitive dysfunction; spatial disorientation; migraine/migrainous headache; pain (especially children); loss of postural control; falls	History; 128 and 256 Hz tuning forks applied to ankles, knees and/or elbows heard or felt in the ear or head; pneumatic otoscopy; cVEMP/oVEMP with reduced threshold with or without increased amplitude, auditory stimuli inducing symptoms; Romberg test while pure tones delivered to individual ear or low frequency tuning fork applied to elbow
Autophony	Resonant voice; chewing; heel strike; pulsatile tinnitus; joints or tendons moving; eyes moving or blinking; comb or brush through hair; face being touched	History
Vestibular dysfunction	Gravitational receptor (otolithic) dysfunction type of vertigo (rocky or wavy motion, tilting, pushed, pulled, tilted, flipped, floor falling out from under); mal de débarquement illusions of movement	History; Dizziness Handicap Inventory (DHI); cVEMP/oVEMP; computerized dynamic posturography; Romberg/sharpened Romberg; head tilt; nuchal muscle tightness
Headache	Migraine/migrainous headache; migraine variants (ocular, hemiplegic or vestibular [true rotational vertigo]); coital cephalagia; photophobia; phonophobia; aura; scotomata	History; Headache Impact Test (HIT-6); Migraine Disability Assessment Test (MIDAS)
Cognitive dysfunction	General cognitive impairment, such as mental fog, dysmetria of thought, mental fatigue; Impaired attention and concentration, poor multitasking (women > men); Executive dysfunction; Language problems including dysnomia, agrammatical speech, aprosidia, verbal fluency; Memory difficulties; Academic difficulty including reading problems and missing days at school or work; Depression and anxiety	History ***Cognitive Screen:*** MoCA and Schmahmann syndrome scale ***IQ:*** WRIT or WAIS2 ***Attention:*** NAB, Attention Module and/or CPT3 ***Memory:*** CVLT2, WMS4, or WRAML2 ***Executive Functioning:*** WCST, TMT, D-KEFS ***Language:*** NAB, Naming ***Visuospatial:*** Benton JLO ***Mood/personality:*** Clinical interview, PHQ-9, GAD-7, ACES, BDI2, BAI, Personality Assessment Inventory (PAI), or Millon Behavioral Diagnostic
Spatial disorientation	Trouble judging distances; detachment/passive observer when interacting with groups of people; out of body experiences; perceiving the walls or floor moving	History; subjective visual vertical
Anxiety	Sense of impending doom	History; GAD-7; BAI
Autonomic dysfunction	Nausea; vomiting; diarrhea; lightheadedness; blood pressure lability; change in temperature regulation; heart rate lability	History; autonomic testing
Endolymphatic hydrops	Ear pressure/fullness not relieved by the Valsalva maneuver; barometric pressure sensitivity	History; Electrocochleography, tympanometry
Hearing	Pseudoconductive hearing loss (bone-conduction hyperacusis)	Comprehensive audiometric evaluation including tympanometry, stapedial reflex testing, speech perception testing, air-conduction and bone-conduction thresholds; magnitude varies by site of dehiscence

ACES, Adverse Childhood Experiences Scale; BAI, Beck Anxiety Inventory; BDI2, Beck Depression Inventory, 2nd edition; Benton JLO, Benton Judgment of Line Orientation; CPT3, Continuous Performance Test, 3rd edition; CVLT2, California Verbal Learning Test, 2nd edition; D-KEFS, Delis-Kaplan Executive Function System; DHI, Dizziness Handicap Inventory; GAD-7, Generalized Anxiety Disorder Screener; HIT-6, Headache Impact Test; MoCA, Montreal Cognitive Assessment; NAB, Neuropsychological Assessment Battery; PAI, Personality Assessment Inventory; PHQ-9, Patient Health Questionnaire; TMT, Trail Making Test; WAIS2, Wechsler Adult Intelligence Scale, 2nd edition; WCST, Wisconsin Card Sorting Test; WMS4, Wechsler Memory Scale, 4th edition; WRAML2, Wide Range Assessment of Memory and Learning, 2nd edition; WRIT, Wide Range Intelligence Test.

foam earphones (E-A-R Link Insert Earphones; E-A-R Auditory Systems, Indianapolis) as described previously (55). Peak-to-peak amplitude was calculated with the Otometrics software after peaks were labeled and the amplitude difference between the two peaks was measured. The threshold was defined as the lowest dB nHL at which a p13 and n23 response could be recorded.

Electrocochleography (ECoG)

Pre-operative ECoG was performed with gold foil tiptrodes (Etymotic Research; Elk Grove Village, Ill.), which were placed adjacent to the tympanic membrane in the external auditory canal and stabilized at the foam tip of the insert audio transducer. Unfiltered clicks of 100 μs duration were presented at an intensity of 85 dB nHL. Two replications of averaged responses elicited by 1,500 clicks presented at a rate of 11.7/s were obtained. Responses were band-pass filtered (20–1,500 Hz) and averaged, and the summating potential to action potential (SP/AP) ratio was calculated. An SP/AP ratio of >0.42 was defined as abnormal for purposes of this study, based on commonly used standards for clinical testing (56).

Statistical Analyses

Statistical analyses were conducted with IBM SPSS Statistics for Windows, Version 24.0 (Armonk, NY: IBM Corp.), with Python

and R extensions. The individual tests performed, results and associated *p*-values are presented in the text.

RESULTS

Subjects, Validated Survey Instruments, and Surgical Intervention

Tables 1, **2** summarize the pre-operative history, symptoms, physical findings and results of diagnostic studies in the 8 patients with CFD who underwent RWR surgery (Group 1). It should be noted that subjects 1, 2, 4, 5, and 8 were previously unrecognized CFD patients who had RWR for what was thought to be a CT– TWS. **Tables 1**, **2** also summarize the pre-operative history, symptoms, physical findings and results of diagnostic studies in the 8 patients with CFD who did not undergo RWR surgery (Group 2). By 6 months post-operatively, no patients had persistent sound-induced dizziness (Tullio phenomenon) or autophony.

High-Resolution Temporal Bone Computed Tomography Findings

The OsiriX MD database built by the neurotologist author (PAW) included 860 studies. Of these, 401 were high-resolution temporal bone CT scans of both temporal bones that were performed to evaluate patients with TWS symptoms. Of the 802 individual temporal bones reviewed, the distribution of otic capsule defects/dehiscence visualized and associated with third window syndrome symptoms in 502 bones were (**Table 4**): SSCD [175]; near-SSCD [121]; CT– TWS [97]; CFD [52]; SSCD and CFD [30]; cochlea-internal auditory canal [5]; CFD and cochlea-internal auditory canal [4]; lateral semicircular canal dehiscence [3]; wide vestibular aqueduct [3]; CFD and wide vestibular aqueduct [2]; posterior semicircular canal [2]; SSCD-superior petrosal sinus [2]; SSCD and posterior semicircular canal and wide vestibular aqueduct [1]; SSCD-subarcuate artery [1]; SSCD and cochlea-internal auditory canal [1]; SSCD and posterior semicircular canal [1]; posterior semicircular canal-jugular bulb [1]; and the modiolus [1]. The SSCD and CT– TWS temporal bones were counted independent of each other; however, there were 22 that had SSCD plugging that later developed CT– TWS.

TABLE 4 | Prevalence of radiographic sites of dehiscence in 502 temporal bones associated with third window syndrome in 401 patients (802 temporal bones).

Location(s)/Site(s)	Prevalence (%)
Superior semicircular canal dehiscence	175/502 (34.9%)
Near-superior semicircular canal dehiscence	121/502 (24.1%)
CT– third window syndrome	97/502 (19.3%)
Cochlea-facial nerve dehiscence	52/502 (10.4%)
Superior semicircular canal dehiscence + Cochlea-facial nerve dehiscence	30/502 (5.98%)
Cochlea-internal auditory canal dehiscence	5/502 (1.0%)
Cochlea-internal auditory canal dehiscence + Cochlea-facial nerve dehiscence	4/502 (0.8%)
Lateral semicircular canal dehiscence	3/502 (0.6%)
Wide vestibular aqueduct	3/502 (0.6%)
Wide vestibular aqueduct + Cochlea-facial nerve dehiscence	2/502 (0.4%)
Posterior semicircular canal dehiscence	2/502 (0.4%)
Superior semicircular canal-Superior petrosal sinus dehiscence	2/502 (0.4%)
Superior semicircular canal dehiscence + Posterior semicircular canal dehiscence + Wide vestibular aqueduct	1/502 (0.2%)
Superior semicircular canal-Subarcuate artery dehiscence	1/502 (0.2%)
Superior semicircular canal dehiscence + Cochlea-internal auditory canal dehiscence	1/502 (0.2%)
Superior semicircular canal dehiscence + Posterior semicircular canal dehiscence	1/502 (0.2%)
Posterior semicircular canal-Jugular bulb dehiscence	1/502 (0.2%)
Modiolus	1/502 (0.2%)

CT–, High-Resolution Temporal Bone Computed Tomography Scan Negative for a Visible Site of Dehiscence.

Two illustrative cases are shown in **Figures 1**, **2**. In **Figure 1**, the images showed a right CFD and a left near-CFD or CFD (**Tables 1**, **2**, Group 1 Patient 3). There are several important points regarding this case that should be emphasized. First, only the right ear had TWS symptoms (sound-induced dizziness and headache; autophony [hearing her eyes blinking, chewing sounding loud in her right ear and hearing her heel strike while walking]), but the left side showed radiographic evidence of a possible CFD and a reduced cVEMP threshold of 80 dB nHL. This underscores the need for clinical judgment and decision-making that integrates clinical symptoms, radiographic features and objective test data before surgical intervention should be pursued. She also was the only patient with electrocochleographic evidence of endolymphatic hydrops in the CFD with RWR surgery group. One notes that it is essential, when possible, to visualize the CFD in the axial, coronal, Pöschl and Stenvers views to minimize the possibility that the appearance of the CFD is a partial volume averaging artifact of the image reconstruction algorithms.

In **Figure 2**, the axial CT images of a male patient with bilateral TWS is shown (**Tables 1**, **2**, Group 1 Patient 2). He had a right CFD and a left CT– TWS that became symptomatic after a snowboarding accident. Bilateral RWR was performed. The images illustrate the CFD on the right and the normally present bony cochlea-facial partition on the left.

Subjects and Surgical Intervention

There were 16 subjects who met the inclusion and exclusion criteria and form the two cohorts included in this study. As shown in **Tables 1**, **2**, there were 8 ears that had RWR procedures performed for 3 left CFD and 5 right CFD. One ear (**Tables 1**, **2**, Group 1 Patient 2) had RWR for a CT– TWS. For the cohort with CFD who were not managed surgically ($n = 8$) (**Tables 1**, **2**), 3 had bilateral CFD while the remaining 5 had left CFD.

Dizziness Handicap Inventory

For the CFD cohort who had RWR procedures performed (Group 1, **Tables 1**, **2**), the pre-operative mean DHI score was 54.3 (SE 4.9, range 30–74). Using the clinical categorical descriptors of the DHI (46, 47), one was at the upper border of mild impairment (score of 30), five subjects had moderate impairment (scores of 40–58) and two subjects had severe impairment (scores >60). The post-operative mean DHI score

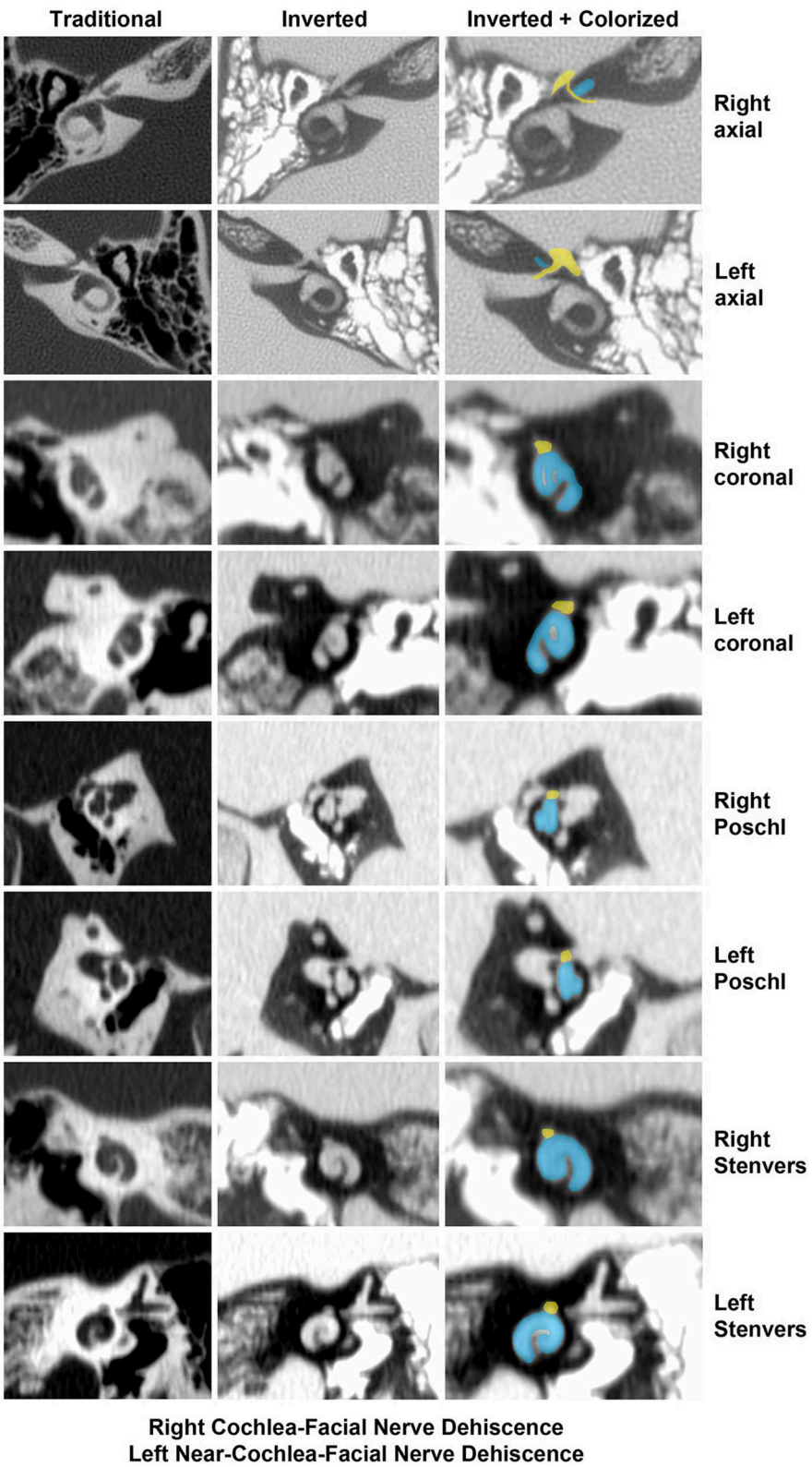

FIGURE 1 | High-resolution temporal bone CT without contrast (**Table 1**, Group 1 Patient 3). Traditional CT images are shown on the far left column. Cochlea (blue) and facial nerve (yellow) have been colorized and superimposed over inverted images in the axial, coronal, Pöschl and Stenvers planes for both the left and right ears. Note that a cochlea-facial nerve dehiscence (CFD) is seen on the left and a near-CFD is seen on the right. The patient has no left-sided third window syndrome symptoms, with resolution of her third window syndrome symptoms after round window reinforcement on the right. Copyright ©P.A. Wackym, used with permission.

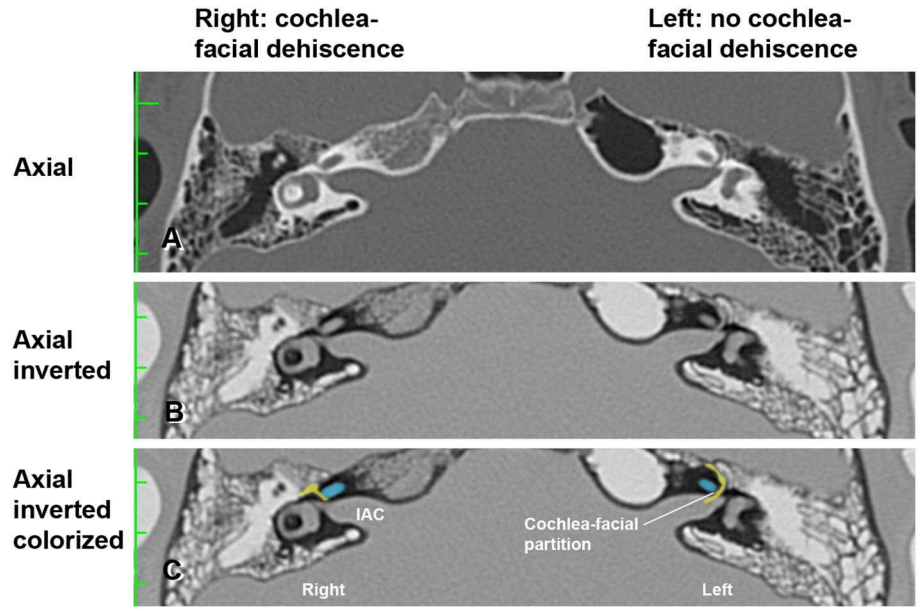

FIGURE 2 | High-resolution temporal bone CT without contrast (**Table 1**, Group 1 Patient 2). **(A)** Traditional axial CT images are shown. **(B)** Inverted axial CT images. **(C)** Cochlea (blue) and facial nerve (yellow) have been colorized and superimposed over inverted images in the axial plane for both the left and right ears. Note that a cochlea-facial nerve dehiscence (CFD) is seen on the right and a cochlea-facial partition between the cochlea and the facial nerve is seen on the left. The patient had left-sided third window syndrome (TWS) symptoms due to a CT negative TWS, with resolution of his TWS symptoms after round window reinforcement on the right and left. IAC, internal auditory canal. Copyright © P.A. Wackym, used with permission.

was 5.5 (SE 4.2, range 0–34), with one subject decreasing from severe to moderate (66 pre-operatively to 34 post-operatively) and the remaining seven showing reductions to the mild range (scores of 0–8). This improvement was highly significant statistically (paired t-test, $p < 0.0001$) (**Figure 3**).

Statistical comparisons were made to determine if specific DHI item scores changed between the pre- and post-treatment scores in the RWR surgery group. This hypothesis was tested by paired t-tests (Bonferroni-corrected p-values for multiple comparisons) between the two test scores. The following items showed significant improvement after surgery:

P4. *Does walking down the aisle of a supermarket increase your problems?* ($p = 0.001$)
F6. *Does your problem significantly restrict your participation in social activities, such as going out to dinner, going to the movies, dancing, or going to parties?* ($p = 0.000$)
F7. *Because of your problem, do you have difficulty reading?* ($p = 001$)
P8. *Does performing more ambitious activities, such as sports, dancing, household chores (sweeping or putting dishes away) increase your problems?* ($p = 0.000$)
F14. *Because of your problem, is it difficult for you to do strenuous homework or yard work?* ($p = 0.000$)
E18. *Because of your problem, is it difficult for you to concentrate?* ($p = 0.000$)
E21. *Because of your problem, do you feel handicapped?* ($p = 0.001$)
F24. *Does your problem interfere with your job or household responsibilities?* ($p = 0.000$)

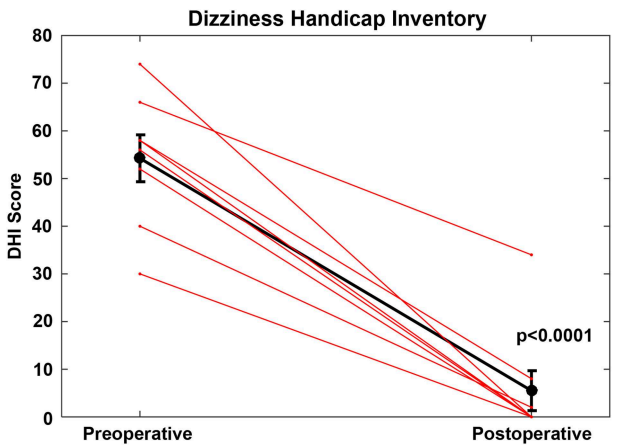

FIGURE 3 | For the cochlea-facial nerve dehiscence cohort who had round window reinforcement procedures performed, the pre-operative mean DHI score was 54.25 (SE 4.9, range 30–74). The post-operative mean DHI score was 5.5 (SE 4.2, range 0–34). This improvement was highly statistically significant (paired t-test, $p < 0.0001$). These data are plotted as a single black line. Individual patients are plotted as separate lines (red). Copyright © P.A. Wackym, used with permission.

As further evidence of the effectiveness of the surgery, the post-operative scores on DHI items P8, F14 and E21 were lower in the operated CFD cohort (t-tests, $p < 0.05$) than the second (repeat) test scores for the CFD cohort who did not choose to have surgery.

For the CFD cohort who did not choose to have surgery (Group 2, **Tables 1**, **2**), the initial mean DHI score was 36.5 (SE 10.6, range 0–100). Four subjects showed mild impairment (scores: 0–26), two subjects reported moderate impairment (scores: 34–36) and two subjects reported severe impairment (scores: 62 and 100). At the second administration, the mean DHI score was 42.5 (SE 11.1, range 12–100). There was no statistically significant difference between the initial and second administration of the DHI in the CFD patients who did not elect to undergo surgery ($p > 0.05$). There were no significant changes on any DHI item between the first and second tests.

Statistical comparison of Group 1 (CFD with RWR) to Group 2 (CFD without RWR) (**Tables 1**, **2**) revealed that the DHI scores at initial presentation were no different between the groups ($p > 0.05$). Further, to determine if there were any significant differences between symptom item endorsements in patients that may be related to election of surgery, we tested the hypothesis that there are significant differences in the first symptom report scores (patterns) between the two patient groups. There were three questions that had a statistically significant difference between the groups: P8 [$F_{(1,14)} = 5.478$, $p < 0.04$], F14 [$F_{(1,14)} = 6.725$, $p < 0.03$], and E21 [$F_{(1,14)} = 5.6$, $p < 0.04$]. For item P8, in the cohort who elected not to have surgery, 2 of 8 had a score of 0, while none electing RWR surgery had a score of 0. For item F14, in the cohort who elected not to have surgery, 3 of 8 had a score of 0, while none electing RWR surgery had a score of 0. For item E21, in the cohort who elected not to have surgery, 6 of 8 had a score of 0; 1 of 8 electing RWR surgery had a score of 0. By binary logistic regression (Wald criterion), P4 and F14 were sufficient to classify 7 of 8 of each group correctly, with F14 alone producing a correct classification of 6 of 8 from each group.

Headache Impact Test

For the CFD cohort who had RWR procedures performed (Group 1, **Tables 1**, **2**), the pre-operative mean HIT-6 score was 64.9 (SE 1.1, range 52–69) and all scores were in the severe impact range (Class IV). The post-operative mean HIT-6 score was 42.4 (SE 2.7, range 36–55); seven subjects shifted into the little or no impact range (<50) (Class I or II) and one subject had a score categorized as Class III. This improvement was highly statistically significant statistically (paired *t*-test, $p < 0.001$) (**Figure 4**). For all of the CFD patients who elected to undergo RWR, they were treated medically as migraine/vestibular migraine patients without resolution of their symptoms before surgical intervention. The duration of medical management ranged from 2.5 to 85 months (mean = 25.2 months).

Statistical comparisons were made to determine if specific HIT-6 scores for individual questions changed between the pre- and post-treatment scores in the RWR surgery group. This hypothesis was tested by paired *t*-tests (Bonferroni-corrected *p*-values) between the two test scores. The following items showed significant improvement after surgery:

HIT-6 Question 2: *How often do headaches limit your ability to do usual daily activities including household work, work, school, or social activities?* ($p = 0.000$)

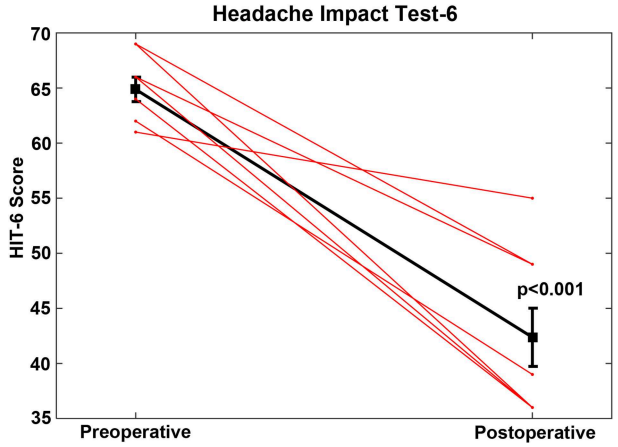

FIGURE 4 | For the cochlea-facial nerve dehiscence cohort who had round window reinforcement procedures performed, the pre-operative mean HIT-6 score was 64.9 (SE 1.1, range 52–69). The post-operative mean HIT-6 score was 42.4 (SE 2.7, range 36–55). This improvement was highly statistically significant (paired *t*-test, $p < 0.001$). These data are plotted as a single black line. Individual patients are plotted as separate lines (red). Copyright © P.A. Wackym, used with permission.

HIT-6 Question 3: *When you have a headache, how often do you wish you could lie down?* ($p = 0.000$)

HIT-6 Question 4: *In the past 4 weeks, how often have you felt too tired to do work or daily activities because of your headaches?* ($p = 0.000$)

HIT-6 Question 5: *In the past 4 weeks, how often have you felt fed up or irritated because of your headaches?* ($p = 0.001$)

For the CFD cohort (Group 2) who did not choose to have surgery (**Tables 1**, **2**), the mean HIT-6 score was initially 61.5 (SE 2.9, range 46–76) and at second administration the mean HIT-6 score was 63.1 (SE 2.9, range 49–76). There was no statistically significant difference between the initial and second administration of the HIT-6 in the CFD patients who did not elect to undergo surgery ($p > 0.05$). Four subjects had scores in the severe impact range, with 1 subject in the significant impact range, 2 subjects in the some impact range, and the remaining subject showing "no or little" impact.

Statistical comparisons to answer the question, "do specific items change between the two HIT-6 test applications in the CFD cohort who did not choose to have surgery group?," tested the hypothesis that there are significant differences in individual symptom report scores in that group in the early vs. later tests. There were no significant changes on any HIT-6 item.

Statistical comparison of Group 1 (CFD with RWR) to Group 2 (CFD without RWR) (**Tables 1**, **2**) revealed that the initial HIT-6 scores were no different between the groups ($p > 0.05$).

Hearing and Balance Testing

Comprehensive Audiometric Testing

Figure 5A shows the pretreatment scattergram of the audiometric data for the 8 patients (9 ears) who underwent

RWR for management of their CFD ($n = 8$) and CT– TWS ($n = 1$). Seven of the 9 ears had a 4-frequency air-bone gap/pseudoconductive hearing loss between 2.5 and 8.75 dB (mean 5.63 dB). One subject (Patient 2) had a true conductive hearing loss with a pretreatment 4-frequency air-bone gap of 42.5 dB in his right ear; which had the CFD (see **Figure 2**). His other ear with the CT– TWS had a pretreatment air-bone gap of 6.25 dB and his pretreatment speech discrimination score was 88% on the left that improved to 100% post-treatment. **Figure 5B** shows the post-treatment scattergram of the audiometric data who underwent RWR for management of CFD ($n = 8$) and CT– TWS ($n = 1$) in 8 subjects. Six ears had no change in word recognition score (WRS), including the 1 ear with a true conductive hearing loss and CFD (Patient 2). This same subject (Patient 2) had a CT– TWS (**Figure 2**) on the left and had a pretreatment speech discrimination score of 88% that improved to 100% post-treatment. Excluding the ear of Patient 2 with the conductive hearing loss, the pseudoconductive hearing loss with the added conductive hearing loss as a result of the RWR procedure had a mean 4-frequency air-bone gap of 10.94 dB (range 5–23.75 dB). As shown in the scatter-plot, 8 ears had modest worsening of the air-bone gap; while only Patient 5 had an improvement from 7.5 to 5 dB for the 4-frequency air-bone gap. There was no statistically significant difference in the 4-frequency air-bone gap pretreatment compared to post-treatment (paired t-test, $p = 0.091$).

Figure 6A shows the pretreatment scattergram of the 4-frequency air-conduction pure tone average audiometric data for the 8 patients who underwent RWR for management of their CFD ($n = 8$). One subject (Group 1 Patient 2) had a true conductive hearing loss with a pretreatment 4-frequency air-conduction pure tone average of 56.25 dB in his right ear; which had the CFD (see **Figure 2**). **Figure 6B** shows the post-treatment scattergram of the audiometric data for 8 patients who underwent RWR for management of CFD. Six ears had no change in word recognition score (WRS), including the 1 ear with a true conductive hearing loss and CFD (Group 1 Patient 2). One had an improvement of speech discrimination ability from 96 to 100%, while another had a decrease in speech discrimination from 96 to 92%. Including the ear of Group 1 Patient 2 with the conductive hearing loss and CFD, the mean pre-operative air-conduction 4-frequency pure tone average was 19.7 dB (range 5–56.25 dB [SE 7.1]), while the mean post-operative air-conduction 4-frequency pure tone average was 22.8 dB (range 5–51.25 dB [SE 5.2]). As shown in the scatterplot (**Figure 6B**), 5 ears had worsening of the 4-frequency air-conduction pure tone average; while 3 stayed the same or improved post-operatively. There was no statistically significant difference in the 4-frequency air-conduction pure tone average pretreatment compared to post-treatment (paired t-test, $p = 0.472$). Six ears had no change in WRS, including the 1 ear with a true conductive hearing loss and CFD (Group 1 Patient 2). One patient had an improved WRS (96–100%) and one patient had a worsened WRS (96–92%). There was no statistically significant difference in the WRS pretreatment compared to post-treatment (paired t-test, $p = 0.402$).

Cervical Vestibular Evoked Myogenic Potentials

The cVEMP thresholds are shown in **Table 1** for the 8 CFD and 1 CT– TWS patients in Group 1 who had RWR surgery. For all 9 ears receiving RWR, the mean cVEMP threshold was 77.2 dB nHL (SD 7.6, range 70–95 dB nHL), excluding the threshold of 95 dB nHL for the single ear with a CFD and a conductive hearing loss of 42.5 dB pre-operatively, the mean cVEMP threshold was 75 dB nHL (SD 3.8, range 70–80 dB nHL). For the non-operated ears reported in **Table 1**, the mean cVEMP threshold was 85.7 dB nHL (SD 10.6, range 70–95 dB nHL). Using a Pairwise Comparison, the unoperated ear cVEMP threshold compared to the operated ear (excluding the large conductive hearing loss cVEMP threshold) the mean difference was 10.7 dB nHL (SE 4.0). This was a statistically significant difference ($p = 0.013$). By a Tukey HSD (honestly significant difference) reduced cVEMP threshold was also statistically lower ($p = 0.034$).

The cVEMP thresholds are shown in **Table 1** for the 8 CFD patients in Group 2 who did not have RWR surgery. For the 8 ears with CFD in Group 2, the mean cVEMP threshold was 76.9 dB nHL (SE 3.0, SD 8.43; range 70–95 dB nHL). For the 5 ears with no CFD the mean cVEMP threshold was 83.0 dB nHL (SE 3.0, SD 6.71; range 80–95 dB nHL). There was no difference in these thresholds using an independent t-test of all values ($p = 0.199$).

As shown in **Table 1**, the amplitudes of the cVEMP responses, in general declined with age. There was also variability of amplitude in the CFD ear relative to the ear without CFD. There were 2 patients in Group 1 who had post-operative cVEMP studies. In patient 1, the cVEMP response was not present in the operated ear after RWR. In patient 4, in the CFD (right) side the amplitude increased from 358 to 403 μV post-operatively and the threshold remained unchanged at 95 dB pre-operatively and post-operatively. This side had a large conductive hearing loss pre-operatively and post-operatively. For the CT– TWS (left) side the amplitude decreased from 466 to 153 μV post-operatively and the threshold normalized from 75 dB pre-operatively to 95 dB post-operatively.

Electrocochleography

As shown in **Table 1**, only 2 ears in Group 1 had abnormal ECoG data suggestive of ELH (SP/AP ratio >0.42). Both of these subjects underwent RWR procedures. One of these subjects (**Table 1**, Patient 2) had electrophysiologic evidence of ELH in his CT– TWS left ear (SP/AP ratio 0.43), while his right ear with the CFD (**Figure 2**) had no evidence of ELH (SP/AP ratio of 0.36). The other subject (**Table 1**, Patient 3, **Figure 1**) had electrophysiologic evidence of ELH in her right CFD ear (SP/AP ratio 0.46), while her left ear with the near-CFD (**Figure 1**) and no TWS symptoms (sound-induced dizziness and headache; autophony [hearing her eyes blinking, chewing sounding loud in her right ear and hearing her heel strike while walking]), had no evidence of endolymphatic hydrops (SP/AP ratio of 0.38).

DISCUSSION

The present report represents the first description of clinical features (**Tables 1**, **2**) and outcomes of CFD managed surgically

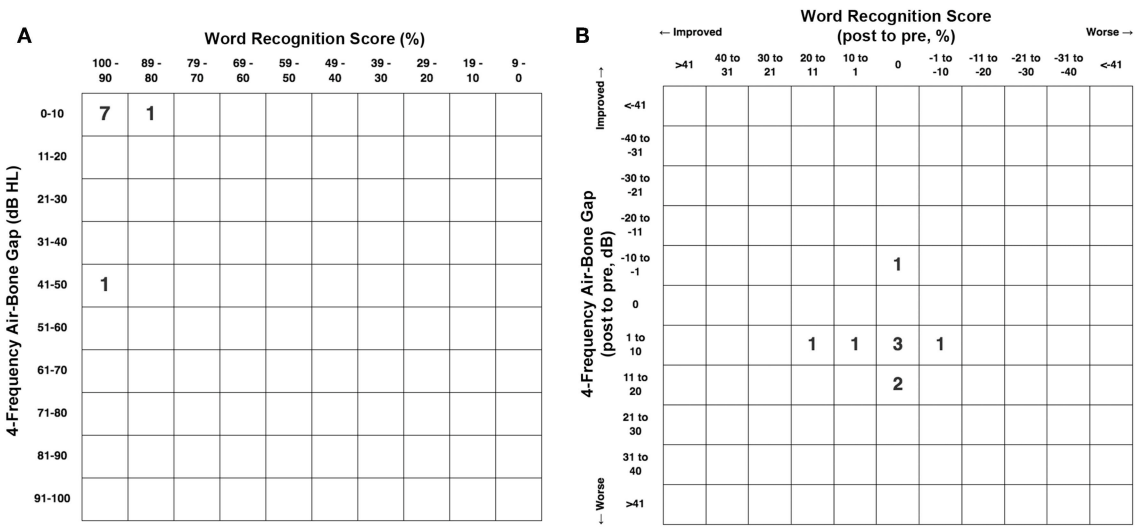

FIGURE 5 | (A) Pretreatment scattergram of audiometric data for the 8 patients (9 ears) who underwent round window reinforcement (RWR) for management of cochlea-facial nerve dehiscence (CFD) ($n = 8$, Group 1) and CT negative (CT–) third window syndrome (TWS) ($n = 1$). Seven of the 9 ears had a 4-frequency air-bone gap/pseudoconductive hearing loss between 2.5 and 8.75 dB (mean 5.63 dB). One subject (**Table 1**, Group 1 Patient 2) had a true conductive hearing loss with a pretreatment 4-frequency air-bone gap of 42.5 dB in his right ear; which had the CFD (see **Figure 2**). His other ear with the CT– TWS had a pretreatment air-bone gap of 6.25 dB and his pretreatment speech discrimination score was 88% on the left that improved to 100% post-treatment. Copyright © P.A. Wackym, used with permission. **(B)** Post-treatment scattergram of audiometric data for 9 patients who underwent round window reinforcement (RWR) for management of cochlea-facial nerve dehiscence (CFD) ($n = 8$) and CT negative (CT–) third window syndrome (TWS) ($n = 1$) in 8 subjects. Six ears had no change in word recognition score (WRS), including the 1 ear with a true conductive hearing loss and CFD (Patient 2). This same subject (Patient 2) had a CT– TWS (**Figure 2**) on the left and had a pretreatment speech discrimination score of 88% that improved to 100% post-treatment. Excluding the ear of Patient 2 with the true conductive hearing loss, the pseudoconductive hearing loss with the added conductive hearing loss as a result of the RWR procedure had a mean 4-frequency air-bone gap of 10.94 dB (range 5–23.75 dB). As shown in the scatterplot, 8 ears had worsening of the air-bone gap; while only Patient 5 had an improvement from 7.5 to 5 dB for the 4-frequency air-bone gap. This likely represents the test-retest variability. There was no statistically significant difference in the 4-frequency air-bone gap pretreatment compared to post-treatment ($p = 0.091$). Copyright © P.A. Wackym, used with permission.

with RWR (**Figures 3**–**6**) and the largest cohort of patients reported to date with CFD who have not had surgical intervention (**Tables 1**, **2**). In the clinical context of TWS, the latter group have decided that the risk of deafness and facial paralysis for a direct surgical plugging of the CFD third window outweighs the perceived impact of the TWS symptoms on their lives. The RWR approach is an alternative surgical procedure to relieve the TWS symptoms with a low risk of morbidity. Although RWR has the potential to change the biomechanical properties of one of the two natural windows (the round window), we found no statistically different hearing outcomes after RWR in our CFD cohort (**Figures 5**, **6**). Further, the efficacy of the procedure in resolving symptoms was demonstrated by clinically meaningful improvement on the DHI and HIT-6 outcome measures (**Figures 3**, **4**, respectively), as well as captured in the pre- and post-operative patient videos (15–19).

Advances in Our Understanding of Third Window Syndrome

Over the past 60 years, we have learned much regarding the clinical features, outcomes measured by validated survey instruments and neuropsychology testing as well as objective diagnostic studies in TWS (2–43). Poe's group observed that 94% of patients with SSCD, or symptoms consistent with SSCD, experienced autophony and aural fullness, while 86% were found to have pseudoconductive hearing loss (20, 21). Interestingly, in their 2007 study, they included four cases of CT– TWS among their series of CT+ SSCD who had also had abnormally low cVEMP thresholds (21). Because of their diagnostic dilemma, they did not manage these patients with surgical intervention. The Wackym group has used the Dizziness Handicap Inventory (DHI), the Headache Impact Test (HIT-6) and comprehensive neuropsychology test batteries pre-operatively and post-operatively to measure the cognitive dysfunction and migraine headache in TWS patients to quantify their dysfunction and recovery outcomes (12–19). Crane and coworkers also reported the reduction of DHI scores after plugging the superior semicircular canal in patients with SSCD (40).

In addition, the Wackym group has reported a delayed development of CT– TWS after surgical plugging and resurfacing of CT+ SSCD TWS (12–14). In a series of near-SSCD patients undergoing plugging and resurfacing procedures at the Johns Hopkins Hospital, all patients noted initial improvement in at least one presenting TWS symptom; however, five subjects (45%) reported the persistence or recurrence of at least one TWS symptom at >1 month after surgery (57). In a larger series of SSCD patients, John Carey's group reported that among 222 patients who underwent plugging procedures for SSCD, there were 21 patients who underwent 23 revision surgeries for failure

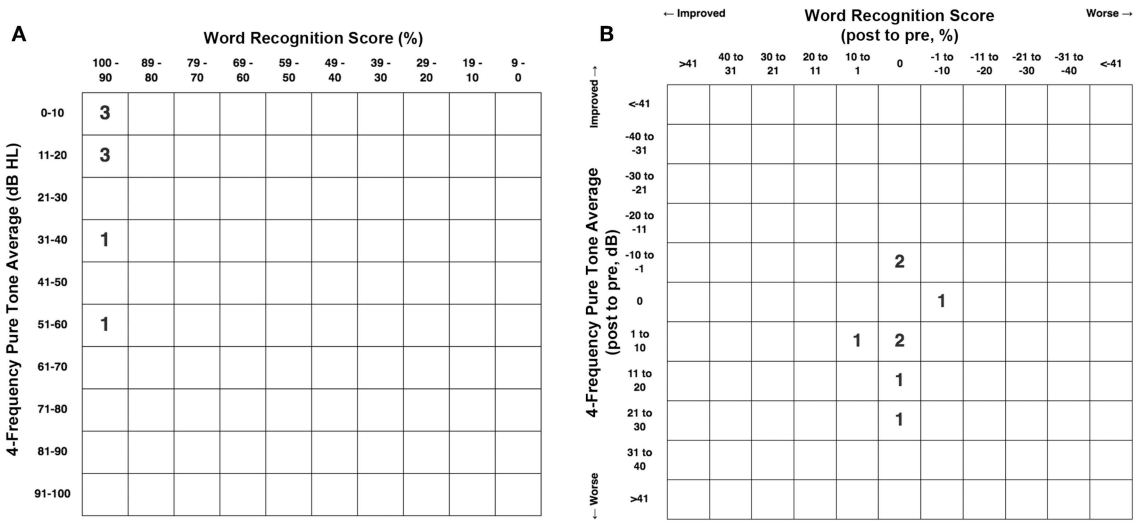

FIGURE 6 | (A) Pretreatment scattergram of the 4-frequency air-conduction pure tone average audiometric data for the 8 patients who underwent RWR for management of their CFD ($n = 8$, Group 1). One subject (**Table 1**, Group 1 Patient 2) had a true conductive hearing loss with a pretreatment 4-frequency air-conduction pure tone average of 56.25 dB in his right ear; which had the CFD (see **Figure 2**). **(B)** Post-treatment scattergram of the audiometric data for 8 patients who underwent RWR for management of CFD. Six ears had no change in word recognition score (WRS), including the 1 ear with a true conductive hearing loss and CFD (Patient 2). One had an improvement of speech discrimination ability from 96 to 100%, while another had a decrease in speech discrimination from 96 to 92%. Including the ear of Patient 2 with the conductive hearing loss and CFD, the mean pre-operative air-conduction 4-frequency pure tone average was 19.7 dB (range 5–56.25 dB), while the mean post-operative air-conduction 4-frequency pure tone average was 22.8 dB (range 5–51.25 dB). As shown in the scatterplot **(B)**, 5 ears had worsening of the 4-frequency air-conduction pure tone average; while 3 stayed the same or improved post-operatively. There was no statistically significant difference in the 4-frequency air-conduction pure tone average pretreatment compared to post-treatment (paired *t*-test, $p = 0.472$). Six ears had no change in WRS, including the 1 ear with a true conductive hearing loss and CFD (Patient 2). One patient had an improved WRS (96–100%) and one patient had a worsened WRS (96–92%). There was no statistically significant difference in the WRS pretreatment compared to post-treatment (paired *t*-test, $p = 0.402$). Copyright © P.A. Wackym, used with permission.

to resolve their TWS symptoms (58). After revision surgery, TWS symptoms were completely resolved in eight (35%), partially resolved in seven (30%), and unresolved in seven (30%) (58). One possible explanation of these findings is that in 14 (61%) of these patients, they also had CT– TWS. It has been suggested that the modiolus may be one site for a CT– TWS (12–14), and Ilmari Pyykkö's and Dennis Poe's demonstration that intratympanic injection of gadolinium subsequently fills the perilymphatic space in mice (59), rats (60), and then exits the inner ear via the modiolus and into the internal auditory canal supports this possibility. Manzari and Scagnelli reported a patient with bilateral SSCD and bilateral dehiscent modioli experiencing bilateral TWS; however, the patient was lost to follow up before surgical intervention (31). Another possible etiology of "CT– TWS" is an unrecognized CFD, as this report underscores.

Naert et al. performed a systematic review of reports of SSCD symptoms and aggregated the most common symptoms into a 22-item common symptom set (41). Among patients with TWS, the same or similar spectrum of symptoms, signs on physical examination and audiological diagnostic findings can be encountered regardless of the site of dehiscence with SSCD, CFD, cochlea-internal carotid artery dehiscence, cochlea-internal auditory canal dehiscence, modiolus, posterior semicircular canal dehiscence, lateral semicircular canal dehiscence, posterior semicircular canal-jugular bulb dehiscence, vestibule-middle ear dehiscence, lateral semicircular canal-facial nerve dehiscence, wide vestibular aqueduct, post-traumatic hypermobile stapes footplate, otosclerosis with internal auditory canal involvement and in patients with CT– TWS. **Table 3** summarizes the spectrum of symptoms, signs, exacerbating factors, diagnostic tools and metrics seen, and used, in patients with TWS caused by a dehiscence at any site (2–43, 57, 58, 61). An important point is that TWS is a clinical entity that presents a symptom spectrum rather than a uniformly observed set of symptoms. Thus, the clinical presentation of an individual patient with TWS is not specific to the site of dehiscence; high-resolution temporal bone CT is necessary to establish the site of dehiscence. This observation, in turn, dictates the range of management options.

Cochlea-Facial Nerve Dehiscence and Other Identified Sites of Dehiscence

Although Jyung and colleagues were the first to identify CFD resulting in TWS in 2014, neither of their two patients were managed surgically (28). As interest in this clinical entity producing TWS has increased, there have been three recent studies focused on the histologic, cadaveric micro-CT and clinical CT prevalence of CFD (32, 44, 45). Fang and coworkers at reported that the histologic prevalence of CFD was 0.59% in 1,020 temporal bone specimens (32). They found that the mean cochlea-facial partition width (CFPW) was 0.23 mm (range 0–0.92 mm, SD 0.15 mm). In particular, 35% of the temporal bones had a CFPW <0.1 mm, which would appear as a CFD on high-resolution temporal bone CT due to current radiographic limitations. They also noted a correlation between a smaller

cross-sectional otic capsule area (OCA) with thinner CFPW, which they speculated may represent a developmental (or scaling) factor and may place older, female and Caucasian patients at greater risk of having a CFD (32).

The Rask-Andersen group in Uppsala, Sweden reported a higher prevalence of CFD in microdissected human temporal bones (43). Of the 282 molds analyzed for CFD, 1.4% (4/282) were found to have a CFD. They also measured the CFPW in 48 silicone molds and 49 resin molds. In the silicone molds, the mean CFPW was 0.20 mm while in the resin molds, the mean CFPW was 0.22 mm; remarkably similar to the histologically measured CFPW in the Fang et al. study (23, 28). They also found one instance of SSCD (1.25%) and two near-SSCD occurrences (2.5%) in 80 microdissected temporal bones that underwent micro-CT and 3D rendering (43). Nikolas Blevins' group at Stanford University recently reported a higher prevalence of CFD in 206 high-resolution temporal bone CT scans (406 ears), identifying 5.4% of ears (22/406 ears) and 9.2% of (19/206 patients) as meeting criteria for CFD; but only 1.4% (3/206 patients) had bilateral CFD (45). The mean CFPW was 0.6 ± 0.2 mm (range 0–0.8 mm), reflecting the lower resolution of their imaging technology (45). This latter issue is illustrated in **Figure 1** where a right near-CFD was seen, yet the patient did not have TWS on the side of the apparent near-CFD. In the Stanford study, they found 33 ears (26 patients, 7 bilateral) with SSCD; of those three ears (2 patients, 1 bilateral) had SSCD and CFD.

The present study identified a fairly high prevalence of otic capsule dehiscence in high resolution temporal images from 401 subjects with TWS symptoms. However, it should be emphasized that all of our patients had TWS symptoms, whereas the status of TWS symptoms was not reported for the subjects in published prevalence studies (32, 44, 45). We identified 463 temporal bones (57.7% [463/802]) with a single site of dehiscence (SSCD, near-SSCD, CT– TWS, CFD, cochlea-internal auditory canal, wide vestibular aqueduct, lateral semicircular canal, modiolus and posterior semicircular canal, SSCD and superior petrosal sinus, SSCD and subarcuate artery). If the CT– TWS temporal bones were excluded, there was single site temporal bone dehiscence found in 366 (366/402 [91.0%]). Regarding multiple sites of dehiscence, there were 38 instances (38/405 [9.38%]) of two site dehiscence (SSCD and CFD, CFD and cochlea-internal auditory canal, CFD and wide vestibular aqueduct, SSCD and cochlea-internal auditory canal, SSCD and posterior semicircular canal-jugular bulb). There was one instance of three sites (3/405 [0.24%]) of dehiscence (SSCD and posterior semicircular canal and wide vestibular aqueduct). The prevalence of multiple-site findings is important to consider when faced with recurrent or incompletely resolved TWS symptoms after plugging a SSCD (12–14, 57, 58). In two of the Johns Hopkins group's publications (57, 58), 45% of their near-SSCD patients and 9.5% of SSCD patients had persistent or recurrent TWS symptoms after surgery via a middle fossa approach and plugging. In light of our recent observations and the histologic, cadaveric and patient CT scan prevalence of CFD and concurrent SSCD and CFD, careful assessment of the presence of CFD in patients with SSCD should be completed and factored into the surgical planning.

Concurrent second otic capsule dehiscence sites in patients with SSCD have been reported previously (12–14, 31, 32, 44, 45). However, because many patients with radiographic evidence of CFD may not have clinical TWS symptoms, the neurotologist author (PAW), does not recommend, or perform, surgical management with RWR of the possible concurrent CFD at the same time as SSCD plugging. It should be noted that even if a SSCD or near-SSCD was found, only about half the patients (52.7%, 175/332) elected to undergo plugging of their SSCD by one of the authors (PAW) between February 2010 and through February 2019. The important point is that surgical management should never be made based solely on the radiographic findings, but rather a combination of objective audiologic test data, clinical symptoms and the measured impact on the patient's life as measured with validated survey instruments, such as the DHI and HIT-6. For many patients, an understanding the source of their TWS symptoms, lifestyle/activity changes and use of an ear plug on the affected side provide sufficient relief for the patient to elect a conservative, non-surgical management approach. The same is true for the other sites of dehiscence found, particularly for CFD. The fact that only 8 patients who had RWR surgery met the inclusion and exclusion criteria used in this study underscores the need to use a comprehensive approach when selecting appropriate surgical candidates.

Subjects, Validated Survey Instruments and Surgical Intervention

For the CFD patients who had RWR surgery, the efficacy of the procedure was demonstrated by the DHI and HIT-6 outcomes (**Figures 3**, **4**, respectively) for symptomatic relief, particularly of a set of items indicating perceived handicap. The improvement is also captured observationally in the pre- and post-operative patient videos (15–19).

Sound-Induced Symptoms

As summarized in **Table 1**, each cohort included patients who had sound-induced dizziness (gravitational receptor dysfunction/asymmetry type of vertigo). This was observed in 75% (6/8) of the patients in either cohort. It should also be noted in both groups that extreme sound sensitivity/pain was common in the children, but not in adults. In addition to sound-induced dizziness, both TWS groups included patients who had sound-induced headache, agitation, confusion or a sense of being overwhelmed. For those CFD patients who elected not to have RWR surgery, or this was not recommended to them, these symptoms were subjectively not as bothersome to the patients.

Hearing Internal Sounds

As summarized in **Table 1**, the typical spectrum of the perception of internal sounds, seen in other TWS etiologies, was observed in the cohort of CFD who underwent RWR surgery. These included self-reports of their voice sounding resonant, hearing loud chewing sounds, hearing their heartbeat, hearing their heel strikes and/or hearing their eyes move or blink. Of the 8 subjects in Group 1, 37.5% (3/8) could hear their eyes move or blink, which is typical of SSCD and CT– TWS patients (9, 12–21).

For the CFD cohort who did not have RWR surgery (**Table 1**, Group 2) only 12.5% (1/8) were able to hear their eyes move or blink. This difference is likely due to the small sample size. For those CFD patients who had RWR surgery, these symptoms resolved post-operatively. For those CFD patients who elected not to have RWR surgery, or this was not recommended to them, these symptoms did not bother the patients sufficiently to offset the perceived risks of surgery.

Trauma, Third Window Syndrome and Perilymphatic Fistula

Victor Goodhill (62) originally, advanced a theory that labyrinthine window ruptures are a possible cause of sudden deafness associated with exertion or trauma. This interest was stimulated by Stroud and Calcaterra's (63) suggestion that increased perilymphatic pressure had caused a window "rupture" in their patients with a "spontaneous" PLF. Over the years the term PLF developed a negative connotation and as described by Hornibrook (64) the evolving controversy produced polarized groups of "believers" and "non-believers" (64–67).

Interestingly there are international and regional differences in the degree of controversy regarding PLF. In the light of our recognition that there are multiple sites where third windows occur in the otic capsule, it is interesting to note that Kohut's definition of a PLF, from over a quarter century ago, still applies to all currently known sites producing a TWS (68); *"A perilymph fistula may be defined as an abnormal opening between the inner ear and the external surface of the labyrinth capsule.…"* Hence, a fistula of the otic capsule (Kohut's definition) can occur in any location that is in communication with perilymph, whether a SSCD, CFD, or any of the well-established sites that can result in a TWS. Patients can have a congenital or acquired TWS. Of those with acquired TWS, there is an unknown but well-recognized percentage of patients who only become symptomatic after a pressure-related event. Therefore, it is more relevant today to consider Goodhill's two proposed mechanisms of explosive and implosive forces. "Explosive" would require an increase in cerebrospinal fluid (CSF) pressure, transmitted from the internal auditory meatus (through the modiolus) or by the cochlear aqueduct. The theory proposed that a force, transmitted through an abnormally patent cochlear aqueduct, could rupture the basilar membrane and/or Reisner membrane into the scala vestibuli, and conceivably injure the utricle, saccule, the semicircular canal system, the round window membrane, or the annular ligament of the stapes. However, these forces could also create a TWS at a site that had not yet become a PLF by delivering an impulse force to that anatomically vulnerable site. Conversely, an "implosive" force would be from a Valsalva maneuver causing sudden air pressure increase through the Eustachian tube, which could elicit a sharp increase in intratympanic pressure and rupture of the round window membrane, annular ligament of the stapes or an anatomically vulnerable site in the otic capsule.

Over a quarter century ago, Black et al. reported that the majority of patients, with what he reported to be middle ear PLF, experienced altered cognitive status (64%) and headache (88%) (39). We have described and quantified similar cognitive changes and headache that recover after surgery for SSCD and CT– TWS (12–14). Video recordings of consenting patients or parents before and after intervention help to further document these obvious alterations in ways that complement standardized neuropsychology testing (15–19). All 8 patients in the CFD with RWR cohort had a pre-TWS history of an explosive or implosive force exposure (**Table 2**). In contrast, only 2 of the 8 patients (25%) in the CFD without RWR surgery group had a history of explosive or implosive forces before presentation (**Table 2**). It should be noted that the same type of mechanisms producing TBI from blast injuries, head trauma or possibly impulsive acoustic energy delivered to the inner ear can produce a TWS or TWS-like symptoms resulting in inner ear dysfunction and asymmetric otolithic input (12–14, 69, 70).

Cervical Vestibular Evoked Myogenic Potentials

The cVEMP thresholds are shown in **Table 1** for the 8 CFD and 1 CT– TWS patients who had RWR surgery. For all 9 ears receiving RWR, the mean cVEMP threshold was 77.2 dB nHL (SD 7.6, range 70–95 dB nHL). Excluding the threshold of 95 dB nHL for the single ear with a CFD and a conductive hearing loss of 42.5 dB pre-operatively, the mean cVEMP threshold was 75 dB nHL (SD 3.8, range 70–80 dB nHL). For the non-operated ears reported in **Table 1**, the mean cVEMP threshold was 85.71 dB nHL (SD 10.6, range 70–95 dB nHL). Within the operated CFD subjects, the mean difference between the unoperated ear cVEMP threshold compared to the operated ear (excluding the large conductive hearing loss cVEMP threshold) was 10.71 dB nHL (SE 4.0), which was statistically significant ($p = 0.013$, Tukey HSD test). By a Tukey HSD the reduced cVEMP threshold was also statistically lower (Tukey HSD test, $p = 0.034$). In the SSCD literature, the cVEMP threshold has been reported to be reduced in most patients, but the cVEMP response can be absent or without a reduced threshold, despite surgical confirmation of the SSCD (9, 11–14, 21). In Minor's 2005 series of 65 SSCD patients (11), the mean reduced threshold for the cVEMP was 81 ± 9 dB nHL—which means there would likely be an unknown, but certain percentage of his patients with SSCD who would not meet the 70 dB nHL threshold standard that some clinicians have advocated anecdotally and would be categorized as "negative." Thus, what might appear to be a "discrepancy" is well-described in the SSCD literature and should be factored into the decision-making when managing patients with TWS due to CFD.

The cVEMP thresholds are shown in **Table 1** for the 8 CFD patients in Group 2 who did not have RWR surgery. For the 8 ears with CFD the mean cVEMP threshold was 76.9 dB nHL (SE 3.0, SD 8.4; range 70–95 dB nHL). There was 1 ear with a CFD that had no cVEMP response (**Table 1**). For the 5 ears with no CFD the mean cVEMP threshold was 83.0 dB nHL (SE 3.0, SD 6.71; range 80–95 dB nHL). There was no difference in these thresholds using an independent *t*-test of all values ($p = 0.199$).

As shown in **Table 1**, the amplitudes of the cVEMP responses, in general declined with age. There was also variability of amplitude in the CFD ear relative to the ear without CFD. Noij et al. found that in SSCD patients, the threshold audiometry and cVEMP data were useful diagnostically and for monitoring outcomes post-operatively, these measures showed no significant

correlation with vestibular and most auditory symptoms or their severity (71).

Because air-conduction cVEMP studies were performed and soft tissue and cartilage were placed in the middle ear and over the RW, post-operative cVEMP studies were not routinely performed in the cohort of patients who had CFD and underwent RWR (Group 1). However, there were 2 of these patients who had post-operative cVEMP studies. In patient 1, the cVEMP response was not present in the operated ear after RWR. In patient 4, in the CFD (right) side the amplitude increased from 358 to 403 μV post-operatively and the threshold remained unchanged at 95 dB pre-operatively and post-operatively. This side had a large conductive hearing loss pre-operatively and post-operatively. For the CT– TWS (left) side the amplitude decreased from 466 to 153 μV post-operatively and the threshold normalized from 75 dB pre-operatively to 95 dB post-operatively.

Dizziness Handicap Inventory

For the CFD cohort who had RWR procedures performed (**Tables 1**, **2**, Group 1), there was a highly statistically significant ($p < 0.0001$) (**Figure 3**) improvement in the mean DHI score. For the CFD cohort who did not choose to have surgery (**Tables 1**, **2**, Group 2), statistical comparison of Group 1 (CFD with RWR) to Group 2 (CFD without RWR) revealed that the DHI scores were no different between the groups ($p > 0.05$) (**Tables 1**, **2**).

We tested the hypothesis that there are significant differences in the first symptom report scores (patterns) between the two patient groups to determine if there were any significant differences between symptom item endorsements in patients that may be related to election of surgery. There were 3 questions related to perceived handicap that were significantly larger in the group electing surgery: *"Does performing more ambitious activities, such as sports, dancing, household chores (sweeping or putting dishes away) increase your problems?"* (P8), *"Because of your problem, is it difficult for you to do strenuous homework or yard work?"* (F14) and *"Because of your problem, do you feel handicapped?"* (E21). By binary logistic regression (Wald criterion), responses to DHI items P4 (*"Does walking down the aisle of a supermarket increase your problems?"*) and F14 (*"Because of your problem, is it difficult for you to do strenuous homework or yard work?"*) were sufficient to classify 7 of 8 of each group correctly, with F14 alone producing a correct classification of 6 of 8 from each group. Based on these findings, the decision to have RWR surgery for CFD appears to be a function of the perceived handicap related to the difficulty of performing tasks that require exertion.

Migraine Headache and Outcomes After Round Window Reinforcement

For the CFD cohort who had RWR procedures performed (**Tables 1**, **2**, Group 1), there was a highly statistically significant ($p < 0.001$) (**Figure 4**) improvement in the HIT-6 score post-operatively. Statistical comparison of Group 1 (CFD with RWR) to Group 2 (CFD without RWR) revealed that the HIT-6 scores were no different between the groups ($p > 0.05$) (**Tables 1**, **2**).

It is approaching one-half century ago that Gordon (67) hypothesized that the migraine headaches seen in PLF patients are caused by reduced spinal fluid pressure. The series published by Black and colleagues (39) 88% of their PLF patients experienced headache. In our longitudinal study of cognitive dysfunction and recovery in TWS, we found that migraine headaches were present in 88% (7/8) of subjects with CT– TWS only, 100% (4/4) of subjects with SSCD and subsequent CT– TWS, and 80% (4/5) of subjects with SSCD only (13). We also reported migraine variants that can occur with the migraine headaches or as separate episodes, including all three variants; ocular migraine, hemiplegic migraine and VM (12–14). We hypothesize that migraines are triggered by the abnormal otolithic input much in the same way that some migraine patients have migraines triggered by trigeminal stimulation. Removal of the abnormal otolithic input would eliminate a trigger, leading to either resolution or improvement of the migraines to the extent that medical management is then successful. Removing the abnormal otolithic input in CFD is achieved by RWR via returning to a two mobile window state rather than the TWS state.

Vestibular migraine (VM), also termed migraine-associated dizziness, has become recognized as a distinct clinical entity that accounts for a high proportion of patients with vestibular symptoms [for review see Furman et al. (72)]. A temporal overlap between vestibular symptoms, such as vertigo and head-movement intolerance, and migraine symptoms, such as headache, photophobia, and phonophobia, is a requisite diagnostic criterion. Physical examination and laboratory testing are usually normal in VM but can be used to rule out other vestibular disorders with overlapping symptoms, such as with the various defects associated with TWS. Vestibular migraine patients typically do not have sound-induced dizziness and nausea or autophony. However, when these patients have endolymphatic hydrops, they can have sound sensitivity that borders on a Tullio phenomenon. For this reason, when a high-resolution temporal bone CT shows no evidence of a bony dehiscence, all patients suspected as having CT– TWS should be treated as a VM patient, since medical management, if successful, avoids unnecessary surgery (12–14). This management strategy is also used by the neurotologist author (PAW) for patients suspected of having a clinically relevant CFD. It should be noted that all 8 patients who elected to undergo RWR for their TWS secondary to their CFD were all treated as vestibular migraine patients before surgery. The mean duration of medical management was 25.2 months (range 2.5–85 months).

Vestibular migraine is an example of the integral overlap between vestibular pathways and migraine circuit triggers and central mechanisms for premonitory symptom generation. Information transmitted by peripheral vestibular sensory organs and the vestibular nerve to the medulla and pons is an external trigger within the migraine circuit construct proposed by Ho and coworkers (73). This model is based upon the distribution of the neuropeptide calcitonin-gene-related-peptide (CGRP), which has a complex distribution within the vestibular periphery (74). One must acknowledge that the use of CGRP-binding monoclonal antibodies as biologics in the clinical practice of migraine management (75, 76) has a potential to produce a side

effect of peripheral vestibular dysfunction or injury due to the impairment of vestibular efferent function.

Migraine headache is nearly always present in patients with gravitational receptor dysfunction type of vertigo caused by TWS. Our study shows that it may also accompany CFD. Migraine seem to be less frequent with rotational receptor dysfunction type of true rotational vertigo (12–19, 39). This is an important concept as CT– TWS, SSCD, and CFD can be associated with three variants of migraine: hemiplegic migraine, ocular migraine and vestibular migraine (12–14, 77). As shown in **Table 2**, all 8 subjects (100%) had migraine headaches and 5/8 (62.5%) CFD patients undergoing RWR experienced migraine variants before surgery (3 CFD patients had intermittent VM episodes and less frequent ocular migraines, while 2 CFD patients had intermittent ocular migraines). For the CFD patients who did not undergo RWR (**Table 2**), 7/8 (87.5%) had migraine headaches and 4/8 (50%) of patients with CFD experienced migraine variants before surgery (2 CFD patients had intermittent VM episodes and less frequent ocular migraines, while 2 CFD patients had VM). In patients with CFD and TWS, the VM episodes can produce a combination of infrequent true rotational vertigo attacks on a background of a gravitational receptor (otolithic) dysfunction type of vertigo. The post-operative HIT-6 results document a profound amelioration of reported headache symptoms in these CFD cases after RWR (**Figure 4**). Because migraine has a high incidence and there are multiple trigger mechanisms, there may only be a marked decrease of the frequency and intensity of the migraines in other cases, but it is often the case that once patients have reached this point they can improve to the point that they come under control with medical management (12–19, 77).

Cognitive Dysfunction and Recovery

Memory, Attention, and Executive Function

Patients with TWS also report symptoms consistent with cognitive dysfunction, spatial disorientation, anxiety and autonomic dysfunction. The degree that these functions and symptoms were impacted in our two cohorts varied as summarized in **Table 2**. A broader description of the range of symptoms and measurement tools available is summarized in **Table 3**.

One possible hypothesis of why these TWS patients experience their cognitive dysfunction and spatial disorientation and recovery of function after surgical intervention is that intermittent aberrant otolithic input to the cerebellum creates an episodic but reversible cerebellar cognitive affective syndrome (78–80). Schmahmann conceptualizes cerebellar cognitive affective syndrome as dysmetria of thought and emotion. He describes impairment of executive function (planning, set-shifting, verbal fluency, abstract reasoning and working memory); spatial cognition (visual spatial organization and memory); personality change (blunting of affect or disinhibited and inappropriate behavior); and language deficits (agrammatism and aprosodia) (78–80). These clinical features closely fit what TWS patients describe and their neuropsychology testing measures (12–19). To varying degrees, TWS patients describe cognitive dysfunction (impaired memory and concentration, word finding and name finding difficulty, occasional slurred speech and for women, the loss of the ability to listen to more than one person speaking at time), spatial disorientation (trouble judging distances, sense of detachment, sometimes perceiving the walls moving/breathing or the floor moving, and less commonly out of body experiences), and anxiety (sense of impending doom). In children and young adults continuing their education, their academic performance typically drops; they miss days of school and are often assigned a psychiatric or neurobehavioral diagnosis (12–19). These symptoms are summarized in **Table 2** for our two cohorts of CFD patients.

In addition, normal vestibular information appears to be important for head direction responses cells in pathways involving the anterodorsal thalamic nucleus. For example, Yoder and Taube (81) showed that the head direction responses are highly abnormal in a genetic mutant mouse without otolith function. The disruption is expected to extend throughout navigation-related pathways, including the hippocampal formation. We suggest that aberrant vestibular information from a unilateral TWS may also lead to disruption of a variety of cognitive processes by disrupting similar responses in our patients. Similar mechanisms may be involved with degraded otolith function in other contexts, for example in aging (82).

In earlier studies of patients undergoing surgery for CT+ SSCD TWS, CT– TWS as well as patients who had surgery for CT+ SSCD TWS and had surgery for a subsequent CT– TWS, we reported impaired executive function and Wide Range Assessment of Memory and Learning, Second Edition (WRAML2) domain abnormalities in these patients pre-operatively and that there was resolution post-operatively (13). We used the DKEFS and found that there was significant post-operative improvement in both the Delis-Kaplan Executive Function System (DKEFS) Motor Speed score [$F_{(2,28)} = 10.31$, $p < 0.01$] and the Number-Letter Switching score [$F_{(2,28)} = 6.04$, $p < 0.05$] (4, 7). These findings are consistent with our hypothesis that aberrant vestibular input in TWS can contribute to signs and symptoms in the cognitive domain.

The role of migraine in these TWS patients may also contribute to the observed cognitive dysfunction and depression. As reviewed by Ravishankar and Demakis (83), research has shown that migraine can affect verbal, visual memory, and selective attention tasks. Cognitive impairments observed in migraineurs have been found to occur during a migraine attack, after the attack, and even when the individual does not exhibit any residual effects of the attack. Individuals with migraine are at a greater risk of developing anxiety and depression. However, the relatively long delay in recovery of cognitive function after surgery for TWS argues against migraine as the cause of the cognitive dysfunction in these patients (13).

Our comorbidity study (14) noted a high rate of psychological comorbidity ($n = 6$). The Millon Behavioral Medicine Diagnostic (MBMD) and the clinical psychology examinations were the most useful in identifying these comorbidities (14). Factitious disorder, functional neurologic symptom disorder (formerly conversion disorder) dissociative motor disorder variant, somatic symptom disorder, attention deficit hyperactivity disorder (ADHD), dissociative identity disorder (DID), major

depressive disorder (MDD), and post-traumatic stress disorder (PTSD) were represented in 6 of the 12 participants in the comorbidity cohort. Suicidal ideation was also common (n = 6) (14). These findings underscore the challenges in sorting out the TWS symptoms caused by the dehiscence, those resulting from other comorbid conditions, or those resulting from interactions between the two factors. Clinically, we have incorporated a staged approach to assessing our TWS patients for comorbidities using baseline cognitive screening with the Montréal Cognitive Assessment (MoCA) as well as depression and anxiety scales. Pre-operative patients also undergo a comprehensive neuropsychological evaluation covering the domains of motor speed, complex attention, processing speed, executive functioning, language, visuospatial abilities, memory, and mood/personality. Results are utilized for a thorough diagnostic differential as well as to identify comorbid factors that may complicate post-surgical outcomes, such as personality disorders and chronic psychiatric illness. Post-operative neuropsychological reevaluations (covering the aforementioned domains with alternative forms) occur at 6–8 months after surgery to determine cognitive symptom improvement as well as to identify residual deficits that may be amenable to neurorehabilitation.

Hearing Outcomes and Electrocochleography

Hearing Outcomes

The magnitude of the pseudoconductive hearing loss was, in general smaller than that seen in cases of SSCD. However, our sample size is much smaller than most series of SSCD addressing this question. The pseudoconductive hearing loss is not always present or can be small in SSCD patients (11–13, 21) and in Poe's series of 65 patients published in 2007 (21), 86% had a pseudoconductive hearing loss, while 14% did not. In Minor's 2005 series, only 70% had a pseudoconductive hearing loss of 10 dB or greater while 30% did not (11). In the current series there was no statistically significant difference in the 4-frequency air-bone gap pretreatment compared to post-treatment (p = 0.091) (**Figure 5B**). There was no statistically significant difference in the WRS pretreatment compared to post-treatment (paired t-test, p = 0.402) (**Figure 6**). While there was no significant difference in the air-bone gap due to the pseudoconductive loss and the post-operative additional conductive hearing loss due to the RWR and the associated 4-frequency pure tone average air-conduction thresholds, when counseling patients considering RWR for CFD, it is typically the case that their other TWS symptoms are so severe that they would be willing to sacrifice hearing to eliminate or reduce their TWS symptoms. Fortunately, our data suggests that they are unlikely to experience this negative hearing outcome after RWR.

Electrocochleography

As shown in **Table 1**, only 2 ears had abnormal electrocochleography suggestive of ELH (SP/AP ratio >0.42). Both of these subjects underwent RWR procedures. One of these subjects (**Table 1**, Group 1 Patient 2) had electrophysiologic signs of endolymphatic hydrops in his CT– TWS left ear (SP/AP ratio 0.43), while his right ear with the CFD (**Figure 2**) had no evidence of endolymphatic hydrops (SP/AP ratio of 0.36). The other subject (**Table 1**, Group 1 Patient 3) had electrophysiologic signs of ELH in her right CFD ear (SP/AP ratio 0.46), while her right ear with the near-CFD (**Figure 1**) and no TWS symptoms, had no evidence of ELH (SP/AP ratio of 0.38). This finding is very different than what is observed in patients with SSCD (12, 13, 57). Arts and colleagues at the University of Michigan were the first to report reversible abnormal ECoG/ELH in patients with SSCD (57). Fourteen of 15 ears confirmed to have SSCD on CT imaging were found to have ECoG evidence of ELH. In all 4 patients who underwent plugging of the SSCD, the ECoG SP/AP ratio normalized post-operatively (57).

Study Limitations

Although this was a retrospective study with a small sample size (n = 16), it is much larger than the 2 published cases of CFD in patients experiencing TWS. There are an additional 5 cases of CFD reported in the context of facial nerve stimulation in cochlear implant recipients. In our study, while cognitive dysfunction, spatial disorientation and anxiety were reported by the patients (**Table 2**), and in many cases captured by their pre-operative videos, objective measurements of these symptoms of TWS were not uniformly or consistently performed, although many underwent formal neuropsychology testing. In addition, tools to measure spatial disorientation and anxiety were not incorporated into their clinical care, so these metrics were not available to compare the patients who underwent RWR surgery and those who did not elect to undergo surgery. Likewise, these metrics were not available to assess outcomes after RWR surgery. The retrospective analysis, though, documents significant clinical features of CFD in patients experiencing TWS that need to be considered in prospective study design.

Conclusions

Overall there was a marked and clinically significant improvement in DHI, HIT-6, and TWS symptoms post-operatively for the CFD cohort who had RWR surgery. A statistically significant reduction in cVEMP thresholds was observed in patients with radiographic evidence of CFD. Surgical management with RWR in patients with CFD was associated with improved symptoms and outcomes measures. There was no statistically significant change of hearing in the patients with CFD who underwent RWR. It is emphasized that radiographic CFD is not in itself an indication for surgery and that the most important factor in decision-making should be in the context of clinical symptoms and other diagnostic findings. There are three important presenting symptoms and physical findings that are critical when identifying a TWS, including CFD: (1) sound-induced dizziness; (2) hearing internal sounds; and (3) hearing or feeling low frequency tuning forks in an involved ear when applied to a patient's knee or elbow. Another important observation in the study was that multiple sites of dehiscence in temporal bones with TWS occurs and this finding is important

to consider when faced with recurrent or incompletely resolved TWS symptoms after plugging a SSCD.

DATA AVAILABILITY STATEMENT

The datasets generated for this study are available on request to the corresponding author.

ETHICS STATEMENT

The studies involving human participants were reviewed and approved by Rutgers New Brunswick Health Sciences Institutional Review Board (Pro2019000726). Written informed consent from the participants' legal guardian/next of kin was not required to participate in this study in accordance with the national legislation and the institutional requirements. Written informed consent was obtained from the individual(s), and minor(s)' legal guardian/next of kin, for the publication of any potentially identifiable images or data included in this article.

AUTHOR CONTRIBUTIONS

PAW and CDB contributed the conception and design of the study. PAW organized the database. CDB performed the statistical analysis. PAW and CDB wrote the first draft of the manuscript. PAW, CDB, PZ, DAS, and JSH wrote the sections of the manuscript. All authors contributed to the manuscript revision, read, and approved the submitted version.

FUNDING

Funds were provided by the Department of Otolaryngology–Head and Neck Surgery, Rutgers Robert Wood Johnson Medical School, and the Ear and Skull Base Center.

SUPPLEMENTARY MATERIAL

The Supplementary Material for this article can be found online at: https://www.frontiersin.org/articles/10.3389/fneur.2019.01281/full#supplementary-material

REFERENCES

1. Tullio P. *Das Ohr und die Entstehung der Sprache und Schrift*. Berlin: Urban & Schwarzenberg (1929). p. 1–455.
2. Huizinga E. The physiological and clinical importance of experimental work on the pigeon's labyrinth. *J Laryngol Otol.* (1955) 69:260–8. doi: 10.1017/S0022215100050635
3. Grieser BJ, Kleiser L, Obrist D. Identifying mechanisms behind the Tullio phenomenon: a computational study based on first principles. *J Assoc Res Otolaryngol.* (2016) 17:103–18. doi: 10.1007/s10162-016-0553-0
4. Fox EJ, Balkany TJ, Arenberg IK. The Tullio phenomenon and perilymph fistula. *Otolaryngol Head Neck Surg.* (1988) 98:88–9. doi: 10.1177/019459988809800115
5. Pyykkö I, Ishizaki H, Aalto H, Starck J. Relevance of the Tullio phenomenon in assessing perilymphatic leak in vertiginous patients. *Am J Otol.* (1992) 13:339–42.
6. Colebatch JG, Rothwell JC, Bronstein A, Ludman H. Click-evoked vestibular activation in the Tullio phenomenon. *J Neurol Neurosurg Psychiatry.* (1994) 57:1538–40. doi: 10.1136/jnnp.57.12.1538
7. Ostrowski VB, Hain TC, Wiet RJ. Pressure-induced ocular torsion. *Arch Otolaryngol Head Neck Surg.* (1997) 123:646–9. doi: 10.1001/archotol.1997.01900060098017
8. Weinreich HM, Carey JP. Perilymphatic fistulas and superior semicircular canal dehiscence syndrome. *Adv Otorhinolaryngol.* (2019) 82:93–100. doi: 10.1159/000490276
9. Ward BK, Carey JP, Minor LB. Superior canal dehiscence syndrome: lessons from the first 20 years. *Front Neurol.* (2017) 8:177. doi: 10.3389/fneur.2017.00177
10. Minor LB, Solomon D, Zinreich JS, Zee DS. Sound- and/or pressure-induced vertigo due to bone dehiscence of the superior semicircular canal. *Arch Otolaryngol Head Neck Surg.* (1998) 124:249–58. doi: 10.1001/archotol.124.3.249
11. Minor LB. Clinical manifestations of superior semicircular canal dehiscence. *Laryngoscope.* (2005) 115:1717–27. doi: 10.1097/01.mlg.0000178324.55729.b7
12. Wackym PA, Wood SJ, Siker DA, Carter DM. Otic capsule dehiscence syndrome: superior canal dehiscence syndrome with no radiographically visible dehiscence. *Ear Nose Throat J.* (2015) 94:E8–24. doi: 10.1177/014556131509400802
13. Wackym PA, Balaban CD, Mackay HT, Wood SJ, Lundell CJ, Carter DM, et al. Longitudinal cognitive and neurobehavioral functional outcomes after repairing otic capsule dehiscence. *Otol Neurotol.* (2016) 37:70–82. doi: 10.1097/MAO.0000000000000928
14. Wackym PA, Mackay-Promitas HT, Demirel S, Gianoli GJ, Gizzi MS, Carter DM, et al. Comorbidities confounding the outcomes of surgery for third window syndrome: outlier analysis. *Laryngoscope Invest Otolaryngol.* (2017) 2:225–53. doi: 10.1002/lio2.89
15. Wackym PA. *Round Window Reinforcement Surgery for Cochlea-Facial Nerve Dehiscence: Symptoms and Testing*. Available online at: https://youtu.be/2z1RJEKZQ1A (accessed November 11, 2019).
16. Wackym PA. *Cochlea-Facial Nerve Dehiscence: Traumatic Third Window Syndrome After a Snowboarding Accident*. Available online at: https://youtu.be/NCDMD5FGf-w (accessed November 11, 2019).
17. Wackym PA. *Right Cochlea-Facial Nerve Dehiscence: 16 Year Old Thought to Have Conversion Disorder*. Available online at: https://youtu.be/fTjsnnUALBw (accessed November 11, 2019).
18. Wackym PA. *Surgery for Cochlea-Facial Nerve Dehiscence: Symptoms and Tuning Fork Testing*. Available online at: https://youtu.be/lFR-zdYlIsY (accessed November 11, 2019).
19. Wackym PA. *Cochlea-Facial Nerve Dehiscence: Third Window Syndrome After a Car Accident*. Available online at: https://youtu.be/eJX2RA3okKc (accessed November 11, 2019).
20. Mikulec AA, Poe DS, McKenna MJ. Operative management of superior semicircular canal dehiscence. *Laryngoscope.* (2005) 115:501–7. doi: 10.1097/01.mlg.0000157844.48036.e7
21. Zhou G, Gopen Q, Poe DS. Clinical and diagnostic characterization of canal dehiscence syndrome: a great otologic mimicker. *Otol Neurotol.* (2007) 28:920–6. doi: 10.1097/MAO.0b013e31814b25f2
22. Young L, Isaacson B. Cochlear and petrous carotid canal erosion secondary to cholesteatoma. *Otol Neurotol.* (2010) 31:697–8. doi: 10.1097/MAO.0b013e31819bd803
23. Meiklejohn DA, Corrales CE, Boldt BM, Sharon JD, Yeom KW, Carey JP, et al. Pediatric semicircular canal dehiscence: radiographic and histologic prevalence, with clinical correlations. *Otol Neurotol.* (2015) 36:1383–9. doi: 10.1097/MAO.0000000000000811
24. Park JJ, Shen A, Loberg C, Westhofen M. The relationship between jugular bulb position and jugular bulb related inner ear dehiscence: a retrospective analysis. *Am J Otolaryngol.* (2015) 36:347–51. doi: 10.1016/j.amjoto.2014.12.006

25. Gopen Q, Zhou G, Poe D, Kenna M, Jones D. Posterior semicircular canal dehiscence: first reported case series. *Otol Neurotol.* (2010) 31:339–44. doi: 10.1097/MAO.0b013e3181be65a4
26. Bear ZW, McEvoy TP, Mikulec AA. Quantification of hearing loss in patients with posterior semicircular canal dehiscence. *Acta Otolaryngol.* (2015) 135:974–7. doi: 10.3109/00016489.2015.1060630
27. Elmali M, Poltat AV, Kucuk H, Atmaca S, Aksoy A. Semicircular canal dehiscence: frequency and distribution on temporal bone CT and its relationship with the clinical outcomes. *Eur J Radiol.* (2013) 82:e606–9. doi: 10.1016/j.ejrad.2013.06.022
28. Blake DM, Tomovic S, Vazquez A, Lee HJ, Jyung RW. Cochlear-facial dehiscence–a newly described entity. *Laryngoscope.* (2014) 124:283–9. doi: 10.1002/lary.24223
29. Fujita T, Kobayashi T, Saito K, Seo T, Ikezono T, Doi K. Vestibule-middle ear dehiscence tested with perilymph-specific protein cochlin-tomoprotein (CTP) detection test. *Front Neurol.* (2019) 10:47. doi: 10.3389/fneur.2019.00047
30. Manzari L. Multiple dehiscences of bony labyrinthine capsule. A rare case report and review of the literature. *Acta Otorhinolaryngol Ital.* (2010) 30:317–20.
31. Manzari L, Scagnelli P. Large bilateral internal auditory meatus associated with bilateral superior semicircular canal dehiscence. *Ear Nose Throat J.* (2013) 92:25–33. doi: 10.1177/014556131309200109
32. Fang CH, Chung SY, Blake DM, Vazquez A, Li C, Carey JP, et al. Prevalence of cochlear-facial dehiscence in a study of 1,020 temporal bone specimens. *Otol Neurotol.* (2016) 37:967–72. doi: 10.1097/MAO.0000000000001057
33. Ho ML, Moonis G, Halpin CF, Curtin HD. Spectrum of third window abnormalities: semicircular canal dehiscence and beyond. *Am J Neuroradiol.* (2017) 38:2–9. doi: 10.3174/ajnr.A4922
34. Koo JW, Hong SK, Kim DK, Kim JS. Superior semicircular canal dehiscence syndrome by the superior petrosal sinus. *J Neurol Neurosurg Psychiatry.* (2010) 81:465–7. doi: 10.1136/jnnp.2008.155564
35. Ionescu EC, Al Tamami N, Neagu A, Ltaief-Boudrigua A, Gallego S, Hermann R, et al. Superior semicircular canal ampullae dehiscence as part of the spectrum of the third window abnormalities: a case study. *Front Neurol.* (2017) 8:683. doi: 10.3389/fneur.2017.00683
36. Dasgupta S, Ratnayake SAB. Functional and objective audiovestibular evaluation of children with apparent semicircular canal dehiscence–a case series in a pediatric vestibular center. *Front Neurol.* (2019) 10:306. doi: 10.3389/fneur.2019.00306
37. Merchant SN, Rosowski JJ. Conductive hearing loss caused by third-window lesions of the inner ear. *Otol Neurotol.* (2008) 29:282–9. doi: 10.1097/MAO.0b013e318161ab24
38. Hornibrook J. *The Balance Abnormality of Chronic Perilymph Fistula*. Available online at: https://www.youtube.com/watch?v=2DXgQMnlgbw (accessed November 11, 2019).
39. Black FO, Pesznecker S, Norton T, Fowler L, Lilly DJ, Shupert C, et al. Surgical management of perilymphatic fistulas: a Portland experience. *Am J Otol.* (1992) 13:254–62.
40. Crane BT, Minor LB, Carey JP. Superior canal dehiscence plugging reduces dizziness handicap. *Laryngoscope.* (2008) 118:1809–13. doi: 10.1097/MLG.0b013e31817f18fa
41. Naert L, Van de Berg R, Van de Heyning P, Bisdorff A, Sharon JD, Ward BK, et al. Aggregating the symptoms of superior semicircular canal dehiscence syndrome. *Laryngoscope.* (2018) 128:1932–8. doi: 10.1002/lary.27062
42. Shim YJ, Bae YJ, An GS, Lee K, Kim Y, Lee SY, et al. Involvement of the internal auditory canal in subjects with cochlear otosclerosis: a less acknowledged third window that affects surgical outcome. *Otol Neurotol.* (2019) 40:e186–90. doi: 10.1097/MAO.0000000000002144
43. Bae YJ, Shim YJ, Choi BS, Kim JH, Koo JW, Song JJ. "Third window" and "single window" effects impede surgical success: analysis of retrofenestral otosclerosis involving the internal auditory canal or round window. *J Clin Med.* (2019) 8:E1182. doi: 10.3390/jcm8081182
44. Schart-Morén N, Larsson S, Rask-Andersen H, Li H. Anatomical characteristics of facial nerve and cochlea interaction. *Audiol Neurootol.* (2017) 22:41–9. doi: 10.1159/000475876
45. Song Y, Alyono JC, Bartholomew RA, Vaisbuch Y, Corrales CE, Blevins NH. Prevalence of radiographic cochlear-facial nerve dehiscence. *Otol Neurotol.* (2018) 39:1319–25. doi: 10.1097/MAO.0000000000002015
46. Fang CH, Chung SY, Mady LJ, Raia N, Lee HJ, Mary Ying YL, et al. Facial nerve stimulation outcomes after cochlear implantation with cochlear-facial dehiscence. *Otolaryngol Case Reports.* (2017) 3:12–4. doi: 10.1016/j.xocr.2017.04.003
47. Schart-Morén N, Hallin K, Agrawal SK, Ladak HM, Eriksson PO, Li H, et al. Peri-operative electrically evoked auditory brainstem response assessment of facial nerve/cochlea interaction at cochlear implantation. *Cochlear Implants Int.* (2018) 19:324–9. doi: 10.1080/14670100.2018.1481179
48. Jacobson GP, Newman CW. The development of the Dizziness Handicap Inventory. *Arch Otolaryngol Head Neck Surg.* (1990) 116:424–7. doi: 10.1001/archotol.1990.01870040046011
49. Whitney SL, Wrisley DM, Brown KE, Furman JM. Is perception of handicap related to functional performance in persons with vestibular dysfunction? *Otol Neurotol.* (2004) 25:139–43. doi: 10.1097/00129492-200403000-00010
50. Yang M, Rendas-Baum R, Varon SF, Kosinski M. Validation of the Headache Impact Test (HIT-6^{TM}) across episodic and chronic migraine. *Cephalalgia.* (2011) 31:357–67. doi: 10.1177/0333102410379890
51. Bayliss M, Batenhorst A. *The HIT-6^{TM}: A User's Guide*. Lincoln, RI: QualityMetric, Inc (2002).
52. Headache Classification Committee of the International Headache Society (IHS). The international classification of headache disorders, 3rd edition. *Cephalalgia.* (2018) 38:1–211. doi: 10.1177/0333102417738202
53. Gurgel RK, Jackler RK, Dobie RA, Popelka GR. A new standardized format for reporting hearing outcome in clinical trials. *Otolaryngol Head Neck Surg.* (2012) 147:803–7. doi: 10.1177/0194599812458401
54. Wackym PA. *Tuning Fork Testing in Otic Capsule Dehiscence Syndrome*. Available online at: https://www.youtube.com/watch?v=Szp_kO8oVos (accessed November 11, 2019).
55. Wackym PA, Ratigan JA, Birck JD, Johnson SH, Doornink J, Bottlang M, et al. Rapid cVEMP and oVEMP responses elicited by a novel head striker and recording device. *Otol Neurotol.* (2012) 33:1392–400. doi: 10.1097/MAO.0b013e318268d234
56. Margolis RH, Rieks D, Fournier EM, Levine SE. Tympanic electrocochleography for diagnosis of Ménière's disease. *Arch Otolaryngol Head Neck Surg.* (1995) 121:44–55. doi: 10.1001/archotol.1995.01890010032007
57. Ward BK, Wenzel A, Ritzl EK, Gutierrez-Hernandez S, Della Santina CC, Minor LB, et al. Near-dehiscence: clinical findings in patients with thin bone over the superior semicircular canal. *Otol Neurotol.* (2013) 34:1421–8. doi: 10.1097/MAO.0b013e318287efe6
58. Sharon JD, Pross SE, Ward BK, Carey JP. Revision surgery for superior canal dehiscence syndrome. *Otol Neurotol.* (2016) 37:1096–103. doi: 10.1097/MAO.0000000000001113
59. Zou J, Zhang W, Poe D, Zhang Y, Ramadan UA, Pyykkö I. Differential passage of gadolinium through the mouse inner ear barriers evaluated with 4.7T MRI. *Hear Res.* (2010) 259:36–43. doi: 10.1016/j.heares.2009.09.015
60. Zou J, Poe D, Ramadan UA, Pyykkö I. Oval window transport of Gd-dOTA from rat middle ear to vestibulum and scala vestibuli visualized by *in vivo* magnetic resonance imaging. *Ann Otol Rhinol Laryngol.* (2012) 121:119–28. doi: 10.1177/000348941212100209
61. Arts HA, Adams ME, Telian SA, El-Kashlan H, Kileny PR. Reversible electrocochleographic abnormalities in superior canal dehiscence. *Otol Neurotol.* (2009) 30:79–86. doi: 10.1097/MAO.0b013e31818d1b51
62. Goodhill V. Sudden deafness and round window rupture. *Laryngoscope.* (1971) 81: 1462–74. doi: 10.1288/00005537-197109000-00010
63. Stroud MH, Calcaterra TC. Spontaneous perilymph fistulas. *Laryngoscope.* (1970) 80:479–87. doi: 10.1288/00005537-197003000-00012
64. Hornibrook J. Perilymph fistula: fifty years of controversy. *ISRN Otolaryngol.* (2012) 2012:281248. doi: 10.5402/2012/281248
65. Friedland DR, Wackym PA. A critical appraisal of spontaneous perilymphatic fistulas of the inner ear. *Am J Otol.* (1999) 20:261–76.
66. Deveze A, Matsuda H, Elziere M, Ikezono T. Diagnosis and treatment of perilymph fistula. In: Lloyd SKW, Donnelly NP, editors. Advances in Hearing Rehabilitation. *Adv Otorhinolaryngol.* (2018) 81:133–45. doi: 10.1159/000485579

67. Gordon AG. Perilymph fistula: a cause of auditory, vestibular, neurological and psychiatric disorder. *Med Hypotheses.* (1976) 2:125–34. doi: 10.1016/0306-9877(76)90067-0
68. Kohut RI. Perilymph fistulas. Clinical criteria. *Arch Otolaryngol Head Neck Surg.* (1992) 118:687–92. doi: 10.1001/archotol.1992.01880070017003
69. Gianoli GJ, Soileau JS, Wackym PA. Neurological symptoms in US government personnel in Cuba. *JAMA.* (2018) 320:603–4. doi: 10.1001/jama.2018.8713
70. Michael E. Hoffer ME, Levin BE, Snapp H, Buskirk J, Balaban CD. Acute findings in an acquired neurosensory dysfunction. *Laryngoscope Invest Otolaryngol.* (2019) 4: 124–31. doi: 10.1002/lio2.231
71. Noij KS, Wong K, Duarte MJ, Masud S, Dewyer NA, Herrmann BS, et al. Audiometric and cVEMP thresholds show little correlation with symptoms in superior semicircular canal dehiscence syndrome. *Otol Neurotol.* (2018) 39:1153–62. doi: 10.1097/MAO.0000000000001910
72. Furman JM, Marcus DA, Balaban CD. Vestibular migraine: clinical aspects and pathophysiology. *Lancet Neurol.* (2013) 12:706–15. doi: 10.1016/S1474-4422(13)70107-8
73. Ho TW, Edvinsson L, Goadsby PJ. CGRP and its receptors provide new insights into migraine pathophysiology. *Nat Rev Neurol.* (2010) 6:573–82. doi: 10.1038/nrneurol.2010.127
74. Wackym PA. Ultrastructural organization of calcitonin gene-related peptide immunoreactive efferent axons and terminals in the rat vestibular periphery. *Am J Otol.* (1993) 14:41–50.
75. Xu D, Chen D, Zhu LN, Tan G, Wang HJ, Zhang Y, et al. Safety and tolerability of calcitonin-gene-related peptide binding monoclonal antibodies for the prevention of episodic migraine–a meta-analysis of randomized controlled trials. *Cephalalgia.* (2019) 39:1164–79. doi: 10.1177/0333102419829007
76. American Headache Society. The American Headache Society position statement on integrating new migraine treatments into clinical practice. *Headache.* (2019) 59:1–18. doi: 10.1111/head.13456
77. Wackym PA, Balaban CD, Mackay HT, Carter DM. Migraine headache and the migraine variants of hemiplegic migraine, ocular migraine and vestibular migraine in otic capsule dehiscence syndrome: outcomes after targeted repair. In: Barbara M and Filipo R, editors. *7th International Symposium on Menière's Disease and Inner Ear Disorders*. Amsterdam: Kugler Publications (2016). p. 77–86.
78. Schmahmann JD. Disorders of the cerebellum: ataxia, dysmetria of thought, and the cerebellar cognitive affective syndrome. *J Neuropsychiatry Clin Neurosci.* (2004) 16:367–78. doi: 10.1176/jnp.16.3.367
79. Hoche F, Guell X, Vangel MG, Sherman JC, Schmahmann JD. The cerebellar cognitive affective/Schmahmann syndrome scale. *Brain.* (2018) 141:248–70. doi: 10.1093/brain/awx317
80. Schmahmann JD. The cerebellum and cognition. *Neurosci Lett.* (2019) 688:62–75. doi: 10.1016/j.neulet.2018.07.005
81. Yoder RM, Taube JS. The vestibular contribution to the head direction signal and navigation. *Front Integr Neurosci.* (2014) 8:32. doi: 10.3389/fnint.2014.00032
82. Kamil RJ, Jacob A, Ratnanather JT, Resnick SM, Agrawal Y. Vestibular function and hippocampal volume in the Baltimore Longitudinal Study of Aging (BLSA). *Otol Neurotol.* (2018) 39:765–71. doi: 10.1097/MAO.0000000000001838
83. Ravishankar N, Demakis GJ. The neuropsychology of migraine. *Dis Mon.* (2007) 53:156–61. doi: 10.1016/j.disamonth.2007.04.006

Conflict of Interest: The authors declare that the research was conducted in the absence of any commercial or financial relationships that could be construed as a potential conflict of interest.

frontiers in Neurology

ORIGINAL RESEARCH
published: 28 May 2020
doi: 10.3389/fneur.2020.00379

Ambient Pressure Tympanometry Wave Patterns in Patients With Superior Semicircular Canal Dehiscence

Anthony Thai[1†], *Zahra N. Sayyid*[1†], *Davood K. Hosseini*[1], *Austin Swanson*[1], *Yifei Ma*[1], *Ksenia A. Aaron*[1] *and Yona Vaisbuch*[1,2*]

[1] *Department of Otolaryngology- Head and Neck Surgery, Stanford University School of Medicine, Stanford, CA, United States,* [2] *Otolaryngology Head and Neck Department, Rambam Medical Center, Haifa, Israel*

Importance: Superior semicircular canal dehiscence (SSCD) is a treatable condition, but current diagnostic modalities have numerous limitations. Clinicians would benefit from an additional tool for diagnostic workup that is both rapid and widely available.

Objective: To assess the utility of ambient pressure tympanometry (APT) in the diagnostic workup of SSCD by determining the sensitivity and specificity of APT for SSCD in comparison to other diagnostic modalities.

Design: Retrospective cohort study of patients who underwent APT and temporal bone computerized tomography (CT) scans from May 2017 to July 2018.

Setting: Tertiary referral center.

Participants: APT was performed as part of routine audiological testing on adult patients. We retrospectively analyzed all patients who received both APT and temporal bone CT scans, and divided ears into SSCD and non-SSCD groups based on the presence or absence of radiographic SSCD. Ears with other radiographic findings that could affect tympanic membrane compliance were excluded.

Exposures: All patients in this study underwent APT and temporal bone CT scans. Some patients also underwent pure tone audiometry and vestibular evoked myogenic potentials (VEMPs).

Main Outcomes and Measures: The primary outcome measures were sensitivity, specificity, and risk ratio of APT for SSCD. Secondary outcome measures include sensitivity of VEMPs and supranormal hearing thresholds.

Results: We describe 52 patients (70 ears) who underwent APT and CT imaging (mean age 47.1 years, 67.1% female). APT detected SSCD with 66.7% sensitivity and 72.1% specificity. In symptomatic patients, sensitivity was 71.4% and specificity was 75%. VEMPs performed best at detecting SSCD when defining a positive test as oVEMP amplitude >17 μV, with a sensitivity of 68.2%, similar to APT ($p > 0.99$). The combination of APT and VEMPs increased sensitivity to 88.9%, better than APT alone ($p = 0.031$) and trending toward better than VEMPs alone ($p = 0.063$).

OPEN ACCESS

Edited by:
Carey David Balaban, University of Pittsburgh, United States

Reviewed by:
Andrea Castellucci, Santa Maria Nuova Hospital, Italy
Cuneyt M. Alper, University of Pittsburgh, United States

****Correspondence:***
Yona Vaisbuch
yona@stanford.edu

[†] *These authors have contributed equally to this work*

Specialty section:
This article was submitted to Neuro-Otology, a section of the journal Frontiers in Neurology

Received: *19 January 2020*
Accepted: *15 April 2020*
Published: *28 May 2020*

Citation:
Thai A, Sayyid ZN, Hosseini DK, Swanson A, Ma Y, Aaron KA and Vaisbuch Y (2020) Ambient Pressure Tympanometry Wave Patterns in Patients With Superior Semicircular Canal Dehiscence. Front. Neurol. 11:379. doi: 10.3389/fneur.2020.00379

Conclusions and Relevance: Rhythmic wave patterns on APT are associated with SSCD and may raise suspicion for this condition in conjunction with consistent results on other diagnostic modalities. Although clinical utility requires confirmation in a larger prospective study, APT is a simple, rapid, and widely available tool warranting further study.

Keywords: ambient pressure tympanometry, superior semicircular canal dehiscence, vertigo, pulsatile tinnitus, autophony, hearing loss, temporal bone CT scan, vestibular evoked myogenic potentials

INTRODUCTION

Superior semicircular canal dehiscence (SSCD) was first described by Minor et al. in 1998 (1). Microscopic SSCD is found in 0.5% of temporal bone specimens (2) and 2–9% of temporal bone computed tomography (CT) scans depending on imaging technique (3–7). Due to a third mobile window effect, patients can present with vestibular and auditory symptoms, including autophony, aural fullness, sound-induced vertigo, pulsatile tinnitus, and hearing loss (1, 8–10). Surgical intervention provides partial or complete symptom resolution in up to 70% of patients (11–15). However, diagnosis is complicated by the variable presentation of SSCD, which may resemble otosclerosis and Meniere's disease (16, 17). Currently, CT imaging is required for diagnosis, but is not always feasible for initial workup due to cost, radiation exposure and limited access in some healthcare settings. Instead, the initial diagnostic algorithm in symptomatic patients involves vestibular examination and audiometry followed by vestibular evoked myogenic potentials (VEMPs) for diagnostic confirmation.

This initial workup has numerous limitations. In particular, it remains controversial which thresholds should be employed during audiologic and vestibular testing. On audiometry, SSCD patients may display low frequency air-bone gaps and supranormal bone conduction thresholds (SNT) above 0 dB (9, 18, 19). On VEMP testing, clinicians rely on abnormally low thresholds or high amplitudes, but precise cut-off values for either parameter remain uncertain (10). A recent study suggested that an ocular VEMP amplitude cutoff of 17 μV displays 100% sensitivity and specificity; although promising, these data have yet to be validated in other studies (20). Moreover, there are discrepancies between self-reported symptoms and imaging findings, poor correlation between vestibular testing and audiometry thresholds, and high false positive rates on CT imaging when compared to cadaveric studies (3–5, 21, 22).

Ambient pressure tympanometry (APT) uses a microphone to record changes in sound intensity in the external ear canal during introduction of a tone. Unlike standard tympanometry, the recording occurs over 15–20 s without alterations in external pressure. This allows for measurement of changes in external ear canal volume over time and indirect detection of tympanic membrane (TM) movement. A positive APT test consists of regular oscillations reflecting repeated TM fluctuations. Clinically, APT is solely employed in the workup of Patulous Eustachian Tube (PET); respiration-synchronous compliance changes have been reported in up to 75% of these patients (23–25). Compliance changes on APT have also been associated in small case series with glomus tumor, myoclonus, jugular bulb dehiscence, carotid artery dehiscence, and SSCD (26–30). Here, we present the first systematic analysis of the association between rhythmic APT wave patterns and SSCD, motivating further study of the utility of APT in the diagnostic workup of SSCD.

Abbreviations: SSCD, superior semicircular canal dehiscence; APT, ambient pressure tympanometry; CT, computerized tomography; cVEMP, cervical vestibular evoked myogenic potential; dB, decibel; oVEMP, ocular vestibular evoked myogenic potential; PCHL, pseudo-conductive hearing loss; PE, pressure equalization; PET, patulous Eustachian tube; ROC, receiver operating characteristic; TM, tympanic membrane; VEMP, vestibular evoked myogenic potential.

MATERIALS AND METHODS

Patients

This study was approved by the Institutional Review Board (IRB-43715). From May 2017 to July 2018, APT was incorporated into routine audiologic testing, and was performed when possible on patients without specific indications or contraindications. Ears with sub-millimeter resolution temporal bone CT imaging were analyzed and divided into SSCD and non-SSCD groups based on the presence or absence of radiographic SSCD as determined by blinded imaging review by a neurotologist. Temporal bone CT scans consisted of images in the coronal, Stenvers view and Poschl views, all with slice thickness of 0.4 mm and maximum collimation of 0.625 mm. Some ears underwent APT twice during our study period. In cases where two tests showed one positive and one negative finding, we analyzed the test displaying rhythmic waves.

Exclusion Criteria

We excluded patients with otologic diagnoses other than SSCD that might generate TM movement, including tegmen dehiscence, encephalocele, cholesteatoma, glomus tumors, jugular bulb dehiscence, sigmoid sinus diverticulum or dehiscence, aberrant carotid artery, carotid artery dehiscence, persistent stapedial artery, posterior semicircular canal dehiscence, middle ear myoclonus, and PET. Similarly, we also excluded patients with otologic conditions that might impair TM compliance, including otosclerosis, middle ear effusion, ossicular chain discontinuity, Meniere's disease, TM perforation and presence of pressure equalization tubes.

TABLE 1 | Diagnostic test characteristics.

	SSCD Group			Symptomatic SSCD		
	Sensitivity (*N*)	**Specificity (*N*)**	**Relative risk, 95% CI, *p*-value**	**Sensitivity (*N*)**	**Specificity (*N*)**	**Relative risk, 95% CI, *p*-value**
APT	66.7% (27)	72.1% (43)	2.67, 1.540 to 5.08, $p = 0.003$	71.4% (21)	75% (12)	2.08, 1.08 to 4.00, $p = 0.028$
cVEMP, thresh < 85 dB (500 Hz)	55.0% (20)	–	–	52.9% (17)	–	–
oVEMP, thresh < 85 dB (500 Hz)	50.0% (20)	–	–	52.9% (17)	–	–
oVEMP amp > 17 μV (500 Hz)	68.2% (22)	–	–	77.8% (18)	–	–
oVEMP, amp > 0 μV (4 kHz)	42.9% (14)	–	–	46.2% (13)	–	–
SNT	50.0% (22)	85.7% (42)	2.77, 1.48 to 5.17, $p = 0.001$,	62.5% (16)	91.7% (12)	2.58, 1.32 to 5.03, $p = 0.006$
APT or, oVEMP amp > 17 μV (500 Hz)	88.9% (27)	–	–	94.4% (18)	–	–

N, total number; SSCD, superior semicircular canal dehiscence; APT, ambient pressure tympanometry; VEMP, vestibular evoked myogenic potential; oVEMP, ocular VEMP; cVEMP, cervical VEMP; amp, amplitude; thresh, threshold; SNT, supranormal threshold; CI, confidence interval.

Audiological Testing

All audiologic measurements were performed by trained audiologists in double-wall audiometric sound booths. APT was completed using Interacoustics Titan (Interacoustics, Audiometer Allé DK 5500 Middelfart) impedance devices controlled using the Titan Suite software v3.4. The software protocol used a 226 Hz probe tone presented at 85 dB to record ipsilaterally for 20 seconds with the instrument's air pump deactivated. The patient remained upright, seated, and quiet throughout the procedure. Hearing evaluations were completed using conventional audiologic procedures. The minimum battery included pure tone air and bone conduction audiometry, speech reception thresholds, and word recognition. Standard tympanometry and ipsilateral acoustic reflex testing were also completed.

VEMP testing was completed using an Intelligent Hearing Systems Smart USB (Intelligent Hearing Systems, 6860 SW 81st Street. Miami, FL 33143. USA) evoked potential system. Cervical (cVEMP) and ocular (oVEMP) VEMP threshold search procedures were completed for each ear. Air conduction 500 Hz tone bursts were used as stimuli. Ipsilateral cVEMP results were obtained with the patient reclined to 30 degrees above horizontal, with the head rotated 45 degrees from the test ear, and held above the exam **Table 1** throughout each run. Contralateral oVEMP recordings were obtained with the patient seated upright with gaze 30 degrees above horizontal. Initial stimulus intensity was 105 dB presented via insert earphones and decreased in 10 dB steps until threshold was obtained. The stimulus rise, plateau and fall were 2, 1, and 2 ms, respectively. The highest intensity inter-amplitude was used for symmetry calculation.

Evaluation of APT Waves

Two authors performed independent, blinded review of APT waves and categorized them as rhythmic or noise. Rhythmic waves consisted of regularly spaced peaks with a frequency of 50–100 peaks per minute, consistent with physiologic heart rate. Noise consisted of fluctuations with no discernible peaks, inconsistently spaced peaks, or a frequency outside of 50–100 peaks per minute. In cases of inconsistent classification of APT tracings between reviewers, the authors came to an agreement following discussion while still blinded to patient diagnosis. For each ear, amplitude and frequency were calculated using a novel algorithm created in RStudio (v1.1.463, RStudio, Inc., Boston, MA, USA). We defined the wave amplitude for each ear as the average height of the waveforms (measured from peak to trough) present throughout the 20 s recording. To account for noise, all heights greater than two standard deviations away from the mean amplitude were discarded as outliers. Frequency was determined by quantifying the number of measured peaks per minute.

Evaluation of Symptoms and Vestibular and Audiometric Tests

Ears were analyzed regarding presence of SNT on audiometry, abnormal VEMPs, and SSCD symptoms. Patients were considered symptomatic if they reported at least one of the following symptoms: pulsatile tinnitus, autophony, ear fullness, sound-induced vertigo. SNT was defined as a bone conduction threshold better than 0 decibels (dB) on pure tone audiometry. Based on previous literature (20) and guidelines at our institution, several definitions were employed for positive VEMP findings: cVEMP threshold at 500 Hz below 85 dB, oVEMP threshold at 500 Hz below 85 dB, oVEMP amplitude at

500 Hz greater than 17 μV, or oVEMP amplitude at 4 kHz greater than 0 μV. Sensitivity for radiographic SSCD was calculated for each of these cutoffs.

Statistical Analysis

The chi-square test was used for inter-group comparison of patient sex. Student's *t*-test was used for inter-group comparison of patient age as well as frequency and amplitude on APT tracings. To examine associations between diagnostic tools and CT results, relative risk and 95% confidence interval were estimated by employing a Poisson regression model with robust sandwich variance estimator that corrects for potentially overestimated standard error (31). Sensitivity and specificity were calculated based on 2 x 2 frequency tables of diagnostic tools and CT results. The McNemar chi-square test was used to compare sensitivity and specificity values between diagnostic tools (32). All analyses were performed using SAS software version 9.4 (SAS Institute, Cary, NC).

RESULTS

Patients

A total of 469 patients (780 ears) underwent APT testing. From this sample, 89 patients (168 ears) underwent temporal bone CT imaging. 98 ears were excluded due to the following diagnoses: tegmen dehiscence (23), otosclerosis (16), middle ear effusion (11), sigmoid dehiscence (9), glomus tumor (6), cholesteatoma (6), myoclonus (4), TM perforation (4), carotid artery dehiscence (4), PE tube placement (4), jugular bulb dehiscence (3), encephalocele (2), and one each of ossicular chain discontinuity, Eustachian tube dysfunction, Meniere's disease, posterior semicircular canal dehiscence, sigmoid diverticulum, and aberrant carotid artery. The study cohort included 52 patients (70 ears) with mean age 47.1 ± 16.7 years and consisting of 47 ears from female patients (67.1%). Based on radiographic findings, ears were divided into SSCD (27 ears) and non-SSCD groups (43 ears). These groups were similar in sex (non-SSCD: 65.1% female, SSCD: 70.4% female, $p = .649$) and age (non-SSCD: 46.7 ± 17.2 years, SSCD: 47.9 ± 16.3 years, $p = 0.777$).

Four ears in each group underwent APT twice during the study period. In the SSCD group, 3 of these 4 ears had inconsistent results between tests (one rhythmic wave and one with noise), compared to 1 of 4 ears in the non-SSCD group.

APT Outcomes

Examples of rhythmic waves and noise are displayed in **Figure 1**. In detecting radiographic SSCD, rhythmic APT waves displayed 66.7% sensitivity (27 SSCD ears) and 72.1% specificity (43 non-SSCD ears) (**Table 1**). The relative risk of radiographic SSCD in ears with rhythmic waves compared to noise was 2.67 ($p = 0.003$). The average amplitude in the SSCD group (0.03 mL) was significantly greater than that of the non-SSCD group (0.015 mL, $p = 0.01$). In symptomatic ears, rhythmic APT waves displayed 71.4% sensitivity (21 SSCD ears) and 75% specificity (12 non-SSCD ears, relative risk 2.08).

In this study, we excluded 16 SSCD ears with comorbid otologic pathologies that may cause TM oscillations. The most common comorbidity was tegmen dehiscence (10 ears, 23.3% of SSCD ears). The sensitivity of APT in these 16 SSCD ears with additional pathology was 50%.

Comparison of APT Results to Other SSCD Screening Tools

In this study cohort, 81.5% of SSCD ears and 23.3% of non-SSCD ears underwent VEMP testing. Due to the small sample of non-SSCD ears undergoing VEMP testing, we do not report the specificity of VEMPs in this study. With regards to sensitivity, several definitions of positive VEMP findings were employed. Of these definitions, oVEMP amplitude > 17 μV at 500 Hz had the highest sensitivity for radiographic SSCD (68.2%), performing similarly to APT ($p > 0.99$). APT also performed similarly to SNT with regards to sensitivity ($p = 0.125$) and specificity ($p = 0.30$). Importantly, the presence of either a positive APT finding or an oVEMP amplitude > 17 μV displayed 88.9% sensitivity, better than APT alone ($p = 0.031$) and trending toward better than oVEMP amplitude > 17 μV alone ($p = 0.063$). However, only 40.9% of ears with radiographic SSCD displayed both rhythmic APT waves and oVEMP amplitude > 17 μV.

In symptomatic patients, oVEMP amplitude > 17 μV displayed 77.8% sensitivity for radiographic SSCD, performing similarly to APT ($p = 0.727$). APT performed similarly to SNT in this subgroup ($p = 0.375$). The presence of either oVEMP amplitude > 17 μV or a rhythmic APT wave displayed 95% sensitivity for radiographic SSCD, higher than VEMPs alone ($p = 0.025$) and trending toward higher than APT alone ($p = 0.063$). 50% of symptomatic SSCD patients displayed both rhythmic APT waves and oVEMP amplitude > 17 μV.

DISCUSSION

Although SSCD is treatable, its diagnosis presents a clinical challenge. CT scans are required for SSCD diagnosis but are time-consuming, not universally available, and associated with a risk of radiation exposure (33). We introduce APT as a simple, rapid and widely available tool that may display rhythmic waves in SSCD patients. To test this association, we rely on CT imaging for confirmation of SSCD diagnosis, as most patients in our cohort lack surgical confirmation. Our initial data suggest an association between rhythmic APT waves and SSCD, particularly in symptomatic patients. Pending validation in a larger prospective study, APT may be a useful addition to the workup of SSCD in conjunction with current diagnostic tools.

The 43 SSCD ears in this study (27 ears with SSCD only and 16 SSCD ears with comorbid pathology) were briefly described in a case series, which did not include a control group or associated data on symptoms, audiometry and vestibular testing (30). To our knowledge, these two studies are the only systematic studies in the English literature that evaluate APT in the workup of conditions other than PET.

APT passively records external ear canal volume over time in resting patients, a proxy for TM movement. In healthy ears, the TM should not move appreciably over this timescale. However, dehiscence of the bony layer overlying the superior canal may

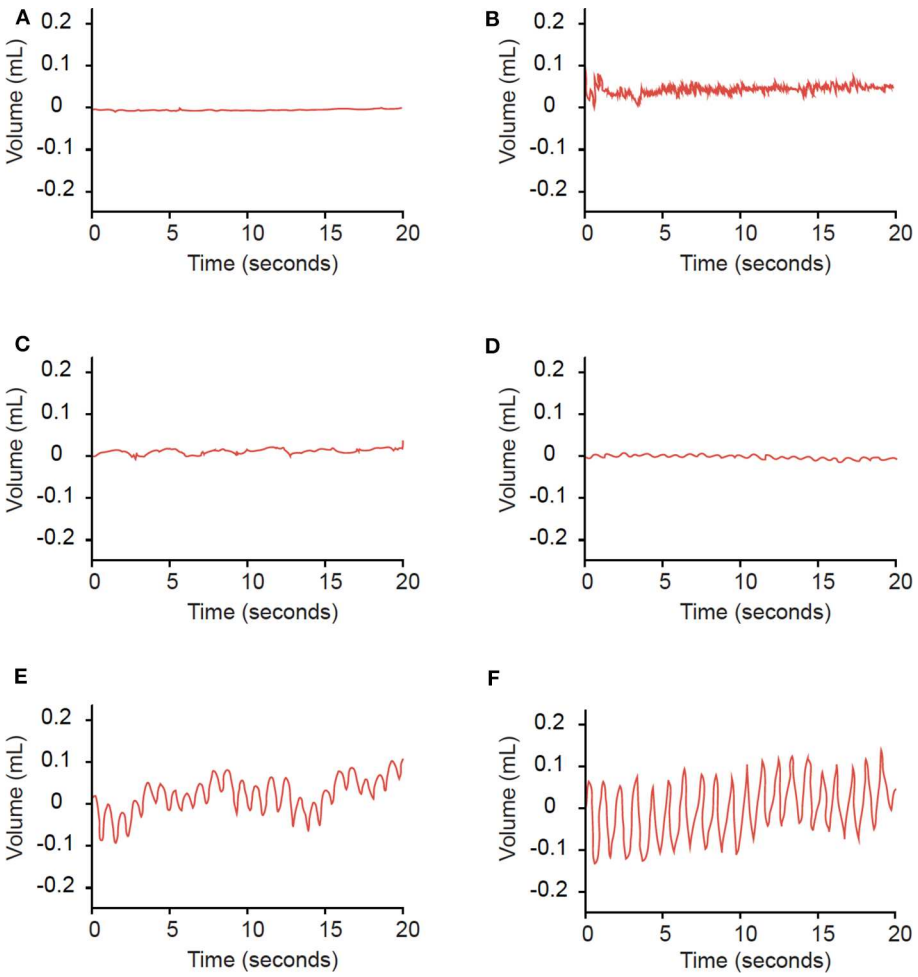

FIGURE 1 | Examples of findings on APT. Findings of a horizontal line **(A)**, no regularly spaced peaks **(B)**, or frequencies outside of 50–100 peaks/minute **(C)** were categorized as noise. Waves with consistently-spaced peaks and frequencies of 50−100 peaks/minute **(D–F)** were categorized as rhythmic waves.

allow transmission of sound pressure from cerebral vessels through this open window (28). These oscillations may propagate sequentially through inner ear fluids, the oval window, the ossicular chain, and the TM (**Figure 2**). Due to this hypothesis, we excluded ears with conditions that might affect TM movement from both SSCD and non-SSCD groups.

APT Outcomes

In this study, APT detected radiographic SSCD with 66.7% sensitivity and 72.1% specificity (**Table 1**). In symptomatic patients, APT displayed sensitivity of 71.4% and specificity of 75%. SSCD workup would only be performed in these symptomatic patients, as no indication currently exists for treatment of asymptomatic SSCD. However, the small size of our cohort should prompt cautious interpretation. Moreover, in SSCD ears with additional pathology, the sensitivity of APT decreases to 50%. Pressure waves from multiple sources may interact and cause noisy TM fluctuation, limiting APT's utility in these patients.

For ears with contradictory results between two APT tests, we analyzed the test with the rhythmic wave, and applied this standard to SSCD and non-SSCD groups. Noise on APT suggests lack of pathology or high levels of noise obscuring existing pathology, while rhythmic waves indicate presence of a source for TM fluctuation. We hypothesize that SSCD ears display rhythmic waves on some but not all APT tests due to technical challenges that decrease the signal to noise ratio, including improper seal formation with the APT probe or excessive patient breathing or movement. In contrast, healthy ears should not occasionally produce rhythmic APT waves. Therefore, for ears with contradictory APT findings, we speculate that noise arises from technical issues and select rhythmic waves for analysis. The equal application of this standard to both groups may lead to increased sensitivity and decreased specificity. To limit noise, we recommend ensuring proper seal formation, instructing patients to limit heavy breathing and movements, and performing APT for longer periods to better detect existing pathology.

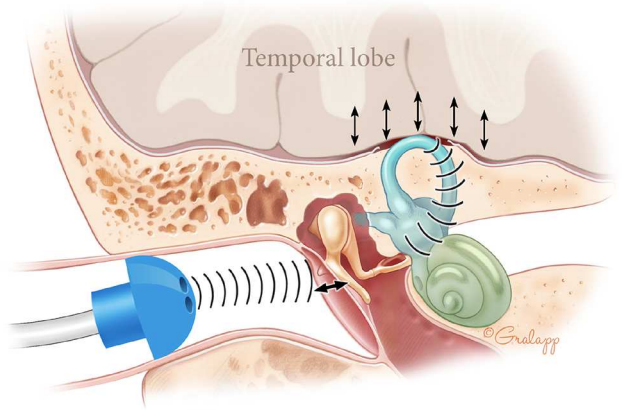

FIGURE 2 | Theory for presence of APT waves in SSCD patients. In SSCD, the brain pounds rhythmically on the dehiscent superior canal. These oscillations propagate sequentially through inner ear fluids, the oval window, and the ossicular chain. This generates rhythmic TM oscillation that may be detected as rhythmic waves on APT.

Aside from these technical challenges, we propose several reasons for the lack of rhythmic waves in some SSCD ears. CT scans may have a high false positive rate for SSCD (4, 5, 22). Therefore, patients in our SSCD group with negative APT findings may have intact but thin superior semicircular canals that appear radiographically dehiscent. In fact, patients with near-dehiscent superior canals can display SSCD symptoms, but may not have APT findings due to an intact barrier preventing transmission of sound pressure (34). Alternatively, small areas of dehiscence may not transmit waves of sufficient amplitude for detection, a hypothesis that cannot be confirmed due to the difficulty of measuring dehiscence area on CT imaging. Moreover, additional pathologies other than those in our exclusion criteria may limit TM mobility.

In addition, several factors may contribute to the presence of rhythmic waves in non-SSCD ears. Most importantly, wave patterns were categorized blindly but subjectively as rhythmic or noise. We may have employed a low threshold for categorizing a wave as rhythmic, leading to overestimation of sensitivity and underestimation of specificity. To address this problem, we have developed a preliminary algorithm to filter out baseline noise and more objectively identify rhythmic waves. This algorithm will need to be validate in a large, prospective sample, which is the focus of a future study. Secondly, APT may constitute an overly sensitive test and detect low amplitude oscillations in healthy ears. Consistent with this reasoning, the wave amplitude in the SSCD group (0.03 mL) was significantly larger than that in the non-SSCD group (0.015 mL, $p = 0.001$). Setting an amplitude threshold for a positive APT test may reduce the false positive rate but would decrease sensitivity. Lastly, other pathologies not considered in our exclusion criteria may cause TM fluctuation in our non-SSCD cohort.

Comparison of APT Results to Other SSCD Screening Tools

In our patient cohort, defining a positive VEMP as oVEMP > 17 μV yielded the highest sensitivity (68.2%), performing similarly to APT (**Table 1**, $p > 0.99$). A previous study described higher VEMPs sensitivity for radiographic SSCD (91%) than reported in our study. This study defined a positive VEMP result as any VEMP threshold < 65 dB at 250, 500, or 1000 Hz (6). Our study evaluated VEMPs performed at 500 Hz; these different frequencies may partially account for the discrepant sensitivities. Another study of 29 patients with surgically confirmed SSCD determined that oVEMP amplitude > 17 μV at 500 Hz displayed a sensitivity of 100%, compared to 68.2% in our study (20). However, the above study performed analysis by patient, while our study analyzed SSCD by ear. SSCD patients undergoing surgery also likely displayed symptoms. When analyzing our symptomatic cohort by patient, sensitivity increased to 84.6% (13 patients). The small sample size and lack of surgical confirmation in our study may account for the remaining gap in sensitivity.

In detecting radiographic SSCD, APT performed similarly to SNT in sensitivity ($p = 0.125$) and specificity ($p = 0.302$). Moreover, APT increases sensitivity and specificity when combined with other SSCD screening tools. The presence of rhythmic APT waves or oVEMP amplitude > 17 μV displayed better sensitivity than APT alone ($p = 0.031$) and trended toward better sensitivity than oVEMP alone ($p = 0.063$). A subgroup of symptomatic patients displayed similar results (**Table 1**). Pending validation of these data, APT testing of symptomatic patients in resource-poor settings may inform whether patients should be recommended for CT imaging.

Limitations

This is a small, single-center retrospective study without routine or randomized CT imaging. While APT was performed routinely, CT imaging was likely performed more frequently in patients with symptoms and/or test results raising suspicion for otologic pathology. With randomized imaging, fewer patients in each group might have symptoms, abnormal VEMPs, or SNT. Therefore, our study may have overestimated sensitivity and underestimated specificity, with an unclear bias on relative risk. In contrast, CT imaging may have high false positive rates for detecting radiographic SSCD (4, 5, 22), which may falsely increase sensitivity and reduce specificity. A prospective study is required to address selection bias and surgical confirmation is needed to correct for false positive rates of CT imaging.

APT is a simple, rapid, and widely available test. Preliminary results suggest that characteristic APT wave patterns may raise suspicion for SSCD in symptomatic patients, in conjunction with consistent results on other diagnostic modalities. These data motivate a prospective study to evaluate the utility of APT in the diagnostic workup of SSCD.

DATA AVAILABILITY STATEMENT

The datasets generated for this study are available on request to the corresponding author.

ETHICS STATEMENT

The studies involving human participants were reviewed and approved by Stanford University Institutional Review Board (IRB-43715). Written informed consent for participation was not required for this study in accordance with the national legislation and the institutional requirements.

AUTHOR CONTRIBUTIONS

AT and ZS conducted data acquisition, analysis, and interpretation, and made significant contributions to the writing and editing of the manuscript. They are designated co-first authors for this study. DH was involved in project conception, manuscript editing and creation of figures. AS contributed to data acquisition, data analysis and manuscript review. YM played a significant role in the statistical analysis of the data and manuscript review. KA was involved in data interpretation and manuscript review. YV led the conception of the study, and made significant contributions to data interpretation and manuscript review.

ACKNOWLEDGMENTS

We thank Chris Gralapp MA, CMI, FAMI and Robert K. Jackler MD for producing the illustration in **Figure 2**.

REFERENCES

1. Minor LB, Solomon D, Zinreich JS, Zee DS. Sound- and/or pressure-induced vertigo due to bone dehiscence of the superior semicircular canal. *Arch Otolaryngol Head Neck Surg.* (1998) 124:249–58. doi: 10.1001/archotol.124.3.249
2. Carey JP, Minor LB, Nager GT. Dehiscence or thinning of bone overlying the superior semicircular canal in a temporal bone survey. *Arch Otolaryngol Head Neck Surg.* (2000) 126:137–47. doi: 10.1001/archotol.126.2.137
3. Masaki Y. The prevalence of superior canal dehiscence syndrome as assessed by temporal bone computed tomography imaging. *Acta Otolaryngol.* (2011) 131:258–62. doi: 10.3109/00016489.2010.526145
4. Sequeira SM, Whiting BR, Shimony JS, Vo KD, Hullar TE. Accuracy of computed tomography detection of superior canal dehiscence. *Otol Neurotol.* (2011) 32:1500–5. doi: 10.1097/MAO.0b013e318238280c
5. Tavassolie TS, Penninger RT, Zuñiga MG, Minor LB, Carey JP. Multislice computed tomography in the diagnosis of superior canal dehiscence: how much error, and how to minimize it? *Otol Neurotol.* (2012) 33:215–22. doi: 10.1097/MAO.0b013e318241c23b
6. Cloutier J-F, Bélair M, Saliba I. Superior semicircular canal dehiscence: positive predictive value of high-resolution cT scanning. *Eur Arch Otorhinolaryngol.* (2008) 265:1455–60. doi: 10.1007/s00405-008-0672-2
7. Williamson RA, Vrabec JT, Coker NJ, Sandlin M. Coronal computed tomography prevalence of superior semicircular canal dehiscence. *Otolaryngol Head Neck Surg.* (2003) 129:481–9. doi: 10.1016/S0194-5998(03)01391-3
8. Minor LB. Superior canal dehiscence syndrome. *Am J Otol.* (2000) 21:9–19. doi: 10.1016/S0196-0709(00)80068-X
9. Merchant SN, Rosowski JJ. Conductive hearing loss caused by third-window lesions of the inner ear. *Otol Neurotol.* (2008) 29:282–9. doi: 10.1097/MAO.0b013e318161ab24
10. Zhou G, Gopen Q, Poe DS. Clinical and diagnostic characterization of canal dehiscence syndrome: a great otologic mimicker. *Otol Neurotol.* (2007) 28:920–6. doi: 10.1097/MAO.0b013e31814b25f2
11. Minor LB. Clinical manifestations of superior semicircular canal dehiscence. *Laryngoscope.* (2005) 115:1717–27. doi: 10.1097/01.mlg.0000178324.55729.b7
12. Ma X-B, Zeng R, Wang G-P, Gong S-S. Transmastoid approach for resurfacing the superior semicircular canal dehiscence with a dumpling structure. *Chin Med J.* (2015) 128:1490–5. doi: 10.4103/0366-6999.157657
13. Rodgers B, Lin J, Staecker H. Transmastoid resurfacing versus middle fossa plugging for repair of superior canal dehiscence: comparison of techniques from a retrospective cohort. *World J Otorhinolaryngol Head Neck Surg.* (2016) 2:161–7. doi: 10.1016/j.wjorl.2016.11.001
14. Succar EF, Manickam PV, Wing S, Walter J, Greene JS, Azeredo WJ. Round window plugging in the treatment of superior semicircular canal dehiscence. *Laryngoscope.* (2018) 128:1445–52. doi: 10.1002/lary.26899
15. Al Afif A, Farmer R, Bance M. Outcomes of transmastoid resurfacing for superior canal dehiscence using a cartilage overlay technique. *Laryngoscope.* (2019) 129:2164–9. doi: 10.1002/lary.27789
16. Merchant SN, Rosowski JJ, McKenna MJ. Superior semicircular canal dehiscence mimicking otosclerotic hearing loss. *Adv Otorhinolaryngol.* (2007) 65:137–45. doi: 10.1159/000098790
17. Brantberg K, Ishiyama A, Baloh RW. Drop attacks secondary to superior canal dehiscence syndrome. *Neurology.* (2005) 64:2126–8. doi: 10.1212/01.WNL.0000165953.48914.B0
18. Brantberg K, Verrecchia L, Westin M. Enhanced auditory sensitivity to body vibrations in superior canal dehiscence syndrome. *Audiol Neurootol.* (2016) 21:365–71. doi: 10.1159/000450936
19. Schmuziger N, Allum J, Buitrago-Téllez C, Probst R. Incapacitating hypersensitivity to one's own body sounds due to a dehiscence of bone overlying the superior semicircular canal. A case report. *Eur Arch Otorhinolaryngol.* (2006) 263:69–74. doi: 10.1007/s00405-005-0939-9
20. Zuniga MG, Janky KL, Nguyen KD, Welgampola MS, Carey JP. Ocular vs. cervical VEMPs in the diagnosis of superior semicircular canal dehiscence syndrome. *Otol Neurotol.* (2013) 34:121–6. doi: 10.1097/MAO.0b013e31827136b0c
21. Noij KS, Wong K, Duarte MJ, Masud S, Dewyer NA, Herrmann BS, et al. Audiometric and cVEMP thresholds show little correlation with symptoms in superior semicircular canal dehiscence syndrome. *Otol Neurotol.* (2018) 39:1153–62. doi: 10.1097/MAO.0000000000001910
22. Crovetto M, Whyte J, Rodriguez OM, Lecumberri I, Martinez C, Eléxpuru J. Anatomo-radiological study of the superior semicircular canal dehiscence radiological considerations of superior and posterior semicircular canals. *Eur J Radiol.* (2010) 76:167–72. doi: 10.1016/j.ejrad.2009.05.038
23. Kumazawa T. A tubotympanometer for evaluation of eustachian tube function. *Ann Otol Rhinol Laryngol.* (1985) 94:24–5. doi: 10.1177/00034894850945S216
24. Finkelstein Y, Talmi YP, Rubel Y, Zohar Y. An objective method for evaluation of the patulous eustachian tube by using the middle ear analyzer. *Arch Otolaryngol Head Neck Surg.* (1988) 114:1134–8. doi: 10.1001/archotol.1988.01860220068026
25. McGrath AP, Michaelides EM. Use of middle ear immittance testing in the evaluation of patulous eustachian tube. *J Am Acad Audiol.* (2011) 22:201–7. doi: 10.3766/jaaa.22.4.2
26. Levenson MJ, Parisier SC, Jacobs M, Edelstein DR. The large vestibular aqueduct syndrome in children. A review of 12 cases and the description of a new clinical entity. *Arch Otolaryngol Head Neck Surg.* (1989) 115:54–8. doi: 10.1001/archotol.1989.01860250056026
27. Yetiser S, Kazkayasi M, Civitci D. Acoustic impedance study of peritubal myoclonus. *Acta Otolaryngol.* (2002) 122:504–9. doi: 10.1080/00016480260092309
28. Hullar TE. Vascular pulsations on impedance audiometry as a sign of a third-mobile window lesion. *Otol Neurotol.* (2010) 31:565–6. doi: 10.1097/MAO.0b013e3181db7324
29. Castellucci A, Brandolini C, Piras G, Fernandez IJ, Giordano D, Pernice C, et al. Superior canal dehiscence with tegmen defect revealed by otoscopy: video clip demonstration of pulsatile tympanic membrane. *Auris Nasus Larynx.* (2018) 45:165–9. doi: 10.1016/j.anl.2016.11.013

30. Sayyid ZN, Thai A, Swanson A, Hosseini DK, Fitzgerald MB, Ma Y, et al. Rhythmic wave patterns on ambient pre11ssure tympanometry in patients with objective tinnitus-associated pathologies. *Otol Neurotol. December. (*2019).
31. Zou G. A modified poisson regression approach to prospective studies with binary data. *Am J Epidemiol.* (2004) 159:702–6. doi: 10.1093/aje/kwh090
32. Trajman A, Luiz RR. McNemar chi2 test revisited: comparing sensitivity and specificity of diagnostic examinations. *Scand J Clin Lab Invest.* (2008) 68:77–80. doi: 10.1080/00365510701666031
33. Zondervan RL, Hahn PF, Sadow CA, Liu B, Lee SI. Frequent body CT scanning of young adults: indications, outcomes, and risk for radiation-induced cancer. *J Am Coll Radiol.* (2011) 8:501–7. doi: 10.1016/j.jacr.2010.12.025
34. Ward BK, Wenzel A, Ritzl EK, Gutierrez-Hernandez S, Della Santina CC, Minor LB, et al. Near-dehiscence: clinical findings in patients with thin bone over the superior semicircular canal. *Otol Neurotol.* (2013) 34:1421–8. doi: 10.1097/MAO.0b013e318287efe6

Conflict of Interest: The authors declare that the research was conducted in the absence of any commercial or financial relationships that could be construed as a potential conflict of interest.

The reviewer CMA and handling editor declared their shared affiliation at the time of the review.

frontiers in Neurology

ORIGINAL RESEARCH
published: 11 June 2020
doi: 10.3389/fneur.2020.00484

Psychometric Tests and Spatial Navigation: Data From the Baltimore Longitudinal Study of Aging

Eric X. Wei[1]*, *Eric R. Anson*[2], *Susan M. Resnick*[3] and *Yuri Agrawal*[1]

[1] Department of Otolaryngology-Head and Neck Surgery, Johns Hopkins University School of Medicine, Baltimore, MD, United States, [2] Department of Otolaryngology, University of Rochester Medical Center School of Medicine and Dentistry, Rochester, NY, United States, [3] Laboratory of Behavioral Neuroscience, National Institute on Aging, Baltimore, MD, United States

Spatial cognition is the process by which individuals interact with their spatial environment. Spatial cognition encompasses the specific skills of spatial memory, spatial orientation, and spatial navigation. Prior studies have shown an association between psychometric tests of spatial ability and self-reported or virtual measures of spatial navigation. In this study, we examined whether psychometric spatial cognitive tests predict performance on a dynamic spatial navigation task that involves movement through an environment. We recruited 151 community-dwelling adult participants [mean (*SD*) age 69.7 (13.6), range 24.6–93.2] from the Baltimore Longitudinal Study of Aging (BLSA). Spatial navigation ability was assessed using the triangle completion task (TCT), and two quantities, the angle and distance of deviation, were computed. Visuospatial cognitive ability was assessed primarily using the Card Rotations Test. Additional tests of executive function, memory, and attention were also administered. In multiple linear regression analyses adjusting for age, sex, race, and education, cognitive tests of visuospatial ability, executive function, and perceptual motor speed and integration were significantly associated with spatial navigation, as determined by performance on the TCT. These findings suggest that dynamic spatial navigation ability is related to spatial memory, executive function, and motor processing speed.

Keywords: spatial cognition, visuospatial ability, triangle completion task, spatial navigation, aging

OPEN ACCESS

Edited by:
Toshihisa Murofushi, Teikyo University, Japan

Reviewed by:
Rachael L. Taylor, The University of Auckland, New Zealand
Arata Horii, Niigata University, Japan

***Correspondence:**
Eric X. Wei
eric.wei@jhmi.edu

Specialty section:
This article was submitted to Neuro-Otology, a section of the journal Frontiers in Neurology

Received: *20 January 2020*
Accepted: *04 May 2020*
Published: *11 June 2020*

Citation:
Wei EX, Anson ER, Resnick SM and Agrawal Y (2020) Psychometric Tests and Spatial Navigation: Data From the Baltimore Longitudinal Study of Aging. Front. Neurol. 11:484. doi: 10.3389/fneur.2020.00484

INTRODUCTION

Spatial cognition is the domain of cognitive function that relates to the processing of information about one's spatial environment. Spatial cognition encompasses the specific skills of spatial orientation (including mental rotation), spatial memory, and spatial navigation. Numerous studies have documented declines in spatial cognition associated with age (1–3), and studies suggest that spatial cognition is among the earliest domains of cognitive function to show impairment during the transition from normal cognitive aging to Alzheimer's disease (4). Impaired spatial cognition has been linked to functional limitations and adverse outcomes in older adults, including driving difficulty, losing, or misplacing objects, difficulty navigating new environments, and falls (5–11).

Static psychometric measures of spatial orientation (and mental rotation), such as the Card Rotations Test, are sometimes used as a proxy in clinical and research settings for assessing spatial cognitive abilities (12, 13). However, it is unclear how these stationary tests of spatial

memory and orientation relate to dynamic spatial cognitive abilities and moreover, whether or not these tests can predict spatial navigation abilities at the scale of environments in which humans interact and move through. In particular, path integration is a critical spatial navigational strategy employed by humans whereby individuals use self-motion cues (e.g., vestibular sensory input and proprioceptive feedback) to maintain a sense of position and orientation. Although it has been shown that psychometric tests of spatial ability are predictive of performance on a virtual maze task (12), it is unclear whether these paper and pencil-based tests are able to predict performance on path integration tasks that require actual movement through space.

In this study, we used data from the Baltimore Longitudinal Study of Aging (BLSA) to assess the cross-sectional association between static psychometric tests that tap into spatial memory and orientation, and spatial navigation as determined by performance on the Triangle Completion Task (TCT). Individual differences in spatial navigational abilities, mediated by a combination of genetic, and environmental influences, are known to be particularly prominent at later stages of life (14), which supports the use of an aging cohort sensitive to variations in individual navigational abilities. The TCT is a dynamic test of spatial navigation that requires participants to create and retain a spatial map of their traveled path using self-motion cues, a process known as path integration (15–18). We hypothesized that visuospatial ability as measured by the Card Rotations Test would be associated with path integration as measured by performance on the TCT. We also examined the relationship between other domains of cognitive function, specifically verbal and non-verbal memory, executive function, language fluency, attention, and visuo-motor scanning, perceptual motor speed and integration, and general mental status, and performance on the TCT. These analyses provide insight into spatial memory, orientation and navigation as closely related vs. discrete abilities, and whether standard psychometric tests reflect path integration ability.

MATERIALS AND METHODS

Study Population

The BLSA is a prospective cohort study followed by the National Institute on Aging (NIA) Intramural Research Program in Baltimore, Maryland. The data are available to the public via the BLSA Investigator's portal. Analysis code will be shared by the corresponding author to other researchers upon request. In this study, a cross-sectional sample of BLSA participants were evaluated who underwent TCT testing and cognitive function testing from January 2016 to March 2017. Participants with cognitive impairment, as determined by Mini-Mental Status Examination (MMSE) score $\leq$ 24, were excluded. Participants were also asked if they were ever told by a doctor that they had osteoporosis, osteoarthritis, and/or spinal stenosis. All participants provided written informed consent, and the study protocol was approved by the institutional review board of the National Institute of Environmental Health Science, National Institutes of Health.

Triangle Completion Task (TCT)

The TCT was developed as a test of egocentric navigation. Test procedures have been described previously in detail (18), and are briefly described here. In brief, participants were asked to walk four triangular paths (twice clockwise, twice counterclockwise) of a 30°-60°-90° configuration with dimensions of 92.5 × 185.5 × 212 cm. Visual and auditory inputs were minimized or attenuated using a blindfold and noise-reducing headphones, respectively. Participants had to rely solely on vestibular, proprioceptive, and motor efference cues to complete the task. The examiner guided the participant through the first two segments including the 90-degree turn of the triangle and were asked to return back to the origin at the end of the second segment. The endpoint for each trial was determined as the midpoint between the anterior tips of the feet. The distance (in cm) between the endpoint and the starting point was averaged over the four trials and termed "distance of deviation." Additionally, the difference between the absolute value of the angle the participant made at the end of the second limb of the triangle and the correct value of the corresponding angle was averaged over the four trials and termed "angle of deviation."

Cognitive Function Tests

Trained, certified examiners performed psychometric testing in the BLSA. The test battery assesses a number of cognitive domains, including verbal memory (California Verbal Learning Test), non-verbal memory (Benton Visual Retention Test), visuospatial ability (Card Rotations Test), executive function (TMT-B, Backward Digit Span, Digit Symbol Substitution Test), language fluency, and executive function (letter and category fluency), attention and visuo-motor scanning (TMT-A, TMT-B, Forward Digit Span), perceptual motor speed and integration (Purdue Pegboard), psychomotor speed (Digit Symbol Substitution Test), and mental status (Mini-Mental State Examination). The procedures for the battery of tests have been published in detail (19), and are briefly described here.

California Verbal Learning Test (CVLT)

The CVLT evaluates verbal learning and memory (20). In this test, a list of 16 shopping list items are read five times, with participants asked to recall the items after each repetition (immediate recall) and then again after 20 min (delayed recall).

Benton Visual Retention Test (BVRT)

The BVRT evaluates non-verbal memory and visuoconstructional skill. In this test, a card with an image of a geometric shape is shown for 10 s. When the card is removed, the participant is asked to draw the shape on a blank piece of paper. The number of errors was measured over 10 trials with 10 different cards (21).

Card Rotations Test

The card rotations test evaluates primarily visuospatial ability. In this test, a reference 2-dimensional geometric shape is shown to the participants. Following, a set of similar 2-dimensional objects are shown, with participants being asked to mentally rotate each object and determine whether it is identical or a mirror image

of the reference object. The outcome of interest was the number of correctly classified objects minus the number of incorrectly classified objects (22).

Trail Making Test Parts A and B (TMT-A and TMT-B)

The TMT-A and TMT-B evaluate attention, processing speed, and visual scanning ability, while the TMT-B also evaluates executive function. In the TMT-A, 25 circles numbered 1–25 are distributed in a random order over a sheet, with participants being asked to draw a trail to connect the numbers in consecutive order (1, 2, 3, etc.) as quickly as possible while maintaining accuracy. In the TMT-B, similarly there are 25 circles with some containing numbers (1–13) and some containing letters (A-L). Participants are asked to draw a trial to connect the numbers and letters in alternating consecutive order (1, A, 2, B, etc.). The outcome of interest was the time to complete each task (23).

Digit Symbol Substitution Test (DSST)

The DSST evaluates executive function, visuospatial ability, and processing speed. Participants are shown nine pairs of digits and symbols, followed by a series of digits, in which participants are asked to draw the correct symbol that matches to each digit in the series. The outcome of interest is the number of correct digit-symbol matches made in 90 s (24).

Category and Letter Fluency Tests

The Category and Letter Fluency Tests evaluate language fluency and executive function. In the Category Fluency test, participants are given a category (animals, fruits, and vegetables) and asked to recite as many words as possible in 1 min that belong in that category. Similarly, in the Letter Fluency test, participants are given a letter (F, A, and S) and asked to recite as many words as possible that begin with that letter. The outcome of interest was the mean number of words recited across the three trials for each test (25).

Forward and Backward Digit Span Test

The digit span test from the Wechsler Adult Intelligence Scale–Revised contains both a forward recall component and a backward recall component. Both components evaluate attention and short-term memory while backward recall also evaluates mental manipulation and executive function. In this test, an increasingly longer lists of digits are recited to the participant who must recall each list immediately afterwards (forwards or backwards), until the participant is no longer able to accurately recall the digits. The outcome of interest is the maximum number of digits recalled correctly (26).

Purdue Pegboard Test

The Purdue Pegboard Test evaluates visuomotor integration as well as manual dexterity of both the dominant and non-dominant hand. Participants are shown a board with small holes and a cup filled with pegs. Participants are asked to insert as many pegs into the board as possible over 30 s using one hand. The outcome of measure is the mean number of pegs placed into the board over two trials with each hand (dominant and non-dominant hands). The mean between the two hands is also calculated (27).

Mini–Mental State Examination

The MMSE evaluates global mental status and is utilized in clinical settings to screen for cognitive impairment and dementia (28). It has a maximum score of 30 points. Participants with MMSE scores of 24 or lower were excluded from the analyses.

Proprioception Testing

Ankle proprioception threshold testing has been previously validated and described in detail (29). In brief, participants, while in a seated position, placed their right foot on a motorized pedal. Participants indicated perception of ankle motion by pressing a button while blindfolded. The test examined the minimal angular displacement (i.e., threshold) required for the participant to recognize passive movement of the ankle joint at an angular speed of 0.3°/s. Testing followed a pre-set sequence of ankle plantar flexion, dorsiflexion, dorsiflexion, and plantar flexion. The proprioception threshold was determined to be the average angular displacement between the last two trials.

Vestibular Evoked Myogenic Potential (VEMP) Testing

Air-conduction evoked cervical VEMP (cVEMP) was performed to assess saccular function. The procedure has previously been described in detail (30). In brief, participants were reclined at 30° from horizontal. Tonic background sternocleidomastoid (SCM) activity was elicited by having participants turn their heads to the right and left. Air-conducted positive polarity tone bursts war delivered monaurally at 500 Hz and 125 dB SPL through a noise-excluding headset. Electromyographic (EMG) signals were recorded with Ag/AgCl electrodes from GN Otometrics (Schaumburg, IL, USA) using a commercial EMG system (Carefusion Synergy, version 14.1, Dublin, OH, USA). An absent cVEMP response was defined as EMG recordings lacking definable p13 waves. Normal saccular function was defined as the presence of a vestibular evoked myogenic potential bilaterally. Abnormal saccular function was defined as either unilaterally or bilaterally absent function.

Statistical Analysis

The main outcome of interest in this study was performance on the TCT. The main predictor variables of interest were performance on cognitive function tests. Descriptive analyses were conducted to examine participant demographics and performance on cognitive function tests. Multiple linear regression models adjusting for demographic characteristics (age, sex, race, and education) were developed to explore the association between performance on each cognitive function test and distance and angle of deviation on the TCT. Postregression estimates and plots were carried out to check that the requirements of multiple linear regression analyses were met. Augmented component-plus-residual plots and Kernel density plots were evaluated to ensure that there was a roughly linear relationship between cognitive variables and TCT performance and an approximately normal distribution of residuals, respectively. Variance inflation factors were calculated to rule out multicollinearity. Cook's distance was used to detect highly influential data points for each regression model, allowing

for the identification of a single observation that was considered a highly influential data point in a majority of regression models involving both angle of deviation and distance of deviation on the TCT. Sensitivity analyses conducted to evaluate the impact of excluding this outlier showed a marginal difference in multiple regression analyses, so the participant was not excluded from the final analyses.

Exploratory factor analysis was performed to identify latent cognitive abilities underlying the battery of cognitive tests. Eigenvalues > 0.8 was used as a cutoff to determine the factors to retain. Multiple linear regression analyses were conducted to assess the association between factors identified and distance and angle of deviation on the TCT. A $p < 0.05$ was considered statistically significant. All analyses were performed using STATA version 14 (College Station, TX, USA).

RESULTS

The study population consisted of 151 participants with a mean age of 69.7 +/– 13.6 years (**Table 1**); 44.4% were female and 65.6% were white. Most participants (83.4%) had a college education or greater. A limited number of participants had missing responses on one or more cognitive function tests; the mean performance of the study sample on each of the cognitive function tests are presented in **Table 1**.

The association between cognitive function testing and deviation on the TCT was evaluated using simple linear regression models (**Table 2**) and multiple linear regression models controlling for age, sex, race, and education (**Table 3**). To facilitate interpretation, cognitive test scores were converted into standardized variables (i.e., z-scores) and the model coefficients were transformed such that a negative coefficient always indicated that better cognitive function was associated with decreased distance or angle of deviation on the TCT. In multiple linear regression analyses, distance of deviation on the TCT was significantly associated with visuospatial ability as determined by the Card Rotations test (β −5.9, $p = 0.03$). Additionally, distance of deviation was significantly associated with tests of executive function, namely the TMT-B (β −5.9, $p = 0.04$) and the DSST (β −10.9, $p = 0.002$), as well as tests of perceptual motor speed and integration, namely the Purdue Pegboard-dominant hand (β −9.2, $p = 0.01$) and the Purdue Pegboard-mean (β −8.3, $p = 0.02$). Notably, the psychometric test demonstrating the strongest relationship with both angular and distance deviation on the TCT was the DSST. Additionally, significant associations were found between angle of deviation on the TCT and performance on the DSST (β −3.4, $p = 0.01$). Performance on the TCT (either distance or angle of deviation) was not significantly associated with verbal or non-verbal memory tests (CVLT and BVRT), language fluency (letter and category fluency), attention and visuo-motor scanning (TMT-A, forward digit span), or global mental status (MMSE) in multiple linear regression models. See **Supplementary Tables 1–15** for coefficients and p-values of other covariates in the multiple regression models. After adjusting for presence of orthopedic issues (osteoarthritis, osteoporosis, and spinal stenosis) and ankle proprioception thresholds, there were no substantial changes in these findings (results not shown). Additionally, to evaluate whether vestibular function might be a confounder in the relationship between performance on psychometric tests and the TCT, we added the cervical vestibular evoked myogenic potential (cVEMP) into the six regression models that demonstrated a significant relationship between performances on psychometric tests and the TCT. In previously published work examining the relationship between vestibular function and the TCT, we found that saccular function, as measured by the cVEMP was significantly associated with both angular and distance errors on the TCT

TABLE 1 | Demographic characteristics and results of cognitive testing in the Baltimore Longitudinal Study of aging ($N = 151$).

	N	Mean (*SD*)	*N* (%)
Sex	151		
Male			84 (55.6%)
Female			67 (44.4%)
Mean age (*SD*)	151	69.7 (13.6)	
Race	151		
White			99 (65.6%)
Non-white			52 (34.4%)
Education	151		
Less than college			25 (16.6%)
College			40 (26.5%)
Greater than college			86 (57.0%)
Learning and memory:			
Verbal: California verbal learning test			
Immediate recall	149	51.8 (11.1)	
Delayed recall	149	10.8 (3.3)	
Figural/non-verbal			
BVRT, errors	151	10.0 (5.8)	
Visuospatial ability			
Card rotations test[a]	145	88.7 (42.4)	
Executive function			
TMT-B, seconds[a,b]	148	74.1 (40.1)	
Backward digit span	151	7.0 (2.2)	
Digit symbol substitution test[a,c]	144	44.6 (12.6)	
Language fluency and executive function			
Letter fluency, mean	150	15.1 (4.0)	
Category fluency, mean	150	15.9 (3.5)	
Attention and visuo-motor scanning			
TMT-A, seconds[a]	151	30.5 (11.6)	
Forward digit span	151	8.2 (2.5)	
Perceptual motor speed and integration			
Purdue pegboard[a]			
Dominant	148	12.8 (2.2)	
Non-dominant	148	12.4 (2.1)	
Mean	147	12.6 (2.0)	
Mental status			
MMSE	150	28.7 (1.3)	

[a] *Tests which have a perceptual motor speed component.*
[b] *TMT-B also has an attention and visuo-motor scanning component.*
[c] *Digit symbol substitution test also has a psychomotor speed component.*

TABLE 2 | Simple linear regression of deviation on the triangle completion task and cognitive function tests in the Baltimore Longitudinal Study on aging.

Cognitive test	Distance of deviation (cm)			Angle of deviation		
	β (95% CI)[a,b]	*p*-value	R^2	β (95% CI) [a,b]	*p*-value	R^2
Learning and memory:						
Verbal: California verbal learning test						
Immediate recall	−2.6 (−7.9, 2.6)	0.32	0.01	−1.4 (−3.2, 0.5)	0.16	0.01
Delayed recall	−1.4 (−6.6, 3.9)	0.6	0.002	−0.9 (−2.8, 1.0)	0.34	0.01
Figural/non-verbal						
BVRT, errors	**−5.7 (−10.9, −0.4)**	**0.03**	**0.03**	**−1.9 (−3.7, −0.01)**	**0.05**	**0.03**
Visuospatial ability						
Card rotations test	**−8.3 (−13.5, −3.2)**	**0.002**	**0.07**	**−2.4 (−4.3, −0.5)**	**0.01**	**0.04**
Executive function						
TMT-B, seconds	**−7.2 (−12.5, −2.0)**	**0.007**	**0.05**	**−2.3 (−4.2, −0.5)**	**0.01**	**0.04**
Backward digit span	−2.5 (−7.8, 2.8)	0.36	0.01	−0.8 (−2.7, 1.1)	0.39	0.005
Digit symbol substitution test	**−12.5 (−17.4, −7.5)**	**<0.001**	**0.15**	**−4.0 (−5.9, −2.2)**	**<0.001**	**0.12**
Language fluency and executive function						
Letter fluency, mean	**−5.2 (−10.4, −0.02)**	**0.05**	**0.03**	**−2.0 (−3.9, −0.2)**	**0.03**	**0.03**
Category fluency, mean	**−8.3 (−13.4, −3.3)**	**0.001**	**0.07**	**−3.1 (−5.0, −1.3)**	**0.001**	**0.07**
Attention and visuo-motor scanning						
TMT-A, seconds	**−5.7 (−10.9, −0.4)**	**0.03**	**0.03**	−1.8 (−3.6, 0.1)	0.06	0.02
Forward digit span	−3.6 (−8.9, 1.7)	0.18	0.01	01.1 (−3.0, 0.7)	0.23	0.01
Perceptual motor speed and integration						
Purdue pegboard						
Dominant	**−11.4 (−16.4, −6.3)**	**<0.001**	**0.12**	**−3.2 (−5.0, −1.4)**	**0.001**	**0.08**
Non-dominant	**−9.0 (−14.2, −3.8)**	**0.001**	**0.07**	**−2.8 (−4.6, −0.9)**	**0.003**	**0.06**
Mean	**−10.8 (−15.9, −5.7)**	**<0.001**	**0.11**	**−3.2 (−5.0, −1.3)**	**0.001**	**0.07**
Mental status						
MMSE	−3.8 (−9.1, 1.5)	0.16	0.01	−1.2 (−3.0, 0.7)	0.23	0.01

[a] *Unadjusted model.*

[b] *Standardized Regression Coefficients were used. Negative* β *coefficients indicate decreased distance of deviation with greater cognitive function.*

The bolded values are significant (as determined by p-value < 0.05).

in healthy older adults (30). Here, we found that after adjusting for vestibular function, the relationship between psychometric measures and the TCT was not substantially attenuated in five out of six of the regression models; only the relationship between the Card Rotations test and distance of deviation on the TCT was mildly attenuated and no longer significant after adding cVEMP to the regression model (from β −5.9, $p = 0.03$ to β −5.1, $p = 0.08$).

Exploratory factor analysis was performed to identify latent cognitive abilities underlying the battery of cognitive tests. One hundred and thirty-four (88.7%) out of 151 participants had complete data on all cognitive tests and contributed to the factor analysis. Factor analysis yielded three factors, which based on the loading structure of the cognitive outcomes, were defined as visuospatial ability, verbal memory, and working memory and attention. The loading structure of the cognitive outcomes on these three factors was similar to the loading structure reported in a previous study that used the same battery of cognitive tests (19). Rotated factor loadings are shown in **Supplementary Table 16**. The visuospatial ability factor and working memory and attention factor were significantly positively correlated ($r = 0.88$, $p < 0.001$). Meanwhile, the verbal memory factor was not significantly correlated with either the visuospatial factor ($r = 0.02$, $p = 0.79$) or the working memory and attention factor ($r = -0.04$, $p = 0.61$). We conducted multivariate analyses controlling for demographic factors to examine the relationship between each of the three factors individually and performance on the TCT. The visuospatial factor was significantly associated with distance of deviation ($\beta = -1.30$, $p < 0.001$) and angle of deviation ($\beta = -0.40$, $p = 0.002$) on the TCT. Similarly, the working memory and attention factor was also significantly associated with distance of deviation ($\beta = -0.85$, $p = 0.003$) and angle of deviation ($\beta = -0.28$, $p = 0.010$) on the TCT. The verbal memory factor was not significantly associated with either distance of deviation or angle of deviation on the TCT. When all three factors were included in a single model along with demographic factors, the visuospatial factor was significantly related to distance of deviation ($\beta = -1.86$, $p = 0.014$) and nearly significantly related to angle of deviation ($\beta = -0.50$, $p = 0.085$) on the TCT. Notably, neither the working memory and attention factor or the verbal memory factor were significantly related to performance on the TCT in this model.

TABLE 3 | Multiple linear regression of deviation on the triangle completion task and cognitive function tests in the Baltimore Longitudinal Study on aging.

Cognitive test	Distance of deviation (cm)			Angle of deviation		
	β (95% CI)[a,b]	*p*-value	R^2	β (95% CI) [a,b]	*p*-value	R^2
Learning and memory:						
Verbal: California verbal learning test						
Immediate recall	2.4 (−3.4, 8.1)	0.42	0.16	0.4 (−1.7, 2.5)	0.71	0.12
Delayed recall	2.4 (−3.1, 7.8)	0.39	0.16	0.5 (−1.5, 2.5)	0.61	0.12
Figural/non-verbal						
BVRT, errors	−3.0 (−8.8, 2.8)	0.31	0.15	−0.8 (−2.8, 1.3)	0.47	0.12
Visuospatial ability						
Card rotations test	**−5.8 (−11.4, −0.2)**	**0.03**	**0.18**	−1.6 (−3.7, 0.5)	0.12	0.13
Executive function						
TMT-B, seconds	**−5.9 (−11.3, −0.4)**	**0.04**	**0.18**	−1.6 (−3.5, 0.4)	0.12	0.14
Backward digit span	−2.0 (−7.3, 3.3)	0.46	0.14	−0.6 (−2.5, 1.3)	0.53	0.12
Digit symbol substitution test	**−10.9 (−17.7, −4.0)**	**0.002**	**0.21**	**−3.4 (−5.9, −0.8)**	**0.01**	**0.15**
Language fluency and executive function						
Letter fluency, mean	−4.8 (−10.0, 0.4)	0.07	0.17	−1.7 (−3.6, 0.2)	0.08	0.13
Category fluency, mean	−4.1 (−10.5, 2.3)	0.21	0.16	−1.7 (−4.1, 0.6)	0.15	0.13
Attention and visuo-motor scanning						
TMT-A, seconds	−2.5 (−7.9, 3.0)	0.37	0.15	−0.6 (−2.5, 1.4)	0.57	0.12
Forward digit span	−2.6 (−7.9, 2.7)	0.34	0.15	−1.0 (−2.9, 0.9)	0.32	0.12
Perceptual motor speed and integration						
Purdue pegboard						
Dominant	**−9.2 (−16.1, −2.3)**	**0.01**	**0.18**	−1.6 (−4.1, 1.0)	0.22	0.12
Non-dominant	−5.1 (−12.0, 1.8)	0.14	0.16	−1.1 (−3.6, 1.4)	0.39	0.12
Mean	**−8.3 (−15.5, −1.1)**	**0.02**	**0.17**	−1.5 (−4.2, 1.1)	0.25	0.12
Mental status						
MMSE	−2.2 (−7.5, 3.2)	0.42	0.15	−0.3 (−2.2, 1.6)	0.76	0.12

[a] *Model adjusted for age, sex, race, and education.*

[b] *Standardized Regression Coefficients were used. Negative* β *coefficients indicate decreased distance of deviation with greater cognitive function.*

The bolded values are significant (as determined by p-value < 0.05).

DISCUSSION

In this study of healthy adults, we observed that cognitive tests of visuospatial ability, as well as executive function and perceptual motor speed and integration were significantly associated with path integration, as determined by performance on the TCT. Spatial navigation is the fundamental process by which humans and other organisms estimate their position in space and track their movement through their environment. Navigation strategies include allocentric navigation, i.e., orientation and movement are calculated relative to visual landmarks and external cues, and egocentric navigation, i.e., individuals use self-motion cues provided by the visual system, vestibular system, and proprioception to track their movement (a process known as path integration) (31–33). Prior studies including from the BLSA have shown a decline in allocentric navigation in a virtual environment with age (34), and have also shown a link between allocentric spatial navigation ability in a virtual environment and measures of mental rotation and verbal and visual memory (35). It has also been demonstrated that path integration ability is also reduced in older relative to younger adults (18), and aging may specifically impair the ability to switch from an egocentric to an allocentric navigational strategy (36). In this study we provide evidence that psychometric measures of visuospatial ability as well as executive function and perceptual motor speed and integration are related to path integration skills.

The appropriateness of using psychometric tests of visuospatial ability as a predictor of spatial navigational abilities has been debated. Whereas, studies of spatial cognition in animals have typically employed maze-learning tasks such as the Morris water navigation task which require actual movement through space, studies of spatial cognition in humans have traditionally employed paper-and-pencil tests of visuospatial ability (12). Indeed, it has been argued that subjective self-reported sense of direction may be a better predictor of spatial navigational abilities than performance on psychometric tests of visuospatial ability, as these tests fail to provide or require self-motion cues, a necessary feature of path integration (13). However, the current findings are more consistent with and build on previous studies that support an association between psychometric tests of visuospatial ability and spatial navigation. One study found highly significant correlations between scores on psychometric tests of spatial ability and performance on a virtual maze test, which simulates visual sensory input and transformations, but not vestibular or proprioceptive information (12). Our findings extend

these previous observations by demonstrating that the Card Rotations Test, a psychometric test of visuospatial ability is associated with performance on a blinded path integration task in which vestibular and proprioceptive sensory inputs were available. Furthermore, in factor analyses, the visuospatial factor was most strongly associated with TCT performance. Notably, despite observing a highly significant relationship between path integration and visuospatial ability as well as other cognitive domains, we note that the R^2 values are low in both simple and multiple regression analyses, consistent with our understanding that path integration is a complex navigational strategy dependent on multiple factors. As such, psychometric tests alone may not be sufficient to predict path integration.

In addition to supporting the association between psychometric tests of visuospatial ability and path integration, our study also demonstrates that path integration is associated with other psychometric measures, notably executive function, and perceptual motor speed and integration in multiple regression analyses. These findings build on an emerging body of evidence that have implicated the role of executive function and other cognitive domains in navigational ability. One study that used a modified TCT in which visual and proprioceptive inputs were removed via wheelchair during the first two legs of the TCT, found that older adults performed worse than younger adults, with 65% of the age-related variance in performance accounted for by performance on the Digit Symbol Substitution test, one of the same tests we used to evaluate executive function in this study (37). Another study in young adults found that performance on a virtual maze test was significantly associated with executive function including measures of inhibitory control and set switching (38). This aforementioned study also found that performance on the Category Fluency test, a measure that taps into language fluency and executive function, was significantly associated with navigational ability, although they did not adjust for important demographic covariates. Similarly, a study using a virtual-reality-based wayfinding task found that measures of executive function specifically working memory and inductive reasoning were significant predictors of performance on the task (39). The underlying mechanism driving the association between executive function and path integration may be related to the utilization of two different path integration strategies: configural vs. continuous. The configural strategy, which requires formation of a working memory representation of the traversed path, has been shown to be more accurate while the continuous strategy, which does not require forming a representation of the path traversed, may permit shorter response times (40). Taken in this context, it is possible that individuals with decreased executive function may be more likely to adopt a continuous navigational strategy over a configural one. Overall our findings build on these studies by demonstrating that associations between multiple cognitive domains and performance on a path integration task are present in a larger study sample and in multiple regression analyses.

Moreover, we found that visuospatial ability and perceptual motor speed were significantly associated with distance of deviation but not angle of deviation on the TCT in multiple regression analyses, while executive function was associated with both distance and angle of deviation. The angular error is made immediately upon ending the guided portion of the TCT and may thus represent immediate path integration ability whereas the distance error occurs at the end of the final segment of the triangle and may pose a greater demand for cognitive resources, specifically encoding spatial information into long-term memory. One study examining the relationship between age and performance on the TCT found that only distance of deviation was reliably correlated with age (37), suggesting that distance of deviation on the TCT may be a more sensitive marker of difficulty with path integration. Our findings thus support that mental rotation, may provide contributions to performance on at least one delayed measure of path integration in a large study sample of healthy adults.

We note several limitations of this study. Although we adjusted for important potential confounders of the association between psychometric tests and the TCT such as age, sex, race, and education level, there remains the possibility of confounding by unmeasured factors. Despite observing highly significant associations between cognitive variables and path integration, we note that the R^2 values are low in multiple regression analyses. Future work is needed to evaluate the relative contributions of different cognitive domains, vestibular function, and proprioception on path integration. This population consisted of cognitively healthy adults and the results presented here may differ for individuals with cognitive impairment. Additionally, although angle and distance of deviation on the TCT were measured in this study, consistent with recent experiments using the TCT (18, 41), some studies have also measured error of the length of the hypotenuse (15, 37). An examination of the relationship of the hypotenuse measure on the TCT and cognitive function would be valuable in future studies.

In summary, we observed that performance in the cognitive domains of visuospatial ability, executive function, and perceptual motor speed and integration were significantly associated with spatial navigation ability, as determined by performance on the TCT. Despite the presence of associations, we observed that psychometric tests explained a relatively low level of the variation in performance on the TCT, suggesting that psychometric tests alone may not be sufficient to predict path integration. Future neuroimaging studies are needed to examine the neuroanatomic networks that may explain the link between psychometric measures of executive function and spatial memory and orientation and dynamic tests of spatial navigation.

DATA AVAILABILITY STATEMENT

Publicly available datasets were analyzed in this study. The data are available to the public via the Baltimore Longitudinal Study of Aging (BLSA) Investigator's portal.

ETHICS STATEMENT

The studies involving human participants were reviewed and approved by National Institute of Environmental Health Science,

National Institutes of Health. The patients/participants provided their written informed consent to participate in this study.

AUTHOR CONTRIBUTIONS

EW: substantial contribution to the conception and design of the work, analysis and interpretation of the data, drafting the manuscript and revising it critically for important intellectual content, final approval of the version to be published, and agreement to be accountable for the work. EA and YA: substantial contribution to the conception and design of the work, acquisition, analysis and interpretation of the data, revising the work critically for important intellectual content, final approval of the version to be published, and agreement to be accountable for the work. SR: substantial contribution to the conception and design of the work, analysis and interpretation of the data, revising the work critically for important intellectual content, final approval of the version to be published, and agreement to be accountable for the work.

FUNDING

EA was funded by a NIH T32 Award (T32 DC000023). YA was funded by NIH/NIA AG057667, NIH/NIDCD DC015583, and NIH/NIDCD DC013056. This study was supported in part by the Intramural Research Program, National Institute on Aging, NIH.

SUPPLEMENTARY MATERIAL

The Supplementary Material for this article can be found online at: https://www.frontiersin.org/articles/10.3389/fneur.2020.00484/full#supplementary-material

REFERENCES

1. Ariel R, Moffat SD. Age-related similarities and differences in monitoring spatial cognition. *Aging Neuropsychol Cognit.* (2017) 25:351–77. doi: 10.1080/13825585.2017.1305086
2. Jansen P, Schmelter A, Heil M. Spatial knowledge acquisition in younger and elderly adults: a study in a virtual environment. *Exp Psychol*. (2009) 57:54–60. doi: 10.1027/1618-3169/a000007
3. Rodgers MK, Sindone JA, Moffat SD. Effects of age on navigation strategy. *Neurobiol Aging.* (2012) 33:21. doi: 10.1016/j.neurobiolaging.2010.07.021
4. Johnson DK, Storandt M, Morris JC, Galvin JE. Longitudinal study of the transition from healthy aging to Alzheimer disease. *Archiv Neurol*. (2009) 66:1254–9. doi: 10.1001/archneurol.2009.158
5. Anderson SW, Aksan N, Dawson JD, Uc EY, Johnson AM, Rizzo M. Neuropsychological assessment of driving safety risk in older adults with and without neurologic disease. *J Clin Exp Neuropsychol*. (2012) 34:895–905. doi: 10.1080/13803395.2011.630654
6. Anstey KJ, Horswill MS, Wood JM, Hatherly C. The role of cognitive and visual abilities as predictors in the Multifactorial Model of Driving Safety. *Accident Anal Prev*. (2012) 45:766–74. doi: 10.1016/j.aap.2011.10.006
7. Dawson JD, Uc EY, Anderson SW, Johnson AM, Rizzo M. Neuropsychological predictors of driving errors in older adults. *J Am Geriatr Soc*. (2010) 58:1090–6. doi: 10.1111/j.1532-5415.2010.02872.x
8. Klencklen G, Després O, Dufour A. What do we know about aging and spatial cognition? Reviews and perspectives. *Ageing Res Rev*. (2012) 11:123–35. doi: 10.1016/j.arr.2011.10.001
9. Liu L, Gauthier L, Gauthier S. Spatial disorientation in persons with early senile dementia of the alzheimer type. *Am J Occup Ther*. (1991) 45:67–74. doi: 10.1016/0197-458090574-J
10. Ott BR, Davis JD, Papandonatos GD, Hewitt S, Festa EK, Heindel WC, et al. Assessment of driving-related skills prediction of unsafe driving in older adults in the office setting. *J Am Geriatr Soc*. (2013) 61:1164–9. doi: 10.1111/jgs.12306
11. Taylor ME, Delbaere K, Lord SR, Mikolaizak AS, Brodaty H, Close JCT. Neuropsychological, physical, and functional mobility measures associated with falls in cognitively impaired older adults. *J Gerontol Ser A Biol Sci Med Sci*. (2014) 69:987–95. doi: 10.1093/gerona/glt166
12. Moffat SD, Hampson E, Hatzipantelis M. Navigation in a "virtual" maze: sex differences and correlation with psychometric measures of spatial ability in humans. *Evol Hum Behav*. (1998) 19:73–87. doi: 10.1016/S1090-513800104-9
13. Wolbers T, Hegarty M. What determines our navigational abilities? *Trends Cognitive Sci*. (2010) 14:138–46. doi: 10.1016/j.tics.2010.01.001
14. Monacelli AM, Cushman LA, Kavcic V, Duffy CJ. Spatial disorientation in Alzheimer's disease the remembrance of things passed. *Neurology*. (2003) 61:1491–7. doi: 10.1212/WNL.61.11.1491
15. Glasauer S, Amorim M-A, Viaud-Delmon I, Berthoz A. Differential effects of labyrinthine dysfunction on distance and direction during blindfolded walking of a triangular path. *Exp Brain Res*. (2002) 145:489–97. doi: 10.1007/s00221-002-1146-1
16. Loomis JM, Klatzky RL, Golledge RG, Cicinelli JG, Pellegrino JW, Fry PA. Nonvisual navigation by blind and sighted: assessment of path integration ability. *J Exp Psychol*. (1993) 122:73–91. doi: 10.1037/0096-3445.122.1.73
17. Marlinsky VV. Vestibular and vestibulo-proprioceptive perception of motion in the horizontal plane in blindfolded man–III. Route inference. *Neuroscience*. (1999) 90:403–11. doi: 10.1016/S0306-452200448-5
18. Xie Y, Bigelow RT, Frankenthaler SF, Studenski SA, Moffat SD, Agrawal Y. Vestibular loss in older adults is associated with impaired spatial navigation: data from the triangle completion task. *Front Neurol.* (2017) 8:1–9. doi: 10.3389/fneur.2017.00173
19. Bigelow RT, Semenov YR, Trevino C, Ferrucci L, Resnick SM, Simonsick EM, et al. Association between visuospatial ability and vestibular function in the Baltimore Longitudinal Study of Aging. *J Am Geriatr Soc*. (2015) 63:1837–44. doi: 10.1111/jgs.13609
20. Delis DC, Kramer J, Kaplan E, Ober BA. *California Verbal Learning Test (CVLT)*. New York, NY: The Psychological Corporation (1987).
21. Benton AL. *Revised Visual Retention Test: Clinical and Experimental Applications*. Iowa City: State University of Iowa (1974). doi: 10.1201/9781420007138
22. Wilson JR, De Fries JC, McClearn GE, Vanderberg SG, Johnson RC, Rashad MN. Cognitive abilities: use of family data as a control to assess sex and age differences in two ethnic groups. *Int J Aging Hum Dev*. (1975) 6:261–76. doi: 10.2190/BBJP-XKUG-C6EW-KYB7
23. Reitan, R. M. (1992). *Trail Making Test: Manual for Administration and Scoring*. Reitan Neuropsychology Laboratory. Available online at: https://books.google.com/books/about/Trail_Making_Test.html?id=K6C4nAEACAAJ (accessed January 20, 2018).
24. Royer FL, Gilmore GC, Gruhn JJ. Normative data for the symbol digit substitution task. *J Clin Psychol*. (1981) 37:608–14. doi: 10.1002/1097-467937:3<608::AID-JCLP2270370328>3.0.CO;2-W
25. Spreen O. *Neurosensory Center Comprehensive Examination for Aphasia (NCCEA) (Revision:)*. Victoria, BC: Neuropsychology Laboratory, University of Victoria (1977).
26. Wechsler D. *Wechsler Adult Intelligence Scale–Revised*. The Psychological Corporation (1981).
27. Tiffin J, Asher EJ. The Purdue pegboard; norms and studies of reliability and validity. *J Appl Psychol*. (1948) 32:234–47. doi: 10.1037/h0061266
28. Folstein MF, Folstein SE, McHugh PR. Mini-mental state. *J Psychiatr Res*. (1975) 12:189–98. doi: 10.1016/0022-395690026-6
29. Ko SU, Simonsick E, Deshpande N, Ferrucci L. Sex-specific age associations of ankle proprioception test performance in older adults: results from

the Baltimore longitudinal study of aging. *Age Ageing*. (2015) 44:485–90. doi: 10.1093/ageing/afv005
30. Anson ER, Ehrenburg MR, Wei EX, Bakar D, Simonsick E, Agrawal Y. Saccular function is associated with both angular and distance errors on the triangle completion test. *Clin Neurophysiol*. (2019) 130:2137–43. doi: 10.1016/j.clinph.2019.08.027
31. Bent LR, Inglis JT, McFadyen BJ. When is vestibular information important during walking? *J Neurophysiol*. (2004) 92:1269–75. doi: 10.1152/jn.01260.2003
32. Bruggeman H, Zosh W, Warren WHH. Optic flow drives human visuo-locomotor adaptation. *Curr Biol*. (2007) 17:2035–40. doi: 10.1016/j.cub.2007.10.059
33. Yang JF, Stein RB, James KB. Contribution of peripheral afferents to the activation of the soleus muscle during walking in humans. *Exp Brain Res*. (1991) 87:679–87. doi: 10.1007/BF00227094
34. Moffat SD, Resnick SM. Effects of age on virtual environment place navigation and allocentric cognitive mapping. *Behav Neurosci*. (2002) 116:851–9. doi: 10.1037//0735-7044.116.5.851
35. Moffat SD, Zonderman AB, Resnick SM. Age differences in spatial memory in a virtual environment navigation task. *Neurobiol Aging*. (2001) 22:787–96. doi: 10.1016/S0197-458000251-2
36. Harris MA, Wiener JM, Wolbers T. Aging specifically impairs switching to an allocentric navigational strategy. *Front Aging Neurosci*. (2012) 4:1–9. doi: 10.3389/fnagi.2012.00029
37. Allen GL, Kirasic KC, Rashotte MA, Haun DBM. Aging and path integration skill: kinesthetic and vestibular contributions to wayfinding. *Perception Psychophys*. (2004) 66:170–9. doi: 10.3758/BF03194870
38. Korthauer LE, Nowak NT, Frahmand M, Driscoll I. Cognitive correlates of spatial navigation: associations between executive functioning and the virtual Morris Water Task. *Behav Brain Res*. (2017) 317:470–8. doi: 10.1016/j.bbr.2016.10.007
39. Taillade M, Sauzéon H, Dejos M, Arvind Pala P, Larrue F, Wallet G, et al. Executive and memory correlates of age-related differences in wayfinding performances using a virtual reality application. *Aging Neuropsychol Cognition*. (2013) 20:298–319. doi: 10.1080/13825585.2012.706247
40. Wiener JM, Berthoz A, Wolbers T. Dissociable cognitive mechanisms underlying human path integration. *Exp Brain Res*. (2011) 208:61–71. doi: 10.1007/s00221-010-2460-7
41. Smith AD, McKeith L, Howard CJ. The development of path integration: combining estimations of distance and heading. *Exp Brain Res*. (2013) 231:445–55. doi: 10.1007/s00221-013-3709-8

Conflict of Interest: The authors declare that the research was conducted in the absence of any commercial or financial relationships that could be construed as a potential conflict of interest.

frontiers in Neurology

REVIEW
published: 21 July 2020
doi: 10.3389/fneur.2020.00695

Vestibular Evoked Myogenic Potential (VEMP) Testing for Diagnosis of Superior Semicircular Canal Dehiscence

Kimberley S. Noij[1] *and Steven D. Rauch*[1,2]*

[1] Department of Otolaryngology, Massachusetts Eye and Ear, Boston, MA, United States, [2] Department of Otolaryngology, Harvard Medical School, Boston, MA, United States

Superior semicircular canal dehiscence is a bony defect of the superior semicircular canal, which can lead to a variety of auditory and vestibular symptoms. The diagnosis of superior semicircular canal dehiscence (SCD) can be challenging, time consuming, and costly. The clinical presentation of SCD patients resembles that of other otologic disease, necessitating objective diagnostics. Although temporal bone CT imaging provides excellent sensitivity for SCD detection, it lacks specificity. Because the treatment of SCD is surgical, it is crucial to use a highly specific test to confirm the diagnosis and avoid false positives and subsequent unnecessary surgery. This review provides an update on recent improvements in vestibular evoked myogenic potential (VEMP) testing for SCD diagnosis. Combining audiometric and conventional cervical VEMP results improves SCD diagnostic accuracy. High frequency VEMP testing is superior to all other methods described to date. It is highly specific for the detection of SCD and may be used to guide decision-making regarding the need for subsequent CT imaging. This algorithmic sequential use of testing can substantially reduce radiation exposure as well as cost associated with SCD diagnosis.

Keywords: third window syndrome, semicircular canal dehiscence syndrome, vestibular evoked myogenic potential, diagnostic, otology

OPEN ACCESS

Edited by:
P. Ashley Wackym, Rutgers, The State University of New Jersey, United States

Reviewed by:
Yuri Agrawal, Johns Hopkins University, United States
Erin Gillikin Piker, James Madison University, United States

***Correspondence:**
Steven D. Rauch
steven_rauch@meei.harvard.edu

Specialty section:
This article was submitted to Neuro-Otology, a section of the journal Frontiers in Neurology

Received: *28 April 2020*
Accepted: *09 June 2020*
Published: *21 July 2020*

Citation:
Noij KS and Rauch SD (2020) Vestibular Evoked Myogenic Potential (VEMP) Testing for Diagnosis of Superior Semicircular Canal Dehiscence. Front. Neurol. 11:695. doi: 10.3389/fneur.2020.00695

INTRODUCTION

Superior semicircular canal dehiscence is a bony defect of the superior semicircular canal (SSC), which can lead to a variety of symptoms, including sound and pressure induced dizziness, aural fullness, hearing loss, autophony, hyperacusis, and pulsatile tinnitus (1). These symptoms are thought to occur due to a "Third Window" mechanism caused by the dehiscence. In the presence of normal bony covering of the semicircular canals, sound stimulation of the ear causes the stapes footplate and oval window to move, resulting in a pressure wave across the basilar membrane in the cochlea and an equal outward motion of the round window. In the presence of a dehiscence, the energy created by stapes footplate and oval window motion is shunted away from its usual route and toward the third window. As a result, the pressure difference across the basilar membrane in the cochlea decreases and energy transmission to the vestibular sense organs increases (2, 3).

In the early twentieth century, Tullio et al. described that fenestration of the semicircular canals in pigeons led to sound-induced eye and head motion in the plane of the fenestrated canal, indicating activation of the vestibulo-ocular and vestibulocollic pathways (4–6). In 1998,

Minor et al. were the first to describe this combination of the anatomical defect and symptoms in humans, dubbed superior semicircular canal syndrome (SCDS). Treatment of SCDS is reserved for patients with disabling or severely intrusive symptoms and consists of surgical plugging of the dehiscence (1).

Many auditory and vestibular symptoms experienced by SCDS patients also occur in other otologic pathologies, such as otosclerosis and Meniere's disease. SCDS patients have even undergone unsuccessful surgical procedures, such as stapedectomies, before being correctly diagnosed (7). It is therefore essential to use objective diagnostics to differentiate SCDS from other pathologies and to confirm diagnosis.

Because there is no single gold standard definitive diagnostic test for SCDS, its diagnosis is generally based on a combination of symptomatology, threshold audiometry, and immittance testing, video-oculography, temporal bone CT imaging, and vestibular evoked myogenic potential (VEMP) testing (3, 8). The choice of diagnostic tools is dependent on their availability and therefore varies per institution. Thus, SCDS diagnosis is often not straightforward, it can be time consuming, and it can be costly.

DIAGNOSTIC TOOLS AND CHALLENGES

The initial cohort of SCDS patients described by Minor et al. suffered from sound- and/or pressure-induced vestibular symptoms (1). Eye movements in the plane of the superior semicircular canal were observed with video-oculography or magnetic field search-coil recordings in 7 of 8 patients. Patients underwent temporal bone CT imaging in the axial and coronal planes (1 mm slice thickness) and all showed a dehiscence of the superior semicircular canal. Brain MRI with and without IV gadolinium performed in 6 patients were normal (1).

Over time, the diagnostic approaches to SCDS patients have been refined and SCDS diagnosis is currently based on a test battery approach (3, 8). Since symptoms that give rise to consideration of the SCDS diagnosis can be auditory, vestibular or both, both auditory and vestibular testing, as well as imaging, play important roles.

TEMPORAL BONE CT IMAGING

Since the issue in SCDS constitutes an anatomical defect, obtaining imaging of the temporal bone to assess the SSC seems a logical diagnostic choice and is widely used to assess patients suspected of SCD, although relatively costly (1). Ideally, CT images are evaluated in the planes parallel (Pöschl) and perpendicular (Stenvers) to the plane of the SSC (**Figure 1**). This diagnostic modality is highly sensitive but lacks specificity; i.e., it is highly likely to detect any true dehiscence but may also give rise to false positives, suggesting dehiscence when none is there. Clinical CT scans overestimate both the presence and size of the dehiscence, especially when the layer of bone covering the canal is thin and when only the Stenvers view is used (9–11). Theoretically, the use of a finer slice thickness would improve the specificity of CT imaging but that is accompanied by an increased risk of motion artifact and increased radiation exposure. Because the treatment of SCDS is surgical, it is crucial to use a highly specific test to confirm the diagnosis and avoid false positives.

AUDIOMETRY

As SCDS patients suffer from auditory symptoms, all should undergo pure tone audiometry testing. Obtaining both air- and bone-conduction thresholds is necessary. If the difference between air- and unmasked bone-conduction thresholds is >10 dB, bone-conduction thresholds should be masked to accurately assess the left and right ear separately. The air-bone gap (ABG) is calculated by subtracting the bone-conduction threshold from the air-conduction threshold. Many, but not all, patients with SCDS suffer from low frequency air-bone gaps (ABG) of ≥ 10 dB, which can be due to low or negative bone-conduction thresholds and/or elevated air-conduction thresholds. The largest ABG is typically seen at 250 Hz (12). Obviously, ABGs are not unique to SCD. They are a common finding in other otologic disorders causing conductive hearing loss, especially those with middle ear pathology (7). Therefore, further evaluation of middle ear function using tympanometry and acoustic reflexes is warranted and aids in differentiating the various causes of the ABG

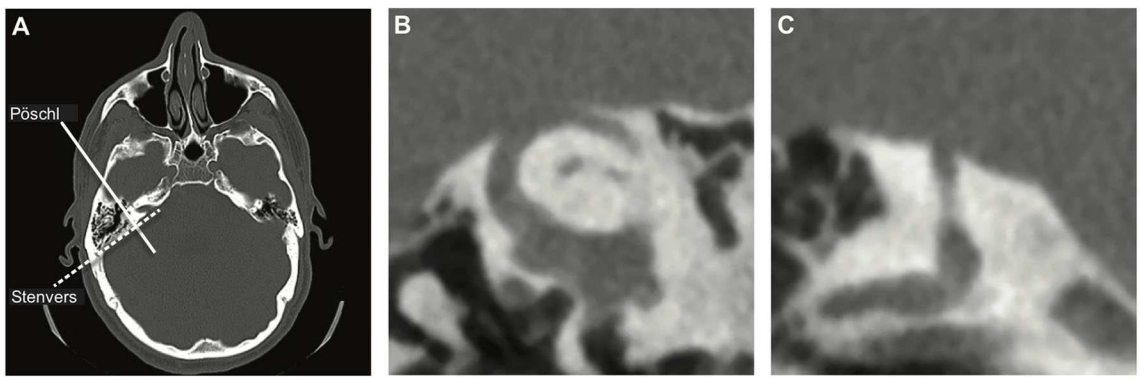

FIGURE 1 | CT images. **(A)** Axial view of the head indicating reformatting planes parallel (Pöschl—solid line) and perpendicular (Stenvers—dashed line) to the plane of the superior semicircular canal (SSC). **(B)** Pöschl view and **(C)** Stenvers view of a dehiscent SSC. The normal bony covering of the SSC is clearly absent in both views.

(7, 10). In contrast to ABG from middle ear pathology that causes abnormalities of tympanometry and/or loss of acoustic reflexes, SCD cases with ABG will exhibit normal tympanometry and preservation of acoustic reflexes. Audiometric testing alone is insufficient for diagnosis of SCD, but can be a valuable diagnostic contributor.

VESTIBULAR EVOKED MYOGENIC POTENTIALS

Tullio et al. described sound-induced activation of the vestibulo-ocular and vestibulocollic pathways in the presence of a third window (4–6). These pathways can be assessed clinically with vestibular evoked myogenic potentials (VEMP), which provide an actual physiological measurement of this phenomenon. The cervical VEMP (cVEMP) relies on the vestibulocollic reflex and assesses saccular and inferior vestibular nerve function through ipsilateral inhibition of the sternocleidomastoid muscle (13). The ocular VEMP (oVEMP) uses vestibulo-ocular projections, allowing for the assessment of utricular and superior vestibular nerve function through contralateral excitation of the inferior oblique eye muscle (14). cVEMP and oVEMP can be obtained during acoustic or vibrational stimulation of the ear while responses are recorded and averaged using surface electromyography of the contracted ipsilateral sternocleidomastoid muscle for cVEMP and contralateral inferior eye muscles during upward gaze for oVEMP (13, 14). Although various types of stimuli have been described, the most commonly used stimulus to obtain a clinical VEMP is a 500 Hz tone burst (15).

The cVEMP response consists of a first positive peak around 13 ms followed by a negative peak around 23 ms after sound stimulus onset (13). The latency of the response is dependent on the rise time of the tone burst (16). The oVEMP response consists of a first negative peak around 10 ms followed by a positive peak around 16 ms (14). The biphasic cVEMP and oVEMP responses can be evaluated using various metrics. The most clinically useful metrics are peak-to-peak amplitude and threshold. The cVEMP peak-to-peak amplitude is greatly affected by muscle contraction effort of the ipsilateral sternocleidomastoid muscle. Stronger muscle contractions correlate with greater peak-to-peak amplitudes. To allow for reliable comparison within and between patients, the peak-to-peak amplitude should be normalized for this muscle contraction effect (13, 17, 18). The oVEMP peak-to-peak amplitude is affected by gaze elevation; i.e., increased gaze elevation correlates with larger peak-to-peak amplitudes (19). Correcting for differences in gaze elevations between and within patients remains a methodologic issue that has not yet been resolved and requires further investigation. VEMPs can be obtained using varying sound frequencies and presentation levels. The VEMP threshold, i.e., the lowest sound level to elicit a response, at any stimulus frequency can provide valuable information regarding otolith function (20).

Since the presence of a third window results in activation of the vestibulo-ocular and vestibulocollic pathways as described by Tullio et al., one would expect VEMP amplitude to increase and threshold to decrease (4–6). In 1994, Colebatch et al. confirmed this prediction: A patient with the Tullio phenomenon demonstrated large cVEMP amplitudes and low cVEMP threshold (21). After Minor et al. first described SCDS, many studies confirmed that, on average, SCDS patients have larger cVEMP and oVEMP amplitudes and lower thresholds compared to healthy controls, although overlap between the SCDS and normal groups is observed (1, 20, 22–30). Until recently, the 500 Hz cVEMP threshold and 500 Hz oVEMP amplitude were found to most accurately differentiate dehiscent ears from healthy controls (20, 23).

ENHANCEMENTS OF VEMP TESTING IN SCD

Several recent studies investigating the use of VEMP testing in SCDS patients explored new methods to improve SCD detection (12, 25, 31–33). As described earlier, there is a need for a highly specific (preferably 100%) test for SCD detection in conjunction with the highly sensitive temporal bone CT imaging.

Both the cochlea and the saccule are affected by the presence of a third window. The mechanism of SCD symptoms, shunting of acoustic energy away from the cochlea and toward the vestibular system is well-known. The resulting audiometric finding of an air-bone gap in combination with auditory symptoms such as autophony and hyperacusis is suggestive but not unique to SCD. Likewise, sound- and pressure-induced vestibular symptoms in combination with a hypersensitive VEMP response is suggestive but not unique to SCD. Multiple studies have shown that ABGs and cVEMP thresholds in SCDS patients are significantly different from healthy controls, although there is still overlap between these two groups for both metrics (1, 20, 23, 25, 26). By combining the two phenomena into one metric objective evidence is sought to demonstrate that sound energy is *both* shunted away from the cochlea and toward the vestibule, a phenomenon that really is (almost) unique to SCD or other vestibular third window disorders. Milojcic et al. investigated whether combining the ABG and cVEMP threshold would improve differentiation between SCD patients and healthy controls. ABGs and cVEMP thresholds were obtained at multiple frequencies and combining cVEMP thresholds and ABG from the same frequency, i.e., subtracting the ABG from the cVEMP threshold, increased positive predictive values at 250, 500, and 1,000 Hz (24). A later retrospective study including 142 SCD ears found that the difference in ABG between dehiscent and healthy control ears was largest at 250 Hz and showed that a calculation subtracting the 250 Hz ABG from the 500 Hz cVEMP threshold (dubbed the "Third Window Indicator") provided better classification between SCD and age-matched healthy controls, with a sensitivity of 82% and a specificity of 100%, compared to a 46% sensitivity, and 100% specificity for the 500 Hz cVEMP threshold alone (12). A smaller prospective study, also using an age-matched healthy control group, found the Third Window Indicator (TWI) to have an 88% sensitivity and 100% specificity [**Table 1**; (32)]. In a group of subjects all suspected to have SCD based on symptoms, the TWI

TABLE 1 | A summary of study results regarding cVEMP and oVEMP testing in a group of SCD patients vs. healthy controls.

		Study	*N*	Cutoff	Sens (%)	Spec (%)	PPV (%)	NPV (%)
cVEMP	500 Hz threshold (12)	Retrospective	142	<98 dB peSPL	46	100	100	35
	TWI (12)	Retrospective	142	<103 dB	82	100	100	59
	500 Hz threshold (32)	Prospective	25	<98 dB peSPL	52	100	100	79
	TWI (32)	Prospective	25	<103 dB	88	100	100	94
	2 kHz VEMPn (32)	Prospective	25	>0.67	96	100	100	98
oVEMP								
	500 Hz amplitude (22)	Retrospective	39	>23.5 μV	68	98	93	87
	4 kHz presence (31)	Prospective	22^	n10 presence	100	100	100	100

^22 patients with unilateral and 4 with bilateral SCD were included, calculations were performed with 22 ears as opposed to 30 ears. It is unclear why the remaining 8 ears were not included. For the calculation of sensitivities and specificities, temporal bone CT imaging was used as the gold standard in all studies.
cVEMP settings: tonebursts were generated using a Blackman gating function with a two cycle rise/fall time (4 ms at 500 Hz, 1 ms at 2 kHz) and no plateau. The 2 kHz VEMP was obtained with a 123 dB peSPL toneburst (12, 32).
oVEMP settings: the 500 Hz amplitude was obtained with using toneburst generated with a Blackman gating function with a two cycle rise/fall time and a one cycle plateau at 95 dB nHL (22). The 4 kHz presence vs. absence was determined using a 7 ms long tone burst (rise/fall times unknown) at 120 dB SPL (31).
cVEMP, cervical vestibular evoked myogenic potential; oVEMP, ocular vestibular evoked myogenic potential; N, number of included SCD patients; Sens, sensitivity; Spec, specificity; PPV, positive predictive value; NPV, negative predictive value; TWI, third window indicator, calculated by subtracting the 250 Hz air-bone gap from the 500 Hz cVEMP threshold; dB, decibel; peSPL, peak sound pressure level.

TABLE 2 | A summary of study results regarding cVEMP and oVEMP testing in a group of SCD patients vs. patients with SCD-like symptoms without a dehiscence (dehiscent vs. not dehiscent on CT).

		Study	*N*	Cutoff	Sens (%)	Spec (%)	PPV (%)	NPV (%)
cVEMP	500 Hz threshold (34)	Retrospective	25	<98 dB peSPL	42	100	100	70
	TWI (34)	Retrospective	25	<103 dB	70	100	100	80
	2 kHz VEMPn (34)	Retrospective	25	>0.67	76	100	100	85
oVEMP								
	500 Hz amplitude (33)	Retrospective	47	Increased^	62	73	47	83
	4 kHz presence (33)	Retrospective	47	n10 presence	83	83	83	93

^Increased 500 Hz oVEMP amplitude is not further defined. For the calculation of sensitivities and specificities, temporal bone CT imaging was used as the gold standard in all studies.
cVEMP settings: tonebursts were generated using a Blackman gating function with a two cycle rise/fall time (4 ms at 500 Hz, 1 ms at 2 kHz) and no plateau. The 2 kHz VEMP was obtained with a 123 dB peSPL toneburst (34).
oVEMP settings: 500 Hz cVEMP thresholds and 4 kHz cVEMPs were obtained using tone bursts with a rise/fall time of 4 ms and no plateau. The 4 kHz cVEMP was obtained at 126 dB SPL (33).
cVEMP, cervical vestibular evoked myogenic potential; oVEMP, ocular vestibular evoked myogenic potential; N, number of included SCD patients; Sens, sensitivity; Spec, specificity; PPV, positive predictive value; NPV, negative predictive value; TWI, third window indicator, calculated by subtracting the 250 Hz air-bone gap from the 500 Hz cVEMP threshold; dB, decibel; peSPL, peak sound pressure level.

differentiated dehiscent from not dehiscent ears with a 70% sensitivity and 100% specificity (**Table 2**). Thus, the Third Window Indicator combines information from two sense organs (the cochlea and the saccule) that are both affected by the presence of a vestibular third window and, therefore, provides better differentiation between SCD and healthy ears compared to either of the two metrics alone.

Another recent investigative interest has been the use of various stimulus frequencies to obtain VEMPs. Two studies found that cVEMP and oVEMP evoked by high frequency tone bursts provide an even better separation between SCD patients and healthy controls (31, 32). The 2 kHz normalized peak-to-peak cVEMP amplitude provided a 96% sensitivity and 100% specificity, compared to 52% sensitivity and 100% specificity of the most commonly used 500 Hz cVEMP threshold (32). The 4 kHz oVEMP (presence vs. absence) provided a 100% sensitivity and specificity, compared to 55% sensitivity, and 100% specificity of the most commonly used 500 Hz oVEMP amplitude [**Table 1**; (22, 31)]. Recent evaluation of these high frequency VEMPs in a clinical population, as opposed to comparison with healthy controls, found them to be highly accurate. Sensitivities, specificities, positive, and negative predictive values were 83, 93, 83, and 93%, respectively, for 4 kHz oVEMP presence vs. absence and 76, 100, 100, and 84.6%, respectively, for the 2 kHz normalized peak-to-peak cVEMP amplitude [**Table 2**; (33, 34)]. The 2 and 4 kHz sound stimuli are at the upper edge of the otolith organ tuning curve. Since the otolith organs are relatively insensitive to acoustic signals at these higher frequencies, vestibular activation produced by a high frequency sound stimulus is usually insufficient to provide consistent responses in normal healthy individuals. However, in the presence of a dehiscent superior semicircular canal, the otolith organ "sees" a much higher "dose" of stimulus energy due to the shunting effect of the third window, resulting in a highly reliable

cVEMP (and oVEMP) response to high frequency stimuli in SCD patients.

A limitation of the studies presented in **Tables 1**, **2** is that CT imaging was used as a gold standard in calculating sensitivities and specificities. As described previously, CT imaging tends to overestimate the presence of the dehiscence and results in inclusion of false positives and therefore could categorize ears as dehiscent that actually do not contain a dehiscence. The alternative is to only include ears with a surgically confirmed dehiscence. This would greatly reduce the number of included ears and result in a small preselected group of patients, as many institutions use the VEMP result to determine surgical eligibility. This would result in an inflation of sensitivity and specificity. Although both methods have pros and cons, we believe that CT imaging is currently the best modality to study VEMP accuracy in detecting SCD, keeping in mind that the sensitivities and specificities may be underestimated using this method. Furthermore, we believe it is clinically relevant and a "best practice" to consider discordance of VEMP and imaging results to be a "red flag" for extra caution in consideration of the SCD diagnosis and/or surgical intervention.

NEAR DEHISCENCE

Besides patients with dehiscent vs. normal SSC, a third group has been identified clinically: those with SCD-like symptoms and radiologic and/or surgical evidence of thin bone covering the SSC, also referred to as "near-dehiscence" (10). Symptomatology in this group can be very similar to patients with a true dehiscence, and with no significant difference in dizziness handicap (DHI) scores between the two groups (35). It is unclear why these patients have symptoms. One suggested explanation has been the potential presence of a pinpoint or "microdehiscence" that could not be observed visually (8). The first report of this phenomenon found that 500 Hz oVEMP amplitudes in 6/9 patients with a near-dehiscence to lie above the 75th percentile of healthy controls, suggesting that the VEMP may provide valuable information in this group (10).

The studies investigating the TWI and the 2 kHz cVEMP included patients with thin bone covering the SSC (i.e., near-dehiscence) as a separate group (12, 32, 34). In all studies, the ABGs, cVEMP thresholds, and normalized peak-to-peak amplitudes of the thin group were very similar to the healthy control group. No significant difference between the thin and healthy control group was found for any of these metrics (12, 32, 34). In the study investigating a clinical population in which all included patients were suspected of having SCD based on symptoms, none of the thin ears met the 2 kHz cVEMP criterion for SCD abnormality (34). This study found autophony to be the only symptom that differed among the dehiscent, thin, and non-dehiscent cohorts, being significantly more common in dehiscent patients with concordant CT and 2 kHz cVEMP evidence of dehiscence than other patients (34). In patients with discordant CT imaging and 2 kHz cVEMP results (dehiscent on CT only, but 2 k Hz cVEMP not reaching threshold for abnormality) migraine was more prevalent (34). A study investigating patients with a surgically confirmed true dehiscence vs. near-dehiscence found the 500 Hz oVEMP amplitude to be significantly higher in the true dehiscence group [$p < 0.001$; (36)]. This study did not provide sensitivities or specificities and did not include a healthy control nor clinical non-dehiscent control group (36). The study investigating the 4 kHz oVEMP in a clinical population included patients with thin bone in their group marked as negative for SCD and it is therefore unknown whether results of this group differed from controls (33). Overall, in patients with symptoms suggestive of SCD and thin bone by CT and/or intraoperative inspection, cVEMP and oVEMP tend to be normal and do not show physiologic evidence of dehiscence. The VEMP is a measure of a physiologic phenomenon of increased acoustic energy delivered to the otolith organs evoking a vestibular reflex response. The absence of an enhanced (low threshold or increased amplitude) VEMP response means energy shunting is not occurring. This seems perfectly plausible if the bone over the SCC is intact, no matter how "thin" it appears radiographically or intraoperatively. The more puzzling question is why these patients have symptoms. It seems that the thin layer of bone is sufficient to maintain normal inner ear physiology and it is unclear what underlying mechanism might account for symptoms is in these patients. This is a topic worthy of further investigation.

COST

Using a one-size-fits-all test battery for diagnostic evaluation of SCDS, comprising audiometric testing, cVEMP and/or oVEMP, and high-resolution CT imaging is costly. An alternative algorithmic sequential testing approach is preferable: Patients suspected of SCDS based upon symptoms and physical findings undergo comprehensive audiometry, including tympanometry and acoustic reflexes, to detect any air-bone gap, and confirm normal middle ear function. They also undergo high frequency VEMP testing. If high frequency VEMP is not available, 500 Hz cVEMP threshold can be obtained and used along with 250 Hz air-bone gap from the pure tone audiogram to calculate the Third Window Indicator. Either of these metrics, the high frequency VEMP or TWI, has extremely high diagnostic accuracy for SCD. Of all patients whose SCDS diagnosis is confirmed in this manner, only a subset will be surgical candidates: Those with significant Tullio phenomenon of sound-induced vertigo or drop attacks, those with other incapacitating vestibular symptoms, and those with severely intrusive auditory symptoms of autophony, hyperacusis, pulsatile tinnitus, and muffled hearing. Many patients with SCDS will have milder symptoms, and once fully informed of the risks vs. benefits of surgical intervention, may elect to forego surgery and live with their symptoms. Only those patients who are surgical candidates need a CT scan for anatomic assessment of their dehiscence. This approach has the dual benefits of only delivering radiation exposure to those patients with a real need and reducing overall cost by reducing the number of unneeded CT scans. Clinical application of this algorithm yielded an estimated cost reduction of 48–65% (34).

CVEMP METHODOLOGY

VEMP testing is still an evolving field. Unlike audiometry, for example, that has been standardized worldwide, VEMP testing equipment and methodology still varies widely from site to site. The interpretation and comparison of VEMP literature is challenged by the heterogeneity of methods used. This makes it particularly challenging for clinicians to determine which settings to use and how to implement a specific VEMP protocol in their clinical practice. To provide clinicians with the available details regarding the settings of each study presented in **Tables 1**, **2**, the figure captions include specific information regarding tone burst settings and sound levels used. Fortunately, the fact that sensitivities and specificities are similar across a number of studies investigating the same VEMP metrics using different stimulus parameters indicates that these methodologic differences may not have that great of an affect VEMP accuracy (**Tables 1**, **2**).

The cutoff values in **Tables 1**, **2** could be used as an example for clinical VEMP protocols, but simply adopting these exact cutoff values into a clinical protocol without local verification may be unwise due to differences in equipment and VEMP programming. The use of newer approaches (TWI and high frequency sound stimuli) in evaluating VEMPs provide better accuracy in detecting SCD. These can be implemented with little or no modification of equipment and testing protocols currently available at many sites and we encourage physicians to implement these in their own clinics.

The studies presented in **Tables 1**, **2** included adult patients and used age-matched control groups. One study investigated the effect of age on cVEMP outcomes in their study group and found the expected decrease in normalized peak-to-peak amplitude and increase in threshold with age in their healthy control group. This age effect was not observed in the dehiscent group and it seems that any age effect on cVEMP outcomes is overwhelmed in the presence of a dehiscence (32). The majority of SCD patients present in their 40s and 50s and although it may not be necessary to obtain different cutoff values within the most commonly studied age range (about 25–70 years old), these cutoff values should be used with caution in "extremes of age," i.e., those younger than 25 and older than 70 years old (12, 32).

DISCUSSION

Based upon the anatomy and physiology of SCD, it was predicted and subsequently confirmed that VEMP testing is a sensitive means to diagnose this anatomic condition. Over the last few years the methods have been refined to optimize both sensitivity and specificity of cVEMP and oVEMP, particularly adoption of high frequency stimuli, making it the most accurate single diagnostic test for SCD. That said, there is additional functional and anatomic information to be had from comprehensive audiometry and CT imaging.

There are several important considerations to keep in mind when using VEMP for evaluation of patients suspected of SCDS. First, it is important to prioritize a high (preferably 100%) specificity for VEMP testing in this patient group. Temporal bone CT imaging is highly sensitive for SCD (9–11). Therefore, a highly specific test adds invaluable information. In addition, SCDS treatment is surgical, making it crucial to use a test with no false positives to avoid unindicated surgery. When 100% specificity is prioritized, sensitivities of the most commonly used 500 Hz cVEMP threshold and oVEMP amplitude, only around 50%, are inadequate for clinical decision making (**Tables 1**, **2**). Several recent developments in VEMP testing have proven to be highly sensitive and specific for SCD detection. A calculation using the 250 Hz ABG and 500 Hz cVEMP thresholds, also known as the "Third Window Indicator" (TWI), provides better differentiation between SCD patients and healthy controls compared to either test alone (12, 32, 34). High frequency cVEMP and oVEMP testing provided even higher sensitivities and specificities (31–34). The advantage of high frequency VEMP testing over TWI is that normalized cVEMP peak-to-peak amplitudes or present vs. absent n10 oVEMP can be used instead of thresholds, requiring only one recording. This reduces sound exposure and testing time.

Regarding the choice of high frequency cVEMP vs. oVEMP, a few things should be considered. At a first glance, accuracy of SCD detection appears comparable for both oVEMP and cVEMP. However, although specificities were high for both testing modalities in a clinical population (cVEMP 100% vs. oVEMP 93%), a test with no false positives is preferred for reasons described above, favoring cVEMP. It is possible that the oVEMP specificity could be improved if a certain amplitude cutoff would be used instead of a presence vs. absence criterion. However, a limitation of using an amplitude cutoff for oVEMP is the current inability to correct for differences in gaze elevation, which may limit accurate intersubject comparison and test-retest reliability.

A serious limitation of both published high frequency oVEMP studies was that some ears were excluded from analysis (31, 33). The high frequency oVEMP study using healthy subjects as the control group described 22 patients with unilateral and 4 patients with bilateral SCD (30 ears in total), while only 22 ears were included in the analysis. It is unclear which ears were excluded and why (31). The high frequency oVEMP study using a clinical control group (i.e., suspected of having SCD based on symptoms) excluded 45 ears, 73% of which were excluded because no identifiable oVEMP at any stimulus frequency or intensity could be obtained (33). It is unclear if any of the excluded ears showed a dehiscence on CT imaging (33). One possible explanation for these missing oVEMPs is subject age. The oVEMP response rate decreases with age and many healthy subjects over age 60 may not have an observable oVEMP response (37, 38).

The high frequency cVEMP studies did not exclude any ears based on cVEMP outcomes and the methods in these studies were therefore more realistic and similar to a true clinical scenario in which absent responses cannot simply be disregarded (32, 34). We do recognize that VEMP testing systems and experience with cVEMP vs. oVEMP differ between

institutions. Regardless of which system or VEMP modality is used, we recommend the use of high frequency VEMP testing for SCD detection.

The cVEMP can reliably differentiate symptomatic patients with actual dehiscence from those with thin or normal bone covering the superior semicircular canal (12, 32, 34). As yet, there is no compelling explanation for clinical symptoms in those patients with thin bone on CT but normal cVEMP response. As CT imaging tends to overestimate the presence of the dehiscence, a discrepancy between CT findings and cVEMP [CT(+)/cVEMP(–)] outcomes should raise suspicion for the presence of a thin layer of bone as there is no physiologic evidence of overactivation of the vestibulocollic pathway. The only studies investigating differences in oVEMP outcomes between thin and dehiscent ears found the 500 Hz oVEMP amplitude was significantly smaller in the thin group compared to the dehiscent group, but it is unclear how much overlap, if any, existed between the two groups (36). These studies did not include patients suspected of SCD with normal CT results (10, 36).

CONCLUSION

Clinical oVEMP and cVEMP testing have seen gradual evolution since they were first demonstrated to be sensitive to the presence of SCD. Based upon the high sensitivity and specificity of high frequency VEMP shown in the clinical setting, we now consider this the gold standard diagnostic screen for SCD. Combined with comprehensive audiometry, and CT if necessary for surgical planning, it is now possible to acquire a detailed physiologic, functional, and anatomic characterization of each patient's superior canal dehiscence that optimizes diagnostic accuracy while simultaneously preserving patient safety and minimizing cost.

AUTHOR CONTRIBUTIONS

KN and SR contributed to the conception and design, analysis, interpretation of data, and participated in drafting the article for important intellectual content. All authors contributed to the article and approved the submitted version.

REFERENCES

1. Minor LB, Solomon D, Zinreich JS, Zee DS. Sound- and/or pressure-induced vertigo due to bone dehiscence of the superior semicircular canal. *Arch Otolaryngol Head Neck Surg.* (1998) 124:249–58. doi: 10.1001/archotol.124.3.249
2. Rosowski JJ, Songer JE, Nakajima HH, Brinsko KM, Merchant SN. Clinical, experimental, and theoretical investigations of the effect of superior semicircular canal dehiscence on hearing mechanisms. *Otol Neurotol.* (2004) 25:323–32. doi: 10.1097/00129492-200405000-00021
3. Ho ML, Moonis G, Halpin CF, Curtin HD. Spectrum of third window abnormalities: semicircular canal dehiscence and beyond. *AJNR Am J Neuroradiol.* (2017) 38:2–9. doi: 10.3174/ajnr.A4922
4. Tullio P. *Das Ohr und die Entstehung der Sprache und Schrift*. Berlin: Germany Urban Schwarzenberg (1929).
5. Huizinga E. On the sound reactions of Tullio. *Acta Otolaryngol.* (1935) 22:359–70. doi: 10.3109/00016483509118116
6. Eunen AJH, Huizinga HC, Huizinga E. Die Tulliosche Reaktion in Zusammenhang mit der Funktion Des Mittelohres. *Acta Otolaryngol.* (1943) 31:265–339. doi: 10.3109/00016484309123252
7. Zhou G, Gopen Q, Poe DS. Clinical and diagnostic characterization of canal dehiscence syndrome: a great otologic mimicker. *Otol Neurotol.* (2007) 28:920–6. doi: 10.1097/MAO.0b013e31814b25f2
8. Ward BK, Carey JP, Minor LB. Superior canal dehiscence syndrome: lessons from the first 20 years. *Front Neurol.* (2017) 8:177. doi: 10.3389/fneur.2017.00177
9. Sequeira SM, Whiting BR, Shimony JS, Vo KD, Hullar TE. Accuracy of computed tomography detection of superior canal dehiscence. *Otol Neurotol.* (2011) 32:1500–5. doi: 10.1097/MAO.0b013e318238280c
10. Ward BK, Wenzel A, Ritzl EK, Gutierrez-Hernandez S, Della Santina CC, Minor LB, et al. Near-dehiscence: clinical findings in patients with thin bone over the superior semicircular canal. *Otol Neurotol.* (2013) 34:1421–8. doi: 10.1097/MAO.0b013e318287efe6
11. Mittmann P, Ernst A, Seidl R, Skulj AF, Mutze S, Windgassen M, et al. Superior canal dehiscence: a comparative postmortem multislice computed tomography study. *OTO Open.* (2018) 2:2473974X18793576. doi: 10.1177/2473974X18793576
12. Noij KS, Duarte MJ, Wong K, Cheng YS, Masud S, Herrmann BS, et al. Toward optimizing cervical vestibular evoked myogenic potentials (cVEMP): combining air-bone gap and cVEMP thresholds to improve diagnosis of superior canal dehiscence. *Otol Neurotol.* (2018) 39:212–20. doi: 10.1097/MAO.0000000000001655
13. Colebatch JG, Halmagyi GM, Skuse NF. Myogenic potentials generated by a click-evoked vestibulocollic reflex. *J Neurol Neurosurg Psychiatry.* (1994) 57:190–7. doi: 10.1136/jnnp.57.2.190
14. Todd NPM, Rosengren SM, Aw ST, Colebatch JG. Ocular vestibular evoked myogenic potentials (OVEMPs) produced by air- and bone-conducted sound. *Clin Neurophysiol.* (2007) 118:381–90. doi: 10.1016/j.clinph.2006.09.025
15. Colebatch JG, Rosengren SM, Welgampola MS. Vestibular-evoked myogenic potentials. *Handb Clin Neurol.* (2016) 137:133–55. doi: 10.1016/B978-0-444-63437-5.00010-8
16. van Tilburg MJ, Herrmann BS, Guinan JJ Jr, Rauch SD. Normalization reduces intersubject variability in cervical vestibular evoked myogenic potentials. *Otol Neurotol.* (2014) 35:e222–7. doi: 10.1097/MAO.0000000000000449
17. van Tilburg MJ, Herrmann BS, Rauch SD, Noij KS, Guinan JJ Jr. Normalizing cVEMPs: which method is the most effective? *Ear Hear.* (2019) 40:878–86. doi: 10.1097/AUD.0000000000000668
18. Noij KS, Herrmann BS, Rauch SD, Guinan JJ Jr. Toward optimizing vestibular evoked myogenic potentials: normalization reduces the need for strong neck muscle contraction. *Audiol Neurootol.* (2017) 22:282–91. doi: 10.1159/000485022
19. Rosengren SM, Colebatch JG, Straumann D, Weber KP. Why do oVEMPs become larger when you look up? Explaining the effect of gaze elevation on the ocular vestibular evoked myogenic potential. *Clin Neurophysiol.* (2013) 124:785–91. doi: 10.1016/j.clinph.2012.10.012
20. Fife TD, Colebatch JG, Kerber KA, Brantberg K, Strupp M, Lee H, et al. Practice guideline: cervical and ocular vestibular evoked myogenic potential testing: report of the guideline development, dissemination, and implementation subcommittee of the American academy of neurology. *Neurology.* (2017) 89:2288–96. doi: 10.1212/WNL.0000000000004690
21. Colebatch JG, Rothwell JC, Bronstein A, Ludman H. Click-evoked vestibular activation in the Tullio phenomenon. *J Neurol Neurosurg Psychiatry.* (1994) 57:1538–40. doi: 10.1136/jnnp.57.12.1538
22. Hunter JB, Patel NS, O'Connell BP, Carlson ML, Shepard NT, McCaslin DL, et al. Cervical and ocular VEMP testing in diagnosing superior semicircular canal dehiscence. *Otolaryngol Head Neck Surg.* (2017) 156:917–23. doi: 10.1177/0194599817690720
23. Benamira LZ, Alzahrani M, Saliba I. Superior canal dehiscence: can we predict the diagnosis? *Otol Neurotol.* (2014) 35:338–43. doi: 10.1097/MAO.0000000000000230

24. Milojcic R, Guinan JJ Jr., Rauch SD, Herrmann BS. Vestibular evoked myogenic potentials in patients with superior semicircular canal dehiscence. *Otol Neurotol.* (2013) 34:360–7. doi: 10.1097/MAO.0b013e31827b4fb5
25. Govender S, Fernando T, Dennis DL, Welgampola MS, Colebatch JG. Properties of 500Hz air- and bone-conducted vestibular evoked myogenic potentials (VEMPs) in superior canal dehiscence. *Clin Neurophysiol.* (2016) 127:2522–31. doi: 10.1016/j.clinph.2016.02.019
26. Roditi RE, Eppsteiner RW, Sauter TB, Lee DJ. Cervical vestibular evoked myogenic potentials (cVEMPs) in patients with superior canal dehiscence syndrome (SCDS). *Otolaryngol Head Neck Surg.* (2009) 141:24–8. doi: 10.1016/j.otohns.2009.03.012
27. Brantberg K, Verrecchia L. Testing vestibular-evoked myogenic potentials with 90-dB clicks is effective in the diagnosis of superior canal dehiscence syndrome. *Audiol Neurootol.* (2009) 14:54–8. doi: 10.1159/000153435
28. Welgampola MS, Myrie OA, Minor LB, Carey JP. Vestibular-evoked myogenic potential thresholds normalize on plugging superior canal dehiscence. *Neurology.* (2008) 70:464–72. doi: 10.1212/01.wnl.0000299084.76250.4a
29. Streubel SO, Cremer PD, Carey JP, Weg N, Minor LB. Vestibular-evoked myogenic potentials in the diagnosis of superior canal dehiscence syndrome. *Acta Otolaryngol Suppl.* (2001) 545:41–9. doi: 10.1080/000164801750388090
30. Brantberg K, Bergenius J, Tribukait A. Vestibular-evoked myogenic potentials in patients with dehiscence of the superior semicircular canal. *Acta Otolaryngol.* (1999) 119:633–40. doi: 10.1080/00016489950180559
31. Manzari L, Burgess AM, McGarvie LA, Curthoys IS. An indicator of probable semicircular canal dehiscence: ocular vestibular evoked myogenic potentials to high frequencies. *Otolaryngol Head Neck Surg.* (2013) 149:142–5. doi: 10.1177/0194599813489494
32. Noij KS, Herrmann BS, Guinan JJ Jr, Rauch SD. Toward optimizing cVEMP: 2,000-Hz tone bursts improve the detection of superior canal dehiscence. *Audiol Neurootol.* (2019) 23:335–44. doi: 10.1159/000493721
33. Lin K, Lahey R, Beckley R, Bojrab 2nd D, Wilkerson B, Johnson E, et al. Validating the utility of high frequency ocular vestibular evoked myogenic potential testing in the diagnosis of superior semicircular canal dehiscence. *Otol Neurotol.* (2019) 40:1353–8. doi: 10.1097/MAO.0000000000002388
34. Noij KS, Remenschneider AK, Herrmann BS, Guinan JJ Jr., Rauch SD. Detecting superior semicircular canal dehiscence syndrome using 2 kHz cVEMP in a clinical population. In: *Poster #264, Presented During Associated for Research in Otolaryngology Mid-Winter Meeting*. San Jose, CA (2020).
35. Mehta R, Klumpp ML, Spear SA, Bowen MA, Arriaga MA, Ying YLM. Subjective and objective findings in patients with true dehiscence versus thin bone over the superior semicircular canal. *Otol Neurotol.* (2015) 36:289–94. doi: 10.1097/MAO.0000000000000654
36. Baxter M, McCorkle C, Trevino Guajardo C, Zuniga MG, Carter AM, Della Santina CC, et al. Clinical and physiologic predictors and postoperative outcomes of near dehiscence syndrome. *Otol Neurotol.* (2019) 40:204–12. doi: 10.1097/MAO.0000000000002077
37. Singh NK, Firdose H. Characterizing the age and stimulus frequency interaction for ocular vestibular-evoked myogenic potentials. *Ear Hear.* (2018) 39:251–9. doi: 10.1097/AUD.0000000000000482
38. Tseng CL, Chou CH, Young YH. Aging effect on the ocular vestibular-evoked myogenic potentials. *Otol Neurotol.* (2010) 31:959–63. doi: 10.1097/MAO.0b013e3181e8fb1a

Conflict of Interest: The authors declare that the research was conducted in the absence of any commercial or financial relationships that could be construed as a potential conflict of interest.

frontiers in Neurology

ORIGINAL RESEARCH
published: 21 July 2020
doi: 10.3389/fneur.2020.00694

Changes in Vestibulo-Ocular Reflex Gain After Surgical Plugging of Superior Semicircular Canal Dehiscence

*Sang-Yeon Lee[1], Yun Jung Bae[2], Minju Kim[1], Jae-Jin Song[1], Byung Yoon Choi[1] and Ja-Won Koo[1,3]**

[1] Department of Otorhinolaryngology-Head and Neck Surgery, Seoul National University Bundang Hospital, Seongnam, South Korea, [2] Department of Radiology, Seoul National University Bundang Hospital, Seongnam, South Korea, [3] Seoul National University Bundang Hospital, Seoul National University College of Medicine, Seoul, South Korea

Superior semicircular canal dehiscence (SCD), which is characterized by a "third mobile window" in the inner ear, causes various vestibular and auditory symptoms and signs. Surgical plugging of the superior semicircular canal (SC) can eliminate the symptoms associated with increased perilymph mobility due to the presence of the third window. However, the natural course of vestibular function after surgical plugging remains unknown. Therefore, we explored longitudinal vestibular function after surgery in 11 subjects with SCD who underwent SC plugging using the middle cranial fossa approach. Changes in vestibulo-ocular reflex (VOR) gain in all planes were measured over 1 year with the video head impulse test. We also evaluated surgical outcomes, including changes in symptoms, audiometric results, and electrophysiological tests, to assess whether plugging eliminated third mobile window effects. The mean VOR gain for the plugged SC decreased from 0.81 ± 0.05 before surgery to 0.65 ± 0.08 on examinations performed within 1 week after surgery but normalized thereafter. Four of seven subjects who were able to perform both VOR tests before surgery and immediately after surgery had pathologic values (SC VOR gain < 0.70). Conversely, the mean VOR gain in the other canals remained unchanged over 1 year. The majority of symptoms and signs were absent or markedly decreased at the last follow-up evaluation, and no complications associated with the surgery were reported. Surgical plugging significantly attenuated the air-bone gap, in particular at low frequencies, because of increased bone conduction thresholds and deceased air conduction thresholds. Moreover, surgical plugging significantly increased vestibular-evoked myogenic potential thresholds and decreased the ratio of summating potential to action potential in plugged ears. Postoperative heavily T2-weighted images were available for two subjects and showed complete obliteration of the T2-bright signal intensity in the patent SC lumen in preoperative imaging based on filling defect at the site of plugging. Our results suggest that successful plugging of dehiscent SCs is closely associated with a transient, rather than persistent, disturbance of labyrinthine activity exclusively involved in plugged SCs, which may have clinical implications for timely and individualized vestibular rehabilitation.

Keywords: superior semicircular canal dehiscence, plugging, vestibulo-ocular reflex, third mobile window, video head impulse test

OPEN ACCESS

Edited by:
P. Ashley Wackym, The State University of New Jersey, United States

Reviewed by:
Quinton Gopen, University of California, United States
Eric Anson, University of Rochester, United States

***Correspondence:**
Ja-Won Koo
jwkoo99@snu.ac.kr

Specialty section:
This article was submitted to Neuro-Otology, a section of the journal Frontiers in Neurology

Received: *01 April 2020*
Accepted: *09 June 2020*
Published: *21 July 2020*

Citation:
Lee S-Y, Bae YJ, Kim M, Song J-J, Choi BY and Koo J-W (2020) Changes in Vestibulo-Ocular Reflex Gain After Surgical Plugging of Superior Semicircular Canal Dehiscence. Front. Neurol. 11:694. doi: 10.3389/fneur.2020.00694

INTRODUCTION

Superior semicircular canal dehiscence (SCD), which is characterized by a "third mobile window" in the inner ear, presents with debilitating vestibulo-cochlear symptoms due to bony dehiscence in the superior canal (SC) (1). The "third mobile window" in the otic capsule is frequently seen in the arcuate eminence facing the middle cranial fossa dura or occasionally seen in the SC close to the common crus by the superior petrosal sinus (2). This pathologic third mobile window increases the vestibular response to various stimuli, such as sound, pressure, and skull vibration (3, 4). Increased sensitivity to bone-conducted sounds can present as autophony and pulsating tinnitus. In addition to subjective symptoms and radiologic evaluation, objective demonstration of cochleo-vestibular hyperresponsiveness can be performed using vestibular-evoked myogenic potentials (VEMP), electrocochleography (ECoG), bone conduction audiometry, and pathologic vestibulo-ocular reflex (VOR) measurements induced by various stimuli. Surgical plugging of the dehiscent SC alleviates the aforementioned symptoms (5–8).

A meta-analysis confirmed that surgical plugging of the dehiscent SC significantly relieves subjective vestibular symptoms in patients with SCD (9). Although the exact mechanism underlying this effect remains unknown, the correction of hypermobile fluid dynamics in the otic capsule by blocking the pressure shunt into the vestibular system may be involved (10, 11). However, surgical plugging in the dehiscent SC may disturb natural fluid dynamics in all semicircular canals (SCCs). Recently, early quantitative video head impulse tests performed within 1 week after surgery showed a tendency for vestibular hypofunction in all ipsilateral canals and some contralateral canals as well as the emergence of compensatory saccades at an early phase (11). The severely reduced VOR gain for plugged SCs remained unchanged over time, whereas the VOR function in other canals generally, if not always, resolved after surgery (11). Nevertheless, the limitations of previous studies, such as relatively short follow-up periods and small sample sizes, render the associations between changes in vestibular function and surgical repair of the SCD speculative and presumptive, in particular for long-term vestibular function. Indeed, no data have been collected on the natural course of vestibular function after surgical plugging of dehiscent SCs.

Therefore, we explored longitudinal vestibular function after surgical plugging via the middle cranial fossa approach in subjects with SCD by measuring changes in VOR gains in all SCCs over time with video head impulse tests. We also evaluated the surgical outcomes of these subjects based on their subjective symptoms, audiometric results, and electrophysiological test findings to assess whether surgical plugging eliminated pathologic third mobile window effects. We observed an immediate deterioration of VOR gain in plugged SCs that stabilized thereafter in the majority of cases, although preserved VOR gains persisted in the other canals. Our results suggest a differential progressive nature of VOR gain between plugged and non-plugged canals following surgical plugging of dehiscent SCs, which paves the way for understanding changes in vestibular function induced by canal plugging in subjects diagnosed with SCD.

METHODS

Participants

The medical records of subjects diagnosed with SCD at Seoul National University Bundang Hospital between January 2015 and December 2019 were retrospectively reviewed. The diagnostic criteria of SCD were based on the combination of dehiscent SC based on high-resolution temporal bone computed tomography (HR-TBCT) images reformatted in the plane of the SC, symptoms and signs relevant to third window syndrome, and at least one objective source documenting abnormal pressure transmission via a third mobile window (1). This study included only subjects in whom SC plugging was performed by a single surgeon (J.W.K.) via a middle fossa approach. Subjects who underwent a video head impulse test before surgery and at least one video head impulse test after surgery were selected to obtain comparison data. Ultimately, 11 subjects were identified. None of the subjects had a history of brain surgery or Meniere's disease, head injury, or neurological disorders. This study was approved by the Seoul National University Bundang Hospital Institutional Review Board (IRB No. B-2004-604-125) and was conducted in accordance with the principles of the Declaration of Helsinki.

Surgical Intervention

Canal plugging was performed with the aim of blocking the abnormal pressure shunt toward the third mobile window. The dehiscent SC was occluded with a combination of soft tissue and bone wax to obtain a watertight seal and then covered with temporalis fascia using the middle cranial fossa approach (**Video S1**).

Video Head Impulse Test: Follow-Up Protocol and Parameters

Head impulse tests were performed with a video system for the acquisition and analysis of eyeball and head movements (ICS Impulse®, GN Otometrics, Denmark), as described in our previous studies. For collection of head impulse data, 20 is the recommended minimum number of head impulses in the standard protocol outlined by the manufacturer. In some cases where we encountered difficulties in collecting acceptable stimulations, video head impulse test responses were analyzed from at least 10 acceptable impulse stimulations. As such, the tests were repeated at least 10 times on each side in an unpredictable direction, using the center-to-outward rotation method, at 5–10° and with peak accelerations of 750–6000°/s (12). Only artifact-free recordings with sufficient head velocity were used for further analyses. The movements of the right eyeball and head were recorded. VOR gain in the video head impulse tests was defined as the ratio of the area under the velocity curves of the right eye to that of the head (13). According to previous studies (14, 15), normal VOR gain is specified by the video head impulse test (ICS Impulse®, GN Otometrics, Denmark) as >0.8 for the lateral canals and >0.7 for the vertical canals. Subjects who underwent surgical plugging were

instructed to undergo serial video head impulse tests before surgery; immediately after surgery (within 1 week); and at 2, 6, and 12 months after surgery, if available.

Pure-Tone Audiometry

All subjects underwent pure-tone audiometry testing before and after surgery. In a soundproof booth, the pure-tone thresholds of bone and air conduction were recorded with standard audiometric testing procedures (ANSI, 1978, New York). The mean hearing threshold was calculated with the average of the hearing thresholds at 0.5, 1, 2, and 4 kHz. Masking was used with the air conduction threshold test if necessary and was used routinely with the bone conduction threshold test in the contralateral ear. Preoperative audiograms were performed an average of 1 day before surgery. The last available postoperative audiogram was used for analyses. Four audiogram parameters were analyzed to obtain comparable data before and after surgery: bone conduction thresholds at 0.25, 0.5, and 1 kHz; air conduction thresholds at 0.25, 0.5, and 1 kHz; air-bone gaps (ABGs) across 0.25, 0.5, and 1 kHz; and ABGs across 0.5, 1, 2, and 4 kHz.

Vestibular Evoked Myogenic Potentials

Cervical VEMPs (cVEMPs) were measured during ipsilateral sternocleidomastoid muscle (SCM) contraction. Subjects were placed in the supine position with their head raised ∼30° from the horizontal and rotated contralaterally to maintain contraction of the ipsilateral SCM. We recorded surface electromyography (EMG) activity from an active electrode placed over the belly of the contracted SCM after subtracting EMG activity from a reference electrode located on the medial clavicle. A ground electrode was attached to the forehead. Alternating tone bursts (500 Hz; rate, 2.1/s; rise-fall time, 2 ms; plateau time, 3 ms; 128 repetitions; Navigation Pro; Biologic Systems, Mundelein, IL, USA) were provided to each ear. The analysis time for each stimulus was 50 ms, and responses elicited by up to 80 stimuli were averaged for each test. We determined the thresholds by lowering the sound stimulus from the 93 dB normalized hearing level (nHL) in 5 dB decrements.

Electrocochleography

Extratympanic ECoG was recorded with a commercial acoustic evoked potential unit (Navigation Pro ver. 7.0.0; Biologic Systems). ER3-26B gold Tiptrodes (Etymotic Research, Elk Grove, IL, USA) were placed close to the tympanic membrane in the external auditory canal. Stimuli consisting of alternating polarity clicks (band-pass filtered, 10e1500 Hz) of 100 ms duration were presented at an intensity of 90 dB nHL. Two replications of averaged responses elicited by 1000–1500 clicks at 7.1 per second were obtained. As mentioned previously, the amplitudes were measured from baseline to summating potential (SP) or action potential (AP) peaks to elicit the SP/AP ratios (16).

Imaging Protocol

All subjects underwent a preoperative HR-TBCT to confirm the dehiscence of the SC. HR-TBCT was performed with a 64-section multidetector CT scanner (Brilliance; Phillips Healthcare, Best, The Netherlands) with the following parameters: collimation, 40 × 0.625 mm; slice thickness, 0.67 mm; increment, 0.33 mm; pitch, 0.825, 120 kVp, 250 mAs. As described by previous reports, images were displayed on an INFINITT PACS system version 3.0.9.1BN9 (INFINITT Healthcare, Seoul, Korea), and 3D multiplanar reconstruction was subsequently used to obtain an oblique coronal reformation image parallel to the SC. The length of the arc of dehiscence, which accounts for SCD size, was measured on a reformatted image in the plane of the SC.

Magnetic resonance imaging (MRI) examinations were performed on a 3 T MR scanner (Ingenia; Philips Healthcare) with a 32-channel SENSE Head Coil (Philips Healthcare). Heavily T2-weighted images (T2-WI) using 3D T2-weighted volume isotropic turbo spin-echo acquisition (T2-VISTA) were used to evaluate the SC structure. The imaging parameters were as follows: repetition time, 2000 ms; echo time, 258 ms; field of view, 160 × 160; acquisition matrix, 228 × 228; flip angle, 90°; echo train length, 74; number of excitations, 1; slice thickness, 0.70 mm; overlap, 0.35 mm. A three-dimensional multiplanar and/or maximum intensity projection (MIP) reconstruction with a slab 5 mm thick was used to evaluate the patency of the SC. MRI was performed at the 1-year follow-up after canal plugging in two subjects.

Statistical Analyses

The data are presented as means ± standard errors of the mean (SEMs). All statistical analyses were performed and illustrated with R (R version 3.5.2 and R Studio 1.0.136, Foundation for Statistical Computing, Vienna, Austria). If the data were normally distributed, one-way within-subjects analysis of variance (ANOVA) and Tukey's *post hoc*-test were used to examine differences in VOR gain over time. In addition, independent *t*-tests were performed to compare cVEMP thresholds and SP/AP ratios between operated and normal ears. Furthermore, paired *t*-tests were used as appropriate to compare cVEMP thresholds, SP/AP ratios, and pure-tone audiometry before and after canal plugging. All statistical tests were two-tailed, and $P < 0.05$ was considered to indicate statistical significance.

RESULTS

Demographic and Clinical Characteristics

The clinical characteristics of the 11 subjects enrolled in this study are summarized in **Table 1**. All 11 subjects underwent surgical plugging for SCD via the middle cranial fossa approach. Their mean age was 49.2 ± 2.97 years (range, 26–61 years), and seven were women. Temporal bone CT images reformatted in the plane of the SC revealed definite evidence of SCD in the affected ears, with a mean dehiscence size of the operated ears of 4.24 ± 0.23 mm (range, 3.07–5.48 mm). Eight subjects presented with unilateral SCD; the remaining three subjects presented with bilateral SCD. Subjects with bilateral SCD underwent canal plugging of the dominant SCD side only via the middle fossa approach. The SCD was located at the arcuate eminence in nine

TABLE 1 | Demographics and clinical characteristics of 11 subjects with superior semicircular canal dehiscence.

Case no.	Sex/age	Side	Dehiscence size (mm)[a]	Follow-up period[b] (months)	Operation	Autophony		Ear fullness		Hearing loss		Dizziness		Tulio/ Hennebert		Pulsating tinnitus	
						Pre	Post	Pre	Post	Pre	Post	Pre	Post	Pre	Post	Pre	Post
1	F/58	R	3.18	46	R) plugging (MFA) T1[c]	NP	NP	NP	NP	•*	○	•	○	•	NP	•*	NP
2	F/61	R	3.93	44	R) plugging (MFA)	•*	NP	•	NP	NP	NP	NP	NP	NP	NP	NP	NP
3	M/56	L	4.01	51	L) plugging (MFA)	•*	NP	•	NP	•	○	NP	NP	NP	NP	•	NP
4	M/26	B	4.33	37	L) plugging (MFA)	•	NP	•	NP○	NP	NP	•*	○	•	NP	•	NP
5	M/47	B	3.9	30	L) plugging (MFA)	•*	NP	•	NP	NP	NP	•	NP	•	NP	•	NP
6	F/45	R	3.07	25	R) plugging (MFA)	•	NP	NP	NP	NP	NP	•*	○	•	NP	•	○
7	F/40	B	4.35	11	R) plugging (MFA)	•*	NP	•	NP	NP	NP	•	NP	NP	NP	•	○
8	F/49	L	5.48	9	L) plugging (MFA) SPS encasing	•*	NP	•	NP	NP	NP	NP	NP	NP	NP	•	NP
9	M/53	L	4.98	7	L) plugging (MFA)	•*	NP	•	NP	NP	NP	•	○	NP	NP	•*	NP
10	F/50	L	4.13	5	L) plugging (MFA) SPS encasing	•*	○	•	NP	•	○	•	NP	NP	NP	•	○
11	M/56	L	5.24	3	L) plugging (MFA)	•*	NP	NP	NP	NP	NP	•	NP	NP	NP	•	NP

*M, male; F, female; R, right; L, left; B, bilateral; MFA, middle fossa approach; SPS, superior petrosal sinus; NP, not present; •, present/ no change; ○, improved; *, chief complaint.*
[a]Note that the length of the arc of superior semicircular canal dehiscence, which accounts for dehiscence size, was measured on a reformatted image in the plane of the superior semicircular canal.
[b]Note that refers to period of follow-up from the surgery to the present. The status if postoperative symptoms after surgery is based on the present.
[c]Note that the case No.1 accompanies chronic otitis media with tympanic membrane perforation. Surgical plugging via middle cranial fossa approach was performed following endaural tympanoplasty type I.

patients (10 sides) and at the level of the superior petrosal sinus in two patients.

Subjective Symptoms Before and After SC Plugging

As summarized in **Table 1**, of the preoperative cochleovestibular symptoms, autophony and pulsatile tinnitus were the most common (90.9% of subjects), followed by ear fullness (72.7%), dizziness (72.7%), Tulio/Hennebert signs (36.4%), and subjective hearing loss (27.3%). Only one subject (subject 1) did not report autophony before surgery, and it is interesting that she had a small tympanic membrane perforation (**Figure S1**).

The average number of debilitating symptoms per subject was three (range, 2–5). After surgery, the median follow-up time was 25 months (range, 3–51 months). No subject had postoperative complications. Most symptoms were absent or markedly relieved at the last follow-up evaluation. In the three subjects with bilateral SCD, lateralized symptoms resolved after surgery, but dizziness persisted in two patients, even after the dominant SC was plugged. During the follow-up period, we suggested that subjects who complain of dizziness after surgery should not be restricted through individual counseling. Specifically, the exercise-based program primarily designed to reduce vertigo, dizziness, and gaze instability, which consists of habituation, gaze stabilization, and balance testing, has not been prescribed to all subjects. Of them, two subjects enrolled in this study (Subject 1 and 3) experienced posterior canal benign paroxysmal positional vertigo (BPPV) in the affected ear for more than 1 year after surgery, which did not seem to be relevant to plugging surgery. All subjects returned to their normal activity.

Longitudinal Changes in VOR Function After SC Plugging

The average VOR gains over 1 year of six canals before and after SC plugging are shown in **Figure 1**. Of the 11 subjects, two had preoperative video head impulse test data from the lateral canals. Before surgery, no significant difference in gain was observed between the operated and normal ears for the SC, HC, and PC. The mean VOR gain of the plugged SCs decreased from 0.81 ± 0.05 before surgery (preoperative evaluation) to 0.65 ± 0.08 on examinations performed within 1 week after surgery (first postoperative evaluation). This represents an approximate 20% attenuation, although this difference was not statistically significant (95% confidence interval [CI] $= -0.36$ to 0.03, $P = 0.092$). Four of the seven subjects who underwent both the preoperative and first postoperative VOR tests contributed to the abnormal gain seen. The mean duration between the preoperative and first postoperative evaluations was 4.2 ± 0.4 days (range, 3–6 days). Compared to the first postoperative evaluation, the mean SC gain increased to 0.78 ± 0.03 during the second postoperative evaluation, a value similar to the preoperative value. The average time to the second postoperative evaluation was 63 ± 3 days (range, 48–78 days). VOR gain for the plugged SC remained unchanged thereafter (third postoperative evaluation, 0.71 ± 0.07; fourth postoperative evaluation, 0.69 ± 0.08). The average time to the third and fourth postoperative evaluations was 184

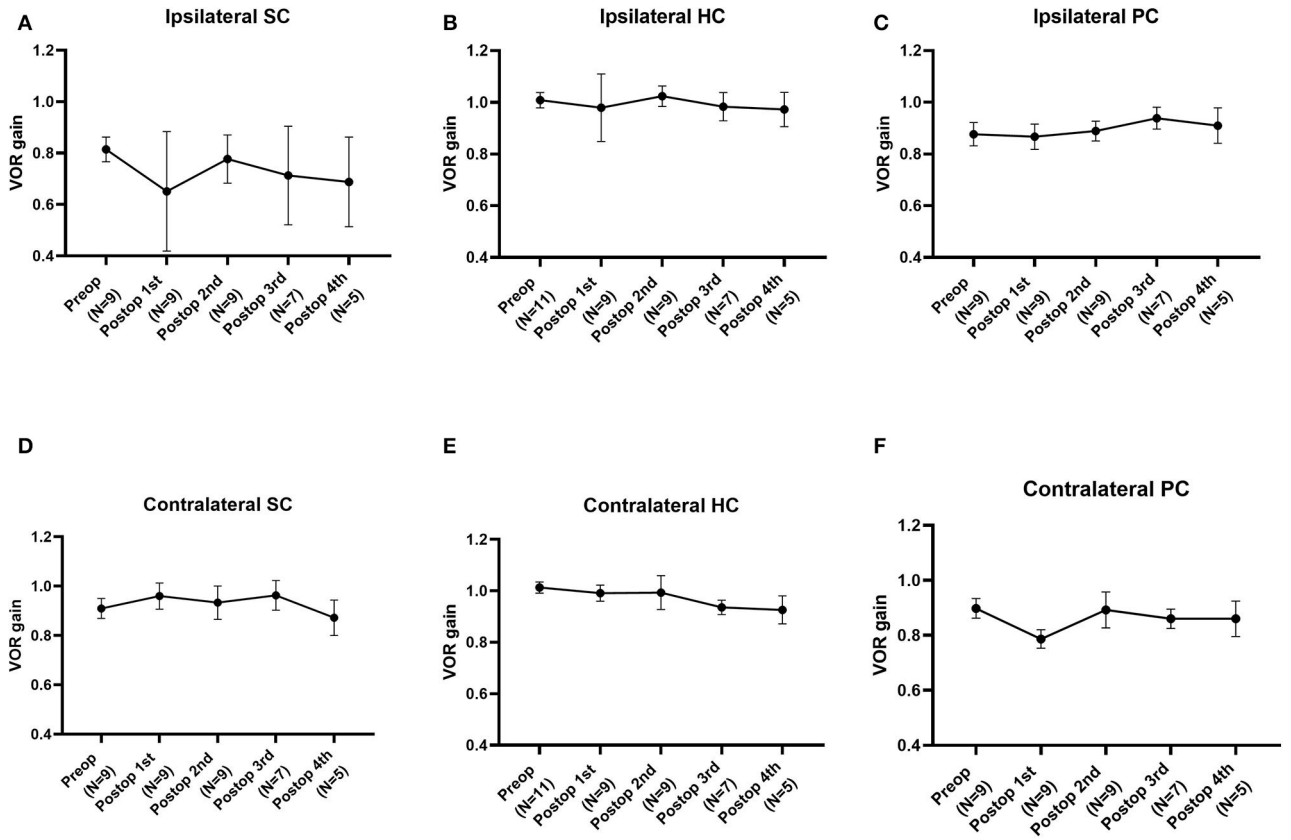

FIGURE 1 | The natural course of the mean vestibulo-ocular reflex (VOR) gain for each semicircular canal (SC) over 1 year before and after plugging of the superior SC. **(A)** The mean VOR gain for plugged SCs decreased immediately within 1 week after surgery but improved over time, similar to the preoperative value. **(B–E)** Compared to the preoperative value, the mean VOR gain for each SC after canal plugging remained unchanged over 1 year of follow-up, without any significant changes between intervals. Data are means ± standard error of the means (SEMs).

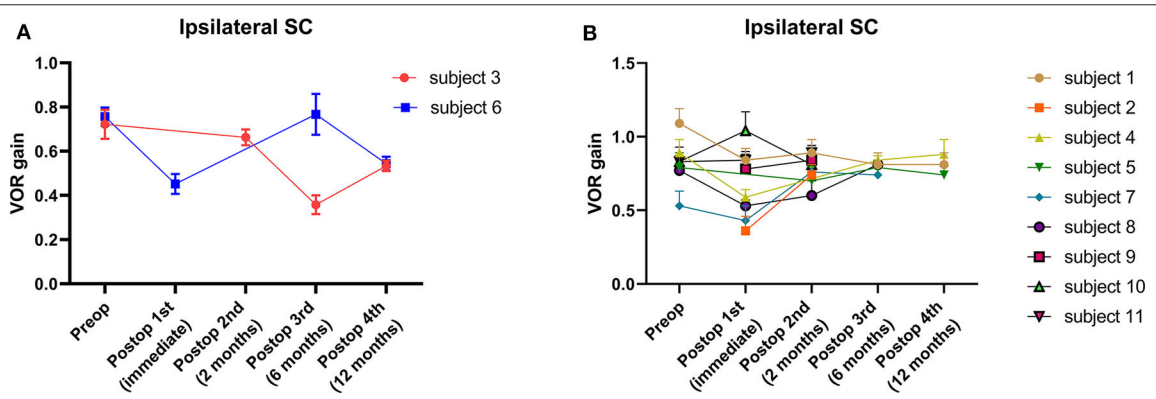

FIGURE 2 | Individual changes in VOR gain for plugged SCs. **(A)** A fluctuating pattern of VOR gain for plugged SCs over time was observed in two subjects. The subjects showed a markedly decreased VOR gain at the 1-year (fourth postoperative) evaluation. **(B)** The typical pattern of VOR gain for plugged SCs over time in nine subjects. Compared to baseline, VOR gains were lower immediately after surgery (first postoperative evaluation) in most cases. Nonetheless, VOR gains for plugged SCs normalized over 1 year, similar to baseline values. In addition, no significant differences in mean VOR gains were observed between intervals at the second, third, and fourth postoperative evaluations. Data are means ± SEMs.

± 6 days (range, 169–215 days) and 376 ± 6 days (range, 355–391 days), respectively. Likewise, individual data showed that the immediate plugged SC gain deteriorated by 1 week after surgery but subsequently normalized thereafter in most subjects, apart from two subjects (subjects 3 and 6; **Figure 2**). VOR gains for plugged SCs in these two subjects exhibited a fluctuating pattern

over time. The subjects showed a markedly decreased VOR gain at the 1-year mark (fourth postoperative evaluation).

Except for the plugged SCs, the mean VOR gain for the semicircular canals did not differ significantly between intervals for each canal, demonstrating nearly equivalent values over 1 year. Although VOR gain in the contralateral PC tended to decrease from the preoperative to the immediate postoperative time point, likely recapitulating VOR gain in the plugged SC, the difference was not statistically significant. In addition, as documented by individual data, no subject had abnormal VOR gain in the contralateral PC that deviated from the normal value throughout the follow-up evaluations. Specifically, one subject (subject 8) exhibited an immediate postoperative reduction in VOR gain in the plugged SC as well as the ipsilateral HC. Although the ipsilateral HC gain was fully recovered thereafter, the reduced VOR gain in the plugged SC remained unchanged at the second postoperative evaluation.

Audiological Characteristics Before and After SC Plugging

Audiometry was performed before surgery and after surgery in all subjects. The average interval between baseline and the last audiogram was 226 days (range, 33–391 days). The mean bone and air conduction thresholds before and after surgical plugging are shown in **Figure 3**. Preoperative audiograms showed significant ABGs in the operated ears, in particular at low frequencies. Note that hypersensitive bone conduction thresholds (<0 dB HL) were observed in six subjects (54.5%) at 250 Hz, two subjects (18.2%) at 500 Hz, and one subject (5.6%) at 1 kHz. Compared to baseline, the average ABGs across 0.25, 0.5, and 1 kHz decreased significantly from 20.0 ± 2.6 to 6.5 ± 2.4 after surgery (95% CI = −20.8 to −6.2, $P = 0.002$), whereas the average ABGs across 0.5, 1, 2, and 4 kHz decreased significantly from 9.0 ± 2.1 to 2.2 ± 0.8 after surgery (95% CI = −12.39 to −1.24, $P = 0.021$) (**Figure 3A**). The bone conduction thresholds at 0.25, 0.5, and 1 kHz increased following surgery, from −3.6 ± 1.5 to 5.9 ± 2.2 ($P < 0.001$), 5.5 ± 3.1 to 12.7 ± 2.1 ($P = 0.009$), and 8.6 ± 4.7 to 14.1 ± 2.7 ($P = 0.119$), respectively. Moreover, only one subject showed bone conduction below 0 dB HL at 0.25 kHz after surgery. In addition, the air conduction thresholds at 0.25, 0.5, and 1 kHz following surgery decreased from 26.8 ± 4.2 to 16.4 ± 3.5 ($P = 0.029$), 23.2 ± 3.1 to 16.4 ± 3.0 ($P = 0.027$), and 20.5 ± 3.6 to 19.6 ± 2.7 ($P = 0.690$), respectively. At the higher frequency range, 15 dB hearing loss at 8 kHz was observed in subject 2 only. Otherwise, significant hearing loss at high frequencies was not observed during follow-up. Collectively, surgical plugging significantly attenuated ABGs, in particular at low frequencies, via increased bone conduction thresholds and decreased air conduction thresholds.

To support our findings with regard to the natural course of audiological recovery, we evaluated the audiological changes with reference to the initial audiogram obtained between 1 and 3 months after plugging surgery. The average interval between baseline and the first audiogram obtained 3 weeks after surgery was 60 days (range, 27–84 days). Unfortunately, pure tone audiometry data obtained between 1 and 3 months after surgery were available for only nine subjects. For the remaining two subjects (Subject 7 and 8), the first audiometry assessments were conducted at 5 and 6 months, respectively. In comparison with the baseline, the average ABGs across 0.25, 0.5, and 1 kHz decreased significantly from 20.0 ± 2.6 to 6.5 ± 2.4 at an average of 60 days (range, 27–84 days) after surgery (95% CI = −15.3 to −10.2, $P < 0.001$) (**Figure 3B**). When comparing audiological results between the initial and the last audiometry assessments, the average ABGs across 0.25, 0.5, and 1 kHz decreased significantly from 7.3 ± 3.1 to 6.5 ± 2.4 after surgery (95% CI = −3.3 to 1.7, $P = 0.506$). In addition, audiological profiles, which included average ABGs across 0.5, 1, 2, and 4 kHz, bone conduction thresholds, and air conduction thresholds at

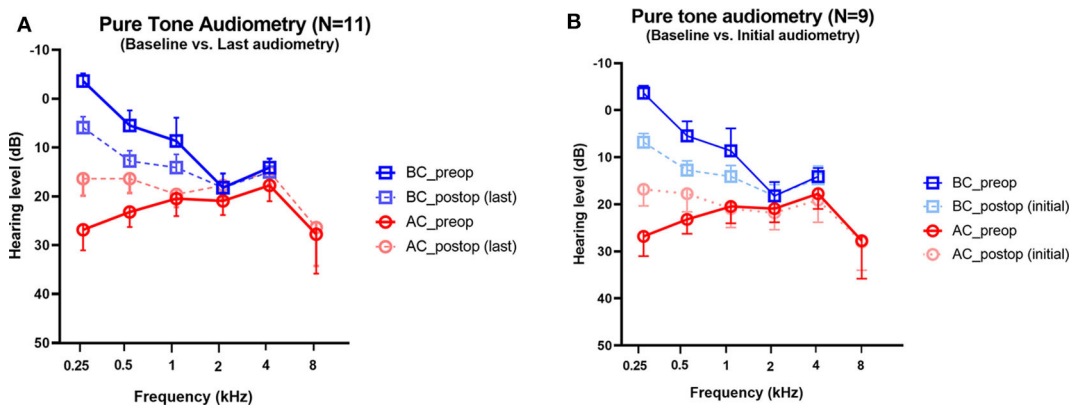

FIGURE 3 | Changes in pure-tone audiometry in the operated ears. Preoperative and postoperative bone conduction and air conduction thresholds are shown for all tested frequencies. **(A)** The postoperative values are based on the last available audiogram. The average interval between baseline and the last audiogram was 226 days (range, 33–391 days). **(B)** The postoperative values are based on the initial available audiogram obtained between 1 and 3 months after plugging surgery. The average interval between baseline and the first audiogram obtained 3 weeks after surgery was 60 days (range, 27–84 days). For two subjects (Subject 7 and 8), the first audiometry assessments were conducted at 5 and 6 months, respectively; thereby, pure tone audiometry data obtained between 1 and 3 months after surgery were available for only nine subjects. Data are means ± SEMs. After surgery, air-bone gaps at 250 and 500 Hz improved significantly ($P < 0.001$, paired *t*-test).

each frequency, did not differ between the initial and last audiometry assessments. Thus, surgical plugging significantly attenuated the air-bone gap, especially at low frequencies, even from the early phase after surgery, and the effects remained unchanged over time.

cVEMP Thresholds and SP/AP Ratios After SC Plugging

All subjects underwent pre- and postoperative cVEMPs and ECoG. The interval between pre- and postoperative evaluations was ∼2 months. As shown in **Figure 4**, mean cVEMP thresholds in the operated and normal ears were 55.7 ± 3.5 dB and 78.0 ± 2.2 dB (95% CI = 13.3 to 31.2, $P < 0.001$), respectively, before surgery and 77.6 ± 3.1 dB and 81.5 ± 2.1 dB (95% CI = −4.1 to 12.0, $P = 0.317$), respectively, after surgery. That is, SC plugging significantly enhanced the mean cVEMP thresholds in the operated ears (95% CI = 14.1 to 29.5, $P < 0.001$). Consistent with this, the mean SP/AP ratio in the operated ears decreased significantly from 0.50 ± 0.04 before surgery to 0.30 ± 0.02 after surgery (95% CI = −0.28 to −0.11, $P < 0.001$). Moreover, mean SP/AP ratios did not differ between operated and normal ears after surgery (95% CI = −0.13 to 0.05, $P = 0.381$).

One subject with tympanic membrane perforation (subject 1) exhibited normal cVEMP threshold and SP/AP ratio before surgery. After successful plugging and tympanoplasty, the cVEMP thresholds and SP/AP ratio remained within normal ranges, whereas the ABG disappeared and the bone conduction threshold normalized (**Figure S1**).

MRI Findings: Structural Changes in SCs After Canal Plugging

Postoperative heavily T2-WIs were available for two subjects and showed complete obliteration of T2-bright signal intensity in the patent SC lumen visible on preoperative imaging with filling of the defects at the site of canal plugging. This indicates successful plugging of peri-lymphatic fluid between the anterior and posterior arms (**Figure 5**). Despite adequate plugging of the SC in these two subjects, one subject (subject 5) had a normal or near-normal VOR gain in the SC and the other (subject 6) showed markedly decreased VOR gains in the plugged SC.

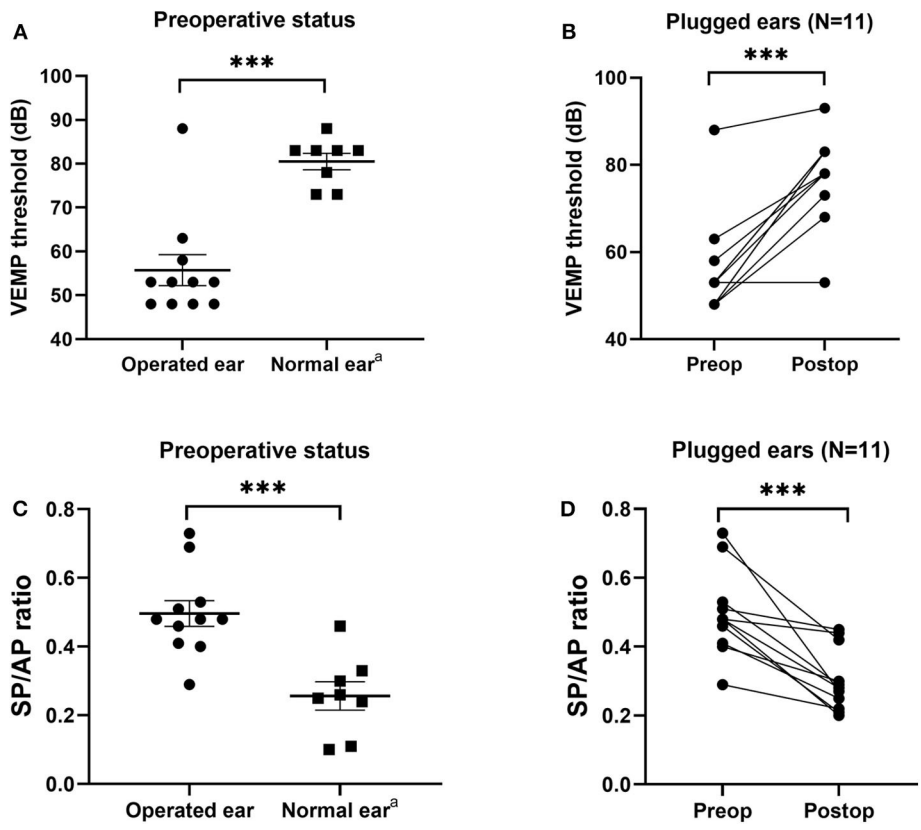

FIGURE 4 | Electrophysiological findings before and after canal plugging. **(A)** Before surgery, the cervical vestibular evoked myogenic potential (cVEMP) threshold differed significantly between operated and normal ears ($P < 0.001$, independent *t*-test). **(B)** Mean cVEMP thresholds before and after surgery for all subjects. Preoperative and postoperative gain values for the same subject are connected by a line. At 2–3 months after surgery, the mean cVEMP thresholds in operated ears increased significantly ($P < 0.001$, paired *t*-test). **(C)** Before surgery, the ratio of summating potential to action potential (SP/AP) differed significantly between operated and normal ears ($P < 0.001$, independent *t*-test). **(D)** SP/AP ratios before and after surgery for all subjects. Preoperative and postoperative gain values for the same subject are connected by a line. At 2–3 months after surgery, the mean SP/AP ratio for operated ears increased significantly ($P < 0.001$, paired *t*-test). Data are means ± SEMs. ***$P < 0.001$. [a]Note that three subjects with bilateral semicircular canal dehiscence (SCD) were excluded from the normal ear analyses.

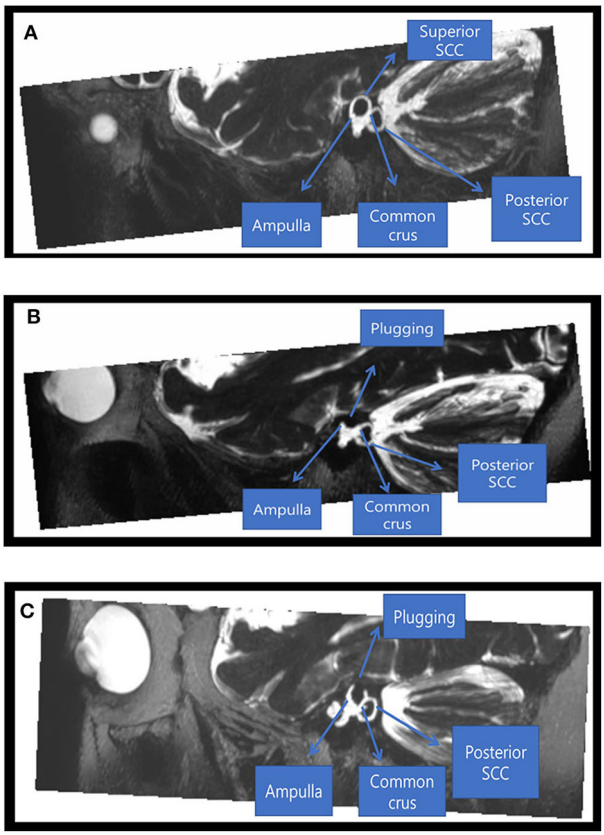

FIGURE 5 | Radiological findings before and after canal plugging. Preoperative **(A)** and postoperative **(B)** images of a 46-year-old male patient who underwent canal plugging. **(A)** Maximum projection intensity reconstruction of oblique sagittal reformatted 3D T2-weighted volume isotropic turbo spin-echo acquisition (T2-VISTA) images (5 mm thick slab) shows T2-bright signal intensity in the patent superior semicircular canal lumen with dehiscence. **(B)** After plugging, the superior semicircular canal lumen was obliterated by filling the defect between the ampulla anteriorly and the common crus posteriorly. **(C)** Postoperative images of a 45-year-old female patient who underwent canal plugging. After plugging, the superior semicircular canal lumen was obliterated by filling the defect between the ampulla anteriorly and the common crus posteriorly.

DISCUSSION

This study explored the postoperative outcomes of individuals with SCD by measuring longitudinal changes in vestibular function after surgical plugging of the dehiscent SC. Consistent with previous reports, individuals with SCD syndrome exhibited marked improvements in terms of subjective symptoms, low-frequency ABGs, cVEMP thresholds, and SP/AP ratios after surgery (2, 16–19). Analyses of repeated quantitative measures of VOR gains over 1 year showed immediate deterioration in VOR gain in the plugged SC that stabilized thereafter in most cases, although VOR gains for the other canals were not affected. Thus, our results suggest that successful plugging of dehiscent SCs is closely associated with a transient, rather than persistent, disturbance of semicircular canal responses exclusively involved in the plugged SC.

It is important to note that we found a propensity for immediate attenuation of VOR gain exclusively in plugged SCs, which suggests that surgical plugging tended to affect the vestibular function of the SC only. Contrary to previous studies (10, 11), VOR gains in the ipsilateral HC and PC were well-preserved in most cases, even immediately after surgery. The plugging procedure led to the elimination of pathologic flow of perilymph in the canal, as evidenced by the complete obliteration of the patent SC lumen by filling the defect at the site of surgical plugging. This finding is consistent with postoperative improvements, which recapitulates the abolishment of the third mobile window effect, including the resolution of associated symptoms, closure of the ABG, and normalization of the cVEMP threshold and SP/AP ratio. In other words, well-preserved VOR gains in the ipsilateral canals, except for plugged SCs, might not be attributed to incomplete compression of the membranous labyrinth (i.e., surgical resurfacing) associated with an increased likelihood of cupula deflection (8). Alternatively, the discrepancy in VOR gains between plugged and non-plugged canals may be associated with a degree in the loss of perilymph during plugging and labyrinthine inflammation.

Unexpectedly, we observed a tendency for a mild decrease in VOR gain in the contralateral PC, although this difference was not statistically significant. A recent study proposed a central compensatory mechanism based on shortened corrective saccade latency and transition from an overt to covert saccade within 1 week after surgical plugging (11). With regard to the presence of refixation saccades, none of the subjects in our cohort had covert and overt saccades during impulses for SC. In this study, nine subjects underwent a video head impulse test immediately after surgery, and five had abnormal VOR gains <0.7 in the plugged SC. Of these subjects, three showed elicitation of compensatory saccades within the first week after surgery; however, the shortening of saccade latency could not be evaluated because of a lack of follow-up during the early phase (**Figure S2**). Contrary to the higher presence of compensatory saccades on postoperative days 1-2 reported by Mantokoudis et al. (11) the relatively higher interval between the preoperative and first postoperative evaluations in this study (4.2 ± 0.4 days; range, 3–6 days) may hinder the investigation of compensatory saccade metrics. In other words, the shortening of saccade latency and occurrence ration revealed by Mantokoudis et al. (11) could not be evaluated because of a lack of follow-up during the early phase. Overall, these findings suggest that a temporarily reduced VOR in the contralateral PC may have occurred given the loss of anti-compensatory inhibition due to central mechanisms (11). However, further confirmation is needed because several factors, including predictive cues in the brain (20, 21), residual VOR gain (22), vestibular rehabilitation treatment (23), and age (24), may be associated with central compensation. As such, future studies investigating the natural course of VOR gains for plugged canals coupled with compensatory saccade metrics after adjusting for confounders are warranted to determine whether the VOR gains for plugged canals are persistently variable.

Our data suggest that the immediate deterioration in VOR gain in the plugged SC was generally a transitory response. The plugged SC gain subsequently stabilized in most cases,

which suggests a two-phase natural course of VOR gain for plugged SCs after surgery. As shown in **Figure 6**, this may be attributable to maintenance of the inertial flow of endolymph across the SC cupula without additional intraluminal fibrosis, despite mechanical obstruction in the middle arm of the SC by surgical plugging. Indeed, previous animal studies have shown that recovery of VOR gain after selective canal plugging could at least be attributable to regained residual sensitivity of the plugged semicircular canals to angular head acceleration (25). Furthermore, it is worth noting that the VOR gain is well-preserved in cases with aplasia or hypoplasia of the horizontal canal or distension of the vestibule, in which cVEMPs and caloric response are not induced (26, 27). Therefore, if not totally absent, trans-cupula inertia may allow cupular displacement by endolymph flow, ultimately normalizing VOR gain via angular rotation. Our findings, coupled with the results of previous studies, support the notion that recovery of SC gain after plugging surgery originates mainly from peripheral recovery processes and changes in the response dynamics of the semicircular canal (i.e., regained trans-cupula inertia) (25, 28). The findings in the animal study further demonstrate that a progressive loss in the VOR gain over the weeks following the additional plugging surgery may be related to fibrosis of the ampulla (25). Given this, adjuvant treatment, such as steroid injections, may be effective in preventing VOR gain from additional intraluminal fibrosis, given the pathologic changes in the inner ear due to the plugging procedure. However, further confirmation is required to clarify these findings. In contrast to our findings, previous studies demonstrated that reduced VOR gain for plugged SCs remained unchanged over time (6, 11). A previous study suggested that global vestibular hypofunction in the immediate postoperative period was largely associated with permanent loss of function over time (10). Similarly, only one subject in the present study showed immediately reduced VOR gain in either the plugged SC or ipsilateral PC after surgery. The reduced VOR gain in the plugged SC then slowly returned to its normal value after ∼2 months compared to other subjects who presented with reduced VOR gain in the plugged SC. That is, the discrepancy in recovery patterns of SC gain among studies may be attributable to the degree of functional deterioration in the labyrinth immediately after surgery. In addition, several limitations of the previous studies, such as small sample sizes and incomplete follow-up data, hinder the ability to draw firm conclusions (11).

In the present study, the results of individual analyses demonstrated that the immediately reduced VOR gains in plugged SCs did not necessarily return to normal baseline values even in the long term (**Figure 3**). Two subjects showed seemingly fluctuating patterns in SC gain over 1 year following surgery. A markedly decreased VOR gain in the plugged SC was found not only immediately after surgery but also at the last follow-up evaluation. However, these subjects did not experience any postoperative complications associated with sensorineural hearing loss. In addition, the normalization of ABGs, SP/AP ratios, and cVEMP thresholds indicated that plugging the dehiscent canal eliminated abnormal pressure transmission via the third mobile window.

In this case series, autophony was the most frequent subjective symptom. Indeed, only one subject did not report autophony before surgery, and this subject had two anterior small tympanic membrane perforations (subject 1). This finding raises the possibility of inserting ventilation tubes to resolve autophony in SCD. Moreover, it is important to take into account clinical manifestations and laboratory findings in patients with SCD complicated by tympanic membrane perforation. Subject 1 had tympanic membrane perforations and a large ABG; however, the SP/AP ration and cVEMP thresholds were within normal range, which can only be expected in SCD. A large ABG may represent the summating effects of tympanic membrane perforation and the presence of a third mobile window. Normal ECoG and cVEMP threshold ranges in this patient can be explained by an increased response of the ECoG and cVEMP threshold by the SCD that was negated by a decreased response due to attenuated mechanical energy delivery through the oval window secondary to tympanic membrane perforation. After plugging, the BC threshold normalized, and the ABG disappeared. However, the SP/AP ratio and cVEMP thresholds remained within the normal range after surgery. The effects of an increased intralabyrinthine response by the SCD and a decreased intralabyrinthine response by the tympanic membrane perforation were similar in this patient.

Moreover, the dehiscence size in those subjects did not differ compared to our subjects. These findings raise the possibility that fluctuating patterns of vestibular function may be due to

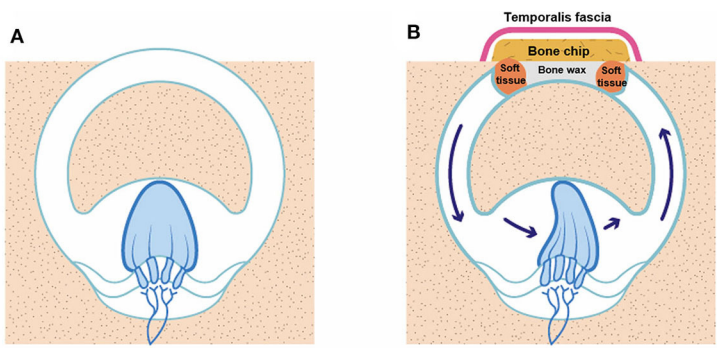

FIGURE 6 | An illustration of how VOR gain is preserved even after canal plugging. **(A)** SCD before surgery, **(B)** SCD after canal plugging. A whole semicircular canal may not be necessary to deflect the cupula on head impulse stimulation.

endolymphatic hydrops in the affected ears (29). Given the higher sample variation in VOR gain in vertical canals, further studies are warranted to validate our findings. Understanding the differential nature of SC gain presenting with fluctuating patterns may provide additional evidence of the necessity for longitudinal and repetitive checkups following surgical plugging in subjects with SCD.

This study has some limitations that should be addressed in future studies. First, it was limited by a relatively small number of subjects and high sample variability of VOR gains, in particular in the vertical canals, which could have potentially led to misinterpretation. Due to the small number of cases involved in video head impulse tests, we identified that our observed SC gains had significant variability and did not exactly follow a Gaussian distribution at each time point (**Table S1**). Moreover, data on longitudinal changes in VOR gain beyond 12 months are needed to confirm the differential pattern of SC gain after surgery among subjects with SCD. Thus, a study with a longer follow-up period and a larger case series is warranted to validate our observations. Second, the interpretation of the two-phase natural course of plugged SC gain was not specified in detail in the current report. Evidence of central compensation for reduced VOR gain based on the occurrence of corrective saccades and decreased latencies of these corrective saccades over 1 week was recently reported (11). Further studies using the longitudinal changes in VOR gain of our subjects as a reference for parameters affecting central compensations may be important for optimizing individualized vestibular strategies.

Despite these limitations, we have elucidated here the changes in auditory and vestibular function that may be relevant to improving debilitating symptoms after successful canal plugging via the middle cranial fossa approach in subjects diagnosed with SCD. To the best of our knowledge, this study is the first to report the differential natural course of VOR gain between plugged SCs and non-plugged canals after surgical plugging. These findings may have clinical implications with respect to timely and individualized rehabilitation treatment.

CONCLUSION

Surgical plugging of dehiscent SCs via the middle cranial fossa approach was an effective treatment option in subjects with SCD. This option ensured that symptoms resolved without significant complications. Indeed, audiometric and electrophysiological findings were normalized after surgery. Specifically, VOR function for plugged SCs decreased immediately after surgical plugging but subsequently normalized in most subjects with SCD. By contrast, non-operated canals tended to remain stable. Understanding the differential natural course of VOR gain, in particular in operated canals, may allow for timely and precise vestibular rehabilitation.

DATA AVAILABILITY STATEMENT

The original contributions presented in the study are included in the article/**Supplementary Material**, further enquiries can be directed to the corresponding author.

ETHICS STATEMENT

The studies involving human participants were reviewed and approved by the Seoul National University Bundang Hospital Institutional Review Board (IRB No. B-2004-604-125) and was conducted in accordance with the principles of the Declaration of Helsinki. The patients/participants provided their written informed consent to participate in this study. Written informed consent was obtained from the individual(s) for the publication of any potentially identifiable images or data included in this article.

AUTHOR CONTRIBUTIONS

J-WK and S-YL: Conceptualization. S-YL: Methodology, Software, Formal Analysis, Project Administration, Writing? Original Draft Preparation, and Investigation. J-WK: Validation, Resources, Funding Acquisition, and Supervision. S-YL, MK, and YB: Data Curation. J-WK, J-JS, and BC: Writing-Review and Editing. S-YL and YB: Visualization. All authors: contributed to the article and approved the submitted version.

FUNDING

This research was supported by SNUBH Grant No. 13-2020-006 (to J-WK).

ACKNOWLEDGMENTS

This work was partly supported by a clinical research grant provided from Seoul National University Bundang Hospital and Seoul National University College of Medicine. The English in this document has been checked by at least two professional editors, both native speakers of English. For a certificate, please see: http://www.textcheck.com/certificate/GFw8rd.

SUPPLEMENTARY MATERIAL

The Supplementary Material for this article can be found online at: https://www.frontiersin.org/articles/10.3389/fneur.2020.00694/full#supplementary-material

Figure S1 | Preoperative and postoperative findings for a 58-year-old female patient with superior canal dehiscence (SCD) and tympanic membrane perforation who underwent superior canal (SC) plugging and type 1 tympanoplasty. **(A)** SCD by the superior petrosal sinus (SPS) shown on high-resolution temporal bone computed tomography images reformatted in the plane of the SC. **(B)** Preoperative tympanic membrane findings. **(C)** Postoperative tympanic membrane findings. **(D)** Pre- and postoperative audiograms.

Figure S2 | Video head impulse tests in the plane of the affected superior canal within the first week after surgery (subjects 6, 7, and 8).

Video S1 | Surgical plugging for superior semicircular dehiscence via the middle cranial fossa approach.

Table S1 | Variability of plugged superior canal (SC) gains at each time point.

REFERENCES

1. Ward BK, Carey JP, Minor LB. Superior canal dehiscence syndrome: lessons from the first 20 years. *Front Neurol*. (2017) 8:177. doi: 10.3389/fneur.2017.00177
2. Park JH, Kang SI, Choi HS, Lee SY, Kim JS, Koo JW. Thickness of the bony otic capsule: etiopathogenetic perspectives on superior canal dehiscence syndrome. *Audiol Neurotol*. (2015) 20:243–50. doi: 10.1159/000371810
3. Songer JE, Rosowski JJ. A superior semicircular canal dehiscence-induced air-bone gap in chinchilla. *Hear Res*. (2010) 269:70–80. doi: 10.1016/j.heares.2010.07.002
4. Minor LB. Superior canal dehiscence syndrome. *Otol Neurotol*. (2000) 21:9–19. doi: 10.1016/S0196-0709(00)80105-2
5. Welgampola MS, Myrie OA, Minor LB, Carey JP. Vestibular-evoked myogenic potential thresholds normalize on plugging superior canal dehiscence. *Neurology*. (2008) 70:464–72. doi: 10.1212/01.wnl.0000299084.76250.4a
6. Carey JP, Migliaccio AA, Minor LB. Semicircular canal function before and after surgery for superior canal dehiscence. *Otol Neurotol*. (2007) 28:356–64. doi: 10.1097/01.mao.0000253284.40995.d8
7. Crane BT, Minor LB, Carey JP. Superior canal dehiscence plugging reduces dizziness handicap. *Laryngoscope*. (2008) 118:1809–13. doi: 10.1097/MLG.0b013e31817f18fa
8. Goddard JC, Wilkinson EP. Outcomes following semicircular canal plugging. *Otolaryngol Head Neck Surg*. (2014) 151:478–83. doi: 10.1177/0194599814538233
9. Vlastarakos PV, Proikas K, Tavoulari E, Kikidis D, Maragoudakis P, Nikolopoulos TP. Efficacy assessment and complications of surgical management for superior semicircular canal dehiscence: a meta-analysis of published interventional studies. *Eur Arch Otorhinolaryngol*. (2009) 266:177. doi: 10.1007/s00405-008-0840-4
10. Agrawal Y, Migliaccio AA, Minor LB, Carey JP. Vestibular hypofunction in the initial postoperative period after surgical treatment of superior semicircular canal dehiscence. *Otol Neurotol*. (2009) 30:502–6. doi: 10.1097/MAO.0b013e3181a32d69
11. Mantokoudis G, Saber Tehrani AS, Wong AL, Agrawal Y, Wenzel A, Carey JP. Adaptation and compensation of vestibular responses following superior canal dehiscence surgery. *Otol Neurotol*. (2016) 37:1399. doi: 10.1097/MAO.0000000000001196
12. Park P, Park JH, Kim JS, Koo JW. Role of video-head impulse test in lateralization of vestibulopathy: comparative study with caloric test. *Auris Nasus Larynx*. (2017) 44:648–54. doi: 10.1016/j.anl.2016.12.003
13. McGarvie LA, MacDougall HG, Halmagyi GM, Burgess AM, Weber KP, Curthoys IS. The video head impulse test (vHIT) of semicircular canal function–age-dependent normative values of VOR gain in healthy subjects. *Front Neurol*. (2015) 6:154. doi: 10.3389/fneur.2015.00154
14. ElSherif M, Reda MI, Saadallah H, Mourad M. Video head impulse test (vHIT) in migraine dizziness. *J Otol*. (2018) 13:65–7. doi: 10.1016/j.joto.2017.12.002
15. Yollu U, Uluduz DU, Yilmaz M, Yener HM, Akil F, Kuzu B, et al. Vestibular migraine screening in a migraine-diagnosed patient population, and assessment of vestibulocochlear function. *Clin Otolaryngol*. (2017) 42:225–33. doi: 10.1111/coa.12699
16. Park JH, Lee SY, Song JJ, Choi BY, Koo JW. Electrocochleographic findings in superior canal dehiscence syndrome. *Hear Res*. (2015) 323:61–7. doi: 10.1016/j.heares.2015.02.001
17. Koo J-W, Hong SK, Kim D-K, Kim JS. Superior semicircular canal dehiscence syndrome by the superior petrosal sinus. *J Neurol Neurosurg Psychiatry*. (2010) 81:465–7. doi: 10.1136/jnnp.2008.155564
18. Park JH, Kim HJ, Kim JS, Koo JW. Costimulation of the horizontal semicircular canal during skull vibrations in superior canal dehiscence syndrome. *Audiol Neurotol*. (2014) 19:175–83. doi: 10.1159/000358002
19. Koo JW. Superior semicircular canal dehiscence syndrome. *Korean J Otorhinolaryngol Head Neck Surg*. (2011) 54:117–23. doi: 10.3342/kjorl-hns.2011.54.2.117
20. Mantokoudis G, Agrawal Y, Newman-Toker DE, Xie L, Saber Tehrani AS, Wong A, et al. Compensatory saccades benefit from prediction during head impulse testing in early recovery from vestibular deafferentation. *Eur Arch Otorhinolaryngol*. (2016) 273:1379–85. doi: 10.1007/s00405-015-3685-7
21. Colagiorgio P, Versino M, Colnaghi S, Quaglieri S, Manfrin M, Zamaro E, et al. New insights into vestibular-saccade interaction based on covert corrective saccades in patients with unilateral vestibular deficits. *J Neurophysiol*. (2017) 117:2324–38. doi: 10.1152/jn.00864.2016
22. Martin-Sanz E, Rueda A, Esteban-Sanchez J, Yanes J, Rey-Martinez J, Sanz-Fernandez R. Vestibular restoration and adaptation in vestibular neuritis and ramsay hunt syndrome with vertigo. *Otol Neurotol*. (2017) 38:e203–8. doi: 10.1097/MAO.0000000000001468
23. Trinidad-Ruiz G, Rey-Martinez J, Batuecas-Caletrio A, Matino-Soler E, Perez-Fernandez N. Visual performance and perception as a target of saccadic strategies in patients with unilateral vestibular loss. *Ear Hear*. (2018) 39:1176–86. doi: 10.1097/AUD.0000000000000576
24. Anson ER, Bigelow RT, Carey JP, Xue QL, Studenski S, Schubert MC, et al. Aging increases compensatory saccade amplitude in the video head impulse test. *Front Neurol*. (2016) 7:113. doi: 10.3389/fneur.2016.00113
25. Hess BJ, Lysakowski A, Minor LB, Angelaki DE. Central versus peripheral origin of vestibuloocular reflex recovery following semicircular canal plugging in rhesus monkeys. *J Neurophysiol*. (2000) 84:3078–82. doi: 10.1152/jn.2000.84.6.3078
26. Shaw B, Raghavan R. Dissociation between caloric and head impulse testing in patients with congenital abnormalities of the semicircular canals. *J Laryngol Otol*. (2018) 132:932–5. doi: 10.1017/S0022215118001317
27. Suzuki M, Saito Y, Ushio M, Yamasoba T, Hatta I, Nakamura M. Vestibulo-ocular reflex (VOR) preserved in bilateral severe vestibular malformations with internal auditory canal stenosis. *Acta Otolaryngol*. (2007) 127:1226–30. doi: 10.1080/00016480701200343
28. Angelaki DE, Hess B, Arai Y, Suzuki J. Adaptation of primate vestibuloocular reflex to altered peripheral vestibular inputs. I Frequency-specific recovery of horizontal VOR after inactivation of the lateral semicircular canals. *J Neurophysiol*. (1996) 76:2941–53. doi: 10.1152/jn.1996.76.5.2941
29. Sone M, Yoshida T, Morimoto K, Teranishi M, Nakashima T, Naganawa S. Endolymphatic hydrops in superior canal dehiscence and large vestibular aqueduct syndromes. *Laryngoscope*. (2016) 126:1446–50. doi: 10.1002/lary.25747

Conflict of Interest: The authors declare that the research was conducted in the absence of any commercial or financial relationships that could be construed as a potential conflict of interest.

frontiers in Neurology

ORIGINAL RESEARCH
published: 20 August 2020
doi: 10.3389/fneur.2020.00871

Membranous or Hypermobile Stapes Footplate: A New Anatomic Site Resulting in Third Window Syndrome

Arun K. Gadre[1], Ingrid R. Edwards[2], Vicky M. Baker[1] and Casey R. Roof[3]*

[1] Department of Otolaryngology—Head and Neck Surgery, Geisinger Medical Center, Geisinger Commonwealth School of Medicine, Danville, PA, United States, [2] Heuser Hearing Institute and Speech and Language Academy, Louisville, KY, United States, [3] Clinical Audiologist, Department of Otolaryngology—Head and Neck Surgery and Communication Sciences, University of Louisville, Louisville, KY, United States

OPEN ACCESS

Edited by:
P. Ashley Wackym, The State University of New Jersey, United States

Reviewed by:
Brian McKinnon, University of Texas Medical Branch at Galveston, United States
Jose N. Fayad, Johns Hopkins Aramco Healthcare (JHAH), Saudi Arabia

****Correspondence:***
Arun K. Gadre
agadre@geisinger.edu

Specialty section:
This article was submitted to Neuro-Otology, a section of the journal Frontiers in Neurology

Received: *15 June 2020*
Accepted: *08 July 2020*
Published: *20 August 2020*

Citation:
Gadre AK, Edwards IR, Baker VM and Roof CR (2020) Membranous or Hypermobile Stapes Footplate: A New Anatomic Site Resulting in Third Window Syndrome. Front. Neurol. 11:871. doi: 10.3389/fneur.2020.00871

Objectives: To describe a potentially underappreciated pathology for post-traumatic persistent intractable dizziness and third window syndrome as well as the methods to diagnose and surgically manage this disorder.

Study Design: Observational analytic case studies review at a tertiary care medical center.

Methods: Patients suffering persistent dizziness following head trauma and demonstrating Tullio phenomena or Hennebert signs are included. All had reportedly normal otic capsules on high resolution temporal bone CT scans (CT). The gray-scale invert function was used to visualize the stapes footplate, which helped determine the diagnosis. Gray-scale inversion can be used to improve visualization of temporal bone anatomy and pathologic changes when diagnoses are in doubt. A search to check for the presence of perilymph leakage was performed in all cases. This was accomplished using intraoperative Valsalva maneuvers. Fat grafting of round and oval windows was performed.

Results: Over an 11-year period between January 2009 and December 2019, 28 patients (33 ears) were treated. Follow-up with balance testing and audiograms were performed 6–8 weeks following surgery. Follow-up ranged from 6 months to 7 years. Prior to surgery all patients reported dizziness in response to loud sounds and/or barometric pressure changes. Seven out of 33 ears had demonstrable perilymph leakage into the middle ear; the rest (26 ears) appeared to have membranous or hypermobile stapes footplates. Membranous stapes footplates were better visualized using the invert function on CT. Thirteen patients had a fistula sign positive bilaterally while 15 had unilateral pathology. Twenty-four of the 28 patients (85.7%) showed both subjective and objective improvement following surgery. No patients suffered from a deterioration in hearing.

Conclusions: A previously underappreciated membranous or hypermobile stapes footplate can occur following head trauma and can cause intractable dizziness typical of third window syndrome (TWS). Durable long term success can be achieved by utilizing fat graft patching of the round and oval windows. High resolution temporal bone CT scans using the gray-scale inversion (invert) function can assist in preoperative diagnosis.

Keywords: head trauma, vertigo, stapes footplate defect, hypermobile stapes, third window syndrome, perilymph fistula, gray-scale invert function CT scan

INTRODUCTION

Acute dizziness may be associated with head trauma, which can even be trivial (1, 2). Following head trauma, persistent, intractable, and sometimes intermittent vertigo or dizziness constitutes a diagnostic and therapeutic challenge. The nature of the injury is often mild and may not result in concussion or loss of consciousness. Many of these patients seek treatment without relief, and when all else fails, they may be inappropriately labeled as suffering from post-concussive syndrome (PCS), or chronic traumatic encephalopathy (CTE). A presumptive diagnosis of perilymph fistula with leakage of perilymph may also be entertained.

We have identified a unique cohort of patients who develop immediate or delayed symptoms which overlap quite closely with those suffering from third window syndrome (TWS) of which superior semicircular canal dehiscence syndrome is best characterized (3). Symptoms include disabling dizziness or vertigo often induced by barometric pressure changes as well as loud sounds. Vertigo spells are generally persistent and are often associated with cognitive deficits. During exploratory surgery we found that presumed leakage of perilymph at the oval or round windows is relatively uncommon; however small or large defects covered over by a membrane are often observed in the stapes footplate. Alternatively, a hypermobile stapes footplate may be discovered.

Our article summarizes clinical and surgical findings in a series of 28 patients. Three illustrative cases have been included. Vestibular testing using bithermal caloric testing is typically non-diagnostic or may show diminished function. However, positive Tullio, and Hennebert tests (fistula test) are often the first clue to diagnosis. The findings on cervical vestibular evoked myogenic potentials (cVEMP) is highly variable and needs to be investigated further. The "invert" function on high resolution CT is suggested as an additional means to identify stapes footplate defects prior to surgery. In a majority of cases fat-grafting of the round and oval windows appears to be curative without resulting in hearing loss.

METHODS

This study represents our experience over an 11-year period (January 1, 2009 through December 31, 2019). The procedures followed were in accordance with the ethical standards of the responsible committee on human experimentation and with the Helsinki Declaration. The Heuser Hearing Institute Institutional Review Board approved these observational analytic case studies (IRB IORG0006526). The Institutional Review Board granted a consent waiver and also approved the use of age and gender as deidentified data. Preliminary findings on the first 9 patients were presented at the 7th International Symposium on Meniere's Disease and Inner Ear Disorders (Rome, Italy October 17–20, 2015) and the Combined Otolaryngology Spring Meeting (COSM Scottsdale, AZ, January 18–20, 2018) but were not published. These cases are included in this scientific paper.

Patients suffering from persistent or intermittent incapacitating vertigo or dizziness following head trauma and demonstrating symptoms suggestive of ear fullness, fluctuating hearing loss, sound intolerance, and hyperacusis are included. Patients sometimes complain of autophony. In addition, several patients reported that the horizon was tilted. They variously described their symptoms as an inability to tolerate loud sounds. They also variously described being dizzy, lightheaded or vertiginous. During waking hours several patients describe a continuous sense of being on a "teeter-totter." Others described being in a "funhouse," "wobbly," "foggy," or describe a "fuzzy- sensation" with an inability to concentrate, where even slight movements of the head would make them dizzy. They all describe the need to hold on to a stable support to avoid falling during standing and ambulation. Patients reporting immediate or delayed onset of dizziness following the inciting trauma are included. None of the patient suffered from dizziness or vestibular symptoms prior to the injury.

All patients underwent a thorough neurotological examination, as well as audiological and vestibular evaluations. This included Siegel's pneumatic otoscopy in the clinic to elicit a Hennebert sign. Vestibular evaluation included a videonystagmography test battery (VNG). All patients underwent testing for subjective or objective Tullio and Hennebert signs. Cervical evoked myogenic potentials (cVEMPs) were added to the diagnostic test battery as these studies became available to our centers.

Audiological assessments included comprehensive audiometry (GSI Audiostar Audiometer, Eden Prairie MN), tympanometry (GSI Tympstar Tympanometer, Eden Prairie MN) in a sound-proof booth, videonystagmography (VNG) including positioning, and caloric irrigations (Micromedical VNG Visual Eyes 4 channel spectrum, Eden Prairie MN). Special testing was completed pre- and post-operatively on a per patient basis with some variability based on patient symptoms, falls risk, patient apprehension, and the examiner. A minority of patients

were tested with cVEMPs pre-and post-operatively. There was a lower rate of follow-up (<50%) for vestibular assessment after surgery due to reported trepidation to repeat testing, loss to follow-up, and patient relocations.

Fistula assessments were utilized as the patient was seated, standing, or on a calibrated foam surface (NeuroCom Balance Manager Dynamic Platform Post-urography system) with vision denied and the use of video eye recording for most patients. Fistula assessments utilized tympanometry as well as ipsilateral and contralateral acoustic reflexes. Acoustic energy utilizing a standard probe tone of 226 Hz was introduced into an ear canal cavity by way of a loudspeaker and a microphone housed within a probe box. The ear canal cavity was hermetically sealed for testing. The pressure transducer, also housed within the probe box was utilized. Measures on tympanometry show maximum mobility of the tympanic membrane when pressure induced into the ear canal equals that in the middle ear (atmospheric pressure relative to middle ear pressure). If a patient reported dizziness during testing, this was a positive subjective Hennebert sign. Ipsilateral and contralateral acoustic reflexes were obtained at loudness intensities of 70–110 dB HL from 500 to 2,000 Hz with a hermetically sealed and pressurized ear from tympanometry recording. During presentation of the acoustic reflex stimuli, a subjective report of dizziness, or objective sway or eye-movements were reported as a positive Tullio phenomenon. Objective recording for nystagmus was also utilized in visually denied patients.

cVEMPs were performed using Bio-logic Navigator Pro Auditory Evoked Potential (AEP) system. The patient was placed supine in a MaxiSelect automatic chair. After skin preparation with 3M Red Dot™ Trace Prep and Nuprep skin gel, Natus jelly tab sensors were attached to Natus Alligator clips and placed in a one channel montage. One electrode was placed over the middle of the sternocleidomastoid (SCM) on the left and right. The ground electrode was placed at the forehead. Air-conducted rarefaction 500 Hz tone bursts were presented unilaterally via an ER 3A-insert earphone. The patient was given instructions to lift the head only and rotate it to the contralateral side producing tonic activation of the SCM muscle. Stimulus was presented at 95 dB nHL to the left ear first. cVEMP response thresholds were recorded from the ipsilateral SCM using a serial down by 10 dB procedure until a presentation stimulus of 65 dB was reached. The same process was then repeated on the right side.

All patients underwent high-resolution temporal bone CT scans without contrast looking specifically for temporal bone fractures, findings of site(s) of dehiscence in the bone of the otic capsule or congenital anomalies. Since intractable dizziness occurred following trauma a presumptive clinical diagnosis of traumatic perilymph fistula with perilymph leakage was made. Only those patients with positive Tullio and/or Hennebert tests were offered surgery. Retrocochlear pathology was ruled out using magnetic resonance imaging (MRI). One patient (**Table 1**, Patient 3) with bilateral superior semicircular dehiscence was included as she was completely asymptomatic prior to head trauma. cVEMPS were not performed in every case due to the lack of availability of the test early in our series.

The gray-scale inversion or "invert" function on the PACS (picture archiving and communication system) which uses the universal DICOM® (Digital Imaging and Communication in Medicine) was used to improve visualization of the stapes footplate on high resolution temporal bone CT scans. Patients who had persistent signs and symptoms suggestive of TWS were offered exploratory surgery. In patients suspected of bilateral pathology the more symptomatic side was operated upon first. If symptoms were controlled or resolved the second side was not operated upon. Exploratory surgery was offered only after a prolonged period of failed conservative management and after a detailed informed consent was obtained.

Middle ear exploration was performed under general anesthesia using both the Carl Zeiss OPMI Pentero 800 microscope (Carl Zeiss Meditec Inc. Dublin, CA) and 4 mm sinus endoscopes (Karl Storz Endoscopy-America, Inc. CA). Still photographs and video recording system using the integrated microscope video camera or a Storz 3-CCD camera (Karl Storz Endoscopy-America, Inc. CA) were used for photo and video documentation. A transcanal exploratory tympanotomy approach was used and the posterior superior bony canal overhang was removed with a curette in order to visualize the oval and round window niches. Mucosal adhesion bands obscuring visualization of the footplate and round window membrane were lysed. Intraoperatively we looked for the presence or absence of perilymph leakage. If none was present, 3 sequential Valsalva maneuvers lasting 5 s were performed by the anesthesiologist 1 min apart. After observing membranous stapes footplates in the first few cases, we began to actively look for their presence in subsequent patients. If present paradoxical movement of the membrane was elicited by gently balloting the posterior crus of the stapes using a Rosen pick or Derlacki mobilizer (**Video 1**). Patients were classified as having a perilymph leak if fluid could be seen actively pooling in the round or oval window niches. A questionable leak was diagnosed if a small amount of fluid was present which did not refill after suctioning despite multiple Valsalva maneuvers. If neither were present a perilymph leak was ruled out. In symptomatic patients, if a membranous stapes footplate or a perilymph leak was not observed, the diagnosis of a hypermobile stapes footplate was inferred.

In all cases the mucosa around the oval and round window niches were denuded. Tiny fat grafts harvested from the cranial aspect of the ear lobule, were packed under the arch of the stapes, and anterior and posterior to the stapes crurae, and also in the round window niche. Gelfoam® (Pharmacia and Upjohn, Kalamazoo, MI) soaked in saline was placed in the middle ear to stabilize the grafts and the tympanomeatal flap was replaced. A small amount of Gelfoam® (Pharmacia and Upjohn, Kalamazoo, MI) soaked in saline was then placed over the incision site.

Post-operatively patients were placed on bed rest and stool softeners for 2 weeks. Patients were cautioned against vigorous nose blowing, straining, and lifting weight heavier than 10 lbs. Follow-up examination was performed in 1 week. At 6–8 weeks the patient's impressions were recorded and a clinical exam included pneumatic otoscopy and an audiometric evaluation was performed. Post-operative testing in the vestibular laboratory was ordered at 2 months.

TABLE 1 | Demographics surgical findings and results.

No	Age (yrs)	Symptom duration (MTS)	Possible etiology	Associated symptoms	Fistula sign	Surgery side	Findings	Results & notes
1	31	26	Pain while snorkeling	Light headed, hyperacusis	AU AD>AS	AD	AD: membranous footplate, no perilymph leak	Complete Resolution, Occasional light headedness
2	55	12	Severe blow over occiput from falling door and frame	Headaches, "foggy feeling," hyperacusis	AU	AU	AD: membranous in center of footplate, no perilymph leak. AS: membranous, no leak	Complete Resolution
3	69	21	Mild head trauma, possible osteoporosis, bilateral SSCD	Spinning sensation, hyperacusis	AD	AD	AD: stapes footplate intact but hypermobile, no perilymph leak	Complete Resolution
4	38	12	Motor vehicle accident	Hyperacusis	AU AD>AS	AD	AD: membranous footplate, no perilymph leak	Complete Resolution
5	36	30	Electric shock at work with fall at work striking head	Hyperacusis	AU AS>AD	AS	AS: membranous footplate, no perilymph leak	Complete Resolution
6	16	2	Weight lifting, concussions playing football	Migraine, light headed, hyperacusis	AS	AS	AS: footplate intact, perilymph fluid leak	Complete Resolution
7	50	26	Motor vehicle accident	Headaches, light headed, hyperacusis	AU AS>AD	AS	AS: footplate intact, perilymph fluid leak	Complete Resolution for 2 months. Now has migraine headaches and recurrent symptoms
8	41	15	Blast injury in Afghanistan, two concussions	Traumatic brain injury, post-concussive migraine	AU AD>AS	AD	AD: membranous defect in center of footplate, no perilymph leak	Complete Resolution, Occasional light headedness
9	39	11	Hit on right temple by engine block on conveyer belt	Cannot ride in an elevator, hyperacusis	AD	AD	AD: membranous footplate, no perilymph leak	Complete Resolution. Has problems tracking fast moving objects and has eye floaters
10	68	28	Possible osteoporosis	Spinning sensation, hyperacusis	AD	AD	AD: stapes footplate intact, perilymph leak	Complete Resolution
11	58	11	Multiple falls and concussion	Migraine, meniere, left BPPV, hyperacusis	AU AD>AS	AD	AD: stapes footplate intact, perilymph leak	Complete Resolution
12	56	21	Concussion, several falls, vehicle accident	Hyperacusis	AU AS>AD	AU	AS: membranous footplate, no perilymph leak, AD: membranous footplate, no perilymph leak	Complete Resolution. Twenty three months later patient involved in MVA. Resolved after revision surgery AS
13	16	32	Heat stroke and fall with occiput hitting concrete	Could not tolerate tuning fork test	AU AD>AS	AD	AD: membranous footplate, no perilymph leak	Complete Resolution
14	49	22	Barotrauma after flight, mild head trauma	Hearing fluctuates, sensation of passing out	AU	AU	AD: membranous footplate posterior half, no leak; AS membranous footplate no leak	Complete Resolution, able to fly to Belgium
15	60	25	Sudden left SNHL of uncertain etiology, possible mild trauma	Spinning sensation with pneumatic otoscopy	AS	AS	AS: two membranous defects in the footplate, no perilymph leakage	Complete Resolution for 7 months then recurred after a coughing fit. Managed conservatively

(Continued)

TABLE 1 | Continued

No	Age (yrs)	Symptom duration (MTS)	Possible etiology	Associated symptoms	Fistula sign	Surgery side	Findings	Results & notes
16	24	37	Head injury from falling out of second floor window	Suggestive of meniere disease, hyperacusis	AS	AS	AS: membranous footplate, with possible perilymph leak	Failed treatment. Two days following treatment lifted 46 lbs. Felt something pop in ears with recurrent symptoms. Lost to followup.
17	43	6	Head injury and unconsciousness from fall, car accident	Heavy metal exposure, history of BPPV	AD	AD	AD: footplate intact hypermobile footplate, no perilymph leak	Complete Resolution. One year post car accident, deployment of airbags, symptoms recurred but resolved completely
18	41	28	Multiple falls and minor head trauma	Migraine, scotomas, hyperacusis,	AD	AD	AD: membranous footplate, no perilymph leak	Complete Resolution. Cervical steal syndrome detected however
19	56	14	Head injury, found unconscious	History of meningitis and mastoiditis	AD	AD	AD: footplate intact, perilymph leak present	Complete Resolution
20	46	62	Severe car accident with loss of consciousness	Hyperacusis, tired, cannot fly	AS	AS	AS: intact footplate with possible perilymph leak	Complete Resolution. Able to fly
21	54	23	Severe car accident with whiplash and loss of consciousness	Spinning, hyperacusis, neck surgery, headaches	AU AS>AD	AS	AS: perilymph fluid contained in sac, possible perilymph leak, but footplate intact and hypermobile	Partial Resolution. Did not keep follow-up
22	27	18	Car accident with whiplash	Hyperacusis with Tullio and Hennebert	AD	AD	AD: irregular membranous deficiency in footplate, hypermobile but no perilymph leak	Complete Resolution
23	54	28	Car accident with whiplash and concussion	BPPV treated, fogginess, hyperacusis	AD	AD	AD: membranous dehiscence in bony footplate, no perilymph leak	Complete Resolution. One week post-op had minimal symptoms which resolved
24	34	30	Car accident with whiplash and multiple fractures and head trauma	BPPV treated, fogginess, hyperacusis	AU	AU	AD: Crack in stapes footplate, no perilymph leak, AS: crack in stapes footplate but perilymph leak at round window	Partial resolution. Patient feels much better but not quite normal. Lost to follow-up
25	24	43	Struck by car and fall from jet ski	BPPV treated, hyperacusis, dysautonomia	AD	AD	AD: crack in footplate, no perilymph leak	Failed treatment. Stayed symptomatic, postural hypotension
26	50	21	Blow to head	Hearing cell phone causes nystagmus	AD	AD	AD: membranous defect in footplate, no perilymph leak	Complete resolution after revision surgery. (Patient had coughing fit 2 weeks after surgery with recurrent symptoms)
27	22	6	Blow to ear with baseball glove	Falls to right with noise. 30% difference in VEMP	AD	AD	AD: ? crack in footplate, no perilymph leak, hypermobile stapes footplate	Complete Resolution
28	62	27	Blow wit football on right side	"Fun house" bending forward results in fall, staggering	AS	As	AS: membranous footplate, no perilymph leak	Complete Resolution. Immediate resolution 24 h post-surgery. VEMP normalized prominent OTR

?, questionable finding.

Illustrative Case 1

A 36-year old male factory worker (**Table 1**, Patient 5) was seen on 15 January 2013 with a 2.5 year history of dizziness and imbalance. The dizziness began a few weeks following a severe electrical shock at work, which caused a fall and he struck his occiput on the concrete floor. This was accompanied by a brief period of unconsciousness, however intracranial hemorrhage was ruled out. The patient was initially diagnosed as suffering from benign paroxysmal positional vertigo (BPPV) and underwent several Epley (4) canalith repositioning maneuvers without relief. Medical therapy for migraine variant dizziness (vestibular migraine) was also unsuccessful. He had not worked for over 2 years. He reported a constant dizzy sensation during all waking hours. Dizziness was associated with headaches, and irritability to both light and sound. Looking up or down and rotation of his head exacerbated his symptoms. Bending down in particular, performing a Valsalva maneuver, and something as trivial as traveling in an elevator worsened his symptoms. He reported the perception of a tilted horizon. Changes in atmospheric pressure such as an incoming storm caused ear fullness and increasing dizziness. He was unable to ride a bicycle. He also reported having to concentrate to avoid falling and feeling exhausted and irritable at the end of the day. As a result he reported feeling extremely depressed and confessed to suicidal ideation.

The patient held his head tilted to the left. Pneumatic otoscopy in the left ear elicited nystagmus associated with nausea. An audiogram demonstrated slightly asymmetric 4 kHz "noise notches" in both ears, but was more pronounced on the left side. Tullio and Hennebert tests were performed in the vestibular lab and found to be positive. The patient reported the sensation of being pushed to the right. Clinically, the possibility of a TWS or a perilymph fistula was suspected. A high resolution temporal bone CT scan was interpreted by the neuroradiologist as being normal. However, one of the authors (AKG) found that a bony defect was observed in the left stapes footplate when compared with the right. This became more apparent when the "invert" function was used on the PACS system (**Figure 1**). On 23 May 2013, he underwent middle ear exploration and a floppy membrane appeared to have replaced the bony stapes footplate. There was no evidence of perilymph leakage. Fat grafts from the lobule were used to reinforce both the round and oval windows as previously described. At follow-up examination in 8 weeks the patient reported that his symptoms had completely resolved (**Video 2**). Hearing fluctuation and noise intolerance resolved completely and he was able to ride a bicycle. Due to a fear of symptom recurrence the patient refused post-operative objective testing. He requested to be released back to work, and was symptom-free for 12 months when he was lost to follow-up.

Illustrative Case 2

A 27-year-old female audiologist (**Table 1**, Patient 22) suffered a whiplash injury after being involved in a motor vehicle collision in February 2014. In August 2014 she began complaining of dizziness which increased progressively. Although her symptoms were not consistent with benign paroxysmal positional vertigo, she underwent several canalith repositioning maneuvers at another institution without relief. In December 2014, she felt extremely nauseated on an airplane flight. She was first seen in our office in June 2015. In addition to intermittent dizziness, she complained of right aural pressure and pain, and an intolerance to loud sounds. Additionally, she also reported cognitive difficulty, and an inability to concentrate on her work. Changing altitude while driving over hilly terrain was particularly disorienting. There was no complaint of a hearing loss or tinnitus. A fistula test using pneumatic otoscopy resulted in nystagmus. The Tullio test was positive and a post-traumatic perilymph fistula was suspected. A high resolution CT scan of the temporal bones was performed and reported as being normal. She consented to right middle ear exploration and surgery was performed on 20 August 2015. Perilymph leakage was not encountered; however, a bony defect in the stapes footplate covered by a thin membrane was observed and patched using fat grafts. At follow-up examination in 8 weeks the patient reported that her vertiginous symptoms had completely resolved, and conductive hearing loss following surgery returned back to baseline (**Video 3**). She also reported a resolution of cognitive issues and was able to test high powered hearing aids as part of her professional duties without suffering dizziness. The patient has been symptom free for 28 months. This was confirmed in the vestibular laboratory.

Illustrative Case 3

A 62-year-old female patient (**Table 1**, Patient 28) presented to our office on 6 June 2019 with a history of dizziness. She reported being struck in the head by a football in September 2017. There was no history of loss of consciousness, but she was seen in the emergency room and was diagnosed with concussion. Soon after the event, she began developing progressively increasing dizziness. She described a sensation of being pushed and had a feeling that she would fall when exposed to something as trivial as a wind gust. During all waking hours she described a feeling of being in a "funhouse," and was extremely unstable on her feet. She was unable to go for rides on her motorcycle because the low-pitched exhaust sounds bothered her. Rolling over in bed occasionally made her dizzy. Dizziness was most pronounced on exposure to loud sounds, and changes in altitude such as riding in an elevator were especially bothersome. While walking she needed to hold on to the wall or her spouse for support. Her symptoms were most pronounced when bending down. She reported an inability to prevent a fall when bending to pick up an object from the floor. Multiple sessions under the care of a physical therapist did not relieve her symptoms. Ear, nose and throat examination was normal, however the patient reported extreme nausea on left-sided pneumatic otoscopy, and a questionable left beating short-lived nystagmus was observed. Bedside vestibular testing and VNG were found to be normal on 9 August 2019. The Hennebert test was equivocal, but with the Tullio test the patient demonstrated pulsion to the right. cVEMP was normal on the right but was abnormal on the left side with increased amplitude and decreased threshold down to 65 dB nHL (**Figures 2C1,C2**). The gray-scale inversion technique on high resolution temporal bone CT scan raised the possibility of a left membranous stapes footplate. The patient consented to surgery and on 5 December 2019 underwent fat graft placement

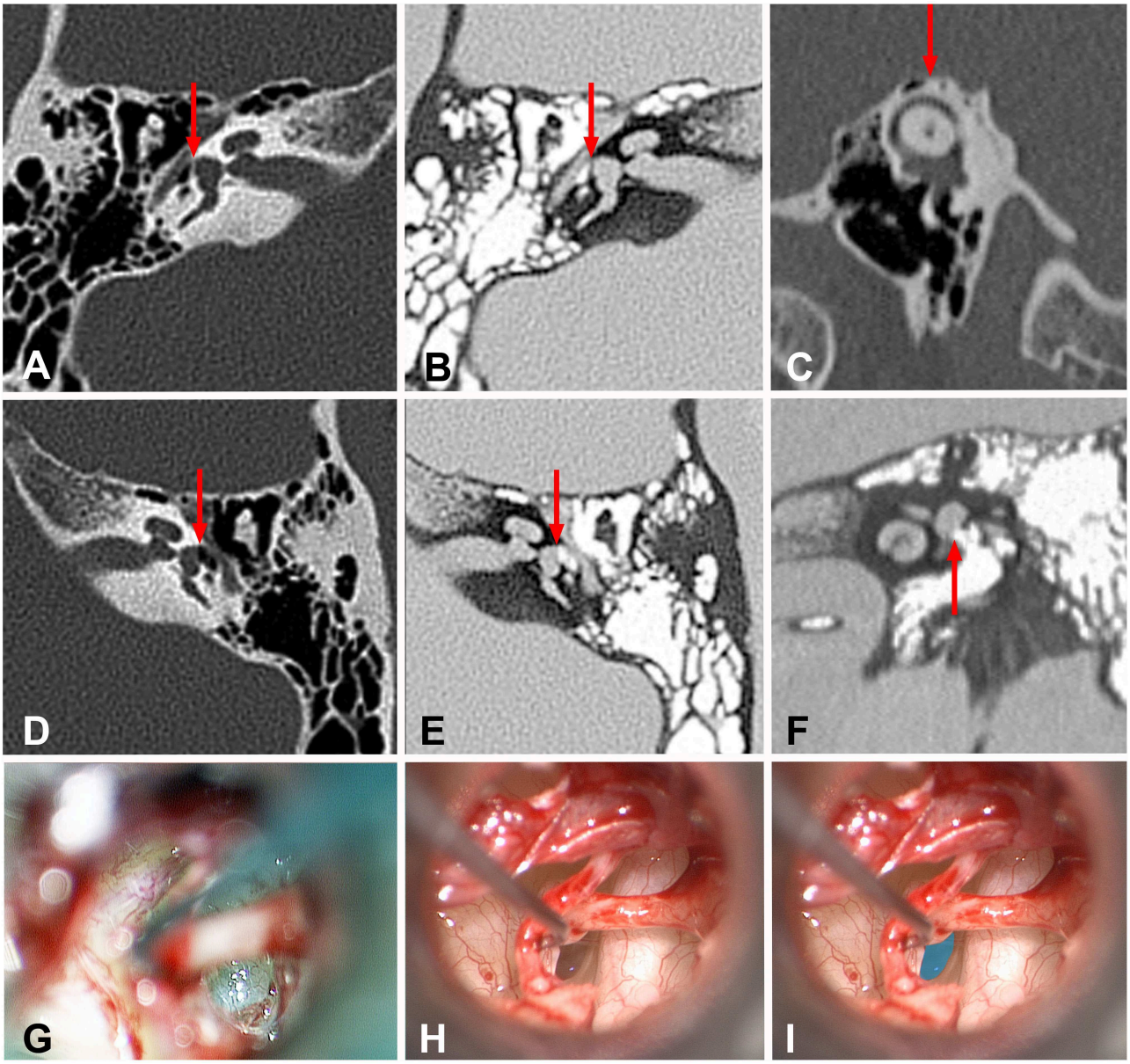

FIGURE 1 | High resolution temporal bone CT images of the normal and abnormal stapes footplate as well as intraoperative images of the hypermobile stapes footplate. **(A)** Traditional axial image of the right temporal bone with bone windows shows the cochlea, internal auditory canal, vestibule, middle ear. Red arrow shows the normal stapes footplate (white line) providing the interface between the vestibule and middle ear. **(B)** Same image as seen in this figure **(A)** using the "invert" function. Note the ease in comparing the air in the middle ear (white) to the fluid-filled vestibule (gray). Red arrow shows the position of the normal stapes footplate (black line) providing the interface between the vestibule and middle ear. **(C)** Traditional Poschl image of the left temporal bone with bone windows shows that in this case of left third window syndrome, there is no superior semicircular canal dehiscence (red arrow). **(D)** Traditional axial image of the left temporal bone with bone windows shows the cochlea, internal auditory canal, vestibule, middle ear. Red arrow shows the position of the membranous stapes footplate providing the interface between the vestibule and middle ear. Note the absence of the white line seen in this figure **(A)**. **(E)** Same image as seen in this figure **(D)** using the "invert" function. Note the ease in comparing the air in the middle ear (white) to the fluid-filled vestibule (gray). Red arrow shows the position of the membranous stapes footplate providing the interface between the vestibule and middle ear. Note the absence of the black line representing the normal stapes footplate seen in this figure **(B)**. **(F)** Inverted coronal image of the left temporal bone with bone windows shows the cochlea, vestibule and middle ear. Red arrow shows the position of the membranous stapes footplate providing the interface between the vestibule and middle ear. Note the absence of the black line representing the normal stapes footplate. **(G)** Intraoperative appearance of a normal stapes footplate. **(H)** Intraoperative appearance of a membranous stapes footplate. Note the translucent appearance of the entire stapes footplate. The bone-covered tympanic segment of the facial nerve can be seen to the right of the stapes footplate. **(I)** The stapes footplate is shaded in blue to illustrate the position of the membranous stapes footplate image seen in this figure **(H)**.

over the oval and round windows (**Figures 2A,B**). While her ear felt plugged following surgery her symptoms of disequilibrium resolved almost immediately. On 14 January 2020 pulsion was not elicited on Tullio testing. Auditory thresholds recovered completely to preoperative levels, and post-operative cVEMP testing demonstrated normal amplitude and threshold on the left side (**Figure 2D**). The patient's and her husband's impressions can be seen and heard in **Videos 4**, **5**. The patient reports that she is almost completely back to normal.

RESULTS

All 28 patients (32 ears) had some level of noise intolerance or hyperacusis associated with varying degrees of dizziness, imbalance, or vertigo. There were 7 males (25.0%) and 21 females (75.0%), whose ages ranged between 16 and 69 years. Our findings are summarized in **Table 1**. All patients had varying degrees of head trauma; In 18 of 28 patients (64%) the trauma could be considered severe with evidence of concussion, or unconsciousness. Audiometric data was variable with no consistent pattern. Most patients developed symptoms several weeks to months following the trauma. Three patients developed immediate symptoms. One patient with prior history of concussions exhibited symptoms while power-lifting. He was found to have a perilymph leak but the stapes footplate was devoid of defects (**Video 6**). Two others patients with immediate onset dizziness (one was struck with a baseball glove on the ear, and another who was hit in the head by a football) did not demonstrate perilymph leakage. One patient in the series also reported a blast injury while in the military. Only one patient (**Table 1**, Patient 3) demonstrated evidence of bilateral superior semicircular canal dehiscence syndrome in addition to a defect in the stapes footplate. The duration of dizziness varied from 2 months in a patient who developed a perilymph fistula while power lifting to 62 months in a patient who was the victim of a severe car accident. The mean duration of symptoms was 22.8 months.

On high resolution temporal bone CT scan none of the patients had identifiable congenital temporal bone anomalies. It is worth mentioning that when the "invert" function was used to visualize the stapes footplate, most patients were observed to have bony defects of variable size on one or both ears. Some of these defects appeared to be subtle gaps or simply cracks without perilymph egress at the time of surgery.

Positive Hennebert or Tullio signs were present in all patients; 12 patients bilaterally (AU), while 11 patients had right-sided (AD), and 5 had left-sided (AS) involvement. Sixteen patients underwent right-sided explorations, 8 had surgery on the left, while 4 had sequential surgery on both ears. Two patients in this series (Patient 12 and Patient 14), required revision surgery as symptoms returned; one following a vehicular accident and the other following a severe bout of coughing. In both, the fat graft had displaced, and their symptoms resolved after revision surgery with new fat grafts being placed.

At the time of surgery, 21 of the 32 (65.6%) ears had what appeared to be bony defects in the stapes footplate which were covered over by a translucent membrane. Some of these defects could be very small and in 4 ears (12.5%) cracks in the footplate without evidence of perilymph leakage were noted. Only 7 of the 32 (21.9%) ears showed evidence of true perilymph leakage (5 involved the oval window, 1 the round window and 1 involved both round and oval windows). The remaining 4 ears (12.5%) had neither leakage of perilymph nor was a membrane present despite being symptomatic. These were determined to have hypermobile stapes footplates. They all exhibited positive Hennebert signs and Tullio phenomena but the stapes footplates were devoid of observable cracks, defects, or membranes. Four ears (12.5%) demonstrated questionable perilymph leaks, and the majority, i.e., 21 ears (65.6%) did not demonstrate any evidence of perilymph leakage. Five of the 7 ears (70.4%) with evidence of perilymph leakage had intact stapes footplates. In contrast only 1 of the 21 ears with membranous footplates showed evidence of perilymph leakage (4.8%).

One patient (**Table 1**, Patient 3) demonstrated a right membranous footplate in addition to bilateral SSCD. She had Tullio and Hennebert signs which were positive on the right side and her symptoms resolved after patching the right oval and round window niches. Therefore, we did not operate on the left ear and did not need to address the radiographic finding of SSCD.

cVEMP testing was performed in 17 ears. Of the 17 symptomatic ears tested, 13 (76%) had subnormal thresholds on cVEMPs, while 4 of the 17 (24%) showed normal thresholds preoperatively. Of the 13 patients with abnormal cVEMPs, 9 (69%) of them had normal threshold results post-operatively. We were unable to obtain post-operative cVEMPs on 4 ears (31%). Post-operatively pneumatic otoscopy was performed on all patients in the clinic; however, several patients did not consent to undergo the Hennebert or Tullio testing in the laboratory because of their anxiety that their symptoms would return. We were able to obtain vestibular post-operative testing in 14 of the 28 patients. Clinically 24 of the 28 patients (85.7%) showed complete amelioration of symptoms and no cases of hearing deterioration occurred in this series. Four of the 33 ears (12.1%) failed to show improvement following surgery.

DISCUSSION

It is widely accepted that BPPV is the most common cause of vertigo after head injury (1, 5). However, we observed that there is a cohort of patients who appear to resist conventional canalith repositioning maneuvers and go on to develop symptoms of persistent incapacitating recalcitrant dizziness. It often becomes de rigueur to label these patients as having post-concussive syndrome (PCS), or chronic traumatic encephalopathy (CTE). It was only after we started obtaining Hennebert and Tullio tests that we began to realize that there could be another etiology for symptoms in addition to BPPV, and post-traumatic vestibular migraines. Hoffer et al. (6) found that after mild head trauma individuals suffered in descending order of frequency from post-traumatic vestibular migraines, post-traumatic positional vertigo, and 19% were classified as suffering from post-traumatic spatial disorientation. This last group was distinguished from

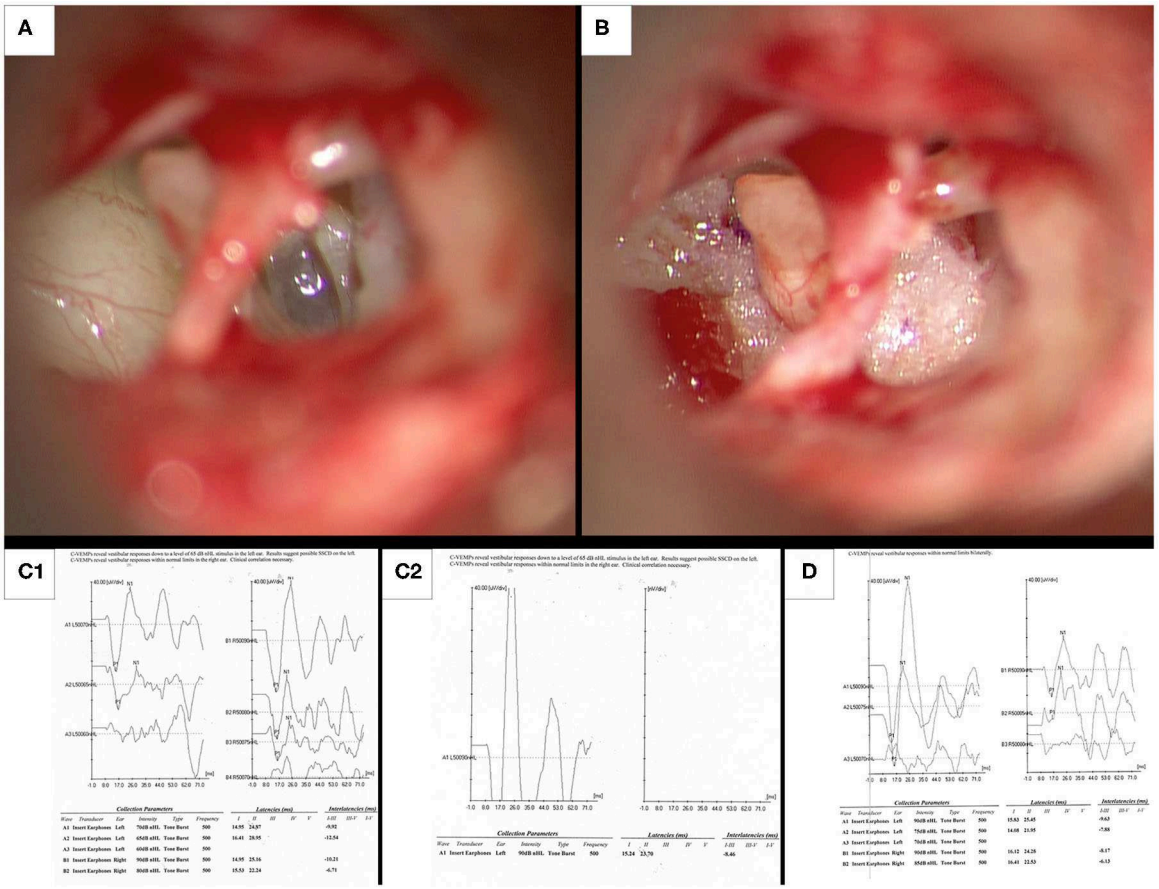

FIGURE 2 | Intraoperative photographs and preoperative and post-operative cVEMP responses in illustrative case 3. **(A)** Intraoperative appearance of a membranous translucent left stapes footplate. **(B)** Fat grafts obtained from the lobule are placed under the arch of the stapes and anterior and posterior to the crurae. **(C1,C2)** Preoperative cVEMPs on the left ear with increased amplitude and decreased threshold down to 65 dB nHL, along with normal cVEMPs in the right ear. **(D)** After auditory thresholds had normalized at 8 weeks following surgery, post-operative cVEMPs shows normalization of thresholds and amplitude on the left side. This suggests that surgery resulted in objective improvement in cVEMPs.

the others by a lack of migraine headaches, a constant feeling of unsteadiness, and abnormalities on static posture testing. They also speculated that individuals who did not recover within 1 year after the injury may have a different pathology and require different treatment modalities. These findings are remarkably similar to patients in our series. However, Tullio and Hennebert tests and the possibility of TWS were not considered as part of their study. The mean duration from the onset of symptoms to getting treated in our series was almost 2 years. The outlier in our series who sought treatment within 2 months was a power weight-lifter who reported hearing a pop in the ear associated with an immediate onset of disequilibrium. The longest duration of symptoms was 62 months in a patient who suffered a severe car accident with life threatening injuries and had unsuccessfully sought care at several institutions. She was diagnosed as having TBI and was forced to resign from employment. Unfortunately she had never been tested for a TWS. Fat grafting of the round and oval windows ameliorated her symptoms.

Tullio and Hennebert tests are known to be positive in several otologic conditions. These include TWS (e.g., superior semicircular canal dehiscence or cochlea-facial nerve dehiscence), perilymph fistula, Menière disease, post-fenestration surgery, vestibulofibrosis, (7) vestibular atelectasis, (8, 9) and also otosyphilis. The diagnosis and management of spontaneous perilymph fistulas is extremely controversial (10). Several prominent surgeons have questioned their existence and surgical repair of the oval and round windows for the management of spontaneous perilymph fistula leaks remains controversial (11, 12). This is not the case for acquired or post-traumatic perilymph fistulas.

It is well-known that post-traumatic perilymph fistulas of the round and oval windows can occur after minor trauma without skull fractures (13, 14) Small defects can occur with dizziness and a positive Hennebert sign despite hearing being normal (15). The symptoms as we found in our series can be quite variable (16, 17). Victor Goodhill (18) first proposed the theory of implosive and explosive forces causing acquired perilymph fistulas. We believe

that most subjects in our series were the result of implosive forces. The exceptions were the power lifter who developed symptoms on straining and the patient who required revision surgery due to coughing.

House (19) observed that surgical exploration was needed to detect perilymph leakage in post-stapedectomy cases. To this day preoperative detection of the site of leakage remains problematic. Tullio test and Hennebert sign can provide a clue that a fistula or TWS may be present but they do not point to a precise site of leakage. Given the history of prior cranial trauma we performed all surgical explorations presuming the diagnosis of perilymph leakage from the inner ear. All patients were operated upon after failed conservative management. At the time of surgery perilymph leakage could be detected in only a minority of cases (21.9%). Instead a membranous stapes or a hypermobile stapes footplate without perilymph leakage was observed in the majority of cases (78.1%). This was unexpected.

A pliable, compliant membranous footplate also appears to protect against perilymph leakage, or may perhaps represent spontaneous healing of an injured footplate. When the footplate was membranous only 4.8% of ears showed demonstrable perilymph egress. Conversely, of the ears with intact footplates 70.4% showed the presence of perilymph leakage. Patients with hypermobile stapes footplates represented a not insignificant minority (12.5%) of explored middle ears. It is noteworthy that they exhibited all clinical characteristics of membranous stapes footplates preoperatively. A mechanical or electronic method to objectively document hypermobility is being explored.

Isolated congenital dehiscence of the stapes footplate has been described in the literature but is exceedingly rare, and usually seen in Mondini deformity (20, 21). We therefore believe that the dehiscences seen in all of our patients were acquired following head trauma. Therefore, our principle hypotheses are: (1) rapid acceleration and deceleration may result in a temporary subluxation of the stapes footplate with disruption of the tiny capillaries supplying the region; and (2) gradual avascular necrosis results in variable sized defects that develop over time. This would also explain the delayed presentation of symptoms in some of our patients. An alternative hypothesis is that trauma results in a fracture which goes on to heal spontaneously. Schucknecht (22) has alluded to similar pathology in human temporal bones and experimental animals, and recommended the early use of connective tissue to patch the defect. He made a similar observation after radiation therapy with an accompanying atrophy of the annular ligament (22).

The work of Minor et al. (23) and Minor (24) in 1998, spawned a great deal of interest in dizziness associated with defects in other areas of the otic capsule. Wackym et al. (3, 25) coined the terms otic capsule dehiscence and third window syndrome (TWS) to describe the spectrum of signs and symptoms observed in these patients. This all-encompassing term correctly alludes to the fact that several other defects in the otic capsule can result in symptoms and a phenotype of the spectrum seen in SSCD patients. The stapes footplate is developmentally part of the otic capsule bone and congenital or acquired dehiscence in the stapes footplate can conceivably represent yet another manifestation of TWS.

The mechanisms for dizziness in membranous or hypermobile stapes footplates has not been well-elucidated. In 1883, Gellé (26) was able to associate dizziness with mobility of the stapes and pathology of the oval and round windows. In 1905, Hennebert (27) demonstrated oculo-vestibular disturbance by changing pressure in otherwise normal appearing ears. A fistulous communication between the perilymph and the middle ear was suspected, but in the absence of magnification could not be demonstrated (28). Bárány (29) therefore concluded that Hennebert's sign was the result of increased stapes mobility.

Dieterich et al. (30) studied a 35-year-old professional horn player who developed an excitatory ocular tilt reaction (OTR), and balance disturbance by tones of 480 +/− 20 Hz at 95 dB. It was manifested as an ipsilateral head tilt, skew deviation of the eyes and ocular torsion, and was characterized as an otolith Tullio phenomenon. At the time of surgery a medially subluxed stapes footplate with hypertrophic stapedius muscle was discovered. However, they did not report the presence of a membranous stapes footplate. The patient's symptoms resolved completely when compressed silastic foam was inserted between the anterior and posterior crurae of the stapes. We utilized the same principle but used autologous lobule fat instead. The presence of fatty tissue perhaps changes impedance and may prevent large medial-lateral displacement of an acquired membranous or hypermobile stapes footplate. In order to make sure that imperceptible perilymph leaks were not missed packing was also performed anterior and posterior to the crurae of the stapes and in the round window. Twenty-four of 28 patients (85.7%) showed complete resolution of symptoms following surgery. Four of the 28 patients failed surgical treatment. These patients may represent an opportunity for future refinement in diagnosis and treatment.

Backous et al. (31) described the relationship of the stapes footplate to the utricle and saccule in 130 temporal bones. However, in none of the specimens was the footplate in contact with either structure. Membranous connections between the utricle and footplate were seen in 34 bones, and pulsion or traction may help explain the otolith Tullio phenomenon. In our series a floppy membrane or hypermobile stapes footplate touching the utricle directly remains a possibility. Alternatively, post-traumatic adhesions may form between the stapes footplate and membranous labyrinth causing symptoms.

Ehmer et al. (32) described the "bulging oval window" sign on CT and MRI. This represents an out-pouching of a fluid filled sac in the region of a stapes footplate defect. We did not specifically look for this sign in our series, but serendipitously found that by using the gray-scale "invert" function, small defects in the stapes footplate could be more readily visualized. Images on CT scan are technically negatives, with air appearing black and bone appearing white. Gray-scale inversion renders a positive image. The physiology literature describes that the human visual system demonstrates optimal contrast perception when a dark object is visualized against a bright background (33). Formal studies utilizing radiologists and otolaryngologists blinded to the diagnosis are necessary to evaluate the sensitivity and specificity of the gray-scale "invert" function as it pertains to this pathology of the stapes footplate. We are further investigating the utility

of this technique to visualize other temporal bone pathologies, which is the subject of another paper. It is our current recommendation that CT scans with the "invert" function, must be utilized in the context of the clinical picture, and should not be used in isolation to make the diagnosis or to recommend surgery.

An inherent limitation of this study is its retrospective nature. An additional limitation is that preoperative vestibular evoked myogenic potentials (cVEMPs) and ocular vestibular evoked myogenic potentials (oVEMPs) were not routinely performed. This was due to the fact that given the clinical history of trauma we were looking for perilymph leaks rather than TWS. Additionally, at the start of our work we did not have the necessary equipment to perform these tests. An additional barrier to cVEMP testing may have been lack of reimbursement for the test. Out of pocket costs may have precluded patient participation in post-operative testing. A multi-institutional prospective study to better characterize ocular movements, and hopefully differentiate between other defects producing symptoms of TWS and membranous and hypermobile stapes footplates is warranted. In illustrative Case 3, (**Figure 2**) we were able to demonstrate a normalization of cVEMP following surgery. Consequently, a systematic use of cVEMPs and oVEMPs is a subject for further research.

While all patients underwent post-operative pneumatic otoscopy in the office, we were able to convince only 50% of our patients to obtain post-operative objective testing. Most patients appeared too nervous to get retested, while three patients had relocated from the area. The use of Tullio and Hennebert tests in post-traumatic dizziness must be encouraged.

CONCLUSION

It is hoped that this article draws attention to an underappreciated clinical entity of post-traumatic membranous and hypermobile stapes footplates that result in symptoms of TWS, including perilymph fistulas. Its pathophysiology and management is discussed. It can cause persistent and often intractable dizziness following head trauma which is often mistaken for traumatic brain injury or post-concussive syndrome. In our experience the presence of true perilymph leak is a relatively uncommon event. Tullio and Hennebert tests help to clue in on the diagnosis and should be performed in every case of persistent dizziness after head trauma. Imaging modalities such as high resolution temporal bone CT scans combined with gray-scale inversion should not be used in isolation but rather used in the context of the clinical history, physical findings and objective audiological and vestibular tests. Fat grafting of the oval and round windows is a low risk procedure with a high probability of curing the condition.

DATA AVAILABILITY STATEMENT

The raw data supporting the conclusions of this article will be made available by the authors, without undue reservation.

ETHICS STATEMENT

The studies involving human participants were reviewed and approved by Heuser Hearing Institute Institutional Review Board. Written informed consent for participation was not required for this study in accordance with the national legislation and the institutional requirements. Written informed consent was obtained from the individual(s) for the publication of any potentially identifiable images or data included in this article.

AUTHOR CONTRIBUTIONS

AG: discovered the condition and performed surgeries and wrote the paper. IE: performed preoperative and post-operative audiology testing and helped analyze data at Heuser Hearing Institute. VB: performed pre and post-operative cVEMP testing and helped analyze data. CR: performed per and post-operative audiology testing and helped edit the paper. All authors contributed to the article and approved the submitted version.

ACKNOWLEDGMENTS

Thanks are due to Ms. Lara A. Hess for her editorial assistance. Thanks are also due to Mr. T. Logan Lindemann for helping with illustrations. The authors wish to thank Dr. Joel Mindel, Mrs. Susan Mindel, Dr. Kenneth Altman, and the Geisinger Health Foundation for supporting publication of the manuscript.

SUPPLEMENTARY MATERIAL

The Supplementary Material for this article can be found online at: https://www.frontiersin.org/articles/10.3389/fneur.2020.00871/full#supplementary-material

REFERENCES

1. Davies RA, Luxon LM. Dizzines following head injury: a neuro-otological study. *J Neurol.* (1995) 242:222–30. doi: 10.1007/BF00919595
2. Fitzgerald DC. Head trauma: hearing loss and dizziness. *J Trauma.* (1996) 40:488–96. doi: 10.1097/00005373-199603000-00034
3. Wackym PA, Balaban CD, Zhang P, Siker DA, Hundal JS. Third window syndrome: surgical management of cochlea-facial nerve dehiscence. *Front Neurol.* (2019) 10:1281. doi: 10.3389/fneur.2019.01281
4. Epley JM. The Canalith repositioning procedure: for treatment of benign paroxysmal positional vertigo. *Otolaryngol Head Neck Surg.* (1992) 107:399–404. doi: 10.1177/019459989210700310
5. Hornibrook J. Immediate onset of positional vertigo following head injury. *N Z Med J.* (1998) 111:1073.
6. Hoffer ME, Gottshall KR, Moore R, Balough BJ, Wester D. Characterizing and treating dizziness after mild head trauma. *Otol Neurotol.* (2004) 25:135–8. doi: 10.1097/00129492-200403000-00009
7. Nadol JB Jr. Positive "fistula sign" with an intact tympanic membrane. Clinical report of three cases and histopathological description of vestibulofibrosis as the probable cause. *Arch Otolaryngol.* (1974) 100:273–8. doi: 10.1001/archotol.1974.00780040283007

8. Wenzel A, Ward BK, Schubert MC, Kheradmand A, Zee DS, Mantokoudis G, et al. Patients with vestibular loss, Tullio phenomenon, and pressure-induced nystagmus: vestibular atelectasis? *Otol Neurotol.* (2014) 35:866–72. doi: 10.1097/MAO.0000000000000366
9. Merchant SN, Schuknecht HF. Vestibular atelectasis. *Ann Otol Rhinol Laryngol.* (1988) 97:565–76. doi: 10.1177/000348948809700601
10. Friedland DR, Wackym PA. A critical appraisal of spontaneous perilymphatic fistulas of the inner ear. *Am J Otol.* (1999) 20:261–79.
11. Shea JJ. The myth of spontaneous perilymph fistula. *Otolaryngol Head Neck Surg.* (1992) 107:613–6. doi: 10.1177/019459989210700501
12. Hughes GB, Sismanis A, House JW. Is there consensus in perilymph fistula management? *Otolaryngol Head Neck Surg.* (1990) 102:111–7. doi: 10.1177/019459989010200203
13. Fee GA. Traumatic perilymphatic fistulas. *Arch Otolaryngol.* (1968) 88:477–80. doi: 10.1001/archotol.1968.00770010479005
14. Tonkin JP, Fagan P. Rupture of the round window membrane. *J Laryngol Otol.* (1975) 89:733–56. doi: 10.1017/S0022215100080944
15. Kohut RI, Waldorf RA, Haenel JL, Thompson JN. Minute perilymph fistulas: dizziness and Hennebert's sign without hearing loss. *Ann Otol Rhinol Laryngol.* (1979) 88:153–9. doi: 10.1177/000348947908800201
16. Thompson JN, Kohut RI. Perilymph fistulae: variability of symptoms and results of surgery. *Otolaryngol Head Neck Surg.* (1979) 87:898–903. doi: 10.1177/019459987908700627
17. Goodhill V. Traumatic fistulae. *J Laryngol Otol.* (1980) 94:123–8. doi: 10.1017/S0022215100088563
18. Goodhill V. Sudden deafness and round window rupture. *Laryngoscope.* (1971) 81:1462–74. doi: 10.1288/00005537-197109000-00010
19. House HP. The fistula problem in otosclerosis surgery. *Laryngoscope.* (1967) 77:1410–26. doi: 10.1288/00005537-196708000-00015
20. Urata S, Kashio A, Sakamoto T, Kakigi A, Yamasoba T. Novel repair of stapedial footplate defect associated with recurrent meningitis. *Otol Neurotol.* (2014) 35:1592–95. doi: 10.1097/MAO.0000000000000549
21. Hoppe F, Hagen R, Hofmann E. Fistula of stapes footplate caused by pulsatile cerebrospinal fluid in inner ear malformation. *ORL.* (1997) 59:115–8. doi: 10.1159/000276920
22. Schuknecht HF. Trauma. In Schuknecht HF, editor. *Pathology of the Ear*. Philadelphia, PA: Lea & Febiger (1993). p. 279–301.
23. Minor LB, Solomon D, Zinreich JS, Zee DS. Sound-and/or pressure-induced dizziness due to bone dehiscence of the superior semicircular canal. *Arch Otolaryngol Head Neck Surg.* (1998) 124:249–58. doi: 10.1001/archotol.124.3.249
24. Minor LB. Clinical Manifestations of superior semicircular canal dehiscence. *Laryngoscope.* (2005) 115:1717–27. doi: 10.1097/01.mlg.0000178324.55729.b7
25. Wackym PA, Wood SJ, Siker DA. Otic capsule dehiscence syndrome: superior semicircular canal dehiscence syndrome with no radiographically visible dehiscence. *Ear Nose Throat J.* (2015) 94:E8–24. doi: 10.1177/014556131509400802
26. Gelle R. Etude Clinique du vertrige de Meniere dans ses rapports avec les lesions des fenestres ovales et rondes. *Arch Neurol.* (1883) 4:273.
27. Hennebert C. Labyrinrinthite double, reflexe moteur oto-ocularie. *Clinique.* (1905) 19:214.
28. Kohut RI. Perilymphatic fistulae: more than a century of notions, conjectures, and critical studies. *Am J Otol.* (1992) 13:38–40. doi: 10.1097/00129492-199201000-00010
29. Barany R. Fall von labyrinthiues. *Monatsschr Ohrenheilkd.* (1910) 11:40.
30. Dieterich M, Brandt TH, Fries W. Otolith function in man. *Brain.* (1989) 112:1377–92. doi: 10.1093/brain/112.5.1377
31. Backous DD, Minor LB, Aboujaoude ES, Nager GT. Relationship of the utriculus and sacculus to the stapes footplate: anatomic implications for sound and/or pressure-induced otolith activation. *Ann Otol Rhinol Laryngol.* (1999) 108:548–53. doi: 10.1177/000348949910800604
32. Ehmer DR Jr, Booth T, Kutz JW Jr, Roland PS. Radiographic diagnosis of trans-stapedial cerebrospinal fluid fistula. *Otolaryngol Head Neck Surg.* (2010) 142:694–8. doi: 10.1016/j.otohns.2009.12.029
33. Blackwell HR. Contrast thresholds of the human eye. *J Opt Soc Am.* (1946) 36:624–43. doi: 10.1364/JOSA.36.000624

Conflict of Interest: The authors declare that the research was conducted in the absence of any commercial or financial relationships that could be construed as a potential conflict of interest.

frontiers in Neurology

REVIEW
published: 25 August 2020
doi: 10.3389/fneur.2020.00891

Biomechanics of Third Window Syndrome

Marta M. Iversen[1]* *and Richard D. Rabbitt*[1,2,3]

[1] Department of Biomedical Engineering, University of Utah, Salt Lake City, UT, United States, [2] Department of Otolaryngology, University of Utah, Salt Lake City, UT, United States, [3] Neuroscience Program, University of Utah, Salt Lake City, UT, United States

Third window syndrome describes a set of vestibular and auditory symptoms that arise when a pathological third mobile window is present in the bony labyrinth of the inner ear. The pathological mobile window (or windows) adds to the oval and round windows, disrupting normal auditory and vestibular function by altering biomechanics of the inner ear. The most commonly occurring third window syndrome arises from superior semicircular canal dehiscence (SSCD), where a section of bone overlying the superior semicircular canal is absent or thinned (near-dehiscence). The presentation of SSCD syndrome is well characterized by clinical audiological and vestibular tests. In this review, we describe how the third compliant window introduced by a SSCD alters the biomechanics of the inner ear and thereby leads to vestibular and auditory symptoms. Understanding the biomechanical origins of SSCD further provides insight into other third window syndromes and the potential of restoring function or reducing symptoms through surgical repair.

Keywords: biomechanics, canal dehiscence, superior semicircular canal dehiscence, third window, vestibular, dizziness, vertigo, air-bone gap

OPEN ACCESS

Edited by:
Tetsuo Ikezono, Saitama Medical University, Japan

Reviewed by:
Andrea Castellucci, Department of Surgery, Santa Maria Nuova Hospital, Italy
Leonardo Manzari, Independent Researcher, Cassino, Italy

***Correspondence:**
Marta M. Iversen
marta.iversen@utah.edu

Specialty section:
This article was submitted to Neuro-Otology, a section of the journal Frontiers in Neurology

Received: *27 April 2020*
Accepted: *13 July 2020*
Published: *25 August 2020*

Citation:
Iversen MM and Rabbitt RD (2020) Biomechanics of Third Window Syndrome. Front. Neurol. 11:891. doi: 10.3389/fneur.2020.00891

INTRODUCTION

The fluid-filled inner ear is almost completely encased in rigid bone, with the exception of a few compliant windows connecting to the middle ear or cranial cavity. The primary and secondary windows are the oval and round windows, which are responsible for sound transmission from the middle ear to the cochlea. The lymph fluids filling the bony labyrinth are nearly incompressible such that, under normal conditions, inward volume velocity at the oval window is accompanied by an equal outward volume velocity at the round window. This fluid flow between the oval and round windows generates a pressure gradient across the cochlear partition that results in a propagating wave toward the apex of the cochlea, activation of cochlear hair cells, and perception of sound (1). Other normal windows of the inner ear include the vestibular aqueduct, cochlear aqueduct, and foramina for blood vessels (2–4), but these windows normally have very high mechanical impedance, owing to their small diameter and long length, and behave mechanically almost as if sealed (5). An enlarged physiologic window (i.e., enlarged vestibular or cochlear aqueduct) or an additional bony dehiscence can create a pathological third window. If sufficiently large, a third window will introduce a low mechanical impedance, thus shunting part of the inner ear fluid pressure and fluid volume flow at the site of the window. The introduction of a compliant third window can have a profound impact on both auditory and vestibular function.

Tullio studied pathologic third window syndrome in the early 20th century, primarily using the pigeon as the animal model. He opened a third window in the semicircular canal bony duct and demonstrated sound-induced eye movements (6). Sound-evoked vertigo or nystagmus are now

termed "Tullio phenomenon," often exhibited as a symptom of third window syndrome. Third window syndrome was first seen in humans with congenital syphilis in the early 20th century who presented with gummatous osteomyelitis and labyrinthine fistulae (7). Hennebert's studies of these patients described eye movements evoked by pressure changes in the external auditory canal, a phenomenon now termed "Hennebert's sign" (8). Since these studies, various causes of the Tullio phenomenon and Hennebert's sign have been reported, such as perilymphatic fistula (9, 10), Ménière's disease (11), and cholesteatoma (12). However, the most common cause is superior semicircular canal dehiscence.

Superior semicircular canal dehiscence (SSCD) in humans was first described by Minor and colleagues in 1998 (13). High-resolution computed-tomography images of the temporal bone revealed dehiscence of the bone above the superior semicircular canal, and imaging was considered the gold standard for diagnosis for a number of years. However, a high rate of false-positive on CT imaging (14–19) motivates the use of physiological indicators of SSCD prior to CT imaging (20), with the most common tests described in subsequent sections. Under current guidelines, patients must present with at least one audiovestibular symptom for a formal diagnosis (21). Symptoms include vestibular indications such as eye movements or dizziness evoked by sound or middle ear/intracranial pressure changes, chronic disequilibrium, oscillopsia; and auditory indications such as autophony, hyperacusis for bone-conducted sounds, conductive hearing loss, and tinnitus. Patients with SSCD can exhibit a variety of these symptoms, though the majority experience some vestibular symptoms (22). Some factors accounting for subject-specific diversity in the array of vestibular and auditory manifestations have been identified, but in most cases, the details are unknown.

A cadaveric survey of 1,000 temporal bones found 0.5% had complete dehiscence, and another 1.4% had significant thinning of bone overlying the superior canal (23). However, clinical presentation of symptoms is less common than anatomic data suggests. Dehiscences vary in size, where even a tiny dehiscence can make vestibular neurons responsive to sound and vibration (24), while a large dehiscence can undergo autoplugging by the dura that dampens lymph motions and superior canal responses (25). Dehiscence can also be complete, or nearly complete (very thin bone), and this likely explains some of the diversity of clinical presentations with SSCD (25).

Other instances of third window syndrome include dehiscence in the posterior or lateral canal and present with clinical symptoms similar to SSCD, though their etiologies can be different (26). The clinical presentation is not specific to the site of a bony defect, and a high-resolution CT is necessary to establish the exact site of dehiscence (20). Other origins include perilymphatic fistula, enlargement of inner ear windows such as the vestibular aqueduct, cochlea-facial nerve dehiscence, and otosclerosis of the internal auditory canal (9, 20, 27–30).

Several studies examining the biomechanical underpinnings of pathologic third window syndrome are useful when interpreting clinical tests and diverse symptoms experienced by SSCD patients (31–34). In this report, we briefly describe clinical audiologic and vestibular tests, and review the biomechanical origins of the third window syndrome.

DISCUSSION

Auditory

Audiometry

Patients with SSCD typically present with an air-bone gap that is largest at low frequencies. There is usually no gap or only a small gap at frequencies >2,000 Hz. Bone conduction thresholds for frequencies <2,000 Hz are sometimes supranormal (0 to −20 dB or more) (35–40). **Figure 1** shows an example audiogram with a 25 dB air-bone gap that resolves after canal plugging (41). It is important to properly calibrate audiometers in order to capture possible bone conduction thresholds below 0 dB hearing level (21). Though audiograms and symptoms vary, there is no significant difference in the air-bone gap between patients with vestibular symptoms and those with exclusively auditory symptoms (22).

Other third window conditions have been shown to present with an air-bone gap on audiometry without middle ear pathological findings including: enlarged vestibular aqueduct (42), posterior canal dehiscence (43–45), carotid canal dehiscence on the scala vestibuli side of the cochlea (46), and Paget disease causing microfractures on the scala vestibuli side of the cochlea (40). An air-bone gap is the most common auditory indicator across different third window syndromes. Presence of a third window also alters the acoustic input impedance of the ear, most easily observed at low frequencies (<600 Hz) by measuring motion of the umbo using laser doppler vibrometry or measuring the acoustic power reflectance in the ear canal (47, 48).

Auditory Biomechanics

SSCD results in conductive hearing loss by the dual mechanism of worsening air-conduction thresholds and improving bone-conduction thresholds. In normal air-conduction, sound enters the oval window through motion of the stapes and exits the round window with equal and outward motion at the round window membrane. The pressure difference across the cochlear partition drives the traveling wave and sensory hair bundle deflection required for sound perception. When a third window lesion is present on the vestibular side of the cochlear partition (SSCD, enlarged vestibular aqueduct, etc.), acoustic energy is shunted away from the cochlea, primarily at low frequencies, and results in lowered sensitivity to air-conducted sound. In bone conduction, vibration of the inner ear lymph fluids evokes a pressure difference across the cochlear partition that is sensitive to the relative impedance difference between the oval and round windows. When a third window lesion is present on the vestibular side, the impedance difference increases, which putatively is responsible for increased sensitivity to bone-conducted sound (49) and autophony experienced by some patients.

Figure 2 shows a simplified lumped parameter network model of the inner and middle ear that models air-conducted and bone-conducted sound transmission with and without a SSCD (49). The model is designed for low frequencies (<4,000 Hz) where the wavelengths are longer than the dimensions of inner

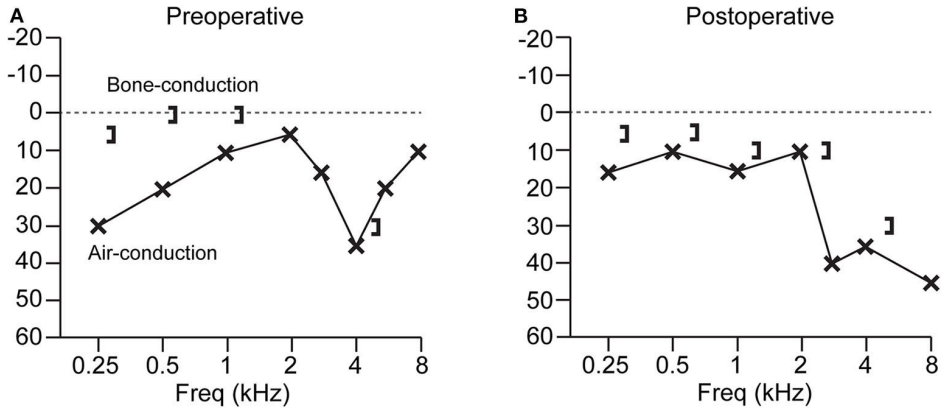

FIGURE 1 | Audiogram from a patient with SSCD before and after superior canal plugging surgery. **(A)** Preoperative audiogram has a low-frequency air-bone gap of up to 25 dB. **(B)** Postoperative audiogram shows resolution of the air-bone gap, with a high-frequency sensorineural loss at 8 kHz. Patient experienced resolution of vestibular symptoms after surgery (41).

ear structures. Further, it neglects deformation of membranous labyrinth as well as the cochlear traveling wave. Canal fluid branches were modeled using a resistor and an inductor to describe fluid viscosity and inertia, respectively. The SSCD is modeled as a compliant window (capacitance) which allows pressure relief and volume velocity through the canal branches of the model. Sound pressure across the basilar membrane is analogous to voltage across the cochlear partition and is used to estimate hearing function. The air-conducted sound audiogram predicted by this model exhibits low-frequency hearing loss due to the impedance through the SSCD, which shunts acoustic energy away from the cochlea (**Figure 2C**). The corner frequency is defined by the transition from low-frequency hearing loss to high-frequency normal hearing, and corresponds to the frequency where the impedance in the dehiscent canal is equal to the cochlear impedance. Above the corner frequency, the SSCD impedance is higher than the cochlear impedance, which effectively stops the shunting of acoustic energy through the canal and leaves air-conducted hearing thresholds unaffected. This corner frequency depends on the location and size of the dehiscence and canal. The predicted bone-conducted audiogram shows low-frequency hypersensitivity that depends on a number of factors: the resonance of the lymph fluids, the middle ear compliance, symmetry in the scala vestibuli and tympani, and symmetry in the round window and middle ear impedances (**Figure 2C**). These mechanical factors likely explain some of the SSCD patient variability seen with audiometry. Finally, the model has been used to predict some low-frequency mechanics where the SSCD shunts lymph volume velocity (**Figure 2D**), but the model neglects the effect of traveling waves along the membranous labyrinth that contribute to vestibular biomechanics in SSCD at higher frequencies as described below (34).

Maximal air-bone gap has been correlated with increased dehiscence length in a large multivariate assessment of SSCD patients (50). A study of intracochlear pressures demonstrates that as dehiscence length increases, the pressure drop across the cochlear partition increases, though the effect saturates at about 2–3 mm in length (51). The authors of the study suggest that as the dehiscence length increases, the impedance at the dehiscence is lowered until other limits dominate, and there is little additional decrease in impedance. This length is likely 1–2 times the diameter of the semicircular canal (31, 51).

Middle ear transmission is not responsible for air-bone gap in SSCD patients, evidenced in part by robust click-evoked VEMP responses (22). Other diagnostic tests and middle ear exploration confirm the lack of pathological middle ear conditions in SSCD (35–38, 52–54).

Vestibular

Eye Movements With Sound and Pressure

Sound- or pressure-evoked eye movements generally align with the plane of the dehiscent semicircular canal (55). However, in cases of large dehiscences ($\geq$5 mm) the alignment of the evoked eye movements can be in other planes, thought to occur due to autoplugging of the dura into the superior canal that compresses the membranous duct and reduces canal function (25, 55). MRI imaging has documented the prolapse of middle fossa dura through a superior canal dehiscence and vestibular-ocular reflex testing shows this prevents high-frequency dynamic response within the superior canal (56). Dehiscence size has been shown to affect the frequency that produces the maximal nystagmus response (57). Additionally, some patients exhibit sound-evoked head movements in the same direction as the ocular slow phase (55).

In SSCD, eye movements can be evoked by low frequency or static (LF) pressure, or an auditory frequency (AF) stimulus. The biomechanics underlying responses to LF vs. AF stimuli differ. Application of increasing middle ear pressure in response to positive external ear canal pressure or nasal Valsalva maneuver drives slowly increasing deflection of the superior canal cupula in the excitatory ampullofugal direction, while decreased middle ear pressure in response to negative pressure exerted on the external ear canal and increased intracranial pressure in

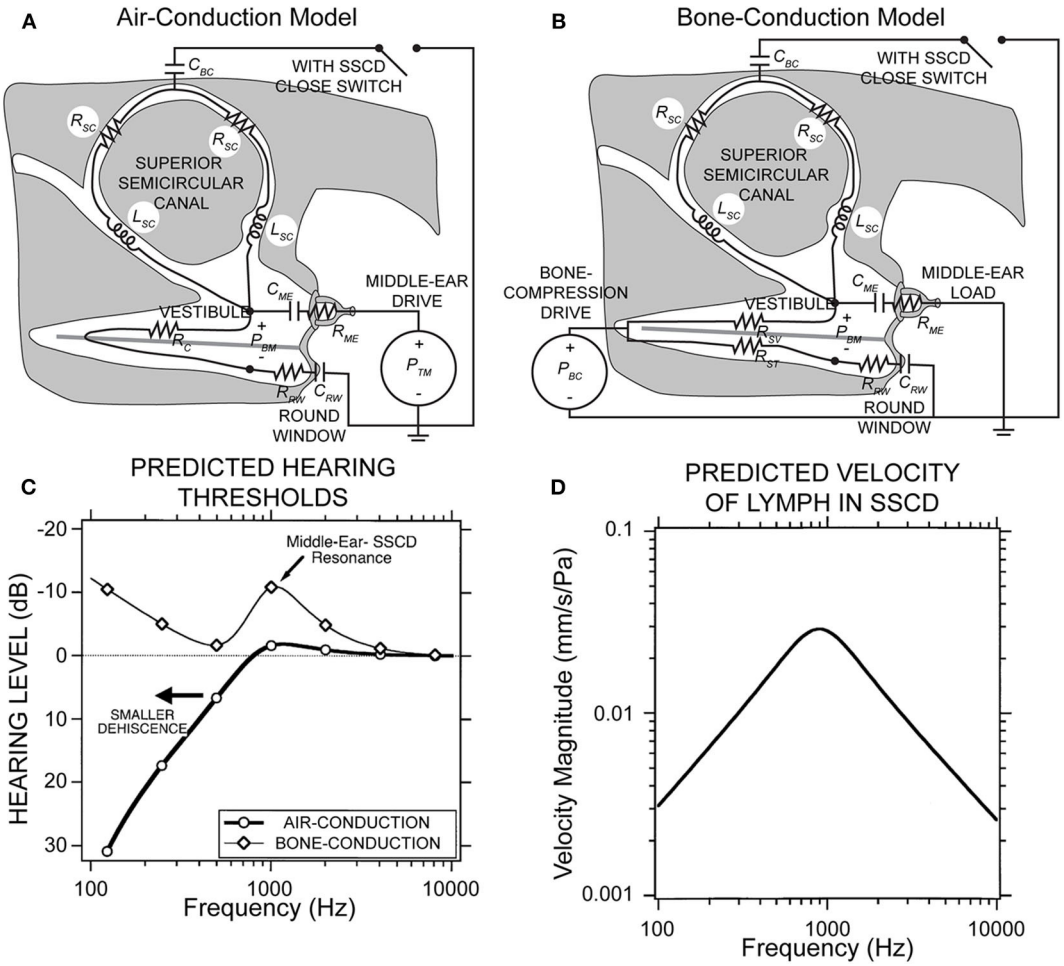

FIGURE 2 | Lumped parameter network model of the inner and middle ear with and without SSCD. **(A)** Air-conduction model where the drive is sound pressure from the ear canal, P_{TM}. **(B)** Bone-conduction model where the drive is effective sound pressure of the vibratory bone-conducted stimulus, P_{BC}. **(C)** The peak in the bone-conduction thresholds is due to a parallel resonance between the compliance of the middle ear load and the inertance of the fluid in the canal limbs. A smaller dehiscence would shift both curves left to lower frequencies. **(D)** Predicted velocity of vestibular lymph fluids in an SSCD with air-conducted sound. Republished from (49), with permission. The Creative Commons license does not apply to this content. Use of the material in any format is prohibited without written permission from the publisher, Wolters Kluwer Health, Inc. Please contact permissions@lww.com for further information.

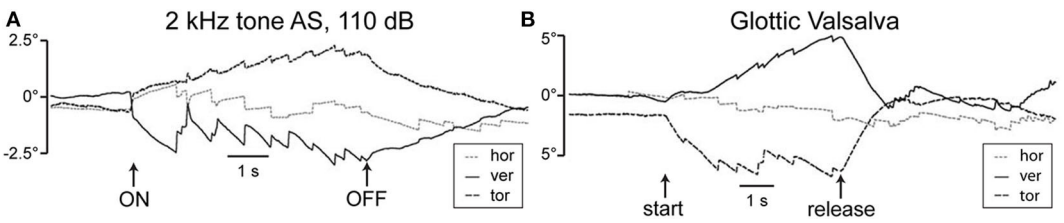

FIGURE 3 | Eye positions recorded from a patient with SSCD. **(A)** Sound-evoked eye movements with 2 kHz tone at 110 dB presented to the left dehiscent ear. Slow phase components are directed upward and clockwise with respect to the patient's point of view, consistent with excitation of the left superior semicircular canal. **(B)** Pressure-evoked eye movements with glottic Valsalva. Slow phase components are principally downward and counterclockwise consistent with inhibition of the left superior semicircular canal. Release causes reversal of the evoked eye movements. Republished from (22), with permission.

response to glottic Valsalva slowly drives the cupula in the inhibitory ampullopetal direction. **Figure 3** demonstrates the slow eye movement with sound (A) or pressure from glottic Valsalva (B). Sound, in contrast, vibrates the cupula leading to excitatory phase-locked canal afferent neuron responses that occur with a short onset latency (34, 58). Sound also triggers wave propagation along the membranous canal that slowly pumps the endolymph in the excitatory or inhibitory direction in a

frequency-dependent manner (34). The magnitude and direction of endolymph pumping are highly sensitive to dehiscence location, morphology of the canal, physical properties, and frequency (34) —factors that would be expected to introduce considerable inter-subject variability. Rapid-onset slow-phase eye movements are excitatory, as vibration-evoked phase-locked neural responses evoked by sound are always excitatory (34, 58, 59). This short-latency excitation is superimposed on a slower component arising from endolymph pumping and cupular deflection (33, 34). The short-latency phase-locked responses cease almost immediately upon termination of the sound, whereas long-latency responses slowly return to baseline following the mechanical time constant of the cupula. Therefore, eye movements after cessation of the sound stimulus are a measure of sustained afferent responses to ampullofugal or ampullopetal cupula displacement, while short-latency eye movements near the onset of the sound are a measure of afferent cycle-by-cycle phase-locked responses to cupula vibration. Nonlinear biomechanics underlying these sound-evoked responses is described in more detail in a later section.

VEMPs

Vestibular Evoked Myogenic Potentials (VEMPs) provide a strong diagnostic indicator of SSCD. The cervical VEMP (cVEMP) pathway is thought to reflect the inhibitory vestibular-colic reflex generated by the activation of saccular macula and potentials are recorded from EMG activity of ipsilateral sternocleidomastoid muscle (60, 61), while the ocular VEMP (oVEMP) is thought to reflect the excitatory vestibular-ocular reflex generated by the activation of utricular macula and responses are recorded from EMG activity of contralateral oblique inferior muscle (62, 63). Both cVEMPs and oVEMPs are diagnostic indicators for SSCD (64), and patients exhibit abnormal, enhanced responses to auditory clicks or tone bursts used in the tests (65). cVEMP amplitudes in the affected labyrinth are increased, and thresholds are lowered (22, 66, 67). oVEMP amplitudes are increased and demonstrate enhanced n10 responses to clicks and 500 Hz tonebursts (68) and 4,000 Hz air-conducted sound or bone-conducted vibration (69). **Figure 4** shows typical cVEMP and oVEMP responses from a patient with unilateral SSCD that demonstrate increased amplitudes and an increased oVEMP response to 4,000 Hz (double arrow). It has been shown directly in animal models that creation of a fistula in the superior canal bony labyrinth makes the canal sensitive to auditory frequency sound and vibration (6, 24), which underlies the enhanced oVEMPs in SSCD. The enhanced response has biomechanical origins as described below. After surgical plugging of the dehisced canal, VEMP thresholds and amplitudes normalize (67).

Enhanced activation of the utricle and saccule by sound used in VEMPs testing is explained by the acoustic energy that is shunted away from the cochlea and into conveyed into the vestibular labyrinth. This energy increases the activation of irregularly discharging otolith afferent neurons that are normally activated only at higher stimulus levels (71). When the canal is repaired, the VEMP thresholds normalize as sound energy is no longer being drawn diverted through the vestibule.

VEMP thresholds can be lower in patients with enlarged vestibular aqueduct (67, 72) and/or perilymphatic fistula (73). However, VEMPs have not been found to accurately or substantively diagnose non-SSCD third window syndromes (74).

Electrocochleography

Electrocochleography (ECoG) shows elevated summating potential (SP) relative to the action potential (AP) in the majority of patients with SSCD (SP/AP ratio > 0.4) (75–78). The

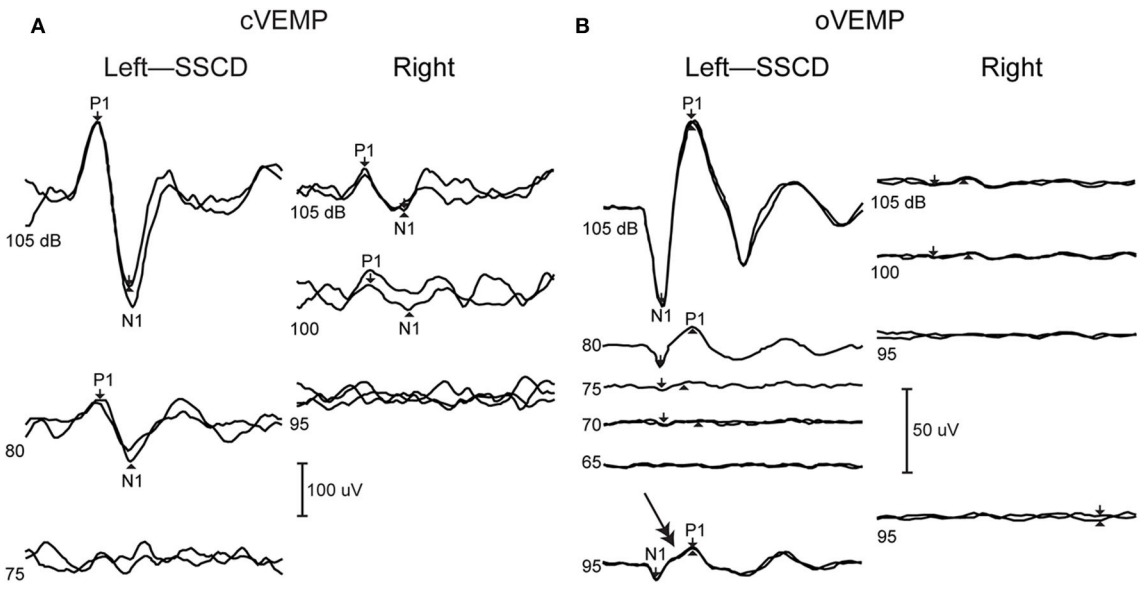

FIGURE 4 | VEMPs from dehiscent (left) and patent (right) ear. **(A)** cVEMP shows increased amplitudes in the dehiscent ear. **(B)** oVEMP shows increased amplitudes as well as abnormal response at super high frequency 4,000 Hz (double arrow). Republished from (70), with permission.

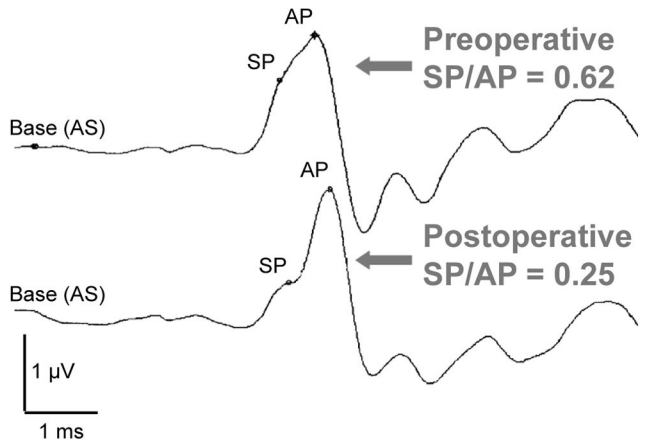

FIGURE 5 | ECoG in a dehiscent ear before and after canal surgery. Preoperative ECoG response shows an elevated SP/AP ratio (>0.4) that normalizes after surgical canal plugging. Republished from (75), with permission. The Creative Commons license does not apply to this content. Use of the material in any format is prohibited without written permission from the publisher, Wolters Kluwer Health, Inc. Please contact permissions@lww.com for further information.

SP/AP ratio usually normalizes after surgical correction (e.g., **Figure 5**) and can be monitored intraoperatively to monitor canal occlusion (75, 76), though symptoms can resolve after surgery without normalization of the ratio (78). The SP value is significantly increased in SSCD patients and decreases after plugging (77, 78). The AP value is likely decreased and increases after plugging in most patients (75, 79). However, the decrease in SP amplitude has a greater effect on SP/AP normalization (75). Though not completely understood, the SP is a short-latency stimulus evoked response and the AP a long-latency response. One hypothesis is that the SP response arises in part from high-frequency responses of the vestibular otolith organs that increase with SSCD, and the AP response arises from cochlear responses that decrease with dehiscence (34). The AP would increase after canal plugging due to the acoustic energy being shunted back into the cochlea. Taken together, these two biomechanical factors could explain the change in the SP/AP ratio.

ECoG has been shown to distinguish SSCD patients from normal subjects, though it has not been shown to be reliable for other third window conditions (77). Cochlea-facial nerve dehiscence and third window syndrome patients described by Wackym et al. usually do not have abnormal ECoG data (20). However, an elevated SP/AP ratio (80) and increased SP value (in 4 of 14 patients) (27) has been reported in a few cases of enlarged vestibular aqueduct. In cases of perilymphatic fistula, the SP/AP ratio is elevated in human (81) and an animal model where it normalizes after healing (82). It is hypothesized that SSCD in these cases induces hydrostatic changes similar to those in endolymphatic hydrops, and therefore has a similar effect on ECoG waveform (76). Though these results describe similar results in some other third window conditions, the complexity of different contributions to the ECoG waveform and the variety of these conditions are responsible for the unreliability of this test in identifying other third window conditions.

Vestibular Biomechanics

Vestibular symptoms evoked by straining or middle ear pressure arise from the pressure driven fluid flow between the oval window and the dehiscence [shown schematically in **Figure 2A**, (49)]. Tullio phenomena and sensitivity to auditory frequency sound arise from a more complex biomechanical mechanism. Sound energy that is diverted toward the dehiscence generates a pressure difference across the membranous vestibular labyrinth that can excite traveling waves (33, 34). Lymph fluids are nearly incompressible and inward volume velocity of fluid at the oval window is balanced by outward volume velocity at the dehiscence, plus the outward volume velocity at the round window. The pressure drop in perilymph from the round window to the dehiscence generates a large pressure gradient both along and across the membranous labyrinth between perilymph and endolymph. This large pressure gradient excites propagating waves that originate at the site of the dehiscence and travel along the membranous duct toward the utricle (34). Though the direction of wave propagation from the dehiscence toward the location of sound stimulus might seem counterintuitive, it arises because conservation of fluid mass converts a low-velocity fluid displacement near the relatively large utricular vestibule into a high-velocity fluid displacement near the fistula. As a result, the highest transmembrane pressure gradients occur near the dehiscence, triggering waves that propagate away from the dehiscence (**Figure 7**).

AF sound-excited waves in the labyrinth have two effects that are demonstrated in recordings of vestibular afferent neurons. First, the waves passing through the ampulla vibrate sensory hair bundles at the sound frequency. Irregularly discharging afferent neurons respond to this auditory-frequency vibration by firing phase-locked action potentials (**Figure 6B**). Second, traveling waves in the membrane interact nonlinearly with the lymph fluids to pump endolymph. Traveling waves are generated on both sides of the dehiscence, but reflections cause one wave to dominate and generate net endolymph flow predominantly in the ampullofugal or ampullopetal direction in a frequency-dependent manner (**Figure 7**). Canal asymmetry is necessary to observe net endolymph pumping. Regularly discharging afferent neurons respond to cupula deflection caused by endolymph pumping by increasing or decreasing their action potential firing rate with a build-up rate that follows the slow mechanical time constant of canal macromechanics (**Figure 6A**).

Phase-locked responses are lost after plugging the canal (24). A biomechanical model predicts that sound-evoked vibration and endolymph pumping is present in normal canals, but is very small and insufficient to evoke neural responses (84), except at very high sound pressure levels (85).

Repair and Plugging

Patients with mild symptoms can reduce exposure to loud sounds and avoid physical straining, and those with pressure sensitivity can benefit from a tympanostomy tube (22). Patients

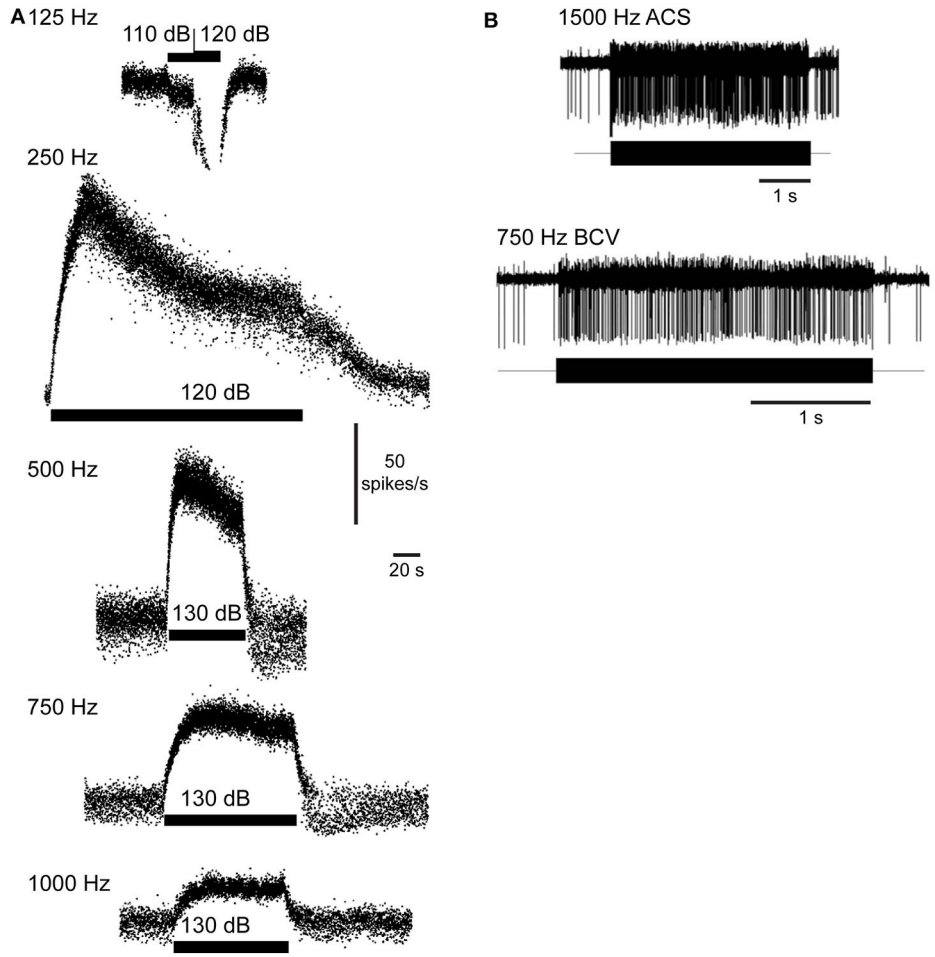

FIGURE 6 | Vestibular afferent neuron responses evoked by fluid vibration and pumping. **(A)** Sustained changes in firing rate in a superior canal afferent neuron after a dehiscence is made in chinchilla superior semicircular canal. Sound evokes a decrease (125 Hz) or increase in afferent firing rate (250, 500, 750, 1,000 Hz). Rise time follows the slow mechanical time constant of the canal. Republished from (83), with permission. **(B)** Phase-locked responses in a superior canal afferent neuron after dehiscence is made in guinea pig superior canal. Sound and bone-conducted vibration at auditory frequencies evoke phase-locking in this irregularly discharging calyx-bearing unit. Republished from (24), with permission. The Creative Commons license does not apply to this content. Use of the material in any format is prohibited without written permission from the publisher, Wolters Kluwer Health, Inc. Please contact permissions@lww.com for further information.

with debilitating symptoms are candidates for surgical repair, and about one-third elect to have surgery (70). Canal plugging achieves long-term control more often than resurfacing and is usually the procedure of choice (22). Patients typically see long-term improvement after canal plugging in symptoms such as sound- or pressure-evoked vertigo (86), autophony (87), dizziness handicap (88), and health-related quality of life (89). Balance measures are impaired immediately after surgical repair (90), but partially recover after 6 weeks to the extent offered by central compensation (91). Compensatory vestibular-ocular reflexes (86) and dynamic visual acuity (92) do not fully recover. Vestibular physical therapy is useful in the postoperative period to aid in recovery (91, 93). In animal models, canal plugging impairs the low frequency VOR and profoundly reduces single unit afferent sensitivity to low-frequency head rotations (>100 fold), but introduces only modest attenuation for high-frequency head rotations (>10 Hz) (94–96). The residual sensitivity at high-frequencies arises from acceleration-induced transmembrane fluid pressure that deforms the labyrinth and deflects the cupula (84). Observations in animal models are consistent with vestibulo-ocular reflexes (VOR) measured postoperatively in patients in that compensatory eye movements are present in response to rotary head thrusts but compromised relative to controls (86, 92, 97, 98). The reduced VOR following surgical plugging putatively reflects broad-band attenuation of sensitivity caused by the procedure, while persistence of a partial VOR reflects residual sensitivity to high-frequency angular head movements. As an alternative to canal plugging, round window reinforcement has been shown to reduce most symptoms in most patients with intractable superior semicircular canal dehiscence with the exception of hearing loss (99).

Mild high-frequency sensorineural hearing loss occurs in ∼25% of patients (100) though significant hearing loss is rare (21). New-onset benign paroxysmal positional vertigo has been reported in up to 25% of postoperative patients likely due

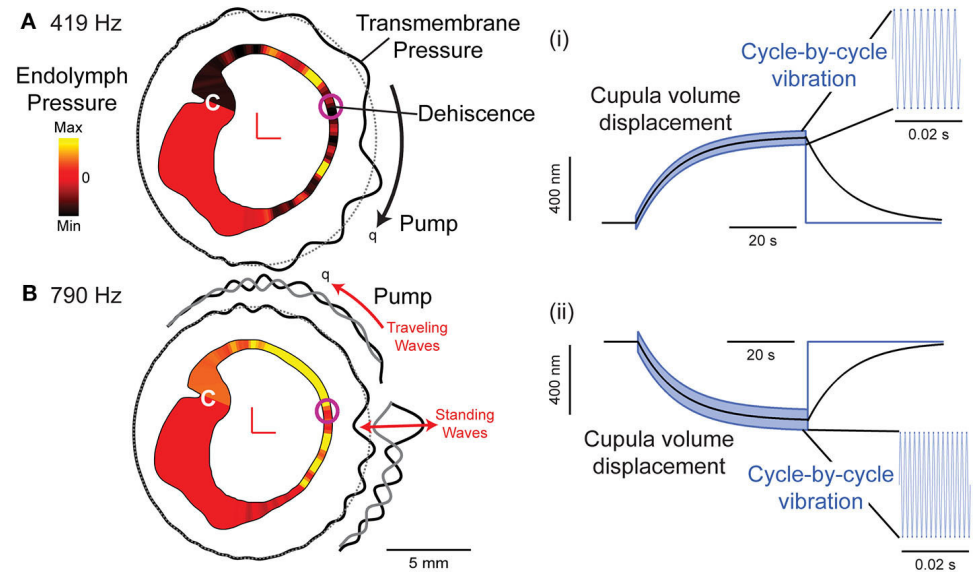

FIGURE 7 | Computational model of a human semicircular canal. **(A,B)** Auditory frequency stimulation at 419 Hz **(A)** and 790 Hz **(B)** evokes slowly developing endolymph pressure distribution (yellow: high; red: zero; and black: low) and a pressure gradient across the cupula (C). Waves travel along the membranous labyrinth away from the site of the dehiscence (transmembrane pressure: black solid line relative to gray dotted line) causing vibration of hair bundles at the stimulus frequency and pumping of endolymph (q) in either direction, ampullofugal for 419 Hz **(A)** and ampullopetal for 790 Hz **(B)**. (i,ii) Cupula displacement where black is the mechanical cupula volume displacement responsible for sustained afferent responses, blue is the cycle-by-cycle cupula vibration responsible for phase-locked afferent responses at 419 Hz (i) and 790 Hz (ii). Based on (34).

to otoconia or plugging material that becomes mobilized in the endolymph (101). Revision surgery is sometimes necessary when symptoms do not cease or reoccur and, in one report, is performed in approximately 10% of cases, though revisions are reported to carry a lower rate of success than primary surgery (102).

CONCLUSION

Superior semicircular canal dehiscence is the most common third-window syndrome. Patients present with sound- or pressure-evoked eye movements and dizziness, decrease in air-conducted hearing, and increase in bone-conducted hearing. The biomechanics of this disorder involves a shunting of acoustic energy away from the cochlea and toward the dehiscent semicircular canal. This increases sound-evoked VEMPs responses, and causes an increase in the audiometric air-bone gap. ECoG tests are consistent with an increase in the short-latency response from the vestibular organs relative to the long-latency response from the cochlea. Various other third window conditions have similar presentations. A dehiscence or fistula located in the bony canal renders the canal sensitive to AF sound and LF pressure. LF responses reflect slow displacements of the cupula in the excitatory or inhibitory direction driven by pressure-evoked deformation of the labyrinth. The specific afferent neurons most sensitive to LF cupula displacements fire action potentials with regularly spaced inter-spike intervals—neurons that provide sustained inputs to the central nervous system. In contrast, AF sound evokes waves that travel along the membranous labyrinth emanating from the site of the dehiscence. The waves vibrate the hair bundles leading to short-latency excitatory phase-locked neuron responses. The specific afferent neurons that are most sensitive to AF vibration fire action potentials with irregularly spaced inter-spike intervals—neurons that provide transient inputs to the central nervous system. These AF sensitive afferent neurons drive short-latency sound-evoked nystagmus in third window patients. In addition, sound generates a slow displacement of the cupula through wave-driven endolymph pumping. This can excite or inhibit regularly discharging afferents, depending on the subject-specific morphology and stimulus frequency, driving a long-latency component that superimposes on top of the short-latency sound-evoked nystagmus. Canal plugging, if complete, removes the third window and eliminates the syndrome.

AUTHOR CONTRIBUTIONS

MI and RR drafted manuscript, edited and revised manuscript, and approved final version of manuscript. MI prepared figures. All authors contributed to the article and approved the submitted version.

FUNDING

This work was supported by National Institute of Deafness and Other Communications Disorders Grant R01-DC-006685 and the National Science Foundation Graduate Research Fellowship #1747505.

REFERENCES

1. Voss SE, Rosowski JJ, Peake WT. Is the pressure difference between the oval and round windows the effective acoustic stimulus for the cochlea? *J Acoust Soc Am*. (1996) 100:1602–16. doi: 10.1121/1.416062
2. Ranke O, Keidel W, Weschke H. Das Höeren bei Verschluss des Runden Fensters. *Z Laryng*. (1952) 31:467–75.
3. Ranke O. Discussion remark to Von a. Meyer zum Gottesberg: Die Schalleitung im Mittelohr in klinischer Sicht. *Z Laryng*. (1958) 37:366–7.
4. Tonndorf J, Tabor JR. Closure of the cochlear windows: its effect upon air-and bone-conduction. *Ann Otol Rhinol Laryngol*. (1962) 71:5–29. doi: 10.1177/000348946207100101
5. Gopen Q, Rosowski JJ, Merchant SN. Anatomy of the normal human cochlear aqueduct with functional implications. *Hear Res*. (1997) 107:9–22. doi: 10.1016/S0378-5955(97)00017-8
6. Tullio P. *Das Ohr und die Entstehung der Sprache und Schrift. [The Ear and the Origin of Language and Writing]*. Oxford: Urban & Schwarzenberg (1929).
7. Hennebert C. Reactions vestibulaires dans les labyrinthites heredo-syphilitiques. *Arch Int Laryngol Otol Rhinol Brocho Oesophagoscopie*. (1909) 28:93–6.
8. Hennebert C. Reflexe oto-oculo-moteur. *Int Zentralblatt Ohrenheilkunde Rhino Laryngol*. (1905) 3:405.
9. Fox EJ, Balkany TJ, Arenberg IK. The Tullio phenomenon and perilymph fistula. *Otolaryngol Head Neck Surg*. (1988) 98:88–9. doi: 10.1177/019459988809800115
10. Hermann M, Coelho DH. Perilymph fistula presenting with contralateral symptoms. *Otol Neurotol*. (2014) 35:301–4. doi: 10.1097/MAO.0b013e3182a43639
11. Ishizaki H, Pyykko I, Aalto H, Starck J. Tullio phenomenon and postural stability: experimental study in normal subjects and patients with vertigo. *Ann Otol Rhinol Laryngol*. (1991) 100:976–83. doi: 10.1177/000348949110001205
12. Hornigold R, Pearch BJ, Gleeson MJ. An osteoma of the middle ear presenting with the tullio phenomenon. *Skull Base*. (2003) 13:113–7. doi: 10.1055/s-2003-40602
13. Minor LB, Solomon D, Zinreich JS, Zee DS. Sound- and/or pressure-induced vertigo due to bone dehiscence of the superior semicircular canal. *Arch Otolaryngol Head Neck Surg*. (1998) 124:249–58. doi: 10.1001/archotol.124.3.249
14. Williamson RA, Vrabec JT, Coker NJ, Sandlin M. Coronal computed tomography prevalence of superior semicircular canal dehiscence. *Otolaryngol Head Neck Surg*. (2003) 129:481–9. doi: 10.1016/S0194-5998(03)01391-3
15. Cloutier JF, Belair M, Saliba I. Superior semicircular canal dehiscence: positive predictive value of high-resolution CT scanning. *Eur Arch Otorhinolaryngol*. (2008) 265:1455–60. doi: 10.1007/s00405-008-0672-2
16. Ceylan N, Bayraktaroglu S, Alper H, Savas R, Bilgen C, Kirazli T, et al. CT imaging of superior semicircular canal dehiscence: added value of reformatted images. *Acta Otolaryngol*. (2010) 130:996–1001. doi: 10.3109/00016481003602108
17. Sequeira SM, Whiting BR, Shimony JS, Vo KD, Hullar TE. Accuracy of computed tomography detection of superior canal dehiscence. *Otol Neurotol*. (2011) 32:1500–5. doi: 10.1097/MAO.0b013e318238280c
18. Tavassolie TS, Penninger RT, Zuniga MG, Minor LB, Carey JP. Multislice computed tomography in the diagnosis of superior canal dehiscence: how much error, and how to minimize it? *Otol Neurotol*. (2012) 33:215–22. doi: 10.1097/MAO.0b013e318241c23b
19. Re M, Gioacchini FM, Salvolini U, Totaro AM, Santarelli A, Mallardi V, et al. Multislice computed tomography overestimates superior semicircular canal dehiscence syndrome. *Ann Otol Rhinol Laryngol*. (2013) 122:625–31. doi: 10.1177/000348941312201005
20. Wackym PA, Balaban CD, Zhang P, Siker DA, Hundal JS. Third window syndrome: surgical management of cochlea-facial nerve dehiscence. *Front Neurol*. (2019) 10:1281. doi: 10.3389/fneur.2019.01281
21. Ward BK, Carey JP, Minor LB. Superior canal dehiscence syndrome: lessons from the first 20 years. *Front Neurol*. (2017) 8:177. doi: 10.3389/fneur.2017.00177
22. Minor LB. Clinical manifestations of superior semicircular canal dehiscence. *Laryngoscope*. (2005) 115:1717–27. doi: 10.1097/01.mlg.0000178324.55729.b7
23. Carey JP, Minor LB, Nager GT. Dehiscence or thinning of bone overlying the superior semicircular canal in a temporal bone survey. *Arch Otolaryngol Head Neck Surg*. (2000) 126:137–47. doi: 10.1001/archotol.126.2.137
24. Dlugaiczyk J, Burgess AM, Goonetilleke SC, Sokolic L, Curthoys IS. Superior canal dehiscence syndrome: relating clinical findings with vestibular neural responses from a guinea pig model. *Otol Neurotol*. (2019) 40:e406–14. doi: 10.1097/MAO.0000000000001940
25. Baxter M, Mccorkle C, Trevino Guajardo C, Zuniga MG, Carter AM, Della Santina CC, et al. Clinical and physiologic predictors and postoperative outcomes of near dehiscence syndrome. *Otol Neurotol*. (2019) 40:204–12. doi: 10.1097/MAO.0000000000002077
26. Chien WW, Carey JP, Minor LB. Canal dehiscence. *Curr Opin Neurol*. (2011) 24:25–31. doi: 10.1097/WCO.0b013e328341ef88
27. Emmett JR. The large vestibular aqueduct syndrome. *Am J Otol*. (1985) 6:387–415.
28. Blake DM, Tomovic S, Vazquez A, Lee HJ, Jyung RW. Cochlear-facial dehiscence–a newly described entity. *Laryngoscope*. (2014) 124:283–9. doi: 10.1002/lary.24223
29. Bae YJ, Shim YJ, Choi BS, Kim JH, Koo JW, Song JJ. "Third Window" and "Single Window" effects impede surgical success: analysis of retrofenestral otosclerosis involving the internal auditory canal or round window. *J Clin Med*. (2019) 8:1182. doi: 10.3390/jcm8081182
30. Shim YJ, Bae YJ, An GS, Lee K, Kim Y, Lee SY, et al. Involvement of the internal auditory canal in subjects with cochlear otosclerosis: a less acknowledged third window that affects surgical outcome. *Otol Neurotol*. (2019) 40:e186–90. doi: 10.1097/MAO.0000000000002144
31. Songer JE, Rosowski JJ. A mechano-acoustic model of the effect of superior canal dehiscence on hearing in chinchilla. *J Acoust Soc Am*. (2007) 122:943–51. doi: 10.1121/1.2747158
32. Kim N, Steele CR, Puria S. Superior-semicircular-canal dehiscence: effects of location, shape, and size on sound conduction. *Hear Res*. (2013) 301:72–84. doi: 10.1016/j.heares.2013.03.008
33. Grieser BJ, Kleiser L, Obrist D. Identifying mechanisms behind the tullio phenomenon: a computational study based on first principles. *J Assoc Res Otolaryngol*. (2016) 17:103–18. doi: 10.1007/s10162-016-0553-0
34. Iversen MM, Zhu H, Zhou W, Della Santina CC, Carey JP, Rabbitt RD. Sound abnormally stimulates the vestibular system in canal dehiscence syndrome by generating pathological fluid-mechanical waves. *Sci Rep*. (2018) 8:10257. doi: 10.1038/s41598-018-28592-7
35. Mikulec AA, Mckenna MJ, Ramsey MJ, Rosowski JJ, Herrmann BS, Rauch SD, et al. Superior semicircular canal dehiscence presenting as conductive hearing loss without vertigo. *Otol Neurotol*. (2004) 25:121–9. doi: 10.1097/00129492-200403000-00007
36. Modugno G, Brandolini C, Savastio G, Ceroni AR, Pirodda A. Superior semicircular canal dehiscence: a series of 13 cases. *ORL J Otorhinolaryngol Relat Spec*. (2005) 67:180–4. doi: 10.1159/000086573
37. Hillman TA, Kertesz TR, Hadley K, Shelton C. Reversible peripheral vestibulopathy: the treatment of superior canal dehiscence. *Otolaryngol Head Neck Surg*. (2006) 134:431–6. doi: 10.1016/j.otohns.2005.10.033
38. Limb CJ, Carey JP, Srireddy S, Minor LB. Auditory function in patients with surgically treated superior semicircular canal dehiscence. *Otol Neurotol*. (2006) 27:969–80. doi: 10.1097/01.mao.0000235376.70492.8e
39. Schmuziger N, Allum J, Buitrago-Téllez C, Probst R. Incapacitating hypersensitivity to one's own body sounds due to a dehiscence of bone overlying the superior semicircular canal. A case report. *Eur Arch Oto Rhino Laryngol Head Neck*. (2006) 263:69–74. doi: 10.1007/s00405-005-0939-9
40. Merchant SN, Rosowski JJ. Conductive hearing loss caused by third-window lesions of the inner ear. *Otol Neurotol*. (2008) 29:282–9. doi: 10.1097/MAO.0b013e318161ab24
41. Merchant SN, Rosowski JJ, Mckenna MJ. Superior semicircular canal dehiscence mimicking otosclerotic hearing loss. *Adv Otorhinolaryngol*. (2007) 65:137–45. doi: 10.1159/000098790
42. Merchant SN, Nakajima HH, Halpin C, Nadol JBJr, Lee DJ, Innis WP, et al. Clinical investigation and mechanism of air-bone gaps in large

vestibular aqueduct syndrome. *Ann Otol Rhinol Laryngol*. (2007) 116:532–41. doi: 10.1177/000348940711600709
43. Bance M. When is a conductive hearing loss not a conductive hearing loss? Causes of a mismatch in air-bone threshold measurements or a "pseudoconductive" hearing loss. *J Otolaryngol*. (2004) 33:135–8. doi: 10.2310/7070.2004.00135
44. Brantberg K, Bagger-Sjöbäck D, Mathiesen T, Witt H, Pansell T. Posterior canal dehiscence syndrome caused by an apex cholesteatoma. *Otol Neurotol*. (2006) 27:531–4. doi: 10.1097/01.mao.0000201433.50122.62
45. Mikulec AA, Poe DS. Operative management of a posterior semicircular canal dehiscence. *Laryngoscope*. (2006) 116:375–8. doi: 10.1097/01.mlg.0000200358.93385.5c
46. Kim HHS, Wilson DF. A third mobile window at the cochlear apex. *Otolaryngol Head Neck Surg*. (2006) 135:965–6. doi: 10.1016/j.otohns.2005.04.006
47. Nakajima HH, Pisano DV, Roosli C, Hamade MA, Merchant GR, Mahfoud L, et al. Comparison of ear-canal reflectance and umbo velocity in patients with conductive hearing loss: a preliminary study. *Ear Hear*. (2012) 33:35–43. doi: 10.1097/AUD.0b013e31822ccba0
48. Merchant GR, Merchant SN, Rosowski JJ, Nakajima HH. Controlled exploration of the effects of conductive hearing loss on wideband acoustic immittance in human cadaveric preparations. *Hear Res*. (2016) 341:19–30. doi: 10.1016/j.heares.2016.07.018
49. Rosowski JJ, Songer JE, Nakajima HH, Brinsko KM, Merchant SN. Clinical, experimental, and theoretical investigations of the effect of superior semicircular canal dehiscence on hearing mechanisms. *Otol Neurotol*. (2004) 25:323–32. doi: 10.1097/00129492-200405000-00021
50. Chien WW, Janky K, Minor LB, Carey JP. Superior canal dehiscence size: multivariate assessment of clinical impact. *Otol Neurotol*. (2012) 33:810–5. doi: 10.1097/MAO.0b013e318248eac4
51. Niesten ME, Stieger C, Lee DJ, Merchant JP, Grolman W, Rosowski JJ, et al. Assessment of the effects of superior canal dehiscence location and size on intracochlear sound pressures. *Audiol Neurootol*. (2015) 20:62–71. doi: 10.1159/000366512
52. Halmagyi GM, Aw ST, Mcgarvie LA, Todd MJ, Bradshaw A, Yavor RA, et al. Superior semicircular canal dehiscence simulating otosclerosis. *J Laryngol Otol*. (2003) 117:553–7. doi: 10.1258/002221503322113003
53. Minor LB, Carey JP, Cremer PD, Lustig LR, Streubel S-O. Dehiscence of bone overlying the superior canal as a cause of apparent conductive hearing loss. *Otol Neurotol*. (2003) 24:270–8. doi: 10.1097/00129492-200303000-00023
54. Mikulec AA, Poe DS, Mckenna MJ. Operative management of superior semicircular canal dehiscence. *Laryngoscope*. (2005) 115:501–7. doi: 10.1097/01.mlg.0000157844.48036.e7
55. Cremer PD, Minor LB, Carey JP, Della Santina CC. Eye movements in patients with superior canal dehiscence syndrome align with the abnormal canal. *Neurology*. (2000) 55:1833–41. doi: 10.1212/WNL.55.12.1833
56. Castellucci A, Brandolini C, Del Vecchio V, Giordano D, Pernice C, Bianchin G, et al. Temporal bone meningocele associated with superior canal dehiscence. *Otol Neurotol*. (2018) 39:e506–8. doi: 10.1097/MAO.0000000000001843
57. Rajan GP, Leaper MR, Goggin L, Atlas MD, Boeddinghaus R, Eikelboom RK. The effects of superior semicircular canal dehiscence on the labyrinth: does size matter? *Otol Neurotol*. (2008) 29:972–5. doi: 10.1097/MAO.0b013e31817f7382
58. Curthoys IS, Vulovic V, Sokolic L, Pogson J, Burgess AM. Irregular primary otolith afferents from the guinea pig utricular and saccular maculae respond to both bone conducted vibration and to air conducted sound. *Brain Res Bull*. (2012) 89:16–21. doi: 10.1016/j.brainresbull.2012.07.007
59. Zhu H, Tang X, Wei W, Maklad A, Mustain W, Rabbitt R, et al. Input-output functions of vestibular afferent responses to air-conducted clicks in rats. *J Assoc Res Otolaryngol*. (2014) 15:73–86. doi: 10.1007/s10162-013-0428-6
60. Colebatch JG, Halmagyi GM, Skuse NF. Myogenic potentials generated by a click-evoked vestibulocollic reflex. *J Neurol Neurosurg Psychiatry*. (1994) 57:190–7. doi: 10.1136/jnnp.57.2.190
61. Murofushi T, Curthoys IS, Topple AN, Colebatch JG, Halmagyi GM. Responses of guinea pig primary vestibular neurons to clicks. *Exp Brain Res*. (1995) 103:174–8. doi: 10.1007/BF00241975
62. Manzari L, Tedesco A, Burgess AM, Curthoys IS. Ocular vestibular-evoked myogenic potentials to bone-conducted vibration in superior vestibular neuritis show utricular function. *Otolaryngol Head Neck Surg*. (2010) 143:274–80. doi: 10.1016/j.otohns.2010.03.020
63. Curthoys IS, Manzari L. Evidence missed: ocular vestibular-evoked myogenic potential and cervical vestibular-evoked myogenic potential differentiate utricular from saccular function. *Otolaryngol Head Neck Surg*. (2011) 144:751–2. doi: 10.1177/0194599810397792
64. Hunter JB, Patel NS, O'connell BP, Carlson ML, Shepard NT, Mccaslin DL, et al. Cervical and ocular VEMP testing in diagnosing superior semicircular canal dehiscence. *Otolaryngol Head Neck Surg*. (2017) 156:917–23. doi: 10.1177/0194599817690720
65. Brantberg K, Bergenius J, Tribukait A. Vestibular-evoked myogenic potentials in patients with dehiscence of the superior semicircular canal. *Acta Otolaryngol*. (1999) 119:633–40. doi: 10.1080/00016489950180559
66. Streubel SO, Cremer PD, Carey JP, Weg N, Minor LB. Vestibular-evoked myogenic potentials in the diagnosis of superior canal dehiscence syndrome. *Acta Otolaryngol Suppl*. (2001) 545:41–9. doi: 10.1080/000164801750388090
67. Welgampola MS, Myrie OA, Minor LB, Carey JP. Vestibular-evoked myogenic potential thresholds normalize on plugging superior canal dehiscence. *Neurology*. (2008) 70:464–72. doi: 10.1212/01.wnl.0000299084.76250.4a
68. Janky KL, Nguyen KD, Welgampola M, Zuniga MG, Carey JP. Air-conducted oVEMPs provide the best separation between intact and superior canal dehiscent labyrinths. *Otol Neurotol*. (2013) 34:127–34. doi: 10.1097/MAO.0b013e318271c32a
69. Manzari L, Burgess AM, Mcgarvie LA, Curthoys IS. An indicator of probable semicircular canal dehiscence: ocular vestibular evoked myogenic potentials to high frequencies. *Otolaryngol Head Neck Surg*. (2013) 149:142–5. doi: 10.1177/0194599813489494
70. Steenerson KK, Crane BT, Minor LB. Superior semicircular canal dehiscence syndrome. *Semin Neurol*. (2020) 40:151–9. doi: 10.1055/s-0039-3402738
71. Curthoys IS. A critical review of the neurophysiological evidence underlying clinical vestibular testing using sound, vibration and galvanic stimuli. *Clin Neurophysiol*. (2010) 121:132–44. doi: 10.1016/j.clinph.2009.09.027
72. Sheykholeslami K, Schmerber S, Habiby Kermany M, Kaga K. Vestibular-evoked myogenic potentials in three patients with large vestibular aqueduct. *Hear Res*. (2004) 190:161–8. doi: 10.1016/S0378-5955(04)00018-8
73. Modugno GC, Magnani G, Brandolini C, Savastio G, Pirodda A. Could vestibular evoked myogenic potentials (VEMPs) also be useful in the diagnosis of perilymphatic fistula? *Eur Arch Otorhinolaryngol*. (2006) 263:552–5. doi: 10.1007/s00405-006-0008-z
74. Fife TD, Colebatch JG, Kerber KA, Brantberg K, Strupp M, Lee H, et al. Practice guideline: cervical and ocular vestibular evoked myogenic potential testing: report of the guideline development, dissemination, and implementation Subcommittee of the American Academy of Neurology. *Neurology*. (2017) 89:2288–96. doi: 10.1212/WNL.0000000000004690
75. Arts HA, Adams ME, Telian SA, El-Kashlan H, Kileny PR. Reversible electrocochleographic abnormalities in superior canal dehiscence. *Otol Neurotol*. (2009) 30:79–86. doi: 10.1097/MAO.0b013e31818d1b51
76. Adams ME, Kileny PR, Telian SA, El-Kashlan HK, Heidenreich KD, Mannarelli GR, et al. Electrocochleography as a diagnostic and intraoperative adjunct in superior semicircular canal dehiscence syndrome. *Otol Neurotol*. (2011) 32:1506–12. doi: 10.1097/MAO.0b013e3182382a7c
77. Park JH, Lee SY, Song JJ, Choi BY, Koo JW. Electrocochleographic findings in superior canal dehiscence syndrome. *Hear Res*. (2015) 323:61–7. doi: 10.1016/j.heares.2015.02.001
78. Wenzel A, Ward BK, Ritzl EK, Gutierrez-Hernandez S, Della Santina CC, Minor LB, et al. Intraoperative neuromonitoring for superior semicircular canal dehiscence and hearing outcomes. *Otol Neurotol*. (2015) 36:139. doi: 10.1097/MAO.0000000000000642
79. Ward BK, Wenzel A, Ritzl EK, Gutierrez-Hernandez S, Della Santina CC, Minor LB, et al. Near-dehiscence: clinical findings in patients with thin bone over the superior semicircular canal. *Otol Neurotol*. (2013) 34:1421–8. doi: 10.1097/MAO.0b013e318287efe6
80. Govaerts PJ, Casselman J, Daemers K, De Ceulaer G, Somers T, Offeciers FE. Audiological findings in large vestibular aqueduct syndrome. *Int J*

Pediatr Otorhinolaryngol. (1999) 51:157–64. doi: 10.1016/S0165-5876(99)00268-2
81. Arenberg IK, Ackley RS, Ferraro J, Muchnik C. ECoG results in perilymphatic fistula: clinical and experimental studies. *Otolaryngol Head Neck Surg*. (1988) 99:435–43. doi: 10.1177/019459988809900501
82. Campbell KC, Savage MM. Electrocochleographic recordings in acute and healed perilymphatic fistula. *Arch Otolaryngol Head Neck Surg*. (1992) 118:301–4. doi: 10.1001/archotol.1992.01880030089018
83. Carey JP, Hirvonen TP, Hullar TE, Minor LB. Acoustic responses of vestibular afferents in a model of superior canal dehiscence. *Otol Neurotol*. (2004) 25:345–52. doi: 10.1097/00129492-200405000-00024
84. Iversen MM, Rabbitt RD. Wave mechanics of the vestibular semicircular canals. *Biophys J*. (2017) 113:1133–49. doi: 10.1016/j.bpj.2017.08.001
85. Zhu H, Tang X, Wei W, Mustain W, Xu Y, Zhou W. Click-evoked responses in vestibular afferents in rats. *J Neurophysiol*. (2011) 106:754–63. doi: 10.1152/jn.00003.2011
86. Carey JP, Migliaccio AA, Minor LB. Semicircular canal function before and after surgery for superior canal dehiscence. *Otol Neurotol*. (2007) 28:356–64. doi: 10.1097/01.mao.0000253284.40995.d8
87. Crane BT, Lin FR, Minor LB, Carey JP. Improvement in autophony symptoms after superior canal dehiscence repair. *Otol Neurotol*. (2010) 31:140–6. doi: 10.1097/MAO.0b013e3181bc39ab
88. Crane BT, Minor LB, Carey JP. Superior canal dehiscence plugging reduces dizziness handicap. *Laryngoscope*. (2008) 118:1809–13. doi: 10.1097/MLG.0b013e31817f18fa
89. Remenschneider AK, Owoc M, Kozin ED, Mckenna MJ, Lee DJ, Jung DH. Health utility improves after surgery for superior canal dehiscence syndrome. *Otol Neurotol*. (2015) 36:1695–701. doi: 10.1097/MAO.0000000000000886
90. Agrawal Y, Migliaccio AA, Minor LB, Carey JP. Vestibular hypofunction in the initial postoperative period after surgical treatment of superior semicircular canal dehiscence. *Otol Neurotol*. (2009) 30:502–6. doi: 10.1097/MAO.0b013e3181a32d69
91. Janky KL, Zuniga MG, Carey JP, Schubert M. Balance dysfunction and recovery after surgery for superior canal dehiscence syndrome. *Arch Otolaryngol Head Neck Surg*. (2012) 138:723–30. doi: 10.1001/archoto.2012.1329
92. Schubert MC, Migliaccio AA, Della Santina CC. Dynamic visual acuity during passive head thrusts in canal planes. *J Assoc Res Otolaryngol*. (2006) 7:329–38. doi: 10.1007/s10162-006-0047-6
93. Carender WJ, Grzesiak M. Vestibular rehabilitation following surgical repair for superior canal dehiscence syndrome: a complicated case report. *Physiother Theory Pract*. (2018) 34:146–56. doi: 10.1080/09593985.2017.1374491
94. Hess BJ, Lysakowski A, Minor LB, Angelaki DE. Central versus peripheral origin of vestibuloocular reflex recovery following semicircular canal plugging in rhesus monkeys. *J Neurophysiol*. (2000) 84:3078–82. doi: 10.1152/jn.2000.84.6.3078
95. Rabbitt RD, Boyle R, Highstein SM. Physiology of the semicircular canals after surgical plugging. *Ann N Y Acad Sci*. (2001) 942:274–86. doi: 10.1111/j.1749-6632.2001.tb03752.x
96. Sadeghi SG, Goldberg JM, Minor LB, Cullen KE. Effects of canal plugging on the vestibuloocular reflex and vestibular nerve discharge during passive and active head rotations. *J Neurophysiol*. (2009) 102:2693–703. doi: 10.1152/jn.00710.2009
97. Mantokoudis G, Saber Tehrani AS, Wong AL, Agrawal Y, Wenzel A, Carey JP. Adaptation and compensation of vestibular responses following superior canal dehiscence surgery. *Otol Neurotol*. (2016) 37:1399–405. doi: 10.1097/MAO.0000000000001196
98. Hassannia F, Douglas-Jones P, Rutka JA. Gauging the effectiveness of canal occlusion surgery: how I do it. *J Laryngol Otol*. 133:1012–6. doi: 10.1017/S0022215119002032
99. Silverstein H, Kartush JM, Parnes LS, Poe DS, Babu SC, Levenson MJ, et al. Round window reinforcement for superior semicircular canal dehiscence: a retrospective multi-center case series. *Am J Otolaryngol*. (2014) 35:286–93. doi: 10.1016/j.amjoto.2014.02.016
100. Ward BK, Agrawal Y, Nguyen E, Della Santina CC, Limb CJ, Francis HW, et al. Hearing outcomes after surgical plugging of the superior semicircular canal by a middle cranial fossa approach. *Otol Neurotol*. (2012) 33:1386–91. doi: 10.1097/MAO.0b013e318268d20d
101. Barber SR, Cheng YS, Owoc M, Lin BM, Remenschneider AK, Kozin ED, et al. Benign paroxysmal positional vertigo commonly occurs following repair of superior canal dehiscence. *Laryngoscope*. (2016) 126:2092–7. doi: 10.1002/lary.25797
102. Sharon JD, Pross SE, Ward BK, Carey JP. Revision surgery for superior canal dehiscence syndrome. *Otol Neurotol*. (2016) 37:1096–103. doi: 10.1097/MAO.0000000000001113

Conflict of Interest: The authors declare that the research was conducted in the absence of any commercial or financial relationships that could be construed as a potential conflict of interest.

frontiers in Neurology

ORIGINAL RESEARCH
published: 25 August 2020
doi: 10.3389/fneur.2020.00879

Ocular Vestibular-Evoked Myogenic Potential Amplitudes Elicited at 4 kHz Optimize Detection of Superior Semicircular Canal Dehiscence

*Emma D. Tran[1], Austin Swanson[1], Jeffrey D. Sharon[2], Yona Vaisbuch[1,3], Nikolas H. Blevins[1], Matthew B. Fitzgerald[1] and Kristen K. Steenerson[1]**

[1] Department of Otolaryngology—Head and Neck Surgery, Stanford University School of Medicine, Stanford, CA, United States, [2] Department of Otolaryngology—Head and Neck Surgery, University of California, San Francisco, San Francisco, CA, United States, [3] Department of Otolaryngology—Head and Neck Surgery, Rambam Medical Center, Haifa, Israel

Introduction: High-resolution temporal bone computed tomography (CT) is considered the gold standard for diagnosing superior semicircular canal dehiscence (SCD). However, CT has been shown over-detect SCD and provide results that may not align with patient-reported symptoms. Ocular vestibular-evoked myogenic potentials (oVEMPs)—most commonly conducted at 500 Hz stimulation—are increasingly used to support the diagnosis and management of SCD. Previous research reported that stimulation at higher frequencies such as 4 kHz can have near-perfect sensitivity and specificity in detecting radiographic SCD. With a larger cohort, we seek to understand the sensitivity and specificity of 4 kHz oVEMPs for detecting clinically significant SCD, as well as subgroups of radiographic, symptomatic, and surgical SCD. We also investigate whether assessing the 4 kHz oVEMP n10-p15 amplitude rather than the binary n10 response alone would optimize the detection of SCD.

Methods: We conducted a cross-sectional study of patients who have undergone oVEMP testing at 4 kHz. Using the diagnostic criteria proposed by Ward et al., patients were determined to have SCD if dehiscence was confirmed on temporal bone CT by two reviewers, patient-reported characteristic symptoms, and if they had at least one positive vestibular or audiometric test suggestive of SCD. Receiver operating characteristic (ROC) analysis was conducted to identify the optimal 4 kHz oVEMP amplitude cut-off. Comparison of 4 kHz oVEMP amplitude across radiographic, symptomatic, and surgical SCD subgroups was conducted using the Mann-Whitney U test.

Results: Nine hundred two patients (*n*, ears = 1,804) underwent 4 kHz oVEMP testing. After evaluating 150 temporal bone CTs, we identified 49 patients (*n*, ears = 61) who had radiographic SCD. Of those, 33 patients (*n*, ears = 37) were determined to have clinically significant SCD. For this study cohort, 4 kHz oVEMP responses had a sensitivity of 86.5% and a specificity of 87.8%. ROC analysis demonstrated that accounting for the inter-amplitude of 4 kHz oVEMP was more accurate in detecting SCD than the presence of n10 response alone (AUC 91 vs. 87%). Additionally, using an amplitude cut-off of 15uV reduces false positive results and improves specificity to 96.8%. Assessing 4 kHz

OPEN ACCESS

Edited by:
P. Ashley Wackym, Rutgers, The State University of New Jersey, United States

Reviewed by:
Chunfu DAI, Fudan University, China
Steven D. Rauch, Harvard Medical School, United States

***Correspondence:**
Kristen K. Steenerson
ksteen@stanford.edu

Specialty section:
This article was submitted to Neuro-Otology, a section of the journal Frontiers in Neurology

Received: *29 May 2020*
Accepted: *09 July 2020*
Published: *25 August 2020*

Citation:
Tran ED, Swanson A, Sharon JD, Vaisbuch Y, Blevins NH, Fitzgerald MB and Steenerson KK (2020) Ocular Vestibular-Evoked Myogenic Potential Amplitudes Elicited at 4 kHz Optimize Detection of Superior Semicircular Canal Dehiscence. Front. Neurol. 11:879. doi: 10.3389/fneur.2020.00879

oVEMP response across SCD subgroups demonstrated that surgical and symptomatic SCD cases had significantly higher amplitudes, while radiographic SCD cases without characteristic symptoms had similar amplitudes compared to cases without evidence of SCD.

Conclusion: Our results suggest that accounting for 4 kHz oVEMP amplitude can improve detection of SCD compared to the binary presence of n10 response. The 4 kHz oVEMP amplitude cut-off that maximizes sensitivity and specificity for our cohort is 15 uV. Our results also suggest that 4 kHz oVEMP amplitudes align better with symptomatic SCD cases compared to cases in which there is radiographic SCD but no characteristic symptoms.

Keywords: superior semicircular canal dehiscence, vestibular evoked myogenic potential, vestibular testing, vestibular dysfunction, third window, computed tomography, temporal bone

INTRODUCTION

In 1998, Minor et al. reported on a series of difficult-to-diagnose patients who experienced sound- or pressure-induced vertigo and demonstrated nystagmus in the plane of the superior semicircular canal (SSC) (1). On computed tomography (CT) imaging, they were found to have a bony dehiscence above the SSC, which was confirmed through surgical exploration and repair. These patients were diagnosed with superior semicircular canal dehiscence (SCD). The opening between the inner ear and cranial cavity creates a novel low-impedance pathway, which re-routes some of the acoustic energy generated from the middle ear to the labyrinth. This phenomenon was described as a third-window effect (2) to which the classic constellation of SCD symptoms (e.g., bone-conduction hyperacusis, pulsatile tinnitus, and sound- or pressure-induced vertigo) is attributed (3, 4).

Since its discovery, SCD has posed a great diagnostic challenge. Identification of the dehiscence on high-resolution temporal bone CT has long been the gold standard of diagnosis but has remained limited by the variability of CT scanner quality, imaging protocols, and interpretations (5). Even with sub-millimeter resolutions, CT scans may still be unable to visualize very thin bone (6). This has led to the radiographic prevalence of SCD (7–9) being considerably higher than those found in cadaveric temporal bone studies (10). In addition, it is thought that many patients with SCD can be asymptomatic or can present with non-specific symptoms potentially related to other etiologies (11). Other vestibular disorders that cause dizziness, including migraine, are often seen in patients with SCD (12, 13). Some are thought to be "sensitized" by SCD or can just occur concomitantly (14). Given that imaging can over-detect dehiscence and SCD symptoms can present variably, Ward et al. proposed diagnostic criteria for clinically significant SCD (hereafter referred to as SCD_{θ}), which required both evidence on CT and specific symptoms characteristic of SCD, as well as a third criterion of a positive finding on physiologic testing. The third criterion can be valuable in the diagnosis and management of SCD when there is uncertainty regarding imaging or symptoms.

Vestibular-evoked myogenic potentials (VEMPs) were first described in 1994 (15). They are thought to reflect a reflex arc in which stimulation of the saccule and utricle generate a myogenic response in the ipsilateral sternocleidomastoid (i.e., cervical or cVEMPs) (15) or the contralateral inferior oblique (i.e., ocular or oVEMPs), respectively (16–18). These organs normally respond to loud acoustic stimuli, but in the setting of a third window, responses are exaggerated (19, 20). Unsurprisingly, then, VEMPs have become an increasingly important part of the diagnostic battery for SCD. Lower cVEMP threshold was the first to be reported to correlate with radiographic SCD (21, 22), and then later, oVEMP amplitude was shown to correlate better with surgically confirmed SCD (23, 24). However, given the variability of these tests due to factors such as age; degree of conductive hearing loss; and even testing equipment, operators, and protocols (25–27); guidelines for incorporating these tests into the diagnostic battery remain ambiguous (28). Manzari et al. demonstrated that the binary presence of the oVEMP n10 response stimulated at a higher frequency such as 4 kHz had a sensitivity and specificity of 100% in 22 patients with radiographic SCD (29). Lin et al. recently validated the superior diagnostic accuracy of 4 kHz oVEMPs n10 response in a similar but larger patient population. However, they were unable to attain the perfect sensitivity and specificity seen by Lin et al. (30).

In this study, we seek to assess the performance of 4 kHz oVEMP in detecting clinically significant SCD_{θ}, as defined by the Ward et al. diagnostic criteria (28), in addition to detecting subgroups of radiographic, symptomatic, and surgical SCD. Given the number of clinical false positives, we also seek to determine whether assessing the amplitude rather than the binary presence of the n10 response for 4 kHz oVEMP can further optimize the detection of SCD.

METHODS

Subjects

We conducted a cross-sectional study of patients seen at our tertiary referral center and who underwent vestibular testing between October 2016 and October 2019. Patients with oVEMP testing conducted at 500 Hz and 4 kHz, cVEMP testing conducted at 500 Hz, audiometric testing, high-resolution computed tomography (CT) imaging, and clinical data including

symptomatology were included in the analysis. Study subjects were excluded if they (1) did not have reliable CT imaging studies, (2) had no measurable response for both cVEMP and oVEMP testing, (3) had 4 kHz oVEMP waveforms that were non-reproducible or lacked either a discernable n10 trough or p15 peak, (4) had abnormal tympanometry, or (5) had a history of ear surgeries or middle-ear conditions that could negate the VEMP response.

Our study cohort was defined by the diagnostic criteria for SCD proposed by Ward et al. (SCD_{θ}), which includes: (1) dehiscence identified on high-resolution CT; (2) at least one of the following characteristic symptoms: autophony or hyperacusis, sound- or pressure-induced vertigo, or pulsatile tinnitus; and (3) at least one of the following audiometric test results: negative bone conduction thresholds on pure-tone audiometry, low cVEMP thresholds, or high oVEMP amplitudes (28). A subject was considered to have negative bone conduction when thresholds were <0 db HL at any frequency. A high oVEMP amplitude was defined as peak-to-peak measurements ≥17 uV at 500 Hz stimulus (23). A cVEMP threshold was considered low when the lowest intensity 500 Hz stimulus that could elicit a reproducible characteristic p13 n23 waveform was ≤75 dB nHL. While third criterion proposed by Ward et al. includes other VEMP testing that may correlate with 4 kHz oVEMP results, these tests are still believed to represent independent physiological responses to different acoustic stimuli. Therefore, we included all three criteria when defining our study cohort.

Through a retrospective chart review, radiographic dehiscence was considered confirmed when both the reading neuroradiologist and diagnosing physician identified a dehiscence on CT imaging. If there was a discrepancy between this initial review of the CT, three expert reviewers (consisting of two neurotologists and one otoneurologist) adjudicated the results through a tie-break protocol. Images that demonstrate thinning or near-dehiscence of the temporal bone were considered negative for SCD. Subjects were considered symptomatic if they had positive dehiscence on CT, as defined by the criteria above; demonstrated symptoms that are characteristic of SCD; and the symptoms were determined to be related to the dehiscence by the diagnosing physician.

Audiometric Procedures

Audiometric data were obtained as part of audiologic evaluations at our institution's audiology clinic. Tests were completed in a double-walled sound booth using GSI Audiostar Pro

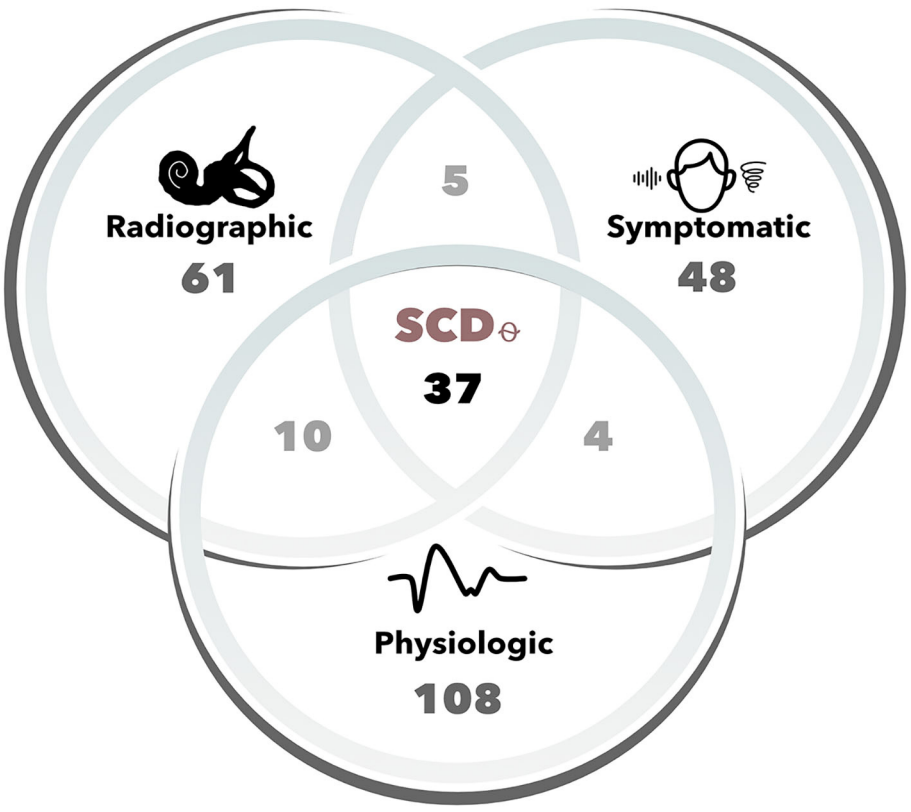

FIGURE 1 | Number of cases for each Ward et al. diagnostic criteria of SCD_{θ}. Cases (i.e., ears) were determined to be radiographically positive based upon two-party review of high-resolution (sub-millimeter) temporal bone computed tomography (CT) scans. Symptomatic cases included one of the following patient-reported symptoms: hyperacusis/autophony, pulsatile tinnitus, sound-, or pressure-induced vertigo. Physiologic cases were those that had either 500 Hz oVEMP amplitude ≥ 17 uV, 500 Hz cVEMP threshold ≤ 75 dB nHL, or negative bone-conduction thresholds. SCD_{θ} refers to our study cohort of clinically significant SCD, as defined by the radiographic, symptomatic, and physiologic diagnostic criteria proposed by Ward et al.

(Grason-Stadler) audiometers and conducted using ER-3A insert earphones or Sennheiser HDA 200 circumaural headphones. A modified Hughson-Westlake method was used to measure air-conduction and bone-conduction thresholds, which could be measured as low as −10 dB HL (31). Bone-conduction testing was conducted with masking if the difference between air- and unmasked bone-conduction thresholds were >10 dB HL. Air-bone gap averages were calculated using the average of the frequencies 250, 500, and 1,000 Hz (32, 33).

VEMP Testing

VEMP testing was completed using an Intelligent Hearing Systems Smart USB (Intelligent Hearing Systems, 6860 SW 81st Street Miami, FL 33143, USA) evoked potential system. Ipsilateral cVEMP results were obtained with the patient reclined to 30 degrees above horizontal, with the head rotated 45 degrees from the test ear, and held above the exam throughout each run. Contralateral oVEMP recordings were obtained with the patient seated upright with head position held level and eye gaze held 30 degrees above horizontal. Air conduction 500 Hz tone bursts were used as stimuli for cVEMP and oVEMP threshold search and inter-amplitude measurement for each ear. Air conduction 4 kHz tone bursts delivered at 95 dB nHL were also used as stimuli for measurement of oVEMP inter-amplitude for each ear. Stimulus envelope characteristics for all VEMP stimuli had a rise, plateau, and fall of 2, 1, and 2 ms, respectively. Amplifier gain was set to 5,000 for cVEMP and 100,000 for oVEMP. The cVEMP high-pass and low-pass filter was set to 10 and 1,500 Hz, respectively. The oVEMP high-pass and low-pass filter was set to 1 and 1,000 Hz, respectively. For threshold search, stimulus intensity was decreased in 10 dB steps until threshold was obtained as the last reproducible response. An evoked potential response is defined as the presence of a reproducible n1 negative peak. The highest inter-amplitude between the n1 and p1 negative and positive peaks, respectively, were manually measured using the software interface. All audiometric data including pure-tone and VEMP testing were prospectively recorded in a custom relational database in Filemaker (Claris International Inc., Santa Clara, CA, USA).

Analysis

R version 3.6.1 (R Foundation for Statistical Computing, Vienna, Austria) (34) was used for statistical analysis with the finalfit (35) package for generation of data tables, ggplot2 (36) package for data visualization, and pROC (37) packages for receiver operating characteristic (ROC) analysis. For the demographics table, we used the Mann-Whitney *U*-test for continuous variables and Pearson's chi-squared test or Fisher's exact test for categorical variables, as appropriate. To identify the optimal diagnostic cut-off for 4 kHz oVEMP amplitude, we conducted a ROC analysis. Sensitivity and specificity were calculated for each amplitude cut-off and the associated 95% confidence interval (CI) are "exact" Clopper-Pearson intervals. Area under the curve was calculated for each cut-off and compared using DeLong's test. Comparisons of 4 kHz oVEMP amplitude across SCD subgroups, as well as characteristic symptoms, were conducted using the Mann-Whitney U test. All results were considered significant at $\alpha = 0.05$.

TABLE 1 | Patient characteristics for patients with superior semicircular canal dehiscence.

		SCD_θ	Control	Total	*p*
Age (%)	<40	7 (18.9)	49 (31.4)	56 (29.0)	0.285
	40–49	12 (32.4)	32 (20.5)	44 (22.8)	
	50–59	9 (24.3)	43 (27.6)	52 (26.9)	
	≥60	9 (24.3)	32 (20.5)	41 (21.2)	
Sex (%)	F	25 (67.6)	108 (69.2)	133 (68.9)	0.844
	M	12 (32.4)	48 (30.8)	60 (31.1)	
Radiographic dehiscence (%)	Absent	0 (0.0)	132 (84.6)	132 (68.4)	<0.001
	Present	37 (100.0)	24 (15.4)	61 (31.6)	
Characteristic symptoms (%)	Absent	0 (0.0)	145 (92.9)	145 (75.1)	<0.001
	Present	37 (100.0)	11 (7.1)	48 (24.9)	
Surgical repair (%)	Not Repaired	27 (73.0)	154 (98.7)	181 (93.8)	<0.001
	Repaired	10 (27.0)	2 (1.3)	12 (6.2)	
500 Hz cVEMP Threshold (dB nHL)	Median (IQR)	75.0 (10.0)	90.0 (15.0)	90.0 (15.0)	<0.001
500 Hz oVEMP Amplitude (uV)	Median (IQR)	88.5 (55.4)	12.5 (23.2)	15.2 (34.3)	<0.001
4 kHz oVEMP Amplitude (uV)	Median (IQR)	23.0 (15.9)	0.0 (0.0)	0.0 (7.5)	<0.001
Negative bone conduction thresholds (%)	Absent	21 (58.3)	126 (84.0)	147 (79.0)	0.001
	Present	15 (41.7)	24 (16.0)	39 (21.0)	
Air-Bone Gap at 250, 500, 1,000 Hz (dB HL)	Median (IQR)	10.8 (14.2)	5.0 (7.5)	5.0 (6.7)	<0.001

SCD_θ refers to our study cohort of clinically significant SCD, as defined by the radiographic, symptomatic, and physiologic diagnostic criteria proposed by Ward et al. Our control cohort are individuals who do not meet these diagnostic criteria.

SCD, superior semicircular canal dehiscence; dB, decibels; nHL, normal hearing loss; HL, hearing loss; F, female; M, male.

RESULTS

Demographics

We identified 1,168 patients (*n*, ears = 2,367) who underwent 500 Hz oVEMP testing and, of those, 902 patients (*n*, ears = 1,804) who also underwent 4 kHz oVEMP testing. High-resolution temporal bone CT scans were available for 150 patients (*n*, ears = 300) for each of whom a detailed chart review was conducted. Four patients (*n*, ears = 6) underwent bilateral SCD repair and were excluded due to lack of pre-operative 4 kHz oVEMP testing. Thirty-three (33) ears were excluded for previous ear surgeries, including 6 ears for unilateral SCD repair without pre-operative 4 kHz oVEMP. Sixty-three (63) ears were excluded due to failure in eliciting any cVEMP or oVEMP responses. Two ears were excluded for abnormal tympanometry.

In total, 49 patients (*n*, ears = 61) were found to have radiographic dehiscence on CT, 44 patients (*n*, ears = 48) reported symptoms characteristic of SCD, and 69 patients (*n*, ears = 108) had positive VEMP findings (**Figure 1**). Of these, 33 patients (*n*, ears = 37) met all three Ward et al. criteria for SCD_{θ}. Patient demographic, audiometric and vestibular testing features are shown for SCD_{θ} patients and controls in **Table 1**.

4 kHz oVEMP and Superior Semicircular Canal Dehiscence

Of the 193 cases (i.e., ears) reviewed, 51 had a positive 4 kHz oVEMP n10 response. There were a total of 37 cases with SCD_{θ} and 157 without SCD_{θ}. **Table 2** presents a frequency table of 4 kHz oVEMP n10 response to SCD_{θ}. Sensitivity for 4 kHz oVEMP response was 86.5% [95% CI: 71.2, 95.5], with 32 out of 37 SCD_{θ} cases demonstrating an n10 response and 19 non-SCD_{θ} cases that were falsely positive. With an estimated prevalence of 1% based on our institution's clinic data, the positive predictive value (PPV) was 6.7% [95% CI: 4.4, 10.0]. Specificity was calculated as 87.8% [95% CI: 81.6, 92.5], with 137 out of 156 non-SCD_{θ} cases without an n10 response and 5 SCD_{θ} cases that were falsely negative. Negative predictive value (NPV) was 99.8% [95% CI: 99.6, 99.9]. **Table 3** summarizes the sensitivity, specificity, PPV, and NPV, and area under the curve (AUC) of 4 kHz oVEMP n10 responses, compared to those of increased 500 Hz oVEMP amplitude and decreased 500 Hz cVEMP thresholds.

ROC-AUC analysis comparing binary 4 kHz oVEMP n10 response (AUC = 87.2%) to 4 kHz oVEMP amplitudes (AUC = 91.0%) found that the accuracy when accounting for the amplitudes was significantly higher ($p < 0.001$) (**Figure 2**). As expected, the 4 kHz oVEMP amplitude for SCD_{θ} cases (median = 23.0 uV, mean = 29.9 uV) is significantly higher than those for non-SCD_{θ} cases (median = 0 uV, mean = 1.8 uV) ($p < 0.001$). However, as demonstrated in **Figure 3**, there are still 19 false positive cases when only considering the presence of 4 kHz oVEMP n10 response. Eleven (58%) of these false positive cases are patients who are <40 years old. To reduce the number of false positive cases, the cut-off amplitude of 15 uV was identified by the ROC analysis to optimize testing accuracy with a sensitivity of 83.8% [95% CI: 68.0, 93.8] and a specificity of 96.8% [95% CI: 92.7, 99.0]. PPV increased to 20.9% [95% CI 9.9, 38.8] and NPV increased slightly to 99.8% [95% CI: 99.6, 99.9] (**Table 4**).

TABLE 2 | Frequency table for 4 kHz oVEMP n10 response for diagnosis of SCD_{θ}.

	Superior semicircular canal dehiscence		
	SCD_{θ}	Control	Total
+ n10 response	32	19	51
– n10 response	5	137	142
Total	37	156	

SCD_{θ} refers to our study cohort of clinically significant SCD, as defined by the radiographic, symptomatic, and physiologic diagnostic criteria proposed by Ward et al. Our control cohort are individuals who do not meet these diagnostic criteria.

4 kHz oVEMP and SCD Symptomatology

Almost a third of our patients (14 out of 49, 32.7%) demonstrated radiographic dehiscence but had no evidence of characteristic symptoms of SCD in their medical chart. To assess how well 4 kHz oVEMP response aligns with patient-reported symptoms, we split the our cohort into 4 mutually exclusive subgroups: (1) negative radiographic SCD (*n*, ears = 132), (2) radiographic dehiscence without characteristic symptoms or "Radiographic SCD" (*n*, ears = 18), (3) radiographic dehiscence with characteristic symptoms or "Symptomatic SCD" (*n*, ears = 31), and (4) surgically confirmed dehiscence or "Surgical SCD" (*n*, ears = 12), which included two cases that did not meet the Ward et al. physiologic diagnostic criterion for SCD_{θ}.

The 4 kHz oVEMP amplitude for symptomatic SCD (median = 19.9 uV, mean = 28.3 uV) and surgical SCD (median = 23.1 uV, mean = 21.7 uV) was significantly higher compared to those without radiographic evidence of SCD (median = 0 uV, mean = 1.34 uV) ($p < 0.001$ for both) (**Figure 4**). However, the 4 kHz oVEMP amplitude for radiographic SCD (median = 0 uV, mean = 4.09 uV) was similar to those without SCD ($p = 0.50$). The amplitude for 4 kHz oVEMP is significantly higher for patients with symptomatic SCD compared to those with radiographic SCD without characteristic symptoms ($p < 0.001$). The ROC curves in **Figure 5** demonstrate the accuracy of 4 kHz oVEMP in detecting all cases of radiographic dehiscence compared to symptomatic and surgical cases.

Comparison of 4 kHz oVEMP amplitudes with symptoms characteristic of SCD demonstrated significantly higher amplitudes associated with aural symptoms of autophony (median 21.5 uV vs. 0 uV, $p = 0.001$) and pulsatile tinnitus (median 21.5 uV vs. 0 uV, $p = 0.01$). Vestibular symptoms such as sound- or pressure-induced vertigo, general vertigo or dizziness, or chronic disequilibrium are not found to be correlated with higher 4 kHz oVEMP amplitudes.

DISCUSSION

Clinicians consider high-resolution CT imaging and patient-reported symptoms in combination when determining whether a patient could benefit from surgical repair of SCD. This decision, however, can be challenging due to varying quality of CT scanners and techniques, as well as the widely diverse

TABLE 3 | VEMP sensitivity and specificity for diagnosis of SCD_{θ}.

	Cut-off (uV)	Sensitivity (%) [95% CI]	Specificity (%) [95% CI]	PPV (%) [95% CI]	NPV (%) [95% CI]	AUC (%) [95% CI]
4 kHz oVEMP n10 response	>0 uV	86.5 [71.2, 95.5]	87.8 [81.6, 92.5]	6.7 [4.4, 10.0]	99.8 [99.6, 99.9]	87.1 [81.0, 93.3]
500 Hz oVEMP amplitude	≥17 uV	91.7 [77.5, 98.2]	62.6 [64.5, 70.2]	2.4 [1.9, 3.0]	99.9 [99.6, 100.0]	77.1 [71.2, 83.1]
500 Hz cVEMP threshold	≤75 dB	55.6 [38.1, 72.1]	96.0 [91.5, 98.5]	12.3 [5.7, 24.5]	99.5 [99.3, 99.7]	75.8 [67.4, 84.1]

SCD, superior semicircular canal dehiscence; PPV, positive predictive value; NPV, negative predictive value; AUC, area under the curve; dB, decibel.

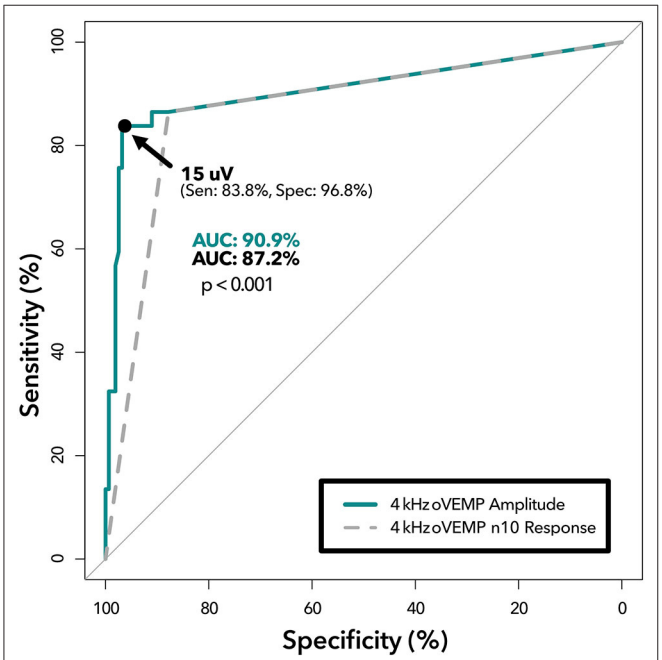

FIGURE 2 | ROC analysis of 4 kHz oVEMP n10 response vs. amplitude. Receiver operating characteristic curves demonstrating diagnostic ability of 4 kHz oVEMP amplitude at various cut-offs (solid line) and 4 kHz oVEMP n10 response (i.e., single amplitude cut-off at >0 uV) (dashed line). The area under the curve (AUC) quantifies the accuracy of detecting SCD for amplitude (top) and n10 response (bottom) with a $p < 0.001$ suggesting significant difference. The data point on the solid line represents the optimal threshold (15 uV) with (sensitivity, specificity) listed.

presentation and severity of SCD symptoms that often do not correlate with CT findings (38). Since a positive VEMP result is suggestive of a physiologically active dehiscence, VEMP testing has become a commonly used tool in the testing battery used to support SCD diagnosis and management. Similar to what has been suggested by Manzari et al. and Lin et al., our results demonstrate that 4 kHz oVEMP performs better in detecting SCD than oVEMP amplitudes and cVEMP thresholds elicited at 500 Hz. Though it is not well-understood why higher frequency VEMPs are more specific to SCD, it may be partially due to the otoliths' increased sensitivity to low-frequency sound and vibration. Higher frequency stimuli would therefore be less likely to stimulate the otoliths unless there is a clear third window phenomenon (39). In this study, we sought to optimize the utility of 4 kHz oVEMP in detecting SCD_{θ}, as defined by the Ward et al. criteria, by accounting for the amplitude rather than the binary presence of the n10 response alone. We found the optimal threshold for detection was 15 uV for our cohort.

Since its introduction, a wide variety of VEMP cut-offs have been proposed in the literature (23–25, 40, 41). However, offering a cut-off can be challenging given the variability occurring between individuals, and its dependence on age, the degree of conductive hearing loss, and testing operator (25–27). When Manzari et al. first reported that 4 kHz n10 response had 100% accuracy to detecting radiographic SCD; the appeal for this high frequency test was not only in its reported accuracy, but also in the simplicity of a binary, all-or-nothing assessment—something that has eluded 500 Hz testing (29) However, in a larger sample size, our study failed to replicate the perfect sensitivity and specificity previously reported by Manzari et al. for 4 kHz n10 responses. In fact, our detection rate of radiographic SCD was much less with an AUC of 76.4%. This is likely because many of our radiographically positive but asymptomatic patients failed to evoke a 4 kHz oVEMP response. Since Manzari et al. did not address symptomatology in their study cohort, we are unable to make an appropriate comparison.

Similarly, the study by Lin et al. looked at the binary presence of 4 kHz oVEMP n10 response in a larger patient population with radiographic SCD and unspecified symptoms (30). Our analysis of this n10 response compared to SCD found a similar sensitivity to Lin et al. but a lower specificity (88 vs. 93%). This is due to a higher number of false positive cases, which was reduced dramatically when raising the 4 kHz oVEMP amplitude cut-off to 15 uV. By using the amplitude cut-off of 15 uV rather than binary n10 response alone, we were able to improve our specificity to 97% (i.e., a 9% improvement). Given that this is a single institution study, we note that our proposed cut-off may not be completely generalizable, and a large-scale, multicenter study can help to validate this cut-off by accounting for the variability across patient populations, testing device, operators, and protocol. Nevertheless, our results do suggest that evaluating the amplitude of 4 kHz oVEMP response rather than the presence of response alone can improve accurate detection of SCD. In **Figure 3**, we visualized age categories to explore the well-documented age-related attenuation of VEMP responses. While our small sample size for each age strata limits our ability to propose age-stratified amplitude cut-offs, the results highlight the trend that younger patients have more robust 4 kHz oVEMP responses, which can lead to false

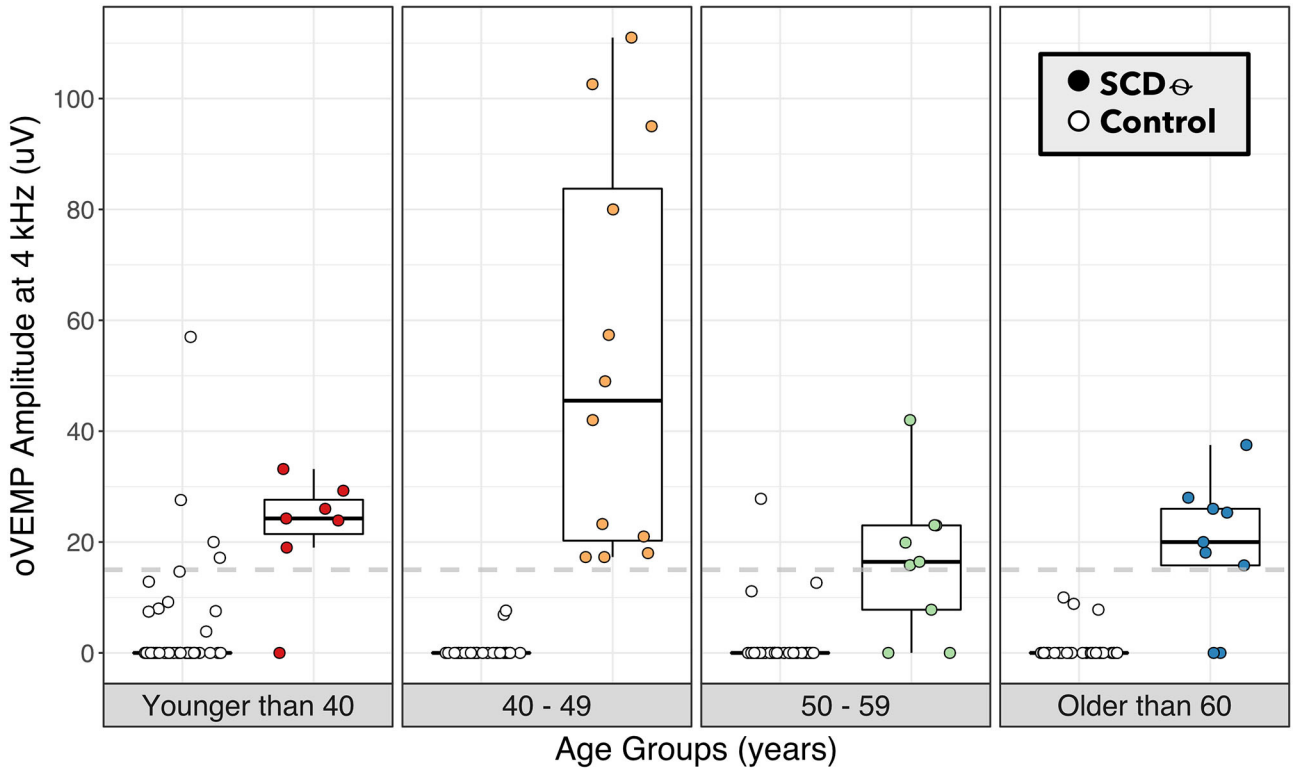

FIGURE 3 | 4 kHz oVEMP amplitude binned by age category for SCD_{θ} and control. 4 kHz oVEMP amplitudes of patients with SCD_{θ} (closed circles) and without SCD_{θ} (open circles) separated into age categories of <40, 40–49, 50–59, and ≥60 years old. Dashed line represents the proposed 4 kHz oVEMP amplitude cut-off of 15 uV for detecting SCD_{θ}.

TABLE 4 | Sensitivity and specificity of various 4 kHz oVEMP amplitude cut-offs for SCD_{θ}.

	Cut-off (uV)	Sensitivity (%) [95% CI]	Specificity (%) [95% CI]	AUC (%) [95% CI]	Accuracy (%)
4 kHz oVEMP amplitude	>0 uV	86.5 [71.2, 95.5]	87.8 [81.6, 92.5]	87.1 [81.0, 93.3]	87.6
	≥10	83.8 [68.0, 93.8]	93.6 [92.7, 99.0]	88.7 [82.4, 95.0]	91.7
	≥15	**83.8** [68.0, 93.8]	**96.8** [92.7, 99.0]	**90.3** [84.1, 96.5]	**94.3**
	≥20	59.5 [42.1, 75.2]	97.4 [93.6, 99.3]	78.5 [70.3, 86.6]	90.2

Sensitivity, specificity, area under the curve (AUC) and accuracy (i.e., percentage of cases correctly classified) are listed for each representative 4 kHz oVEMP amplitude cut-off. AUC and accuracy are highest at the 4 kHz oVEMP amplitude cut-off of 15 uV. Bolded row indicates the sensitivity, specificity, AUC, and accuracy of the optimal 4 kHz oVEMP amplitude cut-off. AUC, area under the curve.

positives, and older patients may have more attenuated, but still reliable, 4 kHz oVEMP responses. This challenges the prevailing notion that older patients should not be given VEMP testing (25, 42, 43).

As a tertiary referral center, we see a high volume of potential SCD patients who have complex and non-classical presentations. Even when adhering to strict criteria to develop our study cohort, we still see a relatively high number of SCD_{θ} false positive ($n = 19$) and radiographic false negative ($n = 24$) cases compared to the literature. Review of these cases revealed interesting patterns that may not solely be a limitation of 4 kHz oVEMP testing but can also reflect the complex pathophysiology of SCD. Younger age, by far, seemed to be the most common trait amongst the false positive cases with 11 out of the 19 cases (57.9%) being younger than 40 years old. We also identified 5 of the 19 cases (26.3%) had evidence of Ehlers-Danlos syndrome (EDS), postural orthostatic tachycardia syndrome (POTS), or some other underlying connective tissue disorder. A small case series described SCD and EDS occurring in patients concomitantly (44) This may suggest an association between the two conditions or, perhaps, represent incidental findings in the context that EDS can lead to symptoms and physiological VEMP findings that are similar to SCD but without actual dehiscence. On review of false negative cases (defined as ears with radiographic dehiscence ± symptoms and negative 4 kHz oVEMPs), 14 of 25 cases (56%) were found in bilateral radiographic SCD patients; and 8 (32%) had wide tegmen dehiscence. The wide tegmen dehiscence and bilateral cases can

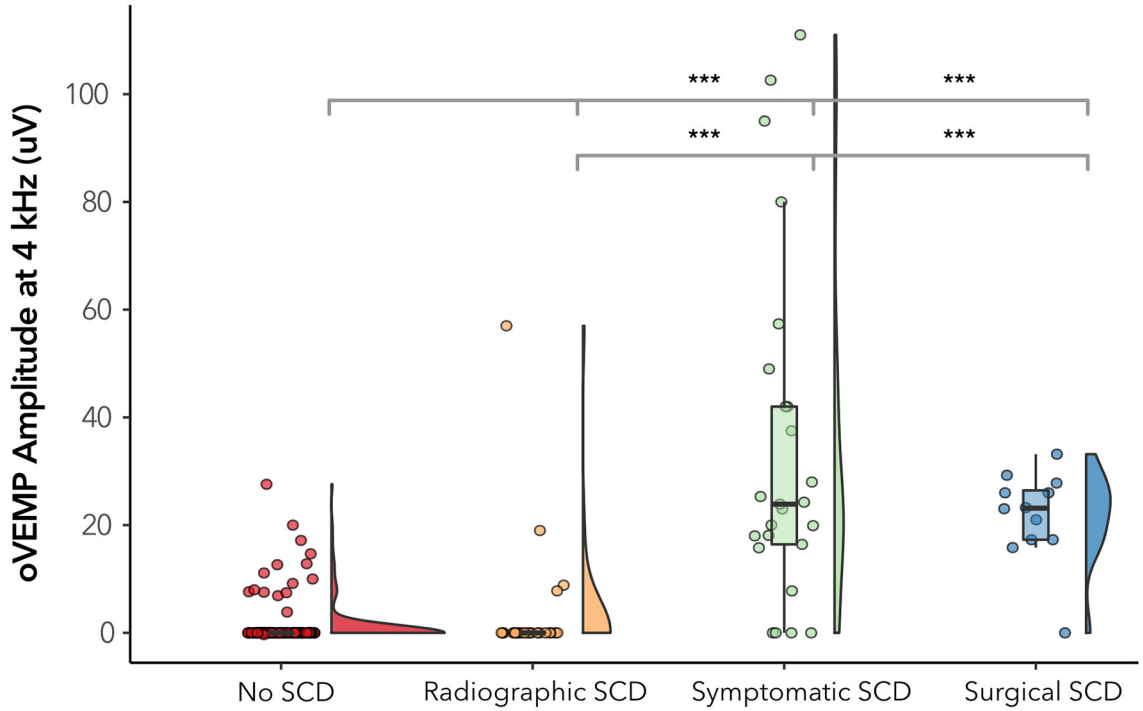

FIGURE 4 | 4 kHz oVEMP amplitude across subgroups of SCD. "No SCD" represents cases without any evidence of dehiscence. "Radiographic SCD" are cases with radiographic dehiscence but no characteristic symptoms. "Symptomatic SCD" are cases with radiographic dehiscence and characteristic symptoms. "Surgical SCD" are cases that have undergone surgical repair of dehiscence. The width of the violin diagram depicts the distribution of data. Absence of asterisk (*) indicated $p > 0.05$ and $^{***}p < 0.001$.

represent extensive disease, which may lead to auto-plugging of the dehiscence by the dura, and a false negative result. This may be more likely given that oVEMP testing is conducted in the upright position (compared to supine with cVEMP testing). Bilateral cases may also have false negative testing if one ear demonstrates a 4 kHz oVEMP response, but the other ear does not—with the more symptomatic ear presumably being more physiologically active. Finally, a few cases had, on average, poorer CT quality or disagreement amongst our CT reviewers. This can call into question whether these cases actually had true dehiscence and may demonstrate the variability in CT quality and interpretation, as well as the tendency for CTs to over-detect dehiscence (5, 11).

Another limitation to our study is that we do not use surgically confirmed SCD to define our study cohort. However, for the subset of 12 surgically confirmed SCD cases, the 4 kHz oVEMP amplitude was shown to be significantly higher than the control. Despite this, our study cohort was defined by radiographic evidence, patient-reported symptoms, and objective test results, which are often used in combination by clinicians to diagnose clinically significant SCD. These diagnostic criteria, however, are not without limitations. For example, 39 cases required additional CT review by our expert panel because the neuro-radiologist and diagnosing physician assessment disagreed or were ambiguous. Many of the patients who underwent 4 kHz oVEMP testing had clinical presentations suggestive of SCD, but by adhering to the strict definition of characteristic symptoms proposed by Ward et al. the number of patients deemed symptomatic was significantly reduced. This suggests a large variability in presenting symptoms for SCD that can go beyond the classical presentation. To define our cohort, we chose 500 Hz oVEMP amplitude and cVEMP threshold cut-offs based upon the literature; however, these cut-offs seem to be much lower than what may be optimal for our patient population and equipment. Despite these limitations, the criteria we used to define our study cohort most accurately reflects the real-life factors clinicians must use in order to determine the patient's surgical candidacy.

We sought to correlate characteristic symptoms collected from chart review with 4 kHz oVEMP amplitudes. This association can be particularly useful in the common situation where presenting symptoms may be multifactorial or due to other comorbidities (38). Some studies have shown that lower cVEMP thresholds were found to correlate with increasing size of dehiscence and higher incidence of vestibular symptoms such as sound-induced vertigo (45, 46). However, the correlation between lower cVEMP thresholds and SCD symptoms have been difficult to reproduce, and many other studies have found that cVEMPs and symptoms do not align (32, 33, 47, 48). Our results suggest that 4 kHz oVEMP amplitudes are significantly higher for patients presenting with classical symptoms of SCD than those patients who have radiographic SCD without these symptoms. One interpretation is that the

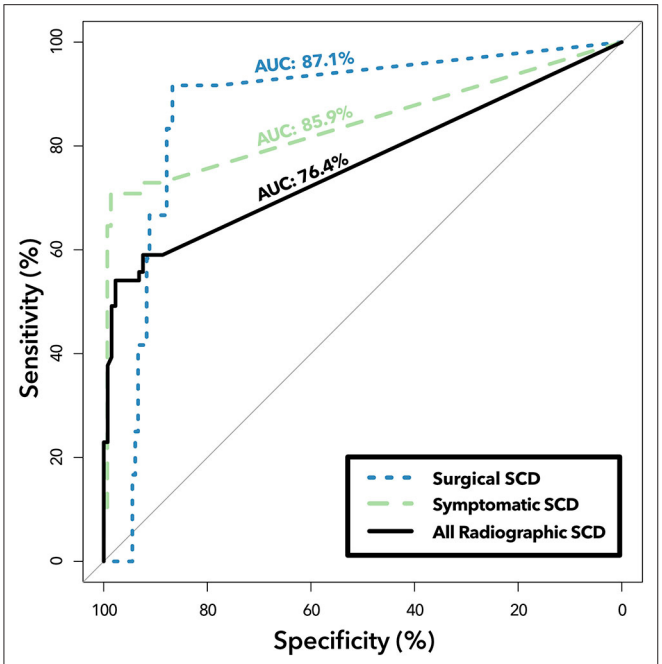

FIGURE 5 | ROC analysis of 4 kHz oVEMP amplitude in detecting subgroups of SCD. Receiver operating characteristic curves demonstrating diagnostic ability of 4 kHz oVEMP amplitude in classifying all cases of radiographic dehiscence ("All Radiographic SCD," solid line), only symptomatic cases with radiographic dehiscence ("Symptomatic SCD," dashed line), and surgically repaired cases of SCD ("Surgical SCD," dotted line). Area under the curve (AUC) quantifies the accuracy for classifying Surgical SCD (top), Symptomatic SCD (middle) and All Radiographic SCD (bottom). The difference between the "All Radiographic SCD" group and the "Symptomatic SCD" group is that patients that have radiographic SCD but without characteristic symptoms are removed from the latter, which improves 4 kHz oVEMP detection performance.

more physiologically active dehiscences (as measured by the VEMPs) have increased shunting of acoustic energy, leading to more noticeable symptoms. Another interpretation is that some of the patients who are asymptomatic or have atypical symptoms may not actually have dehiscence and instead have a false positive CT and a true negative VEMP. This alignment between 4 kHz oVEMP and symptomatic patients may be useful in helping clinicians to determine surgical candidacy.

Additionally, our results suggest that 4 kHz oVEMP amplitude correlate better with patients who present with aural symptoms like autophony and pulsatile tinnitus, but not with vestibular symptoms such as pressure- or sound-induced vertigo, chronic disequilibrium, or generalized vertigo. Given that 4 kHz oVEMP directly tests the stimulation of vestibular organs, the lack of correlation to sound- and pressure induced vertigo was unexpected. This may be due to the low prevalence of patient-reported sound- and pressure-induced vertigo in our SCD population. We acknowledge that given the broad spectrum of symptom presentation, it may be difficult to capture symptomatology from chart review, which may be why the number of patient-reported sound- and pressure-induced vertigo is lower than that seen in the literature (12, 47). This highlights the need for a validated metric to measure symptom severity at presentation and post-intervention in order to more rigorously determine the association between physiological VEMP findings and symptomatology.

CONCLUSION

Here we report the sensitivity and specificity of 4 kHz oVEMP amplitude in detecting clinically significant SCD_{θ}. As previous studies have shown, we found that 4 kHz oVEMP n10 response alone performs better than 500 Hz oVEMP amplitude and cVEMP thresholds. We are able to further improve this detection by assessing 4 kHz oVEMP amplitude and proposing an optimal amplitude cut-off of 15 uV. Our results also suggest that 4 kHz oVEMP amplitudes align better with symptomatic SCD cases, compared to cases in which there is radiographic SCD but no characteristic symptoms. In situations in which there is radiographic evidence of dehiscence but the symptomatic presentation of patients is non-specific, a positive 4 kHz oVEMP can be useful in aiding clinicians in the diagnosis and management of SCD patients.

DATA AVAILABILITY STATEMENT

The raw data supporting the conclusions of this article will be made available by the authors, without undue reservation.

ETHICS STATEMENT

The studies involving human participants were reviewed and approved by Stanford University Institutional Review Board (IRB-50573). Written informed consent for participation was not required for this study in accordance with the national legislation and the institutional requirements.

AUTHOR CONTRIBUTIONS

ET conducted data acquisition, analysis, and interpretation and made significant contributions to the design of the study, as well as the writing and editing of the manuscript. AS designed the audiometric database, conducted data acquisition, and was heavily involved in project design and manuscript editing. JS played a significant role in project design, data review and analysis, and manuscript editing and review. NB reviewed the data and was involved in the editing of the manuscript. MF contributed to the project design and manuscript review. KS led the conception of the study and contributed significantly to the data and manuscript review. All authors contributed to the article and approved the submitted version.

ACKNOWLEDGMENTS

We are deeply grateful for the support of Nobie Redmon, Dan Zylberglejd, and Matthew Winn for helping with data visualization and statistical analyses. We would also like to thank Jason Qian, Tina Munjal and Shayna Cooperman for

their support and input. Finally, we greatly appreciate our audiology team including Mateel Musallam, Michael Smith, Rachael Jocewicz, Daniel Krass, Jannine Larky, Honey Gholami, Jaclyn Moor, Sarah Pirko, Goutham Telukuntla, and Amanda Burke, for all their efforts in collecting and helping us to better understand the data.

REFERENCES

1. Minor LB, Solomon D, Zinreich JS, Zee DS. Sound- and/or pressure-induced vertigo due to bone dehiscence of the superior semicircular canal. *Arch Otolaryngol Neck Surg.* (1998) 124:249–58. doi: 10.1001/archotol.124.3.249
2. Cawthorne T. The effect on hearing in man of removal of the membranous lateral semicircular canal. *Acta Otolaryngol.* (1948) 36:145–9. doi: 10.3109/00016484809122648
3. Minor LB. Superior canal dehiscence syndrome. *Am J Otol.* (2000) 21:9–19. doi: 10.1016/S0196-0709(00)80068-X
4. Minor LB. Clinical manifestations of superior semicircular canal dehiscence. *Laryngoscope.* (2005) 115:1717–27. doi: 10.1097/01.mlg.0000178324.55729.b7
5. Tavassolie T, Penninger R, Zuñiga M, Minor L, Carey J. Multislice computed tomography in the diagnosis of superior canal dehiscence: how much error, and how to minimize it? *Otol Neurotol.* (2012) 33:215–22. doi: 10.1097/MAO.0b013e318241c23b
6. Meiklejohn DA, Corrales CE, Boldt BM, Sharon JD, Yeom KW, Carey JP, et al. Pediatric semicircular canal dehiscence: radiographic and histologic prevalence, with clinical correlation. *Otol Neurotol.* (2015) 36:1383–9. doi: 10.1097/MAO.0000000000000811
7. Williamson RA, Vrabec JT, Coker NJ, Sandlin M. Coronal computed tomography prevalence of superior semicircular canal dehiscence. *Otolaryngol Head Neck Surg Off J Am Acad Otolaryngol Head Neck Surg.* (2003) 129:481–9. doi: 10.1016/S0194-5998(03)01391-3
8. Sequeira SM, Whiting BR, Shimony JS, Vo KD, Hullar TE. Accuracy of computed tomography detection of superior canal dehiscence. *Otol Neurotol Off Publ Am Otol Soc Am Neurotol Soc Eur Acad Otol Neurotol.* (2011) 32:1500–5. doi: 10.1097/MAO.0b013e318238280c
9. Crovetto M, Whyte J, Rodriguez OM, Lecumberri I, Martinez C, Eléxpuru J. Anatomo-radiological study of the superior semicircular canal dehiscence radiological considerations of superior and posterior semicircular canals. *Eur J Radiol.* (2010) 76:167–72. doi: 10.1016/j.ejrad.2009.05.038
10. Carey JP, Minor LB, Nager GT. Dehiscence or thinning of bone overlying the superior semicircular canal in a temporal bone survey. *Arch Otolaryngol Head Neck Surg.* (2000) 126:137–47. doi: 10.1001/archotol.126.2.137
11. Cloutier J-F, Bélair M, Saliba I. Superior semicircular canal dehiscence: positive predictive value of high-resolution CT scanning. *Eur Arch Otorhinolaryngol.* (2008) 265:1455–60. doi: 10.1007/s00405-008-0672-2
12. Chung LK, Ung N, Spasic M, Nagasawa DT, Pelargos PE, Thill K, et al. Clinical outcomes of middle fossa craniotomy for superior semicircular canal dehiscence repair. *J Neurosurg.* (2016) 125:1187–93. doi: 10.3171/2015.8.JNS15391
13. Zhu RT, Van Rompaey V, Ward BK, Van de Berg R, Van de Heyning P, Sharon JD. The interrelations between different causes of dizziness: a conceptual framework for understanding vestibular disorders. *Ann Otol Rhinol Laryngol.* (2019) 128:869–78. doi: 10.1177/0003489419845014
14. Jung DH, Lookabaugh SA, Owoc MS, McKenna MJ, Lee DJ. Dizziness is more prevalent than autophony among patients who have undergone repair of superior canal dehiscence. *Otol Neurotol Off Publ Am Otol Soc Am Neurotol Soc Eur Acad Otol Neurotol.* (2015) 36:126–32. doi: 10.1097/MAO.0000000000000531
15. Colebatch JG, Halmagyi GM, Skuse NF. Myogenic potentials generated by a click-evoked vestibulocollic reflex. *J Neurol Neurosurg Psychiatr.* (1994) 57:190–7. doi: 10.1136/jnnp.57.2.190
16. Manzari L, Burgess AM, Curthoys IS. Dissociation between cVEMP and oVEMP responses: different vestibular origins of each VEMP? *Eur Arch Otorhinolaryngol.* (2010) 267:1487–9. doi: 10.1007/s00405-010-1317-9
17. Curthoys IS, Vulovic V, Burgess AM, Manzari L, Sokolic L, Pogson J, et al. Neural basis of new clinical vestibular tests: otolithic neural responses to sound and vibration. *Clin Exp Pharmacol Physiol.* (2014) 41:371–80. doi: 10.1111/1440-1681.12222
18. Curthoys IS. The interpretation of clinical tests of peripheral vestibular function. *Laryngoscope.* (2012) 122:1342–52. doi: 10.1002/lary.23258
19. Addams-Williams J, Wu K, Ray J. The experiments behind the tullio phenomenon. *J Laryngol Otol.* (2014) 128:223–7. doi: 10.1017/S0022215114000280
20. Huizinga E. The physiological and clinical importance of experimental work on the pigeon's labyrinth. *J Laryngol Otol.* (1955) 69:260–8. doi: 10.1017/S0022215100050635
21. Brantberg K, Bergenius J, Tribukait A. Vestibular-evoked myogenic potentials in patients with dehiscence of the superior semicircular canal. *Acta Otolaryngol.* (1999) 119:633–40. doi: 10.1080/00016489950180559
22. Streubel SO, Cremer PD, Carey JP, Weg N, Minor LB. Vestibular-evoked myogenic potentials in the diagnosis of superior canal dehiscence syndrome. *Acta Oto-Laryngol Suppl.* (2001) 545:41–9. doi: 10.1080/00016480152388090
23. Zuniga MG, Janky KL, Nguyen KD, Welgampola MS, Carey JP. Ocular vs. cervical VEMPs in the diagnosis of superior semicircular canal dehiscence syndrome. *Otol Neurotol Off Publ Am Otol Soc Am Neurotol Soc Eur Acad Otol Neurotol.* (2013) 34:121–6. doi: 10.1097/MAO.0b013e31827136b0
24. Janky KL, Nguyen KD, Welgampola M, Zuniga MG, Carey JP. Air-conducted oVEMPs provide the best separation between intact and superior canal dehiscent labyrinths. *Otol Neurotol Off Publ Am Otol Soc Am Neurotol Soc Eur Acad Otol Neurotol.* (2013) 34:127–34. doi: 10.1097/MAO.0b013e318271c32a
25. Fife TD, Colebatch JG, Kerber KA, Brantberg K, Strupp M, Lee H, et al. Practice guideline: cervical and ocular vestibular evoked myogenic potential testing. *Neurology.* (2017) 89:2288. doi: 10.1212/WNL.0000000000004690
26. Agrawal Y, Zuniga MG, Davalos-Bichara M, Schubert MC, Walston JD, Hughes J, et al. Decline in semicircular canal and otolith function with age. *Otol Neurotol Off Publ Am Otol Soc Am Neurotol Soc Eur Acad Otol Neurotol.* (2012) 33:832–9. doi: 10.1097/MAO.0b013e3182545061
27. Piker EG, Jacobson GP, Burkard RF, McCaslin DL, Hood LJ. Effects of age on the tuning of the cVEMP and oVEMP. *Ear Hear.* (2013) 34:e65–73. doi: 10.1097/AUD.0b013e31828fc9f2
28. Ward BK, Carey JP, Minor LB. Superior canal dehiscence syndrome: lessons from the first 20 years. *Front Neurol.* (2017) 8:177. doi: 10.3389/fneur.2017.00177
29. Manzari L, Burgess AM, McGarvie LA, Curthoys IS. An indicator of probable semicircular canal dehiscence: ocular vestibular evoked myogenic potentials to high frequencies. *Otolaryngol Head Neck Surg Off J Am Acad Otolaryngol Head Neck Surg.* (2013) 149:142–5. doi: 10.1177/0194599813489494
30. Lin K, Lahey R, Beckley R, Bojrab D, Wilkerson B, Johnson E, et al. Validating the utility of high frequency ocular vestibular evoked myogenic potential testing in the diagnosis of superior semicircular canal dehiscence. *Otol Neurotol.* (2019) 40:1353–8. doi: 10.1097/MAO.0000000000002388
31. Carhart R, Jerger J. Preferred method for clinical determination of pure-tone thresholds. *J Speech Hear Disord.* (1959) 24:330–45. doi: 10.1044/jshd.2404.330
32. Chien WW, Janky K, Minor LB, Carey JP. Superior canal dehiscence size: multivariate assessment of clinical impact. *Otol Neurotol Off Publ Am Otol Soc Am Neurotol Soc Eur Acad Otol Neurotol.* (2012) 33:810–5. doi: 10.1097/MAO.0b013e318248eac4
33. Niesten MEF, Hamberg LM, Silverman JB, Lou KV, McCall AA, Windsor A, et al. Superior canal dehiscence length and location influences clinical presentation and audiometric and cervical vestibular-evoked myogenic potential testing. *Audiol Neurootol.* (2014) 19:97–105. doi: 10.1159/000353920
34. R Core Team. *R: A language and environment for statistical computing. R Found Stat Comput* Vienna Austria. (2018)
35. Harrison E, Drake T, Ots R. *finalfit: Quickly Create Elegant Regression Results Tables and Plots when Modelling.* (2019). Available online at: https://CRAN.R-project.org/package=finalfit (accessed January 31, 2020).
36. Wickham H. *ggplot2: Elegant Graphics for Data Analysis.* New York, NY: Springer-Verlag. (2009). doi: 10.1007/978-0-387-98141-3

37. Robin X, Turck N, Hainard A, Tiberti N, Lisacek F, Sanchez J-C, et al. pROC: an open-source package for R and S+ to analyze and compare ROC curves. *BMC Bioinform.* (2011) 12:77. doi: 10.1186/1471-2105-12-77
38. Mau C, Kamal N, Badeti S, Reddy R, Ying Y-LM, Jyung RW, et al. Superior semicircular canal dehiscence: liagnosis and management. *J Clin Neurosci.* (2018) 48:58–65. doi: 10.1016/j.jocn.2017.11.019
39. Todd NPM, Rosengren SM, Colebatch JG. A utricular origin of frequency tuning to low-frequency vibration in the human vestibular system? *Neurosci Lett.* (2009) 451:175–80. doi: 10.1016/j.neulet.2008.12.055
40. Verrecchia L, Westin M, Duan M, Brantberg K. Ocular vestibular evoked myogenic potentials to vertex low frequency vibration as a diagnostic test for superior canal dehiscence. *Clin Neurophysiol.* (2016) 127:2134–9. doi: 10.1016/j.clinph.2016.01.001
41. Verrecchia L, Glad K, Frisk R, Duan M. Vestibular myogenic potentials evoked by air-conducted stimuli at safe acoustic intensity levels retain optimal diagnostic properties for superior canal dehiscence syndrome. *Acta Otolaryngol.* (2019) 139:11–7. doi: 10.1080/00016489.2018.1536297
42. Piker EG, Jacobson GP, McCaslin DL, Hood LJ. Normal characteristics of the ocular vestibular evoked myogenic potential. *J Am Acad Audiol.* (2011) 22:222–30. doi: 10.3766/jaaa.22.4.5
43. Su H-C, Huang T-W, Young Y-H, Cheng P-W. Aging effect on vestibular evoked myogenic potential. *Otol Neurotol Off Publ Am Otol Soc Am Neurotol Soc Eur Acad Otol Neurotol.* (2004) 25:977–80. doi: 10.1097/00129492-200411000-00019
44. Preet K, Udawatta M, Duong C, Gopen Q, Yang I. Bilateral superior semicircular canal dehiscence associated with ehlers-danlos syndrome: a report of 2 cases. *World Neurosurg.* (2019) 122:161–4. doi: 10.1016/j.wneu.2018.10.126
45. Pfammatter A, Darrouzet V, Gärtner M, Somers T, Van Dinther J, Trabalzini F, et al. A superior semicircular canal dehiscence syndrome multicenter study: is there an association between size and symptoms? *Otol Neurotol Off Publ Am Otol Soc Am Neurotol Soc Eur Acad Otol Neurotol.* (2010) 31:447–54. doi: 10.1097/MAO.0b013e3181d27740
46. Lookabaugh S, Niesten MEF, Owoc M, Kozin ED, Grolman W, Lee DJ. Audiologic, cVEMP, and radiologic progression in superior canal dehiscence syndrome. *Otol Neurotol Off Publ Am Otol Soc Am Neurotol Soc Eur Acad Otol Neurotol.* (2016) 37:1393–8. doi: 10.1097/MAO.0000000000001182
47. Noij KS, Wong K, Duarte MJ, Masud S, Dewyer NA, Herrmann BS, et al. Audiometric and cvemp thresholds show little correlation with symptoms in superior semicircular canal dehiscence syndrome. *Otol Neurotol Off Publ Am Otol Soc Am Neurotol Soc Eur Acad Otol Neurotol.* (2018) 39:1153–62. doi: 10.1097/MAO.0000000000001910
48. Mehta R, Klumpp ML, Spear SA, Bowen MA, Arriaga MA, Ying Y-LM. Subjective and objective findings in patients with true dehiscence versus thin bone over the superior semicircular canal. *Otol Neurotol Off Publ Am Otol Soc Am Neurotol Soc Eur Acad Otol Neurotol.* (2015) 36:289–94. doi: 10.1097/MAO.0000000000000654

Conflict of Interest: The authors declare that the research was conducted in the absence of any commercial or financial relationships that could be construed as a potential conflict of interest.

frontiers in Neurology

ORIGINAL RESEARCH
published: 02 September 2020
doi: 10.3389/fneur.2020.00966

Investigation of Mechanisms in Bone Conduction Hyperacusis With Third Window Pathologies Based on Model Predictions

*Stefan Stenfelt**

Department of Biomedical and Clinical Sciences, Linköping University, Linköping, Sweden

A lumped element impedance model of the inner ear with sources based on wave propagation in the skull bone was used to investigate the mechanisms of hearing sensitivity changes with semi-circular canal dehiscence (SSCD) and alterations of the size of the vestibular aqueduct. The model was able to replicate clinical and experimental findings reported in the literature. For air conduction, the reduction in cochlear impedance due to a SSCD reduces the intra-cochlear pressure at low frequencies resulting in a reduced hearing sensation. For bone conduction, the reduced impedance in the vestibular side due to the SSCD facilitates volume velocity caused by inner ear fluid inertia, and this effect dominates BC hearing with a third window opening on the vestibular side. The SSCD effect is generally greater for BC than for AC. Moreover, the effect increases with increased area of the dehiscence, but areas more than the cross section area of the semi-circular canal itself leads to small alterations. The model-predicted air-bone gap for a SSCD of 1 mm^2 is 30 dB at 100 Hz that decreases with frequency and become non-existent at frequencies above 1 kHz. According to the model, this air-bone gap is similar to the air-bone gap of an early stage otosclerosis. The normal variation of the size of the vestibular aqueduct do not affect air conduction hearing, but can vary bone conduction sensitivity by up to 15 dB at low frequencies. Reinforcement of the OW to mitigate hyperacusis with SSCD is inefficient while a RW reinforcement can reset the bone conduction sensitivity to near normal.

Keywords: third window, bone conduction, semi-circular canal dehiscence, model, air-bone gap

OPEN ACCESS

Edited by:
Tetsuo Ikezono,
Saitama Medical University, Japan

Reviewed by:
Habib Georges Rizk,
Medical University of South Carolina, United States
John Joseph Rosowski,
Massachusetts Eye & Ear Infirmary, Harvard Medical School, United States

***Correspondence:**
Stefan Stenfelt
stefan.stenfelt@liu.se

Specialty section:
This article was submitted to Neuro-Otology, a section of the journal Frontiers in Neurology

Received: *28 April 2020*
Accepted: *24 July 2020*
Published: *02 September 2020*

Citation:
Stenfelt S (2020) Investigation of Mechanisms in Bone Conduction Hyperacusis With Third Window Pathologies Based on Model Predictions. Front. Neurol. 11:966. doi: 10.3389/fneur.2020.00966

INTRODUCTION

In normal function of hearing, the ear canal sound pressure is transmitted to the inner ear via the tympanic membrane (TM) and middle ear ossicles. This results in a motion of the stapes in the oval window (OW) that is mimicked in terms of fluid displaced by the motion of the round window (RW), but with opposite phase (1). The equality of fluid displacement at the two windows indicates that the inner ear space is constant and no other in- or outlet displaces fluid. However, this does not mean that there are no other possibilities for fluid displacement in the inner ear beside the OW and the RW. There are two narrow ducts, the cochlear aqueduct close to the RW and the vestibular

aqueduct in the vestibule that connect the inner ear with the fluid in the cranial cavity. Also, blood vessels and neural tissue entering the inner ear may transmit pressure in and out of the inner ear. All these small channels were collectively referred to as the third window by Ranke et al. (2). But for air-conduction (AC) hearing in normal ears, the impedance of these narrow channels are much greater than the impedances of the inner ear fluids, basilar membrane (BM), OW, and RW (3, 4), and they do not affect the volume velocity exciting the BM.

When the stimulation is by bone conduction (BC) (5), i.e., as a vibration to the skull, the equality between the fluid flow at the OW and RW no longer hold (1). One reason for this is that during BC, the bone encapsulating the inner ear moves resulting in a volume alteration of the inner ear space. Another reason is the ability for volume velocity to flow through the vestibular aqueduct at low frequencies (4). Consequently, the vestibular aqueduct facilitates BC hearing at low frequencies when the OW is immobile, for example in ears with otosclerosis (4).

Abnormal conditions exists where a pathological third window arise. The most common such pathological third window is in dehiscence of the semi-circular canal (SSCD) or an enlarged vestibular aqueduct, known as large vestibular aqueduct syndrome (6). Common for these pathologies are that the third window component appears at the vestibular side of the BM, which is important for the hearing outcomes. Symptoms of a third window are decreased sensitivity to low-frequency external sounds while increasing sensitivity to low-frequency internal sounds. This means that AC sound thresholds are elevated at low frequencies while the BC thresholds improve at low frequencies (BC hyperacusis) resulting in a low-frequency air-bone gap (ABG) (7). Other manifestations of a third window in SSCD is autophony (hearing one's own voice as loud or distorted) as well as pulsatile tinnitus and hearing of one's own footsteps (8). Even hearing of eye movements has been reported (9). However, the most severe problem is sound induced vertigo (7), but in the current study only the effects on hearing will be studied.

The low-frequency effect on the AC hearing has been well-investigated in clinical studies (8, 10–12), animal experimental studies (13), cadaveric temporal bone studies (14, 15), and mathematical modeling (16). A usual explanation of the low-frequency AC threshold worsening in SSCD is that the open communication between the vestibule and the cranial space through the semi-circular canal allow sound energy to leak out through this open pathway instead of going to the RW and thereby stimulating the BM. Even if this may serve as a conceptual explanation, it is physically incorrect. The reason for the reduced low-frequency stimulation is that the opening on the vestibule side reduces the cochlear impedance at the OW which leads to a reduction of the intra-cochlear sound pressure that drives the vibration of the BM. This has been shown in intra-cochlear pressure measurement studies on SSCD in cadaveric temporal bones (14, 17).

To mitigate the effects of SSCD in severe cases, surgery can be performed with the aim of sealing the third window, often by plugging the semi-circular canal (18). This is an invasive surgery and others have suggested to reinforce the RW and sometimes also the OW to reduce the effect of the pathological third window (19–21). So far, the outcomes from such reinforcements are unclear and the mechanisms behind the intervention have not been investigated in detail.

The low-frequency effects on BC hearing in SSCD are not equally well-understood as the AC effects. The manifestation of increased low-frequency BC sensitivity, termed BC hyperacusis, is well-established (7, 8) but the mechanisms for this improvement has not been investigated in detail. One suggestion is that the reduced impedance in the vestibule side of the inner ear enhances the volume velocity in the inner ear during BC, known as BC fluid inertia (16, 22). But other mechanisms have also been suggested such as sound pressure transmission from the cranial cavity (8) or that the reduction of the impedance at the OW leads to greater impedance difference between the two sides facilitating BC excitation of the inner ear. Kim et al. (16) investigated the BC inertial effects from SSCD in a finite element model of the ear and found an increased low-frequency BC response. Stenfelt (4) used a lumped-element model to simulate the BC effects from SSCD and reported a low-frequency enhancement. The limitation of both these studies was that they only included one or two contributors to the BC excitation and thereby excluded several other possible contributors. In a later study, the inner ear model by Stenfelt (4) was expanded to include five contributors of BC that have been suggested to be the most important (5, 23).

The aim of this study is to adapt the model in Stenfelt (24) to simulate the effects of inner ear third windows on the five contributors for BC hearing and also for AC hearing. More specifically, the third window effects being studied is dehiscence of the superior semi-circular canal and size variations of the vestibular aqueduct. In addition, the effect from reinforcement of the RW and OW on the predicted hearing results in SSCD is investigated.

MATERIALS AND METHODS

The Model

The basis for the model is that the BC vibration travels as a longitudinal one-dimensional wave in the skull bone. Due to the speed of the propagating wave, different positions vibrate with different phases. As the size of the model is ∼9 mm, attenuation of the bony wave is neglected. This means that all bony parts move with the same amplitude and direction, but differ in phase. This leads to inertial effects and compressional effects. The inertial effects are caused by the mass and acceleration, and are modeled as pressure sources. The compression effects are caused by space alterations due to phase differences of the vibration while the fluid is considered incompressible, so the volume of the space change leads to a net flow of that volume (4). This is modeled as a volume velocity source. The entire layout of the model is depicted in **Figure 1** including the impedances and sources. The skull bone vibrations are taken from the Stenfelt and Goode (25) study as in the previous models.

The sources P_V, P_{SV}, and P_{ST} in **Figure 1** are the sound pressures from the fluid inertia in the vestibule, scala vestibuli, and scala tympani, respectively. The P_{IC_VA} is the sound pressure in the CSF at the vestibular aqueduct opening and the P_{IC_SSC} is

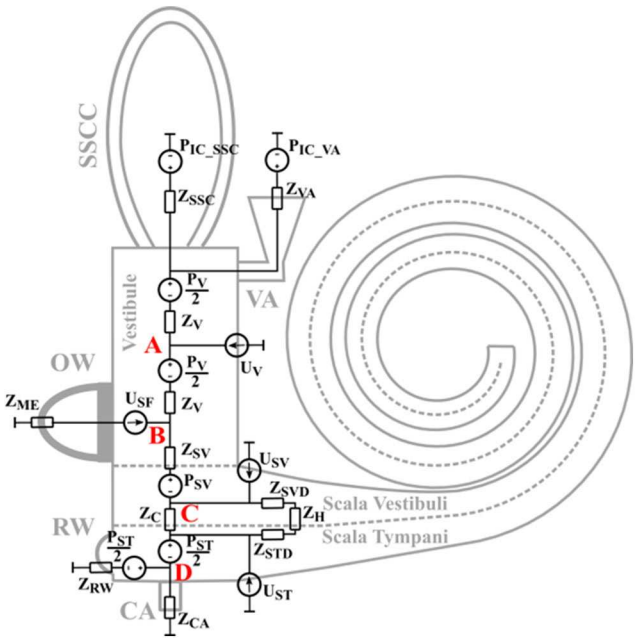

FIGURE 1 | The layout of the lumped element impedance model. The different impedances and sources relate to the physical parts of the inner ear at their approximate positions.

the sound pressure in the CSF at the SSCD. These two sources are the intracranial pressure in the CSF and are modeled equal due to physical closeness. There is no pressure source at the cochlear aqueduct since its contribution was found insignificant compared to the contribution from P_{IC_VA} in Stenfelt (24).

The U_{SF} is a volume velocity source that represents the volume velocity from the stapes motion in the OW when simulating middle ear inertia effects and sound pressure in the ear canal. During AC stimulation, U_{SF} depends on the sound pressure at the TM, a modeled middle-ear transfer function relating stapes velocity to the sound pressure at the TM (26) when the middle-ear is loaded by the inner-ear model of **Figure 1**, and an averaged stapes footplate area of 3.85 mm^2 (27). The same computation is done for the BC external ear component where the ear canal sound pressure in an open ear with BC stimulation is taken from Stenfelt et al. (28). The use of data from occluded ear canals would increase the external-ear contribution to the predicted hearing results. U_{SF} is based on the finite element modeling in Homma et al. (29) when simulating middle ear inertia. This is different from the previous models where the stapes vibration in Stenfelt et al. (30) was used. The benefit of using the data in Homma et al. (29) is that in the measurements of Stenfelt et al. (30), the motion of the stapes may have been influenced by a combination of different BC mechanisms, while the model motion computed by Homma et al. (29), was only driven by middle-ear inertia.

The most significant change from the previous models is the computations of the volume velocity sources U_{SV} and U_{ST}. In the previous models the compression of scala vestibuli and scala tympani was computed in a straight tapered cochlea. In the current model, the estimation of the compressional volume velocity is computed in parameterized coil-shaped ducts (**Figure 2A**). The cross sectional areas of scala tympani and scala vestibuli are modeled as half elliptic where the scala vestibuli width being 1.8 mm and height being 1.2 mm at the base. These dimensions are linearly reduced toward the apex where the width is 1.6 mm and the height is 0.6 mm. The width and height are for scala tympani 2.5 and 1.4 mm, respectively, that become 1.6 and 0.6 mm at the apex. The radius of the outer part of the coiled cochlea is 5 mm at the base that is reduced to 1.6 mm at the apex. The compression is then computed for consecutive 5 degree-wide sections of the coiled cochlea, leading to 180 sections over the 2.5 turns of the cochlea. For each section, based on the space alteration due to the wave propagation, the volume velocities (ΔU_{SV} and ΔU_{ST}) of each section together with the impedances (ΔZ_{SVD} and ΔZ_{STD}, mass of a tube) are computed (**Figure 2B**). Based on the impedances of the scala vestibuli and scala tympani ducts (Z_{SVD} and Z_{STD}, **Figure 2B**), and the cochlear impedances in **Figure 1**, all sections' contributions to U_{SV} and U_{ST} are computed and summed resulting in a final contribution of the volume velocity from U_{SV} and U_{ST} (**Figure 2B**). The impedance of the helicotrema (Z_H, **Figures 1**, **2**) is taken from Marquardt and Hensel (31). The volume velocity source of the vestibule (U_V) is computed similar as in the previous model based on the length of the vestibule (5.8 mm) and an elliptic cross-sectional surface area (radius 1.55 and 2.45 mm).

The impedances in **Figure 1** are either based on the geometry and material properties, or taken from the literature. The impedance of the middle ear seen from inside the OW, Z_{ME}, is obtained from Puria (32) as well as the impedance of the BM. Also included in Z_C is the fluid mass on both sides of the BM, here modeled as $M_{SV}/2$ and $M_{ST}/2$. The other part of the fluid mass in scala tympani is included in the Z_{RW} impedance that also comprises the stiffness of the RW membrane, a value obtained from Merchant et al. (33). Z_{SV} is half the mass of scala vestibuli and Z_V is half the mass of the vestibule.

Third Window

The third window is collectively modeled by three impedances where Z_{CA} represents the cochlear aqueduct, Z_{VA} the vestibular aqueduct, and Z_{SSC} the superior semicircular canal. The position of Z_{CA} is between the RW and the BM, and has half of the scala tympani mass on each side. Z_{CA} is modeled as a straight tube of 10 mm with a diameter of 0.15 mm based on the geometry provided in Gopen et al. (3). The impedance of the vestibular aqueduct changed from the previous models and is here based on the geometries presented in Kämpfe Nordström et al. (34). According to their study, the vestibular aqueduct can be characterized as a two part system where the first part is a 2.3 mm straight tube with 0.3 mm diameter. The second part has a horn-like geometry that is 5.7 mm long extending from the first part, has an elliptic cross-sectional area and an end-opening with radius 3.25 and 0.27 mm. The impedance of the second part was computed by successively adding 0.1 mm sections where the impedance was based on the average cross section area.

The impedance of the SSCD was modeled as a hole in the middle of the semi-circular duct. According to Ifediba et al. (35),

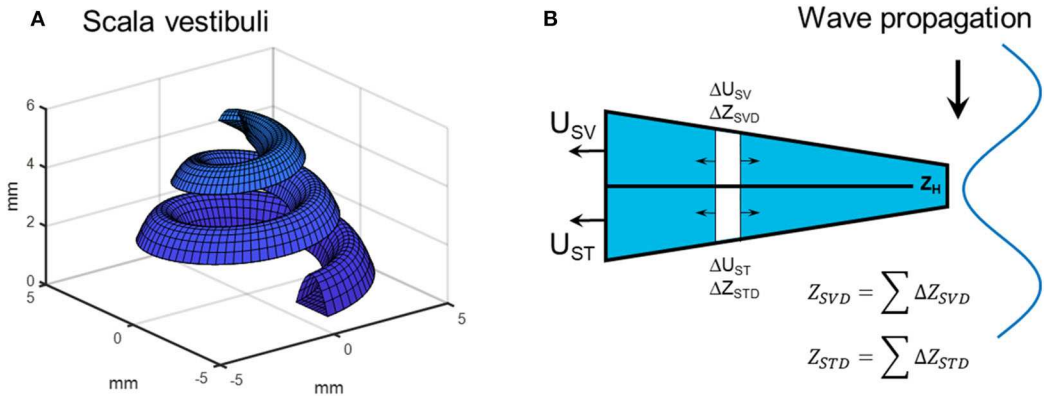

FIGURE 2 | (A) Scala vestibuli as represented by the parametrized geometry. **(B)** The computation of the compression fluid flow based on estimations of small section where the contribution to U_{SV} and U_{ST} from ΔU_{ST} and ΔU_{SV} is based on the wave motion of the bone and the impedances of the ducts as well as on the cochlear load.

the area of the superior semi-circular canal is ∼2 mm^2 close to the common crus and vestibule, and 1 mm^2 at the middle, with a total length of 12 mm. The impedance of the hole between the SSC and the cranial cavity was modeled as a 1 mm long tube with an elliptic cross-section surface where the length of the ellipse was twice the width. This meant that for a SSC without dehiscence, Z_{SSC} was modeled as two 6 mm tubes with areas diminishing from 2 to 1 mm^2 in parallel, terminated by the hole with an infinite impedance (no hole). As the hole became greater, the length of the semi-circular ducts became shorter by the length of the larger radius of the hole. In the current study, the maximum size of the hole had a larger diameter of close to 2 mm, corresponding to a cross-section area of 6 mm^2, and the semi-circular ducts were then reduced to ∼5 mm long. Consequently, the length of the two parallel semi-circular ducts varied between 5 mm for the largest size hole and 6 mm for the no-hole condition. **Table 1** list all impedances.

Simulations

The simulations were conducted using the principal of superposition, where the model was solved for each particular BC stimulus path by turning on all of the sources associated with each BC stimulus mode or AC stimulation and turning the others off. Once the contribution of each stimulus path to the hearing result has been computed, the amplitude squared of the different contributions are summed to compute a quantity proportional to sound power that is used to define the overall hearing result. A more realistic summation would be to add the amplitude and phase of the individual components; however, the phase response of the complex three-dimensional vibration of the real head is not represented in the current model. The computation of a dB change is done according to equation 1

$$dB = 10 \cdot \log_{10}\left(\frac{A^2_{sum}}{A^2_{ref}}\right) \quad (1)$$

where A^2_{sum} is the sum of the contributors' squared amplitudes after the manipulation and A^2_{ref} is the sum of the contributors' squared amplitudes before the manipulation.

It is assumed that the drive of the BM, and thereby the hearing excitation, is caused by the volume velocity through Z_C in the model. This is proportional to the sound pressure difference between scala vestibuli and scala tympani, which has previously been argued to be the drive of the cochlea (14, 17). Therefore, the flow through Z_C is used to compare the contributions from each component and also to investigate changes between conditions.

First, the model itself is validated against experimental data in the normal condition. This is accomplished by comparing intra-cochlear pressures in the model with measurements in cadaveric temporal bones with AC stimulation (14, 36) and BC stimulation (37) and also with BC stimulation in whole human cadaver heads (38). In the experimental datasets the scala vestibuli and scala tympani pressures were measured by small pressure probes inserted into the scalae through tiny holes that were sealed during the measurements (14, 36–38).

The intra-cochlear pressures depend on the exact position of the probes inside the inner ear. In the model, intra-cochlear pressure were extracted at four positions defined as A to D in **Figure 1**. Position A is in the center of the vestibule, position B is at the border between the vestibule and scala vestibuli close to the stapes footplate, position C is at the center of scala vestibuli, and position D is at the center of scala tympani. According to the descriptions of the experiments in the temporal bones, the probe positions were close to positions B and D in the model (14, 36, 37). The exact position of the pressure sensors were not equally well-defined in the Mattingly et al. (38) study. In the AC stimulation comparisons, the ear canal sound pressure is used as reference while the cochlear promontory velocity is used as reference for the BC stimulation compairsons.

Beside the normal condition of the ear, three different conditions are investigated. The first condition is the effect

TABLE 1 | The values of the impedances in **Figure 1**.

Impedance	Value
Z_{SSC}	$j\omega \cdot \left(2.83 \cdot 10^6 + \frac{4 \cdot 10^{-6}}{3 \cdot A_D}\right) + 3.9 \cdot 10^7 + \frac{\pi \cdot 8 \cdot 10^{-6}}{A_D^2}$
Z_{VA}	$j\omega \cdot 5.68 \cdot 10^7 + 1.27 \cdot 10^{10}$
Z_V	$j\omega \cdot 2.43 \cdot 10^5$
Z_{ME}	$j\omega \cdot 4.4 \cdot 10^5 + 1.2 \cdot 10^{12} + \frac{8.1 \cdot 10^{13}}{j\omega}$
Z_{SV}	$j\omega \cdot 2.45 \cdot 10^5$
Z_{SVD}	$j\omega \cdot 2.86 \cdot 10^7$
Z_{STD}	$j\omega \cdot 2.14 \cdot 10^7$
Z_H	$\left(j\omega \cdot 1.7 \cdot 10^7 + 2 \cdot 10^8\right) // \left(2.2 \cdot 10^9 + \frac{1.59 \cdot 10^{12}}{j\omega}\right)$
Z_C	$j\omega \cdot 10.02 \cdot 10^5 + 10^{10}$
Z_{RW}	$j\omega \cdot 4.59 \cdot 10^5 + 5 \cdot 10^8 + \frac{7 \cdot 10^{12}}{j\omega}$

"//" means parallel computing, A_D, area of dehiscence in m^2.

on the AC contribution and the five BC contributors when a hole appears in the superior semi-circular canal, where the hole dimension goes from no-hole to a hole size of 6 mm^2. The second condition explored is a change of the size of the vestibular aqueduct. A large variability is noted in the anatomical studies of the vestibular aqueduct (34), and its effect on the cochlear excitation is examined for variations between half the diameter of the small duct to twice the diameter of the small duct. The third condition investigated in the current study is the effect of OW and RW reinforcement with a present SSCD. This is modeled by increasing the stiffness of the OW and RW separately and jointly, where the increase of the stiffness was either 10 times or 100 times.

RESULTS

Model Validation

The model predictions were compared to experimentally obtained intra-cochlear sound pressures. With AC stimulation, the sound pressures in scala vestibuli and scala tympani in relation to a sound pressure in front of the ear drum are shown in **Figures 3A,B**, respectively. The model-predictions of AC driven intra-cochlear sound pressures at position A and B were nearly identical, and only the sound pressures at positions B and C are included in **Figure 3A**. The sound pressure differences between position B and C are small with almost no difference at the lower frequencies and ∼2 dB lower pressure levels for position C compared to position B at frequencies above 1 kHz. The sound pressures at both positions are in general agreement with the experimentally obtained scala vestibuli sound pressures shown in **Figure 3A**, where the difference between the model-predicted sound pressures and experimentally obtained sound pressures are similar to the difference between the two experimentally obtained sound pressures. The model-predicted scala tympani sound pressure in **Figure 3B** is in line with the experimentally obtained sound pressures. The model predictions in **Figure 3B** are most similar to the Niesten et al. (14) data while the model predicts 5 to 10 dB lower sound pressure at frequencies between 0.5 and 1.0 kHz compared with Nakajima et al. (36).

The model-predicted sound pressures with BC excitation are shown in **Figures 3C,D** together with experimentally obtained BC stimulated intra-cochlear sound pressures in Stieger et al. (37) and Mattingly et al. (38). The scala vestibuli side intra-cochlear sound pressures in relation to the cochlear promontory velocity are shown in **Figure 3C**. The sound pressures at position B and C were within a couple of dBs and only the sound pressures at positions A and B are provided. The sound pressure at position A is relatively close to the experimentally obtained sound pressures while the sound pressure at position B is around 5 dB lower than the position A sound pressure. The model based sound pressure predictions and the Mattingly et al. (38) experimental data indicate an overall 20 dB/decade rise while the Stieger et al. (37) data show a steeper rise at frequencies below 1.5 kHz and a near flat response with frequency at the higher frequencies. The BC model predictions of the scala tympani sound pressure in **Figure 3D** is relatively similar to the Stieger et al. (37) measurements while the Mattingly et al. (38) sound pressures are 5 to 10 dB greater compared to the model predictions.

Model Prediction of BC Contributors

The result in **Figure 4** shows the predicted relative contribution from the five components for BC excitation of the BM in a healthy ear. The general trends are similar to the predictions in Stenfelt (24) with the exception for a few details. The overall most important contributor in the healthy ear is fluid inertia (blue line in **Figure 4**). The middle ear inertia has its major contribution at frequencies between 1 and 2 kHz which is also the frequency range where the middle ear ossicles has its resonance with BC stimulation (29, 30). The use of Homma et al. (29) modeling data for the current simulations increased the middle ear inertia importance around its resonance compared to the earlier model where the Stenfelt et al. (30) data were used. Another difference seen between the current and previous models is the predicted contribution from cochlear compression (red line in **Figure 4**). The use of a coiled cochlea reduced the contribution at the lowest (below 300 Hz) and mid-frequencies, while increasing its contribution at the highest frequencies. The relative contribution from the ear canal sound pressure and intra-cranial pressure is similar to the previous study. It should be noted that the intracranial pressure used here from the Roosli et al. (39) is not the sound pressure in the CSF close to the inner ear but obtained intra-cranially in cadaver heads where the brain was replaced by fluid. Due to uncertainties in the measurements, only CSF pressures at frequencies above 250 Hz is used. However, according to the trajectory, the pressure transmission from the CSF may be important at low frequencies.

Model Predictions of SSCD

Figure 5 shows the simulated effect of a SSCD with different sizes of the dehiscence. The dehiscence size goes from 0.1 to 6 mm^2 and an additional simulation termed "*No imp*" is included that represent the case when Z_{SSC} is zero. This can be seen as a theoretical bound on the greatest change achievable by a SSCD,

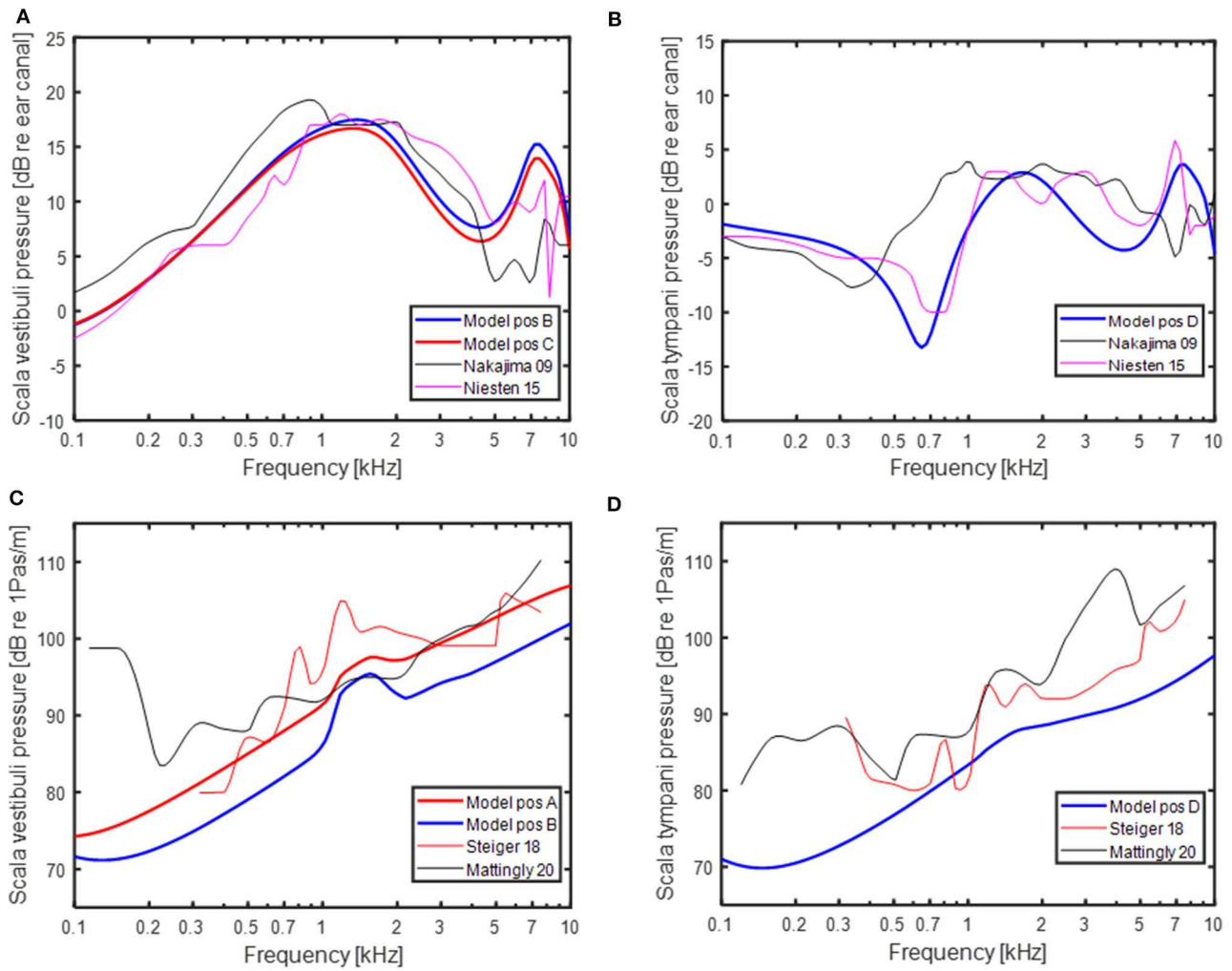

FIGURE 3 | Predictions of intra-cochlear sound pressures with AC stimulation and experimentally measured intra-cochlear sound pressures in Nakajima et al. (36) and Niesten et al. (14) in **(A)** the vestibular side and **(B)** scala tympani. Predictions of intra-cochlear sound pressures with BC stimulation and experimentally measured intra-cochlear sound pressures in Stieger et al. (37) and Mattingly et al. (38) in **(C)** the vestibular side and **(D)** scala tympani. Positions **(A–D)** refer to position in the model schematics in **Figure 1**.

for example a large hole close to the vestibule. In **Figure 5A**, the predicted effect on the AC threshold is shown in relation to a healthy ear. It should be noted that a negative value means worse hearing and a hearing threshold would be increased by that dB level. The AC predictions show a gradually increase in the low-frequency reduction with increasing dehiscence area, but the effect of increased area is small for areas > 3 mm^2. The predicted AC threshold changes are primarily seen at frequencies below 500 Hz where a hole of 1 mm^2 gives a reduction of 3 dB while it results in a reduction of 16 dB at 125 Hz. **Figure 5B** shows the simulated improvement in BC hearing from the SSCD. It indicates a relatively abrupt increase of ∼15 dB at 250 Hz for the smallest dehiscence simulated, and the increase rises with dehiscence dimension up to 23 dB at 300 Hz, the frequency with maximum predicted threshold change. It is noteworthy that the simulations predict less increase at the lowest frequencies and at 100 Hz the increase is ∼10 dB independent of dehiscence dimension.

The predicted ABG is indicated in **Figure 5C** which is the difference between **Figures 5A,B**. The overall morphology shows an increase of the predicted ABG with decreasing frequency between 300 and 1,000 Hz, while the ABG is nearly constant at frequencies below 300 Hz. The predicted ABG has a maximum of 15 dB for the smallest dehiscence simulated (0.1 mm^2) and increases with increasing dimension of the dehiscence reaching just over 30 dB for the largest dehiscence (6 mm^2). In the "No-imp" condition, the maximum ABG reaches 45 dB at 300 Hz.

The predicted changes in the BC contributors with SSCD are shown in **Figure 6**. **Figure 6A** show the relative contribution of the five BC components when the SSCD is 6 mm^2. Compared

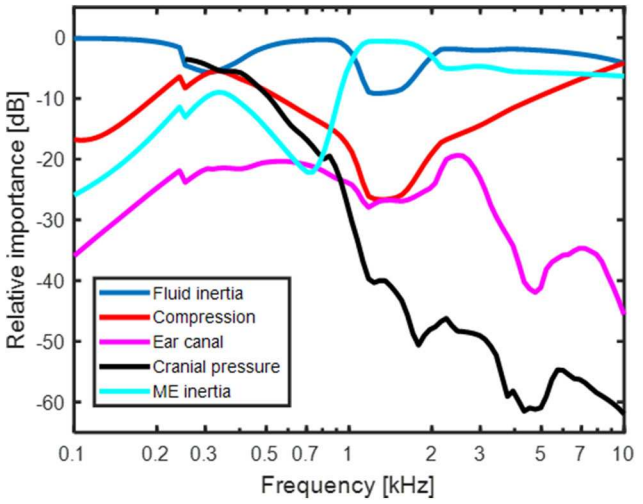

FIGURE 4 | The relative importance from the five contributors of BC sound in a healthy ear.

to **Figure 4** that shows the relative contributions for BC in the healthy ear, the fluid inertia has become even more dominant. The differences seen are, as expected, at frequencies below 1 kHz. The alterations in **Figure 6A** is a combination of the effects seen in **Figures 6B–F**. **Figure 6B** shows the effect for fluid inertia which follows the change in predicted BC thresholds (**Figure 5B**) closely. This prediction is again consistent with fluid inertia as the most important contributor for BC hearing, also in a pathological ear. One interesting observation is the finding at the lowest frequency (100 Hz) where all simulations of a SSCD starts at 10 dB independent of dehiscence size and increases with frequency up to 300 Hz. This is a result of the RW stiffness that restricts the motion of the fluid over the BM at these low frequencies. Consequently, according to this model, the maximum improvement from fluid inertia at frequencies below 300 Hz is determined by the RW stiffness. The inner ear compression component (**Figure 6C**) show nearly an opposite function compared to the fluid inertia, but with less impact. A SSCD result in a decreased BM stimulation from the compression with a minimum of between−5 and−15 dB at frequencies between 200 and 300 Hz. The reduction is primarily a result of U_V and U_{SV} directing the volume velocity toward the SSC instead of over the BM.

The effect of sound pressure in the ear canal with BC (**Figure 6D**) and middle ear inertia (**Figure 6F**) show nearly identical results as with AC stimulation in **Figure 5A** since they all stimulate the inner ear via the stapes velocity (U_{SF}) in the model. The low-frequency reduction coincides with the decrease in cochlear impedance seen at the OW (omitting Z_{ME}). Since the stapes velocity alteration with the change in impedance is small, the reduced cochlear impedance leads to a reduced intra-cochlear sound pressure that decreases the BM excitation. The effect of sound pressure transmission from the CSF to BM vibration (**Figure 6E**) shows the greatest deviation from the other contributors having the greatest impact at the higher frequencies. The increase at 100 Hz is ∼10 dB for all SSCDs simulated that increase further at higher frequencies and a larger dehiscence result in a greater change with around 13 dB for the 0.1 mm^2 dehiscence, 25 dB with 6 mm^2 dehiscence, and 37 dB in the *"No imp"* condition.

Model Predictions of Vestibular Aqueduct Variations

The predicted AC and BC threshold changes with varying size of the vestibular aqueduct are shown in **Figure 7**. In the simulations, the narrow part of the vestibular aqueduct that was modeled as 2.3 mm long tube with a diameter of 0.3 mm was altered with diameters between 0.15 mm (half) and 0.6 mm (double). Since this narrow duct dominates the impedance of the vestibular aqueduct, only the initial cross sectional area of the second horn-like part was altered since it had the same area as the narrow tube. **Figure 7A** indicates that this range of variation did not affect the simulated AC thresholds. The greatest predicted change was around 1 dB appearing at 100 Hz. The predicted BC thresholds in **Figure 7B** were more affected by the dimension of the vestibular aqueduct. In these simulations, the impedance of the semi-circular canal (Z_{SCC}) was infinite and the only volume velocity possible between the vestibule and the cranial cavity was through the vestibular aqueduct. The BC estimations varied between−15 dB and 12 dB at the lowest frequencies, primarily below 500 Hz. A smaller vestibular aqueduct size reduced the predicted BC sensitivity while a greater vestibular aqueduct size improved the predicted BC sensitivity. The explanation for the change in BC sensitivity with vestibular aqueduct alteration is the same as with SSCD, a reduced impedance allow more fluid to be displaced by the fluid inertia thereby improving the BC excitation, while an increase in the impedance restricts the fluid inertia. The middle ear inertia and sound pressure from the ear canal is affected similar as the simulated AC thresholds (**Figure 7A**) while the cochlear compression shows a small low-frequency decrease with larger vestibular aqueduct and a small increase with smaller ducts. The CSF pressure transmission decreases by 12 dB with halving the duct diameter and improves by 10 dB with doubling the duct diameter, almost independent of frequency. These results indicate that the vestibular aqueduct is important for low frequency BC hearing.

Model Predictions of Cochlear Window Reinforcement

The predicted effect of reinforcement of the OW and RW, modeled as an increase in the stiffness, is shown in **Figure 8**. The predicted effect on the AC thresholds is shown in **Figure 8A** for a healthy (no SSCD) ear when the RW and OW stiffness is increased by 10 or 100 times, in isolation or jointly. A stiffness increase of the OW affects the predicted AC thresholds more than a stiffness increase of the RW, where a 10 times increase of the OW stiffness result in similar AC threshold depression as a 100 times increase in the RW stiffness. The greatest decrease is when both the RW and OW stiffnesses are increased 100

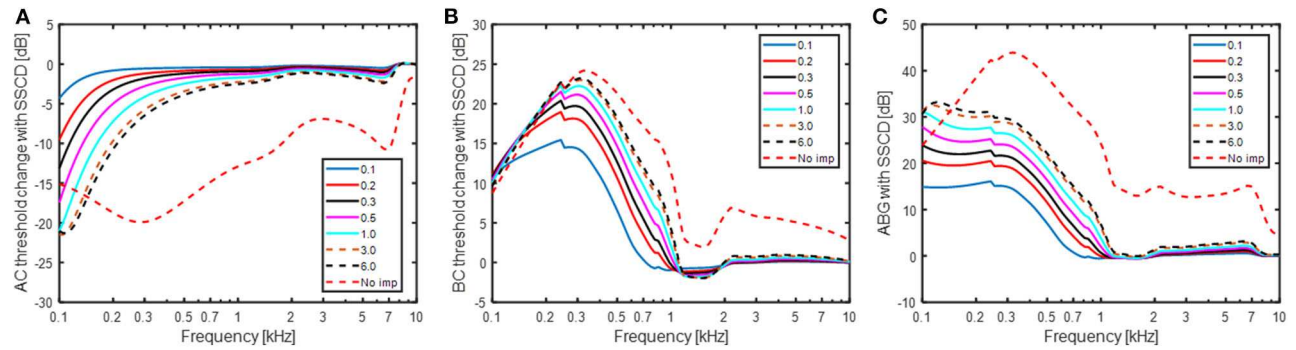

FIGURE 5 | Estimations of **(A)** AC threshold change, **(B)** BC threshold change, and **(C)** ABG for a SSCD based on the model in **Figure 1**. A negative value means decreased sensitivity while a positive value means improved sensitivity in panels **(A,B)**. The legend indicates the dehiscence area in mm^2 and "No imp" refers to the condition where $Z_{SSC} = 0$.

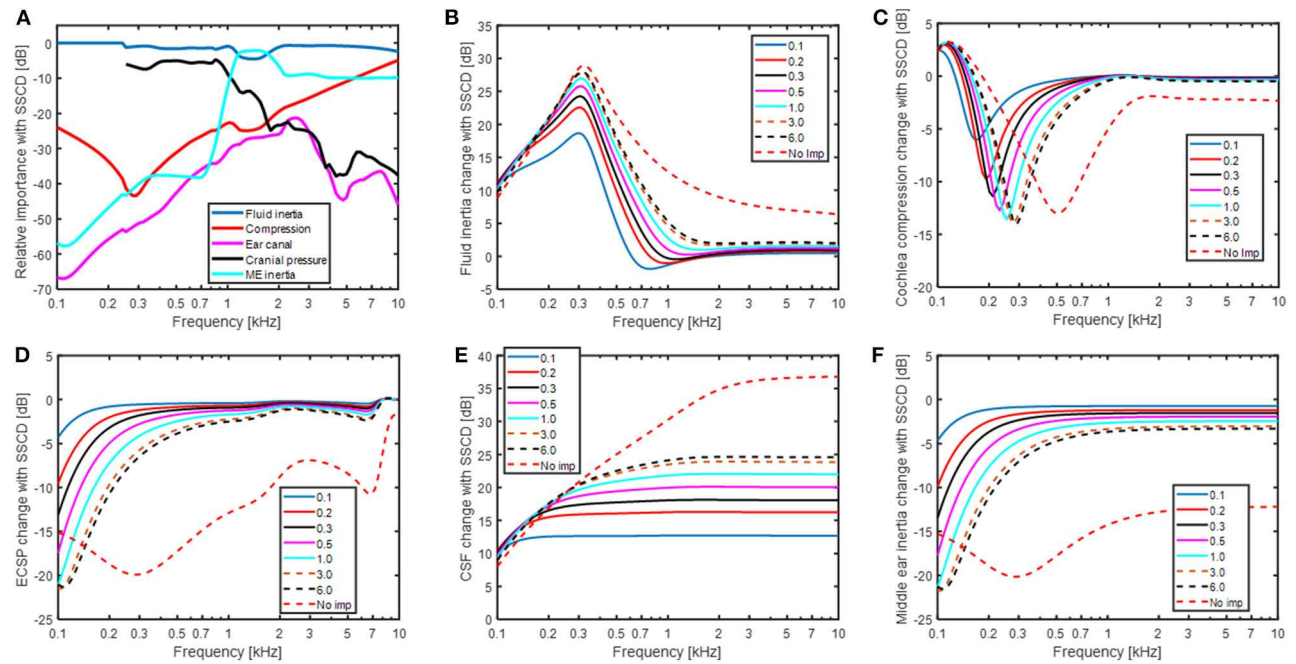

FIGURE 6 | (A) The relative importance for the five contributors to BC sound in a SSCD ear with a dehiscence area of 6 mm^2. **(B–F)** The changes of each individual contributor to BC sound for different areas of a SSCD given in mm^2.

times, resulting in around 60 dB worse predicted thresholds at the lowest frequencies. The predicted result shown in **Figure 8B** is the change in AC thresholds compared with a normal healthy ear, when a SSCD of 3 mm^2 coincides with the alteration of OW and RW stiffness. The normal curve in **Figure 8B** (black dashed line) is the result without changing the stiffness of the RW or OW but with a SSCD of 3 mm^2, i.e., the same as the 3 mm^2 curve in **Figure 5A**. The SSCD boosts the effect from stiffening the RW and OW and a 10 times stiffening of the RW causes a significant predicted AC hearing reduction at the low frequencies. Now, the OW stiffening result in greater reduction at the mid frequencies but affects the lowest frequencies similar as a stiffening of the RW. The combined effect of increasing both the OW and the RW stiffness 100 times result in a reduction of simulated AC hearing by more than 90 dB at the lowest frequencies.

The predicted effects on BC thresholds with OW and RW stiffness increases are shown in **Figures 8C,D**. In the healthy ear (**Figure 8C**), stiffening the RW 10 times gives nearly no effect and stiffening the RW 100 times gives a threshold depression at frequencies below 300 Hz amounting to 17 dB at 100 Hz. Increasing the stiffness of the OW has no effect at the lowest frequencies but decreases the predicted BC thresholds at mid frequencies. Increasing the OW stiffness reduces the inertial contributors and the result is primarily from the cochlear

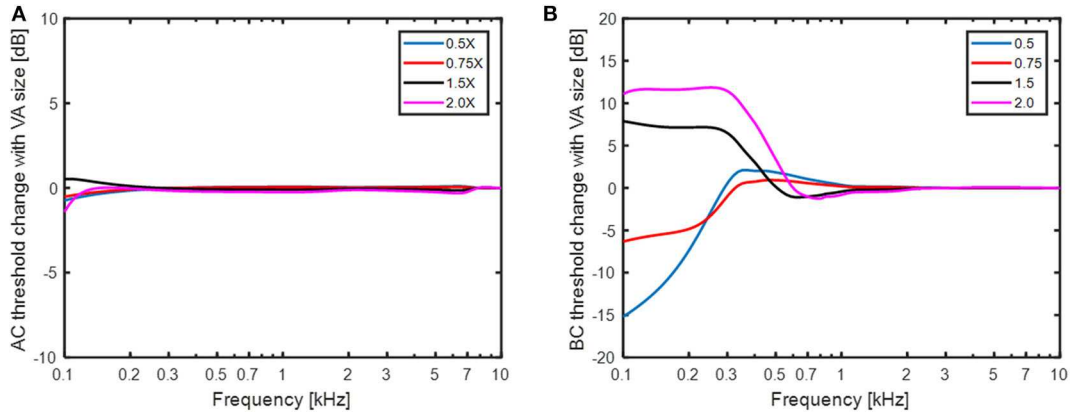

FIGURE 7 | The change in **(A)** AC thresholds and **(B)** BC thresholds when the size of the small duct in the vestibular aqueduct is altered between half diameter (0.5 X) and double diameter (2X).

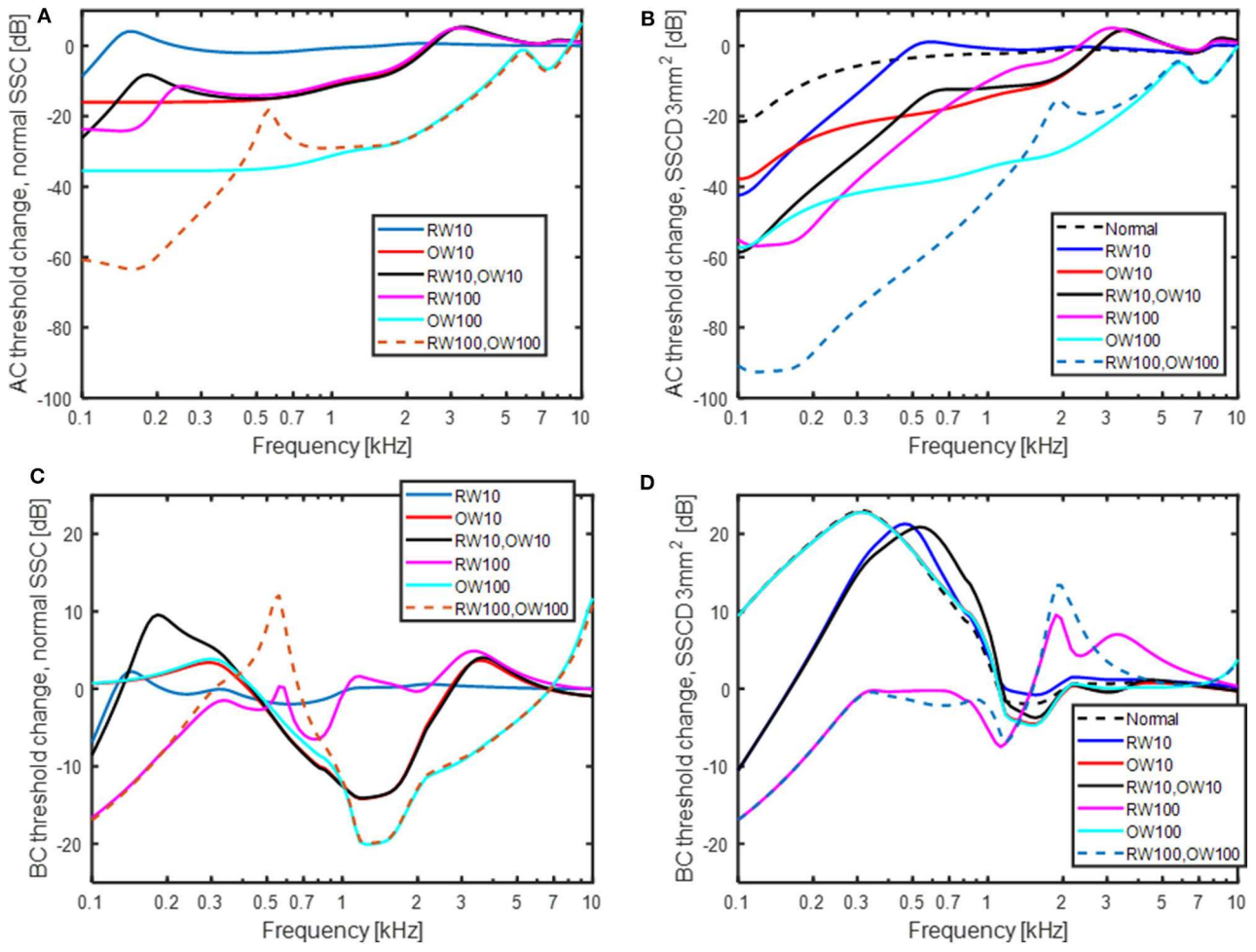

FIGURE 8 | The effect of increasing the stiffness of the OW and RW 10 and 100 times in isolation and jointly. **(A)** AC thresholds with normal semi-circular canal, **(B)** AC thresholds with a SSCD of 3 mm^2, **(C)** BC thresholds with normal semi-circular canal, and **(D)** BC thresholds with a SSCD of 3 mm^2. "Normal" in the legend means no change of OW and RW stiffness.

compression component. The effect with OW and RW stiffness increase is different with SSCD shown in **Figure 8D**. In this case, increasing the OW stiffness has no impact and the curves for 10 times and 100 times stiffness increase falls on top of each other and are nearly identical with the "no stiffness change" curve (here termed normal). Increasing the RW stiffness affect the predicted BC thresholds by reducing the low-frequency BC sensitivity. When the RW stiffness is increased 100 times, the simulated BC thresholds are close to normal at frequencies above 250 Hz and a reduction of 17 dB at 100 Hz is seen.

DISCUSSION

The Model

The current study has investigated the impact from pathological third windows on AC and BC thresholds, and also investigated the mechanisms for the changes. Both the strengths and the weakness of this study are that it is based on a computational model. The strength is that a model facilitates investigations of the mechanisms underlying the results. The weakness of the model is that it is just a model, a simplification of the reality. All models have their limitations and so does this model. For example, the AC transmission is limited to ossicular vibration only and no effect of sound pressure in the middle ear cavity is included. This means that other AC pathways that may become important when the ossicular chain transmission is restricted is omitted in the current model. The model is similar to other lumped-element models of the inner ear where the stimulation is by AC (31, 40, 41). Moreover, the model could predict intra-cochlear sound pressures obtained experimentally in cadaveric temporal bones when the stimulation was a sound pressure in the ear canal (**Figures 3A,B**).

The greatest uncertainty is probably in the representation of the BC model. Models that simulate general BC responses are rare. Most are restricted to a single mode of excitation and have a simplified geometry (42, 43). Whole-head models for BC have been developed (44, 45) but do not include the detailed structures of the inner ear, for example the vestibular and cochlear aqueducts, and is therefore inappropriate for the current study. Even if there are uncertainties with the current model for BC excitation, it has been revised from previous versions (4, 24) by updated geometries, impedances, and excitation patterns, and continue to show similar results.

The model's ability to predict experimental and clinical findings with BC stimulation has been shown in a previous study (4). In the current study, the model validation was done by comparison to experimentally obtained intra-cochlear pressures (**Figures 3C,D**). The model predictions of the intra-cochlear pressures showed similar frequency responses as the experimentally obtained intra-cochlear pressures, but some 5–10 dB overall lower levels. One difference between the model simulations and the experimental measurements with BC stimulation is that the model is restricted to a one-dimensional vibration behavior while the experimental data are obtained with vibration in all three dimension, even if the cochlear promontory vibration is reported as a one-dimensional velocity. The bone encapsulating the inner ear vibrates in all three space dimensions with nearly identical magnitudes (25). Consequently, in the experimental measurements the contribution from three orthogonal vibration directions are summed in the cochlea increasing the overall pressure compared to a one-dimension stimulation. The summation of these contributors in magnitude and phase is unknown, but the addition in sound power from three orthogonal vibrations of equal magnitude is nearly 5 dB. So, part of the discrepancy between the model predictions of intra-cochlear sound pressures and the experimentally measured intra-cochlear sound pressures is caused by the one-dimensional excitation in the model and three-dimensional excitation in the experiments.

There are additional differences between the model simulation of BC sound and the experimental measurements. In Stieger et al. (37) the measurements are conducted in isolated temporal bones excluding the influence from the external ear and CSF pressure. Even if those contributors are not dominating the BC response according to the model simulations in **Figure 4**, the extraction of the temporal bone may affect some of the loading impedances, for example the loading from the vestibular aqueduct or the middle ear ossicles. In Mattingly et al. (38), the measurements were conducted in intact cadaver heads, but the pressure sensors were not rigidly attached to the bone by cement but only with alginate. According to Stieger et al. (37), such attachment introduce artifacts in the measurement of intra-cochlear sound pressure with BC stimulation. This fact introduce uncertainty in the compairson to the Mattingly et al. (38) data.

In the computation of the BC response in the model, the five BC pathways' contributions were added in sound power and not with the individual components' amplitude and phase. This can be seen as a weakness of the model and simulations. However, as stated previously, the bone encapsulating the inner ear vibrates in three dimensions (25), and the amplitude and phase relations between these directions is not well-established. Moreover, the amplitude and phase relation between the directions depend on the exact position of the stimulation. Consequently, if the different contributors in the model were to be added with phase, the phase can be very different in reality due to the influence from vibrations in other directions. It was therefore decided to add the sound power from contributors and neglect the possibility that some of the components may add destructively at specific frequencies. Another aspect is that adding the components with amplitude and phase only influences the results when they are of similar magnitude. When investigating the contribution from the five pathways in **Figure 4** it can be seen that the BC response is mostly dominated by one component. In such case, including the phase in the addition has a minor influence on the final result.

The greatest difference between the current BC model and the previous version was the coiled cochlea and the compressional volume velocity based on volume changes in small sections of the coiled scalae. The cochlear shape was parameterized to facilitate the estimation of volume change based on phase differences in a more correct anatomy. This novel way of estimating the compression during BC changed the effect of compression response in the healthy ear (**Figure 4**). Compared to previous

model predictions, the low and mid-frequency responses were slightly lower and the high-frequency response was increased. The reduction at low frequencies was mainly due to the ability for the volume velocity to flow through the helicotrema instead of forcing all volume velocity toward the cochlea while at high frequencies, the geometrical distribution increased the volume velocity output.

The computations of the coiled scalae also gave impedances for the cochlear duct (Z_{SVD}, Z_H and Z_{STD}, **Figures 1**, **2**) that were included in the computations for all contributors. This series of impedances have a greater magnitude than the impedance over the BM (Z_C, **Figure 1**) that it parallels. It did not impact the computations at the frequencies investigated here, but may influence results at lower frequencies (15, 31). The other larger alteration was the geometry of the vestibular aqueduct that previously consisted of two serial connected tubes with different length and diameters. It was now made by one straight narrow tube and one horn-shaped part that had an increasing elliptic cross-sectional area (34). However, this change did not significantly alter the responses of the BC predictions in **Figure 4**. The thinner tube dominates the impedance of the vestibular aqueduct, and it was similar for the two models. The result in **Figure 4** indicates that for the healthy ear, fluid inertia and middle ear inertia contributes the most.

The results in this study are based on model simulations and need to be interpreted accordingly. The parameters of the model is based on averages from anatomical and physiological measurements. Hence, an individual can deviate from these average data and show different results. However, the trends should be similar and the mechanisms behind the results should also be the same.

Hearing Changes With SSCD

Figure 5 show the predicted changes in AC thresholds, BC thresholds, and ABG with a SSCD. The simulations were done for a dehiscence area of up to 6 mm^2. The limitation to 6 mm^2 was based on the study by Hunter et al. (46) that reported most dehiscence areas to be 6 mm^2 or smaller, with mean areas in different studies ranging from 1.44 to 3.19 mm^2. The ABG in **Figure 5C** show a monotonic increase with increasing size of the dehiscence at frequencies below 1 kHz. This is in line with reports from clinical and experimental studies (14, 46, 47). Hunter et al. (46) computed the correlation between dehiscence size and ABG at 500 Hz and reported it to be $r = 0.27$. When the ABG at 500 Hz in **Figure 5C** is related to dehiscence area a correlation coefficient of $r = 0.77$ is obtained, a value significant higher than the clinical observed correlation. It has also been suggested that when the dehiscence sizes becomes greater than the cross sectional area of the semi-circular canal, it does not add any effect to the ABG (22). This is partially corroborated in the current study where only small changes of the ABG occur once the area has reached 1 mm^2, that is the cross-sectional area of the semi-circular canal for the model (35). Since most sizes of the dehiscence reported clinically are greater than the cross-sectional area of the semi-circular canal (averages ranging between 1.44 and 3.19 mm^2), only weak relations between the dehiscence size and ABG is expected.

The ABG is the difference between the AC and BC thresholds, and according to the model the AC thresholds affect the ABG most at the lowest frequencies while the BC thresholds affect it mostly between 200 and 500 Hz. ABGs for patients with SSCD have been reported up to 50 dB (47), which is greater than the model predicts. If the "No imp" condition is considered, the maximum ABG at 250 and 500 Hz is ∼40 dB. One reason for the limitation of the ABG to ∼30 dB in the model is that the position of the dehiscence is modeled at the middle of the semi-circular canal. Williamson et al. (48) reported the positions of the dehiscence to be approximately equally distributed at the three areas arcuate eminence, posterior aspect, and posterior aspect, of the semi-circular canal. Consequently, the clinically observed spread in the position of the dehiscence add variability to the ABG. For example, Songer and Rosowski (22) reported the difference between a dehiscence close to the vestibule and 5 mm from the vestibule to be about 10 dB. This indicates that the difference in the ABG in **Figure 5C** between 6 mm^2 and "No imp" of ∼10 dB is reasonable and that the model is able to capture ABGs reported clinically.

Niesten et al. (14) reported the intra-cochlear sound pressure in human temporal bones subsequent to SSCD to be reduced 10 to 15 dB at 100 Hz that recovered with frequency and no effect was seen at frequencies above 800 Hz. This is in line with the model predictions in **Figure 5A** where a worsening of the AC threshold of 10 to 20 dB is predicted at 100 Hz, depending on the dehiscence area, that recovers with frequency and is <3 dB at 800 Hz. In a study on chinchillas, Songer and Rosowski (22) showed an abrupt change in the AC threshold when opening the semi-circular canal. That was not found for the model in the AC threshold, but the BC threshold was altered with up to 15 dB when a hole of 0.1 mm^2 was introduced in the model. This can be explained by the impedance difference between the SSCD and the vestibular aqueduct (Z_{SSC} and Z_{VA}) for even a small hole, facilitating fluid inertia at low frequencies. The model predict between 15 and 20 dB BC threshold improvement with a SSCD of 0.5 mm^2 or larger at frequencies between 125 and 500 Hz. Since most audiometers do not measure BC thresholds better than−10 dB HL, an improvement of 20 dB can be difficult to measure if the patient has no sensorineural hearing deficit. This implies that some clinical studies underestimate the ABG due to insufficient dynamic range for the BC testing. Brantberg et al. (8) circumvented this problem by testing the BC thresholds with a minishaker and a load cell to estimate the vibration force applied. When comparing SSCD patients with normal controls they reported BC threshold improvement with SSCD in the range of 15–23 dB at 125 Hz, 17–20 dB at 250 Hz, 5–19 dB at 500 Hz,−4 to 12 dB at 750 Hz, and−4 to 5 dB at 1,000 Hz. These data are in line with the model predicted BC threshold improvement in **Figure 5B**. One possible problem is that the data by Brantberg et al. (8) were obtained with occluded ears which may enhance the low-frequency contribution by the ear canal sound pressure which is affected differently by the SSCD than the BC hearing in general (**Figure 6**) (28, 49).

Since there is a risk of a ceiling effect when clinically measuring BC thresholds in patients with SSCD, and thereby underestimating the ABG, there is a risk of miss-diagnose

patients with SSCD as non-pathological. This risk is even greater if the BC thresholds is not obtained at frequencies below 500 Hz. A solution to this problem is to use a BC transducer that can be used at low frequencies, for example the Radioear B81 BC transducer (50), and measure BC thresholds down to 250 Hz but preferable down to 125 Hz. Also, recalibrating the audiometer for BC transducer use so it permits measurement down to −20 dB HL enable a more correct measure of the BC hyperacusis and a more reliable estimation of the ABG and SSCD diagnosis.

Bone Conduction Contributors With SSCD

The relative importance of the different BC contributors change with the SSCD (cf **Figures 4**, **6A**). In the SSCD ear, the contribution of the fluid inertia dominates the response and only the middle ear inertia contributes at around its resonance frequency. The low-frequency contribution from the middle ear inertia and ear canal sound pressure is reduced similar to the AC thresholds (**Figures 6D,F**). This is caused by the reduction of the cochlear impedance due to the SSCD. According to Chien et al. (47), the stapes velocity increased by 3–5 dB after the introduction of a SSCD, while the RW motion was reduced by 15 dB at 100 Hz. Consequently, the stapes velocity increase after the SSCD cannot compensate for the low-frequency cochlear impedance decrease and the low-frequency intracochlear pressure decreases, which is reflected in the reduced RW motion.

A common complaint by SSCD patients is disturbance by internal sounds such as eye movement, chewing, and bowel sounds (7, 8). It has been hypothesized that internal sounds are transmitted by the intracranial pressure transmission (8). According to the model simulations in **Figure 6**, the sound pressure transmission from the CSF is not dominating the BC response after SSCD and its frequency function is very different from that observed with BC thresholds. The BC thresholds improves at the low frequencies after a SSCD while the sound pressure transmission from the CSF show the greatest improvement at the highest frequencies (**Figure 6E**). This indicates that the internal sounds are not transmitted through the SSCD but is a result of the general BC improvement enhancing internal sounds that cause the skull bone to vibrate.

Hearing as a Function of the Vestibular Aqueduct

The changes in cochlear impedance in the simulations of the vestibular aqueduct in **Figure 7** is less dramatic than those with SSCD in **Figure 6**. This is due to the smaller cross-section area of the vestibular aqueduct compared to the dehiscence areas used to simulate the SSCD. The small tube area of the vestibular aqueduct is 0.07 mm^2 in the normal condition, 0.28 mm^2 in the double-diameter condition, and 0.018 mm^2 in the half-diameter condition. These variations do not affect AC hearing but has an influence on the BC hearing at low frequencies. The standard deviation for the small duct diameter is given in Kämpfe et al. (34) as 0.12 mm which indicates that the normal size +/- 1 SD is almost covered in the 0.5X to 1.5X results. According to the simulations of the BC thresholds, this would indicate a variability of −15 to + 7 dB at 100 Hz. To the author's knowledge, there are no reports on the BC threshold variability at such low frequencies. Clinically, BC thresholds are usually only obtained at 250 Hz and above, and the variation in BC thresholds at 250 Hz due to the spread in vestibular aqueduct size is close to +/- 5 dB, which is lower than the anticipated variability in BC threshold testing (51).

Large vestibular aqueduct syndrome (LVAS) has been reported to result in significant ABGs at frequencies below 1 kHz. Merchant et al. (52) reported LVAS to give an ABG that amounted to 51 dB at 250 Hz that decreased with frequency to 12 dB at 1 kHz. That is far more than what can be expected from the variation of vestibular aqueduct sizes in **Figure 7**, and is more in line with the "No imp" data in **Figure 5C**, indicating a larger opening than 2–4 mm^2 that was modeled as the parallel semicircular canal. Unfortunately, no data on the size of the LVAS was provided in Merchant et al. (52).

Round Window and Oval Window Reinforcement

Stiffening the RW and OW affected the predicted AC thresholds more than the BC thresholds (**Figure 8**). This could be expected as clinically it has been demonstrated that occlusion of the OW [e.g., otosclerosis (53), or RW atresia (54)], affect the AC thresholds significantly but the BC thresholds < 20 dB. For AC, increasing the stiffness of the OW had greater effect than the same stiffness increase of the RW. This can be explained by the two stiffness's being in the AC transmission pathway where the OW stiffness is greater than the RW stiffness, and an increase of the dominating stiffness has the greatest influence. Also, it can be noted that the effect of OW and RW stiffness increase has a greater effect in the SSCD condition (**Figure 8B**) compared to the healthy ear. The predicted loss from the RW stiffness increase in **Figure 8A** is similar to that estimated in Elliott et al. (41), using a similar type of model.

Increasing the stiffness of the RW gives a relatively limited low-frequency effect for the normal ear (**Figure 8C**) while stiffening the OW gives a mid-frequency lowering of the predicted BC thresholds. The increase in OW stiffness can be seen as a model for otosclerosis where the stapes become immobile. The curve for increasing the OW stiffness 100 times in **Figure 8C** do mimic the well-known Carhart notch for BC thresholds in an otosclerotic ear (53). This indicates that the Carhart notch is the reduction of the inertial effect so that the cochlear compression dominates the BC response. Moreover, if an increased OW stiffness is seen as a beginning of an otosclerosis, the predicted ABG of early otosclerosis can be obtained from the predicted AC and BC threshold shifts with OW stiffness in **Figures 8A,C**. **Figure 9** shows the predicted ABG for an OW stiffness increase of 10 times and 100 times together with the ABG for a SSCD with 3.0 mm^2 opening. The morphology of the three curves in **Figure 9** are similar but they differ in magnitude. The ABG for the SSCD falls between the two ABG with OW stiffness increase. This prediction illustrates that it is not possible to distinguish between a SSCD and early stages of otosclerosis based on the ABG alone.

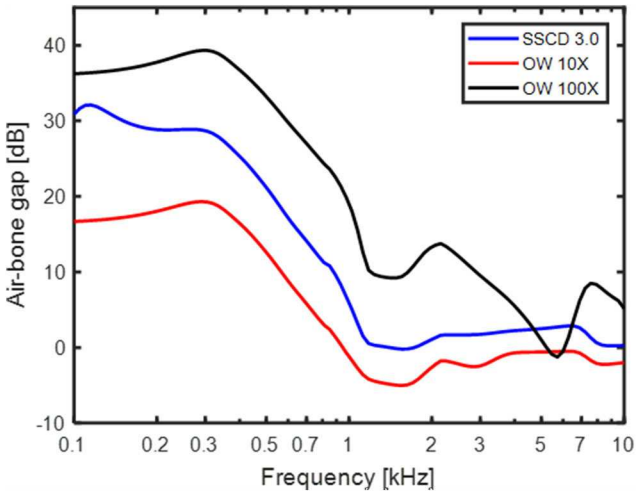

FIGURE 9 | The ABG predicted by the model for a 3 mm^2 SSCD, OW stiffness increase 10 times, and OW stiffness increase 100 times.

The increase in RW and sometimes also OW stiffness have been used to mitigate the adverse effects of SSCD (19–21). When investigating the predicted effects of increased OW stiffness with SSCD in **Figures 8B,D**, it can be seen that for AC stimulation, the OW stiffness increase reduces the hearing threshold over a relative wide range of frequencies. For BC stimulation, it has no effect at all. The model predicts that the volume velocity due to fluid inertia, which dominates the response for BC, flows primarily between the RW and the SSCD, and an increase of the stiffness at the OW does not affect this flow. This is illustrated in **Figure 8D** where the curves for no window stiffness (black dashed line), 10 times OW stiffness (red line) and 100 times OW stiffness (light blue line) nearly overlap. A small increase in RW stiffness (10 times, blue and black lines) reduces the predicted BC response at the lowest frequencies but there is still a 20 dB hyperacusis at around 500 Hz. Once the RW stiffness increase reach 100 times, it reduces the BC sensitivity to near normal values, with a slight depression at the lowest frequencies compared to a healthy ear. These data suggest that for reducing disturbance caused by hyperacusis of internal sounds in SSCD, a reinforcement, or stiffening, at the OW is ineffective, while an increased stiffness at the RW can mitigate the effects once this stiffness increase reach 100 times. Such changes in RW stiffness are predicted to reduce the sensitivity to AC stimulus by more than 20 dB at frequencies <1 kHz. It should be noted that a stiffness increase of the RW by 100 times is significant and would mean that the RW stiffness is 10 times greater than the OW stiffness. Consequently, a stiff plate on the RW would be required to achieve such increased stiffness.

CONCLUSIONS

A lumped element impedance model was able to predict clinical findings in SSCD by both AC and BC stimulation, and gave insight to the mechanisms responsible for the alterations. In general, inertial effects are predicted to be most important for BC hearing in a healthy ear, and the response from fluid inertia becomes even more pronounced in a SSCD case. The SSCD act as a parallel low impedance to the healthy cochlear impedance, which reduces the intra-cochlear sound pressure at low frequencies with a SSCD, leading to worse AC response. The same low impedance from the SSCD improves the volume velocity between the RW and vestibule for BC sound leading to an increased low-frequency BC response. The predicted sound pressure transmission from the cranial cavity to the inner ear via the SSCD seem not to be important for the clinical findings observed.

The normal variability in vestibular aqueduct size do not affect AC hearing and only BC hearing at very low frequencies. The predicted ABG from an early stage of otosclerosis is similar to the ABG from SSCD which indicates the ABGs alone cannot differentiate between these pathologies. The use of window reinforcement to mitigate BC hyperacusis can be effective when the RW is reinforced but has no impact when the OW is reinforced. Such reinforcement do affect AC hearing negatively.

DATA AVAILABILITY STATEMENT

The raw data supporting the conclusions of this article will be made available by the authors, without undue reservation.

AUTHOR CONTRIBUTIONS

SS made the simulations, analyzed the results, and wrote the manuscript.

FUNDING

The grant supporting the research is The Swedish Research Council (Vetenskapsrådet) grant number 2017-06092.

REFERENCES

1. Stenfelt S, Hato N, Goode RL. Fluid volume displacement at the oval and round windows with air and bone conduction stimulation. *J Acoust Soc Am.* (2004) 115:797–812. doi: 10.1121/1.1639903
2. Ranke O, Keidel W, Weschke H. Des Hören beim Verschluss des runden Fensters. *Zeitschrift Laryngol.* (1952) 31:467–75.
3. Gopen Q, Rosowski J, Merchant S. Anatomy of the normal human cochlear aqueduct with functional implications. *Hear Res.* (1997) 107:9–22. doi: 10.1016/S0378-5955(97)00017-8
4. Stenfelt S. Inner ear contribution to bone conduction hearing in the human. *Hear Res.* (2015) 329:41–51. doi: 10.1016/j.heares.2014.12.003
5. Stenfelt S, Goode R. Bone conducted sound: physiological and clinical aspects. *Otol Neurotol.* (2005) 26:1245–61. doi: 10.1097/01.mao.0000187236.10842.d5

6. Merchant S, Rosowski J. Conductive hearing loss caused by third-window lesions of the inner ear. *Otol Neurotol.* (2008) 29:282–9. doi: 10.1097/MAO.0b013e318161ab24
7. Ward B, Carey J, Minor L. Superior canal dehiscence syndrome: lessons from the first 20 years. *Front Neurol.* (2017) 8:1–10. doi: 10.3389/fneur.2017.00177
8. Brantberg K, Verrecchia L, Westin M. Enhanced auditory sensitivity to body vibrations in superior canal dehiscence syndrome. *Audiol Neurotol.* (2016) 21:365–71. doi: 10.1159/000450936
9. Bertholon P, Reynard P, Lelonge Y, Peyron R, Vassal F, Karkas A. Hearing eyeball and/or eyelid movements on the side of a unilateral superior semicircular canal dehiscence. *Eur Arch Otorhinolaryngol.* (2018) 275:629–35. doi: 10.1007/s00405-017-4781-7
10. Minor LB. Superior canal dehiscence syndrome. *Am J Otol.* (2000) 21:9–19. doi: 10.1016/S0196-0709(00)80105-2
11. Brantberg K, Bergenius J, Mendel L, Witt H, Tribukait A, Ygge J. Symptoms, findings and treatment in patients with dehiscence of the superior semicircular canal. *Acta Otolaryngol.* (2001) 121:68–75. doi: 10.1080/000164801300006308
12. Mikulec A, Mckenna M, Ramsey M, Rosowski J, Herrmann B, Rauch S, et al. Superior semicircular canal dehiscence presenting as conductive hearing loss without vertigo. *Otol Neurotol.* (2004) 25:121–9. doi: 10.1097/00129492-200403000-00007
13. Songer J, Rosowski J. A superior semicircular canal dehiscence-induced air-bone gap in chinchilla. *Hear Res.* (2010) 269:70–80. doi: 10.1016/j.heares.2010.07.002
14. Niesten M, Stieger C, Lee D, Merchant J, Grolman W, Rosowski J, et al. Assessment of the effects of superior canal dehiscence location and size on intracochlear sound pressures. *Audiol Neurotol.* (2015) 20:62–71. doi: 10.1159/000366512
15. Raufer S, Masud S, Nakajima H. Infrasound transmission in the human ear: Implications for acoustic and vestibular responses of the normal and dehiscent inner ear. *J Acousti Soc Am.* (2018) 144:332–42. doi: 10.1121/1.5046523
16. Kim N, Steele C, Puria S. Superior-semicircular-canal dehiscence: effects of location, shape, and size on sound conduction. *Hear Res.* (2013) 301:72–84. doi: 10.1016/j.heares.2013.03.008
17. Pisano D, Niesten M, Merchant S, Nakajima H. The effect of superior semicircular canal dehiscence on intracochlear sound pressures. *Audiol Neurotol.* (2012) 17:338–48. doi: 10.1159/000339653
18. Ward B, Agrawal Y, Nguyen E, Della-Santina C, Limb C, Francis H, et al. Hearing outcomes after surgical plugging of the superior semicircular canal by a middle cranial fossa approach. *Otol Neurotol.* (2012) 33:1386–91. doi: 10.1097/MAO.0b013e318268d20d
19. Silverstein H, Kartush J, Parnes L, Poe D, Babu S, Levenson M, et al. Round window reinforcement for superior semicircular canal dehiscence: a retrospective multi-center case series. *Am J Otolaryngol.* (2014) 35:286–93. doi: 10.1016/j.amjoto.2014.02.016
20. Succar E, Manickam P, Wing S, Walter J, Greene J, Azeredo W. Round window plugging in the treatment of superior semicircular canal dehiscence. *Laryngoscope.* (2018) 128:1445–52. doi: 10.1002/lary.26899
21. Suzuki M, Okamoto T, Ushio M, Ota Y. Two cases of tullio phenomenon in which oval and round window reinforcement surgery was effective. *Auris Nasus Larynx.* (2019) 46:636–40. doi: 10.1016/j.anl.2018.10.022
22. Songer J, Rosowski J. A mechano-acoustic model of the effect of superior canal dehiscence on hearing in chinchilla. *J Acousti Soc Am.* (2007) 122:943–51. doi: 10.1121/1.2747158
23. Stenfelt S. Acoustic and physiologic aspects of bone conduction hearing. *Adv Oto-Rhino-Laryngol.* (2011) 71:10–21. doi: 10.1159/000323574
24. Stenfelt S. Model predictions for bone conduction perception in the human. *Hear Res.* (2016) 340:135–43. doi: 10.1016/j.heares.2015.10.014
25. Stenfelt S, Goode RL. Transmission properties of bone conducted sound: measurements in cadaver heads. *J Acousti Soc Am.* (2005) 118:2373–91. doi: 10.1121/1.2005847
26. O'connor K, Puria S. Middle-ear circuit model parameters based on a population of human ears. *J Acousti Soc Am.* (2008) 123:197–211. doi: 10.1121/1.2817358
27. Hato N, Stenfelt S, Goode RL. Three-dimensional stapes footplate motion in human temporal bones. *Audiol Neuro-Otol.* (2003) 8:140–52. doi: 10.1159/000069475
28. Stenfelt S, Wild T, Hato N, Goode RL. Factors contributing to bone conduction: the outer ear. *J Acousti Soc Am.* (2003) 113:902–12. doi: 10.1121/1.1534606
29. Homma K, Du Y, Shimizu Y, Puria S. Ossicular resonance modes of the human middle ear for bone and air conduction. *J Acousti Soc Am.* (2009) 125:968–79. doi: 10.1121/1.3056564
30. Stenfelt S, Hato N, Goode R. Factors contributing to bone conduction: The middle ear. *J Acousti Soc Am.* (2002) 111:947–59. doi: 10.1121/1.1432977
31. Marquardt T, Hensel J. A simple electrical lumped-element model simulates intra-cochlear sound pressures and cochlear impedance below 2 kHz. *J Acousti Soc Am.* (2013) 134:3730–8. doi: 10.1121/1.4824154
32. Puria S. Measurements of human middle ear forward and reverse acoustics: Implications for otoacoustic emissions. *J Acousti Soc Am.* (2003) 113:2773–89. doi: 10.1121/1.1564018
33. Merchant S, Ravicz M, Rosowski J. Acoustic input impedance of the stapes and cochlea in human temporal bones. *Hear Res.* (1996) 97:30–45. doi: 10.1016/S0378-5955(96)80005-0
34. Kämpfe Nordström C, Laurell G, Rask-Andersen H. The human vestibular aqueduct: anatomical characteristics and enlargement criteria. *Otol Neurotol.* (2016) 37:1637–45. doi: 10.1097/MAO.0000000000001203
35. Ifediba M, Rajguru S, Hullar T, Rabbitt RD. The role of 3-canal biomechanics in angular motion transduction by the human vestibular labyrinth. *Annals of Biomedical Engineering.* (2007) 35:1247–63. doi: 10.1007/s10439-007-9277-y
36. Nakajima H, Dong W, Olson E, Merchant S, Ravicz M, Rosowski J. Differential intracochlear sound pressure measurements in normal human temporal bones. *J Assoc Res Otolaryngol.* (2009) 10:23–36. doi: 10.1007/s10162-008-0150-y
37. Stieger C, Guan X, Farahmand R, Page B, Merchant J, Abur D, et al. Intracochlear sound pressure measurements in normal human temporal bones during bone conduction stimulation. *J Assoc Res Otolaryngol.* (2018) 19:523–39. doi: 10.1007/s10162-018-00684-1
38. Mattingly J, Banakis Hartl R, Jenkins H, Tollin D, Cass S, Greene N. A comparison of intracochlear pressures during ipsilateral and contralateral stimulation with a bone conduction implant. *Ear Hear.* (2020) 41:312–22. doi: 10.1097/AUD.0000000000000758
39. Roosli C, Dobrev I, Sim J, Gerig R, Pfiffner F, Stenfelt S, et al. Intracranial pressure and promontory vibration with soft tissue stimulation in cadaveric human whole heads. *Otol Neurotol.* (2015) 37:e384–390. doi: 10.1097/MAO.0000000000001121
40. Rosowski J, Songer J, Nakajima H, Brinsko K, Merchant S. Clinical, experimental, and theoretical investigations of the effect of superior semicircular canal dehiscence on hearing mechanisms. *Otol Neurotol.* (2004) 25:323–32. doi: 10.1097/00129492-200405000-00021
41. Elliott S, Ni G, Verschuur C. Modelling the effect of round window stiffness on residual hearing after cochlear implantation. *Hear Res.* (2016) 341:155–67. doi: 10.1016/j.heares.2016.08.006
42. Bohnke F, Arnold W. Bone conduction in a three-dimensional model of the cochlea. *ORL: J Oto-Rhino-Laryngol Rel Special.* (2006) 68:393–6. doi: 10.1159/000095283
43. Kim N, Homma K, Puria S. Inertial bone conduction: Symmetric and anti-symmetric components. *J Assoc Res Otolaryngol.* (2011) 12:261–79. doi: 10.1007/s10162-011-0258-3
44. Taschke H, Hudde H. A finite element model of the human head for auditory bone conduction simulation. *ORL: J Oto-Rhino-Laryngol Rel Special.* (2006) 68:319–23. doi: 10.1159/000095273
45. Chang Y, Kim N, Stenfelt S. The development of a whole-head human finite-element model for simulation of the transmission of bone-conducted sound. *J Acousti Soc Am.* (2016) 140:1635–51. doi: 10.1121/1.4962443
46. Hunter J, O'connell B, Wang J, Chakravorti S, Makowiec K, Carlson M, et al. Correlation of superior canal dehiscence surface area with vestibular evoked myogenic potentials, audiometric thresholds, and dizziness handicap. *Otol Neurotol.* (2016) 37:1104–10. doi: 10.1097/MAO.0000000000001126
47. Chien W, Ravicz M, Rosowski J, Merchant S. Measurements of human middle- and inner-ear mechanics with dehiscence of the superior semicircular canal. *Otol Neurotol.* (2007) 28:250–7. doi: 10.1097/01.mao.0000244370.47320.9a
48. Williamson R, Vrabec J, Coker N, Sandlin M. Coronal computed tomography prevalence of superior semicircular canal dehiscence. *Otolaryngol Head Neck Surg.* (2003) 129:481–9. doi: 10.1016/S0194-5998(03)01391-3

49. Stenfelt S, Reinfeldt S. A model of the occlusion effect with bone-conducted stimulation. *Int J Audiol.* (2007) 46:595–608. doi: 10.1080/14992020701545880
50. Eichenauer A, Dillon H, Clinch B, Loi T. Effect of bone-conduction harmonic distortions on hearing thresholds. *J Acousti Soc Am.* (2014) 136:EL96–102. doi: 10.1121/1.4885771
51. Jervall L, Arlinger S. A compairson of 2-dB and 5-dB step size in pure-tone audiometry. *Scand Audiol.* (1986) 15:51–6. doi: 10.3109/01050398609045954
52. Merchant S, Nakajima H, Halpin C, Nadol JJ, Lee D, Innis W, et al. Clinical investigation and mechanism of air-bone gaps in large vestibular aqueduct syndrome. *Ann Otol Rhinol Laryngol.* (2007) 116:532–41. doi: 10.1177/000348940711600709
53. Carhart R. Effect of stapes fixation on bone conduction response. In: Otosclerosis, editor. *Schuknecht.* Boston, MA: Little, Brown and Company (1962). p. 175–97.
54. Linder T, Ma F, Huber A. Round window atresia and its effect on sound transmission. *Otol Neurotol.* (2003) 24:259–63. doi: 10.1097/00129492-200303000-00021

Conflict of Interest: The author declares that the research was conducted in the absence of any commercial or financial relationships that could be construed as a potential conflict of interest.

frontiers in Neurology

REVIEW
published: 15 September 2020
doi: 10.3389/fneur.2020.01046

Perilymphatic Fistula: A Review of Classification, Etiology, Diagnosis, and Treatment

Brooke Sarna[1†], *Mehdi Abouzari*[1†], *Catherine Merna*[1], *Shahrnaz Jamshidi*[1], *Tina Saber*[1] *and Hamid R. Djalilian*[1,2*]

[1] Department of Otolaryngology–Head and Neck Surgery, University of California, Irvine, CA, United States, [2] Department of Biomedical Engineering, University of California, Irvine, CA, United States

A perilymphatic fistula (PLF) is an abnormal communication between the perilymph-filled inner ear and the middle ear cavity, mastoid, or intracranial cavity. A PLF most commonly forms when the integrity of the oval or round window is compromised, and it may be trauma-induced or may occur with no known cause (idiopathic). Controversy regarding the diagnosis of idiopathic PLF has persisted for decades, and the presenting symptoms may be vague. However, potential exists for this condition to be one of the few etiologies of dizziness, tinnitus, and hearing loss that can be treated surgically. The aim of this review is to provide an update on classification, diagnosis, and treatment of PLF. Particular attention will be paid to idiopathic PLF and conditions that may have a similar presentation, with subsequent information on how best to distinguish them. Novel diagnostic criteria for PLF and management strategy for PLF and PLF-like symptoms is presented.

Keywords: perilymphatic fistula, perilymph fistula, dizziness, vertigo, tinnitus, association, blood patch

OPEN ACCESS

Edited by:
P. Ashley Wackym, The State University of New Jersey, United States

Reviewed by:
Tetsuo Ikezono, Saitama Medical University, Japan
Gerard Joseph Gianoli, The Ear and Balance Institute, United States
Arun Gadre, Geisinger Medical Center, United States

***Correspondence:**
Hamid R. Djalilian
hdjalili@hs.uci.edu

[†] *These authors share first authorship*

Specialty section:
This article was submitted to Neuro-Otology, a section of the journal Frontiers in Neurology

Received: *27 April 2020*
Accepted: *10 August 2020*
Published: *15 September 2020*

Citation:
Sarna B, Abouzari M, Merna C, Jamshidi S, Saber T and Djalilian HR (2020) Perilymphatic Fistula: A Review of Classification, Etiology, Diagnosis, and Treatment. Front. Neurol. 11:1046. doi: 10.3389/fneur.2020.01046

INTRODUCTION

A perilymphatic fistula (PLF) is an abnormal communication between the perilymph-filled inner ear and outside the inner ear that can allow perilymph to leak from the cochlea or vestibule, most commonly through the round or oval window. PLF commonly causes cochlear and vestibular symptoms. Connections between vestibular symptoms and compromise of the structural integrity of the inner ear have been drawn as early as 1909 (1); however, vague symptoms, lack of a clear diagnostic test, and changes in the description and definition of a PLF have made even the existence of the condition a controversial subject for decades. In his work titled *Perilymph Fistula: Fifty Years of Controversy*, Hornibrook provides a detailed examination of the history of PLF and the sources of controversy surrounding the condition, including associated symptoms and terminology (2).

PLFs are ultimately a rare condition: it is estimated that PLFs has an incidence of 1.5/100,000 of adults, which is similar to that of vestibular schwannoma (3). In children, PLFs caused by congenital anomalies may be a more prominent cause of audiovestibular symptoms and have been thought to occur in up to 6% of children with idiopathic sensorineural hearing loss (4). Difficulties in defining and diagnosing PLFs has led to a dearth of more robust epidemiological information. Part of this problem has been that most methods used to identify PLFs lacked the sensitivity and specificity to provide consistent diagnoses (5). However, improvements in imaging techniques and emerging technology in the form of biomarkers have shown promise as tools to help define and diagnose PLF (6).

TABLE 1 | Categorization of perilymphatic fistula according to etiology based on a nationwide study by Matsuda et al. (23).

Category 1	Linked to trauma, middle and inner ear diseases, middle and/or inner ear surgeries
Category 2	Linked to barotrauma caused by antecedent events of external origin (such as flying or diving)
Category 3	Linked to barotrauma caused by antecedent events of internal origin (such as straining, sneezing, or coughing)
Category 4	Has no apparent antecedent event

Despite their rarity, PLFs hold importance as one of the few potential causes of hearing loss and vestibular disturbance that can be treated surgically. In this review, we will present a compilation of current information on etiology and diagnosis of PLF as well as an update on new and developing treatment techniques.

ETIOLOGY

PLFs can broadly be divided into two categories: those with an identifiable cause and those without. At first, PLFs were observed in post-stapedectomy patients where perilymph would leak around a prosthesis placed into the oval window due to a failure of the seal around or under the prosthesis (7–9). Though techniques for stapes surgery have advanced, PLFs still occur as a complication in ∼1% of stapedotomy procedures (10) and may be present in up to one-third of individuals requiring revision stapedectomies (11).

Shortly after the identification of surgery as a cause of PLFs, Fee observed that PLFs may be present even with no history of prior otologic procedure and attributed their cause to head trauma (12). Potential causes include barotrauma, temporal bone fractures, and penetrating trauma (13–15). In the 1970s, Goodhill discerned implosive (originating from Valsalva force-induced increased pressure in the middle ear) from explosive forces [originating from increased cerebrospinal fluid (CSF) pressure] as causes of inner ear injury (16). In a study by Hidaka et al. that reviewed 51 causes of traumatic PLF in Japan, an estimated 40% were due to blunt head trauma, 35% due to penetrating injury, 5.8% due to barotrauma, and the remainder were iatrogenic (17). Interestingly, these numbers may vary by country, as the use of ear picks and Q-tips is generally higher in Japan (18).

There remained, however, cases in which individuals were found to have PLF symptoms with no history of either surgery or trauma. The exact amount of these "spontaneous" or "idiopathic" cases of PLF varies, but the number may be significant, ranging from 24 to 51% (19–21). Although these cases of PLF were historically called "spontaneous," it is more accurate to refer to them as "idiopathic," as the word "spontaneous" can have small but important differences in its definition that can affect how PLFs are classified (22). Occasionally these cases were still preceded by a specific event, such as sneezing, straining, nose blowing, laughing, or even bending over, prompting controversy over what constitutes an idiopathic PLF (22). Currently, there are no universally accepted formal diagnostic criteria for the diagnosis of PLF; however, in an effort to combat inexactness in the use of "spontaneous" PLF, researchers in Japan have created a modern classification system that divides PLF by cause into four groups (**Table 1**), similar to systems used in the past (16, 24). In this system, PLFs with antecedent events fall into categories 1, 2, and 3, while PLFs with no identifiable antecedent event fall into category 4 and are labeled idiopathic. Using this system, about 38.6% of cases in the study fell into category 4 (23). In contrast to Goodhill's classification (implosive vs. explosive) (16), the classification in **Table 1** is simple and easy-to-use in clinical practice. In some cases of sudden deafness/dizziness following nose blowing, the route of inner ear injury cannot be discerned. In this scenario, nose blowing may increase either middle ear pressure via Eustachian tube (implosive) or intracranial pressure by straining (explosive); however, these types of mistakes cannot be made using the classification in **Table 1**.

The question of what may be provoking idiopathic PLF formation remains. In some cases, congenital malformations and microfissure formation may be a contributing factor (25). Microfissures can develop in multiple areas in the temporal bone, but those that develop between the round window niche and the posterior canal ampulla and around the oval window are theorized as an etiology for PLFs (26–29). Microfissures can be a normal finding (29); however, defective remodeling or anatomical variation in fissure location may distinguish fissures that contribute to PLF and those that are asymptomatic. In a similar manner, perilymph can leak through the fissula ante fenestrum as well. In normal development, the fissula ante fenestrum is a bony cleft present in all individuals that remodels and fills with cartilage and mesenchymal tissue. If this remodeling is altered, it may result in a patent cleft through which perilymph can leak (30). Elevations in intracranial pressure can also increase perilymphatic fluid pressure and cause or exacerbate fistulas (31). In many cases, patients may simply not recall a specific event preceding their symptoms. A more detailed discussion of potential factors is included at the end of this review.

DIAGNOSIS

Diagnosing PLFs has been a difficult task ever since their discovery over a century ago. Generally, they cause acute onset of audiological symptoms, vestibular symptoms, or both. This can include unilateral sudden hearing loss, tinnitus, vertigo, aural fullness, and disequilibrium (19–21). Commonly, patients present with both audiologic and vestibular symptoms, though they can be variable, and aural fullness in particular may be sensitive for PLF (6). There may be a history of head trauma, penetrating ear trauma, barotrauma, or prior otologic surgery. The audiovestibular symptoms can be similar in presentation to conditions such as superior or posterior canal dehiscence, vestibular migraine, endolymphatic hydrops, Meniere's disease, eustachian tube dysfunction, mal de debarquement, and persistent postural-perceptual dizziness, all of which similarly lack precise diagnostic tools. An expanded discussion of third window syndromes and how to distinguish them from PLF is included below. Clinicians should maintain high suspicion

TABLE 2 | Proposed diagnostic criteria for perilymphatic fistula (PLF).

Definite PLF

Fluctuating or non-fluctuating hearing loss, tinnitus, aural fullness, and/or vestibular symptoms immediately preceded by one of the following events #1-3, which fulfills Criteria A or B:

1. Barotrauma caused by external events (e.g., slap/suction to the ear, head trauma, blast, skydiving, underwater diving, or flying, etc.)
2. Barotrauma caused by internal events (e.g., nose-blowing, sneezing, straining, or heavy lifting, etc.)
3. Direct trauma to the inner ear (e.g., Q-tip injury, stapedotomy operation, temporal bone fracture, etc.)

A. Laboratory testing for a perilymph biomarker with high sensitivity and specificity.

B. Observation of perilymph leakage in the middle ear and resolution of symptoms after treatment with intratympanic blood patch or surgical plugging of leak.

Possible PLF

Fluctuating or non-fluctuating hearing loss, tinnitus, aural fullness, and/or vestibular symptoms without antecedent event such as #1-3 above, with third window abnormalities and lack of response to migraine lifestyle, dietary, and prophylaxis therapy, and with resolution of symptoms after treatment with intratympanic blood patch or surgical plugging of leak.

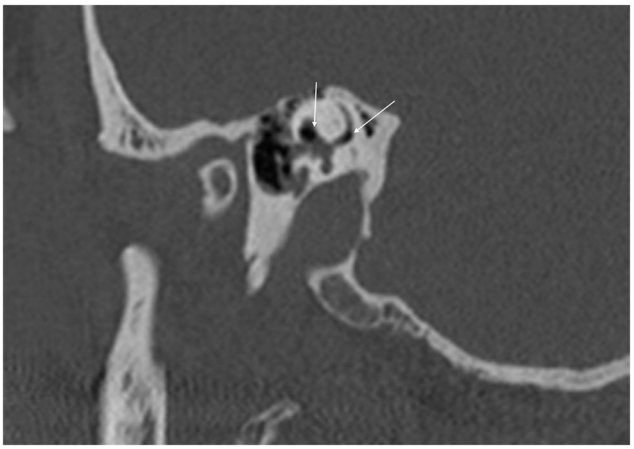

FIGURE 1 | Sagittal CT of temporal bone demonstrating air in the vestibule and the crus communs (arrows) in a patient with perilymph fistula.

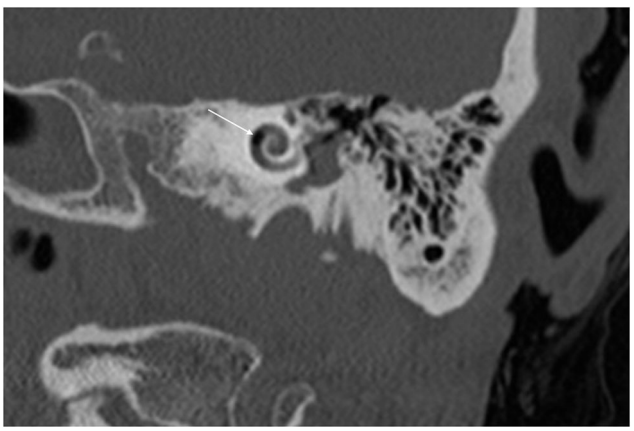

FIGURE 2 | Coronal CT of temporal bone showing air in the second cochlear turn (arrow).

for a PLF when individuals with non-specific audiovestibular symptoms do not respond to conventional medical treatments or vestibular rehabilitation and when there is a history of onset after trauma or an inciting event (32). We have proposed a set of diagnostic criteria for aid in the identification of definite and probable PLF (**Table 2**).

For decades, the gold standard for diagnosis of a PLF has been intra-operative visualization of perilymph leakage with subsequent improvement in symptoms after the leak has been repaired. However, this test is arguably subjective as no established criteria exist for what constitutes a perilymphatic leak on observation (33). The total amount of perilymph in one inner ear is only slightly larger than three drops of water (∼150 μl) (2, 32), prompting questions as to whether liquid observed in the middle ear could represent perilymph, CSF, or even local anesthetic and transudates (34). In our intraoperative observation, because the stapes footplate is placed in a dependent position in the middle ear during surgery, a small amount of transudate from the middle ear mucosa can accumulate in the footplate and create the appearance of a PLF when one does not exist. This transudate can increase as a result of manipulation of the middle ear mucosa or from the heat of a microscope, laser, or endoscope.

With the improvement in the resolution of computed tomography (CT) and magnetic resonance imaging (MRI), the need for exploratory procedures to identify PLFs in traumatic or post-surgical cases has declined. One of the earliest described radiological signs of a PLF is pneumolabyrinth, or air in the cochlea, vestibule, and/or semicircular canals (35). Small bubbles of air can be hard to visualize on typical CT scans, so high resolution scans including coronal or sagittal views may be useful in suspected cases (**Figures 1**–**4**) (13). Fluid in the round and oval window is another reliable sign of a PLF. A study by Venkatasamy et al. (36) evaluated the CT and MRI findings of 17 individuals with surgically confirmed PLFs and found that oval window PLFs most commonly presented with pneumolabyrinth and disorientation of the stapedial footplate, while round window PLFs most commonly presented with effusion of the round window niche. Generally, they found that high resolution CT scanning of the temporal bone has a sensitivity for detection of PLFs of over 80% when compared to intra-operative visualization of leak, and a combination of CT and MRI was reported to diagnose almost 100% of cases. We have found the axial and coronal CISS (constructive interference in steady state) (also called FIESTA (fast imaging employing steady-state acquisition) or MPR (magnetic resonance perfusion) sequence to be the most useful sequences (**Figures 5**–**7**). MRI may be particularly useful for identifying congenital abnormalities that may contribute to PLF formation and reduces the need for CT imaging in children. False negative cases may be due to scarring or intermittent or slow leakage of fluid, whereas false positive cases may be due to normal hypodensities seen in the cochlea (**Figure 8**),

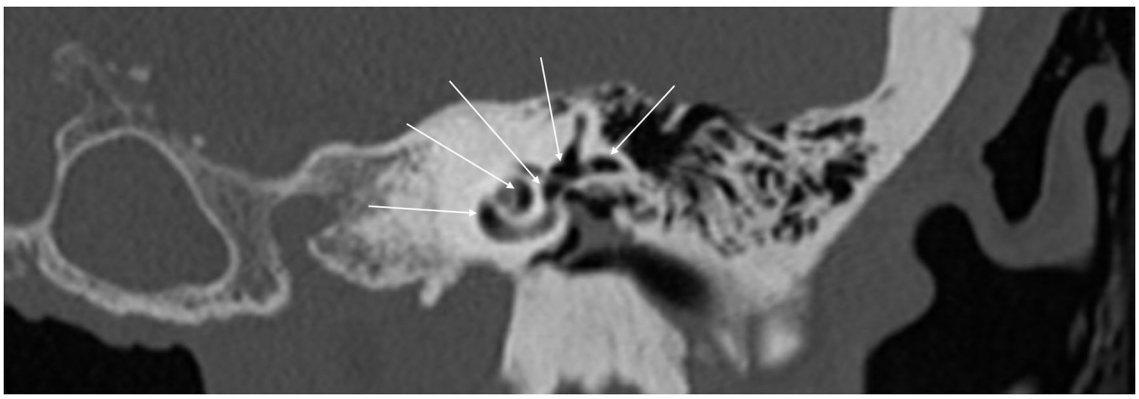

FIGURE 3 | Coronal CT of temporal bone showing extensive air in the cochlea, superior canal, horizontal canal, and vestibule (arrows).

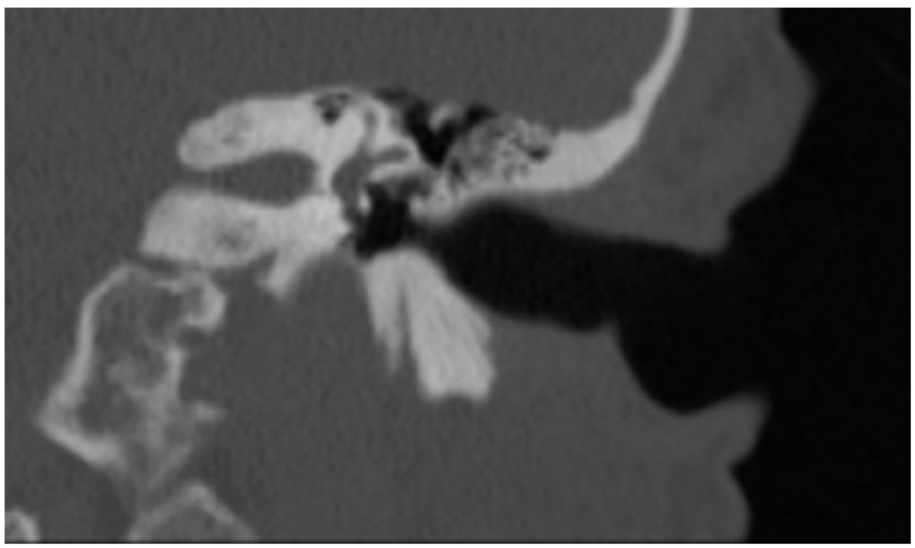

FIGURE 4 | Coronal CT of temporal bone of the same patient in **Figure 3** after perilymph fistula repair procedure. No air is seen in the inner ear.

motion artifacts, or inflammation (36). Clinicians should be mindful of the context of sensitivity and specificity data for diagnosis of PLFs, as it is generally compared using visualization of leaks as a gold standard, which can be unreliable. Additionally, PLF can be intermittent in nature, increasing the amount of false negative cases. Imaging will generally be useful in acute post-traumatic or post-operative patients with larger leaks. In addition, CT is necessary in ruling out other causes of third window syndrome such as superior or posterior canal dehiscence, enlarged vestibular or cochlear aqueduct, and carotid or facial nerve-cochlea fistula, all of which can present similar to idiopathic PLF.

A variety of other testing methods have been used to help diagnose PLFs, including audiometry, cervical vestibular evoked myogenic potential (cVEMP), electrocochleography, and the fistula test, as part of videonystagmography. These methods have varying sensitivity for the diagnosis of PLF but generally may be helpful in localizing the affected side or in distinguishing nystagmus invoked by noise or pressure changes (6). The fistula sign is a clinical finding that has traditionally been used; a positive fistula sign is defined as nystagmus when negative pressure is applied to the external auditory canal. However, its sensitivity may vary from as little as 0% to as high as 77% (19, 32). The platform pressure test (PPT) is yet another specific tool lacks sensitivity that can be used to help diagnose PLFs (37).

New technologies are being continuously explored and developed that may shed light on precise diagnosis of PLFs. Virtual endoscopy is a method that recreates an intraoperative, endoscopic environment using three dimensional spiral CT scans. In a prospective study of 145 patients, Bozorg Grayeli et al. found that virtual endoscopy had a sensitivity and specificity of 75% for diagnosing PLFs when compared to intra-operative visualization or resolution of symptoms after surgery (38). It can be particularly useful for round window PLFs and for

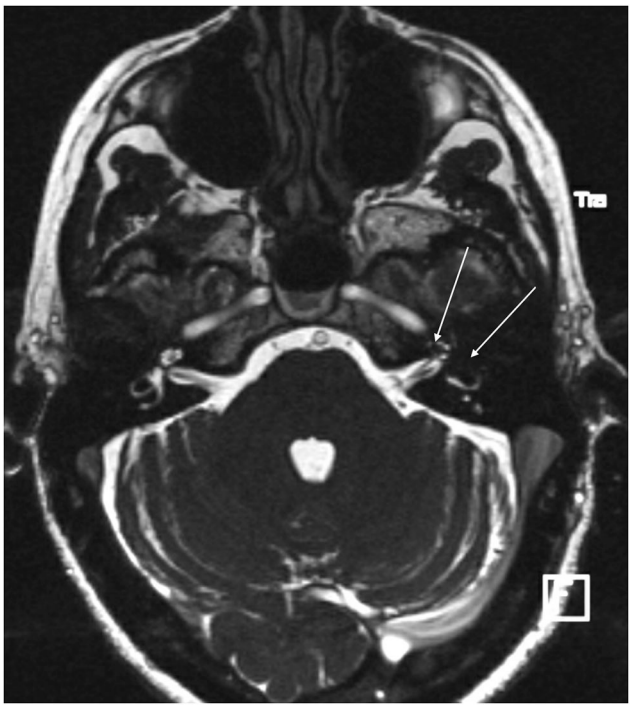

FIGURE 5 | CISS sequence MRI of a patient with PLF showing significant air in the vestibule and the anterior crus of the horizontal canal as well as the second turn of the cochlea (arrows).

FIGURE 6 | CISS sequence MRI of the same patient as **Figure 5** 1 day after blood patch procedure. There is a small amount of air in the distal basal turn of the cochlea (arrow).

small PLFs <0.5 mm in size that are not visible on typical CT scans (39).

The use of biomarkers for the detection of perilymph fluid is similarly under investigation. Beta-2 transferrin and cochlin tomoprotein (CTP) have been targets of research as a potential way to confirm the leakage of perilymph within the middle ear. This test shows great promise and is continuously available as an investigator-initiated trial throughout Japan since first introduced by Ikezono et al. in 2009 (40). Recently in June 2020, the Japan Ministry of Health, Labor, and Welfare approved the CPT ELISA test which has qualities for medical diagnosis (personal communication). However, it still lacks regulatory approval for clinical use worldwide and appears to only be available by SRL Inc., Tokyo, Japan. This has limited its availability and adoption clinically. Beta-2 transferrin is a protein found in higher concentration in CSF, vitreous humor, and perilymph (41). Although some studies showed it may have been a promising marker to identify perilymph in the surgical environment (42, 43), other studies have raised concerns regarding ease of sample contamination with blood, blood plasma, CSF, and beta-1 transferrin (44). Unlike beta-2 transferrin, CTP is a protein found in perilymph but not in appreciable amounts in CSF (45). Western blot and ELISA testing of fluid and lavages from the middle ear for CTP shows promise as a reliable diagnostic tool for PLFs (23, 40, 46, 47). Currently, the test is limited by the presence of CTP in blood, which may represent a route for sample contamination; however, lavage techniques and centrifugation should dilute or remove any blood in the sample enough so as not to affect the final result of the CTP analysis (40).

TREATMENT

Treatment of PLFs essentially falls into two categories: conservative or surgical. The management strategy chosen often depends on the etiology of the PLF and severity of symptoms. Generally, PLF with a known cause is a surgical disease; however, conservative therapy may be considered if no identifiable etiology for the PLF symptoms is known (idiopathic PLF) (32). Conservative therapy generally entails avoiding anything that can increase inner ear or intracranial pressure and potential use of intra-tympanic steroids in acute decompensation (6, 48). It is our belief that PLFs with a known cause should generally be treated surgically to avoid further degradation of hearing. PLFs without a known cause can be treated conservatively or surgically if conservative management fails. There is evidence, particularly in animal models, that some PLFs can heal on their own given adequate removal of factors that provoke high intracranial/intracochlear pressure such as straining (24, 49, 50). The precise characteristics of the PLFs that heal spontaneously have not yet been elucidated. Despite this, research appears to show that the more severe the inciting trauma, the lower the chance of spontaneous healing (51). It is difficult to know what percentage of patients benefit from

conservative therapy alone as research in this area is lacking. We generally do not recommend conservative treatment in patients with known causes of the PLF, given the risk of progression to permanent hearing loss if surgical treatment is delayed (52, 53).

There is a spectrum of surgical treatment options ranging from in-office procedures to operations in a surgical theater, with the common goal of sealing the fistula. Typically, both the oval and round window are grafted using temporalis fascia or tragal perichondrium, regardless of which window contained the fistula. A variety of other materials have been used including fat grafts, areolar tissue, and Gelfoam (Pfizer, New York, NY) (19, 54). In patients operated on by other surgeons, we have seen significant conductive hearing loss when excessive fascia has been used around the oval window. We generally use Gelfoam around the oval window and fascia in the round window after creating a circumferential mucosal trauma with a needle or a defocused laser on low power, when we uncommonly have to perform surgery for these patients. We use fascia in the oval window only in cases of footplate fracture. In cases where an exploratory tympanotomy is used for diagnosis but no leak is visualized, historically up to 78% of clinicians reported that they would still graft the windows in consideration of an occult leak (55). Of note, this survey was conducted in 1990 and management strategies of current neurotologists may have changed.

FIGURE 7 | CISS sequence MRI of the same patient as **Figure 6** at the level of the vestibule demonstrating improvement in the intravestibular air (arrows) compared to **Figure 5**.

Several years ago, a woman who was 12 weeks pregnant presented to us with acute vertigo and loss of hearing after she suffered trauma when a Q-tip was left in her ear. Examination showed trauma to the posterior superior quadrant of the tympanic membrane and a high frequency sensorineural hearing loss. The patient's case presented a dilemma: surgical treatment could place the fetus at risk, whereas conservative, non-surgical treatment could place her hearing at risk. The patient was offered the option of a blood patch procedure to potentially control the PLF. Under topical anesthesia, 0.5 cc of blood was injected into the middle ear and the patient was placed in a position so as to keep the oval window at its most dependent position for 30 min. The patient was given a suction to remove her saliva to prevent swallowing for the duration of the 30 min. The next day, the patient's vertigo had resolved, and her hearing had returned to normal. We have previously published a small report on the use of the blood patch procedure (56), and since our experience with

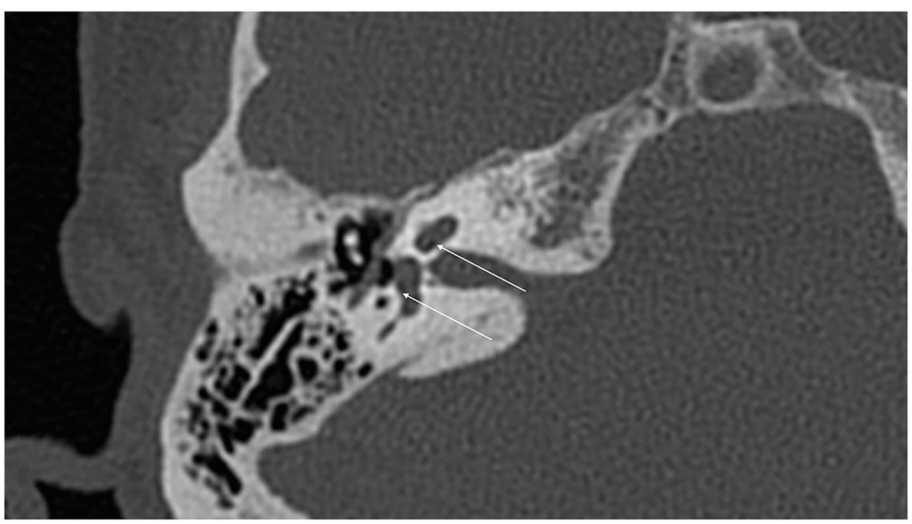

FIGURE 8 | False positive hypodensities (arrows) seen in the cochlea on routine CT of temporal bone.

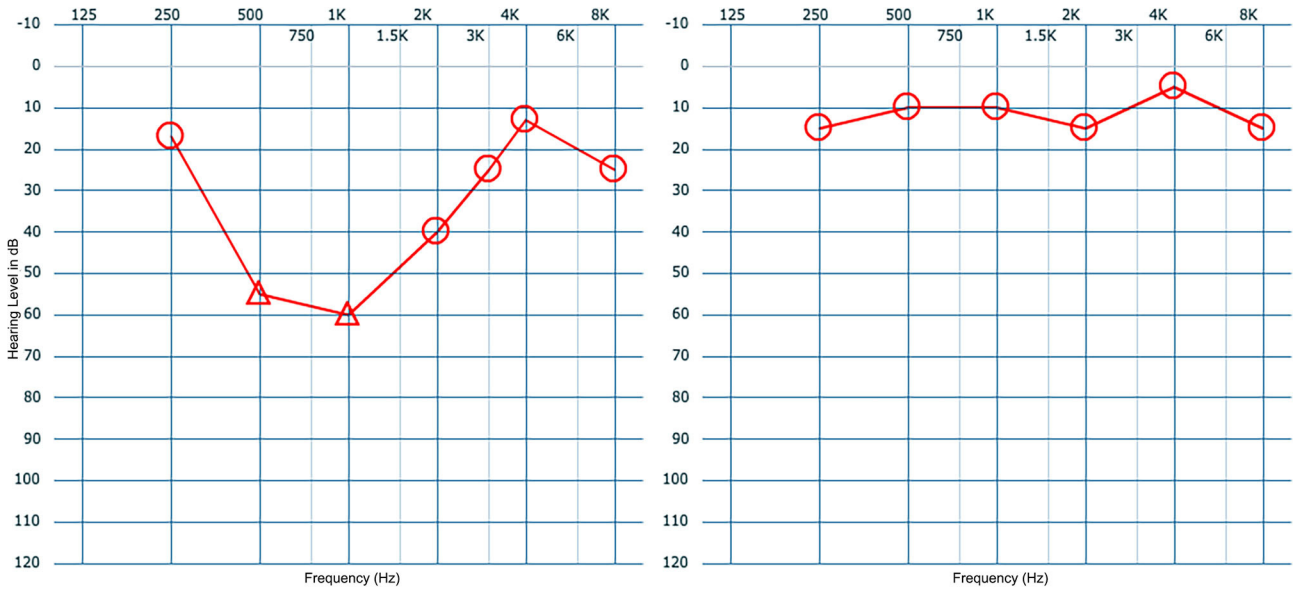

FIGURE 9 | Audiograms of a patient presenting with sudden hearing loss after blowing her nose (left panel) showing improvement of hearing 1 week after a blood patch procedure (right panel).

those patients, we initially perform a blood patch procedure on all patients with suspected PLF. We generally do not perform VEMP testing prior to or after the blood patch procedure. All patients with a post-traumatic PLF have had resolution of their symptoms. This blood patch procedure is also used to rule out PLF in patients, particularly idiopathic PLF where a history of trauma is not present. In our experience, a lack of response to the blood patch procedure is likely suggestive of a lack of a PLF in the first place; however, it is important to be mindful of the fact that PLFs can resolve on their own with time as well as with conservative therapy and that surgical therapy may sometimes result in a negative response even in patients with a true PLF. Surgical therapy is only undertaken if there is a temporary response to the blood patch procedure with relapse of symptoms. The blood patch procedure is performed twice prior to performing a surgical procedure. **Figure 9** demonstrate a typical improvement in hearing seen after a blood patch procedure. We theorize that initially blood covers the round and oval windows and seals them mechanically. After a few days, blood creates an inflammatory reaction that may facilitate granulation tissue formation and adhesion of adjacent tissues.

Surgery is generally effective at reducing or resolving patient symptoms, though vestibular symptoms tend to be improved more often than auditory symptoms. A range of 80–95% of patients experience improvement in vestibular symptoms, and a range of 20–49% experience improvement in hearing (19, 48, 57). The timing of surgery is a controversial subject—some authors recommend urgent corrective surgery within a few days of presentation (58), while others believe urgent surgery is not strictly necessary as improvements in hearing are small (48). Seltzer and McCabe reported that patients' hearing may benefit from surgery even after symptoms have been present for years (19), while other authors have found that prognosis may depend on timeliness of repair (53). The efficacy and timing of surgical repair depends on the particular etiology and location of the PLF. We generally recommend an in-office blood patch procedure upon presentation to the office or the emergency department.

DISCUSSION OF OTHER POTENTIAL CAUSES AND ASSOCIATIONS OF IDIOPATHIC PERILYMPHATIC FISTULA

With potentially more than a third of PLFs being idiopathic in nature (23), it is important for the clinician to differentiate true PLFs from conditions that mimic PLF. It is likely that many cases of idiopathic PLF represent third window syndromes (59). The most common of the third window syndromes is semicircular canal dehiscence (SCD). The majority of canal dehiscence is seen in the superior canal (SSCD) (60), followed by the less common posterior canal dehiscence (PCD) (61). Horizontal canal dehiscence can be caused by chronic otitis media, fracture, neoplasm, or cholesteatoma. An idiopathic dehiscence of the horizontal canal, although rare, has also been described previously in the literature (62, 63). In SCD, thinning of the bone of the semicircular canals causes hearing loss, vertigo, and in some cases increased transmittance of bodily sounds (autophony) (60). The presence of autophony and the provocation of vertigo symptoms by sound or pressure are two features that tend to support a diagnosis of third window syndrome over a PLF.

In SSCD, there is no breakage of the membranes containing perilymph or endolymph in the inner ear, so no true membrane fistula is formed. Rather, the bone of the canal overlying the membrane is thin or dehiscent, creating a "third window" and resulting in symptoms. It was thought that thinning of the

bone is likely congenital or developmental, as opposed to an acquired anomaly (64). However, newer evidence suggests that a higher body mass index (BMI) and obstructive sleep apnea (OSA) are more common in SSCD patients (65) This may be due to a higher intracranial pressure in patients with high BMI and OSA. Though the thin bone is present throughout life, symptoms do not appear until adulthood when trauma, erosion from the temporal lobe, and/or increased elasticity of the dura allows for pressure transference through the bone into the inner membranes (66). Only about 59% of patients with SSCD report a known inciting event (60)—the remaining 41% may present in a similar manner as an idiopathic PLF. SSCD can be distinguished from PLF by visualizing thinned bone over the superior canal on high resolution CT imaging using <0.7 mm slices, but it may be missed on conventional CT scans (67). Video head impulse testing may show decreased function of the affected canal (68). cVEMP testing will show lowered threshold values and increased amplitudes in both SSCD and PLF (69). Electrocochleography may also aid in diagnosis and will show an elevated summating potential (SP) to action potential (AP) ratio; however, this ratio will also be elevated in SSCD and Meniere's disease (70).

Other third window syndromes that can mimic canal dehiscence include carotid artery-cochlear dehiscence (CCD) and cochlea-facial nerve dehiscence (CFD). In CCD, there is thinning of the bone separating the carotid artery canal and the cochlea, most commonly between the basal turn of the cochlea and the petrous internal carotid artery (71). Though it can cause symptoms similar to both SCD and PLF, CCD usually presents with hearing loss and pulsatile tinnitus (72). MRI may not adequately visualize the internal carotid artery, so if suspicion for CCD is high, a high resolution CT scan should be obtained (73). Direct surgical repair of the fistula is not undertaken in these individuals due to proximity of the internal carotid artery (72).

CFD is a similar condition in which there is thinning of the bone between the cochlea and the labyrinthine segment of the facial nerve canal. It may also present with pulsatile tinnitus, fluctuations in or loss of hearing, and vertigo (74). CFD is rare—Fang et al. conducted a study on 1,020 temporal bone specimens and found complete dehiscence in only 0.59% (75). Of 401 temporal bones of patients presenting with a third window syndrome, Wackym et al. found 10.4% to have radiographically visible isolated CFD, with a further 7.8% having simultaneous

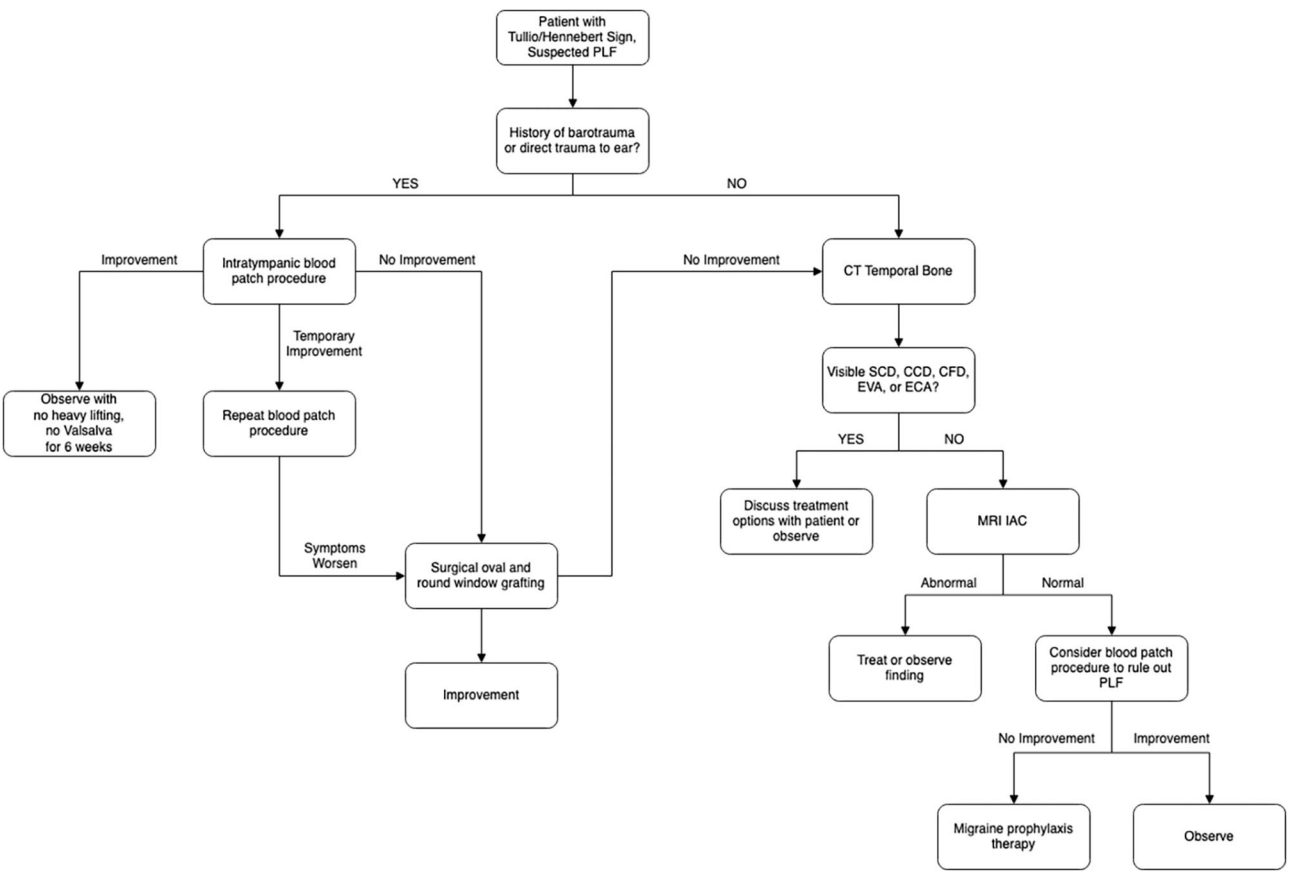

FIGURE 10 | Algorithm for management of suspected perilymphatic fistula (PLF) based on the discussion provided in this review and the authors' experience. Patients with Tullio or Hennebert sign are entered into the algorithm. If the patients have barotrauma or direct trauma, they would be directed to the left side of the algorithm. If they do not have barotrauma or direct trauma, they would be then worked up/treated according to the right side of the algorithm. CT, computed tomography; MRI IAC, magnetic resonance imaging of internal auditory canal; SCD, semicircular canal dehiscence; CCD, carotid artery-cochlear dehiscence; CFD, carotid-facial nerve dehiscence; EVA, enlargement of vestibular aqueduct; ECA, enlargement of cochlear aqueduct.

CFD and another dehiscence (76). Like CCD, CFD is visible on high resolution CT imaging, but not all individuals with visible CFD on imaging will have associated symptoms. Direct surgical treatment of the dehiscence carries a risk of deafness and facial nerve paralysis—round window reinforcement is an alternative procedure that is effective at reducing vertigo and headache symptoms with fewer risks to important nerves (76).

There are third window syndromes which do not involve bony dehiscence, namely enlargement of the vestibular aqueduct (EVA) and enlargement of the cochlear aqueduct (ECA). EVA occurs as a result of a congenital malformation and often presents as mixed hearing loss in childhood (77). The third window effect may be one of many mechanisms via which EVA causes hearing loss (78). The conductive component of the hearing loss in EVA is likely due to the third window. Both MRI and high-resolution CT are sufficient for evaluating EVA (79); however, specific criteria for abnormal aqueduct width range from >1 to >2 mm (80, 81). ECA is a potentially related condition (82) with a similar mechanism of hearing loss. Unlike EVA, ECA is a rare condition that is steeped in some controversy regarding its existence and contribution to symptoms (83). ECA can generally be defined as a diameter >1 mm in the otic capsule portion and can be evaluated with high resolution MRI and CT imaging.

Another similarly presenting group of conditions is Meniere's disease (MD) and migraine. MD is a syndrome defined by a constellation of episodic vertigo, fluctuating hearing loss, tinnitus, and aural fullness. Patients can experience symptoms anywhere for a few minutes to as long as a day (84). Generally, there is a return to baseline between episodes; however, patients may have permanent progressive hearing loss over time. The cause of MD is still unknown, but it has one defining pathological feature: endolymphatic hydrops (85, 86). MD and PLF have been found in close association (87, 88), and PLF-induced changes in perilymph flows may alter the fluid production and balance in the inner ear so as to result in endolymphatic hydrops in some cases (89). Therefore, endolymphatic hydrops may be seen in both MD and PLF, and many patients with a PLF may have an element of MD as well. On the other hand, endolymphatic hydrops by itself does not appear to be sufficient to cause the symptoms of MD (86), and instead a complex interplay of factors including migraine, vascular changes, and interruptions in homeostasis may play a role (90).

Like MD, migraine can present with fluctuating hearing loss, and both conditions can have pressure change induced symptoms (91). There may be significant overlap between the two conditions, with up to 68% of individuals with MD experiencing migraine headache as well (92). Tympanostomy tubes, which equalize the pressure differential between the external and middle ear, may be a potential treatment option for pressure sensitive MD and migraine (93–96). It may be worth exploring other factors such as MD and migraine in seemingly idiopathic PLF patients who do not see significant benefit from window-sealing surgical treatment. A management strategy based on the experience of the authors for suspected PLF is summarized in **Figure 10**.

CONCLUSION

Perilymphatic fistula is an enigmatic condition. Its diagnosis requires a thorough history to evaluate for a preceding event. For now, diagnosis and treatment choice continue to be based on an amalgam of clinical picture, vestibular, auditory, and imaging studies, and response to treatment, but advances in diagnostic criteria, high resolution imaging, and biomarker testing are paving the way for accurate pre-operative diagnosis in the near future. Similarly, surgical treatment techniques are progressing toward quick, in-office treatment for most cases. Though PLFs are rare, it is critical to remain vigilant of them as prompt treatment has the potential to save patients from debilitating vertigo and permanent hearing loss.

AUTHOR CONTRIBUTIONS

BS, MA, and HD contributed the conception and design of the study. BS, MA, CM, SJ, and TS performed review of the literature and collecting relevant information. BS, MA, and HD wrote the first draft of the manuscript. All authors contributed to the manuscript revision, read, and approved the submitted version.

FUNDING

MA was supported by the National Center for Research Resources and the National Center for Advancing Translational Sciences, National Institutes of Health, through Grant TL1TR001415. The content is solely the responsibility of the authors and does not necessarily represent the official views of the NIH.

REFERENCES

1. E. R. Fistel im ovalen Fenester. Monatsschr Ohrenh. (1909) 10:787.
2. Hornibrook J. Perilymph fistula: fifty years of controversy. *ISRN Otolaryngol.* (2012) 2012:281248. doi: 10.5402/2012/281248
3. Fiedler T, Boeger D, Buentzel J, Esser D, Hoffmann K, Jecker P, et al. Middle ear surgery in thuringia, Germany: a population-based regional study on epidemiology and outcome. *Otol Neurotol.* (2013) 34:890–7. doi: 10.1097/MAO.0b013e318280dc55
4. Reilly JS. Congenital perilymphatic fistula: a prospective study in infants and children. *Laryngoscope.* (1989) 99:393–7. doi: 10.1288/00005537-198904000-00006
5. Friedland DR, Wackym PA. A critical appraisal of spontaneous perilymphatic fistulas of the inner ear. *Am J Otol.* (1999) 20:261–76.
6. Deveze A, Matsuda H, Elziere M, Ikezono T. Diagnosis and treatment of perilymphatic fistula. *Adv Otorhinolaryngol.* (2018) 81:133–45. doi: 10.1159/000485579
7. Farrior JB. Abstruce complications of stapes surgery: diagnosis and treatment. In: *Henry Ford Hospital International Symposium on Otoslcerosis.* Chicago, IL: Little Brown Company (1962). p. 509–21.
8. Steffen TN, House HP, Sheehy JL. The slipped strut problem. A review of 52 cases. *Ann Otol Rhinol Laryngol.* (1963) 72:191–205. doi: 10.1177/000348946307200116
9. Shea JJ. Stapedectomy - long-term report. *Ann Otol Rhinol Laryngol.* (1982) 91:516–20. doi: 10.1177/000348948209100510
10. Hall AC, Mandavia R, Selvadurai D. Total endoscopic stapes surgery: systematic review and pooled analysis of audiological outcomes. *Laryngoscope.* (2019) 130:1282–6. doi: 10.1002/lary.28294

11. Betsch C, Ayache D, Decat M, Elbaz P, Gersdorff M. [Revision stapedectomy for otosclerosis: report of 73 cases]. *J Otolaryngol.* (2003) 32:38–47. doi: 10.2310/7070.2003.35383
12. Fee GA. Traumatic perilymphatic fistulas. *Arch Otolaryngol.* (1968) 88:477–80. doi: 10.1001/archotol.1968.00770010479005
13. Kita AE, Kim I, Ishiyama G, Ishiyama A. Perilymphatic fistula after penetrating ear trauma. *Clin Pract Cases Emerg Med.* (2019) 3:115–8. doi: 10.5811/cpcem.2019.1.37404
14. Prisman E, Ramsden JD, Blaser S, Papsin B. Traumatic perilymphatic fistula with pneumolabyrinth: diagnosis and management. *Laryngoscope.* (2011) 121:856–9. doi: 10.1002/lary.21439
15. Pullen FW 2nd. Perilymphatic fistula induced by barotrauma. *Am J Otol.* (1992) 13:270–2.
16. Goodhill V. Labyrinthine membrane ruptures in sudden sensorineural hearing loss. *Proc R Soc Med.* (1976) 69:565–72. doi: 10.1177/003591577606900815
17. Hidaka H, Miyazaki M, Kawase T, Kobayashi T. Traumatic pneumolabyrinth: air location and hearing outcome. *Otol Neurotol.* (2012) 33:123–31. doi: 10.1097/MAO.0b013e318241bc91
18. Hakuba N, Iwanaga M, Tanaka S, Hiratsuka Y, Kumabe Y, Konishi M, et al. Ear-pick injury as a traumatic ossicular damage in Japan. *Eur Arch Otorhinolaryngol.* (2010) 267:1035–9. doi: 10.1007/s00405-009-1162-x
19. Seltzer S, McCabe BF. Perilymph fistula: the Iowa experience. *Laryngoscope.* (1986) 96:37–49. doi: 10.1288/00005537-198601000-00007
20. Shelton C, Simmons FB. Perilymph fistula: the stanford experience. *Ann Otol Rhinol Laryngol.* (1988) 97:105–8. doi: 10.1177/000348948809700201
21. Rizer FM, House JW. Perilymph fistulas: the house ear clinic experience. *Otolaryngol Head Neck Surg.* (1991) 104:239–43. doi: 10.1177/019459989110400213
22. Meyerhoff WL. Spontaneous perilymphatic fistula: myth or fact. *Am J Otol.* (1993) 14:478–81. doi: 10.1097/00129492-199309000-00012
23. Matsuda H, Sakamoto K, Matsumura T, Saito S, Shindo S, Fukushima K, et al. A nationwide multicenter study of the cochlin tomo-protein detection test: clinical characteristics of perilymphatic fistula cases. *Acta Otolaryngol.* (2017) 137:S53–S9. doi: 10.1080/00016489.2017.1300940
24. Althaus SR. Perilymph fistulas. *Laryngoscope.* (1981) 91:538–62. doi: 10.1288/00005537-198104000-00007
25. Weber PC, Perez BA, Bluestone CD. Congenital perilymphatic fistula and associated middle ear abnormalities. *Laryngoscope.* (1993) 103:160–4. doi: 10.1002/lary.5541030207
26. Kohut RI, Hinojosa R, Budetti JA. Perilymphatic fistula: a histopathologic study. *Ann Otol Rhinol Laryngol.* (1986) 95:466–71. doi: 10.1177/000348948609500506
27. Kohut RI, Hinojosa R, Thompson JN, Ryu JH. Idiopathic perilymphatic fistulas. A temporal bone histopathologic study with clinical, surgical, and histopathologic correlations. *Arch Otolaryngol Head Neck Surg.* (1995) 121:412–20. doi: 10.1001/archotol.1995.01890040036006
28. Fujita T, Kobayashi T, Saito K, Seo T, Ikezono T, Doi K. Vestibule-middle ear dehiscence tested with perilymph-specific protein cochlin-tomoprotein (CTP) detection test. *Front Neurol.* (2019) 10:47. doi: 10.3389/fneur.2019.00047
29. Okano Y, Myers EN, Dickson DR. Microfissure between the round window niche and posterior canal ampulla. *Ann Otol Rhinol Laryngol.* (1977) 86:49–57. doi: 10.1177/000348947708600108
30. Toth M, Roesch S, Grimm A, Plachtovics M, Hempel JM, Rasp G. The role of fissula ante fenestram in unilateral sudden hearing loss. *Laryngoscope.* (2016) 126:2823–6. doi: 10.1002/lary.25922
31. Lollis SS, Weider DJ, Phillips JM, Roberts DW. Ventriculoperitoneal shunt insertion for the treatment of refractory perilymphatic fistula. *J Neurosurg.* (2006) 105:1–5. doi: 10.3171/jns.2006.105.1.1
32. Maitland CG. Perilymphatic fistula. *Curr Neurol Neurosci Rep.* (2001) 1:486–91. doi: 10.1007/s11910-001-0111-x
33. Wall C 3rd, Rauch SD. Perilymph fistula pathophysiology. *Otolaryngol Head Neck Surg.* (1995) 112:145–53. doi: 10.1016/S0194-5998(95)70314-4
34. Gibson WP. Spontaneous perilymphatic fistula: electrophysiologic findings in animals and man. *Am J Otol.* (1993) 14:273–7.
35. Mafee MF, Valvassori GE, Kumar A, Yannias DA, Marcus RE. Pneumolabyrinth: a new radiologic sign for fracture of the stapes footplate. *Am J Otol.* (1984) 5:374–5.
36. Venkatasamy A, Al Ohraini Z, Karol A, Karch-Georges A, Riehm S, Rohmer D, et al. CT and MRI for the diagnosis of perilymphatic fistula: a study of 17 surgically confirmed patients. *Eur Arch Otorhinolaryngol.* (2020) 277:1045–51. doi: 10.1007/s00405-020-05820-3
37. Black FO, Lilly DJ, Peterka RJ, Shupert C, Hemenway WG, Pesznecker SC. The dynamic posturographic pressure test for the presumptive diagnosis of perilymph fistulas. *Neurol Clin.* (1990) 8:361–74. doi: 10.1016/S0733-8619(18)30361-X
38. Bozorg Grayeli A, Bensimon JL, Guyon M, Aho-Glele S, Toupet M. Detection of perilymphatic fistula in labyrinthine windows by virtual endoscopy and variation of reconstruction thresholds on CT scan. *Acta Otolaryngol.* (2020) 140:270–6. doi: 10.1080/00016489.2020.1715472
39. Bensimon JL, Grayeli AB, Toupet M, Ferrary E, Sterkers O. Detection of labyrinthine fistulas in human temporal bone by virtual endoscopy and density threshold variation on computed tomographic scan. *Arch Otolaryngol Head Neck Surg.* (2005) 131:681–5. doi: 10.1001/archotol.131.8.681
40. Ikezono T, Matsumura T, Matsuda H, Shikaze S, Saitoh S, Shindo S, et al. The diagnostic performance of a novel ELISA for human CTP (Cochlin-tomoprotein) to detect perilymph leakage. *PLoS ONE.* (2018) 13:e0191498. doi: 10.1371/journal.pone.0191498
41. Thalmann I, Kohut RI, Ryu J, Comegys TH, Senarita M, Thalmann R. Protein profile of human perilymph: in search of markers for the diagnosis of perilymph fistula and other inner ear disease. *Otolaryngol Head Neck Surg.* (1994) 111:273–80. doi: 10.1177/019459989411113P117
42. Weber PC, Kelly RH, Bluestone CD, Bassiouny M. Beta 2-transferrin confirms perilymphatic fistula in children. *Otolaryngol Head Neck Surg.* (1994) 110:381–6. doi: 10.1177/019459989411000405
43. Skedros DG, Cass SP, Hirsch BE, Kelly RH. Beta-2 transferrin assay in clinical management of cerebral spinal fluid and perilymphatic fluid leaks. *J Otolaryngol.* (1993) 22:341–4.
44. Levenson MJ, Desloge RB, Parisier SC. Beta-2 transferrin: limitations of use as a clinical marker for perilymph. *Laryngoscope.* (1996) 106:159–61. doi: 10.1097/00005537-199602000-00010
45. Ikezono T, Shindo S, Sekiguchi S, Hanprasertpong C, Li L, Pawankar R, et al. Cochlin-tomoprotein: a novel perilymph-specific protein and a potential marker for the diagnosis of perilymphatic fistula. *Audiol Neurootol.* (2009) 14:338–44. doi: 10.1159/000212113
46. Kataoka Y, Ikezono T, Fukushima K, Yuen K, Maeda Y, Sugaya A, et al. Cochlin-tomoprotein (CTP) detection test identified perilymph leakage preoperatively in revision stapes surgery. *Auris Nasus Larynx.* (2013) 40:422–4. doi: 10.1016/j.anl.2012.08.001
47. Ikezono T, Shindo S, Sekine K, Shiiba K, Matsuda H, Kusama K, et al. Cochlin-tomoprotein (CTP) detection test identifies traumatic perilymphatic fistula due to penetrating middle ear injury. *Acta Otolaryngol.* (2011) 131:937–44. doi: 10.3109/00016489.2011.575795
48. Goto F, Ogawa K, Kunihiro T, Kurashima K, Kobayashi H, Kanzaki J. Perilymph fistula—45 case analysis. *Auris Nasus Larynx.* (2001) 28:29–33. doi: 10.1016/S0385-8146(00)00089-4
49. Gulya AJ, Boling LS, Mastroianni MA. ECoG and perilymphatic fistulae: an experimental study in the guinea pig. *Otolaryngol Head Neck Surg.* (1990) 102:132–9. doi: 10.1177/019459989010200206
50. Reis HG, Marques RH, Moussalle SK. [Perilymphatic fistula: report of a case which resolved spontaneously in five days and literature review]. *Rev Neurol.* (2002) 34:838–40. doi: 10.33588/rn.3409.2001383
51. Emmett JR, Shea JJ. Traumatic perilymph fistula. *Laryngoscope.* (1980) 90:1513–20. doi: 10.1288/00005537-198009000-00014
52. Comacchio F, Mion M. Sneezing and perilymphatic fistula of the round window: case report and systematic review of the literature. *J Int Adv Otol.* (2018) 14:106–11. doi: 10.5152/iao.2018.4336
53. Komori M, Yamamoto Y, Yaguchi Y, Ikezono T, Kojima H. Cochlin-tomoprotein test and hearing outcomes in surgically treated true idiopathic perilymph fistula. *Acta Otolaryngol.* (2016) 136:901–4. doi: 10.3109/00016489.2016.1165861
54. Weider DJ, Johnson GD. Perilymphatic fistula: a new hampshire experience. *Am J Otol.* (1988) 9:184–96.
55. Hughes GB, Sismanis A, House JW. Is there consensus in perilymph fistula management? *Otolaryngol Head Neck Surg.* (1990) 102:111–7. doi: 10.1177/019459989010200203

56. Garg R, Djalilian HR. Intratympanic injection of autologous blood for traumatic perilymphatic fistulas. *Otolaryngol Head Neck Surg.* (2009) 141:294–5. doi: 10.1016/j.otohns.2009.05.024
57. Fitzgerald DC, Getson P, Brasseux CO. Perilymphatic fistula: a Washington, DC, experience. *Ann Otol Rhinol Laryngol.* (1997) 106:830–7. doi: 10.1177/000348949710601005
58. Park GY, Byun H, Moon IJ, Hong SH, Cho YS, Chung WH. Effects of early surgical exploration in suspected barotraumatic perilymph fistulas. *Clin Exp Otorhinolaryngol.* (2012) 5:74–80. doi: 10.3342/ceo.2012.5.2.74
59. Wackym PA, Wood SJ, Siker DA, Carter DM. Otic capsule dehiscence syndrome: superior semicircular canal dehiscence syndrome with no radiographically visible dehiscence. *Ear Nose Throat J.* (2015) 94:E8–E24. doi: 10.1177/014556131509400802
60. Minor LB, Solomon D, Zinreich JS, Zee DS. Sound- and/or pressure-induced vertigo due to bone dehiscence of the superior semicircular canal. *Arch Otolaryngol Head Neck Surg.* (1998) 124:249–58. doi: 10.1001/archotol.124.3.249
61. Mikulec AA, Poe DS. Operative management of a posterior semicircular canal dehiscence. *Laryngoscope.* (2006) 116:375–8. doi: 10.1097/01.mlg.0000200358.93385.5c
62. Bassim MK PK, Buchman CA. Lateral semicircular canal dehiscence. *Otol Neurotol.* (2007) 28:1155–6. doi: 10.1097/MAO0b013e31809ed965
63. Zhang LC SY, Dai CF. Another etiology for vertigo due to idiopathic lateral semicircular canal bony defect. *Auris Nasus Larynx.* (2011) 38:402–5. doi: 10.1016/j.anl.2010.11.003
64. Carey JP, Minor LB, Nager GT. Dehiscence or thinning of bone overlying the superior semicircular canal in a temporal bone survey. *Arch Otolaryngol Head Neck Surg.* (2000) 126:137–47. doi: 10.1001/archotol.126.2.137
65. Schutt CA, Neubauer P, Samy RN, Pensak ML, Kuhn JJ, Herschovitch M, et al. The correlation between obesity, obstructive sleep apnea, and superior semicircular canal dehiscence: a new explanation for an increasingly common problem. *Otol Neurotol.* (2015) 36:551–4. doi: 10.1097/MAO.0000000000000555
66. Chien WW, Carey JP, Minor LB. Canal dehiscence. *Curr Opin Neurol.* (2011) 24:25–31. doi: 10.1097/WCO.0b013e328341ef88
67. Belden CJ, Weg N, Minor LB, Zinreich SJ. CT evaluation of bone dehiscence of the superior semicircular canal as a cause of sound- and/or pressure-induced vertigo. *Radiology.* (2003) 226:337–43. doi: 10.1148/radiol.2262010897
68. Cremer PD, Minor LB, Carey JP, Della Santina CC. Eye movements in patients with superior canal dehiscence syndrome align with the abnormal canal. *Neurology.* (2000) 55:1833–41. doi: 10.1212/WNL.55.12.1833
69. Modugno GC, Magnani G, Brandolini C, Savastio G, Pirodda A. Could vestibular evoked myogenic potentials (VEMPs) also be useful in the diagnosis of perilymphatic fistula? *Eur Arch Otorhinolaryngol.* (2006) 263:552–5. doi: 10.1007/s00405-006-0008-z
70. Arts HA, Adams ME, Telian SA, El-Kashlan H, Kileny PR. Reversible electrocochleographic abnormalities in superior canal dehiscence. *Otol Neurotol.* (2009) 30:79–86. doi: 10.1097/MAO.0b013e31818d1b51
71. Young RJ, Shatzkes DR, Babb JS, Lalwani AK. The cochlear-carotid interval: anatomic variation and potential clinical implications. *AJNR Am J Neuroradiol.* (2006) 27:1486–90.
72. Lund AD, Palacios SD. Carotid artery-cochlear dehiscence: a review. *Laryngoscope.* (2011) 121:2658–60. doi: 10.1002/lary.22391
73. Rathe M, Govaere F, Forton GEJ. Unilateral pulsatile tinnitus associated with an internal carotid artery-eustachian tube dehiscence. *OTO Open.* (2018) 2:2473974X17753605. doi: 10.1177/2473974X17753605
74. Blake DM, Tomovic S, Vazquez A, Lee HJ, Jyung RW. Cochlear-facial dehiscence–a newly described entity. *Laryngoscope.* (2014) 124:283–9. doi: 10.1002/lary.24223
75. Fang CH, Chung SY, Blake DM, Vazquez A, Li C, Carey JP, et al. Prevalence of cochlear-facial dehiscence in a study of 1,020 temporal bone specimens. *Otol Neurotol.* (2016) 37:967–72. doi: 10.1097/MAO.0000000000001057
76. Wackym PA, Balaban CD, Zhang P, Siker DA, Hundal JS. Third window syndrome: surgical management of cochlea-facial nerve dehiscence. *Front Neurol.* (2019) 10:1281. doi: 10.3389/fneur.2019.01281
77. Steinbach S, Brockmeier SJ, Kiefer J. The large vestibular aqueduct–case report and review of the literature. *Acta Otolaryngol.* (2006) 126:788–95. doi: 10.1080/00016480500527276
78. Merchant SN, Rosowski JJ. Conductive hearing loss caused by third-window lesions of the inner ear. *Otol Neurotol.* (2008) 29:282–9. doi: 10.1097/MAO.0b013e318161ab24
79. Connor SEJ, Dudau C, Pai I, Gaganasiou M. Is CT or MRI the optimal imaging investigation for the diagnosis of large vestibular aqueduct syndrome and large endolymphatic sac anomaly? *Eur Arch Otorhinolaryngol.* (2019) 276:693–702. doi: 10.1007/s00405-019-05279-x
80. Vijayasekaran S, Halsted MJ, Boston M, Meinzen-Derr J, Bardo DM, Greinwald J, et al. When is the vestibular aqueduct enlarged? A statistical analysis of the normative distribution of vestibular aqueduct size. *AJNR Am J Neuroradiol.* (2007) 28:1133–8. doi: 10.3174/ajnr.A0495
81. Valvassori GE, Clemis JD. The large vestibular aqueduct syndrome. *Laryngoscope.* (1978) 88:723–8. doi: 10.1002/lary.1978.88.5.723
82. Kim BG, Sim NS, Kim SH, Kim UK, Kim S, Choi JY. Enlarged cochlear aqueducts: a potential route for CSF gushers in patients with enlarged vestibular aqueducts. *Otol Neurotol.* (2013) 34:1660–5. doi: 10.1097/MAO.0b013e3182a036e4
83. Stimmer H. Enlargement of the cochlear aqueduct: does it exist? *Eur Arch Otorhinolaryngol.* (2011) 268:1655–61. doi: 10.1007/s00405-011-1527-9
84. Lopez-Escamez JA, Carey J, Chung WH, Goebel JA, Magnusson M, Mandala M, et al. Diagnostic criteria for meniere's disease. *J Vestib Res.* (2015) 25:1–7. doi: 10.3233/VES-150549
85. Schuknecht HF, Gulya AJ. Endolymphatic hydrops. An overview and classification. *Ann Otol Rhinol Laryngol Suppl.* (1983) 106:1–20. doi: 10.1177/00034894830920S501
86. Rauch SD, Merchant SN, Thedinger BA. Meniere's syndrome and endolymphatic hydrops. Double-blind temporal bone study. *Ann Otol Rhinol Laryngol.* (1989) 98:873–83. doi: 10.1177/000348948909801108
87. Potter CR, Conner GH. Hydrops following perilymph fistula repair. *Laryngoscope.* (1983) 93:810–2. doi: 10.1288/00005537-198306000-00022
88. Fitzgerald DC. Perilymphatic fistula and meniere's disease. clinical series and literature review. *Ann Otol Rhinol Laryngol.* (2001) 110:430–6. doi: 10.1177/000348940111000507
89. House HP. The fistula problem in otosclerosis surgery. *Laryngoscope.* (1967) 77:1410–26. doi: 10.1288/00005537-196708000-00015
90. Sarna B, Abouzari M, Lin HW, Djalilian HR. A hypothetical proposal for association between migraine and meniere's disease. *Med Hypotheses.* (2020) 134:109430. doi: 10.1016/j.mehy.2019.109430
91. Hoffmann J, Lo H, Neeb L, Martus P, Reuter U. Weather sensitivity in migraineurs. *J Neurol.* (2011) 258:596–602. doi: 10.1007/s00415-010-5798-7
92. Ghavami Y, Mahboubi H, Yau AY, Maducdoc M, Djalilian HR. Migraine features in patients with meniere's disease. *Laryngoscope.* (2016) 126:163–8. doi: 10.1002/lary.25344
93. Ogawa Y, Otsuka K, Hagiwara A, Inagaki A, Shimizu S, Nagai N, et al. Clinical study of tympanostomy tube placement for patients with intractable meniere's disease. *J Laryngol Otol.* (2015) 129:120–5. doi: 10.1017/S0022215115000079
94. Sugawara K, Kitamura K, Ishida T, Sejima T. Insertion of tympanic ventilation tubes as a treating modality for patients with meniere's disease: a short- and long-term follow-up study in seven cases. *Auris Nasus Larynx.* (2003) 30:25–8. doi: 10.1016/S0385-8146(02)00105-0
95. Montandon P, Guillemin P, Hausler R. Prevention of vertigo in meniere's syndrome by means of transtympanic ventilation tubes. *ORL J Otorhinolaryngol Relat Spec.* (1988) 50:377–81. doi: 10.1159/000276016
96. Abouzari M, Parker E, Sarna B, Trent M, Goshtasbi K, Tan D, et al. Tympanostomy tube placement for pressure change-induced vertigo. In: *Poster Presented at: Triological Society. 2020 Combined Sections Meeting.* Coronado, CA (2020).

Conflict of Interest: The authors declare that the research was conducted in the absence of any commercial or financial relationships that could be construed as a potential conflict of interest.

frontiers in Neurology

ORIGINAL RESEARCH
published: 16 September 2020
doi: 10.3389/fneur.2020.00954

Audiovestibular Quantification in Rare Third Window Disorders in Children

Soumit Dasgupta[1], Sudhira Ratnayake[1], Rosa Crunkhorn[1], Javed Iqbal[1], Laura Strachan[1] and Shivaram Avula[2]*

[1] Department of Paediatric Audiology and Audiovestibular Medicine, Alder Hey Children's NHS Foundation Trust, Liverpool, United Kingdom, [2] Department of Paediatric Radiology, Alder Hey Children's NHS Foundation Trust, Liverpool, United Kingdom

Third window disorders are structural abnormalities in the bony otic capsule that establish a connection between the middle/inner ear or the inner ear/cranial cavity. Investigated extensively in adults, they have hardly been studied in children. This study is a retrospective study of children (aged 5–17 years) diagnosed with rare third window disorders (third window disorders reported rarely or not reported in children) in a tertiary pediatric vestibular unit in the United Kingdom. It aimed to investigate audiovestibular function in these children. Final diagnosis was achieved by high resolution CT scan of the temporal bones. Of 920 children attending for audiovestibular assessment over a 42 month period, rare third windows were observed in 8 (<1%). These included posterior semicircular canal dehiscence (n = 3, 0.3%), posterior semicircular canal thinning (n = 2, 0.2%), X linked gusher (n = 2, 0.2%), and a combination of dilated internal auditory meatus/irregular cochlear partition/deficient facial nerve canal (n = 1, 0.1%). The majority of them (87.5%) demonstrated a mixed/conductive hearing loss with an air-bone gap in the presence of normal tympanometry (100%). Transient otoacoustic emissions were absent with a simultaneous cochlear pathology in 50% of the cohort. Features of disequilibrium were observed in 75% and about a third showed deranged vestibular function tests. Video head impulse test abnormalities were detected in 50% localizing to the side of the lesion. Cervical vestibular evoked myogenic potential test abnormalities were observed in all children in the cohort undergoing the test where low thresholds and high amplitudes classically found in third window disorders localized to the side of the defects in 28.5%. In the series, 71.4% also demonstrated absent responses/amplitude asymmetry, some of which did not localize to the ipsilesional side. Two children presented with typical third window symptoms. This study observes 2 new rare pediatric third window phenotypes and the presence of a cochlear hearing loss in these disorders. It emphasizes that these disorders should be considered as an etiology of hearing loss/disequilibrium in children. It also suggests that pediatric third window disorders may not present with classical third window features and are variable in their presentations/audiovestibular functions.

Keywords: third window, semicircular canal dehiscence, X linked gusher, audiovestibular, children, HRCT, vHIT, cVEMP

OPEN ACCESS

Edited by:
P. Ashley Wackym, The State University of New Jersey, United States

Reviewed by:
Fazil Necdet Ardiç, Pamukkale University, Turkey
Armagan Incesulu, Eskişehir Osmangazi University, Turkey
Avi Shupak, University of Haifa, Israel

****Correspondence:***
Soumit Dasgupta
Soumit.dasgupta@alderhey.nhs.uk

Specialty section:
This article was submitted to Neuro-Otology, a section of the journal Frontiers in Neurology

Received: *24 June 2020*
Accepted: *23 July 2020*
Published: *16 September 2020*

Citation:
Dasgupta S, Ratnayake S, Crunkhorn R, Iqbal J, Strachan L and Avula S (2020) Audiovestibular Quantification in Rare Third Window Disorders in Children. Front. Neurol. 11:954. doi: 10.3389/fneur.2020.00954

INTRODUCTION

The human ear consists of 2 mobile normal windows for transmission of sound between the middle and the inner ear, namely the oval window and the round window. There are other windows called third windows that are present, and these windows connect the inner ear to the cranial cavity, for example, the cochlear aqueduct, the vestibular aqueduct, and the numerous bony channels that conduct the nerves and vessels entering or exiting the inner ear from/to the posterior cranial fossa (1). These normal third windows in normal physiological conditions are of high impedance, do not affect inner ear sound conduction, and do not influence the functional sound flow (2).

Pathological third windows, on the other hand, do interfere with transmission of the cochlear traveling wave generated at the oval window, as these windows do not offer high impedance to acoustic transmission. They shunt or deviate the acoustic energy from the middle ear, thereby leading to a drop in air conducted sound thresholds and improve the bone conduction thresholds as they provide an alternate low impedance path, bypassing the oval-round window classical low impedance pathway (1). Invariably, these third windows are due to defects in the bony otic capsule.

Regardless of the anatomical location of the pathological third window, i.e., whether it is a direct physical connection between the middle and the inner ear or between the inner ear and the cranial cavity, these disorders generate typical third window features that include conductive hearing loss, sound, or positive pressure induced dizziness (Tullio's or Hennebert's phenomenon), disequilibrium, autophony, and conductive dysacusis [magnified perception of sounds generated by the body, e.g., gaze evoked tinnitus (3)] in addition to occasional oscillopsia, phonophobia, pulsatile tinnitus, and high amplitude, low threshold vestibular evoked myogenic potentials (4). These are called third window effects; however, although observation of these symptoms constitute the diagnostic criteria, some of them may be absent, especially depending on the functional status of the audiovestibular system (5).

The first pathological third window identified was the dehiscence of the superior semicircular canal in 1998 (6). Since then, there has been plenty of research not only in this particular disorder but also in third windows in general in the adult population. A recent third window was identified by Blake et al. (7) as the cochlear-facial nerve dehiscence (CFD). Several pathological third window disorders have been identified (**Table 1**). The most studied third window disorder remains the superior semicircular canal dehiscence (SSCD).

Intuitively and logically, the etiology of third window disorders can be deemed developmental or traumatic (9–11) if we consider SSCD. The manifestation in SSCD may be late as the dimensions may increase with age, leading to frank symptoms if SSCD is acquired (12). Canal dehiscences may be a part of more extensive cochleovestibular dysplasias, e.g., with hypoplastic cochlear or vestibular system (13) or CDH23 mutations with Usher syndrome (14). Recently, a genetic SSCD has been proposed (15). However, it must be remembered that the prevalence of SSCD with cochleovestibular dysmorphology is the same as SSCD without any other inner ear structural abnormality. This raises the possibility that a third window structural abnormality may be a *de novo* or standalone abnormality (13).

TABLE 1 | Identified third window disorders [after Wackym et al. (3), Scarpa et al. (8)].

1. Superior, posterior, and lateral semicircular canal dehiscence
2. Cochlea-facial nerve dehiscence
3. Cochlea-internal carotid artery dehiscence
4. Cochlea-internal auditory canal dehiscence
5. X linked gusher syndrome
6. Perilymph fistula
7. Facial nerve canal dehiscence
8. Wide vestibular aqueduct in children
9. Posttraumatic hypermobile stapes footplate
10. Otosclerosis with internal auditory canal involvement
11. Bone dyscrasias for example Paget's disease of the bone and osteogenesis imperfecta
12. Endolymphatic hydrops

Structural and bony otic capsule abnormalities can be proposed to possess a similar etiology, although given their rarity, evidence is yet to emerge. The commonest third window disorder in children is the enlarged vestibular aqueduct (EVA) that can accompany a fully blown systemic genetic syndrome, e.g., the CHARGE (coloboma, heart defects, atresia choanae, growth retardation, genital abnormalities, and ear abnormalities) or the BOR (branchio-oto-renal) syndrome and in 20% cases may be a feature of Pendred syndrome (16). X linked gusher is an isolated otic capsule abnormality and is caused by a mutation in POU3F4 gene (17).

The objective confirmation of a third window abnormality is by demonstrating the third window effect by vestibular evoked myogenic potential (VEMP) parameters (lowering of threshold and increase in amplitude in the affected side) and by high resolution computerized tomographic scans (HRCT) of the temporal bones with optimal cuts and special views (9). VEMPS show typical third window characteristics. The lowering of impedance of the acoustic traveling wave and the third window shunted sound energy passing through the vestibular system makes it hyper reactive to the sound (18, 19), generating these typical features. Sensitivity, and specificity to diagnose a third window abnormality is high with VEMPS (20). HRCT is the gold standard of objective confirmation although it may still over diagnose the condition even when taken in slices of <0.625 mm and in the Stenver or Poschl views (9). Another observation proposed by Wackym et al. (21) is that there may be negative CT scans with typical symptoms which are responsive to surgery for third window disorders.

Only EVA as a third window disorder has been studied extensively in children as it is relatively common. In a large series comprising 221 children with mainly sensorineural hearing loss, 8.6% demonstrated an isolated EVA whilst 3.16% showed an EVA that was associated with other inner ear anomalies (22). Gopen et al. (16) in a review article observed that 20–100% of children with EVA may present with a vestibular symptom, and they invariably present with hearing losses.

Other third window disorders are rare in children including canal dehiscences (13). There are limited studies investigating SSCD in children. Dasgupta and Ratnayake (5) pointed out that SSCD in children might not present with classical third window features as they may not be able to describe these symptoms or because the defects might not have attained the dimensions to cause an overt third window symptom. Other researchers have reached similar conslusions (23, 24). In other words, SSCD in children might not generate the classical SSCD syndrome found in adults that by definition is a constellation of clinical symptoms and audiovestibular tests. SSCD has been reported in the case series by Chen et al. (25) who also reported posterior semicircular dehiscences (PSCD) in a cohort of 113 presenting with hearing loss with a 15% prevalence and by Lee et al. (23) who observed that hearing loss and disequilibrium were the commonest presenting features. Meicklejohn et al. (26) in live and cadaveric temporal bone dissections detected that prevalence of radiologic semicircular canal dehiscences declined with increasing age, reinforcing the idea that otic capsule thickens with age. He also observed normal, mixed, and sensorineural hearing losses in his cohort. A 6.2% incidence of SSCD was found in a large multicentre review by Sugihara et al. (27). Near dehiscences or where the semicircular bone is thinned but not frankly dehiscent can generate third window features and respond to third window surgery (28). They are rare and have not been investigated in detail.

There have been isolated case reports and series reports regarding X linked gushers (29). CFD has been reported only in 7 children (3, 30) and after an extensive search of literature, these authors were unable to find any child being reported with any other rare third window disorders, e.g., the carotid artery-cochlear dehiscence (CACD) that is very rare in adults as well (31).

The present study is a retrospective study investigating these rare third window disorders in children. This study reports subjective and objective audiovestibular quantification in a group of children with different but hardly reported or not reported third window structural disorders. This is the first time that we are reporting objective vestibular quantification in some groups of these children from a tertiary pediatric balance unit in the United Kingdom.

PATIENTS AND METHODS

Patients

Children attending the tertiary audiovestibular medicine outpatients in Alder Hey Children's Hospital between February 2016 and July 2019 were studied by a retrospective case note analysis. The research was conducted according to the rules and regulations of the Helsinki declaration relating to research involving live human subjects. The Health Research Authority of England (HRA) and Health and Care Research Wales (HCRW) approved the research (approval number 20/HRA/1289). The HRA also granted a consent waiver. Children with isolated findings of rare third windows were included. We defined these as rare third window disorders as they are the least reported or not reported at all and thus they did not include EVA or SSCD. Children who were diagnosed with a systemic genetic syndrome with third window structural abnormalities and cochleovestibular dysplasias of varying nature were also excluded. The age range for the study was fixed between 5 and 17 years as bony structural abnormalities like SSCD could be a part of normal development up to the age of 5 years (10, 13, 24).

TABLE 2 | Symptoms of pediatric vestibular disease [table adapted from (5)]; children with specific symptoms in the series in brackets and italics.

- Obvious dizziness/vertigo/lightheadedness (usually describable by children above 8 years of age)
- Fright or pallor
- Clutching at objects to steady oneself
- Bumping into things, falling and tripping [*case 1*]
- Clumsiness
- Sudden very brief lasting falls with immediate complete recovery
- Periodic episodes of nausea or vomiting ± migrainous features
- Delayed motor functions
- Loss of postural control or unsteadiness [*cases 2,3,6*]
- Difficulty with ambulating in the dark [*case 2*]
- Difficulty with or avoidance to ride a bike or in amusement park rides due to imbalance [*cases 2 and 4*]
- Abnormal movements during walking, running [*case 7*]
- Abnormal behavior observed up by significant others (care giver, school or peer group)
- Difficulties in challenging movements (swimming, dancing)
- Oscillopsia
- Difficulties in challenging visual environments for example in superstores and in crowded places [*cases 2 and 3*]
- Poor head eye or hand eye coordination
- Motion intolerance or cyclical vomiting [*case 2*]
- Third window symptoms if described by older children—conductive dysacusis (for example, hearing one's own footsteps), gaze evoked tinnitus (audible eye movements [*case 3*]), autophony (altered perception or perverted self-monitoring of own voice [*case 3*]), Tullio's phenomenon (dizziness on hearing loud sounds), Hennebert's phenomenon (pressure induced dizziness for example on coughing and sneezing), pulsatile tinnitus (tinnitus that is synchronous with pulse beat [*cases 3 and 5*])

Methods

Anamnesis

History from patients with third window disorders is crucial to establish a diagnosis. There are characteristic symptoms of the third window effect. However, in children, these may be difficult to elicit and, indeed, obtaining this history is an art in itself driven by several behavioral factors in the child (32). Thus, eliciting this history is often surrogate and dependant on carers or parents who usually are quite reliable and astute to observe hearing and vestibular behavior in the children. A lack of school performance and academia or behavioral reactions to communication was deemed as key indicators of a hearing loss. Sudden falls and trips, lack of spatial awareness, bumping into objects, or inability to ride a bike were taken as indicators of disequilibrium. Wherever possible, children were asked about specific third window symptoms as older children were in a position to narrate these symptoms themselves. A full set of symptoms is shown in **Table 2**.

Audiovestibular Quantification

All children and carers provided full verbal informed consent for clinical examination. The examination was performed by the first three authors, all of whom are experienced clinicians. Complete pediatric examination is an essential part of the holistic assessment of the child, and indeed problems with communication or with balance may result from non-audiovestibular conditions, and the possibilities are vast. A full neurological, oculomotor, and musculoskeletal examination were performed in every child, especially as disequilibrium may be a presenting feature of a neurological, ocular, or musculoskeletal disorder.

Audiological tests performed in every child included behavioral pure tone audiometry and live voice speech tests as well as objective audiometry with tympanometry, acoustic reflexes (ART), and transient otoacoustic emissions. Otoscopy was performed before audiological testing. Pure tone audiometry entailed measurement of air and bone conduction thresholds with masking wherever indicated with the sound delivered through TDH 39 headphones. Up to 20 dBHL thresholds were considered as normal, and a negative bone conduction was indicated by a threshold of below 0 dBHL. Pure tone thresholds were measured from 500 Hz to 4 kHz and were averaged for the study. Transient otoacoustic emissions (TEOAE) were measured by Otodynamics equipment with a stimulus intensity of 80–88 dBSPL.

A full neurovestibular examination was performed first with vision. This included measurement of the subjective visual vertical (measurement of head tilt with respect to the vertical to assess static gravitational sensor function) and any nystagmus with optic fixation (for central function). Videonystagmography (VNG) using the ICS system with and without optic fixation was used to measure smooth pursuits and saccades (for central function), nystagmus (for peripheral vestibular semicircular canal and central function), post passive head shake nystagmus in the horizontal direction (for peripheral lateral semicircular canal function), and in the vertical direction (for central function), the mastoid vibration test induced nystagmus (for peripheral lateral semicicular canal function), the head heave test (otolith counterpart of the high frequency canal head impulse test to assess high frequency utricular function), the ocular counter rolling test (ocular movements in response to head roll to assess gravitational sensor function), the office rotatory chair tests (to assess peripheral vestibulo-ocular reflex or VOR), the optokinetic test (for central function), and the suppression of visual fixation test (for central cerebellar function). Vestibulo-spinal tests were performed with the Romberg, the Unterberger, the tandem gait, the one legged stance, and the sharpened Romberg's tests. A foam cushion was used to eliminate proprioception cues in these tests with eyes closed to elicit a vestibular response in maintaining posture. Dix Hallpike, the supine roll test, and the deep head hanging test were performed to exclude benign positional paroxysmal vertigo (BPPV).

A full 6 canal video head impulse test (vHIT) was performed in every child with a minimum of 10 head thrusts for each canal function with the ICS Impulse system. A VOR gain of 0.8–1 was considered normal for the lateral semicircular canal whilst a VOR gain of 0.6–0.8 was the norm for the vertical canals. Recent studies (33, 34) indicate that vertical canal gains are lower in the pediatric population than in adults similar to what we have also found using similar equipment in children with normal vestibular function (35). Saccades, rather than VOR gain, were deemed as pathological weakness as studies have shown that saccades can occur with normal VOR gain in vestibular hypofunction (36, 37). Two senior clinicians (SDG and SR) analyzed the saccades in the current series independently. Low VOR gain without saccades was deemed as clinically insignificant in the absence of any neurological comorbidity. Compatibility with the test was high. Calorics are not performed in our center due to the distress they cause to children.

Cervical vestibular evoked myogenic potential test (cVEMP) was performed with the Neurosoft software. Air conducted stimuli delivered through Etymotic ER 3A insert ear phones at rarefied 100 dBnHL comprised of 60 sweeps with a stimulation rate of 3–5 Hz were presented to each ear at a tone burst of 500 Hz with a Bartlett Trapezoid rise and fall time of 1 ms. The analysis time window was 50 ms with a sampling rate of 5,000 Hz. Amplitudes were measured after averaging at least 2 runs wherever possible. Adaptive notch filter between 30 and 2,000 Hz was used in the protocol. Rectified amplitudes were also considered when subsequent measurements of asymmetry were performed between the 2 sides. The amplitude asymmetry was calculated as the right amplitude minus left amplitude divided by right amplitude plus left amplitude $\times$ 100. Thresholds were measured wherever possible, but it must be remembered that this is not always possible due to compatibility issues as active sternocleidomastoid contraction becomes strenuous for some children and several runs cannot be implemented. Pediatric norms are variable and the test itself is very operator dependant. The normative value the (38) first paper of its kind as regards mean amplitudes and thresholds in children were different from other publications (39, 40). It was also emphasized that this variability is due to several factors that include VEMP stimulus parameters and local laboratory norms (39). Absolute amplitude values may be misleading due to the lack of these standardized norms and hence we follow the asymmetrical amplitude parameter as a more robust sign than absolute amplitudes, unless these amplitudes are clearly very high and match with symptoms. In our center, we consider 15–150 microvolts as normal amplitude values, up to 25% as normal amplitude asymmetry and 85 dBnHL as the threshold with our test set up in the pediatric population. We are still collecting our own ocular vestibular evoked myogenic potential (oVEMP) norms, so we did not use this test in this series. Interestingly, in a recent study, the authors commented that oVEMPs are more sensitive indicators than cVEMPS to diagnose vestibular dysfunction in children (41).

All children presenting with hearing loss underwent the full set of aetiological investigations as suggested by the British Association of Audiovestibular Physicians

TABLE 3 | Assessment of the vestibular system in children [table adapted from (5)].

I. Audiological tests
• Pure tone audiometry with masking
• Tympanometry
• Acoustic reflexes
• Otoscopy
• Transient otoacoustic emissions
II. Full neurological examination
III. Musculoskeletal examination
IV. Full oculomotor examination
V. Vestibular tests
• Assessment of subjective visual vertical
• Videonystagmography with and without visual fixation for smooth pursuits, saccades, horizontal and vertical head shake, head heave, ocular counter rolling, mastoid vibration test, optokinetic test and ectopic eye movements
• Video head impulse test
• Cervical vestibular evoked myogenic potential test
• Vestibulo-spinal test battery with and without proprioception for Romberg, Unterberger, tandem gait; one legged stance and sharpened Romberg
• Office rotatory chair tests and suppression of visual fixation
• Dix Hallpike, supine roll and deep head hanging tests

(BAAP) (42) that included chromosome karyotyping, molecular biology genetic studies, ophthalmological investigations, and metabolic and inflammatory screens to rule out other causes of hearing loss in children. Some of these tests were also informative of causes of vestibular dysfunction in children, e.g., autoimmune vestibular disorder.

It must be emphasized that pediatric examination and audiovestibular testing is intense and time consuming. Occasionally, the children were brought back for a second appointment. Every effort was made to make the child as comfortable as possible and not put too much strain as, in our experience, tiredness and fatigue during testing invariably leads to less test compatibility with the tests generating incomplete results. This situation is hardly encountered in adults.

Table 3 shows the examination algorithm.

Imaging

Based on the history, clinical examination, and investigations, all children with conductive/mixed hearing losses and normal middle ear function with/without balance problems, third window symptoms, and deranged vestibular function tests underwent HRCT to visualize the bony otic capsule as a first line of investigations. Only sensorineural hearing losses also underwent HRCT if their MRI scans were deemed normal. The CT was acquired using ultrahigh resolution spiral CT with overlapping slices of 0.8 mm with 0.4 mm increment. The images were reconstructed in the axial, coronal, and sagittal planes with oblique views at 0.5 mm. The scans were analyzed by one of the co-authors (SA) who is a senior radiologist specializing in pediatric head and neck radiology. The thickness of the semicircular canal walls was measured and a thickness of at or $<$0.5 mm in at least 2 planes was deemed as a thin semicircular wall or a near dehiscence (26, 43). HRCT provided the final direct visual confirmation of the rare third windows in the children in the series.

Statistical Methods

Descriptive statistics were computed using Quick Statistics Calculators, an online digital portal (https://www.socscistatistics.com/tests). We did not investigate any analytical statistics to explore variations among groups as the number of cases were deemed too small, and there is a danger of running ANOVA with small samples in that it might lead to erroneous conclusions because of a lack of power (44).

RESULTS

The observations in the case series are given in **Tables 4**, **5**, **Figures 1–4** are representative cases in each group (Group A PSCD—**Figure 1**; Group B posterior semiciruclar canal thinning PSCT—**Figure 2**; Group C X linked—**Figure 3**, and Group D Multiple—**Figure 4**).

The total number of children seen for vestibular assessment between the period of February 2016 and July 2019 were 920. Out of these, 19 were diagnosed with SSCD (2.06%), 26 with EVA (2.82%), and 8 with rare third window disorders (0.86%) on HRCT. These rare third window disorders included 3 with isolated posterior semicircular dehiscences (0.32%—cases 1,2,3), 2 with thinned posterior semicircular canal wall (0.2%—cases 4,5), 2 with X linked gusher (0.2%—cases 6,7), and 1 with a combination of a facial nerve canal hypoplasia and a dilated auditory meatus lying very close to the cochlea (0.1%—case 8). The diagnosis of the X linked gusher group was by typical HRCT findings and a typing of the POU3F4 genetic mutation in a family of 2 children with the same mother. Two of the 3 children with frank PSCD also showed high riding jugular bulbs. These children where rare third window disorders were identified were assigned 4 groups: Group A—children with only posterior semicircular canal dehiscence (PSCD); Group B—children with a thinned posterior semicircular canal wall (PSCT); Group C—children with X linked gusher disease; and Group D—children with other rare third window disorders.

Of the whole third window cohort ($n = 53$) that constituted only 5.76% of all children seen, Group B and Group C were observed in 3.77%, Group A in 5.66%, and Group D in 1.88%. There were 4 females and 4 males in the rare third window series ($n = 8$). The average age of the females was 11.75 years (range 6–15 years) and that of the males was 10.75 years (range 6–16 years). Of the 16 ears studied, a third window abnormality was observed in 4 ears on the right, 1 on the left, and in 3 children, it was present bilaterally with 5 ears showing no abnormality.

Children presenting with symptoms of communication difficulties, loss of hearing, and difficulties in understanding speech and instructions in the school set up were observed in 5 children (62.5%) of the cohort of rare third window disorders. There were 3 children who did not present with any symptoms of hearing loss, 2 of them with unilateral hearing losses, and 1 with normal hearing. Six children demonstrated a mixed hearing loss

TABLE 4 | Children in case group.

Child/group	HS	BS	TW	Tymp/ECV	ART	OAE	VNG/VFT	PTA av R AC/BC	PTA av L AC/BC	Type HL	Diagnosis
1/A	Yes	Yes	Nil	Normal	Normal	Absent	Normal	52/46	55/46	Mix B	R PSCD
2/A	Nil	Yes	Nil	Normal	Absent R	N/A	Normal	25/5	6/0	CHL R	R PSCD
3/A	Nil	Yes	Auto/GET/PT	Normal	Normal	Normal	Normal	7/4	5/3	No HL	R PSCD
4/B	Yes	Yes	Nil	Normal	Normal	Normal	Abnormal	36/30	37/26	Mix B	R PSCT
5/B	Yes	Nil	PT	Normal	Normal	Normal	Normal	42.5/30	4/0	Mix R	Bil PSCT
6/C	Yes	Yes	Nil	Normal	Absent L	Absent	Normal	76/51	100/51	Mix B	X linked
7/C	Yes	Yes	CD	Normal	Normal	Absent	Abnormal	80/50	80/50	Mix B	X linked
8/D	Nil	Nil	Nil	Normal	Normal	Absent L	Abnormal	25/10	100/53	Mix L	Multiple L
Mean PTA thresholds								42.93/ 28.25	48.37/ 28.65		

HS, hearing symptoms; BS, balance symptoms; TW, Third window symptoms; Tymp, tympanometry; ECV, external auditory canal volume; ART, acoustic reflex test; OAE, transient otoacoustic emission; VNG, videonystagmography; VFT, vestibular function tests; PTA av R and av L, pure tone audiometry thresholds averaged 500 Hz−4 kHz right and left in dBHL; AC, air conduction; BC, bone conduction; HL, hearing loss; CHL, conductive hearing loss; Mix, mixed; Bil/B, bilateral; R, right; L, left; PSCD, posterior semicircular canal dehiscence; PSCT, posterior semicircular canal thinning; N/A, not available; PT, pulsatile tinnitus; GET, gaze evoked tinnitus; Auto, autophony; CD, conductive dysacusis.

TABLE 5 | Children in case group, vHIT and cVEMP results.

Child/group	VOR L LSCC	VOR R LSCC	VOR L SSCC	VOR R SSCC	VOR L PSCC	VOR R PSCC	Saccades	cVEMP amp/RA R μV	cVEMP amp/RA L μV	Thresh R/L dBnHL
1/A RPSCD	1.16	1.09	0.55	0.75	0.85	0.69	Yes R	254.9/2.9	168.8/2.2	85/85
2/A RPSCD	0.93	0.89	0.56	0.67	0.84	0.54	Nil	42.8/0.9	114.2/2	NA
3/A RPSCD	0.67	0.48	0.62	N/A	N/A	1.46	Nil	NA	NA	NA
4/B RPSCT	0.86	0.9	0.73	0.48	0.54	0.47	Yes R	Nil	Nil	Nil
5/B BPSCT	0.83	0.88	0.58	0.42	0.55	0.56	Nil	Nil	57.7/1.7	Nil/NA
6/C Xlinked	0.72	0.88	0.3	0.41	0.54	0.64	Yes B	92.5/2.9	Nil	85/Nil
7/C Xlinked	1.07	0.95	0.69	0.8	0.95	0.69	Nil	57.3/1.1	58.9/0.8	75/75
8/D LMulti	0.75	0.92	0.69	0.8	0.95	0.69	Yes L	101.2/1.5	Nil	NP/Nil
Mean VOR gain	**0.87**	**0.88**	**0.59**	**0.61**	**0.7**	**0.71**				

VOR, vestibulo-ocular reflex gain; LSCC, lateral semicircular canal; SSCC, superior semicircular canal; PSCC, posterior semicircular canal; amp, amplitude; RA, rectified amplitude; Thresh, threshold; R, right; L, left; NA, not available; PSCD, posterior semicircular canal dehiscence; PSCT, posterior semicircular canal thinning; B, bilateral; Multi, multiple; NA, not available; NP, not performed; Nil, absent response.

(75%) with appreciable air bone gaps in pure tone audiometry. There was 1 child with a conductive hearing loss only. There were 4 bilateral and 3 unilateral hearing losses. Average air conduction thresholds (the mean of the summated averages of air conduction thresholds in each child between 500 Hz and 4 kHz) and average bone conduction thresholds (the mean of the summated averages of bone conduction thresholds in each child) indicated a >10 dBHL air bone gap (**Table 4**). The hearing loss localized to the side of the lesion in 7 children; in 2 children it was also present in the ear without a third window abnormality, and in 1 child it was observed only in 1 ear where there was a bilateral third window abnormality. The child with normal hearing showed a unilateral pathology. In Group B, this asymmetry was most noticed where the hearing loss was present in the ear without a third window and absent in the ear with a third window. Only 2 children, one in Group A and one in Group B presented with a third window symptom of pulsatile tinnitus, and the child in Group A also complained of gaze evoked tinnitus and autophony.

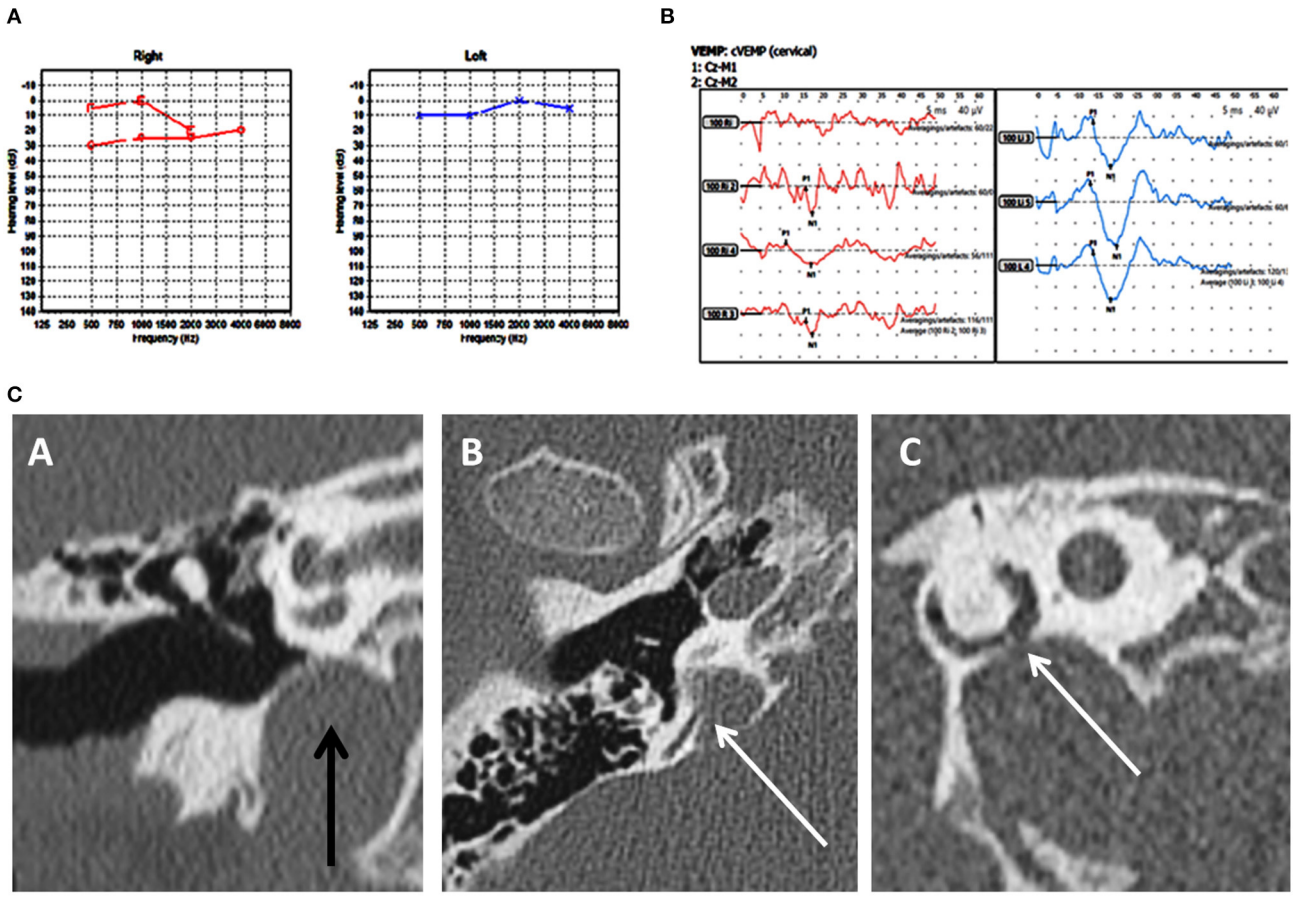

FIGURE 1 | Case number 2—Unilateral right posterior semicircular dehiscence. **(A)**, Pure tone audiometry showing mild conductive low frequency hearing loss on the right. **(B)**, Clinically significant cVEMP amplitude asymmetry with the right weaker than the left. This child perceived significant balance issues but his vestibular tests including the vHIT was normal. **(C)**—CT scan images of the right petrous temporal bone in the coronal plane (A) demonstrates a high riding jugular bulb. The axial image (B) the sagittal oblique reconstruction parallel to the posterior semi-circular canal (C) demonstrate dehiscence of the posterior semi-circular canal at its junction with the jugular bulb.

The most severe mixed hearing loss was detected in Group C, the X linked gusher group where it was bilateral, and in Group D with multiple third windows with a severe mixed hearing loss on the affected side. The least intense hearing loss was in Group B with PSCT group. As regards bone conduction thresholds, none of the children demonstrated a negative bone conduction threshold.

All children ($n = 8$) in the series demonstrated normal otoscopy and normal tympanometry with normal external auditory canal volumes (100%). Six exhibited normal acoustic reflexes—ART; there were 2 children who showed absent reflexes. Three returned normal transient otoacoustic emissions (TEOAE), and 4 showed absent emissions (3 bilateral and 1 unilateral). No data was available for one child.

Six children (75%) in the series presented with one or more features of disequilibrium as enumerated in **Table 2**. The child with multiple third window abnormalities did not complain of any symptoms relating to balance, and neither did the child with the bilateral PSCT. From the group perspective, 100% presented with the symptom(s) in Groups A and C and 50% in Group B. Three children were observed to exhibit abnormal balance function tests excluding the vHIT and VEMP (37.5%). In the vHIT test, 4 (50%) children demonstrated repeatable catch up saccades (i.e., saccades that were consistent and replicable) in at least 1 or more canals with or without normal VOR gain. In all these children the saccades localized to the side of the third window abnormality. This abnormality was detected in 1 child in each group. The average VOR gain in the whole series in the lateral semicircular canal as given in **Table 5** was within the normal range of our laboratory.

cVEMPs could be performed in 7 children. One child in Group A did not undergo the test as we did not possess the facility at the time of diagnosis and the child's subsequent discharge to the adult services. Two children found it too strenuous to complete the threshold test and we could only obtain amplitudes here (cases 2 and 5). In 1 child in Group B, we could only perform one run to obtain amplitudes (case 5, **Figure 2B**), and 1 child did not have thresholds performed on the good ear (case 8, **Figure 4C**). The results were rather heterogeneous to average in this study, but overall cVEMP abnormalities were observed in all

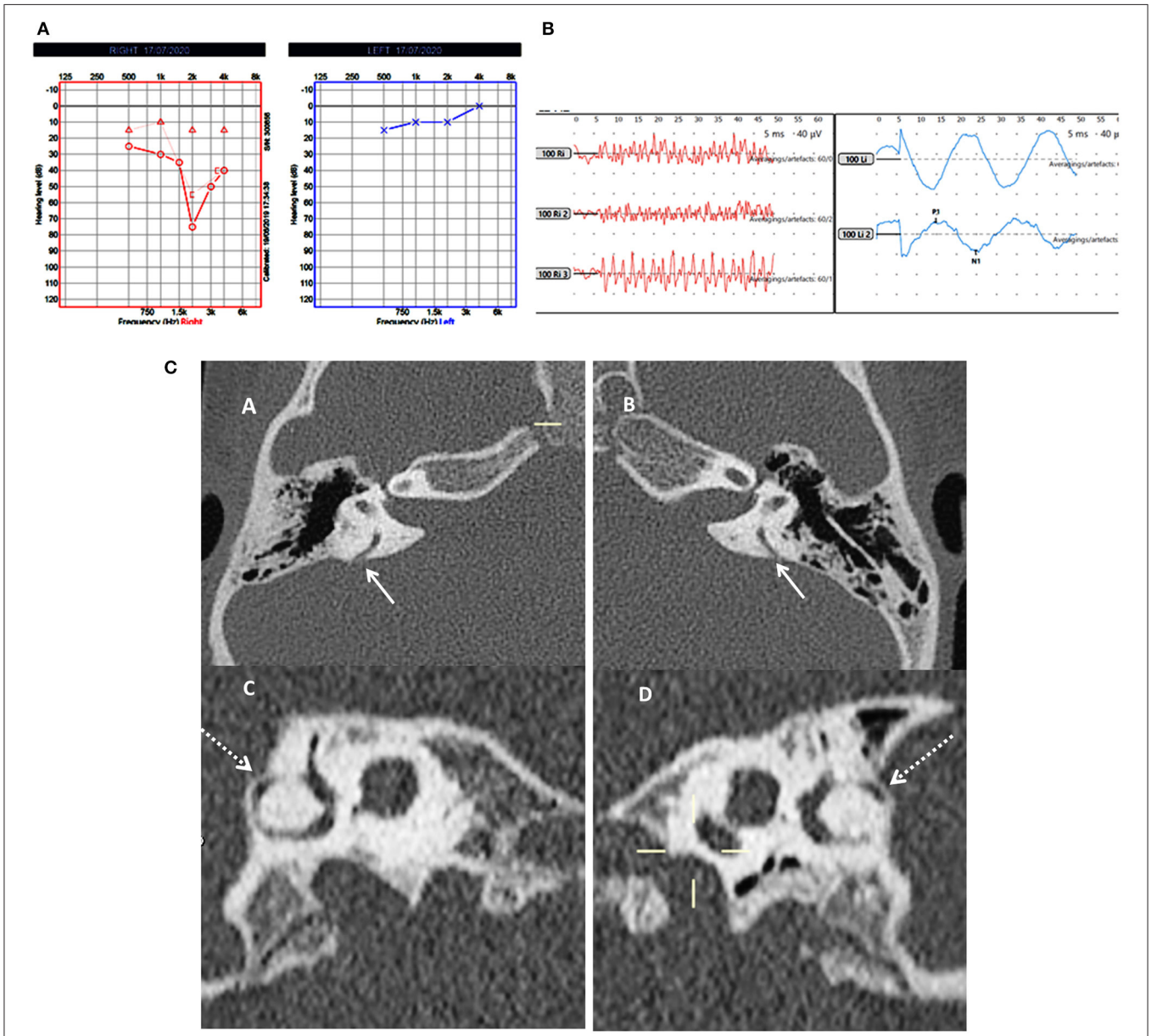

FIGURE 2 | Case number 5—Bilateral posterior semicircular canal thinning. **(A)**, Pure tone audiometry showing right mixed hearing loss. **(B)**, cVEMP showing absent response on the right and normal amplitude on the left; in this child vHIT was normal and there were no symptoms of balance problems. **(C)**—CT scan images of the right (A) and left (B) petrous temporal bone in the axial plane demonstrates apparent dehiscence of the posterior semi-circular canal (white arrows). Sagittal oblique reconstruction of the right (C) and left (D) petrous temporal bone parallel to the plane of the posterior semi-circular canal demonstrates thinning of the overlying bone (dotted arrows) measuring 0.5 mm in thickness on both sides.

7 children. These included increased amplitude on the dehisced side (Group A, case 1); amplitude asymmetry (Group A, case 2); absent response (Group B, cases 4, and 5; Group C, case 6; Group D, case 8), and low thresholds (Group C, case 7). This is given in **Table 5**.

DISCUSSION

In the current study we concentrated on rare third window disorders in children, the definition of which we have described in our Methods section. We observed such abnormalities in 0.8% in a large cohort of children, accounting for only 15.09% of all third windows, making these defects rare.

Whilst in adults and in children, it has been established that frank dehiscences of semicircular canal walls, either superior or posterior, are responsible for the phenotype, yet there are patients where a thinning of the canal walls or near dehiscence may lead to similar symptoms (28). These patients often respond to surgical management of semicircular canal dehiscences. Judging as to what is a thinning can be subjective, and there is no consensus

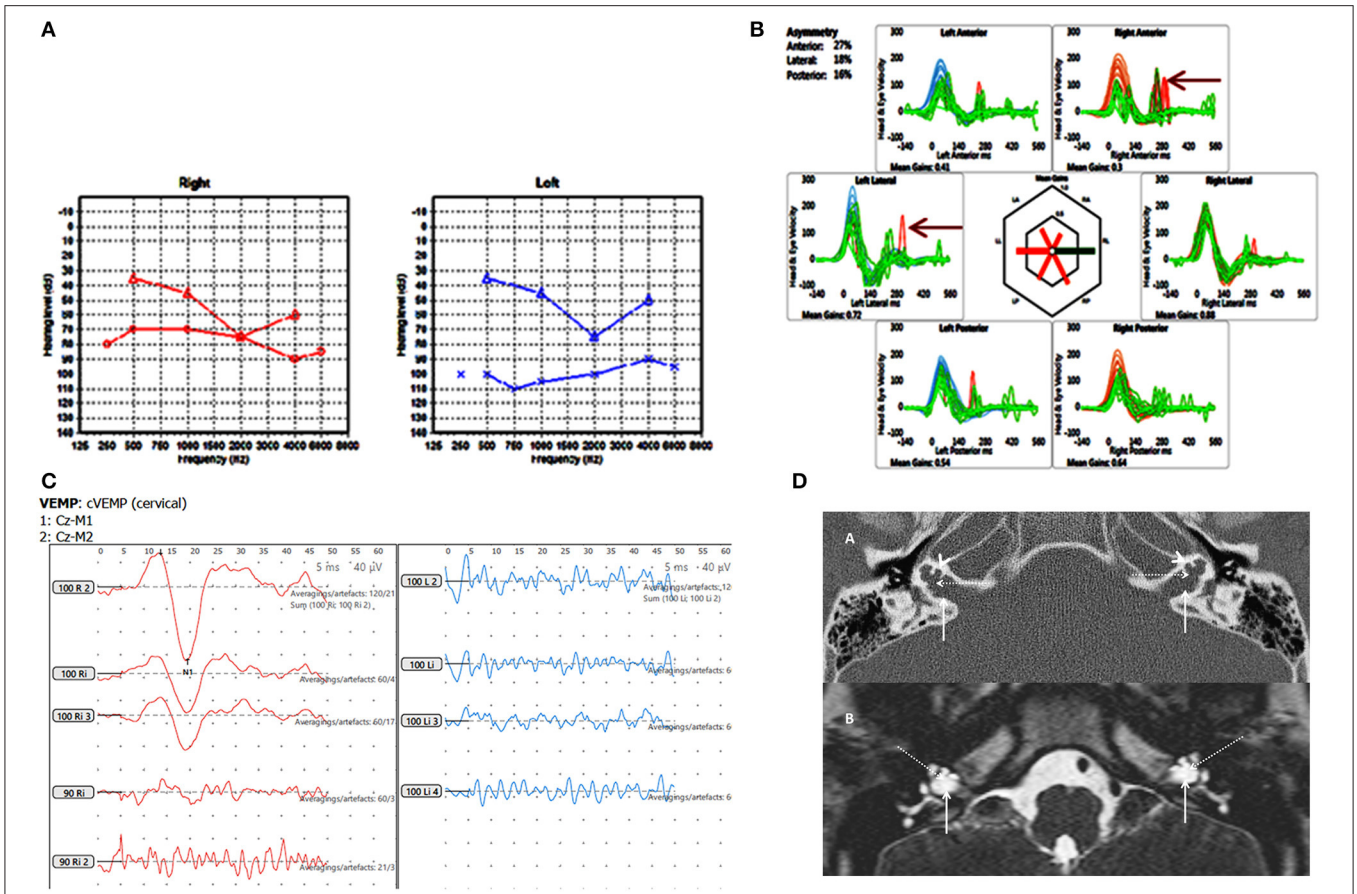

FIGURE 3 | Case number 6, X linked gusher. **(A)**, Pure tone audiometry showing significant bilateral mixed hearing loss. **(B)**, Catch up saccades on both sides on the vHIT (arrow). **(C)**, Absent cVEMP response on the side of the greater hearing loss and normal amplitude and threshold on the other side. **(D)**, Axial CT scan (A) and T2 DRIVE MRI image (B) of the petrous temporal bone demonstrating bilateral bulbous dilatation involving the fundus of the internal auditory canal (arrow) and bilateral incomplete separation of the basal turn of the cochlea (arrow head) from the fundus of the internal acoustic canal (dotted arrow) classical of X linked gusher disorder.

as yet as to what are the physical dimensions of such thinning. For example, Ward (45) considers thinning as a thin strip of bone in their study with adults, whilst Kaur (43) after measuring actual semicircular canal bone thickness observed that thickness ranged from 0.4 to 2.08 mm with an average of about 1.5 mm. Meicklejohn (26) in children above the age of 4 years reported similar observations. Saxby (13) commented that thinning can be developmental but can lead to a dehiscence in the future. Based on these studies, for this study, we postulated that a semicircular canal wall thickness at or below 0.5 mm can be accepted as thinning.

Group A in our study comprised of frank posterior semicircular canal dehiscence as a single inner ear abnormality. This has been hardly reported in children. Meicklejohn (26) in his large series studying CT temporal bones in children from birth did not find any PSCD between the ages of 4–7. In another large series studying temporal bones, PSCD was observed only in 0.6% of children above 3 years (13). In the only case series investigating PSCD in children, 3 children were studied who presented with unilateral PSCD (46). The current series showed a slightly lesser incidence than the one reported in Meicklejohn's (26) series and in Saxby's (13) series due to the fact that these studies included concomitant cochleovestibular dysmorphia that we have excluded from our study. Two out of our three children in Group A also had a high riding jugular bulb that is deemed as an association of PSCD (8, 13, 46, 47) and in both of these children, the point of dehiscence was in contact with the jugular bulb (**Figure 1C**).

Clinical features of PSCD can be variable. In the only pediatric clinical series comprised of 3 children, normal hearing was reported in addition to low frequency conductive hearing loss. They all presented with third window symptoms and all showed cVEMP abnormalities with increased amplitudes and decreased thresholds (46). In the current series, we observed some heterogeneity of symptoms. Mixed hearing loss, conductive hearing loss, and normal hearing were observed. All the children presented with disequilibrium. Rather interestingly, the child with right PSCD perceived quite disproportionate balance problems and showed a significant VEMP amplitude asymmetry with the right side weaker than the left. One reason for this might be due to intrinsic saccular weakness in this child that explains the child's disproportionate balance symptoms. In the child with

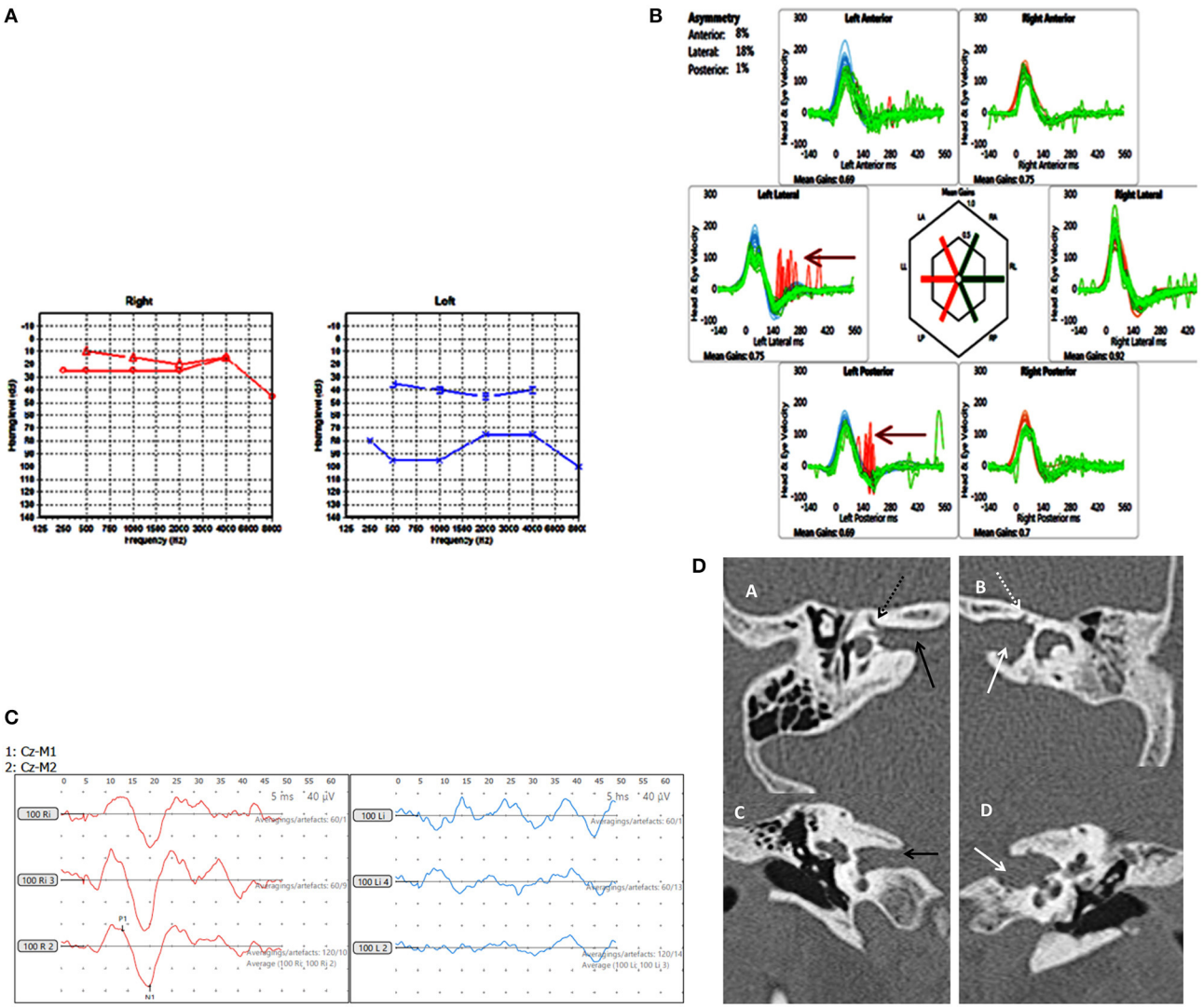

FIGURE 4 | Case number 8, Multiple abnormalities. **(A)**, Pure tone audiometry showing left mixed hearing loss (A) with a normal right side. **(B)**, vHIT showing left sided high frequency multiple canal dysfunction with catch up saccades (arrow) with a normal right side. **(C)**, No response on the cVEMP on the left with a normal right side. **(D)**, CT scan of the left petrous temporal bone in the axial plane (B) and coronal plane (D) demonstrate irregular widening of the internal auditory canal (white arrow) the labyrinthine segment of the left facial nerve canal has an ill-defined bony wall (dotted white arrow). The right petrous temporal bone demonstrates a normal sized internal auditory canal (C black arrow) on the axial and coronal planes and the bony wall of the right facial nerve canal appears normal (A dotted black arrow).

unilateral left PSCD, bilateral mixed hearing loss, abnormal vHIT, and high VEMP amplitudes, it is possible that a structural third window may be evolving, a proposition suggested by Saxby (13). The third child in this group presented with some typical third window features.

Group B in our study consisted of children with PSCT with audiological and balance symptoms that to our knowledge have not been reported in literature. This group was rather homogeneous in terms of their audiovestibular phenotype and yielded some consistency in their VEMP results. They showed absent either unilateral or bilateral VEMP responses. The series with PSCT in adults also observed that about 30% of their subjects did not return a VEMP response (45). Again we propose that this could be due to inherent saccular weakness in this condition. Both children showed bilateral mixed losses with normal OAE and ART.

Group C in our study were the 2 children with a congenital X linked gusher. They both showed identical pathognomonic HRCT features that is usually diagnostic (48). They both presented with bilateral severe mixed hearing losses and balance problems. Both showed a cochlear component to the hearing loss. One child fulfilled the criteria for a third window disorder with lowered VEMP thresholds whilst the other with an abnormal bilateral vHIT showed an absent VEMP response on the side of the greater hearing loss. This may suggest that both cochlear and saccular function can be affected in this disorder.

The third window effect in an X linked gusher is postulated to be due to the absence of lamina cribrosa establishing an

abnormal connection between the perilymphatic space and the subarachnoid space, i.e., a connection between the inner ear and the cranial spaces (8). The condition is rare. A thorough search of the literature yielded circa 89 patients since 1971 (29, 47, 49–58). These children present with progressive mixed hearing losses and varying degrees of vestibular problems as was found in our study. A dilated internal auditory meatus (IAM) in these children accompanied the inner ear phenotype as such dilatations frequently accompany inner ear dysmorphology (59, 60). This is the first time that we are presenting objective quantification of vestibular function in X linked gusher.

Our child in Group D was rather interesting. The severe left sided mixed hearing loss with normal middle ear function suggested inner ear abnormalities with third window structural defects as these are the only pathologies known to generate a non-middle ear origin air bone gap (8). Therefore, we deduced that the conductive element of the mixed hearing loss can come only from a third window defect. The CT showed multiple third window structural abnormalities. We included this child to highlight the observation that occasionally known third window structural abnormalities might not show up clearly on imaging but can be inferred by the effects they generate.

The child in Group D clearly showed deficient vestibular function on the left side, suggesting a cochleo-vestibular pathology. This child was also the one who showed no symptoms from the audiovestibular function point of view. A child may undergo complete vestibular central compensation rendering the child asymptomatic (35) and might not perceive a unilateral hearing loss (61).

About two thirds of children in the present series did not complain of a subjective hearing loss, including children who demonstrated PTA measured mild hearing loss, a unilateral hearing loss, or normal hearing. The majority of children in the current series showed a mixed hearing loss or a conductive hearing loss that is in agreement with other studies who have described similar hearing loss in SSCD in children and third windows (20, 23, 25, 62). The hearing loss correlated well to the side of the lesion in the majority. Negative BC has been postulated to be a diagnostic criteria for third window defects especially SSCD (9). However, Merchant et al. (63) commented that rather than negative BC thresholds, the air bone gap is more important to consider as a diagnostic criteria. In the current series, there were no children with negative BC.

Normal TEOAE was observed in 3 children (1 with normal hearing and 2 with 30 dBHL or less hearing loss). TEOAE are abnormal in hearing losses of cochlear origin above 30 dBHL (64), so probably these 2 children had a mild cochlear component to their hearing loss. TEOAEs are usually preserved in third window disorders unless complicated by a simultaneous significant cochlear pathology that over rides the third window effect (5, 46, 65). The children with mixed losses above 30 dBHL in the series returned absent TEOAEs. Sensorineural hearing loss has been reported in pediatric SCDS (5, 66–68). There was 1 child with normal hearing that has also been reported in third window disorders (5, 68).

Tympanometry and ART are also preserved in third window disorders (69). In our study, tympanometry was normal in all children that virtually eliminated a middle ear disorder explaining a mixed or a conductive hearing loss. ART was present in three-fourths of cases. The sensitivity and specificity of the test is not 100% and we would consider its absence in one-fourths of the cases as a normal variation (70).

In the current series, three-fourths of the children in the series complained of some features of disequilibrium that is characteristic of a third window abnormality (47). However, balance symptoms may be absent altogether (5, 20, 47, 71). We believe that this could be due to central compensation. There were only 2 children who presented with classical third window symptoms in the form of pulsatile tinnitus, gaze evoked tinnitus, and autophony. Dasgupta and Ratnayake (5) in a series with SSCD in children remarked that radiologically established pediatric third window disorders in children might not present with a fully blown clinical syndrome with its classical features as this history may be difficult to elicit or the defect has still not reached the stage where it may lead to classical third window symptoms.

Vestibular function tests other than the vHIT and cVEMP were normal in about 60% of our children but abnormal in about 40%. They were mostly abnormal in children with a possible cochlear abnormality. Vestibular function test except the VEMPs results are variable in third window disorders (8, 47) but curiously they have not been studied in detail. We believe that these tests are more likely to be deranged if the third window abnormality involves a wider anatomical topography of the bony labyrinth.

The vHIT as a tool to assess high frequency all canal function in vestibular diagnostics has revolutionized the diagnostic process and finds wide application (72). Use in children is still limited although the evidence is slowly emerging (35, 73–78). One difficulty in children is the standardization of norms. We have explained about these norms in our Methods section (33–35). The average VOR gain in our series in all canals was mostly normal in the 4 different groups that we have also found in a previous study (5) suggesting that VOR gain is largely preserved in pediatric third window disorders.

The role of saccades in interpreting the vHIT has gathered momentum (79) and we have explained the importance of saccades in the presence of normal VOR gain in our Methods section (36, 37). In the current series, they were deemed pathological in about a half of the cohort localizing accurately to the side of the third window defect. One publication (5) reported the utility of the vHIT in pediatric SSCD, and it appears from this study that indeed this test does add significantly to vestibular information in third windows. For example, in EVA, vHIT can be deranged (80).

VEMP studies have shown that third window VEMP characteristics [i.e., increased amplitude and decreased threshold due to hypersensitivity of the saccule and the urticle to acoustic energy (19)] may be observed in third window disorders that include EVA, SSCD, PSCD, and CFD in the pediatric population (3, 46, 81, 82). We have discussed the variable norms for pediatric cVEMP in our Methods section (38–40) and the difficulties in performing the test in children. For oVEMPS, there are very few studies (83, 84) to establish norms. In the current series, there

were increased amplitudes, absent responses, and low thresholds in the children undergoing cVEMPs in varying percentages in the cohort. This indicates that cVEMPs characteristics in pediatric rare third windows may be rather heterogeneous. Overall, cVEMP abnormalities were detected in all the children who underwent the test. This can suggest that saccular abnormalities may be associated with a high percentage of rare third window disorders in children.

The limitations of this study include the small numbers, but the third window conditions highlighted in the current series are rare in children. Therefore, it will be injudicious to generalize observations based on this study. In addition, this was a retrospective non-controlled study. However, we were careful to avoid inconsistencies as the 2 senior and experienced physicians (SD and SR) managed these children maintaining continuity of observations, thereby eliminating an important bias in the study. Furthermore, the study looked into a defined set of the population unlikely to be influenced by confounding variables.

As the literature suggests, third window disorders in children may present without third window syndromic features (5) which are determined by defined symptoms and objective signs as is found in the literature mainly in adult cohorts (9). A number of factors may account for this, for example, a co-existing cochlear or vestibular dysfunction. It could also be due to a difference in endolymphatic fluid dynamics in children as compared to adults (85). Furthermore, as mentioned earlier, third window symptoms may be difficult to elicit in children. In children, consequently, the diagnosis is based on a holistic process rather than by didactic and set criteria of a third window syndrome so well-defined in adults. However, some features like disequilibrium, conductive component of a hearing loss with normal middle ear studies, and normal TEOAE may be consistent features that should raise the suspicion of a third window. There may be accompanying vestibular dysfunction and VEMP abnormalities.

This study has highlighted a cochlear element to a mixed loss in these rare third windows as a phenotype. It has also observed 2 new entities that present with features of third window disorders. The first one is a PSCT or near dehiscence that behaves like other third window disorders, and the second is a combination of more than 1 possible third window structural abnormality which are as yet unclassified third windows but generate symptoms nevertheless.

It is important to consider the premise that whether HRCT diagnosis of a third window abnormality, especially a canal dehiscence in a child, can be incidental or part of the normal developmental process and therefore deemed non-pathological. Did the HRCTs over diagnose the conditions in our series? Available evidence suggests that dehiscences can be a normal phenomenon until the age of 5 years (13, 26). All our patients were over 5 years, and we feel that an incidental or developmental third window structural defect is unlikely to be the case, as all these children in the series presented with at least one third window feature and were most comprehensively investigated from other causes of a hearing loss. Therefore, by the process of elimination in the medical algorithm, we concluded that their observed third window abnormalities were responsible for their phenotypes. Thus, it is a matter of fine judgement and expertise to diagnose these conditions in children. HRCT remains an important investigation to perform to establish diagnosis that aids significantly in informing the child and the carers as to what is going on and may determine surgery if required.

We believe that it is important to consider third window disorders as concrete diagnoses as this helps in formulating holistic management plans in children. In our center, all these children and their parents/carers receive full counseling on typical third window syndrome symptoms that can occur later in life. Indeed, this dissemination of diagnostic information often participates in a cognitive treatment of the child. One of the children in the current series with autophony and gaze evoked tinnitus who was desperately seeking answers (being labeled as someone having psychological problems with a poor quality of life) was extremely relieved with the diagnosis and devised excellent coping strategies by self-awareness. None of the children in our series required operative intervention, but some did require auditory, vestibular, and cognitive rehabilitation aided by the diagnostic process.

CONCLUSIONS

Rare third window disorders, as the name suggests, are rare and can be missed unless there is a high index of clinical suspicion in a child with disequilibrium, a conductive element to a measured hearing loss with normal middle ear function and abnormal objective vestibulometry that will lead to a confirmation with HRCT. They might not present with classical third window symptoms described well in adults, and their phenotypes might be quite heterogeneous. This study shows that diagnosis of these conditions in children is dependent on a good anamnesis and extensive objective and subjective audiovestibulometry and depends on expert and fine clinical judgement. It also emphasizes that it is important to diagnose rare third window disorders in children for their holistic management.

DATA AVAILABILITY STATEMENT

All datasets generated for this study are included in the article/supplementary material.

ETHICS STATEMENT

The studies involving human participants were reviewed and approved by HRA England and Health and Care Research Wales (HCRW); approval number 20/HRA/1289 dated 19.05.2020; parental/carer consent waived as this was a retrospective case note study. Written informed consent from the participants' legal guardian/next of kin was not required to participate in this study in accordance with the national legislation and the institutional requirements.

AUTHOR CONTRIBUTIONS

SD and SR were the responsible clinicians for the children included in the case series. SD collated the data, collected and analyzed the evidence, and wrote the paper. RC and SR collaborated to write the manuscript and analyse the evidence.

JI and LS were the audiologists and SA was the radiologist responsible for the children in the case series. All authors critically reviewed clinical findings and the manuscript drafts, and contributed to the final version and own responsibility for the integrity of the paper.

FUNDING

This study was funded by Alder Hey Children's NHS Foundation Trust.

ACKNOWLEDGMENTS

We gratefully acknowledge the advice of Ms. Amy Lennox, Consultant Audiologist, Hypatia Dizziness and Balance Center, Liverpool, United Kingdom, for her valuable expertise in pediatric VEMP tests, the research department of Alder Hey NHS Children's NHS Foundation Trust for sponsoring this work, and the assistance rendered to us by the department of Pediatric Audiology in the same hospital, especially Mr. John Wong, senior audiologist.

REFERENCES

1. Merchant SM, Rosowski JJ. Conductive hearing loss caused by third-window lesions of the inner Ear. *Otol Neurotol.* (2008) 29:282–9. doi: 10.1097/MAO.0b013e318161ab24
2. Gopen Q, Rossokowski JJ, Merchant SM. Anatomy of the normal human cochlear aqueduct with functional implications. *Hear Res.* (1997) 107:9–22. doi: 10.1016/S0378-5955(97)00017-8
3. Wackym PA, Balaban C, Zhang P, Siker DA, Hundal JS. Third window syndrome: surgical management of cochlea-facial nerve dehiscence. *Front Neurol.* (2019) 10:1281. doi: 10.3389/fneur.2019.01281
4. Mau C, Kamal N, Badeti S, Reddy R, Ying MY, Jyung RW, et al. Superior semicircular canal dehiscence. diagnosis and management. *J Clin Neurosci.* (2018) 48:58–65. doi: 10.1016/j.jocn.2017.11.019
5. Dasgupta S, Ratnayake SAB. Functional and objective audiovestibular evaluation of children with apparent semicircular canal dehiscence–a case series in a pediatric vestibular center. *Front Neurol.* (2019) 10:306. doi: 10.3389/fneur.2019.00306
6. Minor LB, Solomon D, Zinreich JS, Zee DS. Sound- and/or pressure-induced vertigo due to bone dehiscence of the superior semicircular canal. *Surgery.* (1998) 124:249–58. doi: 10.1001/archotol.124.3.249
7. Blake DM, Tomovic S, Vasquez A, Lee H, Jyung RW. Cochlear-facial dehiscence–a newly described entity. *Laryngoscope.* (2014) 124:283–9. doi: 10.1002/lary.24223
8. Scarpa A, Ralli M, Cassandro C, Gioacchini FM, Di Stadio A, Cavaliere M, et al. Inner-ear disorders presenting with air–bone gaps: a review. *J Int Adv Otol.* (2020) 16:111–6. doi: 10.5152/iao.2020.7764
9. Ward BK, Carey JP, Minor LB. Superior canal dehiscence syndrome: lessons from the first 20 years. *Front Neurol.* (2017) 8:177. doi: 10.3389/fneur.2017.00177
10. Jackson NM, Laveil A, Morell B, Carpenter CC, Givens V, Kakade A, et al. The relationship of age and radiographic incidence of superior semicircular canal dehiscence in pediatric patients. *Otol Neurotol.* (2015) 36:99–105. doi: 10.1097/MAO.0000000000000660
11. Carey JP, Minor LB, Nager GT. Dehiscence or thinning of bone overlying the superior semicircular canal in a temporal bone survey. *Arch Otolaryngol Head Neck Surg.* (2000) 126:137–47. doi: 10.1001/archotol.126.2.137
12. Nadgir RN, Ozonoff A, Devaiah AK, Halderman AA, Sakai O. Superior semicircular canal dehiscence: congenital or acquired condition? *AJNR Am J Neuroradiol.* (2011) 32:947–9. doi: 10.3174/ajnr.A2437
13. Saxby AJ, Gowdy C, Fandino M, Chadha NK, Kozak FK, Sargent MA, et al. Radiological prevalence of superior and posterior semi-circular canal dehiscence in children. *Int J Paediatr Otorhinolaryngol.* (2015) 79:411–8. doi: 10.1016/j.ijporl.2015.01.001
14. Noonan KY, Russo J, Shen J, Rehm H, Halbach S, Hopp E, et al. CDH23 related hearing loss: a new genetic risk factor for semicircular canal dehiscence? *Otol Neurotol.* (2016) 37:1583–8. doi: 10.1097/MAO.0000000000001210
15. Niesten MEF, Lookabaugh S, Curtin H, Marchant SN, McKenna MJ, Grolman W, et al. Familial superior canal dehiscence syndrome. *JAMA Otolaryngol Head Neck Surg.* (2014) 140:363–8. doi: 10.1001/jamaoto.2013.6718
16. Gopen Q, Zhou G, Whittemore K, Kenna M. Enlarged vestibular aqueduct: review of controversial aspects. *Laryngoscope.* (2011) 121:1971–8. doi: 10.1002/lary.22083
17. Hildebrand MS, de Silva MG, Tan YT, Rose E, Nishimura C, Tolmachova T, et al. Molecular characterization of a novel X-linked syndrome involving developmental delay and deafness. *Am J Med Genet.* (2007) 143A:2564–75. doi: 10.1002/ajmg.a.31995
18. Rosengren SM, Colebatch JG, Young AS, Govender S, Welgampola MS. Vestibular evoked myogenic potentials in practice: methods, pitfalls and clinical applications. *Clin Neurophysiol Pract.* (2019) 4:47–68. doi: 10.1016/j.cnp.2019.01.005
19. Manzari L, Burgess AM, Macdougal HG, Curthoys IS. Enhanced otolithic function in semicircular canal dehiscence. *Acta Oto-Laryngol.* (2010) 131:107–12. doi: 10.3109/00016489.2010.507780
20. Zhou G, Ohlms L, Liberman J, Amin M. Superior semicircular canal dehiscence in a young child: implication of developmental defect. *Int J Paediatr Otorhinolaryngol.* (2007) 71:1925–8. doi: 10.1016/j.ijporl.2007.08.009
21. Wackym PA, Wood S, Siker DA, Carter D. Otic capsule dehiscence syndrome: superior canal dehiscence syndrome with no radiographically visible dehiscence. *Ear Nose Throat J.* (2015) 94:E8–24. doi: 10.1177/014556131509400802
22. Arjamand EM, Webber A. Audiometric findings in children with a large vestibular aqueduct. *Arch Otolaryngol Head Neck Surg.* (2004) 130:1169–74. doi: 10.1001/archotol.130.10.1169
23. Lee GS, Zhou G, Poe D, Kenna M, Amin M, Ohlms L, et al. Clinical experience in diagnosis and management of superior semicircular canal dehiscence in children. *Laryngoscope.* (2011) 121:2256–61. doi: 10.1002/lary.22134
24. Hagiwara M, Shaikh J, Fang Y, Fatterpaker G, Roehm PC. Prevalence of radiographic semicircular canal dehiscence in very young children: an evaluation using high-resolution computed tomography of the temporal bones. *Pediatr Radiol.* (2012) 42:1456–64. doi: 10.1007/s00247-012-2489-9
25. Chen EY, Paladin A, Phillips G, Raske M, Vega L, Peterson D, et al. Semicircular canal dehiscence in the paediatric population. *Int J Paediatr Otorhinolaryngol.* (2009) 73:321–7. doi: 10.1016/j.ijporl.2008.10.027
26. Meiklejohn DA, Corrales CE, Boldt BM, Sharon JD, Yeom KW, Carey JP, et al. Pediatric semicircular canal dehiscence: radiographic and histologic prevalence, with clinical correlation. *Otol Neurotol.* (2015) 36:1383–9. doi: 10.1097/MAO.0000000000000811
27. Sugihara EM, Babu SC, Kitsko DJ, Haupert MS, Thottam PJ. Incidence of paediatric superior semi-circular dehiscenceand inner ear anomalies: a large multicentre review. *Otol Neurotol.* (2016) 37:1370–5. doi: 10.1097/MAO.0000000000001194
28. Baxter M, McCorkale C, Guajardo CT, Zuniga MG, Carter AM, Della Santina CC, et al. Clinical and physiologic predictors and postoperative outcomes of near dehiscence syndrome. *Otol Neurotol.* (2018). 40:204–12. doi: 10.1097/MAO.0000000000002077
29. Saylisoy S, Incesulu A, Gurbuz MK, Adapinar B. Computed tomographic findings of X-Linked deafness: a spectrum from child to mother, from young to old, from boy to girl, from mixed to sudden hearing loss. *J Comput Assist Tomogr.* (2014) 38:20–4. doi: 10.1097/RCT.0b013e3182a0d05f
30. Koroulakis DJ, Reilly BK, Whitehead MT. Cochlear–facial dehiscence in a pediatric patient. *Pediatric Radiol.* (2020) 50:750–2. doi: 10.1007/s00247-019-04600-4

31. Lund AD Palacios SD. Carotid artery-cochlear dehiscence: a review. *Laryngoscope*. (2011) 121:2658–60. doi: 10.1002/lary.22391
32. Dasgupta S, Mandala M, Salerni L, Crunkhorn R, Ratnayake S. Dizziness and balance problems in children. *Curr Treat Options Neurol*. (2020) 22:8. doi: 10.1007/s11940-020-0615-9
33. Bachmann K, Sipos K, Lavender K, Hunter V. Video head impulse testing in a pediatric population: normative findings. *J Am Acad Audiol*. (2018) 29:417–26. doi: 10.3766/jaaa.17076
34. Abdullah NA, Wahat NHA, Curthoys IS, Abdullah A, Alias H. The feasibility of testing otoliths and semicircular canals function using VEMPs and vHIT. Malaysian Children. *J Sains Kesihatan Malaysia*. (2017) 15:179–90. doi: 10.17576/jskm-2017-1502-24
35. Dasgupta S. The video head impulse in children - initial experiences in a tertiary centre. *J Int Adv Otol*. (2015) 11 (Suppl.):7–8.
36. Perez-Fernandez N, Eza-Nunez P. Normal gain of VOR with refixation saccades in patients with unilateral vestibulopathy. *J Int Adv Otol*. (2015) 11:133–7. doi: 10.5152/iao.2015.1087
37. Korsager LE, Faber CE, Schmidt JH, Wansscher JH. Refixation saccades with normal gain values: a diagnostic problemin the video head impulse test: a case report. *Front Neurol*. (2017) 8:81. doi: 10.3389/fneur.2017.00081
38. Kelsch TA, Schaefer LA, Esquivel CR. Vestibular evoked myogenic potentials in young children: test parameters and normative data. *Laryngoscope*. (2006) 116:895–900. doi: 10.1097/01.mlg.0000214664.97049.3e
39. Maes L, De Kegel A, van Waelvelde H, Dhooge I. Rotatory and collic vestibular evoked myogenic potential testing in normal-hearing and hearing-impaired children. *Ear Hearing*. (2014) 35:e21–e. doi: 10.1097/AUD.0b013e3182a6ca91
40. Pereira AB, de Melo Silva GS, Assuncao AR, Atherino CCT, Volpe FM, Felipe L. Cervical vestibular evoked myogenic potentials in children. *Braz J Otorhinolaryngol*. (2015) 81:358–62. doi: 10.1016/j.bjorl.2014.08.019
41. Madzharova KI, Beshkova AP. Diagnostic capabilities of the vestibular evoked myogenic potential test in children with vestibular dysfunction. *Int J Otorhinolaryngol Head Neck Surg*. (2020) 6:606–11. doi: 10.18203/issn.2454-5929.ijohns20201275
42. The British Association of Audiovestibular, Physicians. *2015-2018. Guidelines and Clinical Standards*. (2019). Available online at: https://www.baap.org.uk/uploads/1/1/9/7/119752718/guidelines_for_aetiological_investigation_into_mild_to_moderatebilateral_permanent_childhood_hearing_impairment.pdf (accessed 23 June, 2020)
43. Kaur T, Johanis M, Miao T, Romiyo P, Duong C, Sun MZ, et al. CT evaluation of normal bone thickness overlying the superior semicircular canal. *J Clin.Neurosci*. (2019) 66:128–32. doi: 10.1016/j.jocn.2019.05.001
44. Sullivan L, Weinberg J, Keaney JF. Common statistical pitfalls in basic science research. *J Am Heart Assoc*. (2016) 5:e004142. doi: 10.1161/JAHA.116.004142
45. Ward BK, Wenzel A, Ritzi EK, Gutierrez-Hernandez S, Della Santina CC, Minor LLB, et al. Near-dehiscence: clinical findings in patients with thin bone over the superior semicircular canal. *Otol Neurotol*. (2013) 34:1421–8. doi: 10.1097/MAO.0b013e318287efe6
46. Bulck PV, Leupe PJ, Forton GEJ. Children with posterior semicircular canal dehiscence: a case series. *Int J Pediatric Otorhinolaryngol*. (2019) 123:51–6. doi: 10.1016/j.ijporl.2019.03.032
47. Ho ML, Halpin CF, Curtin HD. Spectrum of third window abnormalities: semicircular canal dehiscence and beyond. *Am J Neuroradiol*. (2017) 38:2–9. doi: 10.3174/ajnr.A4922
48. Phelps PD, Reardon W, Pembrey M, Bellman S, Luxon L. X-linked deafness, stapes gushers and a distinctive defect of the inner ear. *Neuroradiology*. (1991) 33:326–30. doi: 10.1007/BF00587816
49. Kumar G, Castillo M, Buchman CA. X-linked stapes gusher: CT findings in one patient. *AJNR Am J Neuroradiol*. (2003) 24:1130–2.
50. Beltagi El AH, Eisherbiny MM, El-Nil, H. Congenital X-linked stapes gusher syndrome. *Neuroradiol J*. (2012) 2:486–8. doi: 10.1177/197140091202500412
51. Altay H, Savas R, Ogut F, Kirzali T, Alper H. CT and MRI findings in X-linked progressive deafness. *Diagn Interv Radiol*. (2008) 14:117–9.
52. Papadaki E, Prassopoulos P, Bizakis J, Karampeikos S, Papadakis H, Gourtsoyiannis N. X-linked deafness with stapes gusher in females. *EurJ Radiol*. (1998) 29:71–5. doi: 10.1016/S0720-048X(98)00027-8
53. Cremers CWRG, Huygens PM. Clinical features of female heterozygotes in the X-linked mixed deafness syndrome (with perilymphatic gusher during stapes surgery). *Int J Pdiatric Otorhinolaryngol*. (1983) 6:179–85. doi: 10.1016/S0165-5876(83)80118-9
54. Wester JL, Merna C, Lewis R, Sepahdari AR, Ishiyama G, Hosokawa K, et al. Facial nerve stimulation following cochlear implantation for X-linked stapes gusher syndrome leading to identification of a novel POU3F mutation. *Int J Pediatric Otorhinolaryngol*. (2016) 91:121e123. doi: 10.1016/j.ijporl.2016.10.003
55. Wallis C, Ballo R, Wallis G, Beighton P, Goldblatt J. X-linked mixed deafness with stapes fixation in a mauritian kindred: linkage to Xq Probe pDP34. *Genomics*. (1988) 3:299–301. doi: 10.1016/0888-7543(88)90119-X
56. Kumar S, Mawby T, Sivapathasingam V, Humphries J, Ramsden J. X-linked deafness: a review of clinical and radiological findings and current management strategies. *World J Otorhinolaryngol*. (2016) 28:19–22 doi: 10.5319/wjo.v6.i1.19
57. Talbot JM, Wislon DF. Computed tomographic diagnosis of X-linked congenital mixed deafness, fixation of the stapedial footplate, and perilymphatic gusher – 4 kids. *Am J Otol*. (1994) 15:177–82.
58. Tang A, Parnes LS. X-linked progressive mixed hearing loss: computed tomography findings. *Ann Otol Rhinol Laryngol*. (1994) 103:655–7. doi: 10.1177/000348949410300814
59. Bisdas S, Lenarz M, Lenarz T, Becker H. The abnormally dilated internal auditory canal: a non-specific finding or a distinctive pathologic entity. *J Neuroradiol*. (2006) 33:275–7. doi: 10.1016/S0150-9861(06)77279-0
60. Alsabih M, Alosaimi K, Halawani R, Alzhrani F. Hearing loss in a child with cystic dilated internal auditory canal. hearing loss in a child with cystic dilated internal auditory canal. *Indian J Otol*. (2019) 25:169–72. doi: 10.4103/indianjotol.INDIANJOTOL_127_18
61. Borton SA, Mauze E, Lieu JE. Quality of life in children with unilateral hearing loss: a pilot study. *Am J Audiol*. (2010) 19:61–72. doi: 10.1044/1059-0889(2010/07-0043)
62. Bevans SE, Chen BS, Crawford JV. Acquired mixed hearing loss. In: Kountakis SE, editors. *Encyclopedia of Otolaryngology, Head and Neck Surgery*. Berlin; Heidelberg: Springer (2013). p. 15–29.
63. Merchant SN, Rosowski JJ, McKenna MJ. Superior semcircualr canal dehiscence mimicking otosclerotic hearing loss. *Adv Otorhinolaryngol*. (2007) 65:137–45. doi: 10.1159/000098790
64. Probst R, Harris FP. A comparison of transiently evoked and distortion-product otoacoustic emissions in humans. *J Am Acad Audiol*. (2018) 29:443–50.
65. Thabet EM. Transient evoked otoacoustic emissions in superior canal dehiscence syndrome. *Eur Arch Otorhinolaryngol*. (2011) 268:137–41. doi: 10.1007/s00405-010-1313-0
66. Lagman C, Ong V, Chung LK, Elhajjmoussa LK, Fong C, Wang AC, et al. Paediatric superior semicircular canal dehiscence: illustrative case and systemic review. *J Neurosurg Paediatr*. (2017) 20:196–203. doi: 10.3171/2017.3.PEDS1734
67. Kanaan AA, Raad RA, Hourani RG, Zaytoun GM. Bilateral superior semicircular canal dehiscence in a child with sensorineural hearing loss and vestibular symptoms. *Int J Paediatr Otorhinolaryngol*. (2011) 75:877–9. doi: 10.1016/j.ijporl.2011.03.019
68. Wenzel A, Stuck BA, Servais JJ, Hormann K, Hulse M, Hulse R. Superior canal dehiscence syndrome in children – a case report. *Int J Paediatr Otorhinolaryngol*. (2015) 79:1573–8. doi: 10.1016/j.ijporl.2015.05.022
69. Castellucci A, Brandolini C, Piras G, Modugno GC. Tympanometric findings in superior semicircular canal dehiscence syndrome. *Acta Otorhinolaryngol Ital*. (2013) 33:112–20.
70. Hunter LL, Ries DT, Schlauch RS, Levine SC, Ward WD. Safety and clinical performance of acoustic reflex tests. *Ear Hear*. (1999) 20:506–14. doi: 10.1097/00003446-199912000-00006
71. Teixeira ED, Fonseca MT. Superior semicircular canal dehiscence without vestibular symptoms. *Int Arch Otorhinolaryngol*. (2014) 18:210–2. doi: 10.1055/s-0033-1351670
72. Halmyagi GM, Chen L, MacDougall HG, Weber KP, McGarvie LA, Curthoys IS. The video head impulse test. *Front Neurol*. (2017) 8:258. doi: 10.3389/fneur.2017.00258
73. Sommerfleck PA, Gonzalez Macchi ME, Weinschelbaum R, De Bagge MD, Bernaldez P, Carmona S. Balance disorders in childhood: main etiologies

according to age. usefulness of the video head impulse test. *Int J Pediatr Otorhinolaryngol.* (2016) 87:148–53. doi: 10.1016/j.ijporl.2016.06.020
74. Hamilton SS, Zhou G, Brodsky JR. Video head impulse testing (VHIT) in the pediatric population. *Int J Pediatr Otorhinolaryngol.* (2015) 79:1283–7. doi: 10.1016/j.ijporl.2015.05.033
75. Alizadeh S, Rahbar N, AhadiM, Sameni SJ. *Normative vestibulo-ocular reflex Data in 6-12 Year-Old Children Using Video Head Impulse Test*. Available online at: https://avr.tums.ac.ir/index.php/avr/article/view/190
76. Bayram A, Kaya A, Mutlu M, Hira I, Tofar M, Ozcan I. Clinical practice of horizontal video head impulse test in healthy children. *Kulak Burun Bogaz Ihtis Derg.* (2017) 27:79–83. doi: 10.5606/kbbihtisas.2017.75725
77. Souza Renata P, Agata PD, Malgorzata S, Wieslaw K. Application of the video head impulse test in the diagnostics of the balance system in children. *Pol Otorhino Rev.* (2015) 4:6–11. doi: 10.5604/20845308.1150794
78. Hulse R, Hormann K, Servais JJ, Hulse M, Wenzel A. Clinical experience with video head impulse test in children. *Int J Pediatr Otorhinolaryngol.* (2015) 79:1288–93. doi: 10.1016/j.ijporl.2015.05.034
79. Curthoys IS, Manzari L. Clinical application of the head impulse test of semicircular canal function. *Hear Balance Commun.* (2017) 15:113–26. doi: 10.1080/21695717.2017.1353774
80. Jung JJ, Suh MJ, Kim SH. Discrepancies between video head impulse and caloric tests in patients with enlarged vestibular aqueduct. *Laryngoscope.* (2017) 127:921–6. doi: 10.1002/lary.26122
81. Zhou G, Gopen Q. Characteristics of vestibular evoked myogenic potentials in children with enlarged vestibular aqueduct. *Laryngoscope.* (2011) 121:220–5. doi: 10.1002/lary.21184
82. Zhou G, Gopen Q, Poe DS. Clinical and diagnostic characterisation of canal dehiscence syndrome: a great otologic mimicker. *Otol Neurotol.* (2007) 28:920–26. doi: 10.1097/MAO.0b013e31814b25f2
83. Kuhn JJ, Lavender VH, Hunter L, McGuire SE, Meinzen-Derr J, Keith R, et al. Ocular vestibular evoked myogenic potentials: normative findings in children. *J Am Acad Audiol.* (2018) 29:443–50. doi: 10.3766/jaaa.17086
84. Rodrigues AI, Thomas MLA, Janky KL. Air-conducted vestibular evoked myogenic potential testing in children, adolescents, and young adults: thresholds, frequency tuning, and effects of sound exposure. *Ear Hear.* (2019) 40:192–203. doi: 10.1097/AUD.0000000000000607
85. Figaji AA. Anatomical and physiological differences between children and adults relevant to traumatic brain injury and the implications for clinical assessment and care. *Front Neurol.* (2017) 8:685. doi: 10.3389/fneur.2017.00685

Conflict of Interest: The authors declare that the research was conducted in the absence of any commercial or financial relationships that could be construed as a potential conflict of interest.

frontiers in Neurology

ORIGINAL RESEARCH
published: 08 October 2020
doi: 10.3389/fneur.2020.552495

Impact of Superior Canal Dehiscence Syndrome on Health Utility Values: A Prospective Case-Control Study

Ibrahim Ocak[1,2], Vedat Topsakal[1,2], Paul Van de Heyning[1,2], Gilles Van Haesendonck[1,2], Cathérine Jorissen[1,2], Raymond van de Berg[1,2,3,4], Olivier M. Vanderveken[1,2] and Vincent Van Rompaey[1,2]*

[1] Department Otorhinolaryngology & Head and Neck Surgery, Antwerp University Hospital, Antwerp, Belgium, [2] Translational Neurosciences, Faculty of Medicine and Health Sciences, University of Antwerp, Antwerp, Belgium, [3] Division of Balance Disorders, Department of Otorhinolaryngology and Head and Neck Surgery, Maastricht University Medical Center, Maastricht, Netherlands, [4] Faculty of Physics, Tomsk State University, Tomsk, Russia

Introduction: Superior canal dehiscence syndrome (SCDS) is a condition characterized by a defect in the bone overlying the superior semicircular canal, creating a third mobile window into the inner ear. Patients can experience disabling symptoms and opt for surgical management. Limited data are available on the impact of SCDS on health-related quality of life (HRQoL) and disease-specific HRQoL more specifically.

Objective: To perform a prospective analysis on generic HRQoL in SCDS patients compared to healthy age-matched controls.

Methods: A prospective study was performed on patients diagnosed with SCDS and who did not undergo reconstructive surgery yet. Patients were recruited between November 2017 and January 2020 and asked to complete the Health Utility Index (HUI) Mark 2 (HUI2)/Mark 3 (HUI3) questionnaire. For the control group, age-matched participants without otovestibular pathology or other chronic pathology were recruited. The multi-attribute utility function (MAUF) score was calculated for the HUI2 and HUI3. Results of both groups were compared using the Mann-Whitney U test.

Results: A total of 20 patients completed the questionnaire. Age ranged from 37 to 79 years with a mean age of 56 years (45% males and 55% females). The control group consisted of 20 participants with a mean age of 56.4 years and ranged from 37 to 82 years (35% males and 65% females). For the case group, median HUI2 MAUF score was 0.75 and median HUI3 MAUF score was 0.65. For the control group, the median scores were 0.88 and 0.86 respectively. There was a statistically significant difference for both HUI2 ($p = 0.024$) and HUI3 ($p = 0.011$). SCDS patients had a worse generic HRQoL than age-matched healthy controls. One patient with unilateral SCDS had a negative HUI3 MAUF score (−0.07), indicating a health-state worse than death.

Conclusion: SCDS patients have significantly lower health utility values than an age-matched control group. This confirms the negative impact of SCDS on generic HRQoL, even when using an instrument that is not designed to be disease-specific but to assess health state in general. These data can be useful to compare impact on HRQoL among diseases.

Keywords: vestibular system, autophony, health-realeted quality of life, labyrinth diseases, vertigo

OPEN ACCESS

Edited by:
Tetsuo Ikezono, Saitama Medical University, Japan

Reviewed by:
Kristen Leigh Janky, Boys Town, United States
Hong Ju Park, University of Ulsan, South Korea
Carleton Eduardo Corrales, Brigham and Women's Hospital and Harvard Medical School, United States

****Correspondence:***
Ibrahim Ocak
ibrahim.ocak@uza.be

Specialty section:
This article was submitted to Neuro-Otology, a section of the journal Frontiers in Neurology

Received: *16 April 2020*
Accepted: *07 September 2020*
Published: *08 October 2020*

Citation:
Ocak I, Topsakal V, Van de Heyning P, Van Haesendonck G, Jorissen C, van de Berg R, Vanderveken OM and Van Rompaey V (2020) Impact of Superior Canal Dehiscence Syndrome on Health Utility Values: A Prospective Case-Control Study. Front. Neurol. 11:552495. doi: 10.3389/fneur.2020.552495

INTRODUCTION

First described by Lloyd Minor in 1998 (1), superior canal dehiscence syndrome (SCDS) is characterized by a defect in the bony cover of the superior semicircular canal, which creates a third mobile window into the inner ear, in addition to the round and oval window (2, 3). This third window alters the physiologic inner ear mechanics and results in a hydroacoustic shunting away from the cochlea, toward the bony defect in the labyrinth, stimulating the vestibular end organs (4). SCDS also causes enhanced bone conduction thresholds, leading to an audiometric air-bone gap, with normal stapedial reflexes (3–5). These pathophysiological features explain the symptoms patients with SCDS can experience, including autophony, aural fullness, pulsatile and non-pulsatile tinnitus, bone conduction hyperacusis, imbalance and vertigo. Gaze-evoked tinnitus, hearing distortion and oscillopsia are also possible symptoms (4, 6).

Management of SCDS depends on the severity of the symptoms. In case of mild symptoms, conservative management may include avoiding symptom triggers or placement of a tympanostomy tube for patients with primarily pressure induced symptoms (7, 8). For patients with disabling symptoms, various surgical options can be offered (9–13). Surgery has not only the potential to improve specific symptoms (14–20), but it can also improve health-related quality of life (HRQoL) (21).

Limited data are available on the impact of SCDS on generic health-related quality of life (HRQoL) and even less on disease-specific HRQoL. A distinction can be made between generic and disease-specific HRQoL instruments. Disease-specific instruments measure the HRQoL for a specific illness, allowing to detect changes after medical and/or surgical treatment or over time when treating conservatively. On the contrary, generic HRQoL instruments are designed to assess the health state in general and are not designed to detect changes in HRQoL due to a specific disease. They can be used to compare HRQoL with other chronic illnesses and a healthy population, which is not possible with a disease specific HRQoL (22). They can also be used to calculate quality adjusted life years (QALYs) and to determine cost-effectiveness of medical treatments (23, 24).

An example of generic HRQoL is the Health Utility Index (HUI). HUI consists of 2 systems, the HUI mark 2 (HUI2) and HUI mark 3 (HUI3), which are complementary to each other. HUI not only measures generic HRQoL scores, but makes it also possible to calculate single-attribute scores of morbidity for each domain of functioning (25).

The aim of this study was to perform a prospective analysis on generic HRQoL in SCDS patients compared to healthy age-matched controls.

MATERIALS AND METHODS

Study Design

Both patients with SCDS and controls received a letter of introduction, an explanation of the purpose of the study, and the Health Utility Value Mark 2/3 questionnaire in Dutch. Informed consent was obtained from each participant as part of the survey. Study approval was obtained from the ethical committee of the University Hospital Antwerp and the University of Antwerp (B30020173349).

Study Population

The study population comprised two groups: case and control. Cases included patients diagnosed with SCDS who had not undergone surgery for SCDS (yet). The diagnosis of SCDS was based on the combination of: (1) Symptoms related to SCDS (bone conduction hyperacusis, and/or pulsatile tinnitus, and/or sound-induced vertigo/oscillopsia, and/or pressure induced vertigo/oscillopsia); (2) Low cervical vestibular evoked myogenic potentials (cVEMPs) thresholds; (3) CT scan showing dehiscence of the superior semicircular canal (3). Surgery for SCDS in the past was an exclusion criterion. Patients younger than 18 years old were also excluded. Subjects were recruited from the tertiary neurotology clinics at the Antwerp University Hospital. The control group contained age-matched healthy controls without SCDS and without ear pathology. Controls were recruited from people accompanying patients at their visit in the department of Otorhinolaryngology and Head & Neck Surgery. Participants were questioned whether they had any hearing or balance disorders or other chronic diseases. Control participants with an otovestibular and/or a chronic disease, e.g., diabetes mellitus, pulmonary disease and cardiovascular pathology, were excluded. Hypertension was not an exclusion criterion because of its high prevalence (26). For both groups, questionnaires with incomplete data were excluded from the study. Questionnaires were sent to, and, collected from both groups between November 2017 and January 2020.

Vestibular Testing and CT Scan

All included patients underwent a cVEMP. At the University Hospital Antwerp, air-conducted 500 Hz tone bursts were delivered monoaurally via insert phones and responses were recorded with an auditory evoked potential system equipped with electromyographic software (Neuro-Audio, Difra, Belgium), with self-adhesives electrodes (Blue sensor, Ambu, Denmark) on the sternocleidomastoid muscle. The delivered high intensity auditory stimuli resulted in a typically biphasic shape. If the wave was absent at 100 dB nHL, cVEMP response was considered to be absent. A cVEMP threshold of $\leq$75 dB nHL (99 dB SPL) was considered to be indicative for the presence of a third mobile window.

For the detection of dehiscence of the superior semicircular canal, a high resolution CT scan (0.625 mm slice thickness) of the temporal bone with reconstructions in the plane of the superior semicircular canal was performed. The scans were interpreted by experienced radiologists.

Health Utility Index Mark 2 (HUI2)/Mark 3 (HUI3)

The HUI measurement system consists of a validated 15-item questionnaire for self-completion. It is designed to collect information required for classification of the participants' health status according to both the HUI2 an HUI3 classification systems.

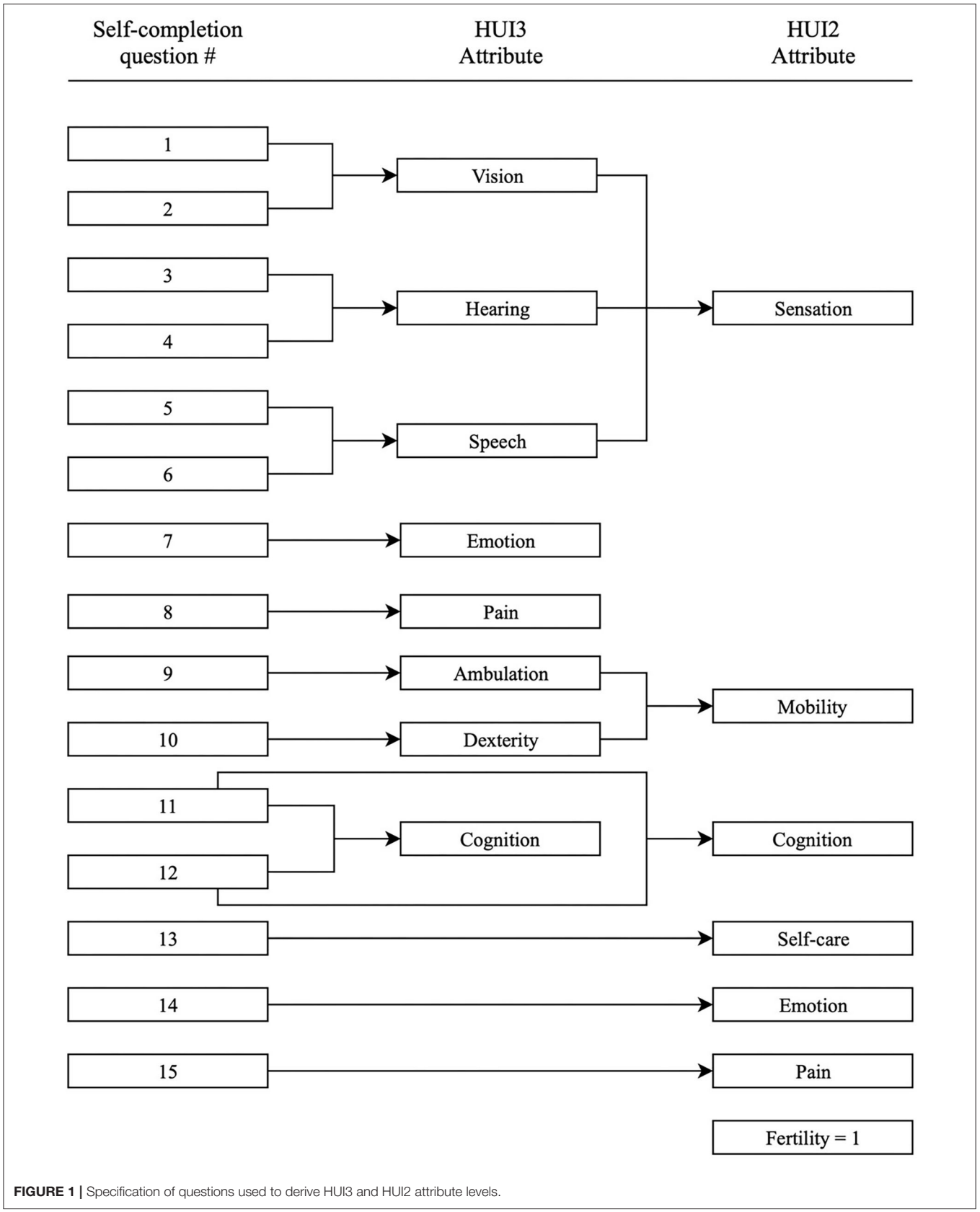

FIGURE 1 | Specification of questions used to derive HUI3 and HUI2 attribute levels.

The HUI2 consists of seven domains of functioning: sensation, mobility, cognition, self-care, emotion, pain and fertility (fertility is assumed to be level 1, "able to have children with a fertile spouse," in the HUI mark 2/mark 3 and is not asked to the subject). The HUI3 contains 8 domains of functioning, namely vision, hearing, speech, emotion, pain, ambulation, dexterity and cognition (**Figure 1**). Each domain has 5 or 6 levels of (dis)ability. In HUI3, sensation is divided in vision, hearing and speech, and mobility is divided in ambulation and dexterity. HUI2 contains self-care and fertility which is not implemented in HUI3. This makes HUI2 and HUI3 complementary to each. For both the HUI2 and HUI3 a multi-attribute utility function (MAUF) score can be calculated, to evaluate the general health state and HRQoL, with 1 equal to perfect health and 0 equal to death. Negative scores are possible and indicate a health state worse than death. The MAUF score can be classified in to disability categories; none, mild, moderate and severe. Different schemes are used for HUI2 and HUI3 as summed up below (25).

	HRQoL scores	Disability category
HUI2	1.00	None
	0.91 through 0.99	Mild
	0.80 through 0.90	Moderate
	<0.80	Severe
HUI3	1.00	None
	0.89 through 0.99	Mild
	0.70 through 0.88	Moderate
	<0.70	Severe

Statistical Analysis

The statistical analysis was carried out on two levels: first, a comparison of responses between the case and control groups, and secondly, analysis of responses within the case group for following variables: uni- and bilateral SCDS, and subjects opting for surgery after completing the questionnaire. All analyses were performed with IBM SPSS statistics version 25 (IBM Corp., Armonk, NY, USA).

Kolmogorov-Smirnov test was used to examine the distribution of HUI2 and HUI3 MAUF scores for both case and control group. Considering the small sample size, and normal distribution of answers (see below), the non-parametric Mann-Whitney U test was performed to compare responses between the case and control groups. The same test was also used to compare differences within the case group. A p-value <0.05 was used to determine statistical significance.

RESULTS

Case Group

The case group consisted of 20 patients diagnosed with SCDS who had not undergone surgery for SCDS. All patients had symptoms related to SCDS, low cVEMP potentials and HRCT scan showing the dehiscence. The age ranged from 37 to 79 years with an average of 55.9 years (median 58.5 years) and standard deviation of 12.6 years. There were 11 (55%) female and 9 (45%) male patients in the case group. From the 20 patients, 17 (85.0%) had a unilateral bony defect over the superior semicircular canal, of which 7 (41.2%) were right-sided and 10 (58.8%) left-sided. Three patients (15.0%) had bilateral defects. A response rate of 100% was achieved for the case group because almost all patients completed the questionnaire directly at the clinic.

Control Group

The control group consisted of 20 age-matched persons without otovestibular pathology or symptomatology and without any

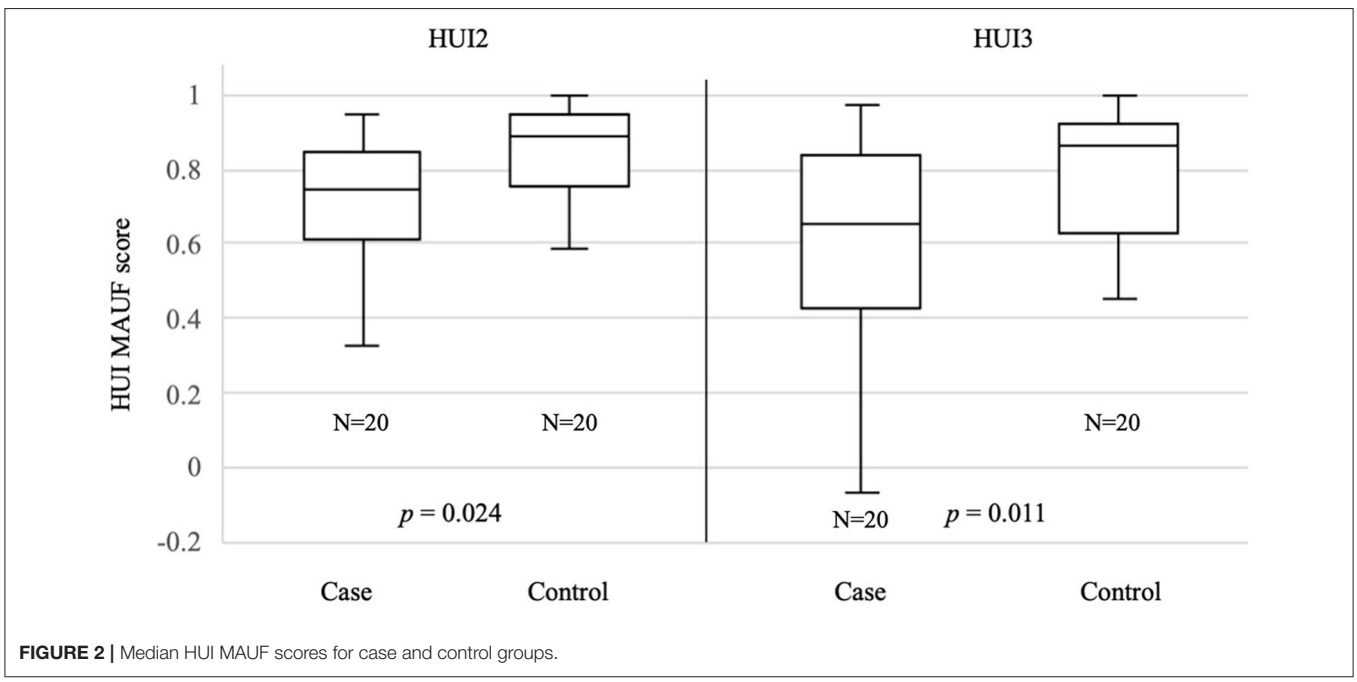

FIGURE 2 | Median HUI MAUF scores for case and control groups.

chronic disease. Age of the individuals in this group ranged from 30 to 82 years with an average of 55.9 years (median 58.5 years) and standard deviation of 12.6 years. The gender distribution was as follows: female 65.0% ($n = 13$) and male 35.0% ($n = 7$). For the control group, a high response rate of 83% was achieved. Four persons refused to participate in this study. A total of 20 healthy participants completed the questionnaire.

HUI2 and HUI3 Multi-Attribute Utility Function (MAUF)

Figure 2 shows the boxplot of HUI2 and HUI3 MAUF for both groups. The median HUI2 MAUF score for case group was 0.75 with a standard deviation (SD) of 0.22. For the control group, the median was 0.88 (SD= 0.14). The median HUI3 MAUF score for the case group was 0.65 (SD = 0.28). Median HUI3 MAUF score for control group was 0.86 (SD = 0.17). Comparison of case and control groups showed significantly difference for both the HUI2 MAUF ($p = 0.024$) and HUI3 MAUF ($p = 0.011$) scores. SCDS patients had a worse HRQoL than age-matched healthy controls. One patient with unilateral SCDS had a negative HUI3 MAUF score (−0.07), indicating a health-state worse than death.

The median and mean of the single attribute scores for each domain of functioning and the MAUF scores are shown in **Table 1**. Analysis of the single attribute scores showed significantly worse scores for HUI2 emotion ($p = 0.023$), HUI2 pain ($p = 0.040$) and HUI3 pain ($p = 0.012$) in the case group.

Comparison of uni- vs. bilateral SCDS and HUI2 showed median MAUF score of 0.75 (SD = 0.21) for the unilateral SCDS group, and 0.64 (SD = 0.28) for the bilateral SCDS group. The median HUI3 MAUF score for the unilateral group was 0.66 (SD = 0.29) and 0.43 (SD = 0.28) for the bilateral group. There was no statistically significant difference for HUI2 ($p = 0.20$) and HUI3 ($p = 0.53$) scores for uni- vs. bilateral SCDS (**Figure 3**).

After completing the questionnaire, 6 patients opted for surgery. Comparison of surgery vs. conservative approach within the case group showed no statistically significant differences for HUI2 ($p = 0.19$) and HUI3 ($p = 0.36$). The median HUI2 MAUF score was 0.79 (SD = 0.22) and median HUI3 MAUF score was 0.66 (SD = 0.32) for the conservative group. The surgery group had a median HUI2 MAUF score 0.69 (SD = 0.21) and a median HUI3 MAUF score of 0.53, with a SD of 0.19 (**Figure 4**). It is important to mention that all the patients completed the questionnaire prior to any treatment. A comparison of pre- and postoperative was not performed.

TABLE 1 | Single and multi-attribute scores of study participants.

	SCDS			Control			
	Mean	**Median**	**SD**	**Mean**	**Median**	**SD**	***p*-value**
HUI2 MAUF*	0.70	0.75	0.22	0.84	0.88	0.14	0.024
Sensation	0.92	0.92	0.05	0.92	0.95	0.08	0.289
Mobility	1.00	1.00	0.01	0.99	1.00	0.04	0.336
Cognition	0.97	1.00	0.04	0.99	1.00	0.02	0.218
Self-care	1.00	1.00	0.01	1.00	1.00	0	0.317
Emotion	0.93	0.93	0.07	0.97	1.00	0.05	0.023
Pain	0.86	0.97	0.20	0.96	1.00	0.09	0.040
HUI3 MAUF	0.59	0.65	0.28	0.80	0.86	0.17	0.011
Vision	0.97	0.98	0.04	0.98	0.98	0.02	0.989
Hearing	0.97	1.00	0.07	0.97	1.00	0.10	0.678
Speech	0.98	1.00	0.04	0.99	1.00	0.02	0.301
Emotion	0.93	0.95	0.09	0.97	1.00	0.05	0.096
Pain	0.89	0.90	0.09	0.96	0.96	0.04	0.012
Ambulation	0.99	1.00	0.03	0.99	1.00	0.03	0.620
Dexterity	1.00	1.00	0.01	1.00	1.00	0	0.799
Cognition	0.91	1.00	0.15	0.98	1.00	0.03	0.355

**Fertility is considered to be 1.*

HUI, Health Utility Index; MAUF, multi-attribute utility function; SCDS, superior canal dehiscence syndrome.

Underlined values are $p < 0.05$ indicating statistical significance.

DISCUSSION

The aim of this study was to perform a prospective analysis on generic HRQoL in SCDS patients compared to healthy age-matched controls. Patients with SCDS can experience a wide variety of symptoms. If the symptoms are disabling and have a negative impact on the HRQoL, surgery can be offered to patients. However, limited data are available on the impact of SCDS on generic HRQoL. Generic HRQoL can, for example, be used to calculate quality adjusted life years (QALYs) and to determine cost-effectiveness of medical treatments, like transmastoid vs. middle cranial fossa approach or plugging vs. resurfacing for SCDS repair (27). Our data set can also be used to calculate QALYs and to compare with other studies. However, a more reliable comparison can be made with a larger data set (multicentric for example).

Comparison of case and control group revealed significant difference in HUI2 and HUI3 MAUF scores, with lower scores for the case group. Analysis of the single attribute levels showed worse scores for HUI2 emotion ($p = 0.023$), HUI2 pain ($p = 0.040$) and HUI3 pain ($p = 0.012$) in the case group. Lower scores for pain may be explained by hyperacusis but further research is needed. Patients with SCDS can also experience depression, as shown in the study of Wackym et al. They investigated the cognitive and neurobehavioral outcome before and after surgical repair of otic capsule dehiscence. Preoperative completion of the Beck Depression Inventory-II showed mild depression, which improved after surgery (28). This can explain the negative impact on the attribute "emotion" in our study population.

The subgroup analysis of the case group did not reveal any statistically significant differences comparing bilateral to unilateral SCDS patients and patients who opted for surgery compared to patients who chose a conservative approach. Surgery has the potential to improve symptoms such as autophony, and pulsatile tinnitus (14, 15, 29). However, these symptoms are not measured by HUI, because it is a generic HRQoL instrument. This could (partially) explain why there was no significant difference in HUI scores between the patients who opted for surgery and the patients who chose a conservative approach. It is important to mention that all the patients completed the questionnaire prior to

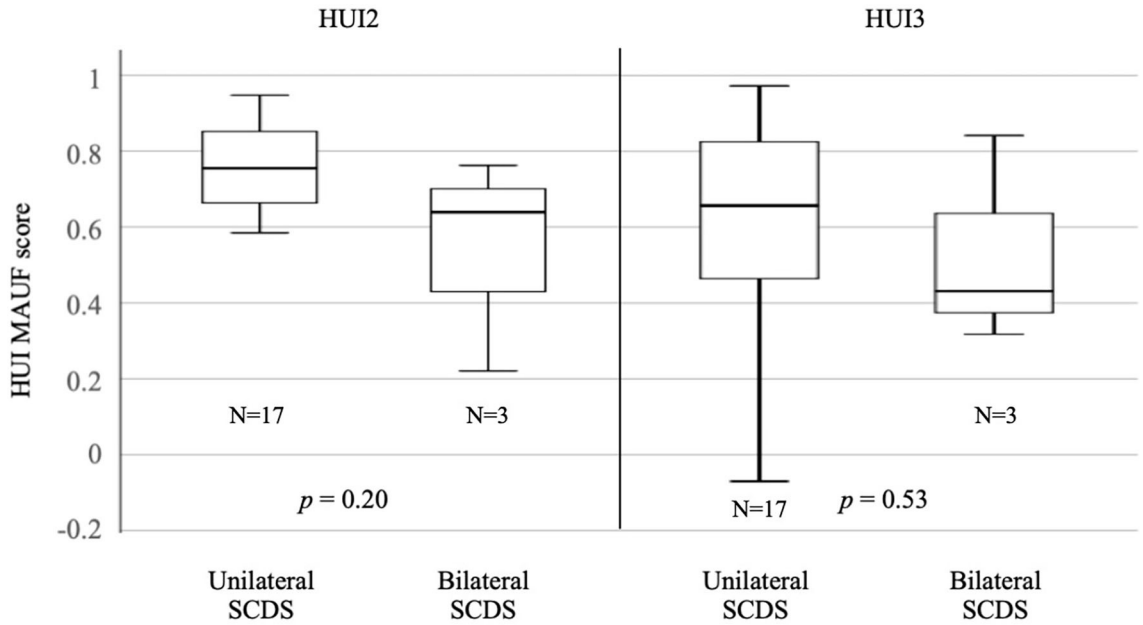

FIGURE 3 | Median HUI MAUF scores for uni- vs. bilateral SCDS.

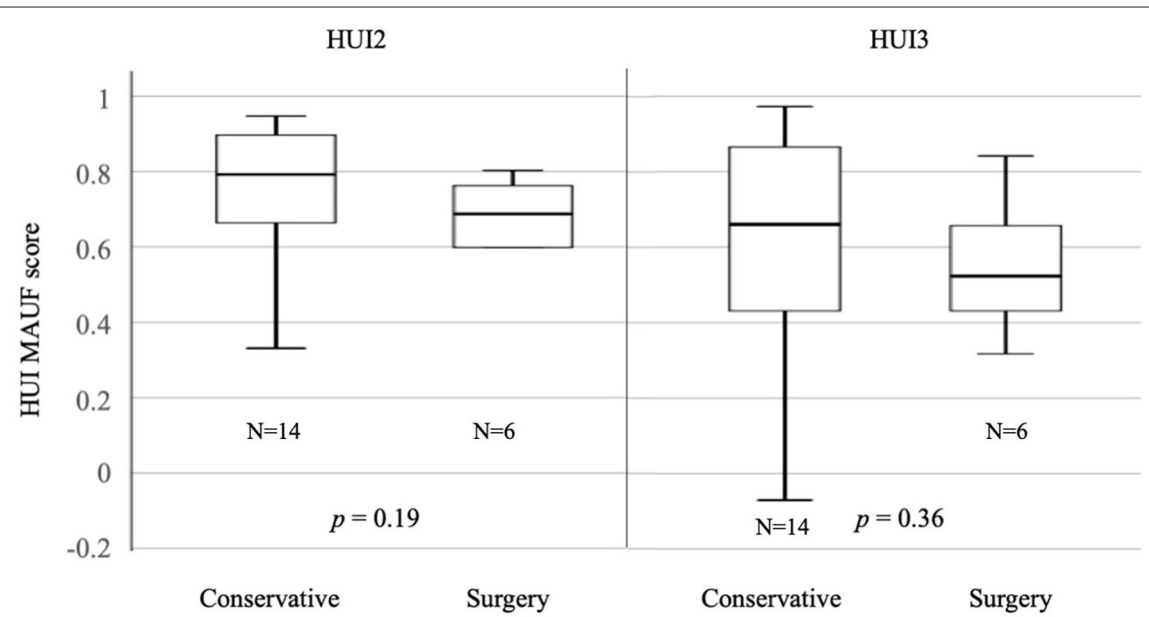

FIGURE 4 | Median HUI2 MAUF scores for conservative vs. surgical approach.

any treatment. A comparison of pre- and postoperative was not performed.

Analysis of health utility values (HUV) after surgery for SCDS was performed by Remenschneider et al. They investigated the HUV in 51 patients with SCDS. The HUV was measured by Short-Form 6 Dimension Questionnaire. Twenty-three of 51 patients opted for surgery. There was no significant difference between the operated and non-operated group preoperatively. We had a similar finding for the preoperative comparison of the HUI values between the conservative and surgery group, however the sample size in our study was lower. Analysis of HUV after surgery showed a significant improvement of the HUV (21). Allsopp et al. investigated QoL outcomes after transmastoid plugging of SCDS retrospectively. Generic HRQoL was calculated

by the Glasgow Benefit Inventory (GBI). Ten patients were enrolled in the study. Postoperative GBI values were significantly better (30). These results indicate that surgery is a good option which can increase the HRQoL in patients with SCDS. In this study, postoperative HUI values were not compared with preoperative results, because postoperative questionnaires were not (yet) filled by the patients who opted for surgery.

Generic HRQoL can also be used to compare HRQoL among different pathologies. Sun et al. compared HRQoL, measured with the dizziness handicap index and HUI3, in 15 patients with bilateral vestibular deficiency (BVD), 22 patients with unilateral vestibular deficiency (UVD) and 23 healthy controls. BVD patients had a significantly decreased HRQoL compared to UVD and healthy controls. The mean HUI3 MAUF score was 0.39 (SD = 0.34) for the BVD, 0.63 (SD = 0.26) for the UVD and 0.94 (SD = 0.09) for the control group (31). Our data demonstrated a median HUI3 MAUF score of 0.65 (SD = 0.28) for the SCDS patients and 0.86 (SD = 0.17) for the control group as shown in **Figure 2**. Patients with SCDS had a worse HUI3 score with statistically significant difference compared to healthy controls. Both BVD and SCDS can have a negative impact on HRQoL and therefore surgical treatments might be considered or developed for SCDS and BVD respectively, in case of disabling symptoms (32, 33).

Carlsson et al. investigated the QoL in 369 patients with sudden sensorineural hearing loss (SSHL). QoL was measured by the EuroQoL 5D, problems impact rating scale and hospital anxiety and depression scale. In patients with tinnitus and remaining vertigo after SSHL, a significant negative impact on all three QoL measurements was found (34).

The major limitation of this study is the rather low sample size. Sample size was even lower when performing subgroup analysis. There were only three patients with bilateral SCDS and six patients opting for surgery after completing the questionnaire. This makes statistical analysis difficult and no statistically significant differences were calculated in the subgroup analysis.

Even though our data highlights that SCDS can have an impact on the generic HRQoL, the syndrome can cause a wide range of symptoms and clinical presentation can be different for each case. It can also be difficult for patients to spontaneously mention some of the "odd" symptoms, like "hearing the eyeballs move." This points to the need of an evidence-based disease-specific patient-reported outcome measure (PROM) (6). With such a measurement, the prevalence and severity of the symptoms can be evaluated, and the impact on HRQoL might be estimated (35).

CONCLUSION

SCDS patients have significantly lower generic HRQoL scores, measured with HUI2 and HUI3, than an age-matched control group. This confirms the negative impact of SCDS on generic HRQoL, even when using an instrument that is not designed to assess disease-specific HRQoL but to assess health state in general. These data can be useful to compare impact on HRQoL among diseases. In addition, there is a need for a disease-specific PROM for SCDS in order to properly investigate the prevalence and severity of symptoms SCDS patients are experiencing. Such a measurement can also be useful to evaluate treatment more objectively over time, than only history taking.

DATA AVAILABILITY STATEMENT

The raw data supporting the conclusions of this article will be made available by the authors, without undue reservation.

ETHICS STATEMENT

The studies involving human participants were reviewed and approved by Antwerp University Hospital/University of Antwerp Ethics Committee. The patients/participants provided their written informed consent to participate in this study.

AUTHOR CONTRIBUTIONS

VVR conceived the idea and developed the theory of the research. IO carried out the study and performed the statistical analysis. Database of patients was started by GVH and updated by VVR and IO. Controls were recruited by IO. Questionnaires were processed and analyzed by IO. CJ helped with the writing of the cVEMP and HUI methodology. The manuscript was reviewed by VT, PVDH, GVH, CJ, OV, RVDB, VVR and IO. All authors contributed to the article and approved the submitted version.

REFERENCES

1. Minor LB, Solomon D, Zinreich JS, Zee DS. Sound- and/or pressure-induced vertigo due to bone dehiscence of the superior semicircular canal. *Arch Otolaryngol Head Neck Surg.* (1998) 124:249–58. doi: 10.1001/archotol.124.3.249
2. Lee GS, Zhou G, Poe D, Kenna M, Amin M, Ohlms L, et al. Clinical experience in diagnosis and management of superior semicircular canal dehiscence in children. *Laryngoscope.* (2011) 121:2256–61. doi: 10.1002/lary.22134
3. Ward BK, Carey JP, Minor LB. Superior canal dehiscence syndrome: lessons from the first 20 years. *Front Neurol.* (2017) 8:177. doi: 10.3389/fneur.2017.00177
4. Bi WL, Brewster R, Poe D, Vernick D, Lee DJ, Eduardo Corrales C, et al. Superior semicircular canal dehiscence syndrome. *J Neurosurg.* (2017) 127:1268–76. doi: 10.3171/2016.9.JNS16503
5. Rosowski JJ, Songer JE, Nakajima HH, Brinsko KM, Merchant SN. Clinical, experimental, and theoretical investigations of the effect of superior semicircular canal dehiscence on hearing mechanisms. *Otol Neurotol.* (2004) 25:323–32. doi: 10.1097/00129492-200405000-00021
6. Naert L, Van de Berg R, Van de Heyning P, Bisdorff A, Sharon JD, Ward BK, et al. Aggregating the symptoms of superior semicircular canal dehiscence syndrome. *Laryngoscope.* (2018) 128:1932–8. doi: 10.1002/lary.27062
7. Chien WW, Carey JP, Minor LB. Canal dehiscence. *Curr Opin Neurol.* (2011) 24:25–31. doi: 10.1097/WCO.0b013e328341ef88
8. Minor LB. Clinical manifestations of superior semicircular canal dehiscence. *Laryngoscope.* (2005) 115:1717–27. doi: 10.1097/01.mlg.0000178324.55729.b7
9. Van Rompaey V, Van de Heyning P. "Superior semicircular canal dehiscence" -syndroom: een nieuwe binnenooraandoening. *Tijdschr voor Geneeskunde.* (2015) 71:1104–9. doi: 10.2143/TVG.71.17.2001934

10. Amoodi HA, Makki FM, McNeil M, Bance M. Transmastoid resurfacing of superior semicircular canal dehiscence. *Laryngoscope.* (2011) 121:1117–23. doi: 10.1002/lary.21398
11. Brantberg K, Bergenius J, Mendel L, Witt H, Tribukait A, Ygge J. Symptoms, findings and treatment in patients with dehiscence of the superior semicircular canal. *Acta Otolaryngol.* (2001) 121:68–75. doi: 10.1080/000164801300006308
12. Van Haesendonck G, Van de Heyning P, Van Rompaey V. Retrospective cohort study on hearing outcome after transmastoid plugging in superior semicircular canal dehiscence syndrome: our experience. *Clin Otolaryngol.* (2016) 41:601–6. doi: 10.1111/coa.12539
13. Silverstein H, Kartush JM, Parnes LS, Poe DS, Babu SC, Levenson MJ, et al. Round window reinforcement for superior semicircular canal dehiscence: a retrospective multi-center case series. *Am J Otolaryngol.* (2014) 35:286–93. doi: 10.1016/j.amjoto.2014.02.016
14. Crane BT, Lin FR, Minor LB, Carey JP. Improvement in autophony symptoms after superior canal dehiscence repair. *Otol Neurotol.* (2010) 31:140–6. doi: 10.1097/MAO.0b013e3181bc39ab
15. Crane BT, Minor LB, Carey JP. Superior canal dehiscence plugging reduces dizziness handicap. *Laryngoscope.* (2008) 118:1809–13. doi: 10.1097/MLG.0b013e31817f18fa
16. Goddard JC, Wilkinson EP. Outcomes following semicircular canal plugging. *Otolaryngol Head Neck Surg.* (2014) 151:478–83. doi: 10.1177/0194599814538233
17. Janky KL, Zuniga MG, Carey JP, Schubert M. Balance dysfunction and recovery after surgery for superior canal dehiscence syndrome. *Arch Otolaryngol Head Neck Surg.* (2012) 138:723–30. doi: 10.1001/archoto.2012.1329
18. Jung DH, Lookabaugh SA, Owoc MS, McKenna MJ, Lee DJ. Dizziness is more prevalent than autophony among patients who have undergone repair of superior canal dehiscence. *Otol Neurotol.* (2015) 36:126–32. doi: 10.1097/MAO.0000000000000531
19. Limb CJ, Carey JP, Srireddy S, Minor LB. Auditory function in patients with surgically treated superior semicircular canal dehiscence. *Otol Neurotol.* (2006) 27:969–80. doi: 10.1097/01.mao.0000235376.70492.8e
20. Ward BK, Agrawal Y, Nguyen E, Della Santina CC, Limb CJ, Francis HW, et al. Hearing outcomes after surgical plugging of the superior semicircular canal by a middle cranial fossa approach. *Otol Neurotol.* (2012) 33:1386–91. doi: 10.1097/MAO.0b013e318268d20d
21. Remenschneider AK, Owoc M, Kozin ED, McKenna MJ, Lee DJ, Jung DH. Health utility improves after surgery for superior canal dehiscence Syndrome. *Otol Neurotol.* (2015) 36:1695–701. doi: 10.1097/MAO.0000000000000886
22. Wells GA, Russell AS, Haraoui B, Bissonnette R, Ware CF. Validity of quality of life measurement tools–from generic to disease-specific. *J Rheumatol Suppl.* (2011) 88:2–6. doi: 10.3899/jrheum.110906
23. Karnon J. Heath state utility values for cost-effectiveness models. *Pharmacoeconomics.* (2017) 35(Suppl. 1):1–3. doi: 10.1007/s40273-017-0537-x
24. Finch AP, Brazier JE, Mukuria C. What is the evidence for the performance of generic preference-based measures? A systematic overview of reviews. *Eur J Health Econ.* (2018) 19:557–70. doi: 10.1007/s10198-017-0902-x
25. Horsman J, Furlong W, Feeny D, Torrance G. The Health Utilities Index (HUI): concepts, measurement properties and applications. *Health Qual Life Outcomes.* (2003) 1:54. doi: 10.1186/1477-7525-1-54
26. Williams B, Mancia G, Spiering W, Agabiti Rosei E, Azizi M, Burnier M, et al. 2018 ESC/ESH Guidelines for the management of arterial hypertension: The Task Force for the management of arterial hypertension of the European Society of Cardiology and the European Society of Hypertension: The Task Force for the management of arterial hypertension of the European Society of Cardiology and the European Society of Hypertension. *J Hypertens.* (2018) 36:1953–2041. doi: 10.1097/HJH.0000000000001940
27. Rodgers B, Lin J, Staecker H. Transmastoid resurfacing versus middle fossa plugging for repair of superior canal dehiscence: comparison of techniques from a retrospective cohort. *World J Otorhinolaryngol Head Neck Surg.* (2016) 2:161–7. doi: 10.1016/j.wjorl.2016.11.001
28. Wackym PA, Balaban CD, Mackay HT, Wood SJ, Lundell CJ, Carter DM, et al. Longitudinal cognitive and neurobehavioral functional outcomes before and after repairing otic capsule dehiscence. *Otol Neurotol.* (2016) 37:70–82. doi: 10.1097/MAO.0000000000000928
29. Thomeer H, Bonnard D, Castetbon V, Franco-Vidal V, Darrouzet P, Darrouzet V. Long-term results of middle fossa plugging of superior semicircular canal dehiscences: clinically and instrumentally demonstrated efficiency in a retrospective series of 16 ears. *Eur Arch Otorhinolaryngol.* (2016) 273:1689–96. doi: 10.1007/s00405-015-3715-5
30. Allsopp T, Kim AH, Robbins AM, Page JC, Dornhoffer JL. Quality of life outcomes after transmastoid plugging of superior semicircular canal dehiscence. *Am J Otolaryngol.* (2020) 41:102287. doi: 10.1016/j.amjoto.2019.102287
31. Sun DQ, Ward BK, Semenov YR, Carey JP, Della Santina CC. Bilateral vestibular deficiency: quality of life and economic implications. *JAMA Otolaryngol Head Neck Surg.* (2014) 140:527–34. doi: 10.1001/jamaoto.2014.490
32. Fujimoto C, Yagi M, Murofushi T. Recent advances in idiopathic bilateral vestibulopathy: a literature review. *Orphanet J Rare Dis.* (2019) 14:202. doi: 10.1186/s13023-019-1180-8
33. van de Berg R, Guinand N, Nguyen TA, Ranieri M, Cavuscens S, Guyot JP, et al. The vestibular implant: frequency-dependency of the electrically evoked vestibulo-ocular reflex in humans. *Front Syst Neurosci.* (2014) 8:255. doi: 10.3389/fnsys.2014.00255
34. Carlsson PI, Hall M, Lind KJ, Danermark B. Quality of life, psychosocial consequences, and audiological rehabilitation after sudden sensorineural hearing loss. *Int J Audiol.* (2011) 50:139–44. doi: 10.3109/14992027.2010.533705
35. Ossen ME, Stokroos R, Kingma H, van Tongeren J, Van Rompaey V, Temel Y, et al. Heterogeneity in reported outcome measures after surgery in superior canal dehiscence syndrome-a systematic literature review. *Front Neurol.* (2017) 8:347. doi: 10.3389/fneur.2017.00347

Conflict of Interest: The authors declare that the research was conducted in the absence of any commercial or financial relationships that could be construed as a potential conflict of interest.

frontiers in Neurology

ORIGINAL RESEARCH
published: 27 October 2020
doi: 10.3389/fneur.2020.549817

Cervical and Ocular Vestibular-Evoked Myogenic Potentials in Patients With Intracochlear Schwannomas

Laura Fröhlich[1], Ian S. Curthoys[2], Sabrina Kösling[3], Dominik Obrist[4], Torsten Rahne[1] and Stefan K. Plontke[1]*

[1] Department of Otorhinolaryngology, Head and Neck Surgery, Martin Luther University Halle-Wittenberg, Halle (Saale), Germany, [2] Vestibular Research Laboratory, School of Psychology, The University of Sydney, Sydney, NSW, Australia, [3] Department of Radiology, Martin Luther University Halle-Wittenberg, Halle (Saale), Germany, [4] ARTORG Center for Biomedical Engineering Research, University of Bern, Bern, Switzerland

OPEN ACCESS

Edited by:
P. Ashley Wackym, The State University of New Jersey, United States

Reviewed by:
Daniel J. Lee, Massachusetts Eye & Ear Infirmary and Harvard Medical School, United States
Denise Utsch Gonçalves, Federal University of Minas Gerais, Brazil

***Correspondence:**
Laura Fröhlich
laura.froehlich@uk-halle.de

Specialty section:
This article was submitted to Neuro-Otology, a section of the journal Frontiers in Neurology

Received: *07 April 2020*
Accepted: *22 September 2020*
Published: *27 October 2020*

Citation:
Fröhlich L, Curthoys IS, Kösling S, Obrist D, Rahne T and Plontke SK (2020) Cervical and Ocular Vestibular-Evoked Myogenic Potentials in Patients With Intracochlear Schwannomas. Front. Neurol. 11:549817. doi: 10.3389/fneur.2020.549817

Objective: To evaluate ocular and cervical vestibular evoked myogenic potentials (oVEMPs and cVEMPs) in patients with solely intracochlear localization of an intralabyrinthine schwannoma (ILS).

Study Design: Retrospective analysis of a series of cases.

Setting: Monocentric study at a tertiary referral center.

Patients: Patients with intracochlear schwannoma (ICS) and VEMP measurements.

Outcome Measures: Signed asymmetry ratio (AR) of cVEMPs and oVEMPs to air conducted sound with AR cut-offs considered to be asymmetrical when exceeding ±30% for cVEMPs and ±40% for oVEMPs with respect to the side affected by the tumor (reduced amplitudes on the affected side indicated by negative values, enhanced amplitudes by positive values); VEMP amplitudes and latencies; tumor localization in the cochlear turn and scala.

Results: Nineteen patients with a solely intracochlear tumor (ICS patients) [10 males, 9 females, mean age 57.1 (SD: 13.4) years] were included in the study. On the affected side, cVEMPs were absent or reduced in 47% of the patients, normal in 32%, and enhanced in 21%. Ocular VEMPs on the affected side were absent or reduced in 53% of the patients, normal in 32% and enhanced in 15%. Latencies for cVEMPs and oVEMPs were not significantly different between the affected and non-affected side. In all patients with enhanced VEMPs, the tumor was located in the scala tympani and scala vestibuli.

Conclusions: As a new and unexpected finding, VEMP amplitudes can be enhanced in patients with intracochlear schwannoma, mimicking the third window syndrome.

Keywords: third window, vestibular schwannoma, intralabyrinthine, intracochlear, VEMP, asymmetry, secondary hydrops, semicircular canal dehiscence

INTRODUCTION

It was observed that intralabyrinthine schwannomas (ILS) can mimic various common cochleovestibular diseases in their symptoms and findings in functional tests. Cochleovestibular schwannomas in general, often also referred to as vestibular schwannomas or acoustic neuromas, are benign tumors that arise from the Schwann cells of the eighth cranial nerve. The schwannomas are referred to as ILS, when they arise from the most peripheral branches of the cochlear or vestibular nerves, i.e., inside the membranous labyrinth (1). ILS can present e.g., with sudden, progressive, or fluctuating hearing loss, pseudo-conductive hearing loss, and/or vertigo, and/or (pulsating) tinnitus, and have been misdiagnosed e.g., as Menière's disease (MD) or sudden hearing loss (2–8). The diagnosis is based on high-resolution magnetic resonance imaging (MRI). Various slightly differing classifications of these tumors have been suggested in the literature (2, 5, 9). The most recent and detailed classification was suggested by Van Abel et al. (5) distinguishing intracochlear, intravestibular, intravestibulocochlear, transmodiolar, transmacular, tympanolabyrinthine, translabyrinthine, and transotic locations or extensions. An extension from the internal auditory canal into the cerebellopontine angle is possible. Van Abel et al. (5) have also described that vertigo and imbalance were commonly reported when the tumors also extended to the vestibular labyrinth but were only reported by 36% of patients with intracochlear schwannomas (ICS). Intracochlear tumor localization seems to be the most common in ILS (2, 9).

The recording of cervical and ocular vestibular evoked myogenic potentials (cVEMPs, oVEMPs) has been described as a screening tool for the assessment of nerve of origin in patients with cochleovestibular schwannoma (10). However, only few data are available on VEMPs in patients with an ILS. Lee et al. (11) described absent or decreased cVEMPs and oVEMPs in patients with ILS without specifying the exact tumor location. Ralli et al. (12) reported an absent oVEMP in a patient with an intravestibular ILS with presence of "a solid mass in the utricle" confirmed by magnetic resonance imaging (MRI). Dubernard et al. (6) analyzed cVEMPs in 36 (32%) of their reported 110 patients with ILS. Twelve patients had an intracochlear tumor and cVEMPs were abnormal, i.e., absent or significantly reduced, in 50% of these patients and preserved in the remaining 50%. To date, there is no study in which both oVEMPs and cVEMPs were systematically analyzed in a series of patients with solely intracochlear tumors.

VEMPs have also been described to be highly sensitive to changes in the inner ear fluid dynamics and to detect defects of the bony labyrinthine wall. In 1998, Minor et al. (13) were the first to report about patients with a defect in the bony wall of the superior semicircular canals, a superior semicircular canal dehiscence (SSCD). Over time, various conditions with a defect of the labyrinthine bony wall have been described in the literature (14–22). These are associated with a similar spectrum of symptoms and objective findings so that these conditions are now summarized under the general term of "third window syndrome" or "third window abnormalities" (23, 24). Wackym et al. (24) defined the following conditions associated with the term of third window syndrome: "SSCD, cochlea-facial nerve dehiscence, cochlea-internal carotid artery dehiscence, cochlea-internal auditory canal dehiscence, lateral semicircular canal-superior semicircular canal ampulla dehiscence, modiolus, perilymph fistula, posterior semicircular canal dehiscence, posterior semicircular canal-jugular bulb dehiscence, SSCD-subarcuate artery dehiscence, SSCD-superior petrosal vein dehiscence, vestibule-middle ear dehiscence, lateral semicircular canal-facial nerve dehiscence, wide vestibular aqueduct in children, post-traumatic hypermobile stapes footplate, otosclerosis with internal auditory canal involvement." The objective findings of increased VEMP amplitudes and/or lower VEMP thresholds have been reported in patients with SSCD (25–28), posterior semicircular canal dehiscence (16, 29), large vestibular aqueduct (30), perilymph fistula (31), cochlea-facial nerve dehiscence (24), posterior semicircular canal-jugular bulb dehiscence (32), and SSCD-superior petrosal vein dehiscence (33). In these patients, the presence of a third window caused by an otic capsule defect changed the mechanical properties, i.e., the fluid dynamics, of the inner ear. It has been shown by measurements and models, that in SSCD ears incoming acoustic energy causes larger fluid displacement in the semicircular canals (34–36). Furthermore, animal studies demonstrated that this results in activation of semicircular canal neurons in addition to otolith neurons (37). These canal afferents project to the contralateral (external ocular) inferior oblique muscle as well as the ipsilateral sternocleidomastoid muscle (inhibitory) and thus their activity contributes to and enhances cVEMPs and oVEMPs (38).

Apart from defects in the bony labyrinth, other inner ear pathologies have the potential to impact inner ear mechanics. Endolymphatic hydrops for instance, which can have various causes (39, 40), is believed to have a huge impact on inner fluid mechanics (41–43). This argument is supported by VEMP studies in patients suffering from clinically diagnosed definite MD. Asymmetric, enhanced cVEMPs (44, 45) but also enhanced oVEMPs in MD patients have been reported (46, 47). These inner ear pathologies can therefore mimic third window syndrome with regard to VEMP test results. While ILS can mimic other cochleovestibular diseases in their symptoms and functional findings, it is unknown, if ILS can also mimic third window syndrome as was described for other inner ear pathologies.

The aim of this study was to review and describe oVEMPs and cVEMPs of patients with solely intracochlear localization of an ILS. By including only ICS patients, we sought to avoid those with direct impact of the intravestibular schwannoma on otolith organs which might lead to a change in VEMP results.

Abbreviations: ILS, intralabyrinthine schwannoma; MD, Menière's disease; MRI, magnetic resonance imaging; ICS, intracochlear schwannoma; cVEMP, cervical vestibular evoked myogenic potential; oVEMP, ocular vestibular evoked myogenic potential; SSCD, superior semicircular canal dehiscence; VEMP, vestibular evoked myogenic potential; EMG, electromyogram; BT, basal turn; MT, middle turn; AT, apical turn; ST, scala tympani; SV, scala vestibuli; CT, computed tomography; AR, asymmetry ratio; AS, affected side; NAS, non-affected side; ICC, intraclass correlation coefficient.

MATERIALS AND METHODS

Study Design and Participants

In this retrospective analysis, patients of a single tertiary referral center were included. In a personal case series (SKP) at the University Hospital Halle of 53 consecutive patients with intralabyrinthine schwannoma (ILS), magnetic resonance images were analyzed for localization of the tumor. Patients with solely intracochlear schwannoma (ICS) in whom VEMP measurements had been performed between August 2015 and January 2020 were included in this study (ICS patient group). Patients without VEMP measurements or with other tumor localizations [see introduction according to Van Abel et al. (5)] were excluded from this study to avoid influence by direct impact of the tumor on the otoliths or by retrocochlear pathology.

Written informed consent was obtained from all patients. The study protocol was reviewed and approved by the responsible institutional review board (ethics committee of the Medical Faculty of Martin Luther University Halle-Wittenberg and the University Hospital Halle, approval number: 2019-26), and conducted according to the Declaration of Helsinki.

VEMP Testing

The VEMP tests of the included patients were reviewed. All VEMP recordings were collected and analyzed using the Eclipse recording platform (Interacoustics A/S, Middelfart, Denmark). Self-adhesive Neuroline 720 surface electrodes (Ambu A/S, Ballerup, Denmark) were used for electromyogram (EMG) recording after the skin was prepared to provide impedances of 5 kΩ or less. For cVEMPs, the electrodes were placed over the middle of the sternocleidomastoid muscle ipsilateral to the stimulated ear and over the sternum. For oVEMP recordings, the electrodes were placed on the infra-orbital ridge 1 cm below the lower eyelid contralateral to the stimulated ear and about 2 cm below the first electrode. The ground electrode was always positioned on the forehead.

During VEMP testing the patients were sitting on a chair. They were asked to turn their head to the contralateral shoulder for cVEMP testing and hold this position to achieve a constant tonic activation of the sternocleidomastoid muscle (50–200 μV) during the whole recording period. During data acquisition the EMG was monitored and appropriate feedback was provided in real time to ensure that sufficient muscular contraction was sustained (48). For oVEMP testing, the patients were asked to keep their head in a neutral position and look up, maintaining an angle of 20–30°.

For both, cVEMP, and oVEMP testing, air-conducted 500 Hz tone bursts (1 cycle rise/fall time, 2 cycles plateau) were delivered by ER-3A insert earphones (3M, St. Paul, MS, USA) at 100 dB nHL.

The EMG signals were recorded in a −20 to 80 ms window relative to the onset of the stimulus. A bandpass filter of 10–1,000 Hz was applied and the artifact rejection level was set to 400 μV. The responses were averaged to at least 200 stimuli and at least two trials were recorded for each VEMP test.

Specifying Tumor Location

All patients underwent MRI of the temporal bone with at least thin-sliced 3D T2-weighted and T1-weighetd images with contrast medium. In all included patients, the MRI was (retrospectively) systematically studied regarding the localization of the tumor. The classification suggested by Van Abel et al. (5) was used to classify tumor localization in the basal turn (BT), middle turn (MT), or apical turn (AT) of the cochlea, including combinations of these localizations. Additionally, localization of the tumor in the scala tympani (ST) and/or scala vestibuli (SV) was specified, if possible. The MRIs originated from different sources, often from outside our hospital, and thus, showed considerable differences in resolution. MRIs were not repeated, if the scans were sufficient for establishing the diagnosis of ICS.

Exclusion of Third Window Syndromes

Temporal bone computed tomography (CT) scans or cone beam CTs were retrospectively analyzed for the presence of semicircular canal dehiscence, enlarged vestibular aqueduct, cochlea-facial nerve dehiscence, and other third window syndromes [see introduction and (24)]. It has to be noted, however, that the intention for performing the CT and cone beam CT scans were solely for preoperative evaluation of the bony anatomy prior to a possible surgery for tumor removal and hearing rehabilitation with a cochlear implant. They were performed after the diagnosis of an ILS was established by MRI and thus they usually did not include specific reconstructions for evaluation of "third windows" of the inner ear, e.g., no planes along the superior semicircular canal.

The patients' medical histories taken at initial presentation including audiological and vestibular complaints were retrospectively evaluated for typical symptoms of third window lesions including vertigo or oscillopsia induced by loud sounds/Tullio phenomenon, increased sensitivity to low frequency sounds, autophony, and pulsating tinnitus.

Data Analysis

A VEMP was ultimately judged as present, when the putative response was clearly larger than the pre-stimulus waveforms, i.e., the background noise. The impact of muscle contraction on cVEMP results was reduced by averaging the root mean square of the EMG signal over the pre-stimulus window and for each recording frame to calculate the background EMG, i.e., the contraction strength.

The p13 n23 for cVEMPs and n10 p15 for oVEMPs were identified and peak latencies as well as peak-to-peak amplitudes were recorded. The p13 n23 peak-to-peak amplitude was normalized to the background EMG. The asymmetry ratio (AR) was calculated from the peak-to-peak amplitudes. In order to account for the side affected by the tumor (AS) and the non-affected side (NAS) and to overcome the drawback of absolute AR, a signed AR was used:

$$AR\,(\%) = \frac{amplitude\ (AS) - amplitude\ (NAS)}{amplitude\ (AS) + amplitude\ (NAS)} * 100.$$

For cVEMPs, the AS refers to the response recorded from the ipsilateral sternocleidomastoid muscle and for oVEMPs the AS

refers to the response recorded from the contralateral inferior oblique muscle. For cVEMPs, ARs above 30% or below −30% were considered abnormal (49). For oVEMPs, abnormal ARs were above 40% or below −40% (50, 51). Positive values of the AR indicate larger responses of the affected ear (enhanced), while negative values indicate smaller responses of the affected ear (reduced), respectively. If no response could be detected, the amplitude was set to 0 μV. For unilateral responses, the AR was therefore 100% or −100%.

VEMP analysis was performed by two blinded examiners. Normal distribution of the amplitude and latency data was confirmed by a Shapiro-Wilk test. The intraclass correlation coefficient [ICC (3, 1)] was calculated for the oVEMP and cVEMP ARs based on the analysis by the two examiners to assess the inter-rater reliability. If no responses could be detected on the AS and NAS, the AR was set to 0% for the statistical test (see following paragraph). Inter-rater agreement was considered "poor" for ICCs below 0.50, "moderate" between 0.50 and 0.75, "good" between 0.75 and 0.90, and "excellent" above 0.90 (52). Good or excellent agreement was considered acceptable for further analysis. The final latencies and amplitudes were the averages of the examiners. For absence of a response rated by one examiner but presence of a response rated by the other examiner, the amplitudes were the averages and the latencies were taken from the one examiner who rated the response to be present. The cVEMP and oVEMP latencies and amplitudes recorded from the AS were compared to the responses from the NAS as control by paired *t*-tests. A confidence level of 95% or above was considered to be significant ($p < 0.05$). SPSS statistics (IBM, Armonk, New York, USA) was used for all statistical analyses.

The VEMP results were related to tumor localization in a hypotheses generating descriptive analysis.

RESULTS

Twenty-six patients with solely intracochlear schwannoma (ICS) were identified. Six patients had not undergone VEMP testing and were therefore excluded. The analysis of the CTs or cone beam CTs (available in 16 patients) revealed a dehiscent superior semicircular canal in one case. This patient was excluded as well. There were no signs for other third mobile windows of the otic capsule. Thus, 19 patients with ICS were included in the study for final analyis. Of those, 10 patients were male, 9 were female. The mean age was 57.1 (SD: 13.4) years. In 8 patients, the left ear was affected, in 11 patients the tumor was located in the right ear. The mean hearing threshold [pure tone average at 0.5, 1, 2, and 4 kHz (4PTA)] was 90.8 (SD: 25.0) dB HL for the affected side (AS) and 18.7 (SD:13.3) dB HL for the non-affected side (NAS). Some of the patients reported pulsating tinnitus and very few patients reported autophony and increased sensitivity for low frequency sounds. Other typical clinical symptoms of third window lesions like oscillopsia or vertigo induced by loud sounds/Tullio phenomenon have not been observed in any of those patients.

Despite the different image resolution of the MRIs, it was possible to specify tumor localization according to basal turn (BT), middle turn (MT), and the apex (apical turn, AT) in all patients. Only in one patient, it was difficult to localize the tumor with respect to the scala tympani (ST), and/or scala vestibuli (SV). Data for all patients are summarized in **Table 1**. The tumor was located in the BT in 2 patients (11%), in the MT in 7 patients (37%), and in the AT in 1 patient (5%). In 4 patients (21%), the tumor was in the BT and MT, in 4 patients (21%) it was in the MT and AT, and in 1 patient (5%) it was in the BT, MT, and AT. With respect to the scalae, tumors were observed solely in ST in 5 patients (26%). In no patient, the tumor was solely located in SV, and in 14 patients (74%) it was located in both, ST, and SV.

Regarding the VEMP analysis, the inter-rater reliability analysis by ICC revealed good to excellent agreement between the two raters. For cVEMPs, the single measure ICC was 0.990 with a 95% confidence interval from 0.996 to 0.975 [$F_{(18)} = 205.248$, $p < 0.001$]. For oVEMPs, the single measure ICC was 0.875 with a 95% confidence interval from 0.706 to 0.950 [$F_{(18)} = 15.052$, $p < 0.001$]. Cervical VEMPs could be recorded from the affected side (AS) in 13 cases (68%). In 4 cases, the response was absent in the non-affected side (NAS) as well. In the other 2 cases, the AS was the only ear without a response (AR = −100%). The oVEMP measurements showed responses of the AS in 10 patients (53%). In 6 cases, it was absent in both, AS and NAS. In 3 cases, the AS was the only side without a response (AR = −100%). The mean p13 n23 cVEMP amplitude was 0.46 (SD: 0.52) for the AS and 0.50 (SD: 0.45) for the NAS. For oVEMPs, the mean n10 p15 amplitude was 2.44 μV (SD: 4.27 μV) for the AS and 1.89 μV (SD: 2.10 μV) for the NAS. The mean cVEMP p13 latencies were 16.5 ms (SD: 1.8 ms) for the AS and 16.1 ms (SD: 1.7 ms) for the NAS, mean n23 latencies were 26.1 ms (SD: 2.9 ms) and 25.6 ms (SD: 2.2 ms), respectively. For oVEMPs, the mean n10 latencies were 12.7 ms (SD: 1.0 ms) for the AS and 12.4 ms (SD: 0.8 ms) for the NAS, and p15 latencies were 18.1 ms (SD: 1.3 ms) and 17.9 ms (SD: 1.2 ms), respectively. Between the AS and NAS, no significant difference was found for p13 and n23 cVEMP latencies [$t_{(12)} = 1.267$, $p = 0.229$; $t_{(12)} = 1.216$, $p = 0.247$] as well as for the n10 and p15 oVEMP latencies [$t_{(9)} = 1.552$, $p = 0.155$; $t_{(9)} = 0.998$, $p = 0.344$]. The results are illustrated in **Figure 1A**.

The VEMP asymmetry ratio (AR) results are given for each patient in **Table 1**. **Figure 1B** illustrates the results in a boxplot. Patients are color coded as they contribute to both the oVEMP and cVEMP AR data. If no response could be recorded on both the AS and NAS, the AR was illustrated at 0% by an empty circle in the plot. The mean AR was −15.6% (SD: 53.6%) for cVEMPs and −15.3% (SD: 64.5%) for oVEMPs. For cVEMPs, the AR was smaller than −30%, i.e., asymmetrical with reduced responses on the AS, in 5 cases (26%), including the 2 cases with ARs of −100%. The AR was larger than 30%, i.e., asymmetrical with enhanced responses in the AS, in 4 cases (21%). Including the 3 cases with ARs of −100%, the oVEMP AR was smaller than −40% in 4 cases (21%) and larger than 40% in 3 cases (16%). In total, VEMPs were enhanced on the AS in 5 patients: in 2 patients only the cVEMPs (#8, #19), in 1 patient only the oVEMPs (#16), and in 2 patients both, the cVEMPs and oVEMPs (#13, #14). The VEMP results of these patients are illustrated in **Figure 2**.

CT or cone beam CT scans were available in four of five patients with enhanced VEMPs (patient #8 declined the CT)

TABLE 1 | Demographic data, oVEMP and cVEMP asymmetry ratio (AR) results, and tumor localization of included patients.

ID	Age range	AS	4PTA hearing level (dB)		VEMP AR (%)		ICS Location	
			AS	NAS	cVEMP	oVEMP	Cochlear turn	Scala
1	45–50	R	75.00	16.25	n.a.	−2	(MT)+AT	ST+SV
2	45–50	R	>110.00	6.25	−87*	n.a.	(BT)+MT+AT	ST+SV
3	50–55	L	73.75	10.00	6	−29	(MT)+AT	ST+SV
4	30–31	L	97.50	2.50	−63*	n.a.	(BT)	ST+SV
5	65–70	R	80.00	28.75	−9	19	(BT)+MT	ST
6	70–75	L	>110.00	22.50	−65*	−100*	BT+(MT)	ST
7	75–80	L	>110.00	62.50	n.a.	n.a.	(MT)	ST+SV
8	55–60	R	>101.25	33.75	38*	7	MT	ST+SV
9	55–60	R	97.5	11.25	12	n.a.	AT	ST+SV
10	70–75	R	>110.00	18.75	−100*	−85*	MT	ST+SV
11	70–75	L	>110.00	23.75	−100*	n.a.	(MT)+(AT)	ST+SV
12	60–65	R	86.25	8.75	8	−100*	(MT)	ST
13	30–35	L	71.25	8.75	59*	76*	(MT)	ST+SV
14	50–55	R	67.50	13.75	38*	67*	(BT)+MT	ST+SV
15	60–65	R	>110.00	15.00	−16	−14	MT	ST
16	65–70	R	>110.00	10.00	n.a.	63*	MT+AT	ST+SV
17	60–65	L	91.25	21.25	12	−1	MT	ST
18	40–45	L	>110.00	23.75	n.a.	−100*	BT	ST+SV
19	55–60	R	92.50	17.50	33*	n.a.	BT+(MT)	ST+SV

*4PTA, pure tone average at 0.5, 1, 3, 4 kHz; AS, affected side; NAS, non-affected side; AR, asymmetry ratio; ICS, intracochlear schwannoma; BT, basal turn; MT, middle turn; AT, apical turn; ST, scala tumpani; SV, scala vestibuli; (), partially; *abnormal AR.*

and did not show any signs of a third mobile window of the otic capsule.

The analysis of enhanced VEMPs and tumor localization showed that in 2 of the 5 patients with enhanced VEMPs only the MT (#8, #13), in 2 patients the BT and MT (#14, #19), and in 1 patient MT and AT (#16) was involved. A correlation of enhanced VEMPs and tumor localization with respect to the cochlear turn could therefore not be observed. With respect to the scala, the tumors were located in both, ST and SV, in all five patients with enhanced VEMPs and in none of the patients where only the ST was affected by the tumor.

DISCUSSION

Only a few studies reported VEMP results in patients with intralabyrinthine schwannoma (ILS) and mostly described absent or decreased cVEMPs and/or oVEMPs in these patients (6, 11, 12). The exact tumor localization and description of VEMP results in patients with solely intracochlear schwannomas (ICS) was done by Dubernard et al. (6) for 12 patients. Cervical VEMPs were absent or significantly reduced in 50% of the patients and "preserved" in the remaining 50%. Patients with intravestibular tumors were also examined in their study and were—not surprisingly—found to have a higher rate of absent or reduced cVEMPs, which is likely due to a direct impact of the tumor mass on the otolith organs. The results from our study are the first to systematically analyze both oVEMPs and cVEMPs in a series of cases with solely intracochlear tumors.

Despite the intracochlear position, the tumor affected the vestibular response which was found to be absent, reduced and in some cases enhanced. We observed absent or reduced cVEMPs in 47% of the patients and normal cVEMPs in 32%. This is in line with the results described by Dubernard et al. (6). The surprising result was that the cVEMPs were enhanced in 21% of the patients in our study. Ocular VEMPs were reduced or absent in 53% and normal in 32%. Enhanced oVEMPs were observed in 15% of the patients.

Many factors can cause reduced or absent VEMP responses. Particularly in central pathology, the VEMPs are absent, reduced and/or prolonged which can be an early indicator of pathology (53–56). Many studies reported reduced or absent VEMPs in patients with cochleovestibular schwannoma (i.e., vestibular schwannoma, see introduction) and reported a strong relationship with tumor size (57). Cervical VEMPs in 38 ears of Neurofibromatosis Type 2 patients with small cochleovestibular schwannomas were described by Holliday et al. (58). Normal results were found in 71% and abnormal cVEMPs were found in 29% of the patients with a correlation between abnormal cVEMPs and tumor size. VEMP asymmetry ratios (ARs) in patients with cochleovestibular schwannomas can also be used as a screening tool for assessing the function of the superior and inferior vestibular nerves before and after surgical intervention (10). VEMP abnormalities in these patients are attributed to compressional and neurotoxic effects on the nerve and reduced vascular supply of the labyrinth. However, retrocochlear pathology or direct impact of the tumor on the otoliths was excluded in our study by

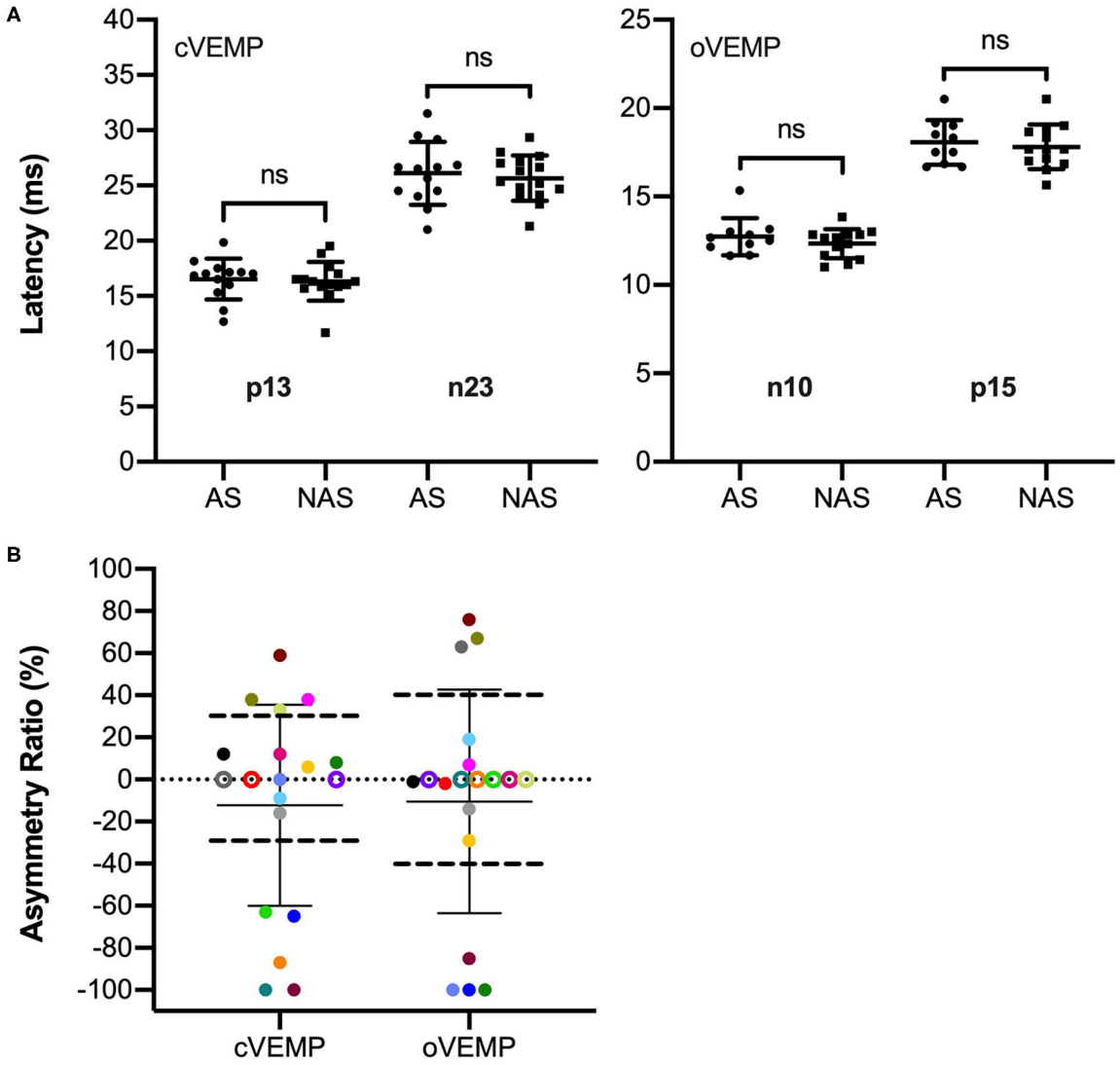

FIGURE 1 | Latency and VEMP asymmetry ratio (AR) results of the included patients ($n = 19$). **(A)** Response latencies with means and standard deviations for the cVEMP p13 and n23 for the side affected by the tumor (AS) ($n = 13$) and the non-affected side (NAS) ($n = 16$) as well as oVEMP n10 and p15 latencies for the AS ($n = 10$) and NAS ($n = 13$). No significant differences were found between latencies of the AS and NAS. **(B)** Signed ARs for cVEMPs and oVEMPs with means and standard deviations. Patients are color coded as they contribute to both the oVEMP and cVEMP AR data. Negative values indicate larger responses on the NAS, positive values indicate larger responses on the AS. For cVEMPs, ARs exceeding ±30% were considered abnormal. For oVEMPs, abnormal ARs were larger/smaller than ±40%. The limits are illustrated by horizontal dashed lines. Data points above the thresholds represent enhanced VEMPs with respect to the AS, data points below the thresholds represent reduced VEMPs in the AS. Patients with absent responses on the AS are shown at AR = −100%. For patients with absent responses on both AS and NAS, the ARs are illustrated at AR = 0% as empty circles.

including only patients with solely intracochlear tumors. In addition, another patient with superior canal dehiscence was excluded, which could have acted as a confounding factor in the VEMP analysis. The pathophysiology of ICS leading to abnormal VEMPs is unknown and can only be speculated about. In patients with cochleovestibular schwannomas (without intracochlear localization of tumors), it has been reported that sensorineural hearing loss is associated with tumor-secreted factors containing pro-inflammatory cytokines which cause cochlear damage (59, 60). This could explain why large cochleovestibular schwannomas sometimes do not cause hearing loss while small ones do. This has not been investigated yet for ICS associated loss of otolith function but could be a similar mechanism. Possibly, the finding of reduced or absent VEMPs in these patients is attributed to a local cytotoxic effect conveyed by the labyrinthine fluids (6).

In the present study, the major and unexpected finding was that the VEMPs in ICS in some patients were enhanced but no latency prolongation was observed. Enhanced VEMPs are commonly seen in patients with third window syndrome. Thus, VEMPs have become a widely used tool in the diagnosis of third window syndrome (16, 24, 29–33) and are enhanced in those

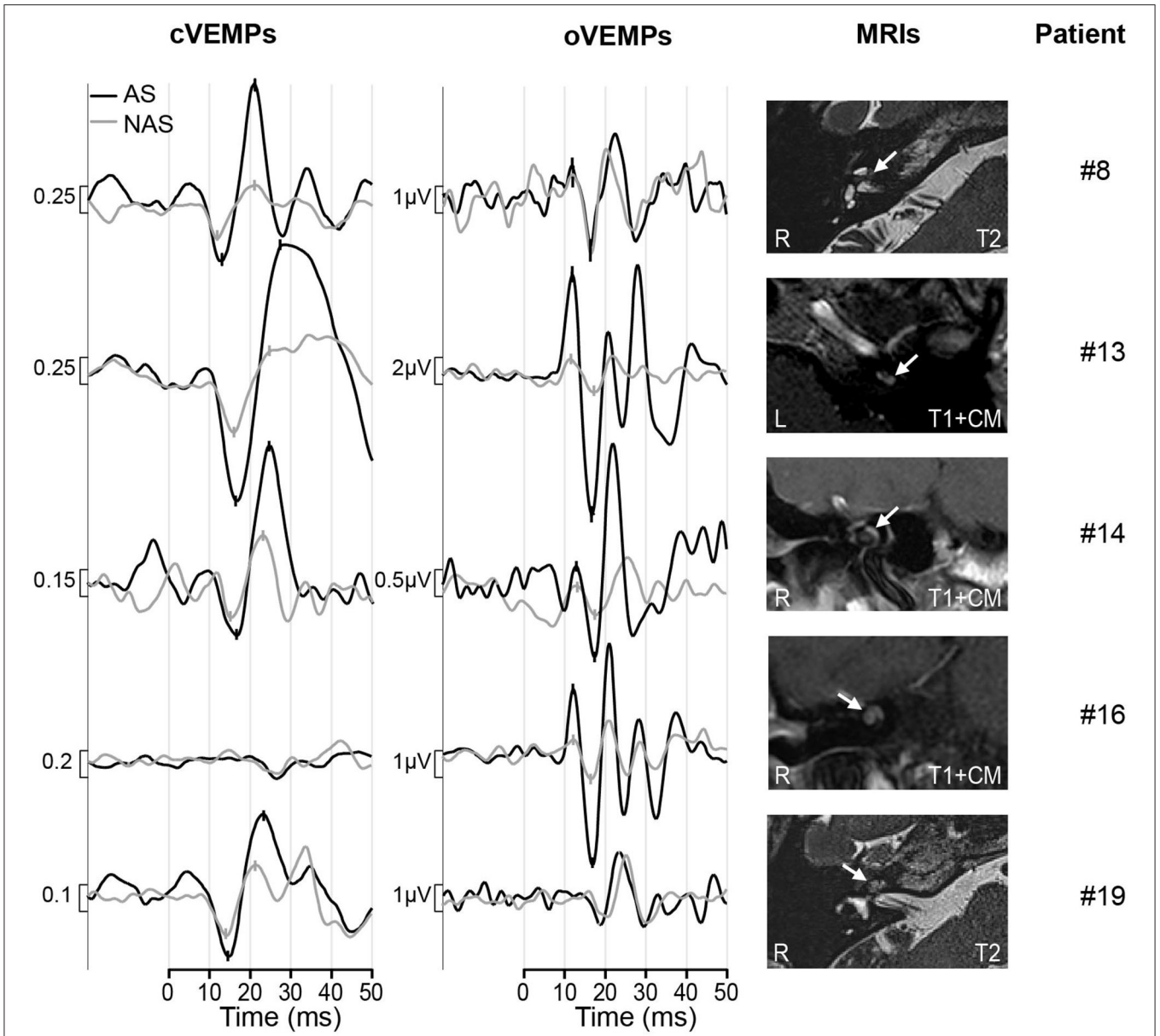

FIGURE 2 | Results of patients with enhanced VEMPs. The black trace shows the response of the affected side (AS), the response from the non-affected side (NAS) is shown by the gray line. The p13, n23 peaks for cVEMPs and n10, p15 peaks for oVEMPs are marked. The MRI scans are shown in the right column with the tumors marked by white arrows. Patient #8, #13, #19: axial, Patient #14 and #16: coronal; R, right; L, left; T1+CM, t1-weighted with contrast medium; T2, t2-weighted.

ears with a defect in the otic capsule (25–28). However, other conditions with endolymphatic hydrops such as Menière's disease have been shown to mimic third window syndrome showing reduced VEMP thresholds and enhanced amplitudes (44–47). To date, it was unknown that—with respect to VEMP results—other inner ear disorders, ICS in particular, have the potential to mimic third window syndrome as well. In our experience, management of patients with ILS is highly individual and detailed functional evaluation of the vestibular labyrinth is important for counseling these patients regarding treatment options (especially with respect to surgical tumor removal) and outcome predictions (61, 62).

To explain the cause of enhanced VEMP amplitudes in ICS patients, we assume that this is due to a change of inner ear (fluid) mechanics caused by the tumor. In this study, we only included ICS patients to avoid bias due to direct influence of the tumor on the otoliths (e.g., as in intravestibular or intravestibulocochlear schwannomas) or by tumor in the internal auditory canal. Measurements, models, and animal studies have shown that in patients with superior semicircular canal dehiscence, a third mobile window leads to larger fluid displacement in the semicircular canals which activates canal neurons contributing to the VEMP and enhancing it (34, 37, 63). This shows that mechanical changes cause enhanced VEMPs.

It also supports the theory that mechanical changes can lead to enhanced VEMPs in patients with endolymphatic hydrops. The exact mechanisms of this observation are yet unknown. Endolymphatic hydrops can have various causes (39, 40). It seems possible that an obstructive tumor mass like an ICS has the potential to cause or act similar to endolymphatic hydrops. This idea is supported by the observation in our study that cVEMPs or oVEMPs were only enhanced, if both scala tympani (ST) and scala vestibuli (SV) were "blocked" by the tumor. This leads to the somehow contradictory observation that—with respect to VEMPs—a "third window syndrome" can act similar to a "minus 1 window syndrome" or "one window syndrome," when the cochlear is "blocked" by a tumor.

In such situations, acoustic stimulation cannot lead to a fully developed traveling wave within the cochlea. Nevertheless, the stapes displacement must still be compensated by a reciprocal displacement of the round window membrane. It is conceivable that this may lead to a perilymph flow which is oscillating more or less directly between the oval window and the round window including a corresponding displacement of the basal basilar membrane. Clearly, in this configuration the fluid dynamics in the basal region of the cochlea would be significantly altered and—similar to the third window syndrome (36)—there would be higher flow velocities close to the saccule which may lead to enhanced VEMPs. It appears also possible that the cochlear blockage leads to a suppression of the piston-like stapes motion (PSM) and that the acoustic stimulation leads only to a "rocking stapes motion" (RSM) which does not create any net fluid displacement within the otic capsule. It has been shown [Figure 5 in Edom et al. (64)] that RSM leads to significantly increased perilymph flow in the basal region of the cochlea which may affect saccular stimulation and be connected to enhanced VEMPs. Computer-modeling of the fluid dynamics of a "blocked" cochlea may have the potential to give answers to the question if the mass effect without concomitant neural damage could cause the enhancement of VEMPs and should be considered in future studies.

Limitations of the study include its retrospective design, which is due to the nature of the observation which was more or less accidental. This is also a reason, why the study did not include threshold measurements. Since VEMPs evoked by bone conducted vibration were not available at that time, only air conduction was used for stimulation. While any third window abnormalities were excluded in most patients, CT scans were not available in 1 of the 5 patients with enhanced VEMPs, and CTs (although thin-sliced) were technically not targeted specifically on exclusion of bony defects of the inner ear. These limitations can be addressed in further studies including specific history taking (i.e., checklists for symptoms of third window syndromes), threshold measurements in all patients with enhanced VEMPs as well as specific CT scans in these patients. Another aspect which has to be considered in further studies is the evolution of VEMPs in these patients. It should be examined, how the VEMP amplitudes and latencies change over time, possibly in the course of tumor growth. Regarding the different outcomes, i.e., especially reduced or absent in contrast to normal or enhanced VEMPs, the tumors' intrinsic biology with respect to tumor secreted factors should be investigated as was done for cochleovestibular schwannomas causing hearing loss (59, 60). This is important to assess the clinical relevance of normal, absent or reduced, and enhanced VEMPs and might become beneficial for counseling ICS patients.

CONCLUSION

We described that enhanced VEMP amplitudes could be observed in patients with intracochlear schwannoma. It was an unexpected novelty that in addition to conditions described by the general term of the third window syndrome, or in Menière's disease, VEMP amplitudes can be enhanced in patients with intracochlear schwannoma. Response latencies were not significantly different between the side affected by the tumor and the non-affected side. Intracochlear tumors should therefore be added to the list of conditions which may cause increased VEMP amplitudes. Since management of patients with intracochlear schwannomas is highly individual, these findings might become beneficial for counseling these patients regarding treatment options and outcome predictions.

DATA AVAILABILITY STATEMENT

The raw data supporting the conclusions of this article will be made available by the authors, without undue reservation.

ETHICS STATEMENT

The studies involving human participants were reviewed and approved by Ethics committee of the Medical Faculty of Martin Luther University Halle-Wittenberg and the University Hospital Halle. The patients/participants provided their written informed consent to participate in this study.

AUTHOR CONTRIBUTIONS

LF and SP contributed the conception and design of the study and organized the database. LF, SP, and SK performed the data analysis. TR contributed to the data analysis and the visualization of results. IC and DO made contributions with interpretation of the results and generation of hypotheses. LF wrote the first draft of the manuscript. All authors contributed to the manuscript revision, read, and approved the submitted version.

FUNDING

The authors acknowledge the financial support of the Open Access Publication Fund of the Martin Luther University Halle-Wittenberg.

ACKNOWLEDGMENTS

The authors thank Karl-Johan Fredén Jansson for support in acquiring data of patient #8 in this study and providing the data plots for this patient.

REFERENCES

1. Merchant SN, McKenna MJ. Schwannoma. In: Merchant SN, Nadol JB, editors. *Schuknecht's Pathology of the Ear*. 3rd ed. Shelton: People's medical publishing house (2010). p. 492–510.
2. Kennedy RJ, Shelton C, Salzman KL, Davidson HC, Harnsberger HR. Intralabyrinthine schwannomas: diagnosis, management, and a new classification system. *Otol Neurotol.* (2004) 25:160–7. doi: 10.1097/00129492-200403000-00014
3. Slattery EL, Babu SC, Chole RA, Zappia JJ. Intralabyrinthine schwannomas mimic cochleovestibular disease: symptoms from tumor mass effect in the labyrinth. *Otol Neurotol.* (2014) 36:167–71. doi: 10.1097/MAO.0000000000000516
4. Tieleman A, Casselman JW, Somers T, Delanote J, Kuhweide R, Ghekiere J, et al. imaging of intralabyrinthine schwannomas: a retrospective study of 52 cases with emphasis on lesion growth. *Am J Neuroradiol.* (2008) 29:898–905. doi: 10.3174/ajnr.A1026
5. Van Abel KM, Carlson ML, Link MJ, Neff BA, Beatty CW, Lohse CM, et al. Primary inner ear schwannomas: a case series and systematic review of the literature: primary inner ear schwannomas. *Laryngoscope.* (2013) 123:1957–66. doi: 10.1002/lary.23928
6. Dubernard X, Somers T, Veros K, Vincent C. Clinical presentation of intralabyrinthine schwannomas: a multicenter study of 110 cases. *Otol Neurotol.* (2014) 35:1641–9. doi: 10.1097/MAO.0000000000000415
7. Jerin C, Krause E, Ertl-Wagner B, Gürkov R. Clinical features of delayed endolymphatic hydrops and intralabyrinthine schwannoma: an imaging-confirmed comparative case series. English version. *HNO.* (2017) 65:41–5. doi: 10.1007/s00106-016-0199-6
8. Plontke SK, Rahne T, Pfister M, Götze G, Heider C, Pazaitis N, et al. Intralabyrinthine schwannomas: surgical management and hearing rehabilitation with cochlear implants. *HNO.* (2017) 65:136–48. doi: 10.1007/s00106-017-0364-6
9. Salzman KL, Childs AM, Davidson HC, Kennedy RJ, Shelton C, Harnsberger HR. Intralabyrinthine schwannomas: imaging diagnosis and classification. *Am J Neuroradiol.* (2012) 33:104–9. doi: 10.3174/ajnr.A2712
10. Rahne T, Plößl S, Plontke SK, Strauss C. Preoperative determination of nerve of origin in patients with vestibular schwannoma. *HNO.* (2018) 66:16–21. doi: 10.1007/s00106-017-0416-y
11. Lee SU, Bae YJ, Kim HJ, Choi JY, Song JJ, Choi BY, et al. Intralabyrinthine schwannoma: distinct features for differential diagnosis. *Front Neurol.* (2019) 10:750. doi: 10.3389/fneur.2019.00750
12. Ralli M, Nola G, Fusconi M, Sparvoli L, Ralli G. ocular vestibular evoked myogenic potentials and intravestibular intralabyrinthine schwannomas. *Ear Nose Throat J.* (2018) 97:E21–5. doi: 10.1177/014556131809700703
13. Minor LB, Solomon D, Zinreich JS, Zee DS. Sound- and/or pressure-induced vertigo due to bone dehiscence of the superior semicircular canal. *Arch Otolaryngol Neck Surg.* (1998) 124:249–58. doi: 10.1001/archotol.124.3.249
14. Young L, Isaacson B. Cochlear and petrous carotid canal erosion secondary to cholesteatoma. *Otol Neurotol.* (2009) 31:697–8. doi: 10.1097/MAO.0b013e31819bd803
15. Park JJH, Shen A, Loberg C, Westhofen M. The relationship between jugular bulb position and jugular bulb related inner ear dehiscence: a retrospective analysis. *Am J Otolaryngol.* (2015) 36:347–51. doi: 10.1016/j.amjoto.2014.12.006
16. Gopen Q, Zhou G, Poe D, Kenna M, Jones D. Posterior semicircular canal dehiscence: first reported case series. *Otol Neurotol.* (2010) 31:339–44. doi: 10.1097/MAO.0b013e3181be65a4
17. Blake DM, Tomovic S, Vazquez A, Lee H, Jyung RW. Cochlear-facial dehiscence—A newly described entity. *Laryngoscope.* (2014) 124:283–9. doi: 10.1002/lary.24223
18. Fujita T, Kobayashi T, Saito K, Seo T, Ikezono T, Doi K. Vestibule-middle ear dehiscence tested with perilymph-specific protein Cochlin-Tomoprotein (CTP) detection test. *Front Neurol.* (2019) 10:47. doi: 10.3389/fneur.2019.00047
19. Manzari L. Multiple dehiscences of bony labyrinthine capsule. A rare case report and review of the literature. *Acta Otorhinolaryngol Ital.* (2010) 30:317–20. doi: 10.3233/VES-140517
20. Manzari L, Scagnelli P. Large bilateral internal auditory meatus associated with bilateral superior semicircular canal dehiscence. *Ear Nose Throat J.* (2013) 92:25–33. doi: 10.1177/014556131309200109
21. Koo JW, Hong SK, Kim DK, Kim JS. Superior semicircular canal dehiscence syndrome by the superior petrosal sinus. *J Neurol Neurosurg Psychiatry.* (2010) 81:465–7. doi: 10.1136/jnnp.2008.155564
22. Ionescu EC, Al Tamami N, Neagu A, Ltaief-Boudrigua A, Gallego S, Hermann R, et al. superior semicircular canal ampullae dehiscence as part of the spectrum of the third window abnormalities: a case study. *Front Neurol.* (2017) 8:683. doi: 10.3389/fneur.2017.00683
23. Ho ML, Moonis G, Halpin CF, Curtin HD. Spectrum of third window abnormalities: semicircular canal dehiscence and beyond. *Am J Neuroradiol.* (2017) 38:2–9. doi: 10.3174/ajnr.A4922
24. Wackym PA, Balaban CD, Zhang P, Siker DA, Hundal JS. Third window syndrome: surgical management of cochlea-facial nerve dehiscence. *Front Neurol.* (2019) 10:1281. doi: 10.3389/fneur.2019.01281
25. Minor LB. Clinical manifestations of superior semicircular canal dehiscence. *Laryngoscope.* (2005) 115:1717–27. doi: 10.1097/01.mlg.0000178324.55729.b7
26. Verrecchia L, Westin M, Duan M, Brantberg K. Ocular vestibular evoked myogenic potentials to vertex low frequency vibration as a diagnostic test for superior canal dehiscence. *Clin Neurophysiol.* (2016) 127:2134–9. doi: 10.1016/j.clinph.2016.01.001
27. Manzari L, Burgess AM, McGarvie LA, Curthoys IS. Ocular and cervical vestibular evoked myogenic potentials to 500 Hz Fz bone-conducted vibration in superior semicircular canal dehiscence. *Ear Hear.* (2012) 33:508–20. doi: 10.1097/AUD.0b013e3182498c09
28. Govender S, Fernando T, Dennis DL, Welgampola MS, Colebatch JG. Properties of 500Hz air- and bone-conducted vestibular evoked myogenic potentials (VEMPs) in superior canal dehiscence. *Clin Neurophysiol.* (2016) 127:2522–31. doi: 10.1016/j.clinph.2016.02.019
29. Aw ST, Welgampola MS, Bradshaw AP, Todd MJ, Magnussen JS, Halmagyi GM. Click-evoked vestibulo-ocular reflex distinguishes posterior from superior canal dehiscence. *Neurology.* (2010) 75:933–5. doi: 10.1212/WNL.0b013e3181f11dfd
30. Taylor RL, Bradshaw AP, Magnussen JS, Gibson WPR, Halmagyi GM, Welgampola MS. Augmented ocular vestibular evoked myogenic potentials to air-conducted sound in large vestibular aqueduct syndrome. *Ear Hear.* (2012) 33:768–71. doi: 10.1097/AUD.0b013e31825ce613
31. Modugno GC, Magnani G, Brandolini C, Savastio G, Pirodda A. Could vestibular evoked myogenic potentials (VEMPs) also be useful in the diagnosis of perilymphatic fistula? *Eur Arch Otorhinolaryngol.* (2006) 263:552–5. doi: 10.1007/s00405-006-0008-z
32. Friedmann DR. A clinical and histopathologic study of jugular bulb abnormalities. *Arch Otolaryngol Neck Surg.* (2012) 138:66–71. doi: 10.1001/archoto.2011.231
33. Schneiders SMD, Rainsbury JW, Hensen EF, Irving RM. Superior petrosal sinus causing superior canal dehiscence syndrome. *J Laryngol Otol.* (2017) 131:593–7. doi: 10.1017/S0022215117001013
34. Rosowski JJ, Songer JE, Nakajima HH, Brinsko KM, Merchant SN. Clinical, experimental, and theoretical investigations of the effect of superior semicircular canal dehiscence on hearing mechanisms. *Otol Neurotol.* (2004) 25:323–32. doi: 10.1097/00129492-200405000-00021
35. Iversen MM, Zhu H, Zhou W, Della Santina CC, Carey JP, Rabbitt RD. Sound abnormally stimulates the vestibular system in canal dehiscence syndrome by generating pathological fluid-mechanical waves. *Sci Rep.* (2018) 8:10257. doi: 10.1038/s41598-018-28592-7
36. Grieser BJ, Kleiser L, Obrist D. Identifying mechanisms behind the tullio phenomenon: a computational study based on first principles. *J Assoc Res Otolaryngol.* (2016) 17:103–18. doi: 10.1007/s10162-016-0553-0
37. Curthoys IS. The new vestibular stimuli: sound and vibration—anatomical, physiological and clinical evidence. *Exp Brain Res.* (2017) 235:957–72. doi: 10.1007/s00221-017-4874-y
38. Curthoys IS, Grant JW, Burgess AM, Pastras CJ, Brown DJ, Manzari L. Otolithic receptor mechanisms for vestibular-evoked myogenic potentials: a review. *Front Neurol.* (2018) 9:366. doi: 10.3389/fneur.2018.00366
39. Ferster APO, Cureoglu S, Keskin N, Paparella MM, Isildak H. Secondary endolymphatic hydrops. *Otol Neurotol.* (2017) 38:774–9. doi: 10.1097/MAO.0000000000001377

40. Smeds H, Eastwood HT, Hampson AJ, Sale P, Campbell LJ, Arhatari BD, et al. Endolymphatic hydrops is prevalent in the first weeks following cochlear implantation. *Hear Res.* (2015) 327:48–57. doi: 10.1016/j.heares.2015.04.017
41. Sufyan Amir Paisal M, Azmi Wahab M, Taib I, Mat Isa N, Ramli Y, Md Seri S, et al. Flow behaviour in normal and Meniere's disease of endolymphatic fluid inside the inner ear. *IOP Conf Ser Mater Sci Eng.* (2017) 243:012033. doi: 10.1088/1757-899X/243/1/012033
42. Grieser BJ, McGarvie LA, Kleiser L, Manzari L, Obrist D, Curthoys IS. Numerical investigations of the effects of endolymphatic hydrops on the VOR response. *J Vestib Res.* (2014) 24:219.
43. Obrist D. Flow phenomena in the inner ear. *Annu Rev Fluid Mech.* (2019) 51:487–510. doi: 10.1146/annurev-fluid-010518-040454
44. Young YH, Wu CC, Wu CH. Augmentation of vestibular evoked myogenic potentials: an indication for distended saccular hydrops. *Laryngoscope.* (2002) 112:509–12. doi: 10.1097/00005537-200203000-00019
45. Taylor RL, Zagami AS, Gibson WP, Black DA, Watson SR, Halmagyi MG, et al. Vestibular evoked myogenic potentials to sound and vibration: characteristics in vestibular migraine that enable separation from Menière's disease. *Cephalalgia.* (2012) 32:213–25. doi: 10.1177/0333102411434166
46. Wen MH, Cheng PW, Young YH. Augmentation of ocular vestibular-evoked myogenic potentials via bone-conducted vibration stimuli in ménière disease. *Otolaryngol Neck Surg.* (2012) 146:797–803. doi: 10.1177/0194599811433982
47. Manzari L, Tedesco AR, Burgess AM, Curthoys IS. Ocular and cervical vestibular-evoked myogenic potentials to bone conducted vibration in Ménière's disease during quiescence vs during acute attacks. *Clin Neurophysiol.* (2010) 121:1092–101. doi: 10.1016/j.clinph.2010.02.003
48. Rahne T, Weiser C, Plontke S. Neurofeedback-Controlled comparison of the head elevation versus head rotation and head-hand methods in eliciting cervical vestibular evoked myogenic potentials. *Audiol Neurotol.* (2014) 19:327–35. doi: 10.1159/000362661
49. McCaslin DL, Fowler A, Jacobson GP. Amplitude normalization reduces Cervical Vestibular Evoked Myogenic Potential (cVEMP) amplitude asymmetries in normal subjects: proof of concept. *J Am Acad Audiol.* (2014) 25:268–77. doi: 10.3766/jaaa.25.3.6
50. Welgampola MS, Colebatch JG. Characteristics and clinical applications of vestibular-evoked myogenic potentials. *Neurology.* (2005) 64:1682–8. doi: 10.1212/01.WNL.0000161876.20552.AA
51. Govender S, Rosengren SM, Colebatch JG. Vestibular neuritis has selective effects on air- and bone-conducted cervical and ocular vestibular evoked myogenic potentials. *Clin Neurophysiol.* (2011) 122:1246–55. doi: 10.1016/j.clinph.2010.12.040
52. Koo TK, Li MY. A guideline of selecting and reporting intraclass correlation coefficients for reliability research. *J Chiropr Med.* (2016) 15:155–63. doi: 10.1016/j.jcm.2016.02.012
53. Oh SY, Kim JS, Lee JM, Shin BS, Hwang SB, Kwak KC, et al. Ocular vestibular evoked myogenic potentials induced by air-conducted sound in patients with acute brainstem lesions. *Clin Neurophysiol.* (2013) 124:770–8. doi: 10.1016/j.clinph.2012.09.026
54. Skorić MK, Adamec I, Madarić VN, Habek M. Evaluation of brainstem involvement in multiple sclerosis. *Can J Neurol Sci.* (2014) 41:346–9. doi: 10.1017/S0317167100017285
55. Oh SY, Kim HJ, Kim JS. Vestibular-evoked myogenic potentials in central vestibular disorders. *J Neurol.* (2016) 263:210–20. doi: 10.1007/s00415-015-7860-y
56. Di Stadio A, Dipietro L, Ralli M, Greco A, Ricci G, Bernitsas E. The role of vestibular evoked myogenic potentials in multiple sclerosis-related vertigo. A systematic review of the literature. *Mult Scler Relat Disord.* (2019) 28:159–64. doi: 10.1016/j.msard.2018.12.031
57. Taylor RL, Kong J, Flanagan S, Pogson J, Croxson G, Pohl D, et al. Prevalence of vestibular dysfunction in patients with vestibular schwannoma using video head-impulses and vestibular-evoked potentials. *J Neurol.* (2015) 262:1228–37. doi: 10.1007/s00415-015-7697-4
58. Holliday MA, Kim HJ, Zalewski CK, Wafa T, Dewan R, King KA, et al. Audiovestibular characteristics of small cochleovestibular schwannomas in neurofibromatosis Type 2. *Otolaryngol Neck Surg.* (2014) 151:117–24. doi: 10.1177/0194599814529081
59. Soares VYR, Atai NA, Fujita T, Dilwali S, Sivaraman S, Landegger LD, et al. Extracellular vesicles derived from human vestibular schwannomas associated with poor hearing damage cochlear cells. *Neuro-Oncol.* (2016) 18:1498–507. doi: 10.1093/neuonc/now099
60. Sagers JE, Sahin MI, Moon I, Ahmed SG, Stemmer-Rachamimov A, Brenner GJ, et al. NLRP3 inflammasome activation in human vestibular schwannoma: implications for tumor-induced hearing loss. *Hear Res.* (2019) 381:107770. doi: 10.1016/j.heares.2019.07.007
61. Plontke SK, Kösling S, Rahne T. Cochlear implantation after partial or subtotal cochleoectomy for intracochlear schwannoma removal—a technical report. *Otol Neurotol.* (2018) 39:365–71. doi: 10.1097/MAO.0000000000001696
62. Plontke SK, Fröhlich L, Wagner L, Kösling S, Götze G, Siebolts U, et al. How much cochlea do you need for cochlear implantation? *Otol Neurotol.* (2020) 41:694–703. doi: 10.1097/MAO.0000000000002614
63. Songer JE, Rosowski JJ. The effect of superior-canal opening on middle-ear input admittance and air-conducted stapes velocity in chinchilla. *J Acoust Soc Am.* (2006) 120:258–69. doi: 10.1121/1.2204356
64. Edom E, Obrist D, Henniger R, Kleiser L, Sim JH, Huber AM. The effect of rocking stapes motions on the cochlear fluid flow and on the basilar membrane motion. *J Acoust Soc Am.* (2013) 134:3749–58. doi: 10.1121/1.4824159

Conflict of Interest: The authors declare that the research was conducted in the absence of any commercial or financial relationships that could be construed as a potential conflict of interest.

frontiers in Neurology

ORIGINAL RESEARCH
published: 29 October 2020
doi: 10.3389/fneur.2020.580184

Bone-Conducted oVEMP Latency Delays Assist in the Differential Diagnosis of Large Air-Conducted oVEMP Amplitudes

*Rachael L. Taylor[1,2], John S. Magnussen[3], Belinda Kwok[2,4], Allison S. Young[2], Berina Ihtijarevic[2,4], Emma C. Argaet[2,4], Nicole Reid[5], Cheryl Rivas[4], Jacob M. Pogson[2,5], Sally M. Rosengren[2,5], G. Michael Halmagyi[2,5] and Miriam S. Welgampola[2,4,5]**

[1] Department of Physiology and Center for Brain Research, The University of Auckland, Auckland, New Zealand, [2] Central Clinical School, Faculty of Medicine and Health, The University of Sydney, Sydney, NSW, Australia, [3] Macquarie Medical Imaging, Macquarie University Hospital, Sydney, NSW, Australia, [4] The Balance Clinic and Laboratory, Sydney, NSW, Australia, [5] Neurology Department and Institute of Clinical Neurosciences, Royal Prince Alfred Hospital, Sydney, NSW, Australia

OPEN ACCESS

Edited by:
P. Ashley Wackym,
The State University of New Jersey,
United States

Reviewed by:
Sun-Young Oh,
Jeonbuk National University,
South Korea
Leonardo Manzari,
MSA ENT Academy Center, Italy

***Correspondence:**
Miriam S. Welgampola
miriam@icn.usyd.edu.au

Specialty section:
This article was submitted to Neuro-Otology, a section of the journal Frontiers in Neurology

Received: 05 July 2020
Accepted: 28 September 2020
Published: 29 October 2020

Citation:
Taylor RL, Magnussen JS, Kwok B, Young AS, Ihtijarevic B, Argaet EC, Reid N, Rivas C, Pogson JM, Rosengren SM, Halmagyi GM and Welgampola MS (2020) Bone-Conducted oVEMP Latency Delays Assist in the Differential Diagnosis of Large Air-Conducted oVEMP Amplitudes. Front. Neurol. 11:580184. doi: 10.3389/fneur.2020.580184

Background: A sensitive test for Superior Semicircular Canal Dehiscence (SCD) is the air-conducted, ocular vestibular evoked myogenic potential (AC oVEMP). However, not all patients with large AC oVEMPs have SCD. This retrospective study sought to identify alternate diagnoses also producing enlarged AC oVEMPs and investigated bone-conducted (BC) oVEMP outcome measures that would help differentiate between these, and cases of SCD.

Methods: We reviewed the clinical records and BC oVEMP results of 65 patients (86 ears) presenting with dizziness or balance problems who underwent CT imaging to investigate enlarged 105 dB nHL click AC oVEMP amplitudes. All patients were tested with BC oVEMPs using two different stimuli (1 ms square-wave pulse and 8 ms 125 Hz sine wave). Logistic regression and odds ratios were used to determine the efficacy of BC oVEMP amplitudes and latencies in differentiating between enlarged AC oVEMP amplitudes due to dehiscence from those with an alternate diagnosis.

Results: Fifty-three ears (61.6%) with enlarged AC oVEMP amplitudes were identified as having frank dehiscence on imaging; 33 (38.4%) had alternate diagnoses that included thinning of the bone covering (near dehiscence, $n = 13$), vestibular migraine ($n = 12$ ears of 10 patients), enlarged vestibular aqueduct syndrome ($n = 2$) and other causes of recurrent episodic vertigo ($n = 6$). BC oVEMP amplitudes of dehiscent and non-dehiscent ears were not significantly different ($p > 0.05$); distributions of both groups overlapped with the range of healthy controls. There were significant differences in BC oVEMP latencies between dehiscent and non-dehiscent ears for both stimuli ($p < 0.001$). A prolonged n1 125 Hz latency (>11.5 ms) was the best predictor of dehiscence (odd ratio = 27.8; 95% CI:7.0-111.4); abnormal n1 latencies were identified in 79.2% of ears with dehiscence compared with 9.1% of ears without dehiscence.

Conclusions: A two-step protocol of click AC oVEMP amplitudes and 125 Hz BC oVEMP latency measures optimizes the specificity of VEMP testing in SCD.

Keywords: vestibular-evoked myogenic potentials, superior semicircular canal dehiscence, tullio phenomenon, vertigo, hyperacusis, bone-conduction

INTRODUCTION

Superior canal dehiscence (SCD) is one of several third-mobile window syndromes characterized by an abnormal communication between the inner ear and the intracranial cavity. Diagnosis is best made using a combination of symptoms, CT imaging, and audiovestibular test results, which often includes the recording of vestibular evoked myogenic potentials (VEMPs) (1). VEMP amplitudes are typically enlarged and/or thresholds are reduced as the opening in the superior semicircular canal renders vestibular receptors more susceptible to stimulation by sound and vibration (2–5). Air-conducted (AC) ocular VEMP (oVEMP) amplitudes, cervical VEMP (cVEMP) thresholds, and high frequency (4000 Hz) AC and bone-conducted (BC) oVEMP amplitudes have high sensitivity in discriminating between dehiscent and normal ears (6–9). As AC oVEMP amplitude measurements require fewer trials and minimal departure from standard clinical protocols, they are advocated as the most efficient means of SCD identification (6).

Despite reports of good sensitivity and specificity, most VEMP studies in SCD have been limited to comparisons with healthy controls. However, pathological VEMPs are not specific to SCD. Amplitudes are sometimes enlarged and/or thresholds are reduced in early Meniere's disease (10), enlarged vestibular aqueduct syndrome (11–14) and dehiscence of the posterior canal (15). According to a recent study, false positive (i.e., enlarged) AC oVEMPs may be recorded in around 11% of the non-dehiscent dizzy population (16). Differentiating between SCD and cases of thin bone (near dehiscence) is of particular interest, as there is some suggestion that the latter may be at greater risk of post-operative complications (17). Whether VEMP protocols can be modified to achieve this distinction is currently unclear.

In a previous study, skull-tap oVEMP latencies were identified as an alternative indicator of SCD (18). Tendon hammer taps applied to the upper forehead of patients with SCD produced marked latency delays with sensitivity comparable to AC oVEMP amplitudes. The source of the latency prolongation, which was approximately 4 ms, was hypothesized to be an additional inhibitory inferior oblique muscle response mediated by superior canal afferents. Skull vibration, like changes in intracranial pressure caused by Valsalva (closed glottis) or straining (19), may conduct through the opening in the canal from the soft tissue of the brain and CSF causing additional *ampullopetal* fluid movement. Combinations of ampullopetal and ampullofugal fluid displacement may cause different patterns of otolith and canal receptor activation, producing changes in oVEMP morphology and latency. Intact bone covering should prevent this pressure transference. Thus, we hypothesize the latency effect of bone-conducted (BC) vibration should be specific to SCD.

In this study we investigated whether latency delays produced by a low frequency BC stimulus could assist in differentiating enlarged AC oVEMPs due to dehiscence, from those arising from other pathology. First, we identified cases seen over a five-year period who underwent imaging due to enlarged AC oVEMPs and sought their diagnosis and associated symptoms. BC oVEMP amplitudes and latencies of ears diagnosed with SCD were then compared to those without SCD (i.e., false positive AC oVEMPs) to determine their diagnostic utility.

MATERIALS AND METHODS

Participants

This study was approved by The Royal Prince Alfred Research Ethics and Governance Office. All controls and thirty-two patients provided written consent. Data collected from the remaining patients were used as per existing waiver of consent. All patients with large oVEMPs were studied using this protocol as standard of care.

Patient Population

Potential participants were identified from the clinical records of neurology clinics at the Royal Prince Alfred Hospital and The Balance Clinic and Laboratory, Sydney Australia. Inclusion criteria required that patients had undergone temporal bone CT imaging at one of two facilities due to enlarged AC oVEMP amplitudes, above the clinical normative range (mean + 2SD of 144 healthy ears; aged 21 to 84 years), *AND* had oVEMP testing with a low-frequency, 125 Hz bone-conducted stimulus. Clinical records of patients meeting these criteria were reviewed for symptom characterization, which was supplemented in most cases by a symptom questionnaire that was administered either face-to-face or over the telephone.

Healthy Controls

Twenty-one healthy controls (15 female) aged 37.2 ± 9.5 years without vestibular symptoms were recruited for comparison of bone-conduction oVEMP data.

Ocular Vestibular Evoked Myogenic Potentials

oVEMPs were recorded using one of two Medelec Synergy evoked-potential systems (software versions 12.2 and 15.0, VIASYS Healthcare UK Ltd). Active (inverting) Ag/AgCl electrodes were placed infra-orbitally beneath the lower lid margin of the contralateral eye, with a reference (non-inverting) electrode placed vertically below it on the cheek. A sternum electrode served as the ground.

Clinical oVEMP testing was undertaken using three stimuli: 0.1 ms air-conducted clicks (140 dB peak-SPL) delivered with alternating polarity using TDH-49 supra-aural head phones,

and bone-conducted vibration consisting of both 1 ms square-wave "minitaps" (MT: 20 V amplitude) and a single cycle 125 Hz sine wave (8 ms duration; 0 ms rise/fall; 20 V peak-peak driving voltage), both with initial condensation polarity. BC stimuli were applied in the midline, close to the hairline (**Figure 1A**), using a hand-held minishaker (model 4810, Bruel & Kjaer) while the participant lay semi-recumbent. Mastoid accelerometery (**Figure 1B**) measured for the 125 Hz stimulus from six participants using triaxial accelerometers (TMS international), indicated maximum acceleration in the naso-occipital direction (*X* axis). Fourier analysis of the acceleration response confirmed a low frequency power spectrum, similar to tendon-hammer taps but lower than for minitaps (described previously in 18).

All stimuli were presented at a rate of 5 Hz while the participant gazed upward as high as possible. Responses to 50 (BC) and 100 (AC) stimuli were amplified, band-pass filtered (3–1000 Hz), and averaged. Latencies and peak-to-peak amplitudes for oVEMPs recorded from each ear were determined from markings placed on the first dominant negative-positive (n1-p1) bi-phasic waveform of the contralateral EMG recording (**Figure 1C**). As in **Figure 1C**, this was sometimes preceded by an additional smaller negative potential (up-going peak), giving the appearance of a double-peaked negativity. This was coined n0 (18), but as it was not consistently present and the positivity (down-going deflection) between the two n0 and n1 peaks did not cross through zero, it was not analyzed in this study.

3D Temporal Bone Imaging and Patient Classification

Temporal bone imaging was undertaken at two facilities. As a minimum requirement for interpretation, all computerized tomography (CT) imaging included ≤0.5 mm cuts reformatted in the plane of all six semicircular canals. CT scans were interpreted by a radiologist with expertise in temporal bone imaging (JM) who was blinded to both the VEMP results and patient symptoms. Scans were classified as N = normal bone covering; 1 = thin bone covering but no dehiscence; 2 = very thin bone covering but no dehiscence; 3 = no visible bone short segment; 4 = no visible bone long segment; 5 = no visible bone; protrudes above tegmen. Imaging results were used to divide patients into two groups. The first group consisted of patients with frank dehiscence (classifications 3–5), representing true positive AC oVEMPs. The second were identified as having intact bone (classifications N, 1 or 2), i.e., false positive AC oVEMPs. Medical records of both groups were reviewed for evidence of alternate or comorbid diagnoses.

Statistical Analysis

Statistical analysis was performed using SPSS, IBM (version 26) software. Effects of patient group (dehiscent vs. non-dehiscent) and stimulus on oVEMP amplitudes and latencies were compared using a General Linear Mixed Model (GLMM, unstructured covariance), while controlling for age as a covariate. GLMM results are reported in the text as adjusted estimated marginal means and standard errors. Descriptive statistics in the tables represent means (SD). The relationship between individual CT classification scores and oVEMP outcome measures was further explored using Spearman's correlation coefficient. Age adjusted odds ratios (OR) were calculated using binary logistic regression to determine the oVEMP outcome measures and symptoms that were predictive of group membership. Statistical significance was set at $p < 0.05$.

RESULTS

Sixty-five patients aged 53 ± 13 years (43 female) fulfilled criteria for inclusion in the study. AC oVEMPs were enlarged bilaterally in 21 patients, and unilaterally in 44, comprising a total of 86 ears. None of the cases demonstrated prolonged AC oVEMP n1 latencies. Patient demographics and oVEMP test results are summarized for each CT imaging classification score in **Table 1**. Fifty-three of 86 ears (61.6%) with enlarged AC oVEMPs (44 patients; 9 bilateral) were diagnosed as dehiscent (classifications 3–5), representing true positive AC oVEMPs. Among the 33 non-dehiscent ears, representing false positive enlarged AC oVEMPs, 13 had near dehiscence (classification 1 or 2). Of the remaining 20 ears (16 patients), 10 patients fulfilled Barany Society criteria (20) for probable or definite vestibular migraine (VM). For four of these patients, VM was the only vestibular diagnosis. Five patients with VM and bilaterally enlarged AC oVEMPs had normal bone-covering on one side and either near or frank dehiscence on the other; another had recovered from a previous episode of vestibular neuritis. A further two patients suffered migraine headaches without fulfilling criteria for VM. Two patients had intractable positional vertigo attributed to BPPV, and another had recurrent spontaneous vertigo of unknown etiology. Enlarged vestibular aqueducts were the probable cause of enlarged AC oVEMP amplitudes in two ears of one patient.

oVEMP Amplitudes

oVEMP amplitudes for dehiscent and non-dehiscent ears are compared in **Figure 2** relative to the clinical normative range (AC stimulus), and results of the 21 control participants (BC stimuli). Analysis of patient results using a GLMM confirmed a significant interaction between stimulus modality and participant group ($F = 9.438$, $p < 0.001$). oVEMP amplitudes in SCD were on average larger in response to AC (70.6 ± 3.5 μV) compared with either BC stimulus (125 Hz = 46.2 ± 3.4 μV; MT = 55.6 ± 3.6 μV), whereas for non-dehiscent patient ears, they were comparable across stimuli. As indicated in **Figure 2**, amplitude distributions for both BC stimuli overlapped with the range of healthy controls and the odds of either group having an enlarged amplitude above the normal range was not significantly different (MT OR = 1.2, CI: 0.5-3.2, $p = 0.671$; 125 Hz OR = 1.1, 95% CI: 0.4-2.8, $p = 0.887$).

BC oVEMP Latencies

Table 2 provides average n1 and p1 latencies for BC stimuli. Compared to the non-dehiscent group, BC oVEMP latencies for n1 and p1 were significantly longer for ears with dehiscence (**Figures 3A,B**, $p < 0.001$). A significant group by stimulus

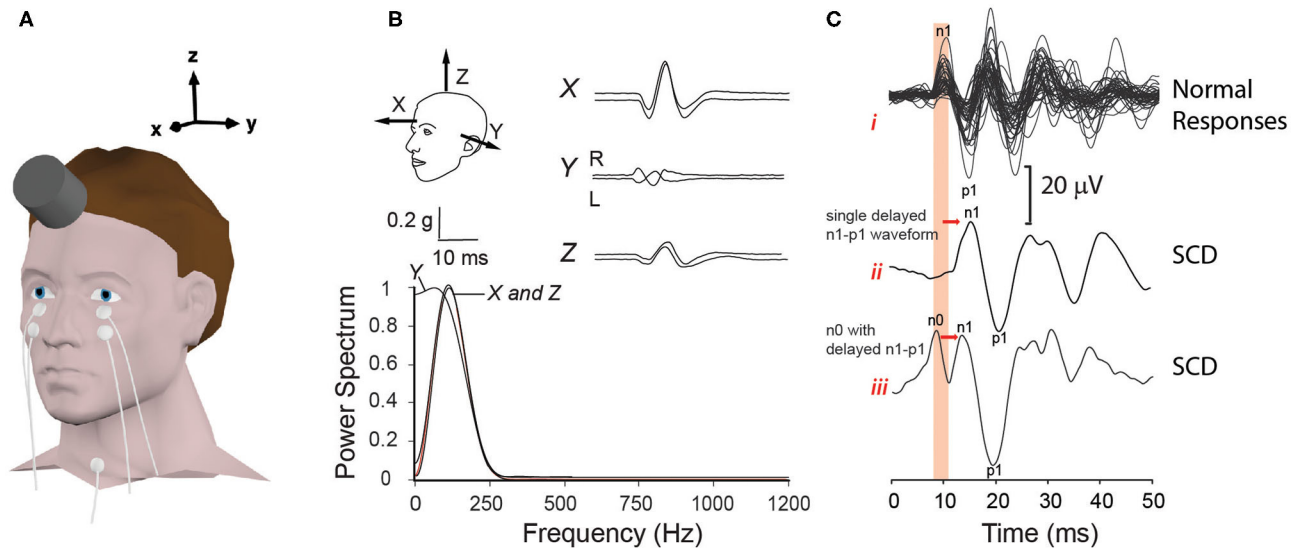

FIGURE 1 | Electrode and transducer details for bone conduction oVEMPs. **(A)** shows the electrode and transducer placement used to record oVEMPs. **(B)** indicates the corresponding three-dimensional (*X, Y* and *Z)* mastoid acceleration (g) response to a 125 Hz sine wave recorded from−10 to +30 ms stimulus onset. Fourier analysis performed over a 10 ms Hanning window, in each axis from stimulus onset, confirms a low frequency power spectrum centered between 125 and 150 Hz. In **(C)**, BC oVEMP waveforms of controls *(i)* are contrasted with two types (*ii* and *iii*) of typical waveforms recorded from SCD patients: *ii* represents a single delayed n1-p1 waveform; in *iii*, the n1-p1 waveform is preceded by an additional up-going n0 potential.

TABLE 1 | Patient demographics, VEMP amplitudes and latencies (mean ± SD) summarized for each CT imaging classification score.

CT Imaging Classification	False Positive AC oVEMPs (non-dehiscent ears)		True Positive AC oVEMPs (dehiscent ears)			Spearman's rho
	N	1 and 2	3	4	5	
Number of ears	20 (11F/5M)	13 (11F/2M)	15 (11F/3M)	10 (5F/5M)	28 (16F/8M)	
Age in years	44 ± 13	49 ± 9	59 ± 10	53 ± 10	57 ± 15	
oVEMP Amplitudes (μV)						
AC oVEMP	36.3 ± 14.2	44.9 ± 20.4	83.4 ± 30.6	77.1 ± 40.0	58.4 ± 21.7	0.40 (<0.001)
MT oVEMP	47.0 ± 22.6	50.1 ± 21.7	58.2 ± 35.9	65.2 ± 36.5	47.7 ± 18.7	0.01(0.950)
125 oVEMP	41.2 ± 23.5	40.8 ± 22.4	44.7 ± 29.6	41.7 ± 24.3	45.5 ± 22.4	0.07 (0.515)
oVEMP Latencies (ms)						
MT oVEMP n1	8.9 ± 0.5	9.5 ± 0.9	10.0 ± 1.1	10.2 ± 0.8	11.1 ± 1.2	0.68 (<0.001)
MT oVEMP p1	13.3 ± 1.1	13.8 ± 1.7	15.3 ± 1.6	15.4 ± 1.2	15.9 ± 1.8	0.59 (<0.001)
125 oVEMP n1	10.0 ± 0.9	10.8 ± 1.4	12.3 ± 1.6	13.1 ± 3.0	13.2 ± 1.9	0.62 (<0.001)
125 oVEMP p1	14.2 ± 0.9	14.9 ± 1.6	16.7 ± 2.0	17.3 ± 3.0	17.6 ± 1.7	0.66 (<0.001)

The final column represents the strength of the correlation (using Spearman's rho) between each VEMP outcome measure and CT classification score. Some patients with bilaterally enlarged AC oVEMPs are represented in two categories of CT imaging.

interaction ($F = 16.927$, $p < 0.001$) further confirmed larger group-mean n1 latency differences for the 125 Hz stimulus (2.3 ± 0.4 ms) than for the MT (1.1 ± 0.2 ms), whereas p1 latency differences for 125 Hz (2.4 ± 0.4 ms) and MT stimuli (1.8 ± 0.4 ms) were more similar ($F = 3.863$, $p = 0.053$). On comparison with the upper normal limits in **Figure 3**, n1 and p1 abnormality rates for dehiscent ears were 79.2 and 75.5% for 125 Hz and 60.4 and 71.7% for MT. For the non-dehiscent group, n1 and/or p1 latencies were prolonged in 3 of 33 ears (9.1%) for 125 Hz stimulation, all with CT classification scores of 2, and in 5 ears (15.2%) for MT stimulation. Compared with the non-dehiscent group, the odds of a prolonged n1 latency for a patient with dehiscence was 27.8 for 125 Hz (OR 95% CI: 7.0-111.4) and 9.9 for MT stimulation (OR 95% CI: 2.6-38.4). Odds of a prolonged p1 latency was similarly increased by a factor of 21.8 (95%CI: 5.4-87.9) for 125 Hz and 9.4 (95%CI: 3.0-30.0) for MT stimuli.

VEMP results for each CT classification are summarized in **Table 1**. Moderate positive correlations were evident between all latency measurements and CT scores. There was no relationship between CT scores and either of the BC stimulus amplitudes, but a weak correlation with AC oVEMP amplitudes.

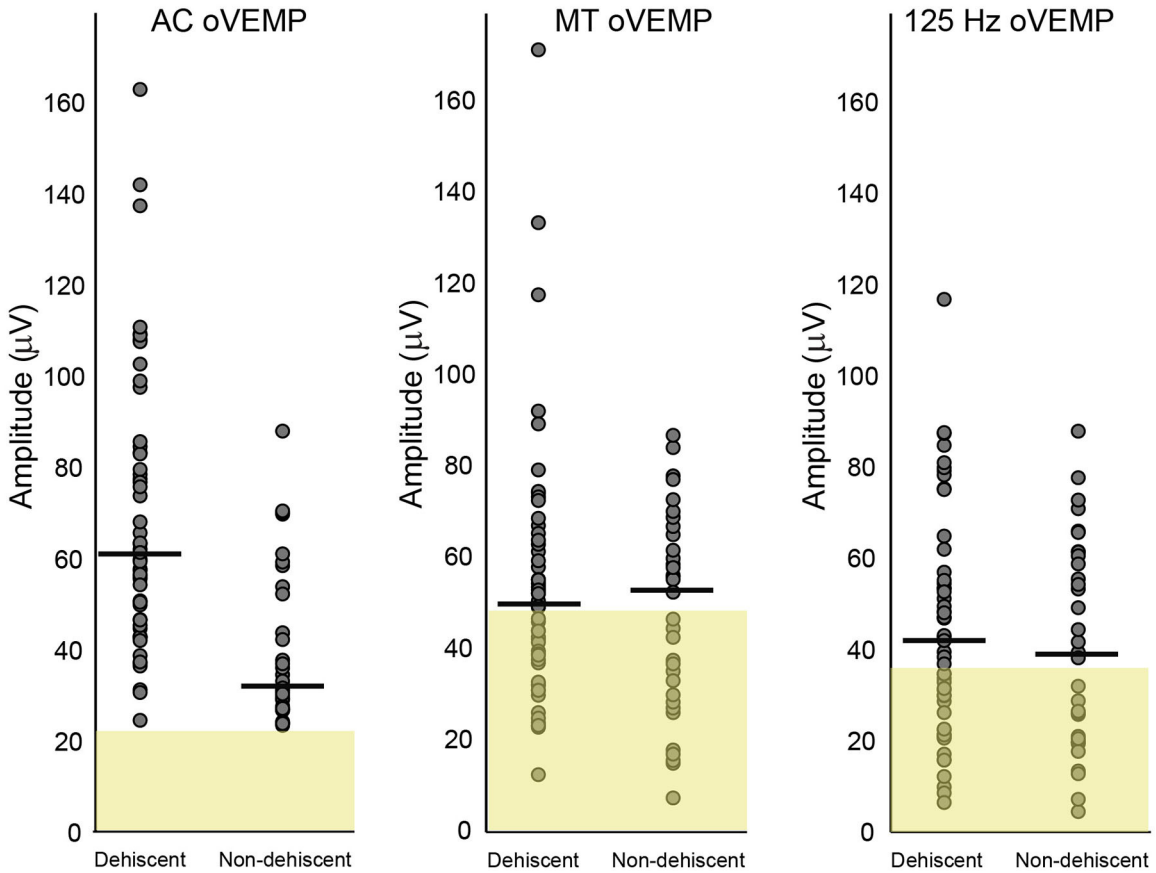

FIGURE 2 | Amplitude comparisons for dehiscent and non-dehiscent ears. Air-conduction oVEMP amplitudes are shown relative to clinical normative data (yellow shaded region) used as recruitment criteria for the study. These data represent the 95% range (mean + 2SD), which defines the upper normal limit as 22.3 microvolts. Normal limits for MT and 125 Hz bone-conduction stimuli represent the mean + 2 SD of the 21 controls recruited in this study, with upper normal limits of 47.6 and 36.2 microvolts, respectively. Horizontal lines indicate group medians.

TABLE 2 | Average BC oVEMP amplitudes and latencies for dehiscent, non-dehiscent and control ears.

	MT			125 Hz		
	Amplitude	**n1**	**p1**	**Amplitude**	**n1**	**p1**
Controls	22.6 ± 12.5	9.0 ± 0.6	13.4 ± 0.8	16.1 ± 10.1	10.3 ± 0.6	14.6 ± 0.8
Dehiscence	54.0 ± 28.4	10.6 ± 1.2	15.7 ± 1.6	44.4 ± 24.5	12.9 ± 2.1	17.3 ± 2.1
Non-dehiscence	48.3 ± 22.0	9.1 ± 0.7	13.5 ± 1.4	41.0 ± 22.7	10.3 ± 1.1	14.4 ± 1.3

Contralateral Ears of Patients With Unilaterally Enlarged AC oVEMPs Due to Frank or Near Dehiscence

CT imaging of the contralateral ears of 35 patients with a positive AC oVEMP and unilateral frank dehiscence revealed 10 cases with normal bone-covering. Sixteen scans revealed thin or very thin bone (classification 1 or 2), three of which were associated with enlarged AC oVEMP amplitudes and were therefore included in the analysis of VEMP results for non-dehiscent ears (**Figures 2**, **3**). A further nine scans were classified as dehiscent despite AC oVEMPs that were either normal or absent (i.e., false *negative* AC oVEMPs), all with a CT classification score of 3 (no visible bone-short segment), normal middle ear function, and normal BC oVEMP latencies. The oVEMP waveforms of a patient with bilateral SCD on CT imaging, showing a false negative AC oVEMP for one ear, are compared in **Figure 4** with the waveforms of a patient with VM and near dehiscence.

Near dehiscence *without* enlargement of AC oVEMP amplitudes was also recorded from the contralateral ears of three patients with unilateral enlarged AC oVEMPs due to near dehiscence. Like the nine patients with frank dehiscence and false negative AC oVEMPs, none of these cases had prolonged BC oVEMP latencies.

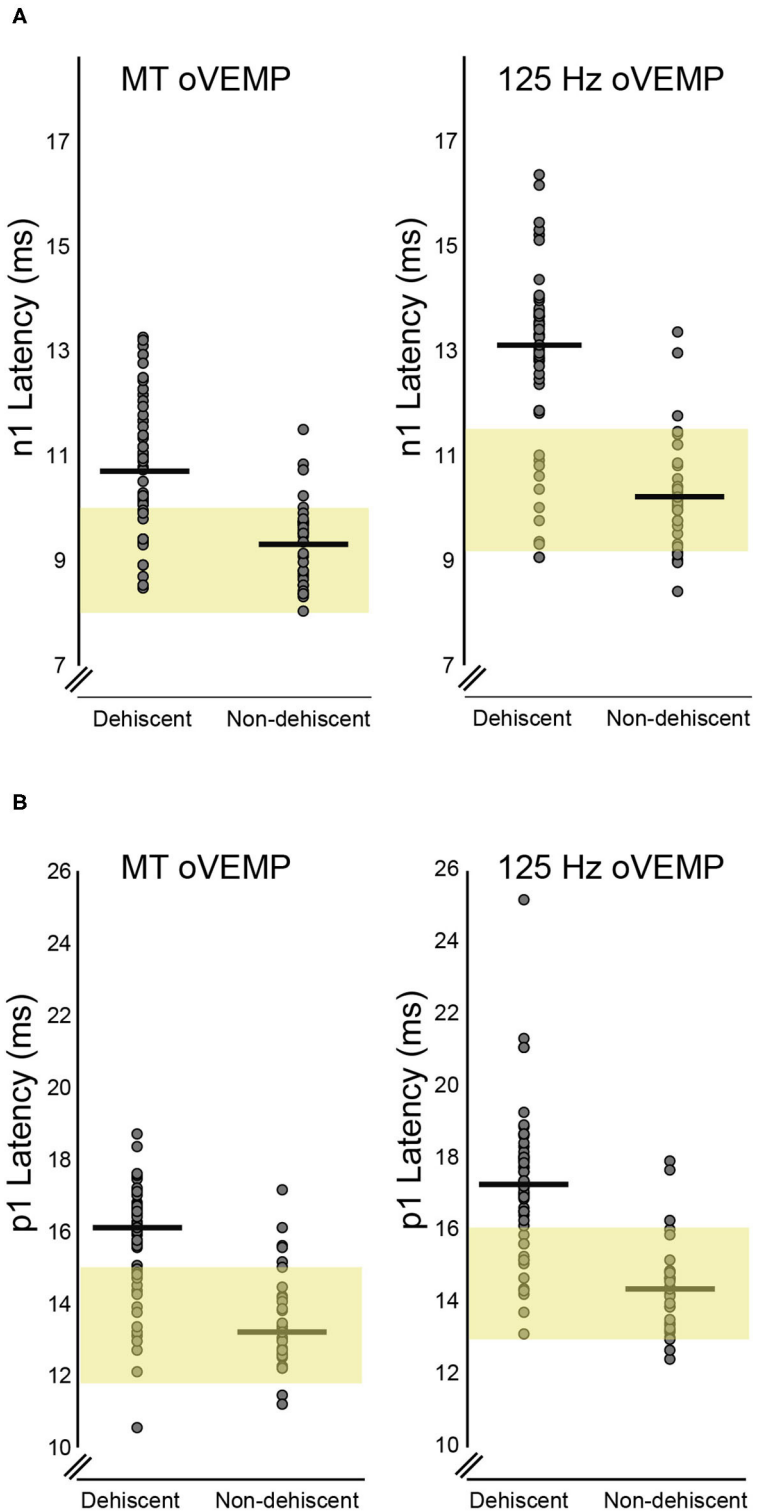

FIGURE 3 | BC Latency comparisons for dehiscent and non-dehiscent ears. **(A)** shows the distribution of n1 latencies for MT and 125 Hz stimuli. Yellow shaded regions correspond to the 95% range (mean +/- 2SD) of values recorded from the 21 controls, which define the upper limit of normal as 10.1 ms for MT and 11.5 ms for 125 Hz stimulation. Median n1 latencies for dehiscent and non-dehiscent ears (horizontal lines) are 10.7 and 9.3 ms for MT and 13.1 and 10.2 ms for 125 Hz. **(B)** shows the latency distributions for p1 potentials relative to the 95% range of control participants. The upper limit of normal for MT and 125 Hz stimulation is defined as 15.0 and 16.1 ms, respectively. Horizontal lines indicate medians of 16.1 and 13.2 ms for dehiscent and non-dehiscent ears for MT stimulation and 17.3 and 14.4 ms for 125 Hz.

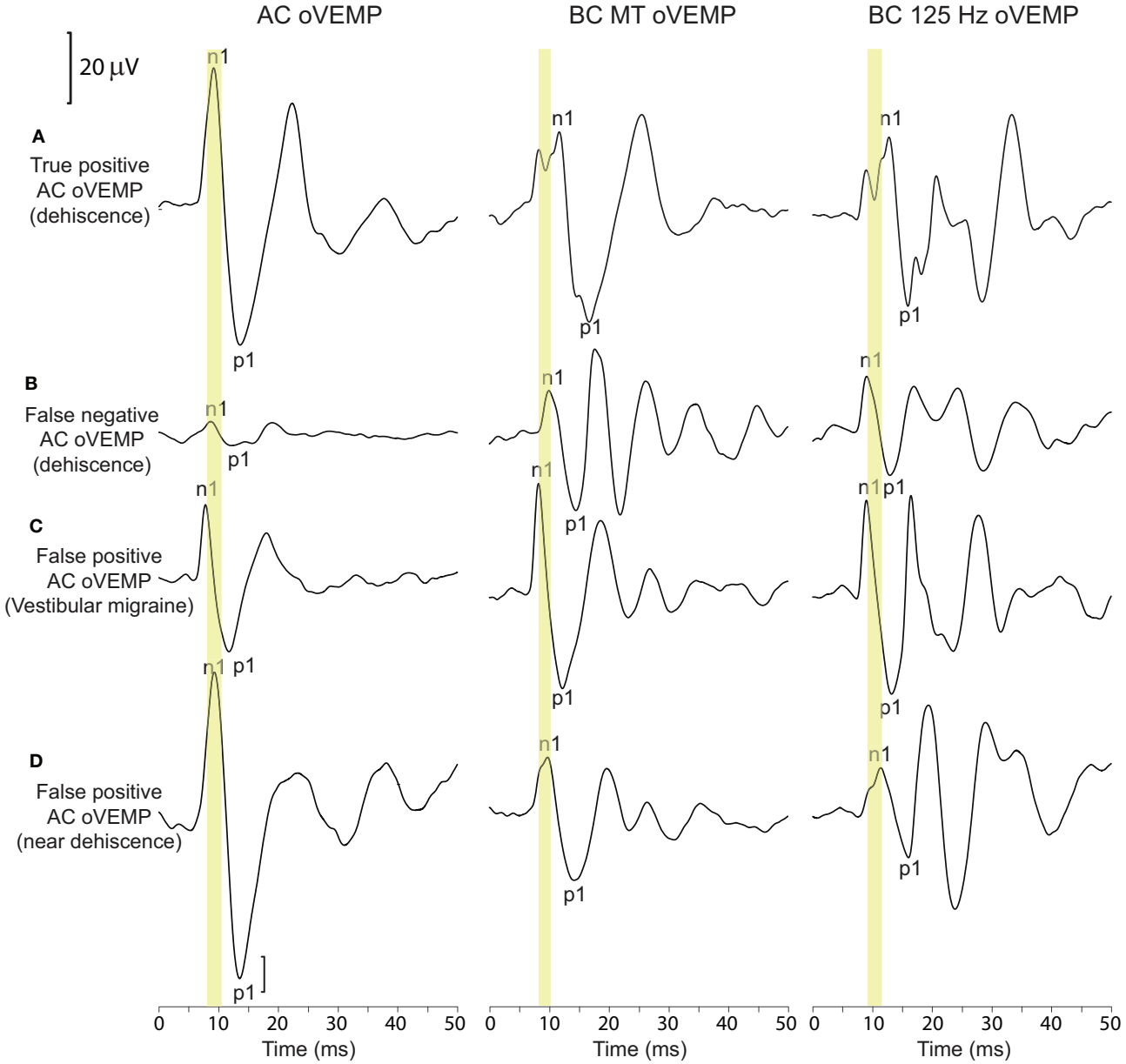

FIGURE 4 | oVEMP waveforms for dehiscent and non-dehiscent ears. **(A, B)** show the corresponding waveforms for the left and right ears of a patient with bilateral dehiscence on CT imaging (classification scores of 4 and 3, respectively). **(A)** represents a true-positive AC oVEMP response. BC oVEMP waveforms show an initial bifid negative potential (described in the methods) with latency delays for both n1 and p1 potentials. The AC oVEMP amplitude in **(B)** falls within normal limits, representing a false negative AC oVEMP; n1 and p1 latencies also fall within the normal range. **(C, D)** show false positive enlarged AC oVEMPs in a patient with vestibular migraine and near dehiscence. BC oVEMP latencies are normal in both cases. The normal n1 latency range is indicated for each stimulus by the yellow shaded region.

Patient Symptoms

Audiovestibular symptoms for dehiscent and non-dehiscent ears are compared in **Table 3**. For both groups, auditory symptoms were more frequently reported than vestibular symptoms. Conductive hyperacusis, the over-hearing of one's own bodily sounds, was the best auditory discriminator, reported by 74.4% of patients with dehiscence compared with 42.8% without it (OR = 3.9, 95% CI:1.3-11.6, $p = 0.013$). Tullio phenomenon, defined as a positive response to one or more questions relating to sound or pressure induced vertigo/oscillopsia, was experienced by 62.8% of patients with dehiscence compared with 33.3% without dehiscence (OR = 3.4, CI: 1.1-10.1, $p = 0.027$). Based

on symptoms and AC oVEMP results, 36 of 43 patients with dehiscence (83.7%)[1] and 12 of 21 patients without dehiscence (57.1%) fulfilled symptom criteria recommended by the Bárány Society (in press) for a diagnosis of superior canal dehiscence *syndrome* (SCDS). Half the non-dehiscent group fulfilling these criteria had near dehiscence. Spearmen's correlations were performed between the number of SCD-type symptoms (**Table 3**: questions 1,2,3,4,6,9) and VEMP results for patients with unilaterally enlarged AC oVEMPs. There was no relationship between the number of SCD symptoms and oVEMP amplitudes or n1 latencies in SCD ($p > 0.3$). In contrast, patients without dehiscence who had more symptoms tended to also have larger AC oVEMP amplitudes (rho = 0.583; $p = 0.047$) and longer BC n1 latencies (rho = 0.634, $p = 0.027$; 125 Hz rho = 0.631, $p = 0.027$).

TABLE 3 | Prevalence of audio-vestibular symptoms.

	Dehiscent		Non-Dehiscent	
	%	Sample size (patients/ears)	%	Sample size (patients/ears)
Vestibular symptoms				
1.*Vertigo-Sound	32.6	43	19	21
2. *Oscillopsia-Sound	25.6	43	19	21
3. *Vertigo-Pressure	48.8	43	28.6	21
4. *Oscillopsia-Pressure	18.6	43	14.3	21
5. Chronic dizziness	45	40	14.3	21
Auditory symptoms				
6. Over-hearing of bodily sounds	74.4	43	42.8	21
7. Loudness discomfort	64.4	43	61.9	21
8. Better than normal hearing	25.5	51	40.6	32
9. Autophony	52.0	25	50.0	4
10.Aural fullness	55.7	52	33.3	33
11.Hearing loss	52.0	50	27.3	33

Percentages indicate the proportion of participants/ears from the total number of available responses (sample size). Percentages for vestibular symptoms, loudness discomfort and hearing of bodily sounds represent the proportion of total patient responses; other auditory symptoms are expressed as a percentage of individual ears. Asterisks indicate symptoms consistent with Tullio phenomenon.

DISCUSSION

In this study of 86 ears with enlarged AC oVEMP amplitudes, the most common diagnosis was frank superior canal dehiscence (SCD). All patients with SCD had vestibular and/or auditory symptoms, and 83.7% had symptoms required to fulfill Barany Society criteria for superior canal dehiscence *syndrome* (SCDS). However, enlarged AC oVEMPs were also recorded in association with near dehiscence, vestibular migraine, enlarged vestibular aqueduct, and in a subset of patients without a definitive diagnosis. Half of these cases had symptoms consistent with SCDS. Most ears (79%) with dehiscence demonstrated BC oVEMP latency delays, compared with <16% of ears without dehiscence. These findings support the use of BC oVEMP latency delays in the differential diagnosis of patients with enlarged AC oVEMP amplitudes.

Delayed BC oVEMPs as a Test of SCD

The findings of this study support the hypothesis that BC oVEMP latency shifts are mediated by a pathological opening in the superior semicircular canal, since they were seen infrequently in other disorders with enlarged AC oVEMP amplitudes. Latency shifts were more pronounced for the 125 Hz stimulus, which is in keeping with previous results using tendon hammer taps which produce a similar low-frequency skull vibration response (18). However, contrasting with results to tendon hammer taps, sensitivity for the 125 Hz stimulus was not 100%. Notably, the sample size in the previous study was smaller and comparisons were made only with healthy controls. Verrecchia et al. (16) similarly found significantly longer Fz 125 Hz latencies for SCD compared with a large group of patients with unselect dizziness, though sensitivity and specificity were lower than for 500 Hz AC oVEMP amplitudes. Whether any of their non-dehiscent patients had both an enlarged AC oVEMP amplitude, and a delayed 125 Hz latency, was not reported. In our study, where an enlarged AC oVEMP was a requirement for inclusion, prolonged 125 Hz n1 latencies >11.5 ms were occasionally recorded in ears with extremely thin bone covering (i.e., near dehiscence). This implies fluid movement through the canal opening is not always necessary. In some cases, flexing of the compliant bone could be sufficient to produce a similar pattern of endolymph displacement and receptor activation, accounting for both the AC oVEMP amplitude enlargement and BC oVEMP latency delay.

Near Dehiscent Ears

Near dehiscence was the most common alternate cause of enlarged AC oVEMPs in this series. Cadaveric studies indicate a prevalence of ∼1.4%, meaning near dehiscence is ∼3-fold more common than frank dehiscence (21). As our data suggest, these cases may or may not be associated with enlarged AC oVEMP amplitudes and SCD-type symptoms. Interest in separating near from frank dehiscence arose following the observation of a possible increase in post-operative complications, which included permanent hearing loss, transient facial nerve palsy and recurrence of symptoms (17). In a subsequent case-controlled study there was no difference in the rate of surgical complications. However, enduring post-operative auditory symptoms were documented in 41% of near dehiscence patients as opposed to 18% with frank dehiscence (22). Thus, distinguishing between etiologies could still be helpful in pre-surgical counseling/planning.

Compared with frank dehiscence, oVEMP amplitudes in near dehiscence tend to be lower (22) and cVEMP thresholds higher (22, 23). This was also observed in the present study for comparisons between AC oVEMP amplitudes of dehiscent and non-dehiscent patient ears. However, the overlapping amplitude distributions make it difficult to establish a definitive cut-off without compromising sensitivity and specificity. Even greater overlap was evident between BC oVEMP amplitude

[1]3 patients with bilaterally enlarged AC oVEMP due to frank dehiscence on one side and near dehiscence on the other, are included in the statistics for the dehiscent group.

distributions, an effect that may be explained by different patterns of endolymph flow, end organ, and receptor activation. Whereas, both stimuli produce combinations of ampullofugal and ampullopetal endolymph pumping and flow (3), eye movement recordings suggest the dominant effect of air-conduction in SCD is otolith and superior canal afferent excitation. The eyes (slow phase) move upward and away from the stimulated ear, reflecting ampullofugal fluid displacement from the oval window of the cochlea toward the dehiscence (24–26).

Low frequency vibration (∼100 Hz) is a less specific stimulus for the otolith afferents (27) that can reach the labyrinth through a combination of inertial, compression, and soft-tissue/fluid pathway mechanisms (28). Distributed patterns of fluid displacement and receptor activation across different parts of the labyrinth probably explains the more modest enhancement in BC oVEMPs and BC-evoked eye movements (8, 26), and the more diverse patterns of nystagmus reported in response to low-frequency BC vibration (29–32).

Latency comparisons were significant not only between patient groups, but in comparison with the upper limit of controls, where a prolonged BC oVEMP latency predicted dehiscence. Previous attempts to discriminate between dehiscence and near dehiscence have met with mixed results. Mehta et al. (23) found no significant differences in DHI scores or objective findings of sound or pressure-evoked nystagmus. In contrast, for a group of patients undergoing SCDS surgery, sound or pressure-evoked nystagmus were more common in frank dehiscence (22). cVEMP thresholds and air-bone gaps on audiometry have been advocated as useful discriminators (22, 23), and oVEMP latencies and amplitudes for BC vertex stimulation can help separate SCD from other causes of dizziness (16). However, threshold seeking and vertex oVEMPs require either additional recordings or a shift in BC stimulation site, and not all neurotologists will have ready access to an audiometer.

Alternate Diagnoses in Patients With Large AC oVEMPs

This study highlights additional diagnoses, other than frank or near dehiscence, that can produce enlarged AC oVEMPs. The finding of two cases with enlarged vestibular aqueducts, another third-window syndrome, is unsurprising and has been described previously (13, 14). Similar to SCD, the enlarged aqueduct creates an additional low impedance pathway, through which sound, vibration and pressure can transmit (33). Absence of a BC oVEMP latency delay in these cases could reflect the different anatomical location of the third window. A low impedance pathway between the aqueduct and cochlear windows (i.e., through the vestibule) could lead to increased otolith hair cell stimulation but without significant fluid displacement and hair cell activation within the superior canal. Further studies involving patients with enlarged vestibular aqueducts are needed to confirm this. No cases of posterior canal dehiscence were identified in this series to determine whether BC oVEMP latency delays occur with increased posterior canal receptor activation.

The finding of enlarged AC oVEMPs in association with VM is more difficult to explain, since there is no third window into the inner ear and VM is a central vestibular disorder (20). VEMP results in VM are variable, ranging from reduced or absent responses (34, 35), to normal responses (36, 37) that sometimes potentiate with repetitive stimulation (38). Potential mechanisms underlying vestibular symptoms and signs are equally diverse and could include any combination of inner ear ischemia due to vasospasm, trigeminal nerve irritation, and central disruptions in sensory processing. In our experience, most VM patients have normal and symmetrical VEMP responses (39). However, just as some VM patients demonstrate hyper-responsivity on caloric testing (40, 41), the enlarged oVEMP responses described herein may represent a subset of patients for whom central mechanisms of vestibular hyperexcitability are dominant. Associated symptoms of aural pressure and hyperacusis (42), further highlight VM as a potential SCD mimic for which adjunct BC oVEMP latency testing could prove useful.

False Negative oVEMPs

This study revealed nine incidental cases of contralateral dehiscence in patients with unilaterally enlarged AC oVEMP amplitudes. This implies AC oVEMP sensitivity is not 100% and may on occasion miss smaller dehiscences. All cases with false negative AC oVEMP results had a CT classification score of 3, suggesting focal dehiscence in the short arm of the canal. Amplitudes and latencies to BC stimuli were also normal in these cases, implying a similar loss of sensitivity. Alternatively, the CT scans for some of these patients may have been classified as dehiscent in error. Even with 0.5 mm collimations, very thin bone can be invisible on CT imaging (23), leading to misdiagnosis of frank dehiscence in up to a third of near dehiscence cases (22). Over-diagnosis of frank dehiscence might also account for some cases in the dehiscence group that were without a BC oVEMP latency prolongation. More studies and case reports are needed to understand how often, and why, false negative AC oVEMPs might occur.

Stimulus Considerations

While both BC stimuli used in this study produced significant latency effects, the effect size was largest for the lower frequency 125 Hz stimulus. Such low frequencies have been used infrequently for BC oVEMP testing and in guinea pigs with an intact bony labyrinth, they activate both irregular discharging otolith and canal afferents (27). We advocate its use, not as a test of otolith function, but as an adjunct test for diagnosing SCD. It is unknown whether differences in stimulus shaping, polarity and duration affect sensitivity and specificity of 125 Hz oVEMPs in SCD. The first studies involving 125 Hz stimulation in SCD used a 10 ms condensation polarity stimulus (2 ms rise/fall) (43, 44). Manzari et al. used a slightly shorter 7 ms 125 Hz stimulus, also of condensation polarity and although latencies were not analyzed, morphological changes (double-peaked configuration) like those reported here were evident in the recordings of a single patient (7). Other investigators have used an unshaped, single cycle (i.e., 8 ms) of either condensation (45) or rarefaction (16) polarity, each proving useful in diagnosing SCD based on different outcome measures. To some extent the choice of stimulus parameters will be influenced by the type of evoked

potential system, many of which require at least one complete stimulus cycle.

Study Limitations

A limitation of this study was that most patients did not undergo surgery to confirm their temporal bone status, meaning the possibility of misdiagnosed frank dehiscence could not be investigated. Other limitations of this study arise mainly from the retrospective design. Patients did not undergo cVEMP threshold testing since our clinic preferentially uses oVEMP for diagnosis of SCD, and those who were imaged at an alternate facility, were not represented. The number and range of alternate diagnoses in this study may differ from other centers and are likely to be influenced by clinic referral patterns and test protocols. For example, enlarged vestibular aqueducts may be less common in a neurology clinic compared with an ENT or audiology clinic, whereas vestibular migraine may be more common. Because we recruited patients based on an enlarged AC oVEMP, we are unable to compare the sensitivity of AC oVEMPs with BC oVEMP amplitudes and latencies. Prospective studies that recruit patients based solely on symptoms, and which are complemented by surgical confirmation of dehiscence, are needed to clarify the sensitivity and specificity of different VEMP outcome measures in SCD.

CONCLUSIONS

Given the established high sensitivity of AC oVEMP amplitudes in SCD, we recommend these recordings continue to be prioritized as a first clinical test of dehiscence. However, as demonstrated in this study, AC oVEMPs can be enlarged for other reasons and in many cases, patients will fulfill symptom criteria for a dehiscence diagnosis. When this occurs, it is helpful to consider other test results. The demonstration of BC oVEMP latency delays in conjunction with an enlarged AC oVEMP amplitude are among the *ad hoc* indicators that can be considered. This may be particularly useful when CT imaging results and/or symptoms are ambiguous.

DATA AVAILABILITY STATEMENT

The raw data supporting the conclusions of this article will be made available by the authors, without undue reservation.

ETHICS STATEMENT

The studies involving human participants were reviewed and approved by the Royal Prince Alfred Research Ethics and Governance Office. Written informed consent for participation was not required for this study in accordance with the national legislation and the institutional requirements.

AUTHOR CONTRIBUTIONS

RT and MW contributed to the conception and design of the study. JM interpreted the CT scans. RT, JM, BK, AY, BI, EA, NR, CR, JP, SR, and MW collected and/or collated data. RT performed the statistical analysis, prepared the figures and tables, and wrote the first manuscript draft. All authors contributed to manuscript revision, read, and approved the submitted version.

FUNDING

RT previously received funding from a University of Sydney Post-Graduate Award and is currently supported by an Aotearoa Fellowship funded by the Center for Brain Research, The University of Auckland, New Zealand. AY receives scholarship funding from the University of Sydney Post-Graduate Award scheme.

REFERENCES

1. Ward BK, Carey JP, Minor LB. Superior canal dehiscence syndrome: lessons from the first 20 years. *Front Neurol.* (2017) 8:177. doi: 10.3389/fneur.2017.00177
2. Carey JP, Hirvonen TP, Hullar TE, Minor LB. Acoustic responses of vestibular afferents in a model of superior canal dehiscence. *Otol Neurotol.* (2004) 25:345–52. doi: 10.1097/00129492-200405000-00024
3. Iversen MM, Zhu H, Zhou W, Della Santina CC, Carey JP, Rabbitt RD. Sound abnormally stimulates the vestibular system in canal dehiscence syndrome by generating pathological fluid-mechanical waves. *Sci Rep.* (2018) 8:10257. doi: 10.1038/s41598-018-28592-7
4. Curthoys IS, Burgess AM, Goonetilleke SC. Phase-locking of irregular guinea pig primary vestibular afferents to high frequency (>250 Hz) sound and vibration. *Hear Res.* (2019) 373:59–70. doi: 10.1016/j.heares.2018.12.009
5. Dlugaiczyk J, Burgess AM, Goonetilleke SC, Sokolic L, Curthoys IS. Superior canal dehiscence syndrome: relating clinical findings with vestibular neural responses from a guinea pig model. *Otol Neurotol.* (2019) 40:e406–14. doi: 10.1097/MAO.0000000000001940
6. Janky KL, Nguyen KD, Welgampola M, Zuniga MG, Carey JP. Air-conducted oVEMPs provide the best separation between intact and superior canal dehiscent labyrinths. *Otol Neurotol.* (2013) 34:127–34. doi: 10.1097/MAO.0b013e318271c32a
7. Manzari L, Burgess AM, Mcgarvie LA, Curthoys IS. An indicator of probable semicircular canal dehiscence: ocular vestibular evoked myogenic potentials to high frequencies. *Otolaryngol Head Neck Surg.* (2013) 149:142–5. doi: 10.1177/0194599813489494
8. Govender S, Fernando T, Dennis DL, Welgampola MS, Colebatch JG. Properties of 500Hz air- and bone-conducted vestibular evoked myogenic potentials (VEMPs) in superior canal dehiscence. *Clin Neurophysiol.* (2016) 127:2522–31. doi: 10.1016/j.clinph.2016.02.019
9. Hunter JB, Patel NS, O'connell BP, Carlson ML, Shepard NT, Mccaslin DL, et al. Cervical and ocular VEMP testing in diagnosing superior semicircular canal dehiscence. *Otolaryngol Head Neck Surg.* (2017) 156:917–23. doi: 10.1177/0194599817690720
10. Young YH, Wu CC, Wu CH. Augmentation of vestibular evoked myogenic potentials: an indication for distended saccular hydrops. *Laryngoscope.* (2002) 112:509–12. doi: 10.1097/00005537-200203000-00019
11. Sheykholeslami K, Schmerber S, Habiby Kermany M, Kaga K. Vestibular-evoked myogenic potentials in three patients with large vestibular aqueduct. *Hear Res.* (2004) 190:161–8. doi: 10.1016/S0378-5955(04)00018-8
12. Manzari L. Vestibular signs and symptoms of volumetric abnormalities of the vestibular aqueduct. *J Laryngol Otol.* (2008) 122:557–63. doi: 10.1017/S0022215107000400
13. Taylor RL, Bradshaw AP, Magnussen JS, Gibson WP, Halmagyi GM, Welgampola MS. Augmented ocular vestibular evoked myogenic potentials to

air-conducted sound in large vestibular aqueduct syndrome. *Ear Hear.* (2012) 33:768–71. doi: 10.1097/AUD.0b013e31825ce613
14. Zhou YJ, Wu YZ, Cong N, Yu J, Gu J, Wang J, et al. Contrasting results of tests of peripheral vestibular function in patients with bilateral large vestibular aqueduct syndrome. *Clin Neurophysiol.* (2017) 128:1513–8. doi: 10.1016/j.clinph.2017.05.016
15. Gopen Q, Zhou G, Poe D, Kenna M, Jones D. Posterior semicircular canal dehiscence: first reported case series. *Otol Neurotol.* (2010) 31:339–44. doi: 10.1097/MAO.0b013e3181be65a4
16. Verrecchia L, Brantberg K, Tawfique Z, Maoli D. Diagnostic accuracy of ocular vestibular evoked myogenic potentials for superior canal dehiscence syndrome in a large cohort of dizzy patients. *Ear Hear.* (2019) 40:287–94. doi: 10.1097/AUD.0000000000000613
17. Ward BK, Wenzel A, Ritzl EK, Gutierrez-Hernandez S, Della Santina CC, Minor LB, et al. Near-dehiscence: clinical findings in patients with thin bone over the superior semicircular canal. *Otol Neurotol.* (2013) 34:1421–8. doi: 10.1097/MAO.0b013e318287efe6
18. Taylor RL, Blaivie C, Bom AP, Holmeslet B, Pansell T, Brantberg K, et al. Ocular vestibular-evoked myogenic potentials (oVEMP) to skull taps in normal and dehiscent ears: mechanisms and markers of superior canal dehiscence. *Exp Brain Res.* (2014) 232:1073–84. doi: 10.1007/s00221-013-3782-z
19. Tilikete C, Krolak-Salmon P, Truy E, Vighetto A. Pulse-synchronous eye oscillations revealing bone superior canal dehiscence. *Ann Neurol.* (2004) 56:556–60. doi: 10.1002/ana.20231
20. Lempert T, Olesen J, Furman J, Waterston J, Seemungal B, Carey J, et al. Vestibular migraine: diagnostic criteria. *J Vestib Res.* (2012) 22:167–72. doi: 10.3233/VES-2012-0453
21. Carey JP, Minor LB, Nager GT. Dehiscence or thinning of bone overlying the superior semicircular canal in a temporal bone survey. *Arch Otolaryngol Head Neck Surg.* (2000) 126:137–47. doi: 10.1001/archotol.126.2.137
22. Baxter M, Mccorkle C, Trevino Guajardo C, Zuniga MG, Carter AM, Della Santina CC, et al. Clinical and physiologic predictors and postoperative outcomes of near dehiscence syndrome. *Otol Neurotol.* (2019) 40:204–12. doi: 10.1097/MAO.0000000000002077
23. Mehta R, Klumpp ML, Spear SA, Bowen MA, Arriaga MA, Ying YL. Subjective and objective findings in patients with true dehiscence vs. thin bone over the superior semicircular canal. *Otol Neurotol.* (2015) 36:289–94. doi: 10.1097/MAO.0000000000000654
24. Cremer PD, Minor LB, Carey JP, Della Santina CC. Eye movements in patients with superior canal dehiscence syndrome align with the abnormal canal. *Neurology.* (2000) 55:1833–41. doi: 10.1212/WNL.55.12.1833
25. Aw ST, Todd MJ, Aw GE, Magnussen JS, Curthoys IS, Halmagyi GM. Click-evoked vestibulo-ocular reflex: stimulus-response properties in superior canal dehiscence. *Neurology.* (2006) 66:1079–87. doi: 10.1212/01.wnl.0000204445.81884.c7
26. Welgampola MS, Migliaccio AA, Myrie OA, Minor LB, Carey JP. The human sound-evoked vestibulo-ocular reflex and its electromyographic correlate. *Clin Neurophysiol.* (2009) 120:158–66. doi: 10.1016/j.clinph.2008.06.020
27. Dlugaiczyk J, Burgess AM, Curthoys IS. Activation of guinea pig irregular semicircular canal afferents by 100 Hz vibration: clinical implications for vibration-induced nystagmus and vestibular-evoked myogenic potentials. *Otol Neurotol.* (2020) 41:e961–70. doi: 10.1097/MAO.0000000000002791
28. Stenfelt S, Goode RL. Bone-conducted sound: physiological and clinical aspects. *Otol Neurotol.* (2005) 26:1245–61. doi: 10.1097/01.mao.0000187236.10842.d5
29. Manzari L, Modugno GC, Brandolini C, Pirodda A. Bone vibration-induced nystagmus is useful in diagnosing superior semicircular canal dehiscence. *Audiol Neurotol.* (2008) 13:379–87. doi: 10.1159/000148201
30. Dumas G, Lion A, Karkas A, Perrin P, Perottino F, Schmerber S. Skull vibration-induced nystagmus test in unilateral superior canal dehiscence and otosclerosis: a vestibular Weber test. *Acta Otolaryngol.* (2014) 134:588–600. doi: 10.3109/00016489.2014.888591
31. Park JH, Kim HJ, Kim JS, Koo JW. Costimulation of the horizontal semicircular canal during skull vibrations in superior canal Dehiscence syndrome. *Audiol Neurootol.* (2014) 19:175–83. doi: 10.1159/000358002
32. Dumas G, Tan H, Dumas L, Perrin P, Lion A, Schmerber S. Skull vibration induced nystagmus in patients with superior semicircular canal dehiscence. *Eur Ann Otorhinolaryngol Head Neck Dis.* (2019) 136:263–72. doi: 10.1016/j.anorl.2019.04.008
33. Merchant SN, Rosowski JJ. Conductive hearing loss caused by third-window lesions of the inner ear. *Otol Neurotol.* (2008) 29:282–9. doi: 10.1097/MAO.0b013e318161ab24
34. Kim CH, Jang MU, Choi HC, Sohn JH. Subclinical vestibular dysfunction in migraine patients: a preliminary study of ocular and rectified cervical vestibular evoked myogenic potentials. *J Headache Pain.* (2015) 16:93. doi: 10.1186/s10194-015-0578-5
35. Zaleski A, Bogle J, Starling A, Zapala DA, Davis L, Wester M, et al. Vestibular evoked myogenic potentials in patients with vestibular migraine. *Otol Neurotol.* (2015) 36:295–302. doi: 10.1097/MAO.0000000000000665
36. Vitkovic J, Paine M, Rance G. Neuro-otological findings in patients with migraine- and nonmigraine-related dizziness. *Audiol Neurootol.* (2008) 13:113–22. doi: 10.1159/000111783
37. Kandemir A, Çelebisoy N, Köse T. Cervical vestibular evoked myogenic potentials in primary headache disorders. *Clinical Neurophysiology.* (2013) 124:779–84. doi: 10.1016/j.clinph.2012.09.027
38. Roceanu A, Allena M, De Pasqua V, Bisdorff A, Schoenen J. Abnormalities of the vestibulo-collic reflex are similar in migraineurs with and without vertigo. *Cephalalgia.* (2008) 28:988–90. doi: 10.1111/j.1468-2982.2008.01641.x
39. Taylor RL, Zagami AS, Gibson WP, Black DA, Watson SR, Halmagyi MG, et al. Vestibular evoked myogenic potentials to sound and vibration: characteristics in vestibular migraine that enable separation from Meniere's disease. *Cephalalgia.* (2012) 32:213–25. doi: 10.1177/0333102411434166
40. Teggi R, Colombo B, Bernasconi L, Bellini C, Comi G, Bussi M. Migrainous vertigo: results of caloric testing and stabilometric findings. *Headache.* (2009) 49:435–44. doi: 10.1111/j.1526-4610.2009.01338.x
41. Nafie Y, Friedman M, Hamid MA. Auditory and vestibular findings in patients with vestibular migraine. *Audiol Med.* (2011) 9:98–102. doi: 10.3109/1651386X.2011.607248
42. Von Brevern M, Zeise D, Neuhauser H, Clarke AH, Lempert T. Acute migrainous vertigo: clinical and oculographic findings. *Brain.* (2005) 128:365–74. doi: 10.1093/brain/awh351
43. Zhang AS, Govender S, Colebatch JG. Superior canal dehiscence causes abnormal vestibular bone-conducted tuning. *Neurology.* (2011) 77:911–3. doi: 10.1212/WNL.0b013e31822c6263
44. Zhang AS, Govender S, Colebatch JG. Tuning of the ocular vestibular evoked myogenic potential (oVEMP) to air- and bone-conducted sound stimulation in superior canal dehiscence. *Exp Brain Res.* (2012) 223:51–64. doi: 10.1007/s00221-012-3240-3
45. Verrecchia L, Westin M, Duan M, Brantberg K. Ocular vestibular evoked myogenic potentials to vertex low frequency vibration as a diagnostic test for superior canal dehiscence. *Clin Neurophysiol.* (2016) 127:2134–9. doi: 10.1016/j.clinph.2016.01.001

Conflict of Interest: The authors declare that the research was conducted in the absence of any commercial or financial relationships that could be construed as a potential conflict of interest.

frontiers in Neurology

CASE REPORT
published: 10 November 2020
doi: 10.3389/fneur.2020.585747

Congenital Membranous Stapes Footplate Producing Episodic Pressure-Induced Perilymphatic Fistula Symptoms

*Han Matsuda[1], Yasuhiko Tanzawa[1], Tatsuro Sekine[1], Tomohiro Matsumura[2], Shiho Saito[1], Susumu Shindo[1], Shin-ichi Usami[3], Yasuhiro Kase[1], Akinori Itoh[1] and Tetsuo Ikezono[1]**

[1] Department of Otorhinolaryngology, Saitama Medical University, Saitama, Japan, [2] Department of Biochemistry and Molecular Biology, Nippon Medical School, Graduate School of Medicine, Tokyo, Japan, [3] Department of Otorhinolaryngology, Shinshu University School of Medicine, Nagano, Japan

OPEN ACCESS

Edited by:
Stefan K. Plontke,
Martin Luther University of Halle-Wittenberg, Germany

Reviewed by:
Ja-Won Koo,
Seoul National University, South Korea
Toru Seo,
St. Marianna University School of Medicine, Japan
Brian McKinnon,
University of Texas Medical Branch at Galveston, United States

***Correspondence:**
Tetsuo Ikezono
ikezono.tetsuo@1972.saitama-med.ac.jp

Specialty section:
This article was submitted to Neuro-Otology, a section of the journal Frontiers in Neurology

Received: 21 July 2020
Accepted: 19 October 2020
Published: 10 November 2020

Citation:
Matsuda H, Tanzawa Y, Sekine T, Matsumura T, Saito S, Shindo S, Usami S-i, Kase Y, Itoh A and Ikezono T (2020) Congenital Membranous Stapes Footplate Producing Episodic Pressure-Induced Perilymphatic Fistula Symptoms. Front. Neurol. 11:585747. doi: 10.3389/fneur.2020.585747

Introduction: Recent third window syndrome studies have revealed that the intact bony labyrinth and differences in the stiffness of the oval and round windows are essential for proper cochlear and vestibular function. Herein we report a patient with a congenital dehiscence of the right stapes footplate. This dehiscence caused long-standing episodic pressure-induced vertigo (Hennebert sign). At the time of presentation, her increased thoracic pressure changes induced the rupture of the membranous stapes footplate. Perilymph leakage was confirmed by imaging and a biochemical test [perilymph-specific protein Cochlin-tomoprotein (CTP) detection test].

Case Report: A 32-year-old woman presented with a sudden onset of right-sided hearing loss and severe true rotational vertigo, which occurred immediately after nose-blowing. CT scan showed a vestibule pneumolabyrinth. Perilymphatic fistula (PLF) repair surgery was performed. During the operation, a bony defect of 0.5 mm at the center of the right stapes footplate, which was covered by a membranous tissue, and a tear was found in this anomalous membrane. A perilymph-specific protein CTP detection test was positive. The fistula in the footplate was sealed. Postoperatively, the vestibular symptoms resolved, and her hearing improved. A more detailed history revealed that, for 15 years, she experienced true rotational vertigo when she would blow her nose. After she stopped blowing her nose, she would again feel normal.

Discussion: There is a spectrum of anomalies that can occur in the middle ear, including the ossicles. The present case had a dehiscence of the stapes, with a small membranous layer of tissue covering a bony defect in the center of the footplate. Before her acute presentation to the hospital, this abnormal footplate with dehiscence induced pathological pressure-evoked fluid-mechanical waves in the inner ear, which resulted in Hennebert sign. When patients have susceptibility (e.g., weak structure) to rupture, such

as that identified in this case, PLF can be caused by seemingly insignificant events such as nose-blowing, coughing, or straining.

Conclusion: This case demonstrates that PLF is a real clinical entity. Appropriate recognition and treatment of PLF can improve a patient's condition and, hence, the quality of life.

Keywords: cochlin-tomoprotein, CTP, pneumolabyrinth, perilymph fistula, PLF, stapes, superior canal dehiscence, third window syndrome

INTRODUCTION

Third window syndrome (TWS) was first identified in patients with superior semicircular canal dehiscence (SCD) (1); now it includes cochlea-internal carotid artery dehiscence and posterior semicircular canal-jugular bulb dehiscence, cochlea-facial nerve dehiscence, and others (2). Wackym et al. classified these conditions as CT+ TWS or CT+ OCDS (i.e., third window syndrome with positive findings on CT imaging or otic capsule dehiscence syndrome with positive findings on CT imaging). The patient reported herein had no visible CT evidence of a bony dehiscence creating a third mobile window. The diagnostic findings and symptoms were similar to those of patients with CT+ TWS (3, 4).

We report a patient identified as a CT- TWS who had a bony defect of 0.5 mm at the center of the right stapes footplate which was covered by a membranous structure. This dehiscence caused a long-standing, pressure-induced vertigo. At the time of presentation, her increased thoracic pressure induced the rupture of the membranous stapes footplate, resulting in severe true rotational vertigo and hearing loss. Perilymph leakage was confirmed by imaging and a biochemical test utilizing a perilymph-specific protein Cochlin-tomoprotein (CTP) detection test.

CASE REPORT

A 32-year-old woman presented to another hospital with a sudden onset of right-sided hearing loss and severe true rotational vertigo, which occurred immediately after nose-blowing. She was treated with corticosteroids and bedrest for 1 week, and her vestibular symptom initially resolved. However, on the 7th day, her severe rotational vertigo recurred, and her hearing loss persisted, and she was referred to our hospital.

An otoscopic examination showed bilateral intact tympanic membranes. Pure tone audiometry showed a severe right-sided mixed hearing loss (**Figure 1**). Left-beating horizontal and rotatory nystagmus was mainly observed in the supine position with Frenzel glasses. A high-resolution temporal bone CT scan on the 10th day showed pneumolabyrinth in the right vestibule (**Figure 2**). She was again treated with bedrest and corticosteroids. After the conservative treatment, however, her vertigo and severe hearing loss did not resolve. Therefore, we decided to perform perilymphatic fistula (PLF) repair surgery on the 17th day. The operation was done under general anesthesia; a transcanal approach with tympanomeatal flap elevation enabled the observation of a dehiscence in the center of the stapes footplate with a bony defect 0.5 mm in diameter, which was covered by a membranous tissue, and a tear was found in this membrane (**Figure 3**). A small amount of perilymph leakage was observed from this tear, and middle ear lavage with 0.3 ml of saline for a CTP detection test was collected during the operation. The fistula in the footplate was sealed with connective tissue, and the round window was reinforced with connective tissue and cartilage to stabilize the labyrinth further. The vestibular symptoms and nystagmus disappeared immediately after the operation, and at her 1-month follow-up assessment, her hearing improved (**Figure 4**). Postoperatively, a CTP detection test revealed a concentration of 0.84 ng/ml, which is positive, with the cutoff criteria being CTP $\geqq$ 0.8 positive, 0.8 > CTP > 0.4 intermediate, and 0.4 > CTP negative (ng/ml) (5).

A more detailed history revealed that, for 15 years, she felt vertigo as if her brain was shaken upward when she would blow her nose. True rotational vertigo would continue for 3 to 4 s. After she stopped blowing her nose, she would again feel normal. She did not hear any internal sounds such as echoing, resonant voice, pulse/heartbeat, or hearing her eyes move or blink. She did not have any history of traumatic events to her head or ears. Based upon her history, intraoperative findings, and postoperative resolution of her vestibular symptoms, the dehiscence of the stapes footplate caused pressure-induced vertigo symptoms. At 1 year after the surgery, she had no recurrence of the vestibular symptoms, and her cochlear function remained unchanged.

DISCUSSION

There is a spectrum of anomalies that can occur in the middle ear, including the ossicles. In mild cases, they can be the cause of conductive hearing loss, and in severe cases, it can cause cerebrospinal fluid (CSF) leakage. Dysplasia of the inner ear is often associated with an abnormal otic capsule, resulting in congenital weakness or fistula formation in the stapes footplate or annular ligament, which is one of the most common causes of cerebrospinal fluid otorrhea and meningitis (6). The present case had normal hearing prior to this episode, and the imaging showed an intact inner/middle ear structure. Intraoperatively, a minor anomaly of the stapes was identified, with a small membranous layer of tissue covering a bony defect in the center of the footplate. This type of congenital anomalous footplate has not been described. Recent developmental studies show that the possibility of this type of anomaly can still exist since the otic capsule may not be involved in the formation of the base of the

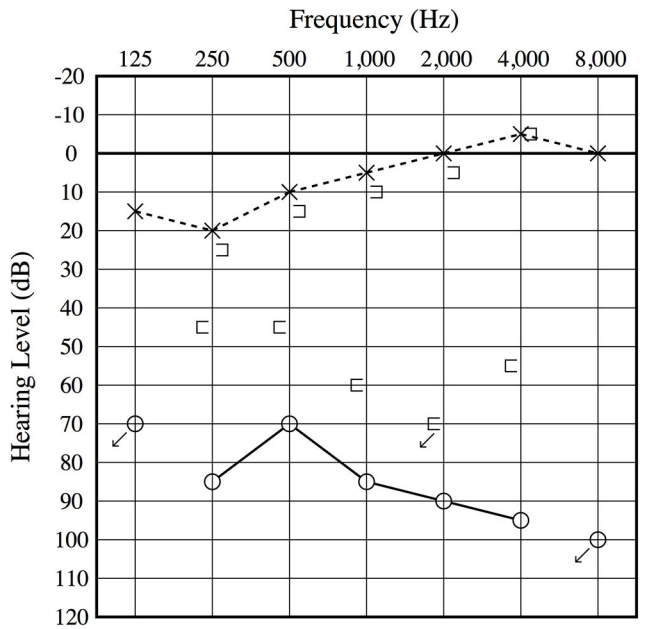

FIGURE 1 | Preoperative audiogram. A severe mixed sensory and conductive hearing loss is observed on the right ear, and an air–bone gap is present at low frequencies.

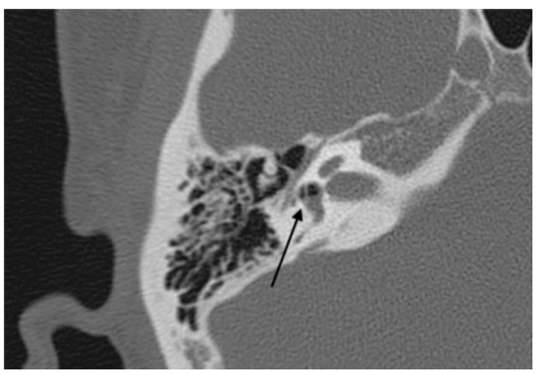

FIGURE 2 | Preoperative CT scan. Air bubbles (arrow) are visible in the vestibule.

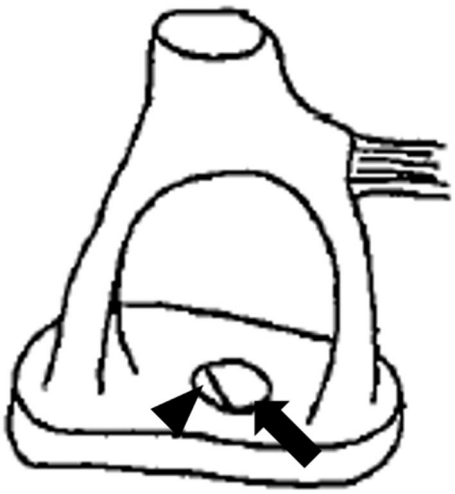

FIGURE 3 | Illustration depicting the anomalous stapes footplate. The arrow illustrates the bony defect, while the arrowhead illustrates a tear in the membranous stapes footplate.

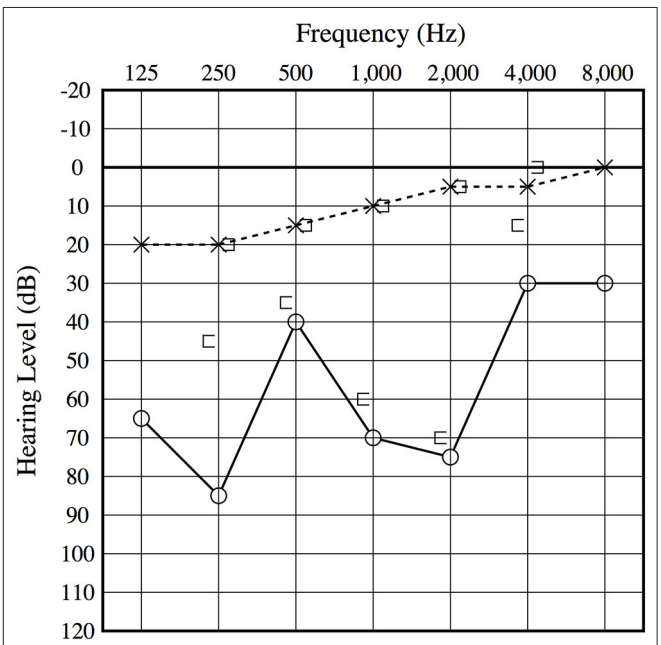

FIGURE 4 | Postoperative audiogram. The 1-month postoperative audiogram had thresholds somewhat improved compared to the preoperative audiogram.

stapes (7, 8). Because of her negative history of past traumatic events to her head or ears, this abnormal finding of the footplate is most probably due to developmental malformation.

Third window syndrome studies revealed that the intact bony labyrinth and differences in the stiffness of the oval and the round windows are essential for proper cochlear and vestibular function (9). Before her acute presentation to the hospital, this dehiscence in the footplate induced pathological pressure-evoked fluid-mechanical waves in the inner ear and caused pressure-induced vertigo, which is one of the TWS symptoms. Although she had vertigo induced by nose-blowing since she was 17 years old, the etiology remained undiagnosed. The rapid change in the middle ear/intracranial pressure by her nose-blowing resulted in membrane rupture, perilymph leakage, and pneumolabyrinth. When patients have susceptibility (e.g., weak structure) to rupture, such as that identified in this case, PLF can be caused by seemingly insignificant events such as nose-blowing.

The diagnosis has been established in CT+ TWS, which has typical symptoms and CT findings. Ward et al. synthesized the diagnostic criteria for SCD (10). On the other hand, the

TABLE 1 | Diagnostic criteria for perilymph fistula (PLF) (based on the criteria of the Intractable Hearing Loss Research Committee of the Ministry of Health and Welfare, Japan revised in 2016).

A. Symptoms

Hearing impairment, tinnitus, aural fullness, and vestibular symptoms are observed in cases who had preceding events as listed below:
(1) Coexisting or pre-existing middle and/or inner ear diseases (trauma, cholesteatoma, tumor, anomaly, SCCD, *etc*.), middle and/or inner ear surgeries
(2) Barotrauma caused by antecedent events of external origin (e.g., blasting, diving, or flying, *etc*.)
(3) Barotrauma caused by antecedent events of internal origin (e.g., nose-blowing, sneezing, straining, or carrying heavy objects, *etc*.)

B. Laboratory findings

(1) Microscopic/endoscopic inspection
Visual identification of fistula(s) between the middle and the inner ear by a microscope or an endoscope. Fistulas can develop at the cochlear window, vestibular window, fracture site, microfissure, malformation, destruction in bony labyrinth caused by inflammation, *etc*.
(2) Biochemical test
Perilymph-specific protein is detected from the middle ear

C. Reference

(1) A perilymph-specific protein; e.g., Cochlin-tomoprotein (CTP) detection test. After myringotomy, the middle ear is rinsed with 0.3 ml saline three times; the fluid was recovered (middle ear lavage, MEL) and tested by polyclonal antibody ELISA. The cutoff criteria: ∼0.4 < CTP-negative; 0.4 ≦ CTP < 0.8 intermediate; 0.8 ≦ CTP-positive
(2) Idiopathic cases may exist
(3) The following symptoms and/or test results may be observed:
1. Streaming water-like tinnitus or feeling of running water in the middle ear
2. A popping sound can be heard at the onset
3. Nystagmus and/or vertigo induced by pressure application to the middle ear (Hennebert's phenomenon, fistula sign)
4. Imaging studies may show a fistula in the bony labyrinth or pneumolabyrinth
5. Progression of hearing impairment, tinnitus, and aural fullness may be acute, progressive, fluctuating, or recurrent
6. The main complaints can be vestibular symptoms without hearing impairment

D. Differential diagnosis

Inner ear diseases with known causes, such as viral infection, genetic, vestibular schwannoma, *etc*.

E. Diagnosis

Probable PLF: only symptoms listed in A
Definite PLF: symptoms and laboratory findings listed in B

clinical entity of PLF with leakage has remained a topic of controversy for more than 50 years due to the lack of specific biomarkers. The manifestations of PLF with leakage include a broad spectrum of neuro-otological symptoms such as hearing loss, vertigo/dizziness, disequilibrium, aural fullness, tinnitus, and cognitive dysfunction. The hearing loss may range from high frequency to low frequency and can mimic Menière disease or cochlear endolymphatic hydrops. Therefore, the difficulty of making a definitive diagnosis of PLF has caused a long-standing debate regarding its prevalence, natural history, management, and even its very existence (11).

We can overcome this controversy if we could make the definite diagnosis of PLF with leakage using an appropriate biomarker. Based on proteomic analysis, we have identified an isoform of Cochlin CTP (12) as a perilymph-specific protein that is not expressed in the blood, CSF, or saliva (13). The leaked perilymph can be recovered by middle ear lavage (MEL) with 0.3 ml of saline. We have developed an ELISA for human CTP and defined the cutoff criteria as CTP ≧ 0.8 positive, 0.8 > CTP ≧ 0.4 intermediate, and 0.4 > CTP negative (ng/ml). The sensitivity and the specificity of the test to detect perilymph leakage was 86.4 and 100%, respectively (5). The detection of CTP in the middle ear indicates the presence of a fistula and perilymph leakage. The CTP test is the most extensively studied biomarker so far. In terms of perilymph-specific expression and diagnostic accuracy, a large-scale study has been reported (14). Using this novel test, the Japanese diagnostic criteria were established (**Table 1**). This test is continuously available as an investigator-initiated trial throughout Japan by Ikezono et al. (5) and funded by Saitama Medical University. In June 2020, the Japanese Ministry of Health Labor Standards approved the CTP ELISA Test, which has qualities for medical diagnosis.

Perilymph leakage may be located in the round or the oval window (15), which may be associated with an anomalous stapes footplate, such as in this case. We have also reported a case with patent fistula ante-fentestram, showing that this microfissure can be the route for perilymph leakage (16). Most pneumolabyrinth patients reported to date were due to temporal bone trauma or otologic surgery (17–19). Pneumolabyrinth was shown by CT imaging in this case, which has a strong diagnostic value for perilymph leakage induced by the barotraumatic event. Imaging by high-resolution temporal bone CT did not show a CT+ TWS or any other inner ear abnormalities, suggesting that the pressure-induced vertigo that she experienced before her acute presentation was due to bony dehiscence of the center of the stapes footplate.

This case demonstrates that PLF is a real clinical entity. It is noteworthy that, unlike other causes of sensorineural hearing loss and dizziness, PLF with leakage is surgically correctable by sealing the fistula. By sealing the fistula, PLF is a surgically curable disease. Also, appropriate recognition and treatment of PLF can improve a patient's condition and, hence, quality of life.

DATA AVAILABILITY STATEMENT

The raw data supporting the conclusions of this article will be made available by the authors, without undue reservation.

ETHICS STATEMENT

The studies involving human participants were reviewed and approved by Institutional Review Board of Saitama Medical University Hospital (IRB No.13086). The patients/participants provided their written informed consent to participate in this study. Written informed consent was obtained from the individual for the publication of any potentially identifiable images or data included in this article.

AUTHOR CONTRIBUTIONS

TI and HM: data curation and conceptualization. TM: formal analysis. TI, S-iU, and YK: funding acquisition. HM, YT, TS, TM, SSa, SSh, YK, AI, and TI: investigation. TI, TM, SSa, and HM: methodology. TI: project administration, resources, supervision, validation, and visualization. HM: writing–original draft. All authors contributed to the article and approved the submitted version.

FUNDING

This work was supported by the Ministry of Health and Welfare, Japan (H29-Nanchitou(Nan)-Ippan-031) (http://www.mhlw.go.jp/english/).

REFERENCES

1. Minor LB, Solomon D, Zinreich JS, Zee DS. Sound- and/or pressure-induced vertigo due to bone dehiscence of the superior semicircular canal. *Arch Otolaryngol Head Neck Surg.* (1998) 124:249–58. doi: 10.1001/archotol.124.3.249
2. Ho ML, Moonis G, Halpin CF, Curtin HD. Spectrum of third window abnormalities: semicircular canal dehiscence and beyond. *AJNR Am J Neuroradiol.* (2017) 38:2–9. doi: 10.3174/ajnr.A4922
3. Wackym PA, Wood SJ, Siker DA, Carter DM. Otic capsule dehiscence syndrome: superior semicircular canal dehiscence syndrome with no radiographically visible dehiscence. *Ear Nose Throat J.* (2015) 94:E8–24. doi: 10.1177/014556131509400802
4. Wackym PA, Balaban CD, Zhang P, Siker DA, Hundal JS. Third window syndrome: surgical management of cochlea-facial nerve dehiscence. *Front Neurol.* (2019) 10:1281. doi: 10.3389/fneur.2019.01281
5. Ikezono T, Matsumura T, Matsuda H, Shikaze S, Saitoh S, Shindo S, et al. The diagnostic performance of a novel ELISA for human CTP (Cochlin-tomoprotein) to detect perilymph leakage. *PLoS ONE.* (2018) 13:e0191498. doi: 10.1371/journal.pone.0191498
6. Wang B, Dai WJ, Cheng XT, Liuyang WY, Yuan YS, Dai CF, et al. Cerebrospinal fluid otorrhea secondary to congenital inner ear dysplasia: diagnosis and management of 18 cases. *J Zhejiang University Sci.* (2019) 20:156–63. doi: 10.1631/jzus.B1800224
7. Rodríguez-Vázquez JF. Development of the stapes and associated structures in human embryos. *J Anatomy.* (2005) 207:165–73. doi: 10.1111/j.1469-7580.2005.00441.x
8. Ozeki-Satoh M, Ishikawa A, Yamada S, Uwabe C, Takakuwa T. Morphogenesis of the middle ear ossicles and spatial relationships with the external and inner ears during the embryonic period. *Anat Rec.* (2016) 299:1325–37. doi: 10.1002/ar.23457
9. Merchant SN, Nakajima HH, Halpin C, Nadol JB Jr, Lee DJ, Innis WP, et al. Clinical investigation and mechanism of air-bone gaps in large vestibular aqueduct syndrome. *Ann Otol Rhinol Laryngology.* (2007) 116:532–41. doi: 10.1177/000348940711600709
10. Ward BK, Carey JP, Minor LB. Superior canal dehiscence syndrome: lessons from the first 20 years. *Front Neurol.* (2017) 8:177. doi: 10.3389/fneur.2017.00177
11. Hornibrook J. Perilymph fistula: fifty years of controversy. *ISRN Otolaryngol.* (2012) 2012:1–9. doi: 10.5402/2012/281248
12. Ikezono T, Shindo S, Sekiguchi S, Hanprasertpong C, Li L, Pawankar R, et al. Cochlin-tomoprotein: a novel perilymph-specific protein and a potential marker for the diagnosis of perilymphatic fistula. *Audiol Neurotol.* (2009) 14:338–44. doi: 10.1159/000212113
13. Ikezono T, Shindo S, Sekiguchi S, Morizane T, Pawankar R, Watanabe A, et al. The performance of Cochlin-tomoprotein detection test in the diagnosis of perilymphatic fistula. *Audiol Neurotol.* (2010) 15:168–74. doi: 10.1159/000241097
14. Matsuda H, Sakamoto K, Matsumura T, Saito S, Shindo S, Fukushima K, et al. A nationwide multicenter study of the Cochlin tomo-protein detection test: clinical characteristics of perilymphatic fistula cases. *Acta Oto-Laryngol (Stockh).* (2017) 137:S53–9. doi: 10.1080/00016489.2017.1300940
15. Kohut RI, Hinojosa R, Howard G, Ryu JH. The accuracy of the clinical diagnosis (predictability) of patencies of the labyrinth capsule (perilymphatic fistulas): a clinical histopathologic study with statistical evaluations. *Acta Oto-Laryngol Suppl.* (1995) 520:235–7. doi: 10.3109/00016489509125236
16. Fujita T, Kobayashi T, Saito K, Seo T, Ikezono T, Doi K. Vestibule-middle ear dehiscence tested with perilymph-specific protein Cochlin-Tomoprotein (CTP) detection test. *Front Neurol.* (2019) 10:47. doi: 10.3389/fneur.2019.00047
17. Achache M, Sanjuan Puchol M, Santini L, Lafont B, Cihanek M, Lavieille JP, et al. Delayed pneumolabyrinth after undiagnosed perilymphatic fistula. A illustrative clinical case justifying a standardised management in an emergency setting. *Eur Ann Otorhinolaryngol Head Neck Dis.* (2013) 130:283–7. doi: 10.1016/j.anorl.2012.04.012
18. Hidaka H, Miyazaki M, Kawase T, Kobayashi T. Traumatic pneumolabyrinth: air location and hearing outcome. *Otol Neurotol.* (2012) 33:123–31. doi: 10.1097/MAO.0b013e318241bc91
19. Ziade G, Barake R, El Natout T, El Natout MA. Late pneumolabyrinth after stapedectomy. *Eur Ann Otorhinolaryngol Head Neck Dis.* (2016) 133:361–3. doi: 10.1016/j.anorl.2015.10.005

Conflict of Interest: TI has a patent on this CTP detection test.

The remaining authors declare that the research was conducted in the absence of any commercial or financial relationships that could be construed as a potential conflict of interest.

frontiers in Neurology

OPINION
published: 20 November 2020
doi: 10.3389/fneur.2020.612075

A Simple Specific Functional Test for SCD: VEMPs to High Frequency (4,000 Hz) Stimuli—Their Origin and Explanation

Ian S. Curthoys[1,2]* *and Leonardo Manzari*[1,2]

[1] Vestibular Research Laboratory, School of Psychology, The University of Sydney, Darlington, NSW, Australia, [2] MSA ENT Academy Center, Cassino, Italy

Keywords: vestibular, otolith, utricular, labyrinth, semicircular canal, VEMP = vestibular-evoked myogenic potential

THE ORIGIN OF VEMP TESTS USING HIGH FREQUENCIES TO IDENTIFY SCD

We fully agree with the statement by Noij et al. (1) that for the detection of semicircular canal dehiscence (SCD) "High frequency VEMP testing is superior to all other methods described to date. It is highly specific for the detection of SCD and may be used to guide decision-making regarding the need for subsequent CT imaging" (1). The ideal is a very fast, innocuous test rather than extended and uncomfortable tests such as determining the threshold for VEMPs. Patients with a dehiscence show larger VEMPs and lower VEMP thresholds to air conducted sound (ACS) and bone conducted vibration (BCV). Standard VEMP stimuli (e.g., 500 Hz short tone bursts) are not optimal for such testing as Noij and Rauch reported. However, we wish to make clear that Manzari et al. (2) were the first to show that for clinical diagnosis of SCD a stimulus of 4,000 Hz is such a very simple very fast test with excellent specificity. We reported a (very short) Brief Communication in *Otolaryngology and Head Neck Surgery* showing the ocular VEMP to high frequency tone burst stimuli (either ACS or BCV) (2) to 4,000 Hz stimuli constituted a fast, simple innocuous functional test with a 100% success in showing SCD in 22 patients with CT verified SCD and the absence of VEMPs in 22 healthy control subjects. The test consisted of 50 presentations of brief (7 ms) tone bursts of high frequency (4,000 Hz) stimuli at a rate of 4/s instead of the standard VEMP test frequency of 500 Hz. Thus, the 4,000 Hz test is very short—a total of only 50 stimulus presentations were given at 4/s so the whole test is complete in 13 s. The sensitivity and specificity of the test was 1.0 and thus, diagnostic accuracy of 100%. In other words, if a patient had an oVEMP response to 4,000 Hz then they had a CT verified SCD. In that group of 22 healthy subjects, none had an oVEMP to 4,000 Hz stimulation. Leonardo Manzari discovered this very simple test at his clinic in Cassino, Italy and validated it on his patients with CT verified SCD and healthy controls. Others have followed his example with minor changes.

Noij and Rauch state in relation to our 2013 paper: "The high frequency oVEMP study using healthy subjects as the control group described 22 patients with unilateral and 4 patients with bilateral SCD (30 ears in total), while only 22 ears were included in the analysis. It is unclear which ears were excluded and why (31)." p.6 and later "A serious limitation of both published high frequency oVEMP studies was that some ears were excluded from analysis."

This is not a serious limitation of our study. There is a very simple explanation for the numbers in the Manzari et al. (2) study. The VEMP data graphed and included in the analysis were for the 22 patients with unilateral SCD. The data for 4 patients with bilateral SCD (8 ears) was not included for the very simple reason that for these 4 patients we could not be certain which ear was

OPEN ACCESS

Edited by:
P. Ashley Wackym, Rutgers, The State University of New Jersey, United States

Reviewed by:
Bryan Kevin Ward, Johns Hopkins University, United States
Steven D. Rauch, Harvard Medical School, United States

***Correspondence:**
Ian S. Curthoys
ian.curthoys@sydney.edu.au

Specialty section:
This article was submitted to Neuro-Otology, a section of the journal Frontiers in Neurology

Received: *30 September 2020*
Accepted: *29 October 2020*
Published: *20 November 2020*

Citation:
Curthoys IS and Manzari L (2020) A Simple Specific Functional Test for SCD: VEMPs to High Frequency (4,000 Hz) Stimuli—Their Origin and Explanation. Front. Neurol. 11:612075. doi: 10.3389/fneur.2020.612075

responsible for the VEMP- the patients had enhanced VEMPs beneath both eyes but there may have been a contribution of the ipsilateral ear to the ipsilateral oVEMP! All the other 22 patients were unilateral SCD so the oVEMP beneath the eye contralateral to the SCD ear uniquely identified it. Rather than include the results (8 ears) from these patients with bilateral SCD who constitute a different group, we chose the conservative approach of not including these data in the graphical and numerical analysis. Had the data from these patients been included then the number of SCD detections would have increased but the sensitivity and specificity cannot increase further because they cannot exceed 1.0!.

THE EXPLANATION OF VEMP RESPONSES TO HIGH FREQUENCIES AFTER SCD

Noij and Rauch attribute the increased VEMP amplitude to the stimulus generating a stronger otolithic response after SCD. They state: "The 2 and 4 kHz sound stimuli are at the upper edge of the otolith organ tuning curve. Since the otolith organs are relatively insensitive to acoustic signals at these higher frequencies, vestibular activation produced by a high frequency sound stimulus is usually insufficient to provide consistent responses in normal healthy individuals. However, in the presence of a dehiscent superior semicircular canal, the otolith organ 'sees' a much higher 'dose' of stimulus energy due to the shunting effect of the third window, resulting in a highly reliable cVEMP (and oVEMP) response to high frequency stimuli in SCD patients."

This statement is correct: recording of single otolithic neurons before and after SCD shows that the SCD does cause enhanced otolithic neural response and that is true for both ACS and BCV stimuli (3) but it is only part of the reason for the enhanced response oVEMP response after SCD. Anatomy and physiology show there is another neural input contributing to the enhanced responses after SCD and clinicians should be aware of this. Superior canal afferent neurons project indirectly to both contralateral inferior oblique via the contralateral III nerve nucleus (the source of oVEMPs) and also to ipsilateral sternocleidomastoid muscle (the source of cVEMPs) (**Figure 1D**). High frequency ACS and BCV at clinically acceptable levels do not cause superior canal neurons to be activated in healthy animals if the labyrinth is encased in bone as it normally is (see **Figures 1A–C**). However, after an SCD these superior canal neurons are activated at low threshold by high frequency stimuli so high frequency stimuli used in clinical testing will cause a marked increase in neural firing of these superior canal neurons which will contribute to both oVEMP and cVEMPs and enhance both VEMPs [it must be noted that very recent evidence shows that in animals with normally encased labyrinths, superior canal afferent neurons can be activated by very low frequencies—less than about 200 Hz (8)].

The evidence for these statements comes from physiological studies. One previous paper had shown this response (10). So Curthoys undertook to confirm and extend the result: in mammals do identified semicircular canal neurons respond to such high frequencies after SCD? The simple answer is yes (5, 6, 9, 11–17). The approach in this work was to record the response of single primary vestibular neurons in guinea pigs to sound and vibration before, during, and after making a dehiscence in the superior semicircular canal (**Figure 1B**). The neurons were identified by their location in Scarpa's ganglion and by their response to angular accelerations in semicircular canal planes or to maintained tilts. These recordings show that superior semicircular canal neurons in healthy guinea pigs with the labyrinth encased in bone (as is normal) are not activated by high frequency ACS or BCV stimulation at levels used in clinical testing. However, after a dehiscence of the bony superior canal there is clear strong increase in neural firing to the same stimulus which was ineffectual before SCD (see **Figure 1C**). Recording from the same neuron before, during, and after shaving away the bone to make a small dehiscence (**Figure 1B**) is an extremely difficult procedure but it provides definitive evidence that superior canal neurons are activated by high frequency sound and vibration after an SCD, but not before. It was repeated in over 70 neurons with the same results. The neurons are activated and show phase locking to these high frequencies (5, 9). The physiological results show that when a dehiscence as small as 0.1 mm diameter is made in the bony wall of the superior canal is made (**Figure 1A)** it causes substantial response to sound and vibration. Recently others have corroborated these results in toadfish (18). These physiological results provide the neural basis for high frequency testing for identifying SCD.

We summarized it thus:

"After SCD the threshold for otolith neurons to ACS and BCV also drops. Compared to normal animals the same stimulus will recruit more otolithic afferent neurons, and superior canal neurons will now also be activated. The superior canal afferents project to contralateral inferior oblique and to ipsilateral SCM. So, after SCD the ACS or BCV stimulus will cause neural drive to these muscles from the superior canal in addition to the enhanced otolithic-IO response. That result explains many clinical phenomena—the enhanced VEMP responses to sound and vibration after an SCD in patients with an SCD, where stimuli with frequencies as high as 4,000 Hz cause oVEMPs and cVEMPs [(2, 3), p. 967]."

CONCLUSION

In conclusion the very simple test that Leonardo Manzari discovered—adjusting the frequency of the audiometer delivering the VEMP stimulus to deliver 4,000 Hz instead of 500 Hz—is a very simple fast and innocuous way of identifying SCD and Manzari's primacy deserves due recognition. What appears to be a minor modification of the test stimulus is in fact

Abbreviations: ACS, air-conducted sound; BCV, bone-conducted vibration; SCD, semicircular canal dehiscence; VEMP, vestibular evoked myogenic potential; oVEMP, ocular vestibular evoked myogenic potential; cVEMP, cervical vestibular evoked myogenic potential.

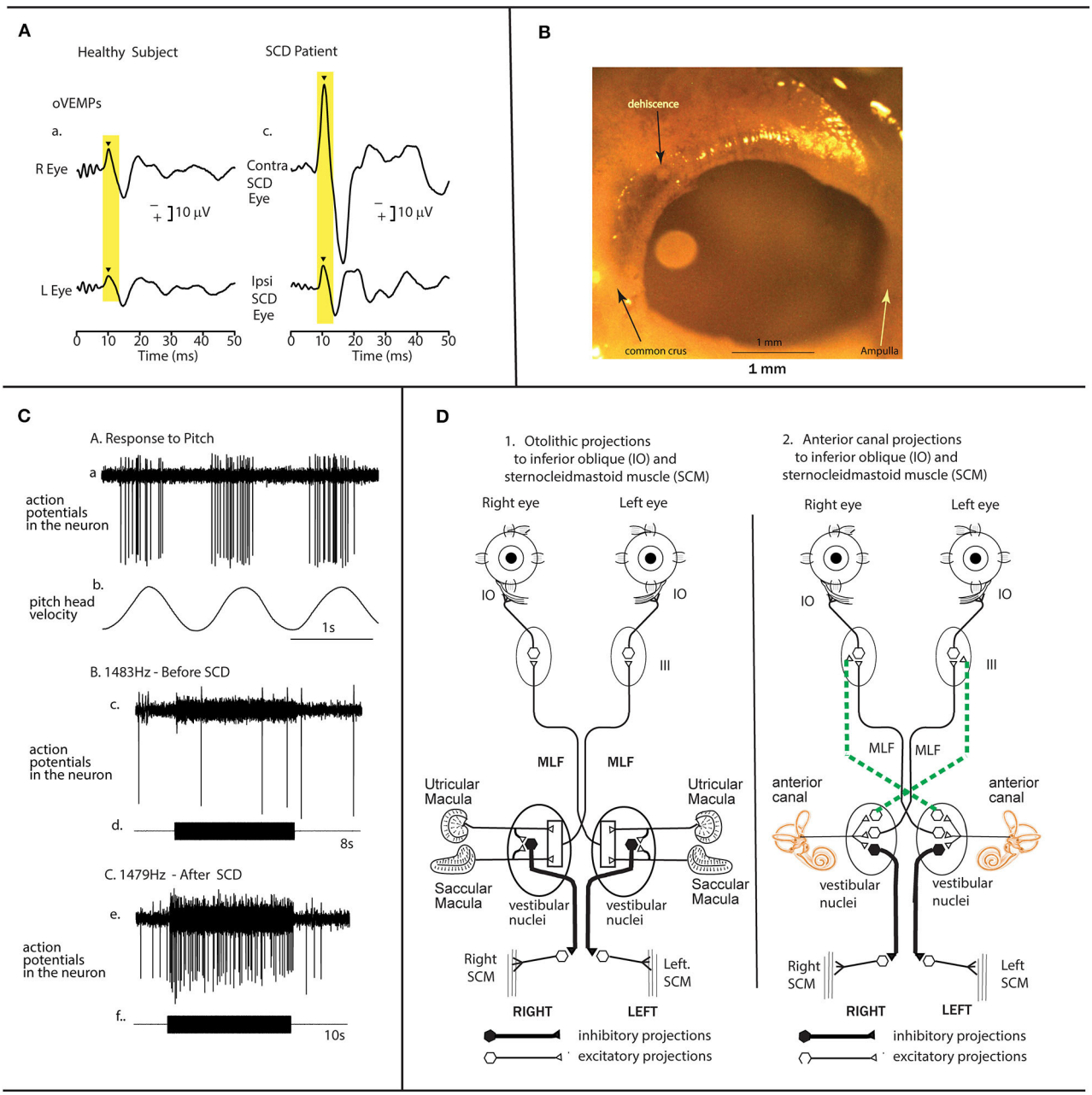

FIGURE 1 | The anatomical and physiological basis for enhanced oVEMP responses after a semicircular canal dehiscence. **(A)** Time series records of the oVEMP response of a patient with an SCD showing a greatly enhanced oVEMP n10 component beneath the eye contralateral to the SCD in response to 500 Hz brief tone bursts. The typical oVEMP n10 response of a healthy subject to the same stimulus shows a much smaller n10 component [reproduced with permission from (4)]. **(B)** A view from a medial view point of the bony wall of the superior semicircular canal in a guinea pig showing the small (0.1 mm diameter) dehiscence of the bony wall of the canal made during the experiment by shaving away the thin bone using a fine scalpel blade, while continuing to record from the same single neuron. In guinea pigs the canal is clearly visible after removal of the overlying cerebellum [reproduced with permission from (5)]. **(C)** After such an SCD, anterior canal neurons with irregular resting activity are activated and phase-lock to ACS and BCV at stimulus levels used for human clinical testing, whereas they do not respond to the same stimuli before SCD (6). In these experiments the same neuron was tested before and after the SCD. The response of one superior canal neuron to high-frequency air-conducted sound, before and after a small dehiscence in the bony wall of the superior canal. (a) The response of the neuron to pitch angular acceleration in the plane of the superior canal identifies the neuron as being a superior canal afferent. (b) Before SCD an 8 s burst of 1,483 Hz ACS has no effect on the neural response—there are very few action potentials during the tone burst. (c) After the SCD a 10 s burst of an air-conducted sound of 1,479 Hz causes strong activation of this same neuron. Reproduced with the permission of John Wiley and Sons Inc., from (3). **(D)** The projections of otolithic (D1) and canal (D2) neurons to IO and SCM [redrawn from (7)]. These are schematic diagrams of a view of the brainstem to show the otolithic projections to IO and SCM on the left (1) and the superior canal projections to IO and SCM on the right (2). These projections were derived from experiments using electrical stimulation to identify the projections. Stimulation in animals with intact labyrinths causes the otolithic neural connections shown in 1 to be activated, so ACS and BCV generate the oVEMP and cVEMP responses without any input from semicircular canal neurons, since canal afferents are not activated by ACS and BCV at frequencies above 200 Hz (8). However, after an SCD,

(Continued)

FIGURE 1 | the otoliths are activated even more strongly but in addition superior semicircular canal neurons are also activated by ACS and BCV as well as the otolithic neurons. Some canal afferents can be activated by frequencies of 3,000 Hz and above (3) (9). The superior canal neurons project to III nucleus by the crossed ventral tegmental tract (dashed lines) and the MLF. This combination of otolithic and canal afferent activation will result in a larger oVEMP 10 (as shown in **A** above). Reproduced with the permission of John Wiley and Sons Inc., from (3).

an entirely new and very specific way of testing SCD and the results from anatomy and physiology show why.

AUTHOR CONTRIBUTIONS

IC wrote the paper and reviewed and approved the final version. LM reviewed and approved the final version. All authors contributed to the article and approved the submitted version.

FUNDING

Supported by a grant from the Garnett Passe and Rodney Williams Memorial Foundation (Grant No. L2907 RP557).

REFERENCES

1. Noij KS, Rauch SD. Vestibular evoked myogenic potential (VEMP) testing for diagnosis of superior semicircular canal dehiscence. *Front Neurol*. (2020) 11:695. doi: 10.3389/fneur.2020.00695
2. Manzari L, Burgess AM, McGarvie LA, Curthoys IS. An indicator of probable semicircular canal dehiscence: ocular vestibular evoked myogenic potentials to high frequencies. *Otolaryngol Head Neck Surg*. (2013) 149:142–5. doi: 10.1177/0194599813489494
3. Curthoys IS. The new vestibular stimuli: sound and vibration-anatomical, physiological and clinical evidence. *Exp Brain Res*. (2017) 235:957–72. doi: 10.1007/s00221-017-4874-y
4. Curthoys IS, Grant JW, Burgess AM, Pastras CJ, Brown DJ, Manzari L. Otolithic receptor mechanisms for vestibular-evoked myogenic potentials: a review. *Front Neurol*. (2018) 9:366. doi: 10.3389/fneur.2018.00366
5. Curthoys IS, Burgess AM, Goonetilleke SC. Phase-locking of irregular guinea pig primary vestibular afferents to high frequency (> 250 Hz) sound and vibration. *Hear Res*. (2019) 373:59–70. doi: 10.1016/j.heares.2018.12.009
6. Dlugaiczyk J, Burgess AM, Goonetilleke S, Sokolic L, Curthoys IS. Superior canal dehiscence syndrome: relating clinical findings with vestibular neural responses from a guinea pig model. *Otol Neurotol*. (2018) 40:e406–14. doi: 10.1097/MAO.0000000000001940
7. Uchino Y, Kushiro K. Differences between otolith- and semicircular canal-activated neural circuitry in the vestibular system. *Neurosci Res*. (2011) 71:315–27. doi: 10.1016/j.neures.2011.09.001
8. Dlugaiczyk J, Burgess AM, Curthoys IS. Activation of guinea pig irregular semicircular canal afferents by 100 hz vibration: clinical implications for vibration-induced nystagmus and vestibular-evoked myogenic potentials. *Otol Neurotol*. (2020) 41:e961–70. doi: 10.1097/MAO.0000000000002791
9. Curthoys IS, Grant JW, Pastras CJ, Brown DJ, Burgess AM, Brichta AM, et al. A review of mechanical and synaptic processes in otolith transduction of sound and vibration for clinical VEMP testing. *J Neurophysiol*. (2019) 122:259–76. doi: 10.1152/jn.00031.2019
10. Carey JP, Hirvonen TP, Hullar TE, Minor LB. Acoustic responses of vestibular afferents in a model of superior canal dehiscence. *Otol Neurotol*. (2004) 25:345–52. doi: 10.1097/00129492-200405000-00024
11. Curthoys IS, Dlugaiczyk J. Physiology, clinical evidence and diagnostic relevance of sound-induced and vibration-induced vestibular stimulation. *Curr Opin Neurol*. (2020) 33:126–35. doi: 10.1097/WCO.0000000000000770
12. Curthoys IS, Grant JW. How does high-frequency sound or vibration activate vestibular receptors? *Exp Brain Res*. (2015) 233:691–9. doi: 10.1007/s00221-014-4192-6
13. Curthoys IS, Vulovic V. Vestibular primary afferent responses to sound and vibration in the guinea pig. *Exp Brain Res*. (2011) 210:347–52. doi: 10.1007/s00221-010-2499-5
14. Curthoys IS, Vulovic V, Burgess AM, Cornell ED, Mezey LE, Macdougall HG, et al. The basis for using bone-conducted vibration or air-conducted sound to test otolithic function. *Ann N Y Acad Sci*. (2011) 1233:231–41. doi: 10.1111/j.1749-6632.2011.06147.x
15. Curthoys IS, Vulovic V, Burgess AM, Manzari L, Sokolic L, Pogson J, et al. Neural basis of new clinical vestibular tests: otolithic neural responses to sound and vibration. *Clin Exp Pharmacol Physiol*. (2014) 41:371–80. doi: 10.1111/1440-1681.12222
16. Curthoys IS, Vulovic V, Burgess AM, Sokolic L, Goonetilleke SC. The response of guinea pig primary utricular and saccular irregular neurons to bone-conducted vibration (BCV) and air-conducted, sound (ACS). *Hear Res*. (2016) 331:131–43. doi: 10.1016/j.heares.2015.10.019
17. Curthoys IS, Vulovic V, Sokolic L, Pogson J, Burgess AM. Irregular primary otolith afferents from the guinea pig utricular and saccular maculae respond to both bone conducted vibration and to air conducted sound*Brain Res Bull*. (2012) 89:16–21. doi: 10.1016/j.brainresbull.2012.07.007
18. Iversen MM, Rabbitt RD. Wave mechanics of the vestibular semicircular canals. *Biophys J*. (2017) 113:1133–49. doi: 10.1016/j.bpj.2017.08.001

Conflict of Interest: The authors declare that the research was conducted in the absence of any commercial or financial relationships that could be construed as a potential conflict of interest.

frontiers in Neurology

CASE REPORT
published: 22 December 2020
doi: 10.3389/fneur.2020.581783

Case Report: Local Anesthesia Round Window Plugging and Simultaneous Vibrant Soundbridge Implant for Superior Semicircular Canal Dehiscence

Giulia Mignacco[1], Lorenzo Salerni[1], Ilaria Bindi[1], Giovanni Monciatti[1], Alfonso Cerase[2] and Marco Mandalà[1]*

[1] Otolaryngology Unit, Department of Medicine, Surgery and Neuroscience, University of Siena, Siena, Italy, [2] Neuroimaging, Diagnostic and Functional Neuroradiology Unit, Department of Neurological and Movement Sciences, University of Siena, Siena, Italy

The aim of the present study is to report the outcomes of round window reinforcement surgery performed with the application of a Vibrant Soundbridge middle ear implant (VSB; MED-EL) in a patient with superior semicircular canal dehiscence (SSCD) who presented with recurrent vertigo, Tullio phenomenon, Hennebert's sign, bone conduction hypersensitivity, and bilateral moderate to severe mixed hearing loss. Vestibular evoked myogenic potentials (VEMPs) and high-resolution computed tomography (HRCT) confirmed bilateral superior semicircular canal dehiscence while this was not seen in magnetic resonance imaging. The surgical procedure was performed in the right ear as it had worse vestibular and auditory symptoms, a poorer hearing threshold, and greatly altered HRCT and VEMPs findings. With local-assisted anesthesia, round window reinforcement surgery (plugging) with perichondrium was performed with simultaneous positioning of a VSB on the round window niche. At the one and 3 months follow-up after surgery, VSB-aided hearing threshold in the right ear improved to mild, and loud sounds did not elicit either dizziness or pain in the patient.

Keywords: superior semicircular canal dehiscence, round window plugging, round window reinforcement, middle ear implant, canal dehiscence syndrome

OPEN ACCESS

Edited by:
P. Ashley Wackym, The State University of New Jersey, United States

Reviewed by:
Sung Huhn Kim, Yonsei University, South Korea
Andrea Castellucci, Santa Maria Nuova Hospital, Italy

****Correspondence:***
Giulia Mignacco
giuliamignacco90@gmail.com

Specialty section:
This article was submitted to Neuro-Otology, a section of the journal Frontiers in Neurology

Received: *09 July 2020*
Accepted: *23 November 2020*
Published: *22 December 2020*

Citation:
Mignacco G, Salerni L, Bindi I, Monciatti G, Cerase A and Mandalà M (2020) Case Report: Local Anesthesia Round Window Plugging and Simultaneous Vibrant Soundbridge Implant for Superior Semicircular Canal Dehiscence. Front. Neurol. 11:581783. doi: 10.3389/fneur.2020.581783

INTRODUCTION

Superior semicircular canal dehiscence (SSCD) was first described by Minor et al. (1), and is characterized by a number of peculiar audio vestibular signs and symptoms (1). Common symptoms are autophony and hyperacusis, aural fullness, dizziness or vertigo/nystagmus induced by intense noises (Tullio phenomenon), or pressure via pneumatic otoscopy (Hennebert's sign). Audiometric findings can include both an air-bone gap or mixed type hearing loss, and/or suprathreshold bone scores. Typical signs and symptoms are secondary to a third window syndrome that results from a dehiscent superior semicircular canal (2).

Both high resolution computed tomography (HRCT) with reconstruction on the plane of the superior canal and vestibular evoked myogenic potentials (VEMPs) are mandatory to confirm the diagnosis of SSCD.

Surgical approaches are not mandatory in SSCD. The decision to treat the pathological canal side is based on various assessments including severity of symptoms, surgical candidacy of patients, and their desire for an improvement in quality of life. Conventional surgery provides direct treatment of the canal fistula through either a transmastoid or middle cranial fossa approach: the most common and well-described surgical treatments include capping, resurfacing, and plugging of the superior semicircular canal (3, 4).

Despite the demonstrated efficacy, these interventions are invasive and imply a potential risk of persistent hearing deterioration and vestibular loss. Both the middle fossa and transmastoid approaches require general anesthesia which might increase the overall surgical and anesthesiologic risk. Recently, it has been proposed that a two-window inner ear system can be restored by directly plugging the round window (RW). This procedure has been demonstrated to be safe, fast, and effective compared to classical SSCD surgical treatments (5, 6).

The Vibrant Soundbridge middle ear implant (VSB; MED-EL, Innsbruck, Austria) is an implantable hearing aid that transduces sounds into electromechanical vibrations to the ossicular chain or directly to the RW. It is indicated for the treatment of conductive or mixed moderate to severe hearing loss (7).

We describe the first case in literature of RW plugging and VSB positioning performed simultaneously under local anesthesia in a patient with bilateral SSCD and severe mixed hearing loss.

CASE DESCRIPTION

A 78-year-old woman was referred to our clinic with bilateral hearing loss with sound distortion, tinnitus and auditory hypersensitivity, recurrent vertigo/dizziness induced by loud noises (Tullio phenomenon), and a diagnosis of bilateral SSCD at the temporal bone HRCT performed in the emergency room (**Figures 2a–c**).

Preoperative audiometry indicated severe mixed hearing loss in the right ear, with moderate conductive hearing impairment in the left ear (**Figure 1**). A pure tone sound of 110 dB at 500 and 1,000 Hz in the right ear, and pneumatically increasing external auditory canal pressure induced dizziness without detectable nystagmus on video-oculographic (or Frenzel goggles) examination. Her tympanogram was bilaterally normal. A stapedial reflex could not be performed due to patient intolerance (dizziness). Mastoid vibration elicited dizziness without detectable nystagmus on video-oculographic (or Frenzel goggles) examination. A temporal bone 1.5-T MRI with 3D reconstruction performed two months before did not show the bilateral dehiscence (**Figures 2d–h**). Air conduction cervical VEMPs (cVEMPs) demonstrated a threshold of 85 dB HL on the right side and 100 dB HL on the left side. The cVEMPs were recorded from both ears using 500 Hz short tone-bursts (STBs). A video head impulse test for horizontal and vertical canals, including both dehiscent SSC, showed normal vestibulo-ocular reflex gain bilaterally (**Table 1**).

TABLE 1 | Pre- and post-operative evaluation steps.

T^0	• Pure tone audiometry: R: severe mixed hearing loss; L: moderate conductive hearing loss • Pure tone audiometry: R: severe mixed hearing loss; L: moderate conductive hearing loss • Air conduction VEMPs: R: threshold of 85 dB HL; L: 100 dB HL • VHIT: normal vestibulo-ocular reflex gain bilaterally • Mastoid vibration: dizziness without Ny
T^1	Radiological assessment: temporal bone 1.5T MRI with 3D reconstruction + temporal bone high resolution multidetector CT
T^2	Round window plugging and simultaneous VSB on right ear
T^3	1-month post-operative follow-up: VSB activation and hearing and vestibular evaluation
T^4	3-months post-operative follow-up: hearing and vestibular evaluation
T^5	6-months post-operative follow-up: hearing and vestibular evaluation

R, right; L, Left; VHIT, video head impulse test; Ny, nystagmus; MRI, magnetic resonance imaging; CT, computerized tomography; VSB, vibrant sound bridge.
T^0, beginning of the evaluation; T^{1-6}, next evaluations.

DIAGNOSTIC ASSESSMENT AND THERAPEUTIC INTERVENTION

Possible surgical procedures (superior canal plugging or resurfacing either through a middle fossa approach or via a transmastoid route, or RW niche plugging) were discussed with the patient. Comorbid cardiopulmonary conditions represented major contraindications for general anesthesia, so the latter procedure was the only possible option to pursue.

Since the patient did not show bilaterally any benefit from an air conduction hearing aid but rather had deteriorating auditory and vestibular symptoms on the right, we decided to perform the surgical procedure in the right ear as it had worse vestibular and auditory symptoms, a poorer hearing threshold, and greatly altered HRCT and VEMPs findings.

With local-assisted anesthesia, we performed a transcanal approach with elevation of the tympanomeatal flap and preservation of the chorda tympani nerve with a minimally invasive retroauricular incision. Ossicular mobility and continuity were assessed, we excluded the stapedial fixation, and no cerebrospinal fluid (CSF) leak was observed during the surgical procedure. After identification and reshaping of the RW niche, a vibroplasty was performed paying particular attention to correctly plugging the round window and coupling it with the floating mass transducer (FMT) of the VSB (**Figure 3**). We opted to couple the FMT with the RW because concomitant RW plugging was performed and from previous studies it seemed to provide a more stable coupling over time than incus (8). No ossicular chain abnormalities or perilymphatic fistula were observed intraoperatively.

The plugging of the round window was achieved using cartilage and perichondrium (tragus). This autologous tissue also helped to seal off the FMT in the round window niche. Furthermore, VSB hearing outcomes were monitored with electrocochleography using a cotton-wick recording electrode placed on the hypotympanum (7) (**Figure 4**).

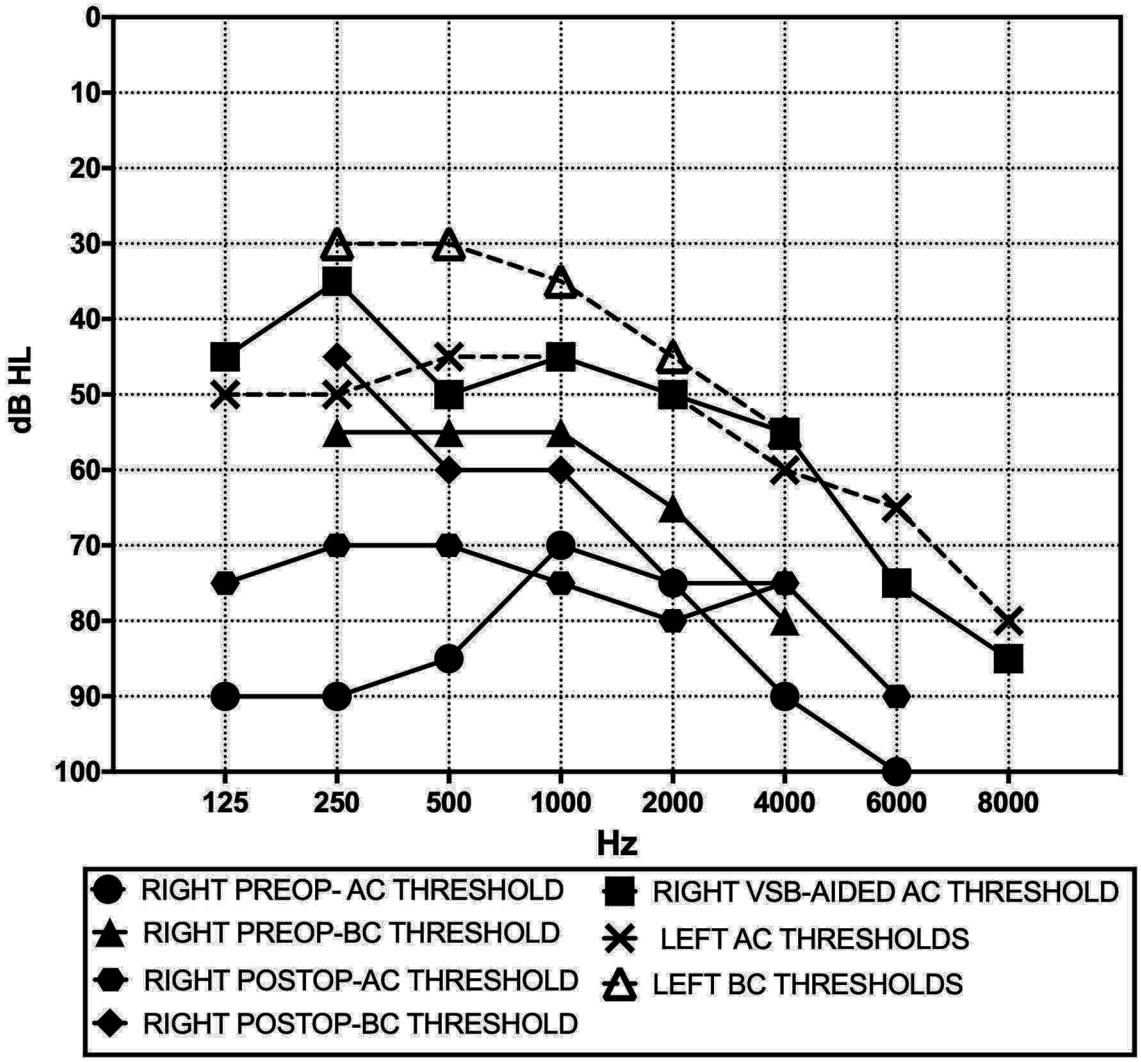

FIGURE 1 | Pre- and postoperative (3-month) pure tone audiograms.

The wire of the VSB was housed in a canal tunnel drilled up to the tympanic attic. Minimal drilling of the cortical temporal bone posterosuperior to the external auditory meatus was necessary to house the implant receiver and extra wire (**Figure 4**). The ear canal tunnel was covered with autologous cartilage and external auditory meatus packing was performed.

This study received an exemption from the ethics committee of the University Hospital of Siena (Comitato Etico Regione Toscana, area vasta Sud Est–AOU Senese, Usl Toscana Sud Est) on 10/21/2019 for publication.

Surgery was uncomplicated, the patient did not complain of any post-operative vestibular symptoms. Sutures and external meatus packing were removed on the 10th postoperative day. At the 1-month follow-up, the patient underwent VSB activation and hearing and vestibular examination. She reported a significant improvement in auditory hypersensitivity and reduced sound distortion although tinnitus remained unchanged. No disabling vestibular symptoms were reported. Neither dizziness nor nystagmus could be observed in response to loud sounds or increased external ear pressure on the right side. The postoperative pure tone audiogram revealed a mild increase at 500, 1,000, and 2,000 Hz and a mild decrease at 250 and 4,000 Hz for bone conduction thresholds (**Figure 1**). An improvement to moderate hearing loss in the VSB-aided hearing threshold was confirmed at 3 months (**Figure 1**). The maximum speech recognition score of bysillabic words at 65 dB HL improved from 10% preoperatively to 70% at the last follow-up. The improvement of hearing and vestibular symptoms was confirmed subjectively by the patient on the right side. Discomfort and mild dizziness associated with loud sounds on the left side remained unchanged. Using a visual analog scale (0–10), the patient reported an improvement in symptoms from

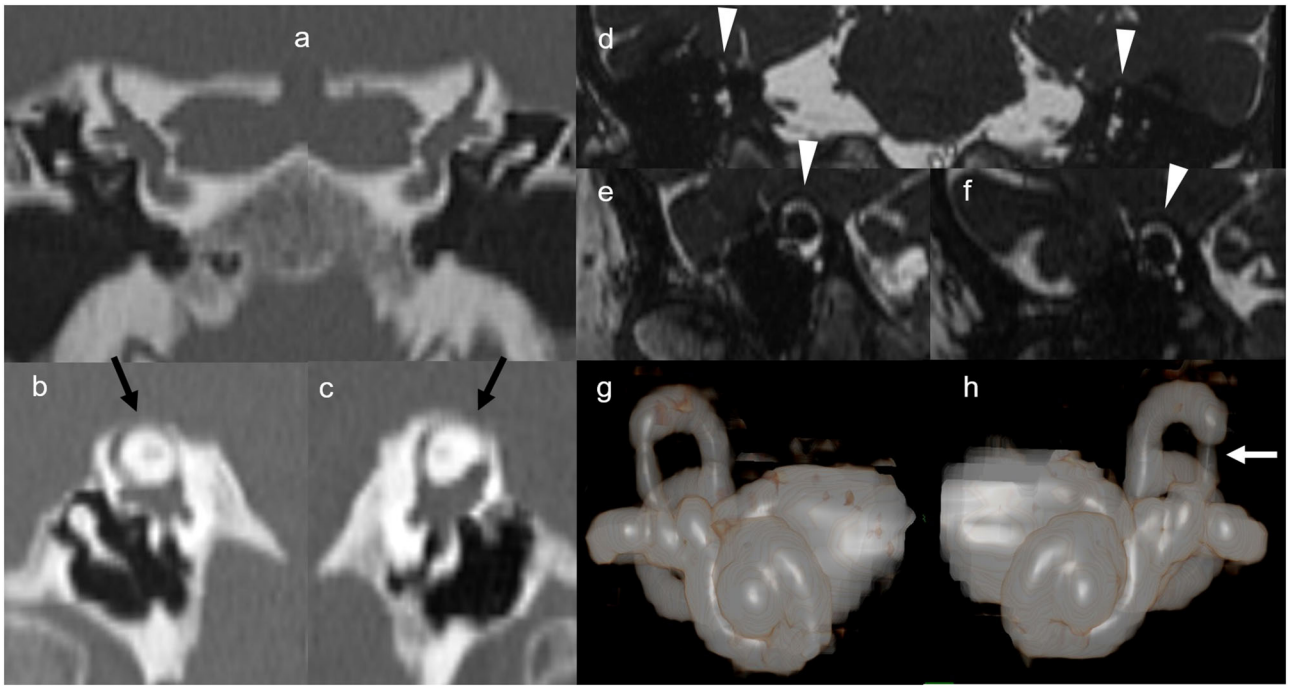

FIGURE 2 | High-resolution computed tomography and magnetic resonance imaging. Multidetector computed tomography 1.0 mm-collimated coronal **(a)**, and 0.5-mm collimated right **(b)** and left **(c)** sagittal oblique (so called Poschl plane) reformatted images obtained at admission in the emergency unit. Images according to the Poschl plane clearly show 5.5 and 3.5 mm-wide dehiscence of the bone overlying the right and the left superior semicircular canals, respectively (black arrows). These findings are consistent with clinical and audiometry findings. 1.5T magnetic resonance 3D-true fast imaging with steady-state free precession coronal **(d)**, right **(e)**, and left **(f)** sagittal oblique reformatted images obtained 2 months before as outpatient did not show the dehiscence (arrowheads). Note that right **(g)** and left **(h)** magnetic resonance 3D volume rendering anterior views shows thinning of both the lateral crus of both the superior semicircular canals, mainly in the left side (white arrow).

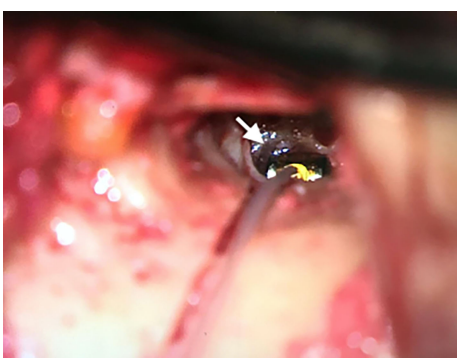

FIGURE 3 | Transcanal identification of round window (white arrow), reshaping of the niche, and positioning of the floating mass transducer of the Vibrant Soundbridge.

10 to 4 and from 9 to 2, respectively, for hearing and vestibular complaints (3-month follow-up). Left side mild symptoms related to dehiscence remained unchanged. No short-term surgical complications such as device extrusion or external or middle ear canal infection/inflammation were identified at the 3-month follow-up (**Table 1**). Control HRCT was not performed since correct positioning of the FMT and plugging of the RW were confirmed by improvements in symptoms and stability of VSB-aided hearing. Air conduction VEMPs were not performed for safety reasons due to the risk of mobilizing the plugging or FMT from the RW.

DISCUSSION

To the best of our knowledge, this is the first report in the literature of local-assisted anesthesia with simultaneous RW reinforcement surgery and VSB positioning in a patient suffering from SSCD. The outcome of this new procedure confirmed the results in terms of safety and improvement in auditory and vestibular symptoms related to SSCD using the minimally invasive procedure for RW plugging reported by Silverstein et al. (6) and Succar et al. (9). The main new finding of this novel procedure is the possibility of using the VSB implant to improve the hearing threshold in patients with associated moderate to severe mixed hearing loss. The adverse effects of a traditional hearing aid fitting motivated us to adopt the vibroplasty procedure because the auditory gain is related to cochlear inner ear fluid movements that ideally do

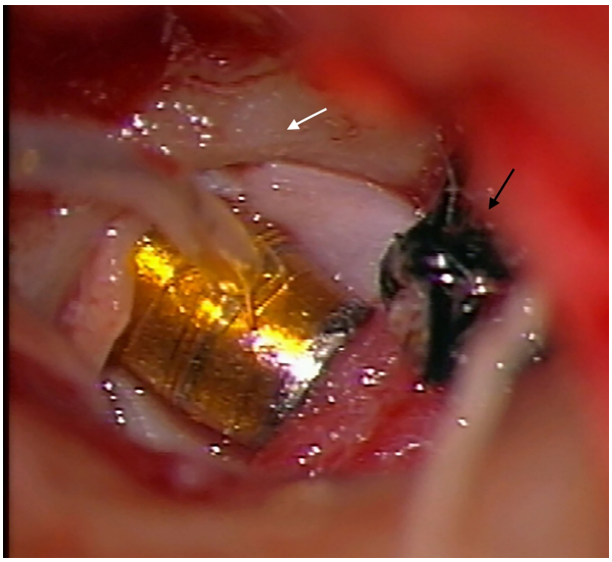

FIGURE 4 | Plugging of the round window with FMT, cartilage, and perichondrium (tragus) (white arrow). These autologous tissues also helped to seal off the floating mass transducer in the round window niche. Intraoperatively hearing evaluation with RW electrocochleography (black arrow).

not determine vestibular end organ activation. The VSB-aided hearing threshold was significantly better than the preoperative value. Furthermore, the minimally invasive RW plugging and implantation procedure can be done with local anesthesia. When performed by experienced surgeons, there is minimal risk of iatrogenic sensorineural hearing loss.

The major improvements in terms of vestibular symptoms over auditory symptoms have been described in the literature for RW plugging vs. superior canal plugging. Several studies (5, 6, 9–11) have indicated that objective hearing outcomes are poorer with the transcanal RW plugging approach compared with canal resurfacing/plugging. In RW plugging, an increase in postoperative air conduction thresholds is common at lower frequencies due to the increased stiffness of the round window. Effects on higher frequencies are negligible because hydromechanical inertia and dissipative impedance of the cochlear fluids plays a major role. The association of VSB implantation with RW transcanal plugging can overcome this issue. The RW-aided gain is similar to that expected for this kind of procedure (7).

The main limitations of the present study are that it is a report on a single case, and there was only a short follow-up period.

In conclusion, simultaneous RW plugging and VSB positioning may be an effective, safe, and rapid surgical approach for SSCD associated with severe mixed hearing loss.

PATIENT PERSPECTIVE

Immediately after the surgical procedure the patient reported an improvement of vestibular symptoms due to loud sounds. She also reported a significant reduction in auditory hypersensitivity and sound distortion. Although tinnitus remained unchanged, the significant improvement in hearing threshold (VSB-aided) led to a higher quality of life.

DATA AVAILABILITY STATEMENT

The raw data supporting the conclusions of this article will be made available by the authors, without undue reservation.

ETHICS STATEMENT

Written, informed consent, including all data and images, was obtained from the patient for the publication of this case report. Surgical procedure was performed in accordance with the Code of Ethics of the World Medical Association (Helsinki Declaration). This study received approval from the ethics committee of the Universitary Hospital of Siena (Comitato Etico Regione Toscana, area vasta Sud Est — AOU Senese, Usl Toscana Sud Est) for the publication on 10/21/2019.

AUTHOR CONTRIBUTIONS

MM performed the surgery. All authors contributed to the preparation and revision of manuscript and analyzed the data.

REFERENCES

1. Minor L, Solomon D, Zinreich J, Zee DS. Sound- and/or pressure-induced vertigo due to bone dehiscence of the superior semicircular canal. *Arch Otolaryngol Head Neck Surg.* (1998) 124:249–58. doi: 10.1001/archotol.124.3.249
2. Minor L. Clinical manifestations of superior semicircular canal dehiscence. *Laryngoscope*. (2005) 115:1717–27. doi: 10.1097/01.mlg.0000178324.55729.b7
3. Nikkar-Esfahani A, Whelan D, Banerjee A. Occlusion of the round window: a novel way to treat hyperacusis symptoms in superior semicircular canal dehiscence syndrome. *J Laryngol Otol.* (2013) 127:705–7. doi: 10.1017/S0022215113001096
4. Mikulec AA, McKenna MJ, Ramsey MJ, Rosowski JJ, Herrmann BS, Rauch SD, et al. Superior semicircular canal dehiscence presenting as conductive hearing loss without vertigo. *Otol Neurotol.* (2004) 25:121–9. doi: 10.1097/00129492-200403000-00007
5. Ziylan F, Kinaci A, Beynon AJ, Kunst HPM. A comparison of surgical treatments for superior semicircular canal dehiscence: a systematic review. *Otol Neurotol.* (2017) 38:1–10. doi: 10.1097/MAO.0000000000001277
6. Silverstein H, Kartush JM, Parnes LS, Poe DS, Babu SC, Levenson MJ, et al. Round window reinforcement forsuperior semicircular canal dehiscence: a retrospective case series. *Am J Otolaryngol.* (2014) 35:286–93. doi: 10.1016/j.amjoto.2014.02.016
7. Colletti V, Mandalà M, Colletti L. Electrocochleography in round window Vibrant Soundbridge implantation. *Otolaryngol Head Neck Surg.* (2012) 146:633–40. doi: 10.1177/0194599811430808
8. Colletti L, Mandalà M, Colletti V. Long-term outcome of round window vibrant sound bridge implantation in extensive ossicular chain defects. *Otolaryngol Head Neck Surg.* (2013) 149:134–41. doi: 10.1177/0194599813486255

9. Succar EF, Manickam PV, Wing S, Walter J, Greene JS, Azeredo WJ. Round window plugging in the treatment of superior semicircular canal dehiscence. *Laryngoscope*. (2018) 128:1445–52. doi: 10.1002/lary.26899
10. Silverstein H, VanEss M. Complete round window niche occlusion for superior semicircular canal dehiscence syndrome: a minimally invasive approach. *Ear Nose Throat J*. (2009) 88:1042–56. doi: 10.1177/014556130908800808
11. Vlastarakos PV, Proikas K, Tavoulari E, Kikidis D, Maragoudakis P, Nikolopoulos TP. Efficacy assessment and complications of surgical management for superior semicircular canal dehiscence: a meta-analysis of published interventional studies. Eur Arch Otorhinolaryngol 2009;266:177–86. doi: 10.1007/s00405-008-0840-4

Conflict of Interest: The authors declare that the research was conducted in the absence of any commercial or financial relationships that could be construed as a potential conflict of interest.

frontiers in Neurology

BRIEF RESEARCH REPORT
published: 11 March 2021
doi: 10.3389/fneur.2021.529661

Detection of Wandering Behaviors Using a Body-Worn Inertial Sensor in Patients With Cognitive Impairment: A Feasibility Study

*Rebecca J. Kamil[1], Dara Bakar[1,2], Matthew Ehrenburg[1], Eric X. Wei[3], Alexandra Pletnikova[4], Grace Xiao[1], Esther S. Oh[4], Martina Mancini[5] and Yuri Agrawal[1]**

[1] Department of Otolaryngology-Head and Neck Surgery, Johns Hopkins University, Baltimore, MD, United States, [2] Warren Alpert Medical School of Brown University, Providence, RI, United States, [3] Johns Hopkins University School of Medicine, Baltimore, MD, United States, [4] Division of Geriatric Medicine and Gerontology, Department of Medicine, Johns Hopkins University, Baltimore, MD, United States, [5] Department of Neurology, Oregon Health and Science University, School of Medicine, Portland, OR, United States

Patients with Alzheimer's disease (AD) and AD related dementias (ADRD) often experience spatial disorientation that can lead to wandering behavior, characterized by aimless or purposeless movement. Wandering behavior has been associated with falls, caregiver burden, and nursing home placement. Despite the substantial clinical consequences of wandering, there is currently no standardized approach to objectively quantify wandering behavior. In this pilot feasibility study, we used a lightweight inertial sensor to examine mobility characteristics of a small group of 12 older adults with ADRD and mild cognitive impairment in their homes. Specifically, we evaluated their compliance with wearing a sensor for a minimum of 4 days. We also examined the ability of the sensor to measure turning frequency and direction changes, given that frequent turns and direction changes during walking have been observed in patients who wander. We found that all patients were able to wear the sensor yielding quantitative turn data including number of turns over time, mean turn duration, mean peak turn speed, and mean turn angle. We found that wanderers make more frequent, quicker turns compared to non-wanderers, which is consistent with pacing or lapping behavior. This study provides preliminary evidence that continuous monitoring in patients with dementia is feasible using a wearable sensor. More studies are needed to explore if objective measures of turning behaviors collected using inertial sensors can be used to identify wandering behavior.

Keywords: dementia, wandering behavior, turning, cognitive impairment, body-worn inertial sensor

OPEN ACCESS

Edited by:
Michael Strupp, Ludwig Maximilian University of Munich, Germany

Reviewed by:
Yoav Gimmon, University of Haifa, Israel
Hamlet Suarez, Hospital Británico, Uruguay

***Correspondence:**
Yuri Agrawal
yagrawa1@jhmi.edu

Specialty section:
This article was submitted to Neuro-Otology, a section of the journal Frontiers in Neurology

Received: *26 January 2020*
Accepted: *25 January 2021*
Published: *11 March 2021*

Citation:
Kamil RJ, Bakar D, Ehrenburg M, Wei EX, Pletnikova A, Xiao G, Oh ES, Mancini M and Agrawal Y (2021) Detection of Wandering Behaviors Using a Body-Worn Inertial Sensor in Patients With Cognitive Impairment: A Feasibility Study. Front. Neurol. 12:529661. doi: 10.3389/fneur.2021.529661

INTRODUCTION

People with Alzheimer's disease (AD) and AD-related dementias (ADRD) can experience impaired spatial awareness and navigation ability, which is thought to lead to wandering behavior (1–4). Wandering may involve repetitive movements including pacing, defined as back-and-forth movement in a limited area, and lapping, defined as repetitive walking in circuitous paths (5, 6). Wandering can also include random movements and increased duration of walking with frequent

episodes of getting lost (2, 6, 7). Wandering has been associated with a myriad of negative outcomes including falls and subsequent injuries, increased caregiver burden, and early institutionalization (8–10). However, currently, there is no standardized approach to objectively describe and measure this behavior. The lack of a precise, objective metric has led to difficulty in studying the risk factors for wandering, the natural history and progression of this behavior, and effectiveness of interventions. Wandering behavior is typically detected by caregiver report, which may be imprecise, as it is based on the caregiver's ability to recognize and report this behavior. Various technologies, such as video surveillance, fluorescent dye–based image processing, wearable global positioning systems (GPSs), and electronic tagging, have been used to physically track wandering patients to help prevent elopement (5, 6, 11–14), but there is currently no standardized approach to objectively measure and quantify the wandering behavior itself.

In the past 10–15 years, wearable sensor technology in the form of inertial measurement units (IMUs) has provided a new avenue for detecting and monitoring the "quantity" and "quality" of mobility and physical activity under natural conditions in a variety of neurological diseases including dementia. These studies used IMUs that were worn by participants to record mobility patterns and quantify gait and turning through accelerations and angular velocity signals (15–20). Although these papers characterized specific impairments in quality of gait over multiple days in people with mild AD (18, 19) and reported reduced quantity of physical activity in people with dementia (21, 22), they did not report information on wandering behaviors. A recent study found that the turning behaviors in older adults with or without cognitive impairment could be successfully characterized with wearable sensors through 7 days of continuous monitoring (23). Characteristics of the turning, including number of turns per hour and speed of turning, were related to the individual's spatial cognitive abilities and also differentiated fallers from non-fallers. Since wandering behavior is associated with repetitive pacing and lapping, which likely affect the frequency and speed of turns, studying turning behavior may offer an objective way to describe the wandering behavior seen in older adults with cognitive impairment. To our knowledge, a link between turning characteristics and wandering has not been studied before. We hypothesize that quantification of turning characteristics using body-worn inertial sensors can provide an objective metric of wandering behavior. As a first step in this line of research, we aimed to assess the feasibility of using objective characteristics of turning quality in real-life conditions as a measure of wandering behavior.

MATERIALS AND METHODS

Participants were recruited from the Johns Hopkins Memory and Alzheimer's Treatment Center (JHMATC). Eligibility criteria included: (1) minimum age of 55 years, (2) a diagnosis of mild cognitive impairment (MCI) or AD based on the 2011 National Institute on Aging—Alzheimer's Association (NIA-AA) criteria (24) or other types of dementia, (3) presence of a caregiver who spends a minimum of 10 h weekly with the participant, and (4) residence within 60 miles of JHMATC given that the accelerometers were set up in patient homes. All of the study participants were diagnosed by dementia specialists at the Johns Hopkins University School of Medicine. We compared our patient data to historical control data obtained as part of a separate study by one of the study investigators (MM), where the same methodology was applied. The control participants were enrolled in the Oregon Center for Aging and Technology (ORCATECH) study of healthy aging and were free of neurological disease or dementia, in contrast to the patients enrolled in the current study.

At the baseline visit, the caregiver and the participant were instructed on how to use and charge a commercial wearable sensor, the Opal (APDM, Portland, OR; **Figure 1**), which was worn on the lower back with an elastic belt against the skin or snuggly around clothing. The Opal is a lightweight (about 22 g) IMU, has a battery life of 12 h, and includes 8 GB of storage. Data from the tri-axial accelerometer and gyroscope was recorded at 128 Hz and stored in the internal memory of the Opal monitors. Participants and/or their caregivers were instructed to wear the device for a minimum of 4 consecutive days for at least 8 h daily during waking hours. The device was battery-operated and charged each night by the participant and/or his/her caregiver. Research staff collected the wearable sensor from the participant's home at the end of the monitoring period, and the devices were cleaned according to manufacturer instructions. The Johns Hopkins Institutional Review Board (IRB) approved this study (Study Number NA_00087648) on 3/18/2014, and informed consent was obtained from the participants and/or their caregivers per established procedures in patients with cognitive impairment (25).

Data were downloaded on a laptop and processed in Matlab (R2016b, Mathworks). The process has been previously validated and described (26, 27). A diagram of the algorithm is presented in **Figure 2**. Gait bouts were defined as periods of walking

FIGURE 1 | Photograph of waist-worn wearable sensor.

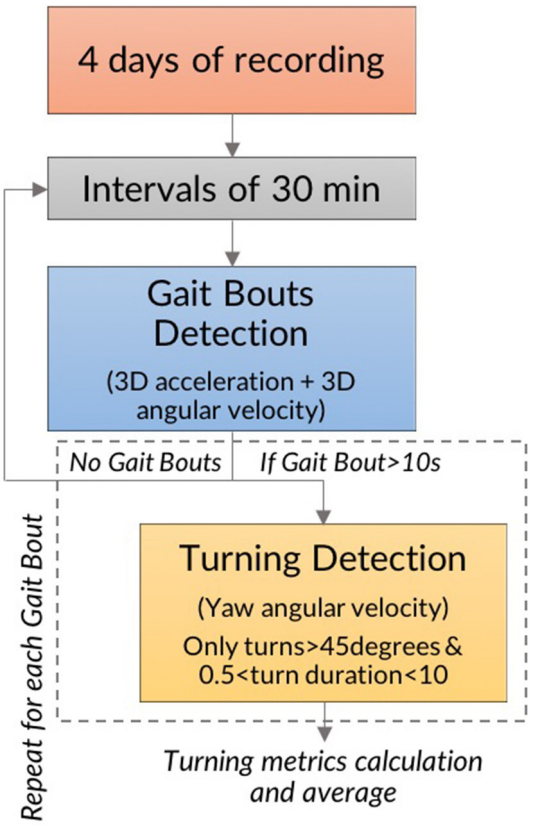

FIGURE 2 | Process for calculation of turning metrics.

10 s or longer as determined by 3D angular velocities and 3D accelerations, in windows of 30 min. Then, the algorithm searched for potential turns within each gait bout by analyzing the horizontal rotational rate. Turning events were defined as a rotation of at least 45 degrees in the horizontal plane (26, 27). Only turning events lasting between 0.5 and 10 s with turn angles of at least 45 degrees were included in the analysis (26, 27). Turn angles were determined by integrating the angular rate of the sensor about the vertical axis (26, 27). The turning characteristics were averaged across time, and data collected included number of hours worn (i.e., total number of analyzed hours, which includes both active and inactive time wearing the sensor), mean number of turns per 30 min interval, mean turn duration, mean peak speed, and mean turn angle (**Figure 2**).

Participant demographic information was obtained from electronic medical records. The Mini-Mental Status Examination (MMSE) score was obtained at the closest clinic visit to study enrollment. A subset of participants and their caregivers were asked about whether the participants wandered, defined as excessive, repetitive walking without a clear goal or purpose (yes or no). Our data were not normally distributed; therefore, the Spearman rank correlation coefficient was used to determine the strength and direction of the relationship between MMSE score and turning characteristic in our study. Two-sample Wilcoxon rank-sum tests were used to determine if there was a difference in various characteristics between non-wanderers and wanderers in a subset of participants. All analyses were performed using Stata 12.1 (College Station, TX).

RESULTS

Twelve participants were recruited for this study. The participants were aged 57–85 years [mean 71.5 (±7.26) years], and 5 of 12 (41.7%) were male (**Table 1**). Participant diagnoses included AD ($n = 8$); vascular dementia (based on a history of multiple strokes, with the diagnosis confirmed by four different neurologists; $n = 1$); Lewy body dementia (DLB) (based on DLB diagnosis criteria laid out by the Consensus Report of the DLB Consortium; $n = 1$) (29); amnestic MCI of AD subtype (based on amyloid positron emission tomography (PET) positivity and diagnosis by a neurologist at the JHMATC; $n = 1$); and dementia due to multiple factors including vasculitis, fibromyalgia, depression, and a previous cerebral vascular accident (diagnosed by a geriatrician at the JHMATC; $n = 1$). MMSE scores ranged from 5 to 29 [mean 18.8 (±7.77)].

All 12 participants wore the device as instructed. Participants wore the device a mean of 32.2 (±8.66) h over the course of 4 days (an average of 8 h daily). The average data from Mancini et al.'s study are described in **Table 1** for direct comparison to our findings (23). Comparing our data to Mancini et al.'s study of older adults with and without cognitive impairment, our cohort of participants with cognitive impairment trended toward having a greater number of turns in 30 min, a shorter mean turn duration, a faster mean peak turning speed, and a smaller mean turn angle (**Table 1**). We also evaluated the Spearman correlation between the MMSE score of our participants and each turning characteristic. We did not observe any significant correlations between MMSE score and length of device use or turning characteristics in this small sample.

Six participants and caregivers provided information about wandering behaviors; three participants were reported to wander by their caregivers, and three participants were reported not to wander. Participants who wandered had significantly lower MMSE scores, higher number of turns in 30 min, and shorter mean turn duration (**Table 2**). No significant associations were observed between wandering and age, mean peak speed, or mean turn angle. Graphs displaying the mean number of turns in 30 min and mean turn duration of non-wanderers (NW) and wanderers (W) are seen in **Figure 3**. Asterisks denote a significant p-value.

DISCUSSION

In this feasibility study, people with MCI and dementia tolerated continuous monitoring of mobility with a wearable sensor and provided evaluable data on turning behavior. Moreover, in a small subset of participants, we observed that participants who wandered had a significantly shorter mean turn duration and higher turn rate (number of turns/30 min) over the entire time

TABLE 1 | Demographic and turning characteristics.

Demographic characteristics					Turning characteristics				
Patient No.	**Diagnosis**	**Age**	**Gender**	**MMSE[f] score**	**Number of hours worn**	**Number of turns/30 min**	**Mean turn duration (seconds)**	**Mean peak speed (degree/second)**	**Mean turn angle (degrees)**
1	VD[a]	77	M	21	45.5	5.25	2.53	63.6	83.5
2	AD[b]	79	M	29	16.5	4.73	1.86	69.3	68.2
3	AD	85	M	14	33.5	1.82	1.56	112.8	82.3
4	LBD[c]	69	M	27	28.5	1.20	2.45	61.2	68.3
5	MCI[d]	67	F	25	42.0	26.8	2.24	80.8	102.5
6	AD	69	F	20	21.0	6.70	2.02	103.7	97.5
7	Multifactorial[e]	71	F	25*	34.0	122.0	1.70	99.4	92.8
8	AD	76	F	23*	35.5	95.0	2.32	64.7	89.0
9	AD	65	F	8	42.5	64.0	1.79	83.0	80.6
10	AD	70	F	5	26.0	88.0	2.04	66.7	81.6
11	AD	73	F	18	30.5	48.0	2.27	78.3	96.7
12	AD	57	M	11*	30.5	76.0	2.05	80.2	93.1
Overall, mean (SD)					32.2 (8.66)	45.0 (43.1)	2.07 (0.30)	80.3 (17.0)	86.3 (11.0)
Data from Mancini et al. study (23)									
Non-fallers, mean (SD)					–	31.8 (8.95)	2.11 (0.17)	75.9 (4.14)	95.2 (2.41)
Recurrent fallers, mean (SD)					–	23.1 (7.10)	2.42 (0.26)	65.6 (9.50)	92.5 (7.21)
Spearman rank correlation coefficient between MMSE score and turning characteristic, *r* (*p*-value)					−0.11 (0.74)	−0.33 (0.30)	0.23 (0.47)	−0.28 (0.38)	−0.08 (0.80)

[a] *VD, vascular dementia.*
[b] *AD, Alzheimer's disease.*
[c] *LBD, Lewy body dementia.*
[d] *MCI, mild cognitive impairment.*
[e] *Multifactorial, Dementia thought to be due to depression, vasculitis, fibromyalgia, and past Cerebrovascular accident (CVA).*
[f] *MMSE, Mini-Mental Status Examination.*
**Montreal Cognitive Assessment (MoCA) scores were obtained in the clinic, and equivalent MMSE scores were reported in this chart (28).*
Participants were dementia patients seen at the Memory Clinic at the Johns Hopkins Department of Geriatrics in 2016–2017.

TABLE 2 | Demographic and turning characteristics in non-wanderers vs. wanderers.

Demographic and turning characteristics	**Non-wanderers ($n = 3$)**	**Wanderers ($n = 3$)**	**Z-score**	***p*-value[a]**	**Probability non-wanderers > wanderers[b]**
	Mean (SD)	**Mean (SD)**			
Age (years)	71.0 (5.29)	64.0 (6.56)	1.09	0.275	77.8%
MMSE score	24.3 (3.06)	8.00 (3.00)	1.96	0.0495	100%
Number of turns/30 min	11.1 (13.8)	76.0 (12.0)	−1.96	0.0495	0.00%
Mean turn duration (seconds)	2.41 (0.15)	1.96 (0.15)	1.96	0.0495	100%
Mean peak speed (degree/second)	68.5 (10.7)	76.6 (8.72)	−1.09	0.275	22.2%
Mean turn angle (degrees)	84.8 (17.2)	85.1 (6.95)	0.218	0.827	55.6%

[a] *Two-sample Wilcoxon rank-sum tests were used to determine if there was a difference between non-wanderers and wanderers. A p-value < 0.05 is considered significant.*
[b] *The probability that the value of the demographic and turning characteristic of non-wanderers is greater than wanderers.*

they were wearing the device relative to participants who did not wander. Although our findings are preliminary, this feasibility study showed that detailed information about the quality of motor behavior under real-life conditions can be collected, such as mean peak speed, mean turn duration, and mean turn angle, in patients with cognitive impairment. In this small sample, we did not observe that severity of cognitive impairment was associated with duration of device use or with any turning characteristics.

Several prior studies have tracked abnormal motor behavior including wandering in patients with dementia. Wandering behavior includes lapping, pacing, directionless movements, and frequently getting lost. One study used wearable sensors to track gait and balance in the laboratory in AD patients (15). Other studies measured path tortuosity using a fractal dimension detected by a sensor network in an assisted living facility occupied by older adults (30, 31). Another group developed an algorithm to detect lapping and pacing wandering behavior using mobile health technology, although this has yet to be validated in patients (5, 32). Lin et al. used GPS traces from GPS-equipped cell phones to define pacing and lapping movements by summing the angles of turning points in a given trajectory and using this value to

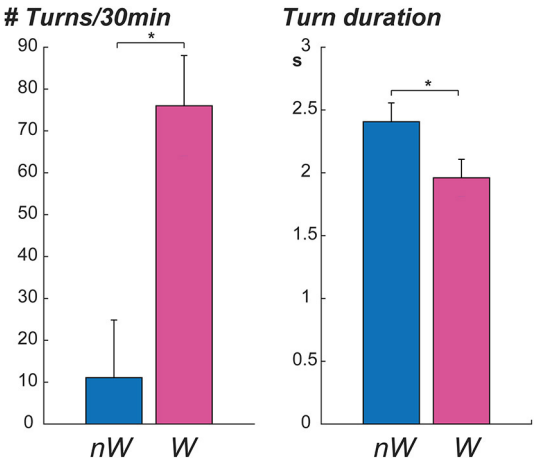

FIGURE 3 | Comparison of turning metrics between wanderers (W) and non-wanderers (nW).

decide if the movement qualifies as pacing or lapping. However, to the best of our knowledge, no previous study characterized turning while walking in people with cognitive impairment in the home environment over multiple days. This small study demonstrates the feasibility of continuous monitoring in patients with cognitive impairment and the potential of using one IMU to objectively define and quantify wandering behavior.

Our data suggest that individuals who wander appear to make more frequent, shorter turns relative to individuals who do not wander, providing further insight into the wandering behavioral phenotype. These findings are consistent with the observation that wanderers often perform pacing and lapping behavior, which could lead to more frequent turns. Wanderers may make shorter turns due to more frequent directionless movement when compared to non-wanderers. Moreover, wanderers often get lost, which could be reflected in more frequent, faster turns employed to find their way or attempt to reorient themselves. However, our sample size is very small, and the extent to which these differences may reflect differences in total motor activity is unclear. Future studies in larger samples will be needed to more definitively establish the relationship between wandering and turning characteristics with more objective measures of wandering such as video surveillance.

Limitations of this study were the small sample size and the inclusion of participants with various etiologies of cognitive impairment. Additionally, although the same device and analysis were used for the control group, the control group was part of a separate study by one of the investigators, which may have limited the comparability of the groups. In future work, we plan to evaluate whether objective measures of turning behaviors collected using the inertial sensor can be used to identify wandering and other abnormal motor behaviors in patients with dementia. Moreover, in a larger sample size, we will consider other characteristics of motor behaviors such as diurnal variability.

DATA AVAILABILITY STATEMENT

The datasets generated for this study are available on request to the corresponding author.

ETHICS STATEMENT

The studies involving human participants were reviewed and approved by Johns Hopkins Institutional Review Board. The patients/participants provided their written informed consent to participate in this study.

AUTHOR CONTRIBUTIONS

YA, MM, DB, GX, and RK contributed to study concept and design, data analysis, and manuscript preparation. EO, EW, and AP participated in data collection. All authors contributed to the article and approved the submitted version.

FUNDING

YA was supported by the NIH NIDCD K23-DC013056. EO was supported by the NIA/NIH K23 Award (1K23AG043504-01), the Roberts Gift Fund, and the Ossoff Family Fund.

REFERENCES

1. Algase DL, Moore DH, Vandeweerd C, Gavin-Dreschnack DJ. Mapping the maze of terms and definitions in dementia-related wandering. *Aging Ment Health.* (2007) 11:686–98. doi: 10.1080/13607860701366434
2. Hope T, Keene J, McShane RH, Fairburn CG, Gedling K, Jacoby R. Wandering in dementia: a longitudinal study. *Int Psychogeriatr.* (2001) 13:137–47. doi: 10.1017/S1041610201007542
3. Klein DA, Steinberg M, Galik E, Steele C, Sheppard JM, Warren A, et al. Wandering behaviour in community-residing persons with dementia. *Int J Geriatr Psychiatry.* (1999) 14:272–9. doi: 10.1002/(SICI)1099-1166(199904)14:4<272::AID-GPS896>3.0.CO;2-P
4. Marcus JF, Cellar JS, Ansari FP, Bliwise DL. Utility of the algase wandering scale in an outpatient alzheimer's disease sample. *Int J Geriatr Psychiatry.* (2007) 22:801–5. doi: 10.1002/gps.1745
5. Lin Q, Zhang D, Huang X, Ni H, Zhou X. Detecting wandering behavior based on GPS traces for elders with dementia. In: *Paper Presented at the ICARCV 2012: 12th International Conference on Control Automation Robotics & Vision.* (2012). 672 p.
6. Martino-Saltzman D, Blasch BB, Morris RD, McNeal LW. Travel behavior of nursing home residents perceived as wanderers and nonwanderers. *Gerontologist.* (1991) 31:666–72. doi: 10.1093/geront/31.5.666
7. Futrell M, Melillo KD, Remington R, Butcher HK. Evidence-based practice guideline: wandering. *J Gerontol Nurs.* (2014) 40:16–23. doi: 10.3928/00989134-20140911-01
8. Ali N, Luther SL, Volicer L, Algase D, Beattie E, Brown LM, et al. Risk assessment of wandering behavior in mild dementia. *Int J Geriatr Psychiatry.* (2016) 31:367–74. doi: 10.1002/gps.4336
9. Cipriani G, Lucetti C, Nuti A, Danti S. Wandering and dementia. *Psychogeriatrics.* (2014) 14:135–42. doi: 10.1111/psyg.12044

10. Colombo M, Vitali S, Cairati M, Perelli-Cippo R, Bessi O, Gioia P, et al. Wanderers: features, findings, issues. *Arch Gerontol Geriatr Suppl.* (2001) 7:99–106. doi: 10.1016/S0167-4943(01)00127-3
11. Mangini L, Wick JY. Wandering: unearthing new tracking devices. *Consult Pharm.* (2017) 32:324–31. doi: 10.4140/TCP.n.2017.324
12. Miskelly F. A novel system of electronic tagging in patients with dementia and wandering. *Age Ageing.* (2004) 33:304–6. doi: 10.1093/ageing/afh084
13. Nishigaki Y, Tanaka K, Kim J, Nakajima K. Development of an image processing support system based on fluorescent dye to prevent elderly people with dementia from wandering. *Annu Int Conf IEEE Eng Med Biol Soc.* (2013) 2013:7302–5. doi: 10.1109/EMBC.2013.6611244
14. Shoval N, Auslander GK, Freytag T, Landau R, Oswald F, Seidl U, et al. The use of advanced tracking technologies for the analysis of mobility in alzheimer's disease and related cognitive diseases. *BMC Geriatr.* (2008) 8:7. doi: 10.1186/1471-2318-8-7
15. Hsu YL, Chung PC, Wang WH, Pai MC, Wang CY, Lin CW, et al. Gait and balance analysis for patients with alzheimer's disease using an inertial-sensor-based wearable instrument. *IEEE J Biomed Health Inform.* (2014) 18:1822–30. doi: 10.1109/JBHI.2014.2325413
16. Kirste T, Hoffmeyer A, Koldrack P, Bauer A, Schubert S, Schroder S, et al. Detecting the effect of alzheimer's disease on everyday motion behavior. *J Alzheimers Dis.* (2014) 38:121–32. doi: 10.3233/JAD-130272
17. Lyons BE, Austin D, Seelye A, Petersen J, Yeargers J, Riley T, et al. Pervasive computing technologies to continuously assess alzheimer's disease progression and intervention efficacy. *Front Aging Neurosci.* (2015) 7:102. doi: 10.3389/fnagi.2015.00232
18. McArdle R, Morris R, Wilson J, Gaina B, Thomas AJ, Rochester L. What can quantitative gait analysis tell us about dementia and its subtypes? A structured review. *J Alzheimers Dis.* (2017) 60:1295–312. doi: 10.3233/JAD-170541
19. McArdle R, Morris R, Hickey A, Del Din S, Koychev I, Gunn RN, et al. Gait in mild Alzheimer's disease: feasibility of multi-center measurement in the clinic and home with body-worn sensors: a pilot study. *J Alzheimers Dis.* (2018) 63:331–41. doi: 10.3233/JAD-189003
20. Schwenk M, Hauer K, Zieschang T, Englert S, Mohler J, Najafi B. Sensor-derived physical activity parameters can predict future falls in people with dementia. *Gerontology.* (2014) 60:483–92. doi: 10.1159/000363136
21. Fleiner T, Haussermann P, Mellone S, Zijlstra W. Sensor-based assessment of mobility-related behavior in dementia: feasibility and relevance in hospital context. *Int Psychogeriatr.* (2016) 28:1687–94. doi: 10.1017/S1041610216001034
22. Fleiner T, Gersie M, Ghosh S, Mellone S, Zijlstra W, Haussermann P. Prominent physical inactivity in acute dementia care: psychopathology seems to be more important than the dose of sedative medication. *Int J Geriatr Psychiatry.* (2019) 34:308–14. doi: 10.1002/gps.5021
23. Mancini M, Schlueter H, El-Gohary M, Mattek N, Duncan C, Kaye J, et al. Continuous monitoring of turning mobility and its association to falls and cognitive function: a pilot study. *J Gerontol A Biol Sci Med Sci.* (2016) 71:1102–8. doi: 10.1093/gerona/glw019
24. Albert MS, DeKosky ST, Dickson D, Dubois B, Feldman HH, Fox NC, et al. The diagnosis of mild cognitive impairment due to alzheimer's disease: recommendations from the national institute on aging-alzheimer's association workgroups on diagnostic guidelines for alzheimer's disease. *Alzheimers Dement.* (2011) 7:270–9. doi: 10.1016/j.jalz.2011.03.008
25. Alzheimer's Association. Research consent for cognitively impaired adults: Recommendations for institutional review boards and investigators. *Alzheimer Dis Assoc Disord.* (2004) 18:171–5. doi: 10.1097/01.wad.0000137520.23370.56
26. El-Gohary M, Pearson S, McNames J, Mancini M, Horak F, et al. Continuous monitoring of turning in patients with movement disability. *Sensors.* (2013) 14:356–69. doi: 10.3390/s140100356
27. Mancini M, Weiss A, Herman T, Hausdorff JM. Turn around freezing: community-living turning behavior in people with parkinson's disease. *Front Neurol.* (2018) 9:18. doi: 10.3389/fneur.2018.00018
28. Saczynski JS, Inouye SK, Guess J, Jones RN, Fong TG, Nemeth E, et al. The Montreal cognitive assessment: creating a crosswalk with the mini-mental state examination. *J Am Geriatr Soc.* (2015) 63:2370–4. doi: 10.1111/jgs.13710
29. McKeith IG, Boeve BF, Dickson DW, Halliday G, Taylor JP, Weintraub D, et al. Diagnosis and management of dementia with Lewy bodies: fourth consensus report of the DLB consortium. *Neurology.* (2017) 89:88–100. doi: 10.1212/WNL.0000000000004058
30. Kearns WD, Nams VO, Fozard JL. Tortuosity in movement paths is related to cognitive impairment. Wireless fractal estimation in assisted living facility residents. *Methods Inf Med.* (2010) 49:592–8. doi: 10.3414/ME09-01-0079
31. Kearns WD, Fozard JL, Becker M, Jasiewicz JM, Craighead JD, Holtsclaw L, et al. Path tortuosity in everyday movements of elderly persons increases fall prediction beyond knowledge of fall history, medication use, and standardized gait and balance assessments. *J Am Med Direct Assoc.* (2012) 13:665.e13. doi: 10.1016/j.jamda.2012.06.010
32. Lin Q, Zhang D, Chen L, Ni H, Zhou X. Managing elders wandering behavior using sensors-based solutions: a survey. *Int J Gerontol.* (2014) 8:49–55. doi: 10.1016/j.ijge.2013.08.007

Conflict of Interest: The authors declare that the research was conducted in the absence of any commercial or financial relationships that could be construed as a potential conflict of interest.

frontiers in Neurology

CASE REPORT
published: 29 March 2021
doi: 10.3389/fneur.2021.634782

Case Report: Could Hennebert's Sign Be Evoked Despite Global Vestibular Impairment on Video Head Impulse Test? Considerations Upon Pathomechanisms Underlying Pressure-Induced Nystagmus due to Labyrinthine Fistula

Andrea Castellucci[1], Cecilia Botti[1,2], Margherita Bettini[3], Ignacio Javier Fernandez[4], Pasquale Malara[5], Salvatore Martellucci[6], Francesco Maria Crocetta[1], Martina Fornaciari[1], Francesca Lusetti[1], Luigi Renna[1], Giovanni Bianchin[3], Enrico Armato[7] and Angelo Ghidini[1]*

[1] *ENT Unit, Department of Surgery, Azienda USL—IRCCS di Reggio Emilia, Reggio Emilia, Italy,* [2] *PhD Proam in Clinical and Experimental Medicine, University of Modena and Reggio Emilia, Modena, Italy,* [3] *Audiology and Ear Surgery Unit, Department of Surgery, Azienda USL—IRCCS di Reggio Emilia, Reggio Emilia, Italy,* [4] *Department of Otolaryngology-Head and Neck Surgery, University Hospital of Modena, University of Modena and Reggio Emilia, Modena, Italy,* [5] *Audiology and Vestibology Service, Centromedico, Bellinzona, Switzerland,* [6] *ENT Unit, Santa Maria Goretti Hospital, Azienda USL Latina, Latina, Italy,* [7] *ENT Unit, SS Giovanni e Paolo Hospital, Venice, Italy*

OPEN ACCESS

Edited by:
Yuri Agrawal, Johns Hopkins University, United States

Reviewed by:
Rachael L. Taylor, The University of Auckland, New Zealand
Desi Phillip Schoo, Johns Hopkins Medicine, United States

***Correspondence:**
Andrea Castellucci
andrea.castellucci@ausl.re.it

Specialty section:
This article was submitted to Neuro-Otology, a section of the journal Frontiers in Neurology

Received: *28 November 2020*
Accepted: *23 February 2021*
Published: *29 March 2021*

Citation:
Castellucci A, Botti C, Bettini M, Fernandez IJ, Malara P, Martellucci S, Crocetta FM, Fornaciari M, Lusetti F, Renna L, Bianchin G, Armato E and Ghidini A (2021) Case Report: Could Hennebert's Sign Be Evoked Despite Global Vestibular Impairment on Video Head Impulse Test? Considerations Upon Pathomechanisms Underlying Pressure-Induced Nystagmus due to Labyrinthine Fistula. Front. Neurol. 12:634782. doi: 10.3389/fneur.2021.634782

We describe a case series of labyrinthine fistula, characterized by Hennebert's sign (HS) elicited by tragal compression despite global hypofunction of semicircular canals (SCs) on a video-head impulse test (vHIT), and review the relevant literature. All three patients presented with different amounts of cochleo-vestibular loss, consistent with labyrinthitis likely induced by labyrinthine fistula due to different temporal bone pathologies (squamous cell carcinoma involving the external auditory canal in one case and middle ear cholesteatoma in two cases). Despite global hypofunction on vHIT proving impaired function for each SC for high accelerations, all patients developed pressure-induced nystagmus, presumably through spared and/or recovered activity for low-velocity canal afferents. In particular, two patients with isolated horizontal SC fistula developed HS with ipsilesional horizontal nystagmus due to resulting excitatory ampullopetal endolymphatic flows within horizontal canals. Conversely, the last patient with bony erosion involving all SCs developed mainly torsional nystagmus directed contralaterally due to additional inhibitory ampullopetal flows within vertical canals. Moreover, despite impaired measurements on vHIT, we found simultaneous direction-changing positional nystagmus likely due to a buoyancy mechanism within the affected horizontal canal in a case and benign paroxysmal positional vertigo involving the dehiscent posterior canal in another case. Based on our findings, we might suggest a functional dissociation between high (impaired) and low (spared/recovered) accelerations for SCs. Therefore, it could be hypothesized that HS in labyrinthine fistula might

be due to the activation of regular ampullary fibers encoding low-velocity inputs, as pressure-induced nystagmus is perfectly aligned with the planes of dehiscent SCs in accordance with Ewald's laws, despite global vestibular impairment on vHIT. Moreover, we showed how pressure-induced nystagmus could present in a rare case of labyrinthine fistulas involving all canals simultaneously. Nevertheless, definite conclusions on the genesis of pressure-induced nystagmus in our patients are prevented due to the lack of objective measurements of both low-acceleration canal responses and otolith function.

Keywords: labyrinthine fistulae, pressure-induced nystagmus, Hennebert's sign, fistula sign, video head impulse test, case report

INTRODUCTION

Pressure-induce nystagmus (PIN), also known as Hennebert's sign (HS), represents a peculiar finding indicating a third window mechanism within the inner ear. It can be elicited either by pressure changes exerted on the external auditory canal (EAC) with tragal compressions or a Politzer bulb, or increasing intracranial/middle-ear pressure through Valsalva maneuvers. It can be found in several labyrinthine disorders with normal otoscopic findings including otosyphilis (1), perilymphatic fistula (2, 3), Meniere's disease (4, 5), vestibular atelectasis (6, 7), hypermobile stapes footplate (8), semicircular canal (SC) dehiscence (9, 10), and other dehiscences between the otic capsule and surrounding structures (11, 12). Similarly, chronic inflammatory pathologies involving the middle ear may lead to labyrinthine fistula (LF) due to otic capsule erosions, accounting for pressure transmission from tympanic cavity into the inner ear (13–19). In the latter case, other classical symptoms and signs of third window syndromes including bone-conducted hyperacusis, sound-induced vertigo (Tullio phenomenon), abnormally enhanced amplitudes and reduced threshold for vestibular evoked myogenic potentials (VEMPs) may be partially or totally hidden by underlying middle ear pathologies.

The pathogenetic mechanism underlying HS is still controversial. In particular, it is unclear whether endolymphatic or perilymphatic flows are involved and which subgroup of hair cells among ampullary and/or otolith receptors represents the target sensor (4–7, 20–28).

Unlike caloric irrigations measuring horizontal SC (HSC) activity in low-acceleration ranges, the video head impulse test (vHIT) represents a recently introduced test assessing the vestibulo-ocular reflex (VOR) of each SC for high accelerations (29). Its diagnostic accuracy is based on Ewalds's laws, stating that stimulation of each canal produces eye rotations around an axis parallel to that of the canal, that ampullopetal endolymphatic flows represent excitatory stimuli for HSC while inhibitory for vertical SCs, and that stronger oculomotor responses are derived from excitatory inputs (30).

Here, we describe three patients with LF due to different temporal bone pathologies presenting with HS and positional nystagmus despite global SCs hypofunction on vHIT. We discuss the possible pathomechanisms underlying PIN and positional nystagmus and we also review the relevant literature.

Abbreviations: BPPV, benign paroxysmal positional vertigo; COM, chronic otitis media; CT, computed tomography; CWD, canal wall down; EAC, external auditory canal; HL, hearing loss; HSC, horizontal semicircular canal; LF, labyrinthine fistula; MRI, magnetic resonance imaging; PIN, pressure-induced nystagmus; PSC, posterior semicircular canal; SC, semicircular canal; SSC, superior semicircular canal; vHIT, video head impulse test; VOR, vestibulo-ocular reflex.

CASE DESCRIPTIONS

Patient 1

An 83-year-old female presented with long-lasting left ear discharge, hearing loss (HL), and recent onset of headache. Her history was consistent with bilateral chronic otitis media (COM) and diabetes mellitus, whereas she denied oscillopsia, pressure-induced vertigo, or other vestibular symptoms. On otoscopy, her left EAC was obliterated by polypoid soft tissue. Pure tone audiometry detected ipsilateral profound HL and right-sided mixed HL (**Figure 1A**). Vestibular examination with video-Frenzel goggles showed neither spontaneous nor positional nystagmus. Nevertheless, left tragal compression evoked strong left-beating horizontal nystagmus that reversed on release of the positive pressure on EAC (**Supplementary Video 1**). Neither glottic nor nasal Valsalva maneuver resulted in detectable nystagmus or vertigo. An ICS Impulse device (Otometrics, Natus Medical Inc, Denmark) was used to measure VOR-gain values for all six SCs on the same day. Gains were considered normal if >0.8 for horizontal SCs and >0.7 for vertical canals (29). vHIT highlighted left global canal deficit and slight right-sided posterior SC (PSC) hypofunction (**Figure 1B**). Bedside oculomotor testing excluded signs of impaired function of central vestibular pathways. Temporal bones CT scan showed soft tissue occupying the left EAC, mastoid, and tympanic cavities with bony erosion involving ossicular chain, HSC, fallopian canal, tympanic medial wall, and tegmen tympani (**Figures 1C,D**). Magnetic resonance imaging (MRI) of the brain showed contrast enhanced tissue invading the intracranial compartment through superior and posteromedial walls of the temporal bone (**Figures 1E,F**). Histologic examination of the polypoid tissue within the left EAC was consistent with squamous cell carcinoma. Diagnosis of T4-stage disease according to the modified Pittsburgh staging system (31) was made, and the patient was addressed to palliative radiation therapy.

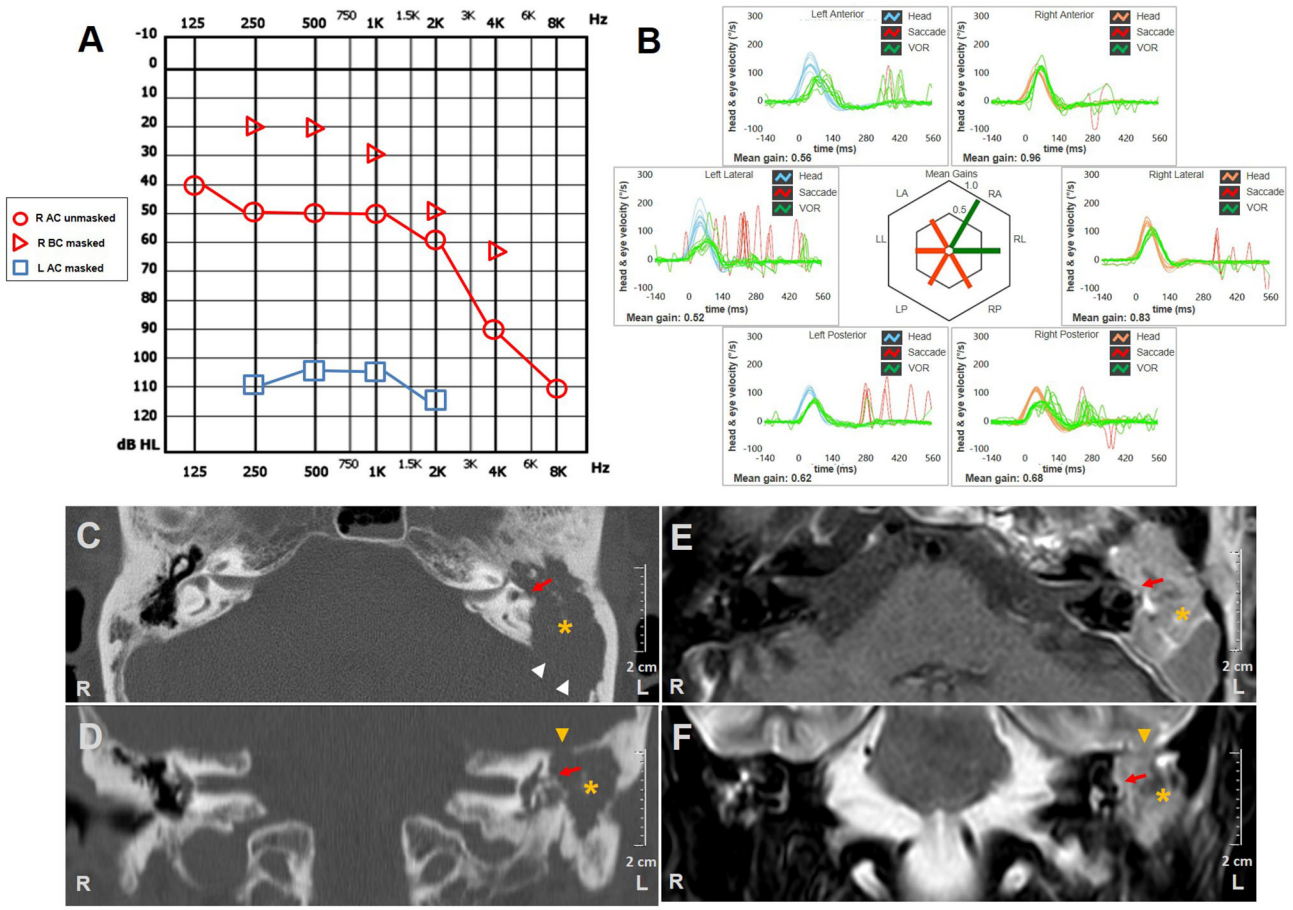

FIGURE 1 | Instrumental and radiological data of case one. **(A)** Audiometry showing mixed HL on the right side and profound HL on the left. **(B)** vHIT measurements. Blue lines represent head impulses exciting left SCs, orange lines correspond to impulses for right SCs, green lines represent eye movements induced by the activation of VOR following each impulse and red lines correspond to corrective saccades. Mean value of VOR-gain (eye velocity/head velocity) is reported for each SC. The hexagonal plot in the center of the figure summarizes mean VOR-gains for each SC; normal gains are shown in green and deficient gains are in red. A global canal hypofunction on the left and a slight reduction of the VOR-gain for contralateral PSC with overt saccades could be clearly observed. Axial **(C)** and coronal **(D)** images of temporal bones CT scans completed with axial T1-weighted **(E)** and coronal T2-weighted **(F)** gadolinium-enhanced brain MRI showing soft tissue density (*yellow asterisks*) within left external/middle-ear and mastoid cavity disrupting surrounding structures. Ossicular chain is not detectable. Bony erosion areas at the posterior fossa (*white arrowheads*) and middle fossa floor (*yellow arrowheads*) with dural infiltration are highlighted. Otic capsule erosion at the left HSC is indicated with *red arrows*. AC, air conduction; BC, bone conduction; CT, computed tomography; HL, hearing loss; HSC, horizontal semicircular canal; L, left; LA, left anterior; LL, left lateral; LP, left posterior; MRI, magnetic resonance imaging; PSC, posterior semicircular canal; R, right; RA, right anterior; RL, right lateral; RP, right posterior; SC, semicircular canal; vHIT, video-head impulse test; VOR, vestibulo-ocular reflex.

Patient 2

A 73-year-old woman referred to our center for a follow-up evaluation of right-sided canal wall down (CWD) mastoidectomy due to a COM with cholesteatoma. The surgical procedure was conducted two years earlier without simultaneous functional stage. She experienced symptoms consistent with right-sided cochleo-vestibular loss following surgery. Pressure-induced unsteadiness and dizziness represented her prominent residual vestibular symptoms. Otoscopy highlighted dry right EAC and well-preserved postoperative conditions. Her audiogram showed right-sided mixed HL with widened air-bone gap at lower frequencies and contralateral age-related sensorineural HL (**Figure 2A**). Although spontaneous nystagmus could not be observed with video-Frenzel goggles, mastoid vibrations elicited left-beating nystagmus. Horizontal nystagmus directed toward the affected side was evoked applying positive pressure on her right EAC, reversing on removal of the pressure. Conversely, no nystagmus could be noticed with Valsalva maneuvers. Even though she denied positional vertigo, left-beating nystagmus could be observed on supine positioning and slightly persistent geotropic direction-changing nystagmus was elicited after head rolls, with stronger amplitude on right-sided positioning (**Supplementary Video 2**). vHIT measurements were taken on the same day, showing VOR-gain reduction for all SCs of the right side and mildly impaired function for left PSC (**Figure 2B**). High-resolution CT scan detected postoperative LF involving right HSC without inflammatory recurrences (**Figures 2C–F**). Although we proposed revision surgery for LF closure and

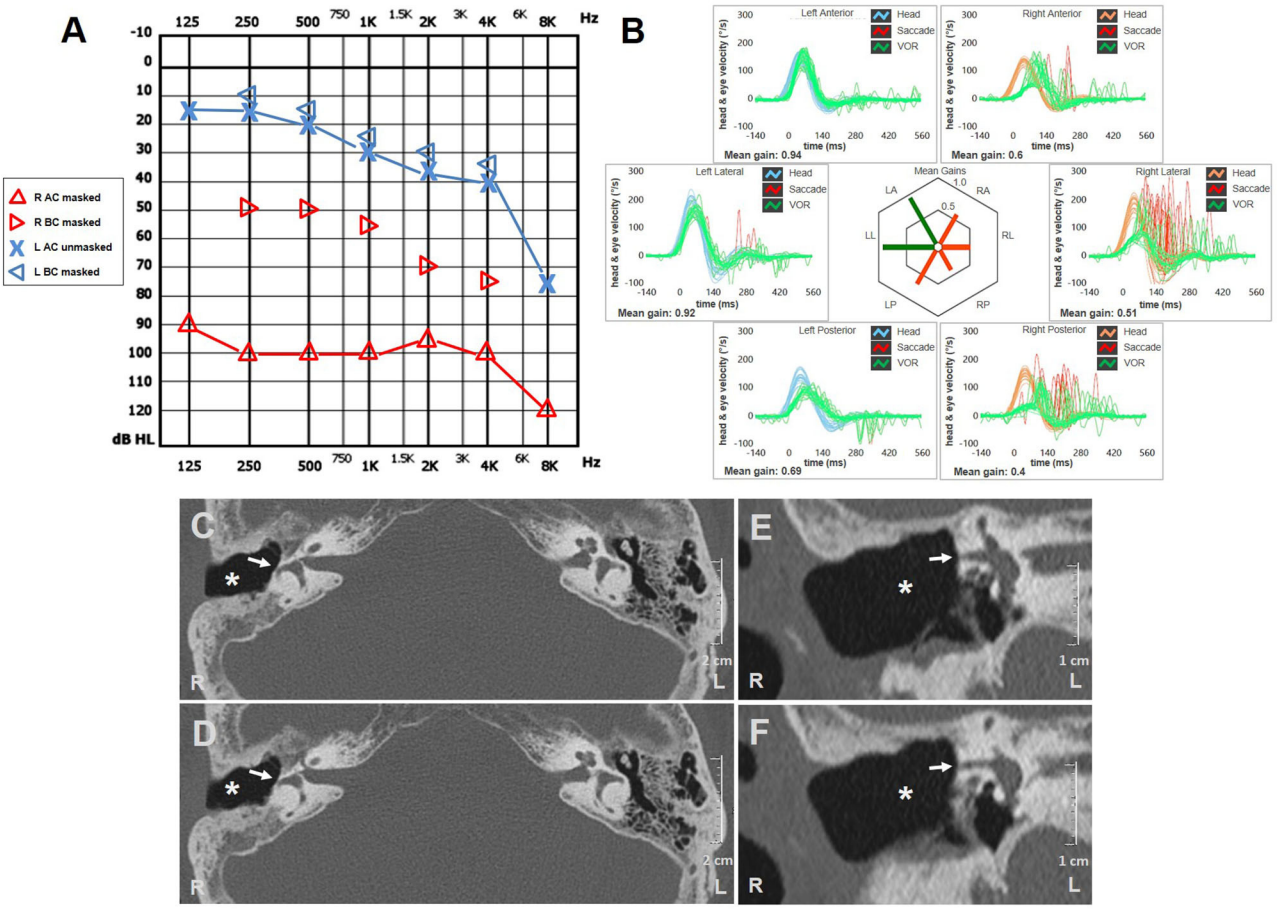

FIGURE 2 | Instrumental and radiological data of case two. **(A)** Audiometric test exhibiting mixed HL on the right with predominant ABG at lower frequencies and left high-frequency sensorineural HL consistent with patient's age. **(B)** vHIT showing reduced VOR-gain values for all right SCs with both overt and covert saccades and slight hypoactive VOR for contralateral PSC without corrective saccades. Axial **(C,D)** and coronal **(E,F)** images of temporal bone CT scans detecting signs of previous CWD mastoidectomy (*white asterisks*) with HSC fistula (*white arrows*). ABG, air-bone gap; AC, air conduction; BC, bone conduction; CWD, canal wall down; CT, computed tomography; HL, hearing loss; HSC, horizontal semicircular canal; L, left; LA, left anterior; LL, left lateral; LP, left posterior; PSC, posterior semicircular canal; R, right; RA, right anterior; RL, right lateral; RP, right posterior; SC, semicircular canal; vHIT, video head impulse test; VOR, vestibulo-ocular reflex.

hearing restoration, she refused additional procedures as audio-vestibular symptoms did not prevent her from leading a normal life.

Patient 3

A 46-year-old man with a history of left ear discharge presented with newly onset HL and vertigo. His medical history was otherwise silent besides head trauma (car accident) that occurred seven months prior to the admission with residual positional vertigo. He denied oscillopsia, pressure-induced vertigo, or other vestibular symptoms. The otoscopy revealed a left thickened tympanic membrane with EAC discharge. Audiometric testing showed down-sloping sensorineural HL on the right and left-sided mixed HL with predominant conductive loss for low frequencies (**Figure 3A**). Right-beating spontaneous nystagmus enhanced by mastoid vibrations consistent with left acute vestibular loss could be observed on video-Frenzel examination. Nystagmus reduced in backward head bending, while increased with downbeat components in forward head tilts. Left Dix-Hallpike maneuver elicited paroxysmal up-beating nystagmus with left torsional components consistent with benign paroxysmal positional vertigo (BPPV) involving left-sided PSC, so he received Epley's repositioning procedures (**Supplementary Video 3**). At the following examination 2 days later, positioning tests were uneventful, whereas right-beating spontaneous nystagmus enhanced by head shakings could be still detectable. Left tragal compression induced right-torsional nystagmus, followed by stronger opposite eye movements on release of the pressure (**Supplementary Video 4**), whereas both nasal and glottic Valsalva maneuvers were uneventful. The patient underwent vHIT measurements on the same day, showing left global hypofunction and slightly reduced VOR-gain for the right PSC (**Figure 3B**). Temporal bones CT scan revealed soft tissue consistent with cholesteatoma obliterating the right-sided tympano-mastoid cavity and eroding ossicular chain, all SCs, sigmoid sinus bony wall, and tegmen tympani

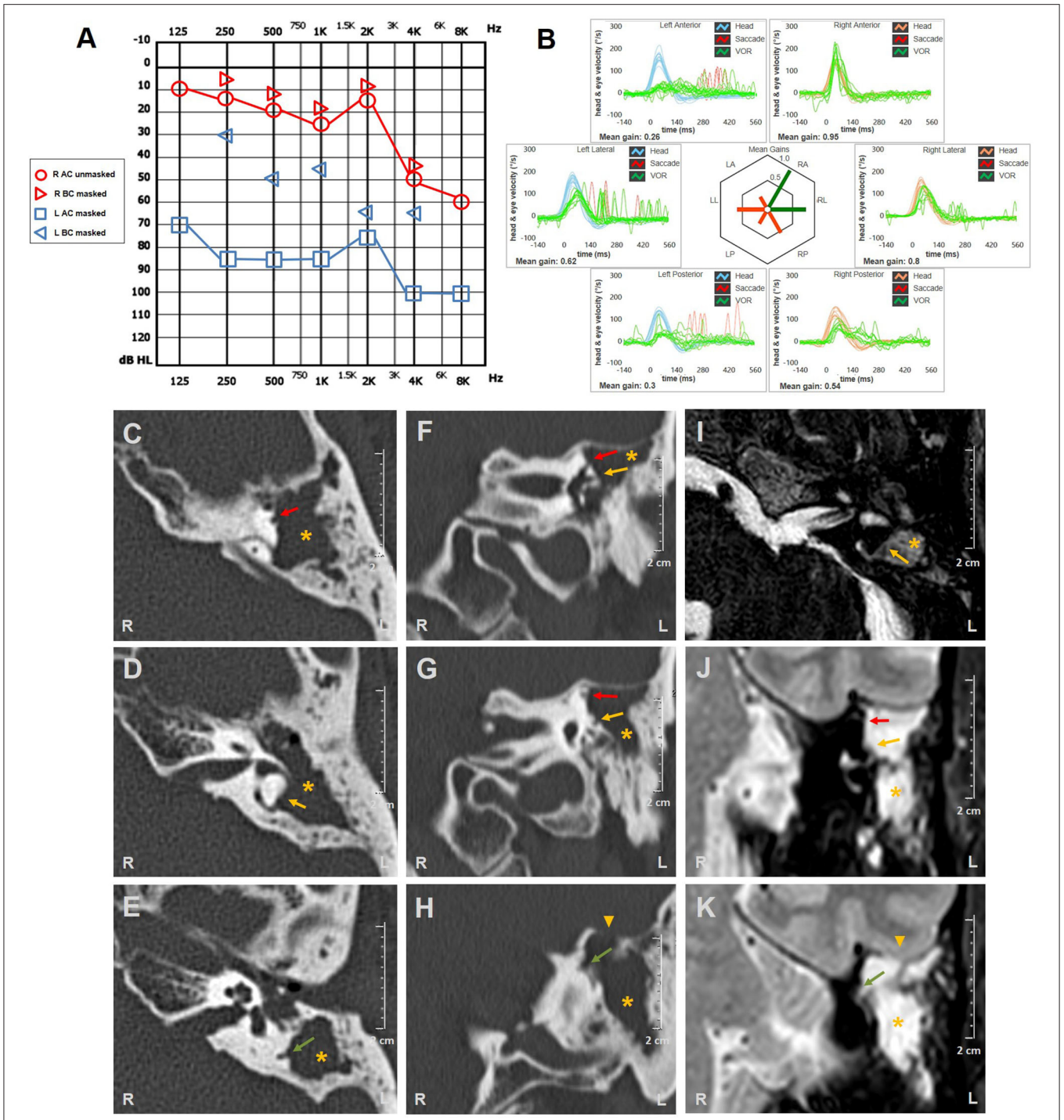

FIGURE 3 | Instrumental and radiological data of case three. **(A)** Audiometric testing showing high-frequency sensorineural HL on the right side and left mixed HL with significant ABG widened for low frequencies and mild-to-moderate down-sloping sensorineural hearing impairment. **(B)** vHIT detecting reduced VOR-gain values for all left SCs with overt saccades and slight hypofunction for contralateral PSC with no corrective saccades. Axial **(C–E)** and coronal **(F–H)** temporal bones CT scans completed with axial **(I)** and coronal **(J,K)** T2-weighted gadolinium-enhanced brain MRI showing soft tissue density (*yellow asterisks*) within left middle-ear and mastoid cavity eroding ossicles and tegmen tympani (*yellow arrowheads*). Bony labyrinthine erosions of left SSC (*red arrows*), HSC (*yellow arrows*), and PSC (*green arrows*) are highlighted. ABG, air-bone gap; AC, air conduction; BC, bone conduction; CT, computed tomography; HL, hearing loss; HSC, horizontal semicircular canal; L, left; LA, left anterior; LL, left lateral; LP, left posterior; MRI, magnetic resonance imaging; PSC, posterior semicircular canal; R, right; RA, right anterior; RL, right lateral; RP, right posterior; SC, semicircular canal; SSC, superior semicircular canal; vHIT, video head impulse test; VOR, vestibulo-ocular reflex.

(**Figures 3C–H**). Angio-MRI of the brain ruled out venous thrombosis and meningeal involvement (**Figures 3I–K**). He received CWD mastoidectomy that evidenced bony erosions of each SC and permitted achievement of cholesteatoma removal. A thin matrix layer was left upon each bony defect, whereas tegmen dehiscence was repaired with bone-pate. Additional procedures for hearing restoration and LF obliteration were postponed at a later stage. Postoperative care included bed rest, intravenous broad-spectrum antibiotics, and corticosteroids tapering for additional two weeks. The patient's conditions progressively recovered and hearing threshold remained unchanged at 30 days. Spontaneous nystagmus was progressively reduced whereas vHIT findings and PIN aligning in the same axis persisted over time.

Written informed consent was obtained from each patient for the publication of this case report, including all data and images.

DISCUSSION

Oval and round windows represent the only sites with reduced impedance in the inner ear, whereas the remaining membranous labyrinth is entirely encased within the otic capsule. Other anatomical openings connecting the inner ear fluid spaces to the surrounding structures, such as the cochlear and vestibular aqueducts, are functionally closed to sound and pressure flows as they usually offer high impedance (11). Additional bony openings such as a labyrinthine dehiscence can result in increased inner ear compliance leading to abnormal pressure transmission into the vestibular system from surrounding compartments (2). LF represents an interruption of the otic capsule connecting perilymphatic spaces with the middle ear. It may occur in <15% of patients affected by COM with cholesteatoma (13–19) or may represent a late complication in subjects being previously submitted to CWD mastoidectomy (32, 33). Affected sites can be identified in <60% of temporal bone CT scans of patients with intraoperative findings of LF (18, 19, 34) while MRI may provide additional information about inner ear involvement (35). Whereas HSC represents the most commonly affected site, both cholesteatoma matrix and inflammatory tissue may sometimes erode other structures as PSC, superior SC (SSC), vestibule, and cochlea (13–18). As LF may also represent a pathway for toxins and pathogens invasion from the middle ear to the membranous labyrinth accounting for serous or suppurative labyrinthitis, symptoms can include variable combinations of vertigo and HL depending on LF location, on the size of bony defects, and on the extent of inner ear damage (13–19, 36). PIN represents a peculiar finding in LF, although it may show a low diagnostic sensitivity. In fact, it might be underestimated due to a possible complete functional loss of inner ear sensors/afferents or the mass-induced canal plug exerted by concurrent middle ear pathologies might prevent pressure change transmissions to the endolymphatic spaces (16, 18, 19, 28, 37). Its pathomechanism is mainly attributed to the stimulation of SC ampulla, according to the site of erosion (14, 20–23, 26–28). On the other hand, HS has been also ascribed to a possible otolith activation in other inner ear disorders, including Meniere's disease, perilymphatic fistula and vestibular atelectasis. In fact, fibrous adhesions between the stapedial footplate and the saccular membranous labyrinth (vestibulofibrosis) either due to a collapse of the membranous labyrinth or due to a saccular distension on a hydropic basis have been hypothesized (4–7, 24, 25). Nevertheless, clinical observations with VEMPs testing in a patient with endolymphatic hydrops (27) and experimental studies on LF in animal models (20) reported the onset of nystagmus after pressure changes despite saccular areflexia and after removal of the otolith membranes, respectively.

All cases herein described presented at our attention with functional loss for all SCs on vHIT besides different degrees of sensorineural HL consistent with global cochleo-vestibular damage. This condition likely represented the result of either previous or current labyrinthitis due to LF, accounting for contralesional nystagmus after mastoid vibrations detected in the second patient and for paretic spontaneous nystagmus enhanced by head shakings in the third case. Conversely, slightly reduced VOR-gains for contralesional PSCs (functionally coupled with affected SSCs) may likely result from the severe functional impairment of injured SSCs, in accordance with studies on contralesional function following vestibular neuritis and vestibular deafferentation, where an involvement of both central compensation processes and peripheral impairment of the "push-pull" mechanism have been hypothesized (38–40). On the other hand, PSC was the only hypoactive canal in the contralateral ear in all cases and the expected corrective saccades after head impulses were lacking in most cases, raising the possibility that our findings might be due to artifacts. Nevertheless, most healthy PSCs exhibited highly reduced VOR-gain values compared to ipsilateral SCs also in larger cohorts with unilateral vestibular loss (41). Moreover, the functional impairment for the PSC of the unaffected ear in the first two cases might reflect the greater effect of aging on PSC VOR-gain compared to the other SCs (42).

Unfortunately, low-acceleration VOR for HSCs could not be assessed with caloric test in the patients of our report due to concurrent external/middle ear pathologies preventing water irrigations. Nevertheless, further HSC VOR responses to different velocity and acceleration ranges could have been provided by rotational testing, but a rotatory chair was not available in our departments. Also, otolith activity could not be measured, as bone-conduction could have been the only possible way to test cervical and ocular VEMPs bypassing middle ear barriers, but it was not available in our institutions. However, given cochlear and SCs impairment, it is reasonable to assume that macular hair cells were also damaged, in accordance with studies in serous labyrinthitis (43–45).

Nevertheless, PIN could still be elicited in all subjects, likewise positional nystagmus in two cases. These apparently incongruent findings might be explained assuming a functional dissociation between ampullary hair cells encoding angular accelerations. In particular, detectable PIN despite SCs impairment on vHIT might imply a spared activity for type II hair cells and regular canal afferents encoding cupular displacements which generates nystagmus (46–48). This hypothesis is supported by studies on animal models of canal dehiscence providing evidence that

sound-evoked eye movements (comparable in principle to PIN) do not only arise from sustained sound-evoked activation of phase-locking irregularly-discharging canal afferents, but also to slowly developing but sustained excitation/inhibition of regularly discharging afferents (48–50). Our assumptions are also in line with data from human temporal bone surveys showing that vestibular degeneration following serous labyrinthitis starts from type I hair-cells (44, 45). Similarly, preserved caloric responses were found in clinical studies on patients with COM (43, 51), perilymphatic fistula (52) or in cases exhibiting HS despite otolith functional loss (27). Conversely, investigations with rotatory testing have mainly documented reduced vestibular responses for the affected ear (53–55), strengthening the hypothesis of a greater impaired function of hair cells encoding for higher range frequencies. On the other hand, it may be assumed that there is a different functional outcome for damaged ampullary hair cells/afferents following acute labyrinthitis, where a selective recovery of sensors encoding for low-velocity inputs was matched by deficient high-acceleration VOR responses at long-term evaluation (38, 56). Nevertheless, a possible role of the residual function of phasic afferents in the genesis of PIN could not be ruled out a priori as all patients herein described did not present with complete canal loss on vHIT. In fact, the amount of residual canal function that is actually needed to still generate a response is not yet fully understood. Moreover, it could not be excluded that the different maximal eye velocities observed during each single canal impulse in each subject could have affected evoked nystagmus amplitudes and the interpretation of eye movements during PIN (26).

Whereas in the first two subjects the easiest explanation for HS is represented by pressure-induced endolymphatic flows toward the ampulla of the involved HSC activating spared/recovered regular afferents (**Figures 4A,B**), simultaneous cupular deflection toward the utricle in all dehiscent SCs could likely account for contralesional torsional nystagmus resulting from left tragal compression in the latter case. In particular, while ipsilesional nystagmus resulting from excitatory pressure-induced input within left HSC was mitigated by underlying baseline spontaneous nystagmus beating in the opposite direction, opposed vertical components generated from simultaneous inhibiting flows within vertical SCs canceled each other. Hence, such a PIN vector (right-torsional nystagmus) could be likely derived from the sum of concurrent inhibitions of left-sided vertical SCs afferents (14, 26) (**Figure 4C**). In accordance with Ewald's laws, pressure removal from the affected ears elicited coplanar weaker opposite nystagmus due to inhibitory ampullofugal flows within HSC in the first two cases. Conversely, the same maneuver generated stronger ipsilesional torsional nystagmus as a result of overlapping excitatory ampullofugal inputs within the left vertical SCs in the latter case (30).

The same reasoning could be applied in the interpretation of nystagmus behavior in the last patient during head movements along the pitch plane. In this case, vertical/torsional positional nystagmus due to simultaneous left-sided PSC BPPV evoked by head bending likely superimposed underlying baseline paretic spontaneous nystagmus (57). In the same patient, paroxysmal nystagmus could be elicited despite PSC VOR-gain loss on vHIT, strengthening the assumption of spared or recovered low-velocity afferents (58). Similarly, in the second case, positional geotropic direction-changing horizontal nystagmus closely matched with the expected oculomotor findings resulting from a buoyancy mechanism likely due to penetration of toxic agents and/or inflammatory mediators into the affected HSC (59–61). On the other hand, positional nystagmus has been reported in patients with labyrinthine-intracranial fistula. In fact, it has been hypothesized that intracranial pressure variations related to sudden changes in head positions could be conveyed into the dehiscent canal and result in excitatory/inhibitory endolymphatic flows accounting for direction-changing nystagmus (62–64). Similarly, head movements have been assumed to evoke subtle mass-induced pressure changes on the membranous labyrinth at the LF area in a patient with cholesteatoma eroding the HSC who presented with geotropic positional horizontal nystagmus (65). Nevertheless, the patient of the second case herein reported should not have developed similar mechanisms, as the LF was in contact neither with intracranial spaces nor with middle ear masses. Furthermore, an outward protrusion of the membranous duct through the right HSC fistula, that should be expected to occur in right-sided head positionings due to the gravity vector, should have resulted in ampullofugal flows, and in turn to apogeotropic nystagmus, which was not the case for our patient.

Although a reverse functional dissociation pattern impairing low-velocity while sparing high-velocity canal VOR has been often observed in several vestibular diseases (66–69), other vestibular pathologies have been related to a loss of sensitivity for high-acceleration head movements while low-acceleration behavior remains intact, likewise LF herein reported (70–72). In particular, SSC dehiscence represents another condition accounting for a third window mechanism that has been demonstrated to result in ocular movements aligning with the plane of the affected canal in response to loud sounds and/or pressure changes despite selectively impaired canal function on vHIT. However, in this condition, either a plug effect exerted by middle fossa structures on membranous labyrinth or dissipation of mechanical energy through the dehiscence have been assumed as underlying factors accounting for reduced high-velocity VOR-gain for the affected canal (73, 74). Whereas this latter mechanism could hypothetically account for the global canal hypofunction on vHIT in the last case with erosion of all the three SCs, it could neither explain the impaired responses in high-velocity domain for vertical canals detected in the first two cases with isolated HSC fistula, nor could it account for the concomitant sensorineural HL.

While both cases 2 and 3 presented with a widened low-frequency air-bone gap, as expected from a third mobile window pathology (11), several symptoms and signs pertaining to the third window spectrum could not be detected in our patients. Whereas the lack of pulsatile tinnitus, own body sounds hyperacusis and vertigo induced by loud sounds could be explained by the masking effect of the underlying middle ear disorders, nystagmus induced by Valsalva maneuvers could have been missing due to the different location of LF created by middle ear disease (as in our patients) compared to SSC

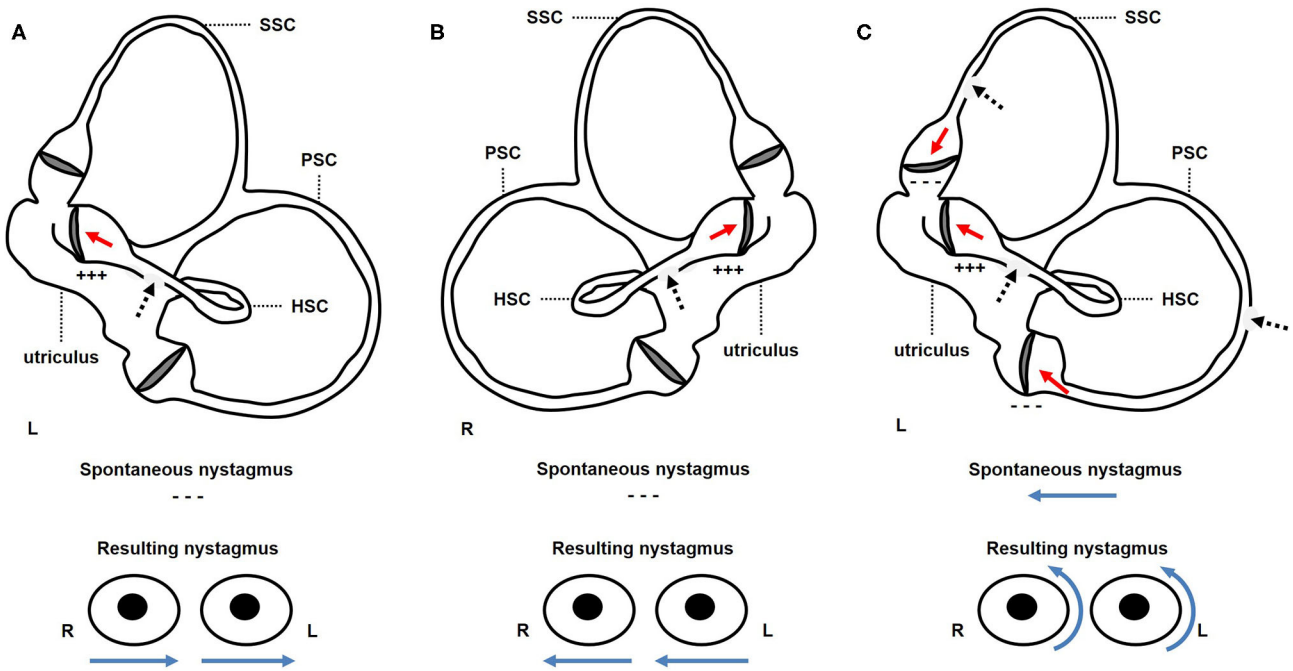

FIGURE 4 | Schematic representation of the membranous labyrinth along the sagittal plane (*above*) to explain the proposed mechanism for pressure-induce eye movements (*below*) in each case. Positive pressure applied over the EAC is represented with *black dashed arrows*, resulting in endolymphatic flows with *red arrows* and direction of nystagmus fast phase with *blue arrows*. **(A)** In the first case, positive pressure applied on the left EAC resulted in ampullopetal endolymphatic flows within left dehiscent HSC, leading to transitory excitation (+ + +) of left HSC afferents. As there were no spontaneous nystagmus, resulting nystagmus was purely horizontal left-beating. **(B)** Likewise, in the second patient, right tragal compression led to ampullopetal excitatory (+ + +) endolymphatic flows within right HSC resulting in transient horizontal right-beating nystagmus. **(C)** In the third case, positive pressure exerted over the patient's left EAC generated simultaneous ampullopetal endolymphatic flows within each dehiscent canal, being excitatory (+ + +) for left HSC and inhibitory for left PSC and SSC (− − −). While horizontal left-beating components coming from left HSC activation opposed to ongoing spontaneous paretic nystagmus, vertical components generated by vertical canal inhibition (upbeat and downbeat for SSC and PSC, respectively) reciprocally canceled. Then, resulting nystagmus mainly reflected torsional rightbeating components coming from inhibition of left vertical canals afferents. EAC, external auditory canal; HSC, horizontal semicircular canal; L, left; PSC, posterior semicircular canal; R, right; SSC, superior semicircular canal.

dehiscence at the arcuate eminence. In fact, the lack of PIN in nasal Valsalva could likely be due to the fact that pressure transmission from the nasal cavity to the middle ear through the Eustachian tube was prevented by the coexistent middle ear pathologies. On the other hand, whereas glottic Valsalva maneuver should generate nystagmus through increased intracranial pressure conveyance to the labyrinthine spaces via SSC dehiscence (9), in no case herein described did LF expose the membranous labyrinth to intracranial cavity. Nevertheless, the lack of video-oculographic recording, providing an accurate detection of subtle eye movements to pressure/sounds and slow phase velocity measures, could have prevented detecting these signs in our study.

In general, the results of our study and literature data suggest that conclusions about SCs activity in the case of vestibular impairment only based on vHIT data could be misleading, as these measurements do not reflect the whole VOR response spectrum and dissociation among afferents encoding high and low-acceleration responses could be possible. In fact, as observed in our patients, HS could be elicited despite global canal hypofunction on vHIT, allowing clinicians to combine the analysis of PIN behavior and imaging to identify the location of LF prior to middle ear surgery (14). According to the same reasoning, vestibular hypofunction on vHIT should never authorize clinicians to neglect evaluating for provoked nystagmus in patients with vestibular symptoms, as residual/spared canal activity could account for ampullary activation to endolymphatic flows despite vHIT data.

Nevertheless, as already evidenced, the main limitation of this study, preventing any definite conclusion on the genesis of PIN in our patients, is the lack of objective measurements of both low-acceleration SCs VOR and otolith function. Despite the unlikelihood of a macular contribution to vestibular responses to pressure changes in the patients herein described, we could not exclude a possible activation of otolith receptors, as it has been described how these structures could modify ongoing ocular movements or generate spontaneous horizontal nystagmus (75, 76), and how they could be functionally spared in case of labyrinthitis with concurrent third window pathologies (77). Additionally, even though the presenting instrumental picture and PIN behavior in the patient with EAC tumor overlapped vestibular findings in the other two individuals with COM, we could not exclude that the two pathologies may result in different labyrinthine lesion patterns. Even though it has been reported

how squamous cell carcinoma of the EAC could result in inner ear invasion through HSC erosions (78) and how middle ear tumors could lead to both labyrinthitis and labyrinthine ischemia (79, 80), inner ear histopathology in the case of temporal bone malignancy is still mostly unknown.

CONCLUSIONS

Although pathomechanisms underlying PIN in LF are still unclear, our case series showing that HS could be detectable even with hypoactive SCs on vHIT might offer additional insights to this aspect. Although vHIT measurements would suggest an impairment of canal function, SCs seem to represent the target sensor of HS in LF as nystagmus axis matched that of the affected canals and its characteristics strictly followed Ewald's laws. In our opinion, this apparently paradoxical finding might be possible through a functional dissociation between low- (active) and high- (impaired) velocity canal afferents. An asymmetrical damage or recovery among different subgroups of hair cells following labyrinthitis might represent the underlying process accounting for this functional behavior. Nevertheless, we strongly believe that further studies on PIN are required to substantiate the assumption that HS in LF results from the stimulation of type II hair-cells and regular afferents of dehiscent SCs.

DATA AVAILABILITY STATEMENT

The original contributions presented in the study are included in the article/**Supplementary Material**, further inquiries can be directed to the corresponding author/s.

ETHICS STATEMENT

The studies involving human participants were reviewed and approved by Area Vasta Nord Emilia Romagna. The patients/participants provided their written informed consent to participate in this study. Written informed consent was obtained from the individual(s) for the publication of any potentially identifiable images or data included in this article.

AUTHOR CONTRIBUTIONS

AC, PM, SM, and EA: conceptualization and data interpretation. AC, CB, PM, SM, FC, MF, and FL: investigation and original draft preparation. AC, CB, MB, IJF, PM, LR, and GB: data acquisition. AC: images and artwork. GB, EA, and AG: supervision and manuscript review. All authors approved the final version of the manuscript.

SUPPLEMENTARY MATERIAL

The Supplementary Material for this article can be found online at: https://www.frontiersin.org/articles/10.3389/fneur.2021.634782/full#supplementary-material

Supplementary Video 1 | Video Frenzel findings in patient 1.

Supplementary Video 2 | Video Frenzel findings in patient 2.

Supplementary Video 3 | Video Frenzel findings in patient 3 (first evaluation).

Supplementary Video 4 | Video Frenzel findings in patient 3 (last evaluation).

REFERENCES

1. Hennebert C. A new syndrome in hereditary syphilis of the labyrinth. *Presse Med Belg Brux.* (1911) 63:467–70.
2. Minor LB. Labyrinthine fistulae: pathobiology and management. *Curr Opin Otolaryngol Head Neck Surg.* (2003) 11:340–6. doi: 10.1097/00020840-200310000-00006
3. Sarna B, Abouzari M, Merna C, Jamshidi S, Saber T, Djalilian HR. Perilymphatic fistula: a review of classification, etiology, diagnosis, and treatment. *Front Neurol.* (2020) 11:1046. doi: 10.3389/fneur.2020.01046
4. Nadol JB Jr. Positive "fistula sign" with intact tympanic membrane. *Arch Otolaryngol.* (1974) 100:273–8. doi: 10.1001/archotol.1974.00780040283007
5. Nadol JB Jr. Positive Hennebert's sign in Ménière's disease. *Arch Otolaryngol.* (1977) 103:524–30. doi: 10.1001/archotol.1977.00780260054005
6. Wenzel A, Ward BK, Schubert MC, Kheradmand A, Zee DS, Mantokoudis G, et al. Patients with vestibular loss, Tullio phenomenon, and pressure-induced nystagmus: vestibular atelectasis? *Otol Neurotol.* (2014) 35:866–72. doi: 10.1097/MAO.0000000000000366
7. Maslovara S, Butkovic-Soldo S, Pajic-Matic I, Sestak A. Vestibular atelectasis: decoding pressure and sound-induced nystagmus with bilateral vestibulopathy. *Laryngoscope.* (2019) 129:1685–88. doi: 10.1002/lary.27724
8. Gadre AK, Edwards IR, Baker VM, Roof CR. Membranous or hypermobile stapes footplate: a new anatomic site resulting in third window syndrome. *Front Neurol.* (2020) 11:871. doi: 10.3389/fneur.2020.00871
9. Minor LB, Solomon D, Zinreich JS, Zee DS. Sound- and/or pressure-induced vertigo due to bone dehiscence of the superior semicircular canal. *Arch Otolaryngol Head Neck Surg.* (1998) 124:249–58. doi: 10.1001/archotol.124.3.249
10. Lee JA, Liu YF, Nguyen SA, McRackan TR, Meyer TA, Rizk HG. Posterior semicircular canal dehiscence: case series and systematic review. *Otol Neurotol.* (2020) 41:511–21. doi: 10.1097/MAO.0000000000002576
11. Merchant SN, Rosowski JJ. Conductive hearing loss caused by third-window lesions of the inner ear. *Otol Neurotol.* (2008) 29:282–9. doi: 10.1097/MAO.0b013e318161ab24
12. Wackym PA, Balaban CD, Zhang P, Siker DA, Hundal JS. Third window syndrome: surgical management of cochlea-facial nerve dehiscence. *Front Neurol.* (2019) 10:1281. doi: 10.3389/fneur.2019.01281
13. Sheehy JL, Brackmann DE. Cholesteatoma surgery: management of the labyrinthine fistula–a report of 97 cases. *Laryngoscope.* (1979) 89:78–87. doi: 10.1288/00005537-197901000-00008
14. McCabe BF. Labyrinthine fistula in chronic mastoiditis. *Ann Otol Rhinol Laryngol Suppl.* (1984) 112:138–41. doi: 10.1177/00034894840930S424
15. Sanna M, Zini C, Bacciu S, Scandellari R, Delogu P, Jemmi G. Management of the labyrinthine fistula in cholesteatoma surgery. *ORL J Otorhinolaryngol Relat Spec.* (1984) 46:165–72. doi: 10.1159/000275704
16. Dornhoffer JL, Milewski C. Management of the open labyrinth. *Otolaryngol Head Neck Surg.* (1995) 112:410–4. doi: 10.1016/S0194-5998(95)70275-X
17. Jang CH, Merchant SN. Histopathology of labyrinthine fistulae in chronic otitis media with clinical implications. *Am J Otol.* (1997) 18:15–25.
18. Busaba NY. Clinical presentation and management of labyrinthine fistula caused by chronic otitis media. *Ann Otol Rhinol Laryngol.* (1999) 108:435–9. doi: 10.1177/000348949910800503
19. Kvestad E, Kvaerner KJ, Mair IW. Labyrinthine fistula detection: the predictive value of vestibular symptoms and computerized tomography. *Acta Otolaryngol.* (2001) 121:622–6. doi: 10.1080/000164801316878935
20. Nylen CO. A clinical study of the labyrinthine fistula symptoms and pseudo-fistula symptoms in otitis. *Acta Otolaryngol.* (1923) 5(Suppl 3):7–511.

21. Dohlman G. The mechanism of the fistula test. *Acta Otolaryngol.* (1953) 43(Suppl 109):22–6. doi: 10.3109/00016485309132494
22. Pursiainen KE. VI. Fistula Tests. *Acta Otolaryngol.* (1954) 43(Suppl 112):44–74. doi: 10.3109/00016485409122089
23. Zwergius E. The mechanism of labyrinthine fistular reactions; experimental investigations. *Acta Otolaryngol.* (1956) 46:74–9. doi: 10.3109/00016485609118171
24. Ostrowski VB, Hain TC, Wiet RJ. Pressure-induced ocular torsion. *Arch Otolaryngol Head Neck Surg.* (1997) 123:646–9. doi: 10.1001/archotol.1997.01900060098017
25. Backous DD, Minor LB, Aboujaoude ES, Nager GT. Relationship of the utriculus and sacculus to the stapes footplate: anatomic implications for sound- and/or pressure-induced otolith activation. *Ann Otol Rhinol Laryngol.* (1999) 108:548–53. doi: 10.1177/000348949910800604
26. Yagi T, Kamura E, Shitara A. Three-dimensional analysis of pressure nystagmus in labyrinthine fistulae. *Acta Otolaryngol.* (1999) 119:150–3. doi: 10.1080/00016489950181558
27. Suzuki M, Kitajima N, Ushio M, Shintani M, Ishibashi T. Changes in the Tullio phenomenon and the fistula sign in the course of endolymphatic hydrops. *ORL J Otorhinolaryngol Relat Spec.* (2003) 65:125–8. doi: 10.1159/000070778
28. Helmchen C, Gehrking E, Gottschalk S, Rambold H. Persistence of perilymph fistula mechanism in a completely paretic posterior semicircular canal. *J Neurol Neurosurg Psychiatry.* (2005) 76:280–2. doi: 10.1136/jnnp.2004.038083
29. Halmagyi GM, Chen L, MacDougall HG, Weber KP, Mc Garvie LA, Curthoys IS. The video head impulse test. *Front Neurol.* (2017) 8:258. doi: 10.3389/fneur.2017.00258
30. Ewald JR. *Physiologische Untersuchungen ueber das Endorgan des Nervus Octavus*. Wiesbaden: Bergmann (1892).
31. Moody SA, Hirsch BE, Myers EN. Squamous cell carcinoma of the external auditory canal: an evaluation of a staging system. *Am J Otol.* (2000) 21:582–8.
32. Hakuba N, Hato N, Shinomori Y, Sato H, Gyo K. Labyrinthine fistula as a late complication of middle ear surgery using the canal wall down technique. *Otol Neurotol.* (2002) 23:832–5. doi: 10.1097/00129492-200211000-00003
33. Portmann D, Rezende Ferreira D. Delayed labyrinthine fistula in canal wall down mastoidectomy. *Rev Laryngol Otol Rhinol (Bord).* (2003) 124:265–8.
34. Fuse T, Tada Y, Aoyagi M, Sugai Y. CT detection of facial canal dehiscence and semicircular canal fistula: comparison with surgical findings. *J Comput Assist Tomogr.* (1996) 20:221–4. doi: 10.1097/00004728-199603000-00009
35. Sone M, Mizuno T, Sugiura M, Naganawa S, Nakashima T. Three-dimensional fluid-attenuated inversion recovery magnetic resonance imaging investigation of inner ear disturbances in cases of middle ear cholesteatoma with labyrinthine fistula. *Otol Neurotol.* (2007) 28:1029–33. doi: 10.1097/MAO.0b013e3181587d95
36. Paparella MM, Brady DR, Hoel R. Sensori-neural hearing loss in chronic otitis media and mastoiditis. *Trans Am Acad Ophthalmol Otolaryngol.* (1970) 74:108–15.
37. D'Albora R, Silveira L, Carmona S, Perez-Fernandez N. Diagnostic bedside vestibuloocular reflex evaluation in the setting of a false negative fistula test in cholesteatoma of the middle ear. *Case Rep Otolaryngol.* (2017) 2017:2919463. doi: 10.1155/2017/2919463
38. Halmagyi GM, Curthoys IS, Cremer PD, Henderson CJ, Todd MJ, Staples MJ, et al. The human horizontal vestibulo-ocular reflex in response to high-acceleration stimulation before and after unilateral vestibular neurectomy. *Exp Brain Res.* (1990) 81:479–90. doi: 10.1007/BF02423496
39. Aw ST, Fetter M, Cremer PD, Karlberg M, Halmagyi GM. Individual semicircular canal function in superior and inferior vestibular neuritis. *Neurology.* (2001) 57:768–74. doi: 10.1212/WNL.57.5.768
40. Palla A, Straumann D. Recovery of the high-acceleration vestibulo-ocular reflex after vestibular neuritis. *J Assoc Res Otolaryngol.* (2004) 5:427–35. doi: 10.1007/s10162-004-4035-4
41. Allum JHJ, Honegger F. Improvement of asymmetric vestibulo-ocular reflex responses following onset of vestibular neuritis is similar across canal planes. *Front Neurol.* (2020) 11:565125. doi: 10.3389/fneur.2020.565125
42. McGarvie LA, MacDougall HG, Halmagyi GM, Burgess AM, Weber KP, Curthoys IS. The Video Head Impulse Test (vHIT) of semicircular canal function - age-dependent normative values of VOR gain in healthy subjects. *Front Neurol.* (2015) 6:154. doi: 10.3389/fneur.2015.00154
43. Chang CW, Cheng PW, Young YH. Inner ear deficits after chronic otitis media. *Eur Arch Otorhinolaryngol.* (2014) 271:2165–70. doi: 10.1007/s00405-013-2714-7
44. da Costa Monsanto R, Erdil M, Pauna HF, Kwon G, Schachern PA, Tsuprun V, et al. Pathologic changes of the peripheral vestibular system secondary to chronic otitis media. *Otolaryngol Head Neck Surg.* (2016) 155:494–500. doi: 10.1177/0194599816646359
45. Kaya S, Schachern PA, Tsuprun V, Paparella MM, Cureoglu S. Deterioration of vestibular cells in labyrinthitis. *Ann Otol Rhinol Laryngol.* (2017) 126:89–95. doi: 10.1177/0003489416675356
46. Goldberg JM, Fernandez C. Physiology of peripheral neurons innervating semicircular canals of the squirrel monkey. I. Resting discharge and response to constant angular accelerations. *J Neurophysiol.* (1971) 34:635–60. doi: 10.1152/jn.1971.34.4.635
47. Sadeghi SG, Chacron MJ, Taylor MC, Cullen KE. Neural variability, detection thresholds, and information transmission in the vestibular system. *J Neurosci.* (2007) 27:771–81. doi: 10.1523/JNEUROSCI.4690-06.2007
48. Rabbitt RD. Semicircular canal biomechanics in health and disease. *J Neurophysiol.* (2019) 121:732–55. doi: 10.1152/jn.00708.2018
49. Carey JP, Hirvonen TP, Hullar TE, Minor LB. Acoustic responses of vestibular afferents in a model of superior canal dehiscence. *Otol Neurotol.* (2004) 25:345–52. doi: 10.1097/00129492-200405000-00024
50. Iversen MM, Zhu H, Zhou W, Della Santina CC, Carey JP, Rabbitt RD. Sound abnormally stimulates the vestibular system in canal dehiscence syndrome by generating pathological fluid-mechanical waves. *Sci Rep.* (2018) 8:10257. doi: 10.1038/s41598-018-28592-7
51. Lee IS, Park HJ, Shin JE, Jeong YS, Kwak HB, Lee YJ. Results of air caloric and other vestibular tests in patients with chronic otitis media. *Clin Exp Otorhinolaryngol.* (2009) 2:145–50. doi: 10.3342/ceo.2009.2.3.145
52. Young Y H, Nomura Y, Hara M. Vestibular pathophysiologic changes in experimental perilymphatic fistula. *Ann Otol Rhinol Laryngol.* (1992) 101:612–6. doi: 10.1177/000348949210100713
53. Bhansali SA, Cass SP, Benitez JT, Mathog RH. Vestibular effects of chronic perilymph fistula in the cat. *Otolaryngol Head Neck Surg.* (1990) 102:701–8. doi: 10.1177/019459989010200613
54. Gianoli GJ, Soileau JS. Chronic suppurative otitis media, caloric testing, and rotational chair testing. *Otol Neurotol.* (2008) 29:13–5. doi: 10.1097/mao.0b013e31815c2589
55. Mostafa BE, Shafik AG, El Makhzangy AM, Taha H, Abdel Mageed HM. Evaluation of vestibular function in patients with chronic suppurative otitis media. *ORL J Otorhinolaryngol Relat Spec.* (2013) 75:357–60. doi: 10.1159/000357475
56. Schmid-Priscoveanu A, Bohmer A, Obzina H, Straumann D. Caloric and search-coil head-impulse testing in patients after vestibular neuritis. *J Assoc Res Otolaryngol.* (2001) 2:72–8. doi: 10.1007/s101620010060
57. Choi S, Choi HR, Nahm H, Han K, Shin JE, Kim CH. Utility of the bow and lean test in predicting subtype of benign paroxysmal positional vertigo. *Laryngoscope.* (2018) 128:2600–4. doi: 10.1002/lary.27142
58. Casani AP, Cerchiai N, Navari E. Paroxysmal positional vertigo despite complete vestibular impairment: the role of instrumental assessment. *Acta Otorhinolaryngol Ital.* (2018) 38:563–8. doi: 10.14639/0392-100X-1549
59. Kim CH, Choi JM, Jung HV, Park HJ, Shin JE. Sudden sensorineural hearing loss with simultaneous positional vertigo showing persistent geotropic direction-changing positional nystagmus. *Otol Neurotol.* (2014) 35:1626–32. doi: 10.1097/MAO.0000000000000457
60. Kim CH, Yang YS, Im D, Shin JE. Nystagmus in patients with unilateral acute otitis media complicated by serous labyrinthitis. *Acta Otolaryngol.* (2016) 136:559–63. doi: 10.3109/00016489.2015.1132845
61. Choi JW, Han K, Nahm H, Shin JE, Kim CH. Direction-changing positional nystagmus in acute otitis media complicated by serous labyrinthitis: new insights into positional nystagmus. *Otol Neurotol.* (2019) 40:e393–e8. doi: 10.1097/MAO.0000000000002104
62. Brantberg K, Bergenius J, Mendel L, Witt H, Tribukait A, Ygge J. Symptoms, findings and treatment in patients with dehiscence of the superior semicircular canal. *Acta Otolaryngol.* (2001) 121:68–75. doi: 10.1080/000164801300006308

63. Suzuki M, Ota Y, Tanaka T, Ota Y. Lateral semicircular canal-enlarged vestibular aqueduct fistula associated with paroxysmal positional nystagmus. *Otol Neurotol.* (2016) 37:e192–3. doi: 10.1097/MAO.0000000000000778
64. Young AS, McMonagle B, Pohl DV, Magnussen J, Welgampola MS. Superior semicircular canal dehiscence presenting with recurrent positional vertigo. *Neurology.* (2019) 93:1070–2. doi: 10.1212/WNL.0000000000008624
65. Shim DB, Ko KM, Song MH, Song CE. A case of labyrinthine fistula by cholesteatoma mimicking lateral canal benign paroxysmal positional vertigo. *Korean J Audiol.* (2014) 18:153–7. doi: 10.7874/kja.2014.18.3.153
66. Mahringer A, Rambold HA. Caloric test and video-head-impulse: a study of vertigo/dizziness patients in a community hospital. *Eur Arch Otorhinolaryngol.* (2014) 271:463–72. doi: 10.1007/s00405-013-2376-5
67. Bartolomeo M, Biboulet R, Pierre G, Mondain M, Uziel A, Venail F. Value of the video head impulse test in assessing vestibular deficits following vestibular neuritis. *Eur Arch Otorhinolaryngol.* (2014) 271:681–8. doi: 10.1007/s00405-013-2451-y
68. Blödow A, Blödow J, Bloching MB, Helbig R, Walther LE. Horizontal VOR function shows frequency dynamics in vestibular schwannoma. *Eur Arch Otorhinolaryngol.* (2015) 272:2143–8. doi: 10.1007/s00405-014-3042-2
69. McGarvie LA, Curthoys IS, MacDougall HG, Halmagyi GM. What does the head impulse test versus caloric dissociation reveal about vestibular dysfunction in Meniere's disease? *Ann N Y Acad Sci.* (2015) 1343:58–62. doi: 10.1111/nyas.12687
70. Prepageran N, Kisilevsky V, Tomlinson D, Ranalli P, Rutka J. Symptomatic high frequency/acceleration vestibular loss: consideration of a new clinical syndrome of vestibular dysfunction. *Acta Otolaryngol.* (2005) 125:48–54. doi: 10.1080/00016480410017981
71. Kirchner H, Kremmyda O, Hüfner K, Stephan T, Zingler V, Brandt T, et al. Clinical, electrophysiological, and MRI findings in patients with cerebellar ataxia and a bilaterally pathological head-impulse test. *Ann N Y Acad Sci.* (2011) 1233:127–38. doi: 10.1111/j.1749-6632.2011.06175.x
72. Castellucci A, Malara P, Martellucci S, Botti C, Delmonte S, Quaglieri S, et al. Feasibility of using the video-head impulse test to detect the involved canal in benign paroxysmal positional vertigo presenting with positional downbeat nystagmus. *Front Neurol.* (2020) 11:578588. doi: 10.3389/fneur.2020.578588
73. Cremer PD, Minor LB, Carey JP, Della Santina CC. Eye movements in patients with superior canal dehiscence syndrome align with the abnormal canal. *Neurology.* (2000) 55:1833–41. doi: 10.1212/WNL.55.12.1833
74. Castellucci A, Piras G, Del Vecchio V, Crocetta FM, Maiolo V, Ferri GG, et al. The effect of superior canal dehiscence size and location on audiometric measurements, vestibular-evoked myogenic potentials and video-head impulse testing. *Eur Arch Otorhinolaryngol.* (2020). doi: 10.1007/s00405-020-06169-3
75. Fluur E, Siegborn J. The otolith organs and the nystagmus problem. *Acta Otolaryngol.* (1973) 76:438–42. doi: 10.3109/00016487309121533
76. Manzari L, MacDougall HG, Burgess AM, Curthoys IS. Selective otolith dysfunctions objectively verified. *J Vestib Res.* (2014) 24:365–73. doi: 10.3233/VES-140537
77. Castellucci A, Botti C, Renna L, Delmonte S, Moratti C, Pascarella R, et al. Enhanced otolith function despite severe labyrinthine damage in a case of pneumolabyrinth and pneumocephalus due to otogenic meningitis associated with superior canal dehiscence. *Otol Neurotol.* (2021) 42:e101–6. doi: 10.1097/MAO.0000000000002835
78. Ungar OJ, Santos F, Nadol JB, Horowitz G, Fliss DM, Faquin WC, et al. Invasion patterns of external auditory canal squamous cell carcinoma: a histopathology study. *Laryngoscope.* (2021) 131:e590–7. doi: 10.1002/lary.28676
79. Hiraide F, Inouye T, Ishii T. Primary squamous cell carcinoma of the middle ear invading the cochlea. A histopathological case report. *Ann Otol Rhinol Laryngol.* (1983) 92(3 Pt 1):290–4. doi: 10.1177/000348948309200315
80. Ogino S, Iino Y, Nakamoto Y, Murakami Y, Toriyama M. Histopathological study of the temporal bones in patients with primary carcinomas of the ear. *Nihon Jibiinkoka Gakkai Kaiho.* (2000) 103:1141–9. doi: 10.3950/jibiinkoka.103.1141

Conflict of Interest: The authors declare that the research was conducted in the absence of any commercial or financial relationships that could be construed as a potential conflict of interest.

frontiers in Neurology

REVIEW
published: 06 April 2021
doi: 10.3389/fneur.2021.638574

Current Trends, Controversies, and Future Directions in the Evaluation and Management of Superior Canal Dehiscence Syndrome

Kristine Elisabeth Eberhard[1,2], *Divya A. Chari*[1], *Hideko Heidi Nakajima*[1], *Mads Klokker*[2,3], *Per Cayé-Thomasen*[2,3] *and Daniel J. Lee*[1]*

[1] Department of Otolaryngology, Massachusetts Eye and Ear, Harvard Medical School, Boston, MA, United States, [2] Copenhagen Hearing and Balance Centre, Department of Otorhinolaryngology, Head and Neck Surgery & Audiology, Copenhagen University Hospital – Rigshospitalet, Copenhagen, Denmark, [3] Faculty of Health and Medical Sciences, University of Copenhagen, Copenhagen, Denmark

Patients with superior canal dehiscence syndrome (SCDS) can present with a range of auditory and/or vestibular signs and symptoms that are associated with a bony defect of the superior semicircular canal (SSC). Over the past two decades, advances in diagnostic techniques have raised the awareness of SCDS and treatment approaches have been refined to improve patient outcomes. However, a number of challenges remain. First, there is currently no standardized clinical testing algorithm for quantifying the effects of superior canal dehiscence (SCD). SCDS mimics a number of common otologic disorders and established metrics such as supranormal bone conduction thresholds and vestibular evoked myogenic potential (VEMP) measurements; although useful in certain cases, have diagnostic limitations. Second, while high-resolution computed tomography (CT) is the gold standard for the detection of SCD, a bony defect does not always result in signs and symptoms. Third, even when SCD repair is indicated, there is a lack of consensus about nomenclature to describe the SCD, ideal surgical approach, specific repair techniques, and type of materials used. Finally, there is no established algorithm in evaluation of SCDS patients who fail primary repair and may be candidates for revision surgery. Herein, we will discuss both contemporary and emerging diagnostic approaches for patients with SCDS and highlight challenges and controversies in the management of this unique patient cohort.

Keywords: superior canal dehiscence, semicircular canal dehiscence, third window syndrome, SCD, SSCD, craniotomy, transmastoid, diagnostic

OPEN ACCESS

Edited by:
P. Ashley Wackym, The State University of New Jersey, United States

Reviewed by:
Arun K. Gadre, Geisinger Medical Center, United States
Andrea Castellucci, Santa Maria Nuova Hospital, Italy

***Correspondence:**
Daniel J. Lee
daniel_lee@meei.harvard.edu

Specialty section:
This article was submitted to Neuro-Otology, a section of the journal Frontiers in Neurology

Received: *07 December 2020*
Accepted: *08 February 2021*
Published: *06 April 2021*

Citation:
Eberhard KE, Chari DA, Nakajima HH, Klokker M, Cayé-Thomasen P and Lee DJ (2021) Current Trends, Controversies, and Future Directions in the Evaluation and Management of Superior Canal Dehiscence Syndrome. Front. Neurol. 12:638574. doi: 10.3389/fneur.2021.638574

INTRODUCTION

Superior semicircular canal dehiscence syndrome (SCDS) was first reported by Minor et al. in 1998 (1). The authors described a series of patients with disequilibrium and sound- and pressure-induced vertigo associated with nystagmus in the plane of the superior semicircular canal (SSC). Computed tomography (CT) imaging revealed a bony defect of the SSC. Symptom improvement was observed in patients who underwent surgical plugging of the defect via middle fossa craniotomy. In subsequent years, auditory symptoms, including autophony, amplification of

bodily sounds, pulsatile tinnitus, conductive hearing loss, hyperacusis, and aural fullness as well as vestibular symptoms of chronic disequilibrium and sound- and pressure-induced vertigo and oscillopsia became hallmarks of SCDS (2–4).

While in most patients symptoms of SCDS can be tolerated and conservative management is reasonable, some individuals suffering from SCDS report decreased quality of life due to challenges in communicating with those around them and completing activities of daily living (5–7). The health utility value (HUV), a measure of general health-related quality of life, ranges from poor health (0.3), to perfect health (1.0). Indeed, HUV is significantly lower in SCDS patients (0.68) compared to the general U.S. population (0.80) (5). For patients with debilitating symptoms, definitive treatment involves surgical repair of the dehiscence. However, the diagnostic evaluation of patients with suspected SCDS can sometimes be difficult to interpret. Established clinical testing that reveals supranormal bone conduction thresholds, low frequency air-bone gap (ABG) with present acoustic reflexes, low threshold cervical vestibular evoked myogenic potentials (cVEMP) and increased ocular VEMP (oVEMP) amplitudes are useful in guiding management options in symptomatic patients with radiologic superior canal dehiscence (SCD). However, some symptomatic patients do not have findings suggesting a classic third window. Furthermore, while clinicians agree that primary (and revision) surgery is a reasonable option for patients with persistent localizing signs and symptoms, the optimal approach, repair technique and materials are the subject of debate and confusion amongst both providers and patients.

Herein, we will review the pathophysiology and etiology of SCD, present current trends in its diagnosis and management, discuss novel approaches, and finally highlight some of the remaining challenges and controversies. Illustrative cases are provided to complement the literature.

Pathophysiology

Symptoms produced in SCDS are thought to occur by a "third window" phenomenon of the inner ear. In a normal ear, sound is transmitted through the ossicular chain resulting in volume velocity into the cochlea through the oval window and eventually toward the round window (bold arrows in **Figure 1A**). SCD results in a third mobile window that enables acoustic stimuli at the oval window to dissipate through the vestibular labyrinth, leading to vertigo, and dizziness (**Figure 1B**). Intracranial pressure changes may also inadvertently stimulate vestibular end organs (**Figure 1C**) (2, 3, 8, 9). Response to air conduction is reduced resulting in low-frequency hearing loss, and response to bone conduction is increased resulting in hyperacusis, autophony, and amplification of bodily sounds (e.g., hearing eye movements or footfalls). Dural pulsations across the dehiscence are the likely cause of pulsatile tinnitus (a common auditory symptom in SCDS patients). The pathophysiology of SCDS remains incompletely understood, especially with regard to the variability in symptomatology among patients, but remains the focus of a number of research studies (8–11, 17, 18).

Third window lesions may occur in different anatomic locations including the posterior or horizontal semicircular canals, bony vestibule, or the cochlea. An enlarged vestibular aqueduct (EVA) can cause a third window phenomenon in children and adults. A pathologically widened vestibular aqueduct produces a communication between the bony vestibule and intracranial cavity that can result in an ABG and mechanical characteristics similar to that observed in patients with SCDS (**Figure 1D**) (13). Patients with EVA present with normal hearing thresholds, conductive hearing loss, mixed hearing loss, or sensorineural hearing loss (SNHL) (13–15). Additionally, a dehiscence between the cochlea and the carotid canal, the cochlea and the facial nerve, and between the posterior semicircular canal or the vestibular aqueduct and the jugular bulb/jugular bulb diverticulum have been hypothesized to act as pathological third windows, dissipating acoustic energy away from the cochlear partition (19–22). Third window-like symptoms have also been described in cases of post-traumatic membranous or hypermobile stapes footplate (23).

Etiology

The etiology of SCD is unknown, but two theories have been proposed in the literature: congenital and acquired. The congenital theory of SCD proposes that failure of fetal and postnatal bone development of the temporal bone predisposes to and causes SCD. Proponents of the congenital theory cite temporal bone histopathology studies that show thinning or dehiscence over the superior canal without evidence of bony remodeling (24). Additionally, there is a high prevalence of radiologic SCD in infants, although these findings usually resolve in the first decade of life with the final postnatal bone development (24–27). Some patients with SCD have generalized thin bone throughout the lateral skull base, multiple tegmen defects, and develop SCDs bilaterally, which may further support the congenital theory (24, 28, 29). It has been hypothesized that congenital thin bone of the lateral skull base predisposes a patient to develop SCD due to a second event later in life. For example, head trauma could disrupt the seal over the endosteum or membraneous labyrinth created by the dura, thus resulting in symptomatic SCDS (4, 24, 28, 29). Concomitant tegmen defects are important to recognize as they may alter the findings of audiometric and vestibular testing (**Figure 2**).

There have been reports of a high prevalence of SCD in patients with a variant of Usher syndrome and overrepresentation of SCD in some families, suggesting that there may be genetic correlates that have not been completely identified (4, 30–32).

The acquired theory of SCD proposes that increased intracranial hypertension and repeated pulsations could degrade the bone overlying the SSC over time. Of note, however, a clear association between intracranial hypertension and SCDS has not been established (33–37). Furthermore, there is not a tendency of obesity among patients who undergo SCD repair (33). Causes of acquired SCD also include: neoplasms such as meningioma (38), vascular malformations (39), chronic osteomyelitis (40),

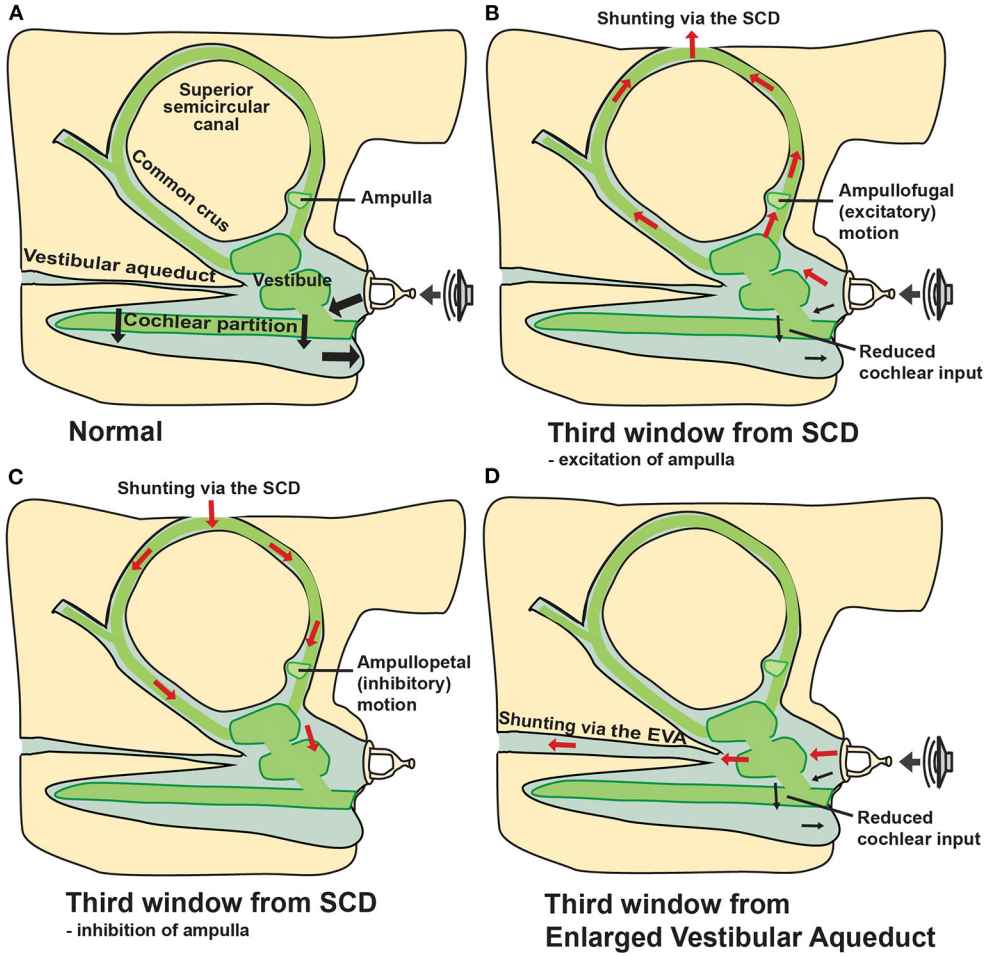

FIGURE 1 | "Third window" mechanism due to SCD and enlarged vestibular aqueduct. Schematic representations illustrate inner ear volume velocity with arrows. **(A)** Normal anatomy allows volume velocity across the cochlear partition from the oval to the round window (two windows). **(B)** Air conducted sound stimulation results in volume velocity from the stapes to be shunted toward the SCD (third window) and away from the cochlea, resulting in increased air-conduction thresholds at low frequencies and/or sound-induced vertigo (Tullio's phenomenon). Positive static pressure in the middle-ear cavity may result in ampullofugal fluid motion exciting the ampulla, resulting in nystagmus (Hennebert sign) and oscillopsia/vertigo (1, 2, 8–12). **(C)** Elevated intracranial pressure from Valsalva against closed glottis (e.g., straining, heaving lifting) may result in ampullopetal endolymphatic fluid motion, inhibition of the ampulla, also leading to nystagmus (Hennebert sign) and oscillopsia/vertigo (1, 8, 11). **(D)** Enlarged vestibular aqueduct (EVA) can also act as a third window, shunting volume velocity away from the cochlear partition and toward the widened vestibular aqueduct (2, 13–15). *Modified from Cheng et al. (16) and Rosowski et al. (8).

fibrous dysplasia (41), and head trauma with temporal bone fractures (42).

DIAGNOSTIC ADVANCEMENTS AND DILEMMAS IN SCDS

Diagnosing SCDS can be challenging as symptoms vary greatly and may mimic other otologic and neurotologic conditions. The most common symptoms of SCDS are autophony (>50% of patients), amplification of bodily sounds (e.g., hearing eye movements or footfalls, >50% of patients), sound- or pressure-induced vertigo (>50%), aural fullness (>60%), conductive hearing loss (∼25–60%), and pulsatile tinnitus (∼20–50%) (4, 43–45). Patients also report symptoms of chronic disequilibrium and "brain fog," that may be related to impaired cognition and a diminished ability to integrate multisensory information (46, 47). The mechanism by which SCD produces such a wide range in symptoms among individuals remains poorly understood (9, 43, 48, 49). A detailed history may reveal symptoms concerning for SCDS and objective findings of the biomechanical effect of SCD, i.e., audiometric testing, VEMP testing, and other novel approaches, can help narrow the differential diagnosis. CT findings of a bony dehiscence over the SSC are diagnostic; however, it is important to recognize that not all individuals with radiologic evidence of dehiscence have relevant symptoms and suffer from SCDS (24, 50).

The diagnostic work-up of SCDS at most centers includes pure tone thresholds to air and masked bone conduction, supranormal bone conduction threshold testing, tympanometry,

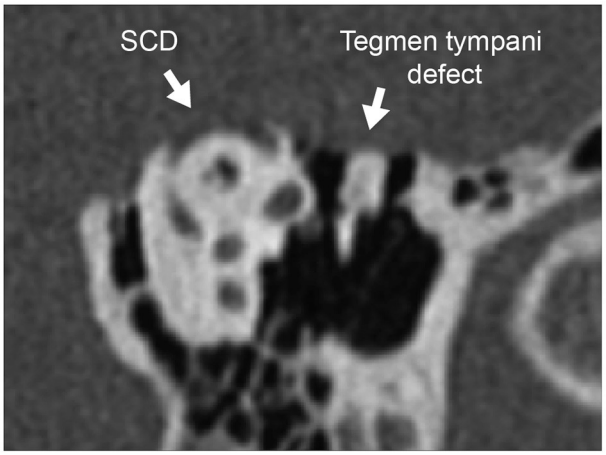

FIGURE 2 | Concomitant tegmen tympani defect with dural herniation. CT of the left ear reformatted to the Pöschl plane demonstrates tegmen tympani bony defect of the skull base and SCD of the arcuate eminence. Herniation of the temporal lobe into the epitympanum can reduce ossicular motion, contributing additionally to the air-bone gap due to SCD and elevating cVEMP threshold (thus masking the lowered cVEMP threshold effect of SCD).

acoustic reflex testing, cervical, and/or ocular VEMP testing, and CT imaging. In this section, we will (1) discuss the advantages and disadvantages of each of these established testing modalities to narrow the differential diagnosis, and (2) review emerging modalities including wideband acoustic immittance and electrocochleography for evaluating patients with third-window symptoms.

Audiometric Testing

In the office, bone conduction testing with a 512 Hz tuning fork often lateralizes to the affected (or worse) ear, further supporting the theory that SCD generates a pseudo-conductive hearing loss. Some patients even have the ability to hear (rather than feel) the tuning fork when placed on the malleolus of the ankle ("ankle Weber") (51). In patients with SCD, pure tone audiometry will often reveal a low frequency ($\leq$1 kHz) ABG, usually in the 15–30 dB range but ABG up to 50 dB has been reported (43, 48, 50, 52, 53). ABG has shown to increase with decreasing frequency, and larger ABG is associated with larger SCD size (9, 12, 48, 54). Furthermore, some SCD patients will have supranormal low frequency (<1 kHz) bone conduction thresholds at −5 to −10 dB HL (8, 11, 18, 50, 53). Low-frequency ABG due to SCD are caused by the combined effects of two separate mechanisms verified by consistency of clinical, temporal bone, and computational modeling data. The low-frequency decrease in air conduction hearing (higher air conduction thresholds) is due to volume velocity shunting via the SCD (**Figure 1B**) (9, 10). The low-frequency increase in bone conduction hearing (lower bone conduction thresholds) is due to altered inner-ear volume velocities and pressures in response to vibration of the skull and altered mass of the inner ear fluid as determined recently in Guan et al. (11, 18).

The presence of low-frequency conductive hearing loss and other SCDS-related symptoms such as autophony and aural fullness are also seen in patients with otosclerosis, Eustachian tube dysfunction, patulous Eustachian tube, and other middle ear pathologies (43). Acoustic reflex testing and tympanometry are essential to rule out middle-ear pathology or Eustachian tube dysfunction (50, 55). Of note, SCD effects on audiometric, immittance, and VEMP testing may be masked by concomitant middle ear abnormalities or tegmen tympani defects with dural herniation into the middle ear because these conditions affect sound transmission (**Figure 2**). For example, the dura encroaching into the middle-ear cavity can reduce ossicular motion, thereby increasing the ABG, elevating VEMP thresholds, and decreasing VEMP amplitude. This would obscure SCD-related findings (**Figure 2**). During impedance measurements such as 226 Hz tympanometry, pulse-synchronous waves have been observed in some SCD patients (56–58).

Vestibular Evoked Myogenic Potential (VEMP) Testing

VEMP testing assesses the function of the otolith organs of the vestibular periphery by measuring surface electromyography responses to acoustic stimulation. In cVEMP testing, the saccule is stimulated leading to an inhibitory response in the ipsilateral sternocleidomastoid muscle modulated by the inferior vestibular nerve. In oVEMP testing, the utricle is stimulated leading to activation of the contralateral eye muscles. The use of VEMP testing has increased to assess patients with a suspected third window, and many, but not all patients with SCDS, have lowered VEMP thresholds and increased VEMP amplitudes in response to an air-conduction stimulus (depending on selected cutoff values and study populations, cVEMP and oVEMP have a sensitivity and specificity above 70%) (59, 60). A number of studies have demonstrated that the diagnostic utility of cVEMP thresholds and oVEMP amplitudes is better than the diagnostic utility of cVEMP amplitudes and oVEMP thresholds, when using a 500 Hz tone burst or a click stimuli (59, 61–63). However, one challenge is the considerable overlap in VEMP threshold and amplitude between patients with SCDS and healthy, normal ears or asymptomatic ears with radiologic SCD (64).

In an effort to improve the diagnostic accuracy of cVEMP testing, Noij et al. (65) proposed a new diagnostic "third window indicator" (TWI) that combines magnitude of the ABG and cVEMP threshold (**Figure 3**). The TWI is defined as the absolute difference of the ABG threshold at 250 Hz and the cVEMP threshold at 500 Hz. The authors found that the TWI detected patients with SCDS with greater accuracy compared to ABG and cVEMP thresholds alone (65). Another initiative to improve the diagnostic accuracy of cVEMP was the use 2,000 Hz stimulus instead of the commonly used 500 Hz tone burst. By using a 2,000 Hz tone burst, the authors of the TWI were able to increase the sensitivity and specificity (sensitivity of 92% and specificity of 100% using TWI at 2 kHz vs. 88 and 100% using TWI at 500 Hz), and they furthermore showed that cVEMP amplitude (as a normalized peak-to-peak amplitude) generated superior results (60, 66). High frequency stimuli in oVEMP testing has

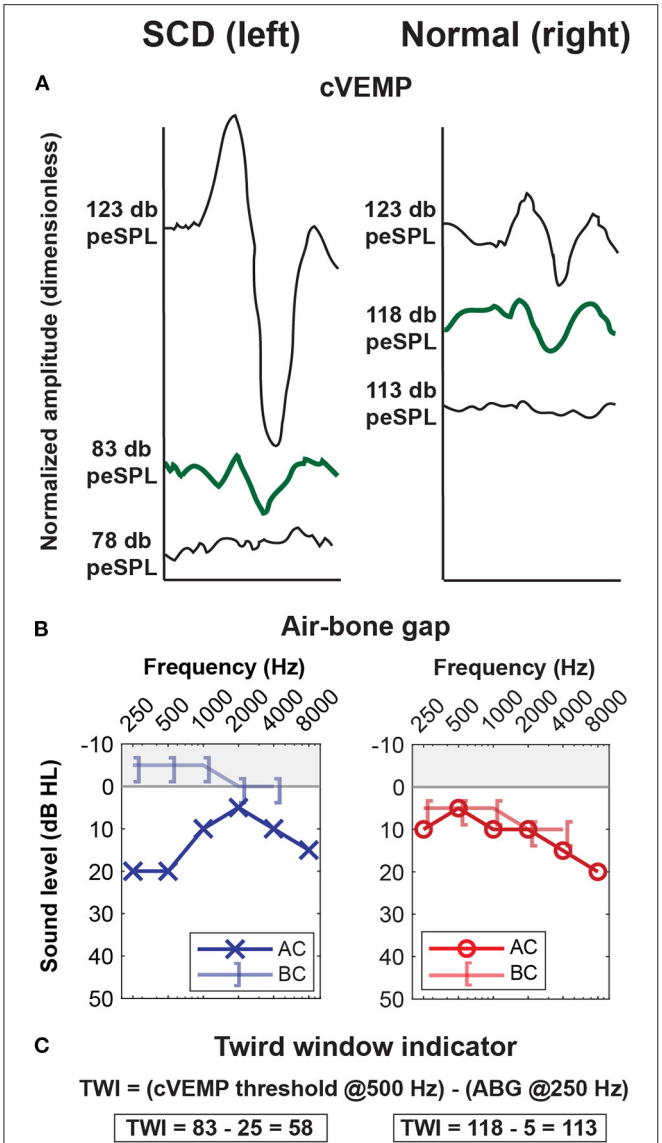

FIGURE 3 | Third Window Indicator (TWI) improves ability to differentiate SCD ears from non-third window ears. Example of an adult patient with symptoms of left-sided SCDS. **(A)** Low threshold cVEMP of 83 dB peSPL [peak sound pressure level, 123 dB peSPL is equivalent to 90 dB HL (65)] at 500 Hz in the left SCDS ear and 118 peSPL in the unaffected right ear. **(B)** Air-bone gap of 25 dB HL at 250 Hz in the left SCDS ear, compared to 5 dB HL in the unaffected right ear. **(C)** The TWI is the difference between the cVEMP threshold at 500 Hz and the air-bone gap at 250 Hz (65). In this case, the TWI is **58** dB for the left SCDS ear, and **113** dB for the unaffected right ear. *Modified from Noij et al. (65).

also shown to be effective in differentiating patients with SCDS from normal controls (one study found sensitivity of 83% and specificity of 93% using 4,000 Hz oVEMP responses vs. 62 and 73% using 500 Hz responses) (67, 68).

Bone-conducted VEMP testing is an alternative approach in cases of concurrent middle ear pathology. oVEMP achieves a higher sensitivity and specificity for both amplitude and threshold testing than cVEMP when a bone-conducted stimulus is used (sensitivity and specificity above 80%) (69).

Despite these diagnostic advancements, there are limitations to the clinical utility of VEMP testing in the evaluation of a patient with suspected SCD. First, VEMP responses assume normal sound transmission through the middle ear, inner ear, otolith organs, and vestibular nerves. Patients with vestibular hypofunction may not demonstrate lowered thresholds or increased amplitudes on VEMP testing of the affected side (70–72), and thus the test may not be used with a high degree of accuracy in this patient population. As vestibular deficits have been observed in some patients following surgical repair of SCD, VEMP testing after surgery can be difficult to interpret. For example, evaluation of patients for revision surgery can be difficult because the thresholds can be elevated for various reasons. VEMP responses are dependent on normal sound transmission to the oval window, which may not be the case if there is middle ear pathology, obscuring the SCD-related changes (**Figures 2**, **4**). Second, VEMP responses decrease with age, although the SCD effect seems to dominate the age effect (60), and conversely, stronger sternocleidomastoid muscle contraction is correlated with larger cVEMP amplitude (60). Third, there is no known association between cVEMP thresholds and severity of auditory or vestibular symptoms (40). Finally, due to lack of standardization in measurement conditions, comparisons of VEMP data across institutions remains challenging and no standard cutoff values for threshold and amplitude exist (60, 70, 77).

Vestibular Testing

Vestibular function testing, including calorics and vestibular ocular reflexes (VOR) (e.g., video or magnetic scleral search coil head impulse or rotary chair testing), may help exclude other vestibular diagnoses with SCD-mimicking symptoms or global vestibular hypofunction, and provides baseline data for the contralateral ear. For example, patients with contralateral vestibular hypofunction (based on calorics and VEMPs) are at risk for prolonged recovery following surgical repair (78). Vestibular testing is critical in the evaluation of patients for revision SCD surgery. For example, caloric testing will assay the residual function of the *superior* vestibular nerve (cVEMPs measure *inferior* vestibular nerve function) in the operated ear and provides baseline data on the function of the contralateral ear. In patients with bilateral SCD, evaluation of residual vestibular function of the operated ear is useful prior to consideration for surgery in the second ear (79).

A vertical torsional nystagmus (in the plane of the SSC) elicited by sound and/or pressure stimuli (e.g., using pneumatic otoscopy or tragal pressure) can be examined using Frenzel lenses, magnetic scleral search coil, or video nystagmography (1, 78, 80). Indeed not all patients have sound- and pressure-induced vertigo or nystagmus, and even in patients with subjective vertigo to sound and pressure stimuli, a nystagmus may not be detected (of note, there is limited literature on the prevalence of this finding in SCDS patients) (1, 78, 80).

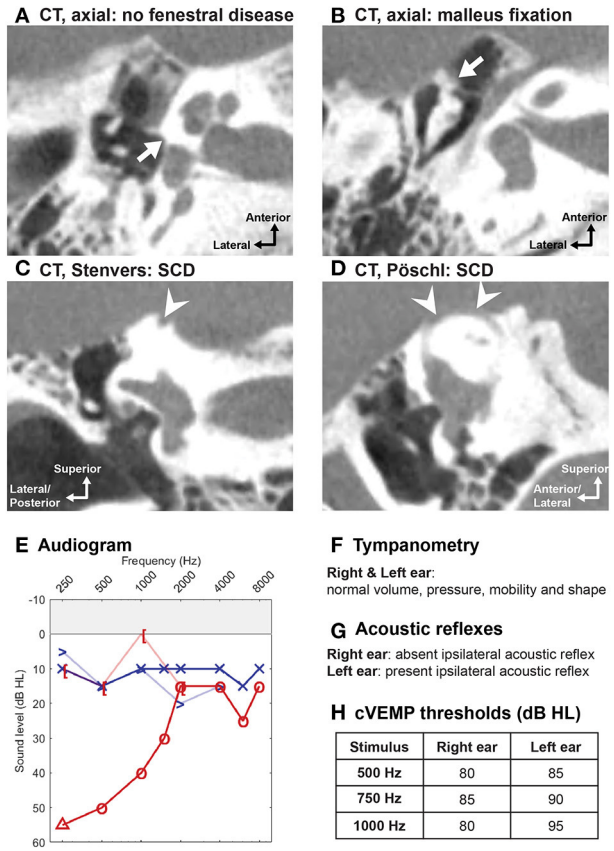

Stimulus	Right ear	Left ear
500 Hz	80	85
750 Hz	85	90
1000 Hz	80	95

FIGURE 4 | Concomitant SCD and malleus fixation. A 57-year-old woman presented with the sole complaint of hearing loss in the right ear. High-resolution CT scans in right ear: **(A)** absence of fenestral disease [though otosclerosis cannot be excluded or diagnosed on radiologic findings alone (73, 74)] and **(B)** malleus fixation to the anterior epitympanic wall; both **(C)** in the plane of Stenvers and **(D)** in the plane of Pöschl showed SCD at the arcuate eminence. **(E)** Large low-frequency air-bone gap on the right. **(F)** Normal tympanometry bilaterally. **(G)** Absent acoustic reflexes in right ear. **(H)** cVEMP thesholds within normal range (80–85 dB HL) in the right pathological ear, which may reflect a combination of lowered cVEMP thresholds from the SCD and elevated cVEMP thresholds from malleus fixation (64). However, when using the third window indicator and 2,000 Hz stimulus, cVEMP responses were consistent with SCD [Of note, in cases of extensive ossicular chain fixation, cVEMP will be absent (64, 75)]. Given concerns of possible *"unmasking"* of SCD symptoms following ossiculoplasty, conservative management with a hearing aid was recommended for this patient (76).

In some patients with a large dehiscence, the VOR response to e.g., head impulse testing may be reduced compared to normal (one study suggested relevance for SCDs ≥5 mm) (80–82). This inverse relationship between SCD size and VOR gain could be explained by "auto-plugging": in ears with a large dehiscence dura may herniate through the dehiscence, compress the membranous labyrinth, and thus impede endolymph flow during head rotation (80–82). In patients who experience sound- and/or pressure-induced vertigo this "auto-plugging" may be incomplete or intermittent. This relationship has implications when interpreting VOR in the presence of a large SCD.

Wideband Acoustic Immittance (WAI)

WAI is a non-invasive measure of the mechano-acoustic impedance of the middle and inner ear. While standard tympanometry uses a single frequency acoustic stimulus, WAI measures function across a range of acoustic frequencies. Wideband tympanometry is WAI measured at different static pressures. One of the most commonly computed metric of WAI is *absorbance*, a measure of the power ratio of reflected sound from the eardrum and the forward sound stimulus presented at the ear canal (**Figure 5A**) (85).

SCD, a mechanical pathology, decreases inner ear impedance, resulting in a peak in absorbance around 1 kHz (**Figure 5B**). Thus WAI is a potential screening tool for SCDS (83, 84). Improved diagnostic accuracy has been achieved with WAI by using advanced analytical techniques such as structure-based computational modeling and machine learning algorithms (86). These methods also serve to automate the diagnostic capability of WAI, especially if combined with audiometric and/or other measurements. Limitation of WAI is that it measures the sum of the impedances of the ear, thus is sensitive to biomechanical effects of the middle ear. For example, a hypermobile tympanic membrane or the presence of ossicular fixation will affect the WAI.

Because SCD is a mechanical pathology affecting the acoustics of the inner ear, WAI may serve an important role in the evaluation of patients with residual signs and symptoms following primary SCD repair. Following surgical repair of SCD where the dehiscence is successfully sealed, the SCD-related changes in WAI will disappear (86). Unlike VEMP measurements that require a functional inferior vestibular nerve pathway, WAI is a mechanical measure of inner ear impendance and may be useful in the assessment of a revision SCD candidate who may have vestibular dysfunction following primary repair.

To date, only few institutions use WAI for diagnosing etiologies of conductive hearing loss. One barrier to widespread use of WAI is due to the complexity of data interpretation. As additional tools are developed to analyze the data and automate diagnoses, WAI may become more widely used.

Electrocochleography (ECochG)

ECochG measures the electric potentials of the cochlea and the cochlear nerve in response to sound stimulation. The electrode is placed either on the surface of the tympanic membrane or in the middle-ear cavity on the promontory of the cochlea or near the round window during a transcanal approach. Various electrical phenomena have been observed: summating potential (SP) reflects direct current (DC), cochlear microphonic reflects the alternating current (AC), while action potential (AP) waveform reflects auditory nerve activity. Historically, ECochG was used to evaluate patients with suspected Menières disease. When SCD is present, the relative static pressure of perilymph in scala vestibuli and scala tympani is reduced compared to static pressures in the endolymph of scala media, thus mimicking the conditions of endolymphatic hydrops (87). These hydrostatic changes of the inner ear are thought to lead to similar ECochG measurements of elevated SP amplitude and SP to AP amplitude ratio (87, 88).

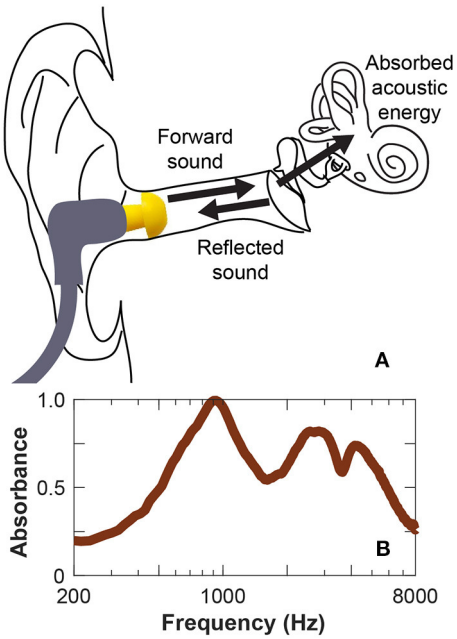

FIGURE 5 | Wideband acoustic immittance testing. Wideband acoustic immittance is a non-invasive measurement that can quantify the acoustic influence of a third window on the impedance of the ear. **(A)** *Absorbance*, or absorbed acoustic energy is measured by presenting acoustic stimulus to the ear canal and measuring reflected sound. **(B)** SCD increases absorbance where a characteristic peak in absorbance around 1 kHz is observed (83, 84).

A number of studies have shown that SP/AP amplitude ratio in most cases can be used to differentiate between SCDS ears and normal or unaffected ears (sensitivity and specificity > 70%) (87, 88). The elevated SP/AP amplitude ratio reverses following surgical plugging of the affected canal (three studies, total of 18 patients with elevated SP/AP ratio preoperatively, 17/18 patients with normalized SP/AP postoperatively, 1/18 with SNHL following surgery, four patients potentially contributed to two studies) (87–89).

ECochG has been used intraoperatively to 1) monitor hearing during SCD repair and 2) confirm canal occlusion. An immediate reduction in the SP/AP amplitude ratio is seen when the canal is occluded (statistically significant, total of 42 ears) (87, 90). While it appears that ECochG may provide intraoperative feedback following canal occlusion, intraoperative ECochG monitoring has not yet been correlated with postoperative symptom resolution or hearing preservation (90).

Imaging—CT Classification of SCD

The gold standard for the radiologic diagnosis of SCD is high-resolution CT. Our group has proposed a CT classification scheme to standardize the description of the dehiscence along the SSC and aid in surgical planning (**Figure 6**) (91). The approach for SCD repair is influenced by the location of the bony defect and its relationship to surrounding tegmen topography. In an analysis of 316 ears with SCDS, the most common location for SCD (on CT) was the arcuate eminence (59%), followed by medial descending limb (29%), lateral ascending limb (8%), and descending limb associated with the superior petrosal sinus (4%). In rare cases, bony defects at two separate locations are observed (<1%) (91).

Imaging—Improving CT Diagnosis of SCD

Due to the effect of volume averaging, routine temporal bone imaging may falsely detect a dehiscence, particularly when the bone overlying the canal is thin (92–94). Several methods have been developed to detect thin bone and dehiscence accurately: (1) decreasing the collimation thickness from 1 to 0.5 mm; (2) reformatting the images from the coronal and axial planes to the plane of the superior canal (Pöschl) and orthogonal to it (Stenvers); (3) assessing density of pixels along the roof of the superior canal to account for volume averaging; and (4) utilizing gray-scale inversion (invert function) to improve visualization and contrast of subtle changes (95–98). It has also been suggested to set a criterion of bony dehiscence in at least two consecutive CT slices (91).

Improvements in imaging modalities have increased the accuracy of detecting a bony defect of the superior canal. Multislice CT (MSCT) scans are commonly used to evaluate patients with a suspected third window but newer approaches using flat panel detector (cone-beam) CT (FPCT) are more accurate (linear correlation for FPCT estimates of SCD length and surgical measurement, $R^2 = 0.93$; linear correlation for MSCT estimate and surgical measurement, $R^2 = 0.28$ with MSCT tending to overestimate SCD length) (99). However, a radiologic dehiscence may be an incidental finding without clinically relevant symptoms. It is hypothesized that in these patients, the dura creates a tight seal above the canal, which protects from the acoustic impedance changes caused by the dehiscence (24). Radiologic canal dehiscence in the absence of symptomatic SCDS does not warrant surgical intervention (4, 78). SCDS must be diagnosed based on localizing signs and symptoms and objective testing, i.e., audiometric and VEMP testing (44, 78). Sole evidence of dehiscence on imaging is insufficient to make a diagnosis of SCDS or surgical intervention.

Role of MRI in the Initial Evaluation of Patients With SCD

Magnetic resonance imaging (MRI) is used increasingly in the preoperative assessment of patients with SCDS and provides complimentary imaging data to CT. Used as a sole modality in the assessment of a suspected third window, high-resolution T2-weighted temporal bone MRI (CISS, FIESTA, etc.) can *exclude* the presence of SCD (and avoid the need for CT in some cases) but it may also falsely detect canal dehiscence in ears with thin bone overlying the canal as seen on CT (e.g., in two studies, 20–39% of ears with SCD seen on MRI had bony covering of the SSC on CT) (100, 101). MRI is important to rule out associated intracranial pathology that may influence surgical decision making. For example, MRI can exclude the presence of a temporal encephalocele, vestibular schwannoma, vascular malformation, or a lateral skull base meningioma (a rare cause of SCD) (**Figure 7**) (38, 40).

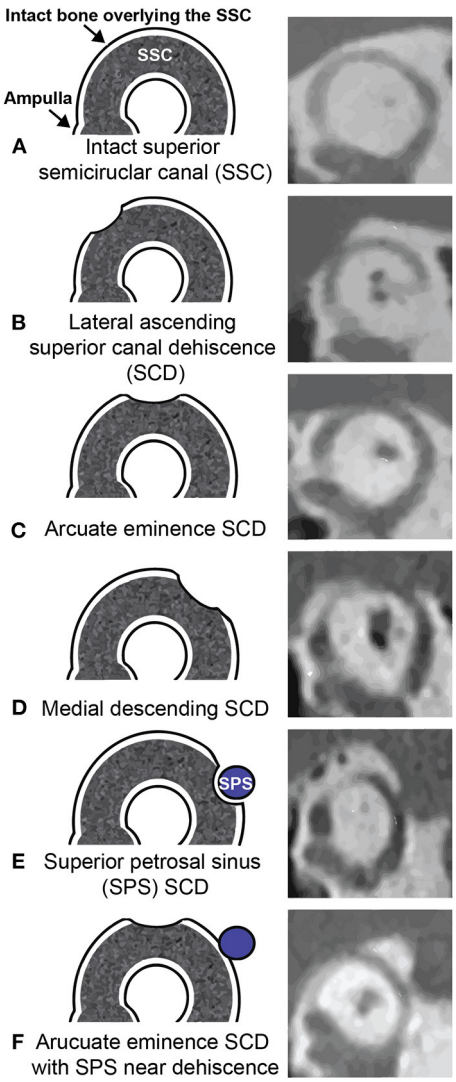

FIGURE 6 | Massachusetts Eye and Ear CT classification of SCD. **Left column (A–F)** illustrates the location of superior semicircular canal defect corresponding to the **right column (A-F)** CT images in the Pöschl plane. SCD size and location are important parameters to consider for surgical planning. *Adapted with permission from Wolters Kluwer Health, Inc.: Lookabaugh et al. (91).

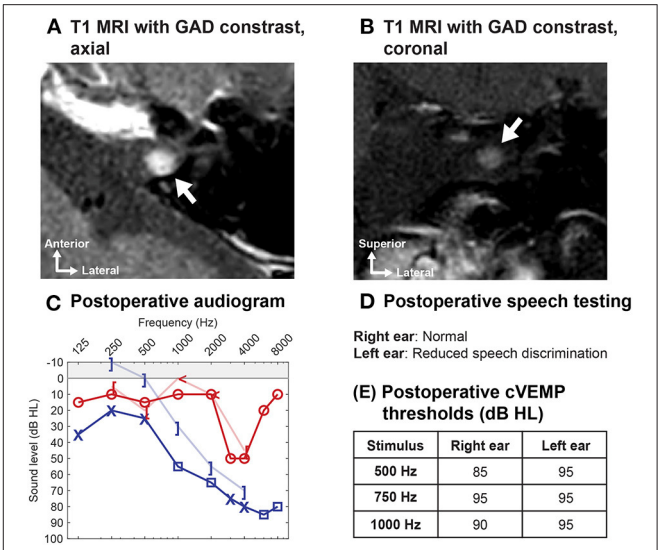

Stimulus	Right ear	Left ear
500 Hz	85	95
750 Hz	95	95
1000 Hz	90	95

FIGURE 7 | Utility of MRI in preoperative evaluation of SCD. A patient who underwent transmastoid SCD repair for symptomatic left ear SCDS reported progressive hearing loss several months after surgery. **(A,B)** Postoperative high-resolution temporal bone MRI with gadolinium (GAD) contrast revealed a focal enhancing lesion of the left internal auditory canal, consistent with a possible superior vestibular nerve schwannoma (arrow). **(C,D)** Audiogram 1 year after SCD repair shows left-sided mixed hearing loss with poor speech discrimination score (progression compared to preoperatively). **(E)** The cVEMP thresholds show preservation of function in the operated left ear. As this small tumor involved the superior vestibular nerve, cVEMP thresholds (driven by the inferior vestibular nerve) would be preserved (or elevated due to SCD surgery). SCD surgery would *not* have been offered if the diagnosis of schwannoma was made preoperatively in either ear, underscoring the importance of a contrast-enhanced high-resolution temporal bone MRI in the workup of SCD. In rare cases, a lateral skull base tumor (e.g., meningioma) found on MRI has been associated with erosion into the superior semicircular canal and SCD symptoms (38).

Utility of Temporal Bone MRI in Patients Who Are Candidates for Revision SCD Repair

MRI is a valuable diagnostic modality in the evaluation of patients considering revision surgery for SCDS. Postoperative CT provides little information on the extent of the SCD repair because most materials used to repair SCD (e.g., bone wax, fascia, cartilage) are not radio-opaque (except when bone chips or bone cement are used to plug or resurface/cap the canal). However, high-resolution T2-weighted MRI formatted to the plane of Pöschl can be used to evaluate the extent of surgical occlusion and identify any residual defects by assessing the fluid void (lack of fluid flow) within the SSC (a proxy for extent of SCD plugging) (**Figure 8**) (102–104). By using both MRI and CT, the fluid void on Pöschl MRI views can be compared to the location and length of the bony dehiscence seen on Pöschl CT to determine if revision surgery may be indicated (by using this method, a residual defect was found in ∼6/9 patients with symptom recurrence vs. 1/4 patients with complete symptom resolution following SCD occlusion repair) (102).

The posterior-medial (descending) limb of the SSC is the most common region with residual defects following middle fossa craniotomy (5/9 ears with residual defect in posterior-medial limb vs. 3/9 ears with residual defect in anterior-lateral limb) (102). If the Pöschl MRI demonstrates a fluid void that does not fully encompass the bony defect on Pöschl CT (consistent with insufficient occlusion and persistent defect), a transmastoid approach to occlude the remaining limb may be indicated (102, 103). One should be aware that aggressive repair with autologous or non-autologous repair materials at the antero-lateral (ascending) limb toward the ampullated end of the SSC could injure the neuroepithelium of the ampulla (102).

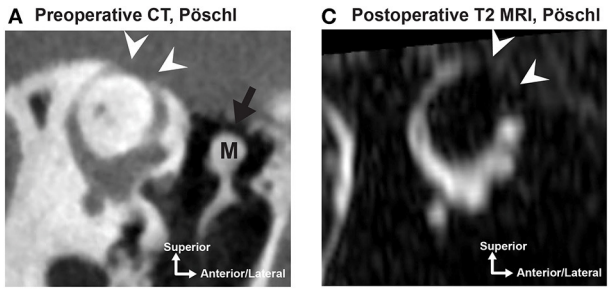

B Preoperative cVEMP thresholds (dB HL)

Stimulus	Right ear	Left ear
500 Hz	75	65
750 Hz	80	65
1000 Hz	90	65

D Postoperative cVEMP thresholds (dB HL)

Stimulus	Right ear	Left ear
500 Hz	80	75
750 Hz	85	85
1000 Hz	85	85

FIGURE 8 | MRI can assess the extent of repair following SCD surgery. **(A)** Preoperative high-resolution CT in the Pöschl plane in a 56-year old male patient with left-sided SCDS. Arcuate eminence defect (white arrowheads). Tegmen tympani dehiscence (black arrow) without dural contact to the malleus (M). **(B)** Preoperative cVEMP thresholds of the left ear at 500, 750, and 1,000 Hz were *lower* (mean: 65 dB HL) than the asymptomatic right ear (mean: 82 dB HL). **(C)** Postoperative T2-weighted MRI in the Pöschl plane illustrates a *fluid void* (no fluid signal) extending beyond the original SCD region seen on preoperative CT, confirming occlusion of the SCD following uneventful surgery with middle cranial fossa approach. **(D)** Postoperative cVEMP thresholds show *elevation* (normalization) in the operated ear (mean: 82 dB HL). Patient also had resolution of primary complaint.

SURGICAL MANAGEMENT: CONSIDERATIONS AND CONTROVERSIES

As there are no known effective medical therapies for SCDS, surgery remains a reasonable treatment option for patients with intractable vestibular and/or auditory symptoms that localize to the side of the radiologic SCD. The goal of surgery is to reduce or eliminate the third mobile window phenomenon. Durable and effective SCD repair must create a watertight seal at the dehiscence site. This is most commonly achieved by occluding the SCD by direct exposure and repair via middle fossa craniotomy (MFC) (**Figures 9A,B**) or directly or indirectly using a transmastoid approach (**Figure 9C**). A resurfacing or capping technique can be used as well from either surgical corridor (**Figure 9D**) but is associated with a higher failure rate (44, 50, 105, 106). However, there remains a relative lack of consensus in the literature about the optimal surgical technique (106, 107).

Surgical Outcomes

Resolution of the chief complaint (either vestibular or auditory) is observed in most patients who undergo SCD repair (33/33 patients) (45). However, mechanically-induced symptoms such as low-frequency conductive hearing loss, autophony, pulsatile tinnitus, and sound- and pressure-induced vertigo appear to resolve more readily compared to symptoms of headaches, chronic disequilibrium, and brain fog (5, 45, 108–111) (i.e., three studies with a total of 124 patients reported postoperative resolution of symptoms of autophony, pulsatile tinnitus and sound- and pressure-induced vertigo in the range of 73–100%, compared to 63–95% for general disequilibrium and aural fullness) (45, 109, 110).

The reported risk of major complications following SCD surgery is low (107, 110, 112, 113). The most common complications include SNHL [profound SNHL ∼2.5%;(112) mild SNHL ∼25%(114)] and balance dysfunction [studies report that 39–80% of patients have balance dysfunction in the first postoperative week with resolution in more than half (115, 116), and that transient room-spinning vertigo due to benign paroxysmal positional vertigo (BPPV) is seen in 4.5–24%(107, 110, 112, 113, 117)]. Rare complications include facial nerve paralysis (reported following MFC), epidural hematoma (reported following MFC), dural tear (reported following both approaches) and surgical site infection (reported following both), and overall the rare complication rate is <1.5% (45, 107, 109, 112).

Postoperative audiometric, VEMP, and vestibular testing are routine measures to assess auditory and vestibular function following surgery. Reversal of SCD effects on audiometric and VEMP testing are observed: (1) Closure of the ABG (mean preoperative low-frequency ABG of 16 dB vs. 8 dB postoperatively, 43 ears) (114); (2) normalization of supranormal bone conduction thresholds (median preoperative thresholds of −5 dB HL vs. +5 dB HL postoperatively, 43 ears) (114); and (3) normalization of cVEMP thresholds and oVEMP amplitudes (significant among 12 subjects) (118) have been associated with successful symptom resolution. Several validated questionnaires have been used to quantify pre- and postoperative SCD signs and symptoms, including the Autophony Index (119), Dizziness Handicap Inventory (DHI) (120), Hearing Handicap Inventory (HHI) (121, 122), and Tinnitus Handicap Inventory (123). As mentioned previously, high-resolution T2-weighted MRI (with Pöschl reformats) is useful to evaluate the extent of canal occlusion following surgery and identify any residual defects that can be associated with residual symptoms (102–104). **Figure 8** highlights the correlation of radiologic confirmation of SCD repair with reversal of diagnostic indicators in a patient with durable symptom control after surgery.

Risk of Postoperative Sensorineural Hearing Loss

Transient SNHL postoperatively has been reported (113, 114, 124) and can accompany labyrinthine hypofunction (114, 124). One study (43 patients) reported that about 50% of surgical SCD patients had at least a mild SNHL measured at 7–10 days after surgery. Bone conduction thresholds tend to increase: at low frequencies bone conduction thresholds normalize from supranormal or low thresholds, and at higher frequencies thresholds may increase above normal range (114). About 25 % of patients treated with systemic steroids for 10–14 days continue to have some SNHL (>1 month) (114).

Persistent mild SNHL following primary surgical repair of dehiscence is not uncommon and typically manifests as a high frequency loss (78, 107, 114, 125) i.e., two studies

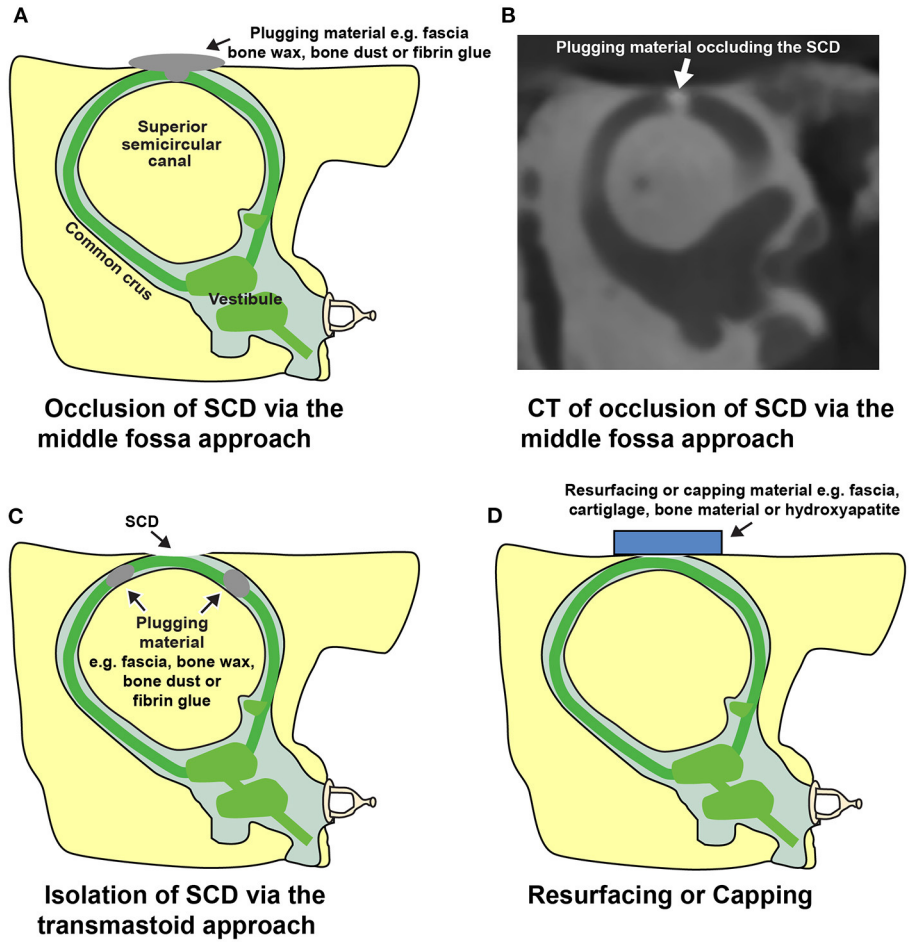

FIGURE 9 | Illustrations depicting surgical repairs of SCD. **(A)** Plugging or occlusion of an arcuate eminence defect via middle fossa craniotomy approach. **(B)** CT image in the Pöschl view following repair. Occlusion was performed in a cadaveric temporal bone model of SCD using contrast-infused surgical bone wax. **(C)** Transmastoid approach for repair of SCD. A labyrinthotomy is created in the ascending and descending limbs of the superior semicircular canal and plugged to isolate the SCD. **(D)** Resurfacing or capping an arcuate eminence defect. This approach attempts to create a seal without occluding the superior semicircular canal lumen. *Modified from Cheng et al. (16).

(43+34 patients) reported a mean 10 dB elevation of air conduction thresholds at 4–8 kHz (significant), which did not affect speech discrimination, and mild SNHL in ∼25% (114, 125). Postoperative moderate to profound SNHL is rare (44, 112, 114), likely around 2.5% (6/242 patients) (112), and can present in a delayed fashion (e.g., 1 week postoperatively) (44, 126). Some reports have indicated an increased risk of SNHL with multiple inner ear surgeries (i.e., revision SCD surgery or SCD surgery following stapedotomy) (103, 112, 114, 127). The largest study reported profound SNHL in 2.3% (5/220 patients) of primary repair cases and in 4.5% of revision repairs (112), while another study showed (though not significant) larger decrease in speech discrimination and pure tone average thresholds among revision cases (21 patients) than primary repairs (27 patients) (103). In summary, in the majority of patients undergoing primary repair, hearing thresholds remain stable or are minimally affected, and word recognition scores are unchanged (110, 113, 114, 127, 128).

Some centers perform intraoperative ECochG and auditory brainstem responses (ABR). However, neither ECochG SP/AP amplitude nor ABR latency appear to successfully predict postoperative hearing outcome (90). Conversely, intraoperative ECochG monitoring in which an instantaneous SP/AP amplitude reduction is achieved upon repair of the dehiscence may provide an objective measurement of successful repair (87, 90).

Cochlear implantation in the presence of SCD does not appear to unmask or worsen SCD symptoms. However, patients with radiologic dehiscence or SCDS had worse speech perception than patients without canal dehiscence (129).

Risk of Dizziness and Balance Impairment After SCD Repair

Vestibular impairment in the acute postoperative setting is commonly reported (39–80% of patients) (115, 116). The

mechanism of this phenomenon and of transient SNHL is unknown. It is hypothesized to be related to the surgical trauma. Potential mechanisms include: (1) labyrinthitis, (2) loss of perilymph disturbing labyrinthine function, (3) compression of the membranous labyrinth with displacement of endolymph causing a "hydrops-like" condition, and (4) membranous labyrinth tears allowing ion exchange between the otherwise confined compartments (111, 115, 116, 130, 131). Additionally, a reduction of SSC function from occlusion repair may cause acute vestibular impairment. In most cases, vestibular impairment resolves or the patient is able to compensate for loss of function within several months [one study found resolution in 70%(116)] (78, 115, 116). Patients with ipsilateral vestibular hypofunction and concomitant SNHL may suffer from labyrinthitis, and treatment with steroids and vestibular therapy can be beneficial [one study reported 2/19 patients with global vestibular hypofunction (81), and another reported 3/16 ears with postoperative SNHL and vestibular hypofunction that resolved on a steroid taper (124)]. Vestibular examination within the first postoperative week will likely show spontaneous and/or post-head-shaking nystagmus (90% of patients), and often as an irritative nystagmus indicating increased excitability (70% of patients), alternatively as a paralytic nystagmus indicating hypofunction (only data on patients with repair by occlusion technique) (115). VOR testing following surgical repair by occlusion will most often show reduced function of the SSC (4/4 and 4/7 patients with reduced VOR gain) (130, 131) and may also show decreased function of the ipsilateral posterior and horizontal semicircular canals (116, 130). This is consistent with vestibular impairment in the acute postoperative setting. One study suggested that over time (months), VOR gain for the SSC can normalize to preoperative values (11 patients) (131), whereas other studies show sustained reduction and only partial improvement in SSC function (19, 5 and 10 patients) (81, 130, 132). Reduced SSC function alone can likely not explain cases of prolonged vestibular impairment.

Prolonged vestibular impairment is common among patients with a concomitant migraine diagnosis or with bilateral SCDS (one study found prolonged vestibular impairment in 13/13 migraine patients vs. 8/25 non-migraine patients) (133), likely due to the more generalized vestibular impairment prior to surgery and a reduced ability of central compensation (45, 133). Patients with bilateral SCD repair are also at risk of persistent oscillopsia, suggesting increased risk of chronic oscillopsia in patients with contralateral vestibular hypofunction (2/4 patients) (79). The ipsilateral horizontal and posterior semicircular canal impairment observed in some patients in the acute postoperative setting is often normalized at long term follow-up (months) (81, 116, 130–132), though sustained reduction of posterior semicircular canal function is seen (81, 130). This stresses the importance of vestibular testing prior to second-sided surgery. Prolonged balance dysfunction may also be exacerbated by episodic BPPV, which occurs not infrequently following SCD repair (4.5–24%, two studies with 242 and 84 subjects, respectively) (112, 117).

Middle Fossa Craniotomy (MFC) and Transmastoid Approaches

The original publication on SCDS by Minor et al. described repair by MFC approach (**Figures 9A,B**) (1). They used a "plugging" technique to achieve resolution of symptoms but "resurfacing" and "capping" techniques have also been described. The repair techniques are discussed in greater detail in subsequent sections.

As an alternative to the MFC approach, the SSC may also be accessed either directly or indirectly by transmastoid approach (**Figure 9C**) (109, 113). The selection of surgical approach is often influenced by the anatomy surrounding the defect and the experience of the surgeon. Lookabaugh et al. (91), who proposed a CT classification of SCD (**Figure 6**), suggested that the location of the dehiscence can be used to determine surgical approach (91). For example, an arcuate eminence defect (59% of SCDS) may be safely reached using the MFC approach (**Figure 10A**), and a contracted mastoid or a low-lying tegmen are suited for an MFC. In contrast, a bony dehiscence along the posterior-medial (descending) limb of the superior canal (29% of SCDs), and associated with the superior petrosal sinus (4% of SCDs) are ideally repaired using a transmastoid corridor to avoid direct manipulation of a skull base venous sinus via MFC (**Figure 10B**) (these defects often do not have a low lying tegmen or associated skull base bony defects).

An important advantage of the MFC is that it enables the surgeon to directly visualize the dehiscence and associated tegmen defects, but may carry a slightly increased risk of cerebrospinal fluid (CSF) leak, stroke and other complications related to craniotomy (45, 112, 136, 137). The transmastoid approach is less invasive than the MFC approach and may be performed in the outpatient setting (132, 134).

Skull base endoscopy using a 0 degree or angled Hopkins rod telescope can be a valuable adjunct to traditional line of sight microscopic-assisted (or exoscopic) SCD repair methods when attempting to visualize "hidden" superior canal defects (135, 138–140). In patients where the arcuate eminence defect is associated with a downsloping tegmen, the microscopic view is limited, necessitating a large craniotomy or extensive temporal lobe retraction (135, 139). An endoscope (e.g., angled) can be utilized through a smaller MFC or keyhole craniotomy to provide superior transillumination of the skull base and identification and characterization of the bony dehiscence (135, 138–140). An example of a defect that is located toward the posterior limb of the superior canal along a downsloping tegmen is shown in **Figure 10C**. Endoscopic transillumination of a blue-lined dehiscence case has been described, suggesting that locating the bony defect may be more facile and accurate with the endoscope (135, 139).

Due to high variability among studies, it is currently difficult to determine if a specific surgical approach is associated with better outcomes.

Canal Plugging and Resurfacing/Capping

To restore labyrinthine biomechanics and reverse the third mobile window effects, a tight fluid seal must be created (12, 141). Several groups have reported plugging of the SSC to obtain a

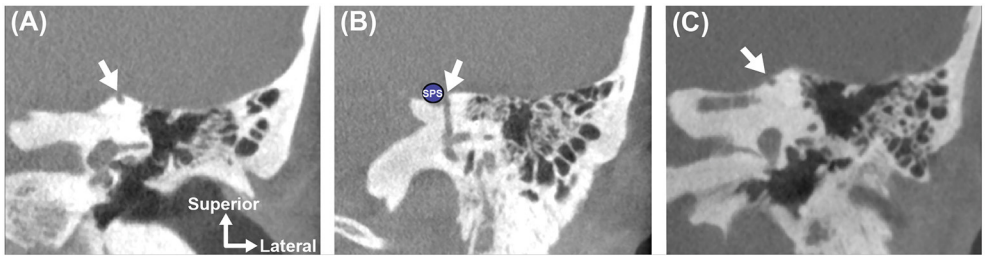

FIGURE 10 | Anatomic location of SCD influences surgical approach and can predict challenging dissection. Coronal high-resolution CT imaging highlights three distinct left ear superior canal defects. **(A)** SCD involving the *arcuate eminence*. This defect is easily accessed and directly visualized via the middle fossa craniotomy approach. **(B)** SCD involving the superior petrosal sinus (SPS). This defect should be repaired using a transmastoid approach with plugging of the ascending and descending limbs of the superior semicircular canal to isolate the defect around the SPS and avoid disrupting the sinus (134). **(C)** SCD involving the *medial* surface of the arcuate eminence along a downsloping tegmen. This defect may be difficult to visualize with a microscopic-assisted middle fossa craniotomy approach unless a large craniotomy and significant brain retraction are performed. To safely identify and repair this type of defect, an endoscopic-assisted middle fossa craniotomy (135) or transmastoid approach may be used.

tight fluid seal (**Figures 9A–C**) and durable symptom control (in general >80% but varying rate of resolution among symptoms, studies including total of 108 patients) (78, 106, 109, 113, 124, 132, 142). Various plugging materials have been used and no material appears to demonstrate clear superiority (78, 106, 109, 113, 124, 132, 142, 143). The most commonly used materials include bone wax (78, 124, 132), bone dust (109, 113), fibrin glue, or fascia (142, 143). Most of these materials are not radiopaque and therefore a postoperative CT scan will not be useful to assess the repair. As described, assessing the fluid void (lack of fluid signal) on T2-weighted MRI scans can help determine the extent of repair (**Figure 8**) (102, 103). Interestingly, an experimental study in human temporal bones showed that an exceedingly small volume of bone wax (3.0–4.0 mm^2) was needed to adequately plug a dehiscence of 1.5–3.5 mm in length via the MFC approach, and that multiple applications of bone wax resulted in extension of wax along the long axis of the superior canal into the ampulla and common crus. Extensive plugging of the defect, as shown in this model, could increase the risk of vestibular complications (141). Another study also suggested that overly-exuberant plugging may involve the common crus and lead to reduced function of both the superior and posterior canal (one reported case) (81).

The theory behind resurfacing techniques involves reinforcing the bone overlying the canal defect (**Figure 9D**). This technique has also been used with successful results (7/11 patients) (44). Resurfacing material varies and includes fascia (44), cartilage (132), bone (44), and hydroxyapatite (144). In theory, resurfacing aims to avoid occlusion of the membranous canal, thus allowing the patient to retain function of the superior canal. While some authors report maintenance of canal function following resurfacing (video head impulse testing showed normal gain in ears with SCD resurfacing repair vs. significantly reduced canal function ears with plugging, 29 ears) (132), others report decreased canal function likely associated with a partial canal plugging (1 reported case) (81), as also illustrated by the case in **Figure 11**. Symptom recurrence is higher with resurfacing: success rate following canal occlusion is reported >80% (studies including total of 108 patients) vs. 50–64% (42 patients) following resurfacing, perhaps due to dislocation or resorption of the graft material (44, 50, 105, 106). One study reported that symptom recurrence occurred in 4/11 patients, who underwent resurfacing, and in none of the nine patients, who underwent plugging procedure (44). Reinforcement of the resurfacing repair with hydroxyapatite, sometimes termed capping, appears to have a higher success rate than resurfacing alone, and can be performed with bone cement alone or in combination with autologous material (106, 145). A literature review comprising 13 studies and case reports found successful symptom resolution in 32/33 patients with canal plugging, 8/16 with resurfacing, and 14/15 with capping (106).

Future methods of SCD repair may include the use of customized 3D-printed prostheses and biological adhesives to preserve the superior canal lumen and canal function and to seal the defect (146). This customized, fixed-length prosthesis was designed to lock into position and occlude the bony defect (146). Refinement of the design and materials is required before translation of this concept into clinical use.

Round Window Reinforcement

Round window reinforcement procedures have been offered by some surgeons in an effort to decrease symptoms of SCDS (147–149). The procedure has historically been used to treat symptoms associated with perilymphatic fistula (148, 149). The round window is commonly accessed by a transcanal tympanotomy approach. Stiffening of the round window is thought to dampen one of the three inner ear windows, restoring the inner ear to a non-physiologic two-window system with the oval window and the dehiscence as the remaining windows (148). In a series of 19 patients, symptom severity of autophony, sound- and pressure-induced vertigo, pulsatile tinnitus, aural fullness, and generalized disequilibrium improved following round window reinforcement with a mean improvement of two points on a seven-point scale (148). However, other reports describe a large variability in patient outcome, with some patients experiencing no resolution of symptoms or only temporary relief of symptoms (149). Furthermore, occlusion of the round window may introduce conductive hearing loss by alteration of the round window

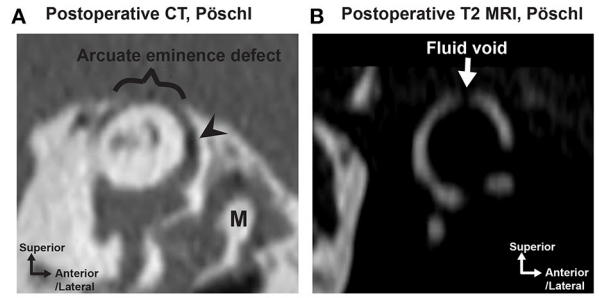

C Postoperative audiogram

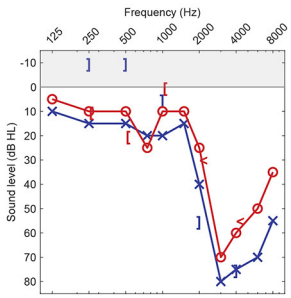

D Postoperative tympanometry

Right & Left ear:
normal volume, pressure, mobility and shape

E Postoperative acoustic reflexes

Right & Left ear:
present ipsilateral acoustic reflexes to 95 dB HL broadband stimulation

F Postoperative cVEMP thresholds (dB HL)

Stimulus	Right ear	Left ear
250 Hz	75	50
500 Hz	70	55
750 Hz	80	55
1000 Hz	80	65

FIGURE 11 | Utility of MRI in the evaluation of patients with persistent or recurrent symptoms following primary SCD repair. A 52-year old male patient underwent middle fossa craniotomy and SCD repair with resurfacing technique at the first institution. He initially experienced symptom resolution after surgery, but symptoms of left-sided aural fullness, pulsatile tinnitus, and sound-induced vertigo recurred 2 weeks later. **(A)** Postoperative (after primary SCD repair) high-resolution CT in the plane of Pöschl shows arcuate eminence defect (bracket) and focal pneumolabyrinth (arrowhead). Malleus indicated with "M." Note that most SCD repair materials are not radio-opaque. **(B)** Postoperative T2-weighted MRI in the plane of Pöschl reveals a focal fluid void (arrow) associated with partial plugging of the superior semicircular canal that does not span the entire length of the defect. **(C–F)** Postoperative (after primary SCD repair) audiometric and vestibular testing. **(C)** Threshold audiogram reveals supranormal bone conduction thresholds (−10 dB at 250 and 500 Hz) of the left ear. **(D)** Normal tympanometry bilaterally. **(E)** Present bilateral acoustic reflexes. **(F)** cVEMP potentials demonstrate low thresholds of 50, 55, 55, and 65 dB HL in response to 250, 500, 750, and 1,000 Hz tone burst stimuli. The patient underwent revision SCD repair at the second institution with plugging of the superior canal using a transmastoid approach with stable symptom improvement 5 years after surgery.

impedance (150, 151). Based on current literature, there is sparse evidence to support round window reinforcement as a viable surgery for mitigation of SCDS-related symptoms. This approach has since fallen out of favor at most centers.

CHALLENGES IN SCDS MANAGEMENT

Patients With Bilateral SCDS

Patients with symptomatic bilateral SCDS must be carefully counseled. The priorities of the clinical treatment team are to: (1) confirm that both ears with SCD are associated with localizing signs and symptoms and supporting findings on audiometric and VEMP testing (44, 78); (2) determine if there is a "worse" ear (44, 78); (3) rule out co-morbid factors such as migraines that can prolong recovery if surgery is offered, as bilateral SCD itself prolongs recovery; (4) discuss that bilateral SCDS is associated with a lower rate of complete symptom resolution (108); and (5) communicate the concerns that bilateral sequential repair could be associated with chronic balance impairment, as patients who undergo surgery bilaterally are at higher risk of vestibular hypofunction (45, 79). Another concern for some patients with bilateral radiologic SCD who undergo surgery for the only side with symptoms of SCDS is, that they may experience "unmasking" of SCD symptoms in the originally asymptomatic contralateral ear (49).

When patients have asymmetric symptoms and the more symptomatic side also demonstrates abnormal findings on audiometric and VEMP testing, selecting the surgical side is straightforward (44, 78). In a study including seven symptomatic patients with bilateral SCDS, cVEMP thresholds were lower in the more symptomatic ear, while thresholds in the contralateral ear were similar to ears without SCD (statistically significant) (125). The physical exam is also useful in these cases, as the Weber often lateralizes to the more severely affected ear in bilateral SCDS. In patients with equivocal symptoms or non-localizing signs and symptoms, the decisions for surgery and surgical side become more challenging.

Patients with bilateral SCDS report less improvement in symptoms following surgical repair compared to patients with unilateral SCDS (complete symptom resolution of primary complaint in patients with unilateral SCDS and repair: ∼48%, bilateral SCDS with unilateral repair: ∼12%, bilateral SCDS with sequential repair: ∼20%) (108). Some studies suggest that poorer outcomes in bilateral SCDS patients may be attributable to a more generalized vestibular impairment prior to surgery and a reduced ability to compensate postoperatively, resulting in increased risk of vestibular dysfunction. One study found prolonged vestibular recovery (>4 months) in 6/11 patients with bilateral SCD and unilateral repair compared to 0/22 patients with unilateral SCD and repair) (45, 133). Also, postoperative dizziness and imbalance, and oscillopsia appear to be more prevalent in patients who undergo second-sided surgery for SCDS (∼3/4 patients) (79). Preoperative vestibular testing in this cohort of patients is therefore critical prior to the first and the second surgery (if candidate for bilateral repair). This testing battery should include assessment of both the inferior and superior vestibular pathways and of semicircular canal function in all planes bilaterally, by VEMP, caloric, and VOR testing.

Patients With Near Dehiscence Syndrome

Patients with very thin bone (sometimes called "near dehiscence") overlying the SSC may exhibit signs and symptoms of SCDS (**Figure 12**) (152). While the pathophysiology underlying this phenomenon is not entirely elucidated, several authors have argued that this variant of SCDS may reflect increased compliance of the thin bone overlying the canal or a pinpoint dehiscence (152). Indeed, pinpoint dehiscence has been found to affect inner ear acoustics in experimental cadaveric studies (12).

Diagnosing patients with near dehiscence can be challenging because the resolution of CT images does not allow one to distinguish pinpoint dehiscence vs. thin bone (as discussed previously under *Imaging—improving CT diagnosis of SCD*) (94). Several studies have shown that symptomatic patients with near

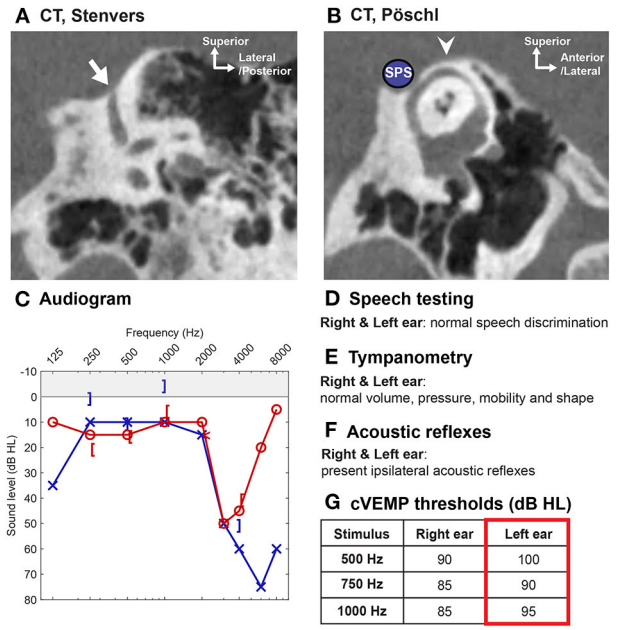

Stimulus	Right ear	Left ear
500 Hz	90	100
750 Hz	85	90
1000 Hz	85	95

FIGURE 12 | "Near dehiscence" of the superior semicircular canal. In this case, a 55-year old male presented with left-sided hearing loss, aural fullness, and vertigo. **(A)** High-resolution CT scan in the Stenvers plane with thin bone overlying the descending limb of the superior semicircular canal (arrow). **(B)** CT scan in the Pöschl view shows an intact arcuate eminence (arrowhead) and thin bone between superior semicircular canal and superior petrosal sinus (SPS, shown by blue circle). **(C–G)** Audiometric and vestibular testing confirm **(C)** a mild left-sided conductive hearing loss (high-frequency dip in thresholds not related to SCD), **(E)** normal tympanometry, **(F)** present acoustic reflex, and **(G)** normal to high cVEMP thresholds.

dehiscence have audiometric and vestibular testing results similar to normal non-dehiscent ears and significantly different from ears with frank dehiscence, suggesting that near dehiscence does not have the same effect on inner ear biomechanics (three studies with a total of 223 SCDS ears, 90 near dehiscence syndrome ears and 83 normal ears; only one study assessed SCDS ears vs. normal ears) (65, 94, 153). By contrast, there are reports of patients with near dehiscence demonstrating supranormal bone conduction thresholds, reduced cVEMP thresholds and increased oVEMP amplitudes, suggesting that these findings may be inconsistent in this patient population (11 and 86 ears) (152, 154). ECochG has also been shown to be produce an increased SP to AP ratio among patients with near dehiscence (153). Altogether, patients with suspected near dehiscence syndrome must be carefully examined to exclude other otologic and neurotologic conditions as the condition can easily be misdiagnosed.

Repair of near dehiscence is accomplished by either reinforcing the thin bone overlying the near dehiscence or creating a small opening in the canal that may be plugged (152). In a study of 10 patients (11 ears) with near dehiscence syndrome who underwent surgical plugging and/or resurfacing, autophony improved or resolved in all cases, pulsatile tinnitus improved or resolved in 8/9 affected ears, and vertigo or disequilibrium induced by sound or pressure improved or resolved in 6/8 patients (152). Two of the 10 patients in this study suffered symptom recurrence and one patient developed unmasking of SCD symptoms in the contralateral ear (152). Of note, surgically opening the near dehiscence does not appear to worsen postoperative vestibular function (115), and complication rates have been found to be similar between surgical management of frank dehiscence and near dehiscence (insignificant difference in complication rate between 34 SCDS ears and 17 near dehiscence syndrome ears for complications including postoperative vestibular hypofunction, BPPV, posterior semicircular canal impairment and facial nerve paresis) (94).

Management of Patients With Concurrent SCDS and Migraine

Patients with concurrent SCDS and migraine present a diagnostic and management challenge. Among patients with SCDS who undergo surgical repair, the prevalence of migraine is estimated to be 34–45% (45, 133). Several studies note that patients with concurrent SCDS and migraine appear to have prolonged recovery after surgery (45, 133). Jung et al. (133) measured the postoperative Dizziness Handicap Inventory (DHI) scores and found that more than 50% of patients with a DHI score >30 suffered from migraine (133).

It is unknown whether a pathophysiological link exists between migraine and SCD. Patients with vestibular migraine and SCDS tend to have overlapping symptoms, and thus it is hypothesized that vestibular migraine may be under-diagnosed among patients with SCDS (108). Patients with symptoms of SCDS such as generalized dizziness, imbalance, headache, and brain fog demonstrate the least degree of improvement following surgery (108). Interestingly, these patients tend to also have vestibular migraine (108).

Management of Patients With Concurrent SCD and Otosclerosis

Patients with concurrent otosclerosis and SCD are rare, but present a diagnostic and management challenge (76, 155–161). In general, patients with concurrent otosclerosis and SCD present with conductive hearing loss, with or without SCD symptoms, absent acoustic reflexes (due to fixation of the stapes) and evidence of radiologic SCD with or without fenestral/antefenestral otosclerosis on CT (73, 74, 76, 155–158, 161). Fixation of an ossicle, stapes or malleus, reduces air-conducted sound transmission through the oval window, minimizing the occurrence of SCD symptomatology (**Figure 4**). Also due to decreased sound transmission, VEMP testing may have limited utility (64). While the SCD will lower VEMP thresholds, the stapes fixation will increase the thresholds, and both low, normal and high cVEMP thresholds have been observed in patients with concurrent otosclerosis and SCD (159, 161).

The largest case series of patients with concurrent otosclerosis and asymptomatic radiologic SCD described eight patients (ten ears), where seven patients (eight ears, one patient with bilateral SCD) underwent stapedotomy because SCD had not been diagnosed prior to the initial stapedotomy (76). Following

stapedotomy, four patients developed unmasking of SCD symptoms. One patient did not experience unmasking of SCD symptoms, and also had near-complete closure of the ABG. Three patients (4 ears) experienced partial closure of ABG, one experienced no change and two patients had worse hearing outcome with enlarged ABG following stapedotomy (both also unmasked SCD symptoms).

For patients with concurrent SCD and otosclerosis, preoperative counseling is challenging, as undoubtedly stapedotomy carries a risk of unmasking of SCD symptoms. However, it is important to note that the true incidence of concurrent otosclerosis and radiologic SCD is unknown, as many otologists and neurotologists do not routinely obtain imaging for the work-up of conductive hearing loss and suspicion of otosclerosis (162). Current literature comprises retrospective case reports and case series, in which preoperative CT was not always obtained. In the largest case serie, 5/8 patients were diagnosed with concurrent disease because of persistent ABG after stapedotomy or unmasking of SCD symptoms, and only three were diagnosed with concurrent disease on preoperative CT. It is possible that literature is biased toward cases where ABG persisted or SCD symptoms were unmasked, which triggered CT imaging and subsequent diagnosis of concurrent otosclerosis and radiologic SCD (76, 161).

Patients who experience unmasking of SCD symptoms following stapedotomy may be candidates for surgical repair of the canal dehiscence (two cases of successful resolution of unmasked SCD symptoms have been described) (76, 156). However, multiple surgeries that involve manipulation of the inner ear could increase the risk of SNHL (127).

Management of Children With SCDS

The occurrence of SCDS in children is rare, but there are a few reports that describe the diagnostic work-up and management of the condition in the pediatric population (163–165). The largest series included 13 children (15 ears) with radiologic SCD and symptoms of hearing loss and/or vestibular impairment (164). Ages ranged from 6 to 17 years with a mean of 11 years. Conductive or mixed hearing loss was present in seven children (nine ears). Vestibular symptoms were observed in five children and included general disequilibrium, vertigo, delayed onset of walking and other motor functions. In another series of seven children (15 ears), ranging from 5 to 11 years of age with a mean of 7 years, one child underwent surgical repair with improvement in both auditory and vestibular symptoms postoperatively (163). In a series of patients with SCDS associated the superior petrosal sinus, a 15 year old female underwent uneventful transmastoid SCD repair with durable symptom control (134). Of note, however, improvement in vestibular symptoms and stable hearing were also noted in one child at 1-year follow-up after conservative observation (163).

Behavioral observations (e.g., sudden very brief falls with immediate recovery, difficulty with or avoidance of balance-demanding activities, and delayed development of motor skills) by caregivers are important to collect, especially in younger children, when evaluating pediatric SCD, because symptom reporting is often non-specific in this patient population. Older children (typically >8 years of age) tend to report typical SCD symptoms, including autophony, amplification of bodily sounds, pulsatile tinnitus, and sound- and pressure-induced vertigo (134, 163, 164). Differences in clinical presentation of SCDS in young children and adults may warrant the development of modified diagnostic criteria for children with suspected SCDS.

Histological and radiologic studies of temporal bones have noted a higher prevalence of dehiscent and thin bone in infants and small children than in adults. One temporal bone study found that specimens from infants demonstrated uniformly thin bone over the SSC, with gradual thickening until 3 years of age (24). CT imaging studies in children (age <18 years) have demonstrated that the prevalence of radiologic near dehiscence and frank dehiscence decreases with age (25, 26). The chance of incidental SCD in young children is therefore increased compared to an adult population, and radiologic findings should be correlated with localizing signs and symptoms, audiometric testing and caregiver observations. Finally, there is currently no evidence that SCD in children is associated with other inner ear anomalies (25).

Revision Surgery

Revision surgeries for SCDS appear to be less successful in resolving symptoms and improving quality of life compared to primary surgeries (5). In a study of 21 patients (23 ears) undergoing revision surgery for SCDS, Sharon et al. (103) found that approximately one-third of patients experienced complete symptom resolution (103). In contrast, about two-thirds of patients undergoing primary surgery for SCDS will experience complete symptom resolution (45). In both primary and revision surgeries, mechanically-explained symptoms of sound- or pressure-induced vertigo, autophony, amplification of bodily sounds, and pulsatile tinnitus are more likely to resolve than chronic disequilibrium, headaches, or fatigue (103, 108). For example, Sharon et al. found that mechanically explained symptoms resolved in 22/23 of revision cases, except for autophony which resolved in 13/17 patients, whereas a symptom like aural fullness only resolved in 7/11 patients (103).

Some case series suggest that revision surgery for SCDS carries a slightly higher risk of moderate to severe SNHL and reduced speech discrimination (two studies, 20 and 2 patients, respectively) (44, 127). Other larger studies note a similar risk of SNHL between patients undergoing primary or revision surgery (one study found no statistically significant difference in risk of profound SNHL) (103, 112). Studies may lack power to detect a difference because of small numbers. It is hypothesized that the inner ear may be sensitive to repetitive surgical trauma, and that scarring and adhesions at the surgical site may increase the trauma to the inner ear during revision surgery (103, 127). For this reason, some surgeons prefer accessing the SSC from a different approach during revision surgery (102).

Selecting appropriate candidates for revision surgery is challenging, particularly as there is some evidence of lower success rates and higher complication rates. Moreover, patients with concurrent migraine or chronic disequilibrium may present with similar symptoms. As described previously, analysis of the

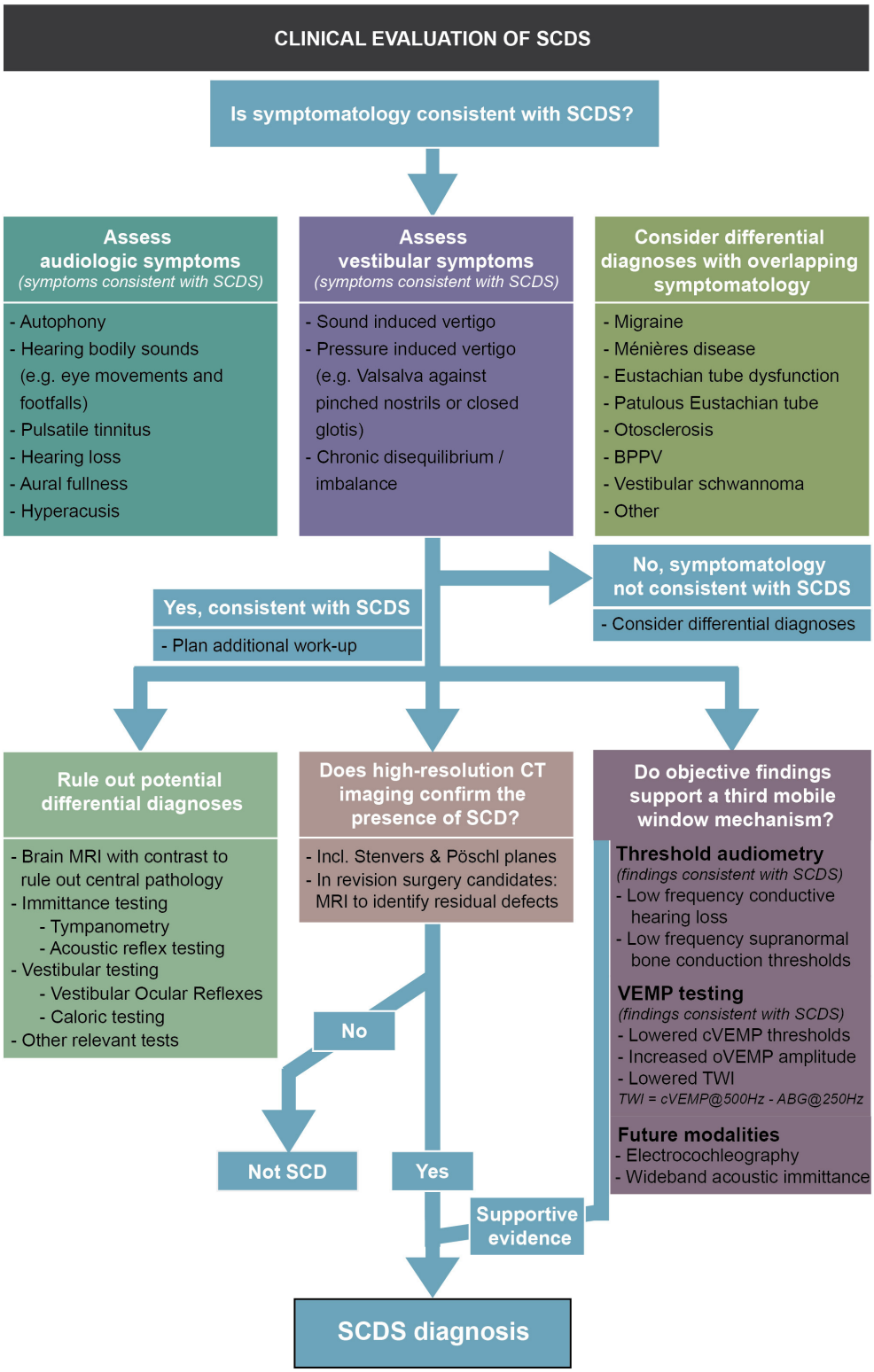

FIGURE 13 | SCD diagnostic algorithm. Evaluation scheme to guide the clinician through a thorough and complete clinical evaluation of a potential SCDS patient.

fluid void of the SSC using T2-weighted MRI imaging can be used to evaluate for residual canal dehiscence following primary surgical repair (**Figures 8**, **11**) (102).

The utility of oVEMP and cVEMP testing in assessing candidacy for revision surgery appear to be limited because SCD effects on VEMP can be obscured by peripheral vestibular deficits following the primary SCD repair (102, 103). One study found that only 4/17 patients with unresolved/recurrent symptoms had elevated oVEMP amplitudes after primary repair/before revision surgery (103) and another study demonstrated low cVEMP thresholds in 4/9 revision surgery candidates (102). However, normalization of VEMP thresholds after successful primary repair (and revision repair) has been reported, which suggests that continued low threshold (high amplitude) VEMP indicates unsuccessful repair (two studies, total of nine patients all with normalization postoperatively) (118, 166). It is possible that VEMP thresholds are less sensitive following initial surgical manipulation and may not change following revision surgery (103).

FUTURE CONSIDERATIONS

While tremendous progress has been made over the past two decades in the diagnosis and management of SCDS, there are a number of important research questions that are still unanswered.

First, the etiology and pathophysiology of SCDS are incompletely understood. There are a wide range of vestibular and auditory symptoms, as well as symptom severity, among SCDS patients that does not always correlate with size and location of the defect. Additionally, some patients may have developed maladaptive behaviors and cognition in response to ongoing symptoms, which complicates symptom presentation.

Second, contemporary diagnostic measures such as audiometric and VEMP testing do not fully capture changes in inner ear biomechanics among patients with SCD, and atypical signs and symptoms, near dehiscence, bilateral dehiscence, and determining candidates for revision repair pose diagnostic challenges. Studies investigating novel diagnostic methods independent of innate vestibular or auditory function are important in solving these challenges.

Third, surgical needs include the ability to create a durable tight fluid seal like SCD plugging but without affecting fluid motion of the SSC, and to reduce the associated complications including dizziness and hearing loss. Customized 3D-prostheses may represent a future approach (146).

Large cohort studies comparing surgical approaches are lacking, in part due to the rarity of the disease, but also due to high variability in technique among surgeons. Additionally, a disease-specific outcome measure in SCDS has not been identified. As current studies rely on a variety of outcome measures, comparing results among studies is challenging. Developing a consensus on the diagnostic criteria and outcome measures is critical to allow clinical outcomes research of SCDS to progress forward. In **Figure 13**, we proposed an evaluation scheme to guide the clinician through a thorough and complete clinical evaluation of a potential SCDS patient.

CONCLUSIONS

SCD has been increasingly recognized as a treatable cause of vestibular and auditory dysfunction. Remarkable strides have been made in understanding the pathophysiology of this unusual third window condition. Improvements in CT resolution as well as more widespread supranormal bone conduction threshold testing, coupled with refinements in cervical and ocular VEMPs have improved the diagnostic yield in the evaluation of patients with a suspected third window. Temporal bone MRI is a valuable imaging modality in the assessment of the patient with a new SCDS diagnosis or in the evaluation of a patient who may be a candidate for revision surgery. WAI and ECochG have been investigated as novel measures to assess SCD biomechanics. Operative management of SCDS has seen advances in the use of minimally invasive surgical corridors, skull base endoscopy, and a variety of repair materials, although debates persist about the optimal surgical approach, technique, and material. Plugging of the defect, rather than resurfacing, is associated with longterm symptom control in most cases. Finally, comparative outcome studies are needed to assess challenging cases, such as patients with bilateral dehiscence, near dehiscence, revision cases, and concurrent SCDS and migraine disorder.

AUTHOR CONTRIBUTIONS

KE and DL concepted the review. KE drafted the manuscript. KE, DC, HN, MK, PC-T, and DL critically revised the manuscript. All authors gave final approval.

FUNDING

Funding was provided by the William Demant Foundation and Copenhagen Hearing and Balance Centre at the Department of Otorhinolaryngology, Head and Neck Surgery & Audiology, Copenhagen University Hospital - Rigshospitalet (KE); and by NIH/NIDCD R01 DC004798 (HN).

ACKNOWLEDGMENTS

We would like to thank Yew Song Cheng for the schematic illustrations and figures.

REFERENCES

1. Minor LB, Solomon D, Zinreich JS, Zee DS. Sound- and/or pressure-induced vertigo due to bone dehiscence of the superior semicircular canal. *Arch Otolaryngol - Head Neck Surg.* (1998) 124:249–58. doi: 10.1001/archotol.124.3.249
2. Merchant SN, Rosowski JJ. Conductive hearing loss caused by third-window lesions of the inner ear. *Otol Neurotol.* (2008) 29:282–9. doi: 10.1097/MAO.0b013e318161ab24
3. Minor LB. Superior canal dehiscence syndrome. *Am J Oto.* (2000) 21:9–19. doi: 10.1016/S0196-0709(00)80068-X

4. Ward BK, Carey JP, Minor LB. Superior canal dehiscence syndrome: lessons from the first 20 yearS. *Front Neurol.* (2017) 8:177. doi: 10.3389/fneur.2017.00177
5. Remenschneider AK, Owoc M, Kozin ED, McKenna MJ, Lee DJ, Jung DH. Health utility improves after surgery for superior canal dehiscence syndrome. *Otol Neurotol.* (2015) 36:1695–701. doi: 10.1097/MAO.0000000000000886
6. Harun A, Semenov YR, Agrawal Y. Vestibular function and activities of daily living. *Gerontol Geriatr Med.* (2015) 1:2333721415607124. doi: 10.1177/2333721415607124
7. Öhman J, Forssén A, Sörlin A, Tano K. Patients' experiences of living with superior canal dehiscence syndrome. *Int J Audiol.* (2018) 57:825–30. doi: 10.1080/14992027.2018.1487086
8. Rosowski JJ, Songer JE, Nakajima HH, Brinsko KM, Merchant SN. Clinical, experimental, and theoretical investigations of the effect of superior semicircular canal dehiscence on hearing mechanisms. *Otol Neurotol.* (2004) 25:323–32. doi: 10.1097/00129492-200405000-00021
9. Cheng YS, Raufer S, Guan X, Halpin CF, Lee DJ, Nakajima HH. Superior canal dehiscence similarly affects cochlear pressures in temporal bones and audiograms in patients. *Ear Hear.* (2020) 41:804–10. doi: 10.1097/AUD.0000000000000799
10. Raufer S, Masud SF, Nakajima HH. Infrasound transmission in the human ear: Implications for acoustic and vestibular responses of the normal and dehiscent inner ear. *J Acoust Soc Am.* (2018) 144:332–42. doi: 10.1121/1.5046523
11. Guan X, Cheng YS, Galaiya DJ, Rosowski JJ, Lee DJ, Nakajima HH. Bone-conduction hyperacusis induced by superior canal dehiscence in human: the underlying mechanism. *Sci Rep.* (2020) 10:1–11. doi: 10.1038/s41598-020-73565-4
12. Pisano D V., Niesten MEF, Merchant SN, Nakajima HH. The effect of superior semicircular canal dehiscence on intracochlear sound pressures. *Audiol Neurotol.* (2012) 17:338–48. doi: 10.1159/000339653
13. Merchant SN, Nakajima HH, Halpin C, Nadol Jr. JB, Lee DJ, Innis WP, et al. Clinical investigation and mechanism of air-bone gaps in large vestibular aqueduct syndrome. *Ann Otol Rhinol Laryngol.* (2007) 116:532–41. doi: 10.1177/000348940711600709
14. Puls T, Van Frayenhoven L. Large vestibular aqueduct syndrome with mixed hearing loss: a case report. *Acta Otorhinolaryngol Belg.* (1997) 51:185–9.
15. Govaerts PJ, Casselman J, Daemers K, De Ceulaer G, Somers T, Offeciers FE. Audiological findings in large vestibular aqueduct syndrome. *Int J Pediatr Otorhinolaryngol.* (1999) 51:157–64. doi: 10.1016/S0165-5876(99)00268-2
16. Cheng YS, Kozin ED, Nakajima HH, Lee DJ. Síndrome da terceira janela como causa de perda auditiva condutiva. In: Lessa MM, Pinna FR, Abrahão M, Caldas Neto SS, editors. *PRO-ORL – Programa de Atualização em Otorrinolaringologia Ciclo 12 Volume.* Alegre: Artmed Panamericana (2018) p. 9–44.
17. Niesten MEF, Stieger C, Lee DJ, Merchant JP, Grolman W, Rosowski JJ, et al. Assessment of the effects of superior canal dehiscence location and size on intracochlear sound pressures. *Audiol Neurotol.* (2015) 20:62–71. doi: 10.1159/000366512
18. Stenfelt S. Investigation of mechanisms in bone conduction hyperacusis with third window pathologies based on model predictions. *Front Neurol.* (2020) 11:966 doi: 10.3389/fneur.2020.00966
19. Kim HHS, Wilson DF. A third mobile window at the cochlear apex. *Otolaryngol - Head Neck Surg.* (2006) 135:965–6. doi: 10.1016/j.otohns.2005.04.006
20. Blake DM, Tomovic S, Vazquez A, Lee HJ, Jyung RW. Cochlear-facial dehiscence - a newly described entity. *Laryngoscope.* (2014) 124:283–9. doi: 10.1002/lary.24223
21. Wackym PA, Balaban CD, Zhang P, Siker DA, Hundal JS. Third window syndrome: surgical management of cochlea-facial nerve dehiscence. *Front Neurol.* (2019) 10:1281. doi: 10.3389/fneur.2019.01281
22. Friedmann DR, Le BT, Pramanik BK, Lalwani AK. Clinical spectrum of patients with erosion of the inner ear by jugular bulb abnormalities. *Laryngoscope.* (2010) 120:365–72. doi: 10.1002/lary.20699
23. Gadre AK, Edwards IR, Baker VM, Roof CR. Membranous or hypermobile stapes footplate: a new anatomic site resulting in third window syndrome. *Front Neurol.* (2020) 11:871. doi: 10.3389/fneur.2020.00871
24. Carey JP, Minor LB, Nager GT. Dehiscence or thinning of bone overlying the superior semicircular canal in a temporal bone survey. *Arch Otolaryngol Head Neck Surg.* (2000) 126:137–47. doi: 10.1001/archotol.126.2.137
25. Sugihara EM, Babu SC, Kitsko DJ, Haupert MS, Thottam PJ. Incidence of pediatric superior semicircular canal dehiscence and inner ear anomalies: a large multicenter review. *Otol Neurotol.* (2016) 37:1370–5. doi: 10.1097/MAO.0000000000001194
26. Jackson NM, Allen LM, Morell B, Carpenter CC, Givens VB, Kakade A, et al. The relationship of age and radiographic incidence of superior semicircular canal dehiscence in pediatric patients. *Otol Neurotol.* (2015) 36:99–105. doi: 10.1097/MAO.0000000000000660
27. Chen EY, Paladin A, Phillips G, Raske M, Vega L, Peterson D, et al. Semicircular canal dehiscence in the pediatric population. *Int J Pediatr Otorhinolaryngol.* (2009) 73:321–7. doi: 10.1016/j.ijporl.2008.10.027
28. Hirvonen TP, Weg N, James Zinreich S, Minor LB. High-resolution CT findings suggest a developmental abnormality underlying superior canal dehiscence syndrome. *Acta Otolaryngol.* (2003) 123:477–81. doi: 10.1080/0036554021000028099
29. Stevens SM, Hock K, Samy RN, Pensak ML. Are patients with spontaneous CSF otorrhea and superior canal dehiscence congenitally predisposed to their disorders? *Otolaryngol - Head Neck Surg.* (2018) 159:543–52. doi: 10.1177/0194599818769875
30. Heidenreich KD, Kileny PR, Ahmed S, El-Kashlan HK, Melendez TL, Basura GJ, et al. Superior canal dehiscence syndrome affecting 3 families. *JAMA Otolaryngol - Head Neck Surg.* (2017) 143:656–62. doi: 10.1001/jamaoto.2016.4743
31. Niesten MEF, Lookabaugh S, Curtin H, Merchant SN, McKenna MJ, Grolman W, et al. Familial superior canal dehiscence syndrome. *JAMA Otolaryngol - Head Neck Surg.* (2014) 140:363–8. doi: 10.1001/jamaoto.2013.6718
32. Noonan KY, Russo J, Shen J, Rehm H, Halbach S, Hopp E, et al. CDH23 related hearing loss: A new genetic risk factor for semicircular canal dehiscence? *Otol Neurotol.* (2016) 37:1583–8. doi: 10.1097/MAO.0000000000001210
33. Jan TA, Cheng YS, Landegger LD, Lin BM, Srikanth P, Niesten MEF, et al. Relationship between surgically treated superior canal dehiscence syndrome and body mass index. *Otolaryngol - Head Neck Surg.* (2017) 156:722–7. doi: 10.1177/0194599816686563
34. Schutt CA, Neubauer P, Samy RN, Pensak ML, Kuhn JJ, Herschovitch M, et al. The correlation between obesity, obstructive sleep apnea, and superior semicircular canal dehiscence. *Otol Neurotol.* (2015) 36:551–4. doi: 10.1097/MAO.0000000000000555
35. Goddard JC, Meyer T, Nguyen S, Lambert PR. New considerations in the cause of spontaneous cerebrospinal fluid otorrhea. *Otol Neurotol.* (2010) 31:940–5. doi: 10.1097/MAO.0b013e3181e8f36c
36. LeVay AJ, Kveton JF. Relationship between obesity, obstructive sleep apnea, and spontaneous cerebrospinal fluid otorrhea. *Laryngoscope.* (2008) 118:275–8. doi: 10.1097/MLG.0b013e31815937a6
37. Nelson RF, Gantz BJ, Hansen MR. The rising incidence of spontaneous cerebrospinal fluid leaks in the United States and the association with obesity and obstructive sleep apnea. *Otol Neurotol.* (2015) 36:476–80. doi: 10.1097/MAO.0000000000000535
38. Crane BT, Carey JP, McMenomey S, Minor LB. Meningioma causing superior canal dehiscence syndrome. *Otol Neurotol.* (2010) 31:1009–10. doi: 10.1097/MAO.0b013e3181a32d85
39. Brantberg K, Greitz D, Pansell T. Subarcuate venous malformation causing audio-vestibular symptoms similar to those in superior canal dehiscence syndrome. *Otol Neurotol.* (2004) 25:993–7. doi: 10.1097/00129492-200411000-00022
40. Bae JS, Lim HW, An YS, Park HJ. Acquired superior semicircular canal dehiscence confirmed by sequential CT scans. *Otol Neurotol.* (2013) 34:45–6. doi: 10.1097/MAO.0b013e31828d6753
41. Goddard JC, Go JL, Friedman RA. Imaging case of the month: fibrous dysplasia causing superior canal dehiscence. *Otol Neurotol.* (2013) 34:2012–3. doi: 10.1097/MAO.0b013e3182355642

42. Peng KA, Ahmed S, Yang I, Gopen Q. Temporal bone fracture causing superior semicircular canal dehiscence. *Case Rep Otolaryngol.* (2014) 2014:1–4. doi: 10.1155/2014/817291
43. Zhou G, Gopen Q, Poe DS. Clinical and diagnostic characterization of canal dehiscence syndrome: a great otologic mimicker. *Otol Neurotol.* (2007) 28:920–6. doi: 10.1097/MAO.0b013e31814b25f2
44. Minor LB. Clinical manifestations of superior semicircular canal dehiscence. *Laryngoscope.* (2005) 115:1717–27. doi: 10.1097/01.mlg.0000178324.55729.b7
45. Niesten MEF, Mckenna MJ, Grolman W, Lee DJ. Clinical factors associated with prolonged recovery after superior canal dehiscence surgery. *Otol Neurotol.* (2012) 33:824–31. doi: 10.1097/MAO.0b013e3182544c9e
46. Bigelow RT, Agrawal Y. Vestibular involvement in cognition: Visuospatial ability, attention, executive function, and memory. *J Vestib Res Equilib Orientat.* (2015) 25:73–89. doi: 10.3233/VES-150544
47. Ashley Wackym P, Balaban CD, Mackay HT, Wood SJ, Lundell CJ, Carter DM, et al. Longitudinal cognitive and neurobehavioral functional outcomes before and after repairing otic capsule dehiscence. *Otol Neurotol.* (2016) 37:70–82. doi: 10.1097/MAO.0000000000000928
48. Niesten MEF, Hamberg LM, Silverman JB, Lou K V, McCall AA, Windsor A, et al. Superior canal dehiscence length and location influences clinical presentation and audiometric and cervical vestibular-evoked myogenic potential testing. *Audiol Neurotol.* (2014) 19:97–105. doi: 10.1159/000353920
49. Pfammatter A, Darrouzet V, Gärtner M, Somers T, Van Dinther J, Trabalzini F, et al. A superior semicircular canal dehiscence syndrome multicenter study: is there an association between size and symptoms? *Otol Neurotol.* (2010) 31:447–54. doi: 10.1097/MAO.0b013e3181d27740
50. Mikulec AA, Mckenna MJ, Ramsey MJ, Rosowski JJ, Herrmann BS, Rauch SD, et al. Superior semicircular canal dehiscence presenting as conductive hearing loss without vertigo. *Otol Neurotol.* (2004) 25:121–9. doi: 10.1097/00129492-200403000-00007
51. Watson SRD, Halmagyi GM, Colebatch JG. Vestibular hypersensitivity to sound (Tullio phenomenon) Structural and functional assessment. *Neurology.* (2000) 54:722–8. doi: 10.1212/WNL.54.3.722
52. Noij KS, Wong K, Duarte MJ, Masud S, Dewyer NA, Herrmann BS, et al. Audiometric and cVEMP thresholds show little correlation with symptoms in superior semicircular canal dehiscence syndrome. *Otol Neurotol.* (2018) 39:1153–62. doi: 10.1097/MAO.0000000000001910
53. Chien WW, Janky K, Minor LB, Carey JP. Superior canal dehiscence size: multivariate assessment of clinical impact. *Otol Neurotol.* (2012) 33:810–5. doi: 10.1097/MAO.0b013e318248eac4
54. Yuen HW, Boeddinghaus R, Eikelboom RH, Atlas MD. The relationship between the air-bone gap and the size of superior semicircular canal dehiscence. *Otolaryngol - Head Neck Surg.* (2009) 141:689–94. doi: 10.1016/j.otohns.2009.08.029
55. Minor LB, Carey JP, Cremer PD, Lustig LR, Streubel SO, Ruckenstein MJ. Dehiscence of bone overlying the superior canal as a cause of apparent conductive hearing loss. *Otol Neurotol.* (2003) 24:270–8. doi: 10.1097/00129492-200303000-00023
56. Hullar TE. Vascular pulsations on impedance audiometry as a sign of a third-mobile window lesion. *Otol Neurotol.* (2010) 31:565–6. doi: 10.1097/MAO.0b013e3181db7324
57. Thai A, Sayyid ZN, Hosseini DK, Swanson A, Ma Y, Aaron KA, et al. Ambient pressure tympanometry wave patterns in patients with superior semicircular canal dehiscence. *Front Neurol.* (2020) 11:379. doi: 10.3389/fneur.2020.00379
58. Castellucci A, Brandolini C, Piras G, Fernandez IJ, Giordano D, Pernice C, et al. Superior canal dehiscence with tegmen defect revealed by otoscopy: video clip demonstration of pulsatile tympanic membrane. *Auris Nasus Larynx.* (2018) 45:165–9. doi: 10.1016/j.anl.2016.11.013
59. Hunter JB, Patel NS, O'Connell BP, Carlson ML, Shepard NT, McCaslin DL, et al. Cervical and ocular vemp testing in diagnosing superior semicircular canal dehiscence. *Otolaryngol - Head Neck Surg.* (2017) 156:917–23. doi: 10.1177/0194599817690720
60. Noij KS, Rauch SD. Vestibular Evoked Myogenic Potential (VEMP) testing for diagnosis of superior semicircular canal dehiscence. *Front Neurol.* (2020) 11:695. doi: 10.3389/fneur.2020.00695
61. Zuniga MG, Janky KL, Nguyen KD, Welgampola MS, Carey JP. Ocular versus cervical VEMPs in the diagnosis of superior semicircular canal dehiscence syndrome. *Otol Neurotol.* (2013) 34:121–6. doi: 10.1097/MAO.0b013e31827136b0
62. Fife TD, Colebatch JG, Kerber KA, Brantberg K, Strupp M, Lee H, et al. Practice guideline: Cervical and ocular vestibular evokedmyogenic potential testing: report of the guideline development, dissemination, and implementation subcommittee of the American Academy of Neurology. *Neurology.* (2017) 89:2288–96. doi: 10.1212/WNL.0000000000004690
63. Janky KL, Nguyen KD, Welgampola M, Zuniga MG, Carey JP. Air-conducted oVEMPs provide the best separation between intact and superior canal dehiscent labyrinths. *Otol Neurotol.* (2013) 34:127–34. doi: 10.1097/MAO.0b013e318271c32a
64. Milojcic R, Guinan JJ, Rauch SD, Herrmann BS. Vestibular evoked myogenic potentials in patients with superior semicircular canal dehiscence. *Otol Neurotol.* (2013) 34:360–7. doi: 10.1097/MAO.0b013e31827b4fb5
65. Noij KS, Duarte MJ, Wong K, Cheng YS, Masud S, Herrmann BS, et al. Toward Optimizing Cervical Vestibular Evoked Myogenic Potentials (cVEMP): combining air-bone gap and cVEMP thresholds to improve diagnosis of superior canal dehiscence. *Otol Neurotol.* (2018) 39:212–20. doi: 10.1097/MAO.0000000000001655
66. Noij KS, Herrmann S, Jr JG. Toward optimizing cVEMP: 2,000-Hz tone bursts improve the detection of superior canal dehiscence. *Audiol Neurotol.* (2019) 24:49. doi: 10.1159/000493721
67. Lin K, Lahey R, Beckley R, Ii DB, Wilkerson B, Johnson E, et al. Validating the utility of high frequency ocular vestibular evoked myogenic potential testing in the diagnosis of superior semicircular canal dehiscence. *Otol Neurotol.* (2019) 40:1353–8. doi: 10.1097/MAO.0000000000002388
68. Manzari L, Burgess AM, McGarvie LA, Curthoys IS. An indicator of probable semicircular canal dehiscence: ocular vestibular evoked myogenic potentials to high frequencies. *Otolaryngol - Head Neck Surg.* (2013) 149:142–5. doi: 10.1177/0194599813489494
69. Govender S, Fernando T, Dennis DL, Welgampola MS, Colebatch JG. Properties of 500 Hz air- and bone-conducted vestibular evoked myogenic potentials (VEMPs) in superior canal dehiscence. *Clin Neurophysiol.* (2016) 127:2522–31. doi: 10.1016/j.clinph.2016.02.019
70. McCaslin DL, Jacobson GP. Vestibular-Evoked Myogenic Potentials (VEMPs). In: Jacobson GP, Shepard NT, Barin K, Janky K, McCaslin D, Burkard RF, editors. *Balance Function Assessment and Management. 3rd ed.* San Diego, CA: Plural Publishing Inc. (2019) p. 399–438.
71. Ruckenstein MJ, Davis S, (editors). Tests of Otolith Function. In: *Rapid Interpretation of Balance Function Tests.* San Diego, CA: Plural Publishing Inc. (2014) p. 131–43.
72. Serra AP, Dorigueto RS, De Almeida RR, Ganança FF. Vestibular evoked myogenic potential in unilateral vestibular hypofunction. *Acta Otolaryngol.* (2012) 132:732–8. doi: 10.3109/00016489.2012.659283
73. Juliano AF, Ginat DT, Moonis G. Imaging review of the temporal bone: Part II. traumatic, postoperative, and noninflammatory nonneoplastic conditions. *Radiology.* (2015) 276:655–72. doi: 10.1148/radiol.2015140800
74. Quesnel AM, Moonis G, Appel J, O'Malley JT, McKenna MJ, Curtin HD, et al. Correlation of computed tomography with histopathology in otosclerosis. *Otol Neurotol.* (2013) 34:22–8. doi: 10.1097/MAO.0b013e318277a1f7
75. Nakajima HH, Ravicz ME, Merchant SN, Peake WT, Rosowski JJ. Experimental ossicular fixations and the middle ear's response to sound : Evidence for a flexible ossicular chain. *Hear Res.* (2005) 204:60–77. doi: 10.1016/j.heares.2005.01.002
76. Dewyer NA, Quesnel AM, Santos F. A case series of patients with concurrent otosclerosis and superior semicircular canal dehiscence. *Otol Neurotol.* (2020) 41:e172–81. doi: 10.1097/MAO.0000000000002487
77. Blakley BW, Wong V. Normal values for cervical vestibular-evoked myogenic potentials. *Otol Neurotol.* (2015) 36:1069–73. doi: 10.1097/MAO.0000000000000752
78. Mikulec AA, Poe DS, McKenna MJ. Operative management of superior semicircular canal dehiscence. *Laryngoscope.* (2005) 115:501–7. doi: 10.1097/01.mlg.0000157844.48036.e7
79. Agrawal Y, Minor LB, Schubert MC, Janky KL, Davalos-Bichara M, Carey JP. Second-side surgery in superior canal dehiscence syndrome. *Otol Neurotol.* (2012) 33:72–7. doi: 10.1097/MAO.0b013e31823c9182

80. Cremer PD, Minor LB, Carey JP, Della Santina CC. Eye movements in patients with superior canal dehiscence syndrome align with the abnormal canal. *Neurology.* (2000) 55:1833–41. doi: 10.1212/WNL.55.12.1833
81. Carey JP, Migliaccio AA, Minor LB. Semicircular canal function before and after surgery for superior canal dehiscence. *Otol Neurotol.* (2007) 28:356–64. doi: 10.1097/01.mao.0000253284.40995.d8
82. Castellucci A, Piras G, Del Vecchio V, Crocetta FM, Maiolo V, Ferri GG, et al. The effect of superior canal dehiscence size and location on audiometric measurements, vestibular-evoked myogenic potentials and video-head impulse testing. *Eur Arch Oto-Rhino-Laryngol.* (2020). doi: 10.1007/s00405-020-06169-3
83. Nakajima HH, Rosowski JJ, Shahnaz N, Voss SE. Assessment of ear disorders using power reflectance. *Ear Hear.* (2013) 34(Suppl. 1):48S−53S. doi: 10.1097/AUD.0b013e31829c964d
84. Merchant GR, Roösli C, Niesten MEF, Hamade MA, Lee DJ, McKinnon ML, et al. Power reflectance as a screening tool for the diagnosis of superior semicircular canal dehiscence. *Otol Neurotol.* (2015) 36:172–7. doi: 10.1097/MAO.0000000000000294
85. Rosowski JJ, Stenfelt S, Lilly D. An overview of wideband immittance measurements techniques and terminology: you say absorbance, i say reflectance. *Ear Hear.* (2013) 34(Suppl 1):9S–16S. doi: 10.1097/AUD.0b013e31829d5a14
86. Masud SF. *Diagnosis of Mechanical Ear Pathologies Using Structure-Based Modeling and Machine Learning Techniques* [dissertation] [Internet]. Harvard University, United States (2020). Available online at: https://dash.harvard.edu/handle/1/37365115 (accessed February 17, 2021).
87. Adams ME, Kileny PR, Telian SA, El-Kashlan HK, Heidenreich KD, Mannarelli GR, et al. Electrocochleography as a diagnostic and intraoperative adjunct in superior semicircular canal dehiscence syndrome. *Otol Neurotol.* (2011) 32:1506–12. doi: 10.1097/MAO.0b013e3182382a7c
88. Park JH, Lee SY, Song JJ, Choi BY, Koo JW. Electrocochleographic findings in superior canal dehiscence syndrome. *Hear Res.* (2015) 323:61–7. doi: 10.1016/j.heares.2015.02.001
89. Arts HA, Adams ME, Telian SA, El-Kashlan H, Kileny PR. Reversible electrocochleographic abnormalities in superior canal dehiscence. *Otol Neurotol.* (2009) 30:79–86. doi: 10.1097/MAO.0b013e31818d1b51
90. Wenzel A, Ward BK, Ritzl EK, Gutierrez-Hernandez S, Santina CCD, Minor LB, et al. Intraoperative neuromonitoring for superior semicircular canal dehiscence and hearing outcomes. *Otol Neurotol.* (2015) 36:139–45. doi: 10.1097/MAO.0000000000000642
91. Lookabaugh S, Kelly HR, Carter MS, Niesten MEF, McKenna MJ, Curtin H, et al. Radiologic classification of superior canal dehiscence: implications for surgical repair. *Otol Neurotol.* (2015) 36:118–25. doi: 10.1097/MAO.0000000000000523
92. Crovetto M, Whyte J, Rodriguez OM, Lecumberri I, Martinez C, Eléxpuru J, et al. Anatomo-radiological study of the superior semicircular canal dehiscence: radiological considerations of superior and posterior semicircular canals. *Eur J Radiol.* (2010) 76:167–72. doi: 10.1016/j.ejrad.2009.05.038
93. Sequeira SM, Whiting BR, Shimony JS, Vo KD, Hullar TE. Accuracy of computed tomography detection of superior canal dehiscence. *Otol Neurotol.* (2011) 32:1500–5. doi: 10.1097/MAO.0b013e318238280c
94. Baxter M, McCorkle C, Trevino Guajardo C, Zuniga MG, Carter AM, Della Santina CC, et al. Clinical and physiologic predictors and postoperative outcomes of near dehiscence syndrome. *Otol Neurotol.* (2019) 40:204–12. doi: 10.1097/MAO.0000000000002077
95. Belden CJ, Weg N, Minor LB, Zinreich SJ. SCC dehiscence radiology. *Radiology.* (2003) 226:337–43. doi: 10.1148/radiol.2262010897
96. Curtin HD. Superior semicircular canal dehiscence syndrome and multi–detector row CT. *Radiology.* (2003) 226:312–4. doi: 10.1148/radiol.2262021327
97. Tavassolie TS, Penninger RT, Zuñiga MG, Minor LB, Carey JP. Multislice computed tomography in the diagnosis of superior canal dehiscence: how much error, and how to minimize it? *Otol Neurotol.* (2012) 33:215–22. doi: 10.1097/MAO.0b013e318241c23b
98. Schwartz T, Lindemann T, Mongelluzzo G, Wackym P, Gadre A. Gray-scale inversion on high resolution computed tomography of the temporal bone: an observational study. *Ann Otol Rhinol Laryngol.* (in press).
99. Tunkel AE, Carey JP, Pearl M. Flat panel computed tomography in the diagnosis of superior semicircular canal dehiscence syndrome. *Otol Neurotol.* (2019) 40:213–7. doi: 10.1097/MAO.0000000000002076
100. Browayes P, Larson TL, Wong ML, Patel U. Can MRI replace ct in evaluating semicircular canal dehiscence. *AJNR Am J Neuroradiol.* (2013) 34:1421–7. doi: 10.3174/ajnr.A3459
101. Inal M, Burulday V, Bayar Muluk N, Kaya A, Simşek G, Ünal Daphan B. Magnetic resonance imaging and computed tomography for diagnosing semicircular canal dehiscence. *J Cranio-Maxillofacial Surg.* (2016) 44:998–1002. doi: 10.1016/j.jcms.2016.06.006
102. Chemtob RA, Epprecht L, Reinshagen KL, Huber A, Caye-Thomasen P, Nakajima HH, et al. Utility of postoperative magnetic resonance imaging in patients who fail superior canal dehiscence surgery. *Otol Neurotol.* (2019) 40:130–8. doi: 10.1097/MAO.0000000000002051
103. Sharon JD, Pross SE, Ward BK, Carey JP. Revision surgery for superior canal dehiscence syndrome. *Otol Neurotol.* (2016) 37:1096–103. doi: 10.1097/MAO.0000000000001113
104. Seroussi J, Hautefort C, Gillibert A, Kania R, Guichard JP, Vitaux H, et al. Postoperative MR imaging features after superior semicircular canal plugging in minor syndrome. *Diagn Interv Imaging.* (2018) 99:679–87. doi: 10.1016/j.diii.2018.08.008
105. Friedland DR, Michel MA. Cranial thickness in superior canal dehiscence syndrome: Implications for canal resurfacing surgery. *Otol Neurotol.* (2006) 27:346–54. doi: 10.1097/00129492-200604000-00010
106. Vlastarakos P V., Proikas K, Tavoulari E, Kikidis D, Maragoudakis P, Nikolopoulos TP. Efficacy assessment and complications of surgical management for superior semicircular canal dehiscence: a meta-analysis of published interventional studies. *Eur Arch Oto-Rhino-Laryngology.* (2009) 266:177–86. doi: 10.1007/s00405-008-0840-4
107. Ziylan F, Kinaci A, Beynon AJ, Kunst HPM. A comparison of surgical treatments for superior semicircular canal dehiscence: a systematic review. *Otol Neurotol.* (2017) 38:1–10. doi: 10.1097/MAO.0000000000001277
108. Alkhafaji MS, Varma S, Pross SE, Sharon JD, Nellis JC, Della Santina CC, et al. Long-term patient-reported outcomes after surgery for superior canal dehiscence syndrome. *Otol Neurotol.* (2017) 38:1319–26. doi: 10.1097/MAO.0000000000001550
109. Schwartz SR, Almosnino G, Noonan KY, Banakis Hartl RM, Zeitler DM, Saunders JE, et al. Comparison of transmastoid and middle fossa approaches for superior canal dehiscence repair: a multi-institutional study. *Otolaryngol - Head Neck Surg.* (2019) 161:130–6. doi: 10.1177/0194599819835173
110. Goddard JC, Wilkinson EP. Outcomes following semicircular canal plugging. *Otolaryngol - Head Neck Surg.* (2014) 151:478–83. doi: 10.1177/0194599814538233
111. Crane BT, Minor LB, Carey JP. Superior canal dehiscence plugging reduces dizziness handicap. *Laryngoscope.* (2008) 118:1809–13. doi: 10.1097/MLG.0b013e31817f18fa
112. Xie Y, Sharon JD, Pross SE, Abt NB, Varma S, Della Santina CC, et al. Surgical complications from superior canal dehiscence syndrome repair: two decades of experience. *Otolaryngol - Head Neck Surg.* (2017) 157:273–80. doi: 10.1177/0194599817706491
113. Beyea JA, Agrawal SK, Parnes LS. Transmastoid semicircular canal occlusion: a safe and highly effective treatment for benign paroxysmal positional vertigo and superior canal dehiscence. *Laryngoscope.* (2012) 122:1862–6. doi: 10.1002/lary.23390
114. Ward BK, Agrawal Y, Nguyen E, Della Santina CC, Limb CJ, Francis HW, et al. Hearing outcomes after surgical plugging of the superior semicircular canal by a middle cranial fossa approach. *Otol Neurotol.* (2012) 33:1386–91. doi: 10.1097/MAO.0b013e318268d20d
115. Janky KL, Zuniga MG, Carey JP, Schubert M. Balance dysfunction and recovery after surgery for superior canal dehiscence syndrome. *Arch Otolaryngol - Head Neck Surg.* (2012) 138:723–30. doi: 10.1001/archoto.2012.1329
116. Agrawal Y, Migliaccio AA, Minor LB, Carey JP. Vestibular hypofunction in the initial postoperative period after surgical treatment of superior

semicircular canal dehiscence. *Otol Neurotol.* (2009) 30:502–6. doi: 10.1097/MAO.0b013e3181a32d69
117. Barber SR, Cheng YS, Owoc M, Lin BM, Remenschneider AK, Kozin ED, et al. Benign paroxysmal positional vertigo commonly occurs following repair of superior canal dehiscence. *Laryngoscope.* (2016) 126:2092–7. doi: 10.1002/lary.25797
118. Welgampola MS, Myrie OA, Minor LB, Carey JP. Vestibular-evoked myogenic potential thresholds normalize on plugging superior canal dehiscence. *Neurology.* (2008) 70:464–72. doi: 10.1212/01.wnl.0000299084.76250.4a
119. Crane BT, Lin FR, Minor LB, Carey JP. Improvement in autophony symptoms after superior canal dehiscence repair. *Otol Neurotol.* (2010) 31:140–6. doi: 10.1097/MAO.0b013e3181bc39ab
120. Jacobson G, Newman C. The development of the dizziness handicap inventory. *Arch Otolaryngol Head Neck Surg.* (1990) 116:424–7. doi: 10.1001/archotol.1990.01870040046011
121. Ventry I, Weinstein B. The hearing handicap inventory for the elderly: a new tool. *Ear Hear.* (1982) 3:128–34. doi: 10.1097/00003446-198205000-00006
122. Newman CW, Weinstein BE, Jacobson GP, Hug GA. The hearing handicap inventory for adults: psychometric adequacy and audiometric correlates. *Ear Hear.* (1990) 11:430–3. doi: 10.1097/00003446-199012000-00004
123. Newman CW, Jacobsen GP, Spitzer JB. Development of the tinnitus handicap inventory. *Arch Otolaryngol Head Neck Surg.* (1996) 122:143–8. doi: 10.1001/archotol.1996.01890140029007
124. Thomeer H, Bonnard D, Castetbon V, Franco-Vidal V, Darrouzet P, Darrouzet V. Long-term results of middle fossa plugging of superior semicircular canal dehiscences: clinically and instrumentally demonstrated efficiency in a retrospective series of 16 ears. *Eur Arch Oto-Rhino-Laryngology.* (2016) 273:1689–96. doi: 10.1007/s00405-015-3715-5
125. Niesten MEF, McKenna MJ, Herrmann BS, Grolman W, Lee DJ. Utility of cVEMPs in bilateral superior canal dehiscence syndrome. *Laryngoscope.* (2013) 123:226–32. doi: 10.1002/lary.23550
126. Mueller SA, Vibert D, Haeusler R, Raabe A, Caversaccio M. Surgical capping of superior semicircular canal dehiscence. *Eur Arch Oto-Rhino-Laryngol.* (2014) 271:1369–74. doi: 10.1007/s00405-013-2533-x
127. Limb CJ, Carey JP, Srireddy S, Minor LB. Auditory function in patients with surgically treated superior semicircular canal dehiscence. *Otol Neurotol.* (2006) 27:969–80. doi: 10.1097/01.mao.0000235376.70492.8e
128. Van Haesendonck G, Van de Heyning P, Van Rompaey V. Retrospective cohort study on hearing outcome after transmastoid plugging in superior semicircular canal dehiscence syndrome: Our Experience. *Clin Otolaryngol.* (2016) 41:601–6. doi: 10.1111/coa.12539
129. Puram S, Roberts D, Niesten M, Dilger A, Lee D. Cochlear implant outcomes in patients with superior canal dehiscence. *Cochlear Implant Int.* (2015) 16:213–21. doi: 10.1179/1754762813Y.0000000044
130. Mantokoudis G, Saber Tehrani AS, Wong AL, Agrawal Y, Wenzel A, Carey JP. Adaptation and compensation of vestibular responses following superior canal dehiscence surgery. *Otol Neurotol.* (2016) 37:1399–405. doi: 10.1097/MAO.0000000000001196
131. Lee SY, Bae YJ, Kim M, Song JJ, Choi BY, Koo JW. Changes in vestibulo-ocular reflex gain after surgical plugging of superior semicircular canal dehiscence. *Front Neurol.* (2020) 11:694. doi: 10.3389/fneur.2020.00694
132. Rodgers B, Lin J, Staecker H. Transmastoid resurfacing versus middle fossa plugging for repair of superior canal dehiscence: comparison of techniques from a retrospective cohort. *World J Otorhinolaryngol - Head Neck Surg.* (2016) 2:161–7. doi: 10.1016/j.wjorl.2016.11.001
133. Jung DH, Lookabaugh SA, Owoc MS, McKenna MJ, Lee DJ. Dizziness is more prevalent than autophony among patients who have undergone repair of superior canal dehiscence. *Otol Neurotol.* (2015) 36:126–32. doi: 10.1097/MAO.0000000000000531
134. McCall AA, McKenna MJ, Merchant SN, Curtin HD, Lee DJ. Superior canal dehiscence syndrome associated with the superior petrosal sinus in pediatric and adult patients. *Otol Neurotol.* (2011) 32:1312–9. doi: 10.1097/MAO.0b013e31822e5b0a
135. Carter MS, Lookabaugh S, Lee DJ. Endoscopic-assisted repair of superior canal dehiscence syndrome. *Laryngoscope.* (2014) 124:1464–8. doi: 10.1002/lary.24523
136. Ung N, Chung LK, Lagman C, Bhatt NS, Barnette NE, Ong V, et al. Outcomes of middle fossa craniotomy for the repair of superior semicircular canal dehiscence. *J Clin Neurosci.* (2017) 43:103–7. doi: 10.1016/j.jocn.2017.05.003
137. Chemtob RA, Barber SR, Zhu AW, Kozin ED, Lee DJ. Transmastoid approach for surgical repair of superior canal dehiscence syndrome. *Oper Tech Otolaryngol Head Neck Surg.* (2019) 30:212–6. doi: 10.1016/j.otot.2019.07.007
138. Shaia WT, Diaz RC. Evolution in surgical management of superior canal dehiscence syndrome. *Curr Opin Otolaryngol Head Neck Surg.* (2013) 21:497–502. doi: 10.1097/MOO.0b013e328364b3ff
139. Cheng YS, Kozin ED, Lee DJ. Endoscopic-assisted repair of superior canal dehiscence. *Otolaryngol Clin North Am.* (2016) 49:1189–204. doi: 10.1016/j.otc.2016.05.010
140. Liming BJ, Westbrook B, Bakken H, Crawford J V. Cadaveric study of an endoscopic keyhole middle fossa craniotomy approach to the superior semicircular canal. *Otol Neurotol.* (2016) 37:533–8. doi: 10.1097/MAO.0000000000000995
141. Cheng YS, Kozin ED, Remenschneider AK, Nakajima HH, Lee DJ. Characteristics of wax occlusion in the surgical repair of superior canal dehiscence in human temporal bone specimens. *Otol Neurotol.* (2016) 37:83–8. doi: 10.1097/MAO.0000000000000916
142. Zhao YC, Somers T, Van Dinther J, Vanspauwen R, Husseman J, Briggs R. Transmastoid repair of superior semicircular canal dehiscence. *J Neurol Surgery, Part B Skull Base.* (2012) 73:225–9. doi: 10.1055/s-0032-1312713
143. Brantberg K, Bergenius J, Mendel L, Witt H, Tribukait A, Ygge J. Symptoms, findings and treatment in patients with dehiscence of the superior semicircular canal. *Acta Otolaryngol.* (2001) 121:68–75. doi: 10.1080/000164801300006308
144. Hillman TA, Kertesz TR, Hadley K, Shelton C. Reversible peripheral vestibulopathy: the treatment of superior canal dehiscence. *Otolaryngol - Head Neck Surg.* (2006) 134:436. doi: 10.1016/j.otohns.2005.10.033
145. Hahn Y, Zappia J. Modified resurfacing repair for superior semicircular canal dehiscence. *Otolaryngol - Head Neck Surg.* (2010) 142:763–4. doi: 10.1016/j.otohns.2010.01.011
146. Kozin ED, Remenschneider AK, Cheng S, Heidi Nakajima H, Lee DJ. Three-dimensional printed prosthesis for repair of superior canal dehiscence. *Otolaryngol Neck Surg.* (2015) 153:616–9. doi: 10.1177/0194599815592602
147. Silverstein H, Van Ess MJ. Complete round window niche occlusion for superior semicircular canal dehiscence syndrome: a minimally invasive approach. *Ear Nose Throat J.* (2009) 88:1042–56. doi: 10.1177/014556130908800808
148. Silverstein H, Kartush JM, Parnes LS, Poe DS, Babu SC, Levenson MJ, et al. Round window reinforcement for superior semicircular canal dehiscence: a retrospective multi-center case series. *Am J Otolaryngol - Head Neck Med Surg.* (2014) 35:286–93. doi: 10.1016/j.amjoto.2014.02.016
149. Succar EF, Manickam P V., Wing S, Walter J, Greene JS, Azeredo WJ. Round window plugging in the treatment of superior semicircular canal dehiscence. *Laryngoscope.* (2018) 128:1445–52. doi: 10.1002/lary.26899
150. Borrmann A, Arnold W. Non-syndromal round window atresia: an autosomal dominant genetic disorder with variable penetrance? *Eur Arch Oto-Rhino-Laryngol.* (2007) 264:1103–8. doi: 10.1007/s00405-007-0305-1
151. Elliott SJ, Ni G, Verschuur CA. Modelling the effect of round window stiffness on residual hearing after cochlear implantation. *Hear Res.* (2016) 341:155–67. doi: 10.1016/j.heares.2016.08.006
152. Ward BK, Wenzel A, Ritzl EK, Gutierrez-Hernandez S, Della Santina CC, Minor LB, et al. Near-dehiscence: clinical findings in patients with thin bone over the superior semicircular canal. *Otol Neurotol.* (2013) 34:1421–8. doi: 10.1097/MAO.0b013e318287efe6
153. Mehta R, Klumpp ML, Spear SA, Bowen MA, Arriaga MA, Ying YLM. Subjective and objective findings in patients with true dehiscence versus thin bone over the superior semicircular canal. *Otol Neurotol.* (2015) 36:289–94. doi: 10.1097/MAO.0000000000000654
154. Taylor RL, Magnussen JS, Kwok B, Young AS, Ihtijarevic B, Argaet EC, et al. Bone-Conducted oVEMP latency delays assist in the differential diagnosis of large air-conducted oVEMP amplitudes. *Front Neurol.* (2020) 11:580184. doi: 10.3389/fneur.2020.580184

155. Pritchett CV, Spector ME, Kileny PR, Heidenreich KD, El-Kashlan HK. Surgical treatment of hearing loss when otosclerosis coexists with superior semicircular canal dehiscence syndrome. *Otol Neurotol.* (2014) 35:1163–7. doi: 10.1097/MAO.0000000000000470
156. Hope A, Fagan P. Latent superior canal dehiscence syndrome unmasked by stapedotomy for otosclerosis. *J Laryngol Otol.* (2010) 124:428–30. doi: 10.1017/S0022215109991654
157. Ungar OJ, Handzel O, Cavel O, Oron Y. Superior semicircular canal dehiscence with concomitant otosclerosis—A literature review and case discussion. *Clin Case Rep.* (2018) 6:2364–70. doi: 10.1002/ccr3.1822
158. Yong M, Zaia E, Westerberg B, Lea J. Diagnosis of superior semicircular canal dehiscence in the presence of concomitant otosclerosis. *Otol Neurotol.* (2017) 38:1071–5. doi: 10.1097/MAO.0000000000001490
159. Maxwell AK, Slattery WH, Gopen QS, Miller ME. Failure to close the gap: concomitant superior canal dehiscence in otosclerosis patients. *Laryngoscope.* (2020) 130:1023–7. doi: 10.1002/lary.28167
160. Hong RS, Metz CM, Bojrab DI, Babu SC, Zappia J, Sargent EW, et al. Acoustic reflex screening of conductive hearing loss for third window disorders. *Otolaryngol Head Neck Surg.* (2016) 154:343–8. doi: 10.1177/0194599815620162
161. Fernandez IJ, Molinari G, Presutti L. Decision making in patients with concomitant otosclerosis and superior semicircular canal dehiscence: a systematic review of the literature. *Otol Neurotol.* (2021) 42:e1–9. doi: 10.1097/MAO.0000000000002897
162. de Souza C, Glasscock ME, (editors). Radiological imaging of otosclerosis. In: *Otosclerosis and Stapedectomy: Diagnosis, Management, and Complications*. Stuttgart; New York, NY; Delhi: Thieme (2004) p. 41–9. doi: 10.1055/b-002-43894
163. Lee GS, Zhou G, Poe D, Kenna M, Amin M, Ohlms L, et al. Clinical experience in diagnosis and management of superior semicircular canal dehiscence in children. *Laryngoscope.* (2011) 121:2256–61. doi: 10.1002/lary.22134
164. Dasgupta S, Ratnayake SAB. Functional and objective audiovestibular evaluation of children with apparent semicircular canal dehiscence–a case series in a pediatric vestibular center. *Front Neurol.* (2019) 10:306. doi: 10.3389/fneur.2019.00306
165. Zhou G, Ohlms L, Liberman J, Amin M. Superior semicircular canal dehiscence in a young child: implication of developmental defect. *Int J Pediatr Otorhinolaryngol.* (2007) 71:1925–8. doi: 10.1016/j.ijporl.2007.08.009
166. Phillips DJ, Souter MA, Vitkovitch J, Briggs RJ. Diagnosis and outcomes of middle cranial fossa repair for patients with superior semicircular canal dehiscence syndrome. *J Clin Neurosci.* (2010) 17:339–41. doi: 10.1016/j.jocn.2009.06.021

Conflict of Interest: The authors declare that the research was conducted in the absence of any commercial or financial relationships that could be construed as a potential conflict of interest.

Advantages of publishing in Frontiers

OPEN ACCESS
Articles are free to read for greatest visibility and readership

FAST PUBLICATION
Around 90 days from submission to decision

HIGH QUALITY PEER-REVIEW
Rigorous, collaborative, and constructive peer-review

TRANSPARENT PEER-REVIEW
Editors and reviewers acknowledged by name on published articles

Frontiers
Avenue du Tribunal-Fédéral 34
1005 Lausanne | Switzerland

Visit us: www.frontiersin.org
Contact us: frontiersin.org/about/contact

REPRODUCIBILITY OF RESEARCH
Support open data and methods to enhance research reproducibility

DIGITAL PUBLISHING
Articles designed for optimal readership across devices

FOLLOW US
@frontiersin

IMPACT METRICS
Advanced article metrics track visibility across digital media

EXTENSIVE PROMOTION
Marketing and promotion of impactful research

LOOP RESEARCH NETWORK
Our network increases your article's readership